Vol. 148, April 1, 1983
Complete in one issue

ISSN 0003-2670

ANALYTICA CHIMICA ACTA

International journal devoted to all branches of analytical chemistry

ELSEVIER SCIENTIFIC PUBLISHING COMPANY

ANALYTICA CHIMICA ACTA

International journal devoted to all branches of analytical chemistry
Revue internationale consacrée à tous les domaines de la chimie analytique
Internationale Zeitschrift für alle Gebiete der analytischen Chemie

PUBLICATION SCHEDULE FOR 1983

	J	F	M	A	M	J	J	A	S	O	N	D
Analytica Chimica Acta	145	146	147	148	149	150/1 150/2	151	152	153/1	153/2	154	155

Scope. *Analytica Chimica Acta* publishes original papers, short communications, and reviews dealing with every aspect of modern chemical analysis, both fundamental and applied.

Submission of Papers. Manuscripts (three copies) should be submitted as designated below for rapid and efficient handling:

Papers from the Americas to: Professor Harry L. Pardue, Department of Chemistry, Purdue University, West Lafayette, IN 47907, U.S.A.

Papers from all other countries to: Dr. A. M. G. Macdonald, Department of Chemistry, The University, P.O. Box 363, Birmingham B15 2TT, England. Papers dealing particularly with computer techniques to: Professor J. T. Clerc, Universität Bern, Pharmazeutisches Institut, Sahlistrasse 10, CH-3012 Bern, Switzerland.

Submission of an article is understood to imply that the article is original and unpublished and is not being considered for publication elsewhere. Upon acceptance of an article by the journal, authors resident in the U.S.A. will be asked to transfer the copyright of the article to the publisher. This transfer will ensure the widest dissemination of information under the U.S. Copyright Law.

Information for Authors. Papers in English, French and German are published. There are no page charges. Manuscripts should conform in layout and style to the papers published in this Volume. Authors should consult Vol. 132, p. 239 for detailed information. Reprints of this information are available from the Editors or from: Elsevier Editorial Services Ltd., Mayfield House, 256 Banbury Road, Oxford OX2 7DH (Great Britain).

Reprints. Fifty reprints will be supplied free of charge. Additional reprints (minimum 100) can be ordered. An order form containing price quotations will be sent to the authors together with the proofs of their article.

Advertisements. Advertisement rates are available from the publisher.

Subscriptions. Subscriptions should be sent to: Elsevier Science Publishers B.V., P.O. Box 211, 1000 AE Amsterdam, The Netherlands.

Publication. *Analytica Chimica Acta* appears in 11 volumes in 1983. The subscription for 1983 (Vols. 145–155) is Dfl. 1980.00 plus Dfl. 220.00 (postage) (total approx. U.S. $880.00). Journals are sent automatically by airmail to the U.S.A. and Canada at no extra cost and to Japan, Australia and New Zealand for a small additional postal charge. All earlier volumes (Vols. 1–144) except Vols. 23 and 28 are available at Dfl. 182.00 (U.S. $72.80), plus Dfl. 14.00 (U.S. $5.60) postage and handling, per volume.

Claims for issues not received should be made within three months of publication of the issue, otherwise they cannot be honoured free of charge.

Customers in the U.S.A. and Canada who wish to obtain additional bibliographic information on this and other Elsevier journals should contact Elsevier Science Publishing Company Inc., Journal Information Center, 52 Vanderbilt Avenue, New York, NY 10017. Tel: (212) 867-9040.

ANALYTICA CHIMICA ACTA
VOL. 148 (1983)

ANALYTICA CHIMICA ACTA

International journal devoted to all branches of analytical chemistry

ELSEVIER - AMSTERDAM - OXFORD - NEW YORK

Anal. Chim. Acta, Vol. 148 (1983)

Printed in The Netherlands.

Analytica Chimica Acta, 148 (1983) 1—12
Elsevier Science Publishers B.V., Amsterdam — Printed in The Netherlands

STABILIZED BACTERIA-BASED POTENTIOMETRIC ELECTRODE FOR PYRUVATE

C. L. DI PAOLANTONIO[a] and G. A. RECHNITZ*
Department of Chemistry, University of Delaware, Newark, DE 19711 (U.S.A.)
(Received 10th September 1982)

SUMMARY

A bacteria-based potentiometric electrode is described which demonstrates a strategy for adapting an unstable enzyme system for use as a practical biocatalyst. *Streptococcus faecium* (ATCC 9790), containing the pyruvate dehydrogenase multienzyme complex, serves to convert pyruvate to carbon dioxide, which is detected by a gas-sensing electrode. The probe has an average slope of 41 mV per concentration decade over a range from 2.2×10^{-4} to 3.2×10^{-2} M pyruvate, and a lower limit of detection of 1.3×10^{-4} M pyruvate. Response times varied from 6—9 min for a new electrode to a maximum of 8—12 min during the probe lifetime of two weeks. Electrode storage at 4° C in a pH 5.5 buffer containing phosphate anions was critical in maintaining optimal probe response characteristics. The *Streptococcus faecium* electrode is compared and contrasted with other potentiometric pyruvate electrodes reported employing isolated enzyme, dual enzyme—cofactor, or plant tissue biocatalysts.

Since 1978, bacteria-based potentiometric electrodes have been reported which respond to several compounds of clinical interest, such as amino acids. Frequently, the enzymatic activity in the intact cells is sufficiently high that response characteristics of the cell-based probe are similar to those of comparable isolated enzyme electrodes, while the lifetime of the former is much enhanced owing to the minimal disruption of the native environment of the enzyme. In bacterial electrodes involving particularly unstable or rigidly regulated enzymes, however, response characteristics may be sufficiently poor that manipulation of biocatalyst growth, assay, and storage conditions is required in order to prepare a workable electrode. Because enzymes which are unstable in the cellular environment are generally even more unstable in the isolated form, efforts to optimize the operation of the bacterial sensor involved may represent the most worthwhile strategy for the development of a quantitatively useful probe.

A sensitive enzyme complex found in plant, animal, and microorganism systems is pyruvate dehydrogenase, which is known to catalyze the reaction sequence [1, 2]:

$$\text{Pyruvate} + \text{TPP-E1} \rightarrow CO_2 + \text{Hydroxyethyl-TPP-E1} \qquad (1)$$

[a]Present address: Diagnostics Division, Abbott Laboratories, North Chicago, IL 60064 (U.S.A.)

0003-2670/83/$03.00

Hydroxyethyl-TPP-E1 + Lipoyl-E2 → *S*-acetyldihydrolipoyl-E2 + TPP-E1 (2)

S-acetyldihydrolipoyl-E2 + CoA → Acetyl-CoA + Dihydrolipoyl-E2 (3)

Dihydrolipoyl-E2 + FAD-E3 → Lipoyl-E2 + FAD(red.)-E3 (4)

FAD(red.)-E3 + NAD^+ → FAD-E3 + NADH + H^+ (5)

to give the overall reaction

Pyruvate + NAD^+ + CoA → Acetyl CoA + NADH + H^+ + CO_2 (6)

In both microbial and mammalian pyruvate dehydrogenase complexes, there exist several subunits each of E1, pyruvate dehydrogenase (E.C. 1.2.4.1), E2, dihydrolipoamide acetyltransferase (E.C. 2.3.1.12) and E3, dihydrolipoamide dehydrogenase (E.C. 1.6.4.3). The five cofactors, thiamine pyrophosphate (TPP), lipoic acid, coenzyme A (CoA), flavin adenine dinucleotide (FAD), nicotinamide adenine dinucleotide (NAD^+), endogenous in the cellular cytoplasm, work in concert with the enzymes to effect the complicated conversion. In addition, the pyruvate dehydrogenase enzyme subunits are known to be allosteric, containing two distinct catalytic sites [3], and to be activated by a divalent cation such as magnesium or manganese [4].

A good source of the enzyme complex is the bacterium *Streptococcus faecium* (ATCC 9790), an easily propagated Group D *Streptococcus* strain. These homofermentative organisms are reported to implement the pyruvate dehydrogenase complex in a dismutation pathway [5, 6]:

$$\text{Pyruvate} + NAD^+ + \text{CoA} \xrightleftharpoons{\text{pyruvate dehydrogenase complex}} \text{Acetyl-CoA} + \text{NADH} + H^+ + CO_2 \quad (6)$$

$$\text{Acetyl-CoA} + \text{phosphate} \xrightleftharpoons[\text{E.C.2.3.1.8}]{\text{phosphate acetyl transferase}} \text{Acetyl phosphate} + \text{CoA} \quad (7)$$

$$\text{Pyruvate} + \text{NADH} + H^+ \xrightarrow[\text{E.C. 1.1.1.27}]{\text{lactate dehydrogenase}} \text{Lactate} + NAD^+ \quad (8)$$

to give the net reaction

2 Pyruvate + phosphate ⇌ Acetyl phosphate + Lactate + CO_2 (9)

Although the potentiometric detector senses the carbon dioxide liberated by the first step of the pyruvate dehydrogenase sequence (Eqn. 1), it is necessary to stabilize the entire fermentative pathway in order to maintain useful biocatalytic activity. It is shown in this paper that the particular sensitivity of pyruvate dehydrogenase complex to changes in its environment makes it a realistic example to illustrate approaches for bioselective membrane electrode development based on bacterial cells.

EXPERIMENTAL

Apparatus

All potentiometric measurements were made with a Corning model 12 pH/mV meter in conjunction with a Heath-Schlumberger model 240 potentio-

metric recorder. Measurements were made in a thermostatted vessel controlled at 25 ± 0.1°C with a Haake model FS water bath. The carbon dioxide sensor used for all work was the Orion model 95-02 electrode. An IEC model HT centrifuge was modified for refrigerated use. The bacteria were grown in a New Brunswick Scientific model G76 gyrotary water bath shaker adjusted to 37°C.

Reagents

All solutions were prepared with distilled, deionized water. Analytical-grade reagents were used except where otherwise noted. L-Pyruvate, all amino acids, malate, citrulline, ornithine, oxalate, tyramine, thiamine pyrophosphate, and 2(*N*-morpholino)-ethanesulfonic acid (MES) were all from Sigma Chemical Co. D-Glucose, magnesium sulfate, potassium hydrogenphthalate, and ethylenediaminetetraacetic acid (EDTA) were from Fisher. Yeast extract and bacto-peptone were from Difco Laboratories, (Detroit, MI), and the bacterium *Streptococcus faecium* (ATCC 9790) was from the American Type Culture Collection (Rockville, MD).

Procedures

Growth and preparation of the bacterial biocatalysts. Streptococcus faecium was grown in a distilled water medium [7] containing 0.5% bacto-peptone, 2.0% yeast extract, 0.05% KH_2PO_4, and 0.05% K_2HPO_4, adjusted to pH 7.0, which was divided among 125-ml culture flasks, and autoclaved at 15 psi for 20 min. The flasks were cooled to room temperature, supplemented with 0.5% D-glucose, and inoculated with 5 ml of a 1—5-day old refrigerated stationary culture of bacteria. The cultures were placed in a shaker bath rotating at approximately one-third of the maximum rate. Under these conditions, the bacterial growth profile revealed a lag phase for the first hour, logarithmic growth for the next four hours with a stationary phase following that period; cells were harvested 3—3.5 h after inoculation at the mid-logarithmic point of multiplication. The growth profile was ascertained by measuring the culture turbidity spectrophotometrically at 660 nm, using distilled deionized water as the reference. The bacteria were washed twice at 4°C in a pH 7.0, 0.2 M sodium phosphate buffer, collected as a paste by centrifugation, and approximately 10 μl (25 mg) was applied to the gas-permeable membrane of a carbon dioxide electrode. The cells were supported at the gas-permeable membrane with a circular dialysis membrane, as previously described [8]. The electrode filling solution consisted of 3.0×10^{-2} M $NaHCO_3$ in 1.7×10^{-1} M NaCl.

The probe was conditioned for one hour and used for pyruvate measurements in a 0.1 M potassium hydrogenphthalate—0.1 M potassium phosphate buffer adjusted to pH 5.5 with potassium hydroxide. The electrode was stored in assay buffer at 4°C.

Optimization of electrode decarboxylating activity. The pH dependence of the pyruvate sensor was established using the previously described initial

rate method [9]. Several 10.00-ml volumes of citrate- and phthalate-based buffers containing 1.0×10^{-3} M thiamine pyrophosphate and 1.2×10^{-3} M pyruvate were tested in the pH range 3.5—6.0. The initial rate of production of carbon dioxide was obtained from a potential vs. time curve as previously described [10]. Measurements of this type yield information regarding the efficiency of both the biocatalyst and the carbon dioxide gas-sensor, allowing optimization of pH with respect to each. Other experimental conditions were varied independently during assay and/or storage while changes in pyruvate response characteristics, such as slope of the calibration graph and response time, were monitored.

Determination of apparent non-immobilized bacterial pyruvate dehydrogenase activity. Four flasks of cells were grown, harvested separately, and washed twice in pH 7.0, 0.2 M sodium phosphate buffer, and each was resuspended in 3.5 ml of wash buffer. Four lengths of 3500 m.w. cutoff dialysis tubing were boiled to remove sulfides; each cell suspension was placed in a dialysis bag; and the four were dialyzed at 4°C against a common 1-l volume of storage buffer, as described above. The buffer was replaced daily with fresh, pre-cooled aliquots. The initial rate of decarboxylation was then measured by adding 1.00 ml of bacterial cell suspension to a thermostatted cell containing 10.00 ml of assay buffer (as described above) and 5×10^{-3} M pyruvate.

RESULTS AND DISCUSSION

Bacterial probe characteristics

The potentiometric response to pyruvate of carbon dioxide electrodes with and without immobilized bacteria is shown in Fig. 1. Calibration graphs obtained for the bacterial electrode in a pH 5.5, 0.1 M potassium hydrogenphthalate—0.1 M potassium dihydrogenphosphate buffer at 25°C, summarized in Table 1, showed an average slope of 41 mV per decade change in pyruvate concentration between 2.2×10^{-4} and 3.2×10^{-2} M pyruvate, lower limit of detection of 1.29×10^{-4} M pyruvate, and response times of 6—9 min on day one and 8—10 min on day 2.

Probe pH dependence

A pH profile, shown in Fig. 2, reflects an optimum at pH 4.5 in citrate buffer, although repetitive kinetic experiments at each pH value below 5.0 resulted in successively lower rates of decarboxylation, as indicated by the error bars. This pH-dependent inactivation of the pyruvate decarboxylase was confirmed by a time study, in which the response of a new bacterial electrode conditioned in pH 3.5 citrate buffer was measured at 60, 90 and 120 min. A rapid decrease in decarboxylation rate was evident, as only 25% of the activity measured at 60 min remained at 120 min. Similar citrate inhibition of the pyruvate dehydrogenase complex has been noted by other workers and attributed either to competition for a limiting cofactor by

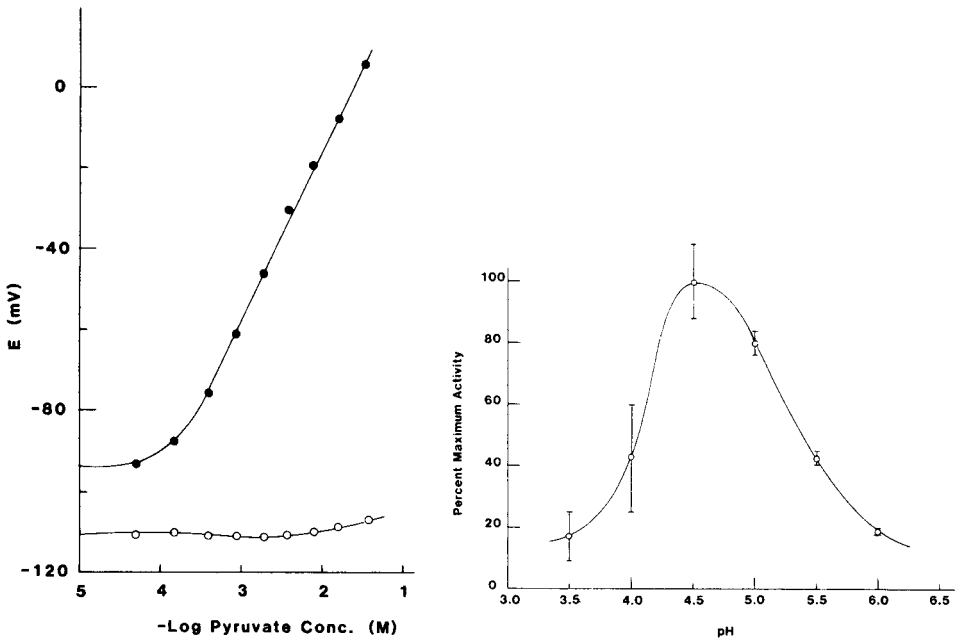

Fig. 1. Responses to pyruvate of a carbon dioxide sensor: (•) with immobilized bacteria; (○) without bacteria.

Fig. 2. Effect of pH on the response of the bacterial electrode using 0.1 M citric acid—sodium citrate buffer. Error bars represent decreasing percent maximum activity resulting from three successive assays at a particular pH.

citrate or its metabolite [11], or to nonspecific regulation of the cellular energy production system [12]. The time-dependent responses of six other bacterial probes were determined in 0.1 M citrate and 0.1 M phthalate buffers at different pH values; the results are summarized in Fig. 3. In each case, degeneration of the enzyme occurs to a greater extent as the pH is lowered, with only 60—70% of the original activity remaining after one day.

Stabilization of the bacterial pyruvate sensor

The dismutation pathway outlined in Eqns. (6—8) is reported to be the pyruvate degradative sequence when *Streptococcus faecalis* is grown in non-vigorously aerated complex media containing lipoic acid [5, 6]. Lipoate was present in the yeast extract component of the growth medium and supplementation of assay or storage buffers was not needed to maintain pyruvate dehydrogenase complex reactions. In fact, assay buffers containing 1×10^{-3} M lipoate almost completely inactivated the probe, possibly because of the same "erratic utilization" of pyruvate reported when the organism was grown in synthetic containing similarly high concentrations of the cofactor [13].

TABLE 1

Pyruvate response characteristics of electrodes based on *Streptococcus faecium* (Calibration conditions chosen: 10.00 ml of pH 5.5, 0.1 M potassium hydrogenphthalate–0.1 M KH_2PO_4—KOH at 25°C.)

Electrode	Slope (mV/decade)	r^2	Lower limit of detection, (10^{-4} M)	Response times[a] (min)		Response times[b] (min)	
1	39.6	0.9982	1.16	8		6	
1[c]	40.4	0.9977	1.28		11		7
2	40.4	0.9986	1.06	8		6	
3	42.5	0.9969	1.69	9		7	
3[c]	41.5	0.9974	1.40		10		8
4	40.3	0.9976	1.24	9		6	
5	39.4	0.9979	1.04	9		7	
6[c]	41.2	0.9940	1.16		12		8
7	42.5	0.9976	1.44	9		6	
7[c]	42.0	0.9974	1.43		10		8
Av. ± s.d.	41.0 ± 1.2		(1.29 ± 0.20) × 10^{-4}	9 ± 1	10 ± 2	6 ± 1	8 ± 1

[a]Response time when changing the pyruvate concentration from 3.98 × 10^{-4} to 8.91 × 10^{-4} M. [b]Response time when changing the pyruvate concentration from 3.72 × 10^{-3} M to 8.13 × 10^{-3} M. [c]Electrode response tested on day 2.

Inorganic phosphate was necessary to maintain optimal probe response characteristics; its role in regenerating coenzyme A (Eqn. 7) for use in the third step of the pyruvate dehydrogenase reaction sequence (Eqn. 3) may deplete cellular stores quickly, requiring outside addition of the anion. Supplementation of a pH 5.5 potassium hydrogenphthalate buffer with 0.1 M potassium phosphate resulted in retention of 72% of the original activity after 4.5 days. Kinetic experiments using a 0.1 M MES–0.1 M

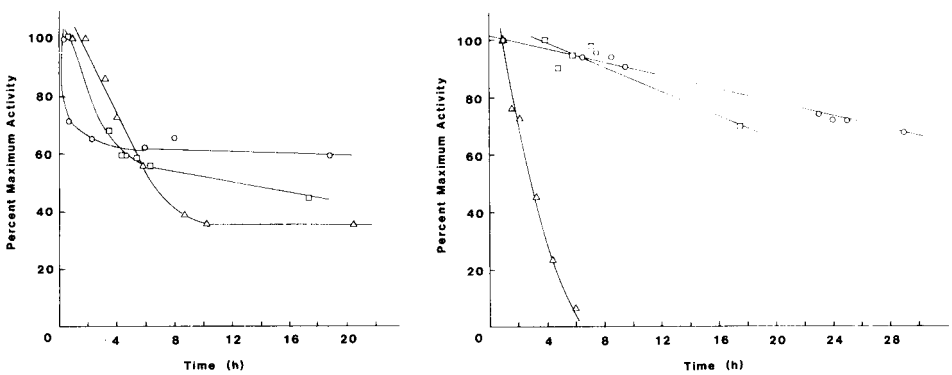

Fig. 3. Effect of buffer composition and pH on the stability of three bacterial pyruvate electrodes. (A) 0.1 M citric acid—sodium citrate buffers; (B) 0.1 M potassium hydrogenphthalate—sodium hydroxide buffers. pH values: (△) 4.5; (□) 5.0; (○) 5.5.

sodium phosphate buffer reflected similar electrode stability, indicating a phosphate rather than potassium dependence. Because no difference in electrode response or stability resulted when a 0.1 M potassium hydrogenphthalate buffer was supplemented with 0.05 M, 0.15 M, or 0.20 M phosphate, all subsequent work was done with a 0.1 M hydrogenphthalate—0.1 M phosphate buffer composition.

Streptococcus faecalis, a parent streptococcal strain, is known to metabolize pyruvate via three main pathways [14], including the pyruvate dehydrogenase complex, a formate acetyltransferase (E.C. 2.3.1.54), and a lipoate-independent pyruvate dehydrogenating system existing in cultures containing iron(II) sulfate or ascorbate. Growth media did not contain the latter components, so the streptococcus was believed to utilize mainly the first two pathways. As formate acetyltransferase converts pyruvate and coenzyme A to formate and acetyl-coenzyme A, high concentrations of formate in the assay buffer would be expected to inhibit this particular enzyme. Supplementation of assay buffer with 0.1 M sodium formate caused no change in pyruvate decarboxylation response characteristics, indicating either inherently low *Streptococcus faecium* formate acyltransferase activity or a lack of feedback inhibition by the reaction end-product. *Streptococcus faecium* and *Streptococcus faecalis* are also reported to convert pyruvate to acetate and carbon dioxide when grown in vigorously aerated glucose media [15]. This may account for some fraction of the pyruvate decarboxylation, as oxygen was not excluded during microbe growth.

Electrode lifetime

The potentiometric response of bacterial probes stored as outlined above at 25° C deteriorated after about two days, with less negative starting potentials, slower steady-state response times, and decreased slopes. An activation treatment consisting of dialysis for 1 h in pH 6.5 phosphate buffer containing 5×10^{-3} M thiamine pyrophosphate and 5×10^{-3} M magnesium ions used to condition the plant tissue-based pyruvate sensor [16], proved unsuccessful for the bacterial probe. Similarly, electrode incubation in pH 6.5 buffers containing either 0.1 M imidazole or 0.1 M MES failed to activate the dehydrogenase complex. Electrode storage between uses at 4° C was effective, however, in maintaining both baseline potentials and calibration graph slopes; virtually the same response characteristics were exhibited with or without supplementation of storage buffers by enzyme cofactors. The two-week useful lifetime is shown by successive calibration curves in Fig. 4; response times for day 13 were between 8 and 12 min at concentrations of 8.13×10^{-3} M and 8.91×10^{-4} M pyruvate (Table 1). Conditioning of the probe in 1.0×10^{-2} M NAD^+-assay buffer or supplementing the working buffer with NAD^+ failed to extend the lifetime of the sensor beyond the two-week period; this may indicate either no uptake of NAD^+ by the cells or general inactivation of the enzyme complex, rather than lack of a specific nucleotide cofactor.

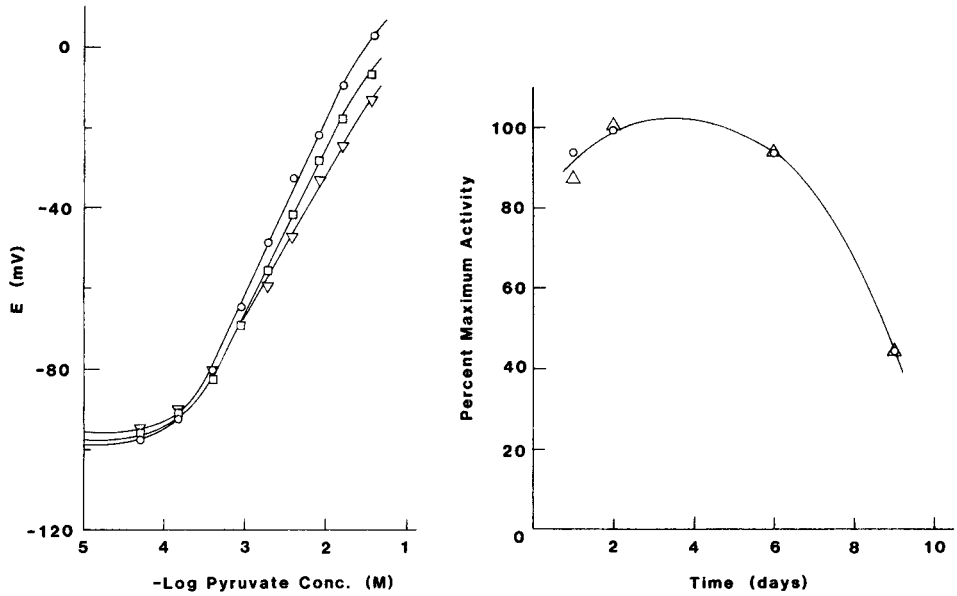

Fig. 4. Responses of the bacterial electrode to pyruvate: (○) day 2; (□) day 7; (▽) day 13.

Fig. 5. Effect of exposure to 4° C, pH 5.5 storage buffer on the pyruvate decarboxylating activity of non-immobilized bacterial cells: (△) trial 1; (○) trial 2.

Apparent non-immobilized bacterial enzyme activity

Long-term degradation of bacterial electrode response can be the result of either general loss of enzyme activity or contact with specific denaturants, such as inhibitory reaction end products, pH extremes in the macro- or micro-environment, or temperature fluctuations. In order to differentiate between the two cases, a large pool of bacterial cells was dialyzed against storage buffer at 4° C and periodically tested by measuring the initial rate of homogeneous decarboxylation. Results of the study, shown in Fig. 5, indicate that a general loss of pyruvate decarboxylating activity occurs after about six days. Thermostable inhibitor(s) of the pyruvate dehydrogenase complex have been identified in the *Streptococcus faecalis* parent strain [17], possibly contributing to the eventual inactivation. Although a substantial fraction of the initially available activity is lost after the first week, sufficient activity remains for an immobilized electrode to perform well throughout the two-week period.

Optimization of sensor assay conditions

Because pyruvate dehydrogenase from both procaryotic and eucaryotic sources is reported [18, 19] to require a divalent cation in order to ensure the stereochemically correct union of apoenzyme with the thiamine pyrophosphate cofactor [1, 20], electrode-kinetic and steady-state responses

were monitored as a function of magnesium ion concentration in the buffer. No change in the rate of decarboxylation was observed when the electrode was preconditioned and used in buffers containing 1×10^{-5}—1×10^{-2} M Mg^{2+}, probably because of sufficient cellular concentrations of the ion. Repeated probe dialysis in 4°C storage buffer containing 1×10^{-2} M EDTA, changed on a daily basis, resulted in no degradation of response characteristics after four days. This indicates that the magnesium contained within the bacteria is either in the bound form and not chelated by the EDTA or is in high enough concentration to allow maximum decarboxylase activity despite considerable ion removal by the chelating agent. Because added magnesium ions had no effect on electrode response, magnesium ion was omitted from all buffers. Similarly, calcium ions proved to be ineffective in activating the streptococcal pyruvate dehydrogenase, as was reported with *E. coli*-derived enzyme, although calcium ion is a strong stimulator of mammalian pyruvate dehydrogenase systems [4].

The effect of a high-energy-yielding source such as glucose on pyruvate decarboxylation of the *Streptococcus* electrode was also examined. A carbon source such as a hexose is metabolized by many bacterial strains to form phosphate-containing products, such as adenosine 5′-triphosphate which can later be expended during cellular biosynthesis. The addition of 0.05% glucose to the assay buffer reduced the response time of the probe at all pyruvate concentrations to about 4 min, one-third to one-half of the time required when no glucose was present. However, the supplementation also caused a tenfold increase in the lower limit of detection of pyruvate and a shift in the logarithmic range of response, which nullifies any advantage gained by the shorter response time. Higher glucose concentrations also stimulated non-pyruvate-dependent carbon dioxide production, reflecting some bacterial respiration and is discussed in the context of selectivity below.

Additional experimental parameters varied included volume of assay buffer, temperature of assay buffer, and bacterial growth period. Essentially the same electrode response was achieved in assay volumes ranging from 2.00 to 10.00 ml, making this probe adaptable to smaller sample sizes. No advantage was gained in raising the buffer temperature from 25°C to 30°C, because carbon dioxide gas is fairly insoluble in aqueous solutions. Finally, mid-logarithmic phase cell harvests yielded sufficient biocatalyst, while late logarithmic and stationary phase harvests required longer growth periods with no concomitant gain in enzyme activity.

Selectivity

The *Streptococcus faecium* electrode was tested for response to several compounds structurally related to pyruvate, including glutamate, lysine, histidine, ornithine, citrulline, oxalate, tyrosine, malate, and glucose (Table 2). Significant responses to 2.0×10^{-3} M glucose, tyrosine, and malate probably indicate the presence of microbial respiratory enzymes, tyrosine decarboxylase (E.C. 4.1.1.25), and malate dehydrogenase (E.C. 1.1.1.39),

TABLE 2

Selectivity of the electrode based on *Streptococcus faecium*[a]

Compound[b]	Deviation from baseline potential (mV)	Compound[b]	Deviation from baseline potential (mV)
Pyruvate	49.5	Oxalate	0.0
Glutamate	0.8	Tyrosine	23.4
Lysine	0.5	Tyrosine[c]	8.0
Histidine	0.2	Malate	31.4
Ornithine	0.5	Glucose	25.4
Citrulline	0.7	Glucose[d]	0.0

[a]Selectivities measured in 0.1 M potassium hydrogenphthalate—0.1 M KH_2PO_4 at pH 5.5. [b]Concentration of each compound tested was 2.0×10^{-3} M. [c]Response measured in assay buffer supplemented with 0.1 M tyramine. [d]Response measured following probe exposure to 0.01 M iodoacetamide in the assay buffer for several hours at 4°C.

respectively. Hexoses are reported to be primary carbon sources for this strain [13] and therefore are easily metabolized, while the tyrosine- and malate-degrading enzymes have been identified in Group D streptococci [21, 22]. Elimination of microbial respiration in order to avoid the glucose interference, as was implemented in a glutamate-selective sensor by vigorous deaeration of working buffers [23], would not be expected to be a viable alternative in this case, as the homofermentative respiration pathway discussed earlier is oxygen-indifferent. Exposure of a new probe to 0.01 M iodoacetamide (in assay buffer), a known glycolysis inhibitor [24, 25], for several hours at 4°C served completely to suppress the glucose interference while good pyruvate response characteristics were maintained. Its irreversibility as an inhibitor was confirmed after exposure of the probe for several days to storage buffers without iodoacetamide, as no glucose response returned, while the pyruvate-decarboxylating activity remained strong. Feedback inhibition of tyrosine decarboxylase through supplementation of assay buffers with 0.1 M tyramine, the end-product of the interfering reaction, effectively suppressed the tyrosine response. The electrode response to pyruvate was similarly unaffected by this treatment, while any steps capable of reducing its malate-decarboxylating activity also inhibited the pyruvate dehydrogenase complex.

Comparison with other potentiometric pyruvate electrodes

A pyruvate sensor based on immobilized lactate dehydrogenase, glutamate dehydrogenase, and nicotinamide adenine dinucleotide was introduced in 1974 [26]. The presence of glutamate in the assay buffer caused ammonium ions to be generated, which were measured by a glass cation-sensing electrode. The measurable range for pyruvate was one concentration decade, from 10^{-4} to 10^{-3} M, while the slope of an electrode stored at 4°C was 15.3 mV/decade

on day 1 and 7.2 mV/decade on day 15. In addition, sodium and potassium ions had to be removed from all buffers and standards, as these ions interfere severely with the ammonium probe. A plant tissue-based sensor in which pyruvate decarboxylase in corn kernel slices serves as biocatalyst to convert pyruvate to carbon dioxide was also reported [16]. Many response characteristics are similar for the bacteria- and tissue-based electrodes, such as average slope, lower limit of detection, and range of response; however, the tissue electrode showed double to triple the response time and had half the useful lifetime when stored at room temperature. Neither tissue nor isolated enzyme biocatalysts are subject to interference by structurally related compounds, although continuous degradation of enzyme electrode slope renders the enzyme electrode impractical [16].

Conclusion

The bacterial electrode described for pyruvate demonstrates a viable approach to adapting a complicated, unstable enzyme system for quantitative use. The biocatalyst lifetime is enhanced and electrode response characteristics are maintained by taking advantage of both inhibitors of metabolic regulatory enzymes, phosphate anions, and the use of enzyme stabilizers, such as buffers of moderate pH and cold storage.

We gratefully acknowledge the support of National Institutes of Health Grant GM-25312.

REFERENCES

1 A. L. Lehninger, Biochemistry, 2nd edn., Worth Publishers, New York, 1975, pp. 450—453.
2 C. J. Stanley, L. C. Packman, M. J. Danson, C. E. Henderson and R. N. Perham, Biochem. J., 195 (1981) 715.
3 H. Bisswanger, J. Biol. Chem., 256 (1981) 815.
4 T. Hayakawa, M. Hirashima, M. Hamada and M. Koike, Biochim. Biophys. Acta, 123 (1966) 574.
5 S. Korkes, A. delCampillo, I. C. Gunsalus and S. Ochoa, J. Biol. Chem., 193 (1951) 721.
6 L. J. Reed, F. R. Leach and M. Koike, J. Biol. Chem., 232 (1958) 123.
7 T. D. Brock and G. Moo-Penn, Arch. Biochem. Biophys., 98 (1962) 183.
8 D. S. Papastathopoulos and G. A. Rechnitz, Anal. Chim. Acta, 79 (1975) 17.
9 M. A. Arnold and G. A. Rechnitz, Anal. Chem., 53 (1981) 515.
10 P. D'Orazio, M. E. Meyerhoff and G. A. Rechnitz, Anal. Chem., 50 (1978) 153.
11 R. J. Haslam, in J. M. Tager, S. Papa, E. Quagliariello and E. C. Slater (Eds.), Regulation of Metabolic Processes in Mitochondria, Elsevier, Amsterdam, 1966, p. 108.
12 C. K. Silbert and D. B. Martin, Biochim. Biophys. Acta, 31 (1968) 818.
13 H. H. Moustafa and E. B. Collins, J. Bacteriol., 97 (1969) 1496.
14 A. Yamazaki, K. Watanabe, Y. Nishimura and T. Kamihara, FEBS Lett., 64 (1976) 364.
15 J. London and M. D. Appleman, J. Bacteriol., 84 (1962) 597.
16 S. Kuriyama, M. A. Arnold and G. A. Rechnitz, J. Membr. Sci., 12 (1983) 269.
17 A. Yamazaki, Y. Nishimiura and T. Kamihara, FEBS Lett., 74 (1977) 62.

18 D. S. Goldman, Biochim. Biophys. Acta, 27 (1958) 506.
19 R. S. Schweet and K. Cheslock, J. Biol. Chem., 199 (1952) 749.
20 D. E. Metzler, Biochemistry, Academic Press, New York, 1977, p. 441.
21 E. F. Gale, in F. F. Nord (Ed.), Advances in Enzymology, Vol. 6, Interscience, New York, 1946, pp. 1—32.
22 R. H. Deibel, Bacteriol. Rev., 28 (1964) 330.
23 M. Hikuma, H. Obana, T. Yasuda, I. Karube and S. Suzuki, Anal. Chim. Acta, 116 (1980) 61.
24 M. Dixon and E. C. Webb, Enzymes, Academic Press, New York, 1964, pp. 341—343.
25 J. L. Webb, Enzyme and Metabolic Inhibitors, Vol. 3, Academic Press, New York, 1966, pp. 61—86.
26 P. Davies and K. Mosbach, Biochim. Biophys. Acta, 370 (1974) 329.

Analytica Chimica Acta, 148 (1983) 13—18
Elsevier Science Publishers B.V., Amsterdam — Printed in The Netherlands

THE DETERMINATION OF GLUCOSE, HYPOXANTHINE AND URIC ACID WITH USE OF BI-ENZYME AMPEROMETRIC ELECTRODES

J. J. KULYS*, V.-S. A. LAURINAVIČIUS, M. V. PESLIAKIENE and V. V. GUREVIČIENE

Institute of Biochemistry, Lithuanian Academy of Sciences, Vilnius (U.S.S.R.)

(Received 22nd October 1982)

SUMMARY

Bi-enzyme electrodes sensitive to 0.01—1.6 mM glucose, 0.01—0.28 mM hypoxanthine and 0.005—0.13 mM uric acid are described which operate at 0.0 V vs. Ag/AgCl. Ascorbic acid, uric acid and other substances do not influence the determination of glucose content in 10-times diluted blood. The flow-through glucose-sensitive electrode is useful for the determination of glucose in pure buffer solutions for 2—3 months and in a 10-fold diluted blood flow for 7 days.

Electrodes with actions based on the electrochemical oxidation of hydrogen peroxide, the product of oxidase reactions, are the most widely used of all amperometric enzyme electrodes [1]. As the hydrogen peroxide oxidation is irreversible, enzyme electrodes operate at 0.6—0.7 V vs. Ag/AgCl [2]. At such a high potential, many organic compounds, including ascorbic and uric acids, urea and amino acids, which are common components of biological fluids, are oxidized at the noble metal electrode [3]. Hence, the selectivity of such enzyme electrodes is low. To improve the selectivity, a complex membrane of three layers, one of which has a decreased permeability to organic compounds, has been used [4]. Such electrodes are used in the Yellow Spring Instrument glucose analyser [4] and as glucose sensors in the Biostator glucose-controlled insulin infusion system (Miles Laboratories) [5]. However, the selectivity of electrodes with a three-layer membrane is inadequate, because various substances, including blood stabilizers, influence the glucose determination [6]. The main problem remaining is to increase further the selectivity of the electrodes, the solution to which may lie in decreasing the electrode potential.

Blaedel and Olson [7] suggested the determination of glucose with glucose oxidase and peroxidase in the presence of hexacyanoferrate(II). A distinctive feature of such a bi-enzyme system is the decreased potential. An analogous bi-enzyme system consisting of cholesterol oxidase and peroxidase has been used for the determination of cholesterol in blood plasma by means of a tubular carbon electrode [8]. Parameters of bi-enzyme electrodes sensitive to glucose, hypoxanthine and uric acid and data on the continuous

0003-2670/83/$03.00

determination of glucose in diluted blood are presented in this paper. Some results concerning the electrochemical studies of bi-enzyme electrodes sensitive to glucose have already been described [9].

EXPERIMENTAL

Materials

Xanthine oxidase (E.C.1.2.3.2) from cream with an activity of 0.74 U mg^{-1} and uricase (E.C.1.7.3.3) with an activity of 0.012 U mg^{-1} (both from Serva, G.F.R.), crystalline glucose oxidase (E.C.1.1.3.4, 180—220 U mg^{-1}; All Union Research Institute of Applied Enzymology, U.S.S.R.), peroxidase (E.C.1.11.1.7) from horseradish (360 U mg^{-1}; Reanal, Hungary), catalase (E.C.1.11.1.6), and bovine serum albumin (both from Chemical Reagents Plant, Olaine, U.S.S.R.), and heparin (Richter, Hungary) were used without further purification. Other reagents were of analytical grade or of the highest purity.

Enzyme electrode preparation

Rods of glassy carbon for the electrode (SU-1200, U.S.S.R.), 3 mm in diameter, were glued into a plastic tube. The electrode was polished with a fine corundum abrasive or Vienna lime. A bi-enzyme membrane (4 mm diameter) or a 10-μl solution of oxidase (50 μg) and peroxidase (50 μg) in the phosphate buffer was applied to the electrode surface. The glucose oxidase/peroxidase membrane was prepared as described previously [9]. The xanthine oxidase/peroxidase membrane was prepared as follows: 6 mg of peroxidase and 12 mg of albumin were dissolved in 0.1 ml of the phosphate buffer solution, 0.1 ml of a 25 mg ml^{-1} solution of xanthine oxidase and 0.04 ml of a 25% glutaraldehyde solution were added to the mixture, which was poured onto a glass plate (3 × 3 cm). After 24 h at 4°C, the membrane formed was cut into pieces. The membranes were held over the electrode surface by a dialysis membrane (55 μm thick).

The diameter of the glassy carbon electrode in the flow-through enzyme electrode was 1.5 mm. The electrode had a flow-through volume of 0.1 ml.

Measurement technique

The electrode current was determined at 0.0 V (vs. Ag/AgCl/saturated KCl) by a LP-7e polarograph. The flow-through electrode operated at 0.0 V (vs. Ag/AgCl/0.1 M KCl). The current from the flow-through electrode and the maximal derivative current value were determined by a specially made device with a digital display and printer. Measurements were made in 0.01 M phosphate buffer, pH 7.2, containing 0.1 M KCl and 1 mM potassium hexacyanoferrate(II) or in the same buffer without the hexacyanoferrate.

For determining substrates, the enzyme and reference electrodes were immersed in 9 ml of buffer solution until the establishment of a constant current (2—5 min) before 10 μl of substrate (glucose, hypoxanthine or uric

acid) was introduced into the cell. After 3 min, the increase in the stationary cathodic current was recorded and the values obtained were used to plot the calibration graphs. In measurements with the flow-through electrode, solutions containing different concentrations of glucose were prepared and pumped through the electrode at 0.3 ml min^{-1} by a peristaltic pump (ELMED-304, Poland). For determining glucose in heparinized blood (10 U heparin ml^{-1}), freshly prepared bovine blood was diluted 10 times with buffer solution and run through the electrode.

To eliminate glucose in blood, glucose oxidase (2 mg) and catalase (2 mg) were introduced into 10 ml of blood. After intensive stirring (30 min) with a magnetic stirrer the mixture was diluted 10 times with buffer solution containing hexacyanoferrate(II) and run through the electrode.

RESULTS

Glucose electrode

In the buffer solution containing hexacyanoferrate(II), the residual current of the glucose electrode based on immobilized enzymes is 5—10 nA. On the introduction of substrate, the constant current, which is established in 1.5—4 min, increases to 200—300 nA (Fig. 1). The current dependence on the substrate concentration exhibits a plateau, but is linear in the range 0.1—1.6 mM (Table 1). The electrodes containing soluble enzymes have shorter response times, but the upper limit of linear response is decreased to 1.2 mM. Their sensitivity, however, is 3—4 times higher than that of the

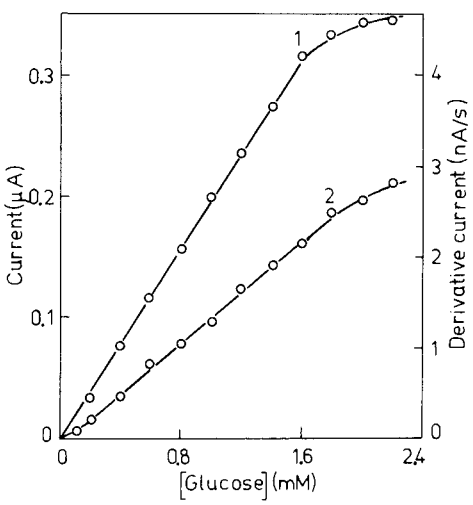

Fig. 1. The dependence of (1) the stationary current and (2) the peak derivative current from the glucose oxidase/peroxidase electrode on glucose concentration. (Glassy carbon electrode, immobilized bi-enzyme system, 0.01 M phosphate buffer pH 7.2, 0.1 M KCl, 1 mM potassium hexacyanoferrate(II), 0.0 V vs. Ag/AgCl.)

TABLE 1

Parameters for the bi-enzyme electrodes

Electrode	Biocatalyst	$Fe(CN)_6^{4-}$ conc. (mM)	Response time[a] (min)	Conc. interval, (mM)	Sensitivity (nA mM^{-1})
Glucose oxidase	Membrane	1.0	2.5	0.1—1.6	205
	Soluble	1.0	1.5	0.1—1.2	860
	enzymes	0	1.5	0.01—0.04	710
Glucose oxidase[b]	Membrane	1.0	3.0	0.1—1.2	56
Xanthine oxidase	Membrane	1.0	3.0	0.02—0.28	3250
	Soluble	1.0	1.0	0.01—0.11	5600
	enzymes	0	1.0	0.01—0.11	2800
Uricase	Soluble	1.0	3.0	0.005—0.035	440
	enzymes	0	3.0	0.01—0.13	120

[a]Time to reach 95% of the stationary current. [b]Flow-through system.

electrodes containing immobilized enzymes. On introduction of glucose, the current increase is also observed in electrodes with soluble enzymes and buffer solution containing no hexacyanoferrate(II). However, the upper linear calibration limit is only 0.04 mM. At low glucose concentrations, the sensitivity of such an electrode is similar to that in the presence of hexacyanoferrate(II) (Table 1).

The selectivity of the electrodes was tested with ascorbic acid (1 mM) and uric acid (0.03 mM), the two most important electroactive compounds in blood. The results obtained indicate that the electrode current in the presence of these substrates is less than 1% of the current at the same glucose concentration. On the removal of glucose from blood by glucose oxidase and catalase, the electrode response does not exceed the residual current. The selectivity of the flow-through glucose sensitive electrode is close to that of the electrode containing immobilized enzymes.

The dependence of the peak derivative current of the bi-enzyme glucose oxidase/peroxidase (immobilized) electrodes on glucose (Fig. 1) and hypoxanthine concentrations is sigmoidal. The slope of the calibration graph decreases above 1.8 mM glucose. Such recording of the peak derivative current decreases the response time of the electrode to 15 s.

Hypoxanthine and uric acid electrodes

The calibration graphs of enzyme electrodes containing xanthine oxidase and peroxidase, or uricase and peroxidase, show lower detection limits for the substrate than the glucose-sensitive electrodes. Their sensitivity in the linear region of the calibration graphs reaches 5 μA/mM xanthine (Table 1) which is much more sensitive than the glucose oxidase electrode; and unlike the latter, the presence of hexacyanoferrate(II) does not change the linear calibration range significantly, although it greatly increases the sensitivity.

During constant passage (8 h) of blood diluted with buffer solution containing hexacyanoferrate(II) through the flow-through glucose electrode, its sensitivity decreased linearly by 30% in 7 days. The same decrease of sensitivity was observed after 2—3 months of use, when a 1 mM glucose solution in the same buffer was used. Enzyme electrodes containing soluble glucose oxidase and peroxidase lost 30% of their initial activity in the course of 3—4 weeks. Electrodes with soluble xanthine oxidase or uricase lost 40—50% of their activity in 2—4 days and with immobilized xanthine oxidase, in 1—2 months.

DISCUSSION

The action of the hexacyanoferrate(II)-mediated bi-enzyme electrodes is based on two reactions [9]:

$$\text{Glucose} + O_2 \xrightarrow{\text{glucose oxidase}} \delta\text{-gluconolactone} + H_2O_2$$

$$H_2O_2 + 2[Fe(CN)_6]^{4-} + 2H^+ \xrightarrow{\text{peroxidase}} 2[Fe(CN)_6]^{3-} + 2H_2O$$

The hexacyanoferrate(III) formed is reduced at a glassy carbon electrode at 0.0 V. Without a mediator, the generated cathodic current is determined by direct reduction of hydrogen peroxide in the presence of peroxidase [9].

The parameters of the bi-enzyme electrodes are established by the kinetic properties of the oxidases as well as of peroxidases. Calculations indicate that at low substrate concentrations (lower than K_m for the enzyme) the stationary current is directly proportional to the substrate concentration [9]. At high concentrations, the stationary current becomes limiting, owing to saturation of the oxidase by the substrate or by hydrogen peroxide which is the product of the oxidase reaction. In glucose oxidase electrodes, the limiting stage is glucose oxidation because the semisaturation concentration with respect to this substrate considerably exceeds the K_m value for peroxidase ($K_m \approx 80$ μM [10]) and is close to that of native glucose oxidase (K_m = 5.9 mM [11]). This conclusion confirms the similar sensitivity of the mediated and unmediated electrodes observed at low glucose concentrations. For the unmediated electrode at high substrate concentration the reduction of hydrogen peroxide becomes rate-limiting. This occurs at a lower hydrogen peroxide concentration in the absence of hexacyanoferrate(II).

The action of the xanthine oxidase and uricase electrodes is also governed by oxidases. However, the use of high protein concentrations and their adsorption on the electrode result in a slower unmediated reduction of hydrogen peroxide than when hexacyanoferrate(II) is used. For this reason there is a considerable difference in sensitivity between the mediated and unmediated electrodes. The linear calibration range is limited by the low values of the Michaelis constant K_m for these enzymes.

The sigmoidal calibration graph obtained by plotting the maximum value from the derivative signal is established by the consecutive conversion of

substrate and its diffusion into the catalytic membrane. This process is similar to the consecutive conversion of substances in a homogeneous medium where the concentration dependence of an end-product with time is sigmoidal [12]. At high substrate concentrations, the linear calibration limit is again determined by the K_m value for the oxidase.

Because bi-enzyme electrodes operate at 0.0 V they are highly selective. This was indicated by the results obtained for the electrode current in the presence of electrochemically active compounds as well as by the zero residual current of these electrodes when diluted blood was used after elimination of glucose. The glucose oxidase electrode also exhibited a high stability in pure solutions. The decrease in the stability of the flow-through electrode in a diluted blood flow was due to the attachment of blood cells to the membrane and to the change in its permeability, as observed with a scanning microscope. The change in the external membrane also considerably reduced (by 20%) the initial sensitivity of the electrodes.

The high selectivity and stability of the bi-enzyme glucose electrodes enables them to be used as sensors for the determination and correction of sugar in blood.

REFERENCES

1 L. C. Clark, Jr., in P. W. Cheung, D. G. Fleming, W. H. Ko and M. R. Neuman (Eds.), Theory, Design and Biomedical Applications of Solid State Chemical Sensors, CRC Press, Cleveland, 1978, p. 183.
2 G. G. Guilbault and G. J. Lubrano, Anal. Chim. Acta, 64 (1973) 439.
3 D. A. Gough, F. L. Anderson, J. Giner, C. K. Colton and J. S. Soeldner, Anal. Chem., 50 (1978) 941.
4 M. H. Keyes, F. E. Semersky and D. N. Gray, Enzyme Microb. Technol. 1 (1979) 91.
5 A. H. Clemens and P. H. Chang, in proceedings of XIVth International Congress of Therapeutics, Montpellier (France), 1977, p. 45.
6 P. M. Hall and J. G. H. Cook, Clin. Chem., 28 (1982) 387.
7 W. J. Blaedel and C. L. Olson, U.S. Patent 3,367,849 (1968).
8 Y. Hahn and C. L. Olson, Anal. Chem., 51 (1979) 444.
9 J. J. Kulys, M. V. Pesliakiene and A. S. Samalius, Bioelectrochem. Bioenerget., 8 (1981) 81.
10 J. J. Kulys and A. S. Samalius, Liet. TSR Mokslu Akad. Darb. Ser. B., 2 (1982) 3.
11 V. F. Akulova, R. K. Vaitkevičius, B. S. Kurtinaitiene and J. J. Kulys, Prikl. Biokhim. Mikrobiol., 14 (1978) 377.
12 S. W. Benson, The Foundations of Chemical Kinetics, McGraw-Hill, New York, 1960.

Analytica Chimica Acta, 148 (1983) 19—25
Elsevier Science Publishers B.V., Amsterdam — Printed in The Netherlands

SOME POTENTIOMETRIC SENSORS WITH LOW OUTPUT IMPEDANCE

JAN LANGMAIER and KAREL ŠTULÍK*

Department of Analytical Chemistry, Charles University, Albertov 2030, 128 40 Prague 2 (Czechoslovakia)

ROBERT KALVODA

J. Heyrovský Institute of Physical Chemistry and Electrochemistry, Czechoslovak Academy of Sciences, Vlašská 9, 110 00 Prague 1 (Czechoslovakia)

(Received 5th October 1982)

SUMMARY

Several electronic circuits were constructed and tested for use in the body of ion-selective electrodes to convert the high-impedance output signal to a low-impedance one, in order to improve the signal-to-noise ratio. The signal was transmitted in analog form or was digitized and transmitted either by a classical electric cable or by an optical link. Good results were obtained by all three methods; transmission of the digitized signal led to a somewhat better precision and use of the optical link decreased the noise level. The reproducibility of measurement and the response rate were not adversely affected by the electronic circuits used. These electrodes are suitable for applications in which the signal is to be transmitted over long distances, such as in automated environmental analyses, industrial analyzers or geological prospecting.

Modern analytical practice increasingly requires automated measurements with transmission of the signal over long distances, e.g. in environmental control, computer-controlled production lines, clinical analyses or in situ analyses in deep bores in geological prospecting. Ion-selective electrodes are well suited for these purposes, but their high output impedance is a serious drawback that places great demands on the electric insulation and shielding and leads to generation of considerable noise in the electric connections (for a more detailed discussion see, e.g., Veselý et al. [1]). This disadvantage can be substantially alleviated when the sensor is combined with a signal-modifying circuit, from which a low-impedance signal is fed into the connecting line, and the analog signal is digitized, to suppress the effect of the noise picked up in the connecting lines.

This immediate connection of sensor and signal modifier has been used in some commercial instruments, e.g., for measurement of the temperature or pressure or for spectral measurements. In measurements with ion-selective electrodes, the signal modifier should consist of an impedance converter which should have the highest possible input impedance and the lowest possible drift, noise and output impedance (see, e.g., Kalvoda [2, 3]).

0003-2670/83/$03.00

Potentiometric sensors combined with signal modifiers and meters are commercially available for physiological [4] and pH [5] measurements. Another approach is either conversion of the voltage signal to current, as in the ion-selective field-effect transistor (ISFET [6]), or use of an electrode with a solid-state membrane that is directly connected with an uncovered chip of a FET operational amplifier [7]. However, these devices suffer from signal instability and difficulties are encountered in preparing ion-selective membranes on ISFET's and in insulating the amplifier chip. Immediate connection of polarographic sensors [3], Clark oxygen electrodes (SFS/9721; Orion Research, Cambridge, MA) or reference electrodes in polarographic circuits (Model 178 Electrometer Probe, Princeton Applied Research, Princeton, NJ) with operational amplifiers has also been described.

This paper describes the construction of a composite sensor containing an ion-selective electrode and an impedance converter, and possibly also a voltage-to-frequency converter, and its operation under laboratory conditions. Further, systems for signal transmission over long distances, based on classical electric conductors and on use of an optical link, are described and tested. The system is based on an operational amplifier (OA) built into the body of the ion-selective electrode and functioning as a voltage follower in various circuits. The non-inverting OA input is connected to the sensor; in combined ion-selective reference electrodes, the grounding input is connected to the reference electrode. The sensor output then consists of the low-impedance signal output of the voltage follower and the grounding lead or the reference electrode output in a combined ion-selective electrode.

EXPERIMENTAL

Equipment

The potentiometric sensors tested were a combined glass pH electrode (GK2301B, Radiometer, Denmark), a commercial fluoride-selective electrode (Crytur 09-17, Monokrystaly, Czechoslovakia) and a laboratory-made fluoride-selective electrode prepared by cementing a cylindrical single-crystal lanthanum fluoride element into a glass tube with a chloroprene rubber cement. Both the fluoride-selective electrodes were of the classical type with an internal standard solution and an internal silver chloride electrode. Some experiments were done with a specially constructed Clark oxygen sensor.

The measurements were made with an Electroanalytical Operational Amplifier Modular Kit (J. Heyrovský Institute of Physical Chemistry and Electrochemistry, Czechoslovakia), an MT100 digital voltmeter (Metra, Czechoslovakia) and BM370 and BM463 oscillographs (Tesla, Czechoslovakia). The impedance converter, built into the ion-selective electrode, contained a CA3140 MOSFET OA (BiMOS operational amplifiers, RCA Company, Somerville, U.S.A.) that is characterized by an extremely high input impedance of 1.5 TΩ, an input bias current of 10 pA and an acceptable temperature drift of 8 μV K^{-1}. The voltage offset was low and constant and

thus was not compensated. The common mode rejection ratio equals 90 dB. Digital measurements were made after conversion of the voltage signal to a train of pulses with a frequency proportional to the voltage, by using a 9400 voltage-to-frequency converter (Model 276-1790; Archer, Fort Worth, TX), combined with a BM520 pulse counter (Tesla, Czechoslovakia).

The long-distance transmission of the sensor analog and digitized signal was tested using a 50-m six-conductor, unshielded telephone cable (1 conductor used for the signal, 2 for the powering voltage and 3 for grounding) that was exposed to various noise sources (electric and electromagnetic fields, inside and outside the laboratory), and a 20-m optical link (Fibre Optic Kit GPK-10M, Optronics, Cambridge, England) with transmitter and receiver.

General procedures

For the fluoride measurements, solutions of sodium fluoride were prepared at concentrations of 1×10^{-2}—5×10^{-5} M with a constant ionic strength of 0.1 maintained by additions of potassium nitrate. The pH measurements were tested with the McIlvaine universal buffer with pH values of 2.2—7.0, maintaining a constant ionic strength of 0.5 with potassium chloride. All the chemicals were of analytical-grade purity (Lachema, Czechoslovakia). The measurements were made at laboratory temperature and the potentials were related to the saturated calomel electrode.

RESULTS

Analog measurements

To construct the voltage follower, the CA3140 OA was used with output connected to the inverting input through a 3 900 Ω resistor. The signal was brought to the non-inverting input through a 1 000 Ω resistor. However, when the signal was measured at a distance greater than 2 m from the amplifier output, the circuit began to oscillate at a high frequency, because of loading of the amplifier. These oscillations were successfully suppressed by connecting a 3.3 pF capacitor in the negative feedback. The resultant circuit (circuit A, Fig. 1) was placed in a teflon case and connected directly to the signal source (either a reference voltage or an ion-selective electrode). The signal was measured with a digital voltmeter at the end of a 50-m unshielded cable (see Experimental). The results of the measurements are given in Table 1. The reproducibility of the measurement was not affected by any noise source (switching on and off of electric appliances, placing the connecting cable outside the laboratory). The only drawback was the need to disconnect the source of powering voltage whenever the system of indicator and the separate reference electrodes was removed from the solution, to prevent excitation of the operational amplifier to the saturation voltage. This problem was eliminated by using a combined indicator-reference electrode.

It may sometimes be undesirable to ground one of the electrodes. It is

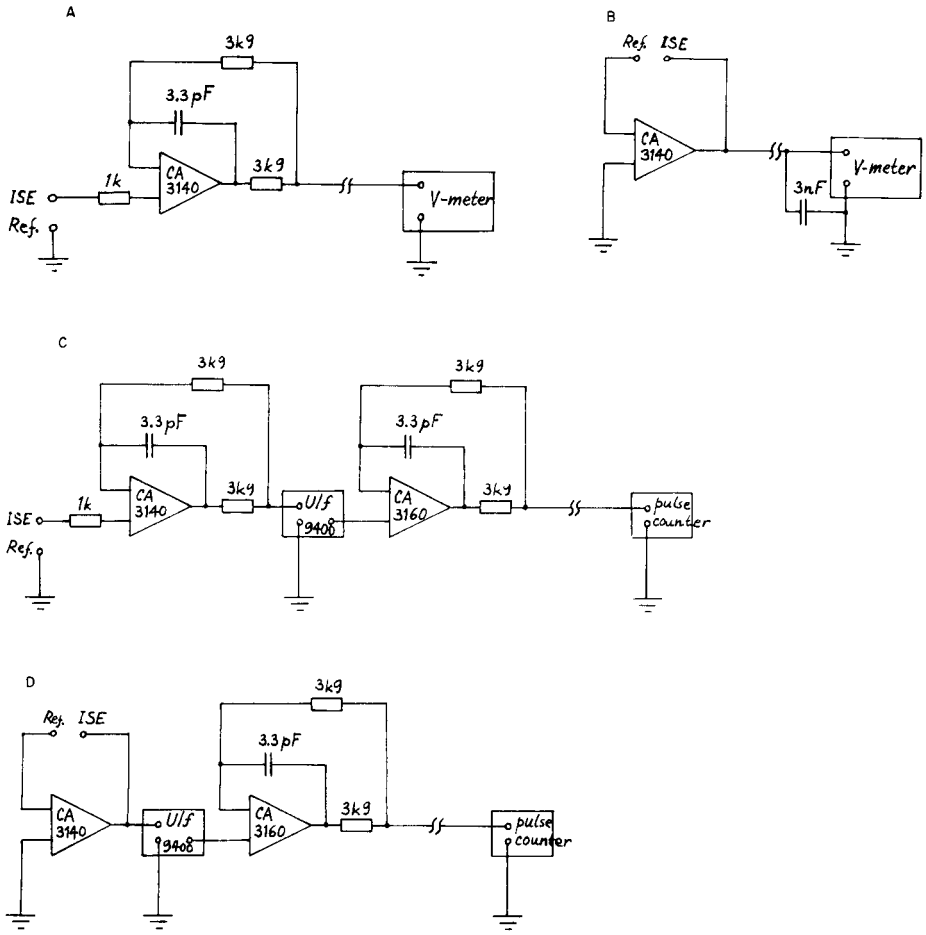

Fig. 1. The impedance converter with different circuits: (A) with the analog output; (B) with the analog output and with the floating source in the negative feedback; (C) with the digital output; (D) with the digital output and with the floating source in the negative feedback.

then advantageous to connect the electrode system in the OA negative feedback (circuit B, Fig. 1). In contrast to circuit A, circuit B did not exhibit a tendency to oscillate and the unmodified signal could be led to the meter separated by a 50-m cable. A 3000-pF capacitor was connected between the output at the end of the cable and the common ground, to prevent possible oscillations arising from noise in the cable. It can be seen from Table 1 that the results of measurements are quite similar to those obtained with circuit A. When separate indicator and reference electrodes are used, the power source must be switched off when the electrodes are removed from the solution, as for circuit A.

TABLE 1

Statistical parameters of analog measurements with the proposed circuits (ten measurements)

Circuit	Type of measurement	Slope (mV/pc)	Intercept (mV)	Corr. coeff.	Mean r.s.d. (%)
A	Ref. voltage, 0—500 mV	1.000	0.8	1.000	0.009
	F^--electrode, pF=2.00—4.31	58.82	—16.4	0.999	0.11
	pH-electrode, pH=2.20—7.00	57.59	—359.2	0.999	0.18
B	Ref. voltage, 0—500 mV	1.000	0.2	1.000	0.046
	F^--electrode, pF=2.00—4.31	57.72	—14.4	1.000	0.13
	pH-electrode, pH=2.20—7.00	57.40	—315.4	1.000	0.14

Digital measurements

In these measurements, the voltage follower circuits depicted in Fig. 1A and B, were connected to the voltage-to-frequency converter. As the Archer 9400 converter has a low power output leading to disappearance of the signal on transmission over greater distances, another voltage follower (rapid OA, RCA type CA3160), was connected between the voltage-to-frequency converter and the cable, to remove this problem. These circuits are depicted in Fig. 1C (circuit C, reference electrode grounded) and Fig. 1D (circuit D, electrode system in the OA negative feedback). The performance of these circuits was tested in the same way as for circuits A and B and the results are given in Table 2 (only the fluoride-selective electrode was tested). No interference from external sources of noise was observed. Comparison of the results in Tables 1 and 2 indicates that the digital measurement is slightly more reproducible.

Signal transmission by optical link

In these measurements, the signal from circuit A was fed through the voltage-to-frequency converter to the transmitter of the optical link, the optical signal was reconverted to a train of pulses in the receiver and fed to the pulse counter (Fig. 2, circuit E). The results are given in Table 3. No interference from external noise sources was observed and the additional OA (CA3160)

TABLE 2

Statistical parameters of digital measurements with the proposed circuits (ten measurements)

Circuit	Type of measurement	Slope (Hz/pc)	Intercept (Hz)	Corr. coeff.	Mean r.s.d. (%)
C	Ref. voltage, 0—500 mV	9.98	0.57	0.999	0.02
	F^--electrode, pF=2.00—4.31	590.8	—130.1	0.999	0.065
D	Ref. voltage, 0—500 mV	9.99	4.01	0.999	0.02
	F^--electrode, pF=2.00—4.31	597.5	—162.4	0.999	0.070

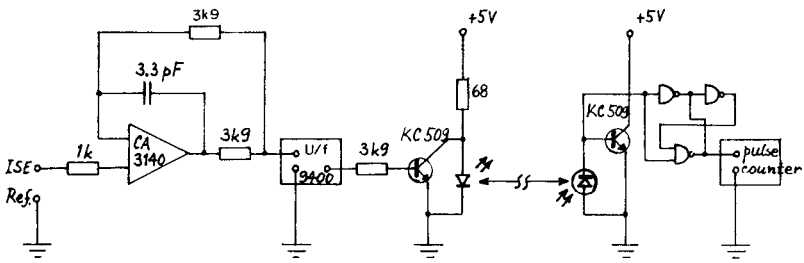

Fig. 2. The transmission of the low-impedance, digitized signal by an optical link (circuit E).

TABLE 3

Statistical parameters of digital measurements with the proposed circuits and with signal transmission by an optical link (ten measurements)

Circuit	Type of measurement	Slope (Hz/pc)	Intercept (Hz)	Corr. coeff.	Mean r.s.d. (%)
E	Ref. voltage, 0—500 mV	9.94	28.81	0.999	0.009
	F^--electrode, pF=2.00—4.31	562.0	1.83	0.998	0.057

for amplification of the signal was unnecessary. Circuit E was also tested for a sensor with a current output, the Clark oxygen electrode. The operational amplifier was then connected as a current follower, with a 100M resistor in the feedback. Some test measurements of the oxygen content in water yielded satisfactory results.

DISCUSSION

It can be seen from the results that the above-described circuits allow measurements with high-impedance voltage sources, such as ion-selective electrodes, to be achieved without deterioration of the information content of the signal even when the signal is transmitted over large distances. Moreover, the signal can be handled by low-impedance instruments. The precision, as well as the response time, of the measurement is unaffected by the electronic circuitry employed. The precision of the measurements increases in the order, analog transmission < digital transmission < digital—optical transmission. The line is not subject to any electrical noise.

The necessity of switching off the power source on removal of the electrodes from the solution can be avoided by using combined electrodes. However, this problem is not encountered in continuous flow measurements, where the electrodes are always immersed in a solution. Some preliminary measurements with the Clark oxygen electrode indicate that the proposed circuitry is also readily applicable to sensors with current output.

The authors are grateful to Dr. M. Herout of the J. Heyrovský Institute of Physical Chemistry and Electrochemistry, Czechoslovak Academy of Sciences, for technical assistance.

REFERENCES

1 J. Veselý, D. Weiss and K. Štulík, Analysis with Ion-Selective Electrodes, Ellis Horwood, Chichester, 1978.
2 R. Kalvoda, Operational Amplifiers in Chemical Instrumentation, Ellis Horwood, Chichester, 1975.
3 R. Kalvoda, Fortschritte in der elektrochemischen Analytik, Analytiktreffen 1979, K. Marx Universität, Leipzig, 1980, p.223.
4 Probe Electrometers, W-P Instruments (catalogue DS 7706), New Haven, U.S.A.
5 Camlab Portable pH-meter, Camlab, Cambridge, England, 1980.
6 J. Janata and R. J. Huber, Ion-Selective Electrode Reviews, 1 (1979) 31.
7 T. A. Fjeldly, K. Nagy and J. S. Johannessen, J. Electrochem. Soc., 126 (1979) 793.

Analytica Chimica Acta, 148 (1983) 27—33
Elsevier Science Publishers B.V., Amsterdam — Printed in The Netherlands

A CHEMICALLY-MODIFIED ENZYME MEMBRANE ELECTRODE AS AN AMPEROMETRIC GLUCOSE SENSOR

TOSHIO YAO

Department of Applied Chemistry, College of Engineering, University of Osaka Prefecture, Mozu-Umemachi, Sakai, Osaka 591 (Japan)

(Received 28th April 1982)

SUMMARY

A chemically-modified enzyme membrane electrode for glucose was constructed by cross-linking glucose oxidase with bovine serum albumin using glutaraldehyde onto a platinum electrode silanized with 3-aminopropyltriethoxysilane. The response time is only 10 s, the calibration graph is linear for 10^{-7}—2×10^{-3} M glucose, and the sensor can be used repeatedly at room temperature for at least 30 days with little deterioration in response.

Highly selective methods for biochemical analysis have been reported by coupling an immobilized-enzyme membrane with an electrochemical sensor. This technique combines the specificity of enzyme catalysis with the sensitivity of potentiometric and amperometric electrodes to yield devices capable of repetitive, cheap assays. Most enzyme electrodes have been fabricated by holding a thin layer over an electrode with some type of enzyme membrane [1].

In recent years, much research has been done in the field of chemically modified electrodes (CME). Such chemical modification involves the strong binding (via irreversible adsorption, polymer coating, or covalent bonding) of a chemical reagent to the surface of an electrode in order to give some particular characteristic. This area has attracted unusual interest because of potential applications to electrocatalysis [2, 3], electrosynthesis [4], and photosensitization [5, 6]. Yet, only a few applications have involved CMEs as potentiometric sensors [7—11].

Ianniello and Yacynych [12] constructed a CME with immobilized enzyme by covalently bonding glucose oxidase to a chemically modified graphite electrode via a cyanuric chloride linkage and evaluated the various response characteristics as an amperometric sensor. In this paper, glucose oxidase is co-cross-linked with bovine serum albumin (BSA) by means of glutaraldehyde on a platinum electrode surface silanized with 3-aminopropyltriethoxysilane. The resulting glucose oxidase—BSA cross-linked membrane is covalently bonded to the electrode surface to yield a glucose sensor. The immobilized glucose oxidase catalyzes the oxidation of glucose in the presence of oxygen

0003-2670/83/$03.00

to yield hydrogen peroxide as one of the products, which is electrochemically oxidized to give a measurable steady-state current. Membrane compositions, response time, linearity, temperature, pH response characteristics, long-term stability and selectivity are examined herein.

EXPERIMENTAL

Reagents and apparatus

Glucose oxidase (130 IU mg^{-1}, from *Aspergillus niger*; P-L Biochemicals) was used. A stock 0.1 M solution of D-glucose (Wako Pure Chemical Co.) was allowed to mutarotate overnight before use. All dilutions were made in the appropriate buffer. Hydrogen peroxide (Wako Pure Chemical Co.; ca. 30%) was used to prepare stock peroxide solutions, which were then assayed by titration with standard potassium permanganate. The BSA powder was 96—99% albumin (Sigma Chemical Co.; fraction V). Glutaraldehyde was an aqueous 20% solution (Wako Pure Chemical Co.). 3-Aminopropyltriethoxysilane was obtained from the Tokyo Kasei Kogyo Co. Controlled human serum (Hyland; OMEGA Control Serum II, Lot. No. 4822Y006A) was used as a standard. All other chemicals were of analytical-reagent grade.

A Yanagimoto P-8 type polarograph was used to apply a constant potential to a two-electrode system. The CMEME and a commercial saturated calomel electrode were used as the working electrode and reference electrode, respectively.

Preparation of electrodes

Preparation of alkylamino-bonded platinum plate electrode. Electrodes were constructed from platinum plate (5 × 5 mm). These electrodes were prepared for chemical modification by cycling between hydrogen and oxygen discharge potentials until the characteristic clean platinum wave pattern [13] was obtained. The electrodes were next anodized for 1 h at 2.50 V vs. SCE in 0.1 M sulfuric acid. The anodized electrodes were removed from the cell, washed thoroughly with distilled water, dried, and refluxed for 1 h in an anhydrous ca. 10% (v/v) solution of 3-aminopropyltriethoxysilane in toluene. The resulting silanized electrodes were rinsed thoroughly with toluene and ethanol.

Preparation of the chemically modified enzyme-membrane electrode. A 1.5-μl aliquot of aqueous 20% (w/v) BSA and 2.0 μl of 4% (w/v) glucose oxidase in pH 5.5 acetate buffer were spread on both sides of the alkylamino-bonded platinum electrode. Then 1.0 μl of aqueous 2.0% (v/v) glutaraldehyde was added to the center of each side of the platinum plate. The solutions were mixed rapidly with a thin glass rod. The membrane was allowed to form at room temperature, open to the atmosphere, for up to 2 h, by which time the water had completely evaporated. The electrode was washed several times in acetate buffer (pH 5.5), followed by cycling between hydrogen and oxygen discharge potentials in 0.1 M tetraethylammonium

perchlorate for 10 min. When not in use, the electrode was stored in pH 7.5 phosphate buffer at ca. 4° C.

Glucose determination

The enzyme-membrane CME was placed in 5 ml of pH 7.5 phosphate buffer, 0.1 M in sodium chloride, stirred with a 3-mm magnetic stirring bar. The electrode was then poised at 0.7 V vs. SCE. After the background current had decayed to a steady-state value, aliquots of the glucose solution were rapidly added from a microsyringe. Steady-state currents (I_{ss}) were obtained after ca. 10 s.

RESULTS AND DISCUSSION

Membrane compositions

Data obtained by e.s.c.a. [14, 15] for platinum oxide electrodes suggested that anodization in aqueous sulfuric acid yeilded a surface layer of PtO or PtO_2. The platinum oxide produced by the anodization at 2.50 V vs. SCE in 0.1 M sulfuric acid, gave a cathodic stripping peak at 0.53 V vs. SCE in aqueous 0.1 M tetraethylammonium perchlorate. This cathodic peak completely disappeared after treatment with the silylating reagent. This shows that the chemical modification produces surface Pt—O—Si bonds which are chemically stable and electrochemically stable, as suggested previously [16].

The enzyme-modified electrodes were prepared by co-cross-linking glucose oxidase with BSA using glutaraldehyde on the silanized platinum electrodes. The resulting membranes were covalently bonded to the electrode surface, as shown in Fig. 1. Table 1 shows the effect of different membrane compositions on the electrode response. As expected, the highest response was obtained with a combination of thin membrane, low glutaraldehyde concentration, and high glucose oxidase activity. Therefore, the membrane composition of electrode E2 was used throughout this work. Typical steady-state responses of the electrode are shown in Fig. 2; the steady-state response was reached in ca. 10 s, which is very rapid compared to previously reported amperometric enzyme electrodes [17—25].

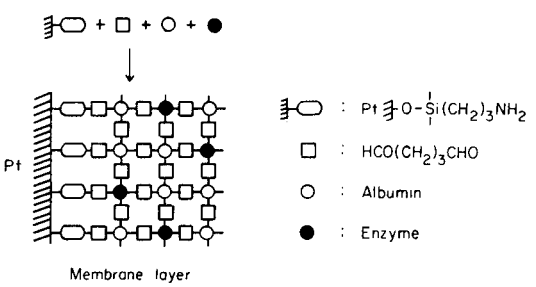

Fig. 1. Schematic representation of the enzyme-membrane CME.

TABLE 1

Effect of membrane compositions on the electrode response

Electrode	BSA[a] (μl)	Glucose oxidase[b] (μl)	Glutaraldehyde[c] (μl)	Steady-state current[d] (μA)	Response time[e] (s)
E1	1.0	2.0	1.0	2.3	5.0
E2	1.5	2.0	1.0	2.9	7.1
E3	2.5	2.0	1.0	2.4	7.3
E4	4.0	2.0	1.0	1.7	8.0
E5	1.5	2.0	0.5	2.8	5.9
E6	1.5	2.0	1.5	2.0	6.9
E7	1.5	2.0	2.0	2.0	6.8
E8	1.5	1.0	1.0	1.8	6.9
E9	1.5	4.0	1.0	2.6	7.0

[a]Aqueous 20% (w/w) solution. [b]2 mg glucose oxidase/50 μl pH 5.5 acetate buffer. [c]Aqueous 2% (v/v) solution. [d]Response to 2×10^{-4} M glucose. [e]Time required to reach 95% of the steady-state current.

Optimal conditions for glucose determinations

The effect of pH on the steady-state response of the enzyme-modified electrode was studied from 4.5 to 9.6. As shown in Fig. 3, the maximum response was at pH 7.5. Compared to soluble glucose oxidase [26], the pH maximum was shifted ca. 2 pH units more alkaline. Between 0 and 1.0 M sodium chloride in the buffer, the variation in the steady-state current was only 2—3%. In this study, a 0.1 M phosphate buffer (pH 7.5) 0.1 M in sodium chloride was used.

The diffusion current plateau of hydrogen peroxide at solid electrodes has previously been reported [27]. Because low levels of hydrogen peroxide are produced during the enzymatic reaction, the exact potential region of this current plateau must be known in order to obtain maximum sensitivity. Figure 4 shows a linear-sweep voltammogram for the enzyme-membrane CME in the presence of 0.2 mM glucose. The current plateau was observed

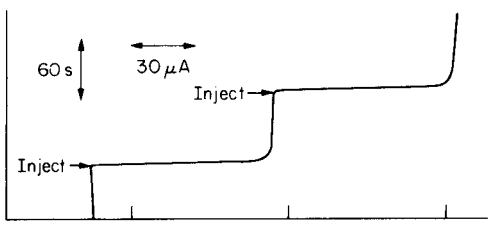

Fig. 2. Typical steady-state current response of the enzyme-membrane CME. (50 μl of 0.2 mM glucose injected into 5 ml of pH 7.5 phosphate buffer, 0.1 M in NaCl; E_{app} = 0.7 V vs. SCE; background current = 3 nA.)

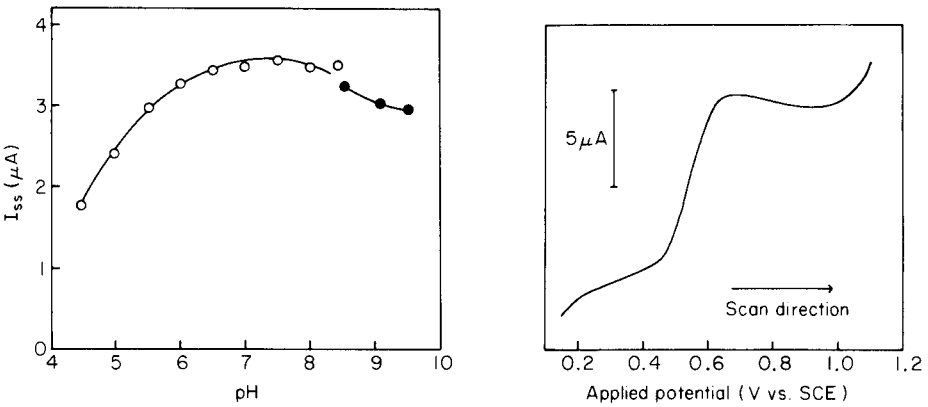

Fig. 3. Effect of pH on the electrode response for (○) phosphate buffer and (●) pyrophosphate buffer. (50 μl of 10 mM glucose injected into 5 ml of buffer.)

Fig. 4. Linear-sweep voltammogram of H_2O_2 decomposition at the electrode in pH 7.5 phosphate buffer 0.1 M in NaCl (2×10^{-4} M glucose, scan rate 10 mV s^{-1}).

at ca. 0.7 V vs. SCE, so this potential was applied to the electrode for hydrogen peroxide monitoring.

Linearity of calibration graph, and precision

The steady-state current responses to various concentrations of glucose were employed to construct calibration graphs for glucose. The graphs were linear from about 10^{-7} M to 2×10^{-3} M. Above the latter value, a response was obtained but the current increase was no longer proportional to the glucose concentration. Slope, intercept, and linear correlation coefficient were 17.8 μA mM^{-1}, 2.0 nA and 0.9999, respectively. The limit of detection depended on the noise level, which was mainly related to the irregularity of stirring rate of the test solutions. The lowest glucose concentration which could be detected by this electrode was 0.9×10^{-8} M, when the signal-to-noise ratio was 2. The relative standard deviations for sets of 10 injections were 1.1 and 1.7% at final concentrations of 5×10^{-5} and 5×10^{-6} M glucose, respectively.

Selectivity and temperature effect

The selectivity depends on both the enzyme and the electrochemical detection method. Glucose oxidase is almost specific for β-D-glucose; the selectivity coefficients are 2×10^{-4}, 0.8×10^{-4} and 10^{-4} for glucose over fructose, lactose, and sucrose, respectively. Because species other than enzymatically-generated hydrogen peroxide may diffuse through the membrane and be oxidized on platinum at 0.7 V, there were the slight interferences from electroactive species such as ascorbate, urate, tyrosine, cysteine, glutathione and bilirubin. However, these electrochemical interferences might be eliminated by subtracting the interfering current, measured with a com-

pensating electrode modified with a non-enzymatic membrane, from the response current of the enzyme-modified electrode. This method was applied to the determination of glucose in a commercial human control serum. The average amount found was 263 ± 2.1 mg dl^{-1} (n = 10), which is in good agreement with the manufacturer's data (267 ± 11 mg dl^{-1}).

The response of the enzyme-modified electrode to glucose was examined at different temperatures. The current increased linearly with increasing temperature according to the equation I_{ss} (μA) = 0.133T(°C) + 0.26 over the temperature range 18—42°C. Therefore, the enzyme-modified electrode may be used over a reasonably large temperature range, though it is necessary to thermostat the solutions carefully.

Long-term stability of the enzyme-modified electrode

The electrodes were stored at 4°C in pH 7.5 phosphate buffer when not in use. Long-term stabilities were studied by periodically testing their response to 0.2 mM glucose. A slight increase in response was observed over the first 2 or 3 days. This behavior has been observed in the past with enzyme electrodes and possible explanations were the establishment of diffusion channels in the membrane, and changes in conformation of the fraction of enzyme immobilized in an inactive conformation to the more stable and preferred active conformation [17]. The stability of the enzyme-modified electrodes was good and even after 30 days they retained most of their original activity.

The electrodes displayed a large steady-state current (17.8 μA mM^{-1}), rapid response (ca. 10 s), and also a low background current (3 nA) compared to the large base-line current (80 μA) of the CME of Ianniello and Yacynych [12]. In conclusion, the enzyme-modified electrode reported in this study displayed a dynamic response range of about 4 decades in glucose concentration and a low detection limit. Also, because of the flexibility in the choice of electrode dimensions, the electrode could easily be used as an electrochemical detector in flow injection analysis. Further applications will be reported later.

The author thanks Mr. Yoshiyuki Matsuda for his help in the experimental work.

REFERENCES

1 P. W. Carr and L. D. Bowers, Immobilized Enzymes in Analytical and Clinical Chemistry, Wiley—Interscience, New York, 1980.
2 J. F. Stargardt, F. M. Hawkridge and H. L. Landrum, Anal. Chem., 50 (1978) 930.
3 H. Jaegfeldt, A. B. C. Torstensson, L. G. O. Gorton and G. Johansson, Anal. Chem., 53 (1981) 1979.
4 B. E. Firth, L. L. Miller, J. Lennox and R. W. Murray, J. Am. Chem. Soc., 98 (1976) 8271.
5 M. S. Wrighton, R. G. Austin, A. B. Bocarsky, J. M. Bolts, O. Haas, K. D. Legg, L. Nadjo and M. Palazzotto, J. Am. Chem. Soc., 100 (1978) 1602.

6 M. Fujihira, T. Osa, D. Hursh and T. Kuwana, J. Electroanal. Chem., 88 (1978) 285.
7 N. Yamamoto, Y. Nagasawa, M. Sawai, T. Sudo and H. Tsubomura, J. Immunol. Methods, 22 (1978) 309.
8 H. A. Laitinen and T. M. Hseu, Anal. Chem., 51 (1979) 1550.
9 N. Yamamoto, S. Shuto and H. Tsubomura, Nippon Kagaku Kaishi, (1980) 1562.
10 W. R. Heineman, H. J. Wieck and A. M. Yacynych, Anal. Chem., 52 (1980) 345.
11 R. M. Ianniello and A. M. Yacynych, Anal. Chim. Acta, 131 (1981) 123.
12 R. M. Ianniello and A. M. Yacynych, Anal. Chem., 53 (1981) 2090.
13 H. Angerstein-Kozlowska, B. E. Conway and W. B. A. Sharp, J. Electroanal. Chem., 43 (1973) 9.
14 G. C. Allen, P. M. Tucker, A. Capon and R. Parsons, J. Electroanal. Chem., 50 (1974) 335.
15 K. S. Kim, N. Winograd and R. E. Davis, J. Am. Chem. Soc., 93 (1971) 6296.
16 J. R. Lenhard and R. W. Murray, J. Electroanal. Chem., 78 (1977) 195.
17 G. G. Guilbault and G. J. Lubrano, Anal. Chim. Acta, 64 (1973) 439.
18 G. G. Guilbault and G. J. Lubrano, Anal. Chim. Acta, 69 (1974) 183.
19 G. J. Lubrano and G. G. Guilbault, Anal. Chim. Acta, 97 (1978) 229.
20 D. R. Thévenot, R. Sternberg, P. R. Coulet, J. Laurent and D. C. Gautheron, Anal. Chem., 51 (1979) 96.
21 L. D. Mell and J. T. Maloy, Anal. Chem., 47 (1975) 299; 48 (1976) 1597.
22 F. R. Shu and G. S. Wilson, Anal. Chem., 48 (1976) 1679.
23 R. A. Kamin and G. S. Wilson, Anal. Chem., 52 (1980) 1198.
24 C. Bourdillon, J. P. Bourgeois and D. Thomas, Biotechnol. Bioeng., 21 (1979) 1877; J. Am. Chem. Soc., 102 (1980) 4231.
25 M. Nanjo and G. G. Guilbault, Anal. Chim. Acta, 73 (1974) 367.
26 T. E. Barman, Enzyme Handbook, Vol. 1, Springer-Verlag, New York, 1969, p. 112.
27 A. Hickling and W. H. Wilson, J. Electrochem. Soc., 98 (1951) 425.

Analytica Chimica Acta, 148 (1983) 35—40
Elsevier Science Publishers B.V., Amsterdam — Printed in The Netherlands

A TRICHLOROMERCURATE(II) ION-SELECTIVE ELECTRODE BASED ON THE TETRADECYLPHOSPHONIUM SALT IN POLYVINYL CHLORIDE

A. V. KOPYTIN, P. GÁBOR-KLATSMÁNYI, V. P. IZVEKOV and E. PUNGOR*

Institute for General and Analytical Chemistry, Technical University of Budapest, 1111-Budapest (Hungary)

G. A. YAGODIN

Mendeleev University, 125047-Moscow (U.S.S.R.)

(Received 1st October 1982)

SUMMARY

An improved trichloromercurate(II) ion-selective electrode based on the tetradecylphosphonium trichloromercurate(II) ion-pair complex in a PVC membrane is described. No plasticizer is used. The composition of the electroactive material was checked by its far-infrared spectra. The electrode response is nearly Nernstian down to 10^{-5}—10^{-6} mol dm^{-3}, depending on the conditions and is unaffected by pH in the range 1.5—6. Under controlled conditions, the electrode is suitable for determining mercury(II) in hydrochloric acid solutions.

In the preparation of ion-selective electrodes, various attempts have been made to apply organic quaternary salts as the active material for measurements of the activity of anions [1—3] or anionic complexes [4—7]. These electroactive components were usually contained in a PVC membrane with a plasticizer, e.g., dibutyl phthalate [2, 4, 8]. The properties of the organic solvents used as plasticizers can have considerable influence on the electrochemical parameters of the electrode [9]. As is known [9—11], the sensitivity and selectivity of ion-selective electrodes which are based on organic liquids (e.g., liquid ion-exchangers in solvents immiscible with water) can be predicted from the relevant extraction data. Solvation and hydration processes in the membrane phase cause deviations from Nernstian response [9, 11]. The behaviour of the PVC-based trichloromercurate(II) ion-selective electrode containing dibutyl phthalate or dibutyl sebacate as plasticizer [8] can be interpreted in terms of this theory.

The present paper is concerned with an investigation of the preparation, properties and application of an improved PVC-based trichloromercurate(II) ion-selective electrode without plasticizer.

0003-2670/83/$03.00

EXPERIMENTAL

Reagents

Electroactive material. The tetradecylphosphonium trichloromercurate(II) complex was prepared as follows:

$$(C_{10}H_{21})_4PNO_3 + HgCl_2 \xrightarrow{HCl} (C_{10}H_{21})_4P[HgCl_3] + HNO_3$$

Tetradecylphosphonium nitrate (10^{-2} mol dm^{-3} in chloroform) and mercury(II) chloride (5×10^{-2} mol dm^{-3} in 10^{-1} mol dm^{-3} hydrochloric acid) were shaken vigorously in a separatory funnel; the ratio of the organic to the aqueous phase was 1:2. The organic phase was shaken another three times (5 min each) with fresh portions of mercury(II) chloride solution. Under these conditions, the $[HgCl_3]^-$ complex anion is transferred to the organic phase [12]. After the last separation, the organic phase was collected in a Petri dish and left at room temperature until the solvent evaporated. In this way, a viscous transparent liquid, the tetradecylphosphonium trichloromercurate(II) complex was obtained.

The separated compound was characterized from its far-infrared spectrum (Fig. 1, curve a). The intense absorption at 277 cm^{-1} can be ascribed to the $[HgCl_3]^-$ ion. There was no band at 225 cm^{-1} from the $[HgCl_4]^{2-}$ ion (see later) [13].

All the chemicals were of analytical grade. The PVC powder was Breon-113 (B.P. Chemicals, England), and the solvent was cyclohexanone.

All calibration solutions were prepared in 0.1 mol dm^{-3} hydrochloric acid to obtain constant ionic strength.

Electrodes and equipment

A double-junction silver—silver chloride electrode (Radelkis, OP-08203) was used as reference. A combined glass electrode (Radelkis OP-08083) was

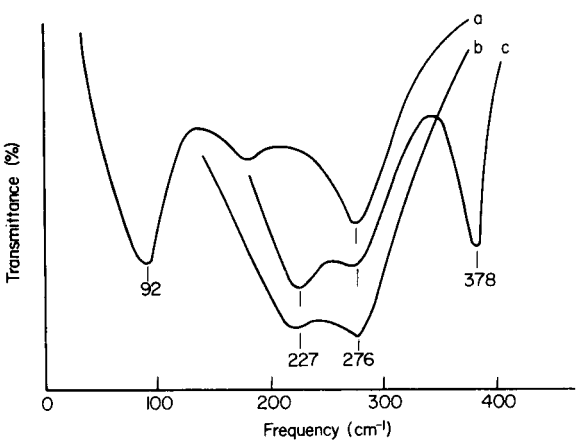

Fig. 1. Far-infrared spectra: (a) tetradecylphosphonium trichloromercurate(II); (b) membrane pretreated in 4 mol dm^{-3} hydrochloric acid; (c) membrane pretreated in 5 mol dm^{-3} hydrochloric acid.

used for pH measurements. The PVC membrane of the $[HgCl_3]^-$-selective electrode was made in the usual manner [14]. The membrane discs (5 mm diameter) were fixed to PVC tubes with a PVC solution in cyclohexanone that also contained the complex compound. The compositions of the electrodes investigated are summarized in Table 1.

Potentials were measured with a digital pH meter (Radelkis, OP-208). The far-infrared spectra were measured in the range 40—400 cm^{-1} with a Fourier-transform spectrometer (IS-3, Grubb-Parsons, England). A PVC film without plasticizer was used as reference.

RESULTS AND DISCUSSION

Composition of the membrane

The calibration curves of the trichloromercurate(II) ion-selective electrodes of different compositions are shown in Fig. 2, while the appropriate data (composition of the membranes, slopes of calibration curves, etc.) are summarized in Table 1. The slopes were calculated by means of the least-squares method for the linear part of the calibration curves. These data show that the slope increases with increasing content of the electroactive material in the membrane. The variation causes not only a change in the electrode response, but also a shift in the E°_{ISE} value. It should be noted that when the content of active component exceeds 60%, the membrane itself cannot be formed properly. The best electrode function was obtained with the compositions 40—60% PVC and 60—40% tetradecylphosphonium trichloromercurate(II). When the amount of the active component was less than 40%, the electrode response deteriorated and the resistance of the membrane increased. Thus, under optimal conditions, trichloromercurate(II) anions, and mercury(II) ions after formation of the chloro complex, can be determined potentiometrically with the electrode.

In view of the above-mentioned possibility of the existence of other chloromercurate(II) complexes in the membrane, the behaviour of the

TABLE 1

Composition of the membranes and some electroanalytical parameters of the trichloromercurate(II) ion-selective electrode

No.	$(C_{10}H_{21})_4P[HgCl_3]$ (%)	PVC (%)	Slope mV/pHg	Lower detection limit (mol dm^{-3})
1	60	40	57	2.3×10^{-5}
2	50	50	56	2.5×10^{-5}
3	40	60	55	3.3×10^{-5}
4[a]	30	70	51	3.7×10^{-5}
5[a,b]	20	80	44	4.0×10^{-5}

[a]The response was not reproducible. [b]High resistance.

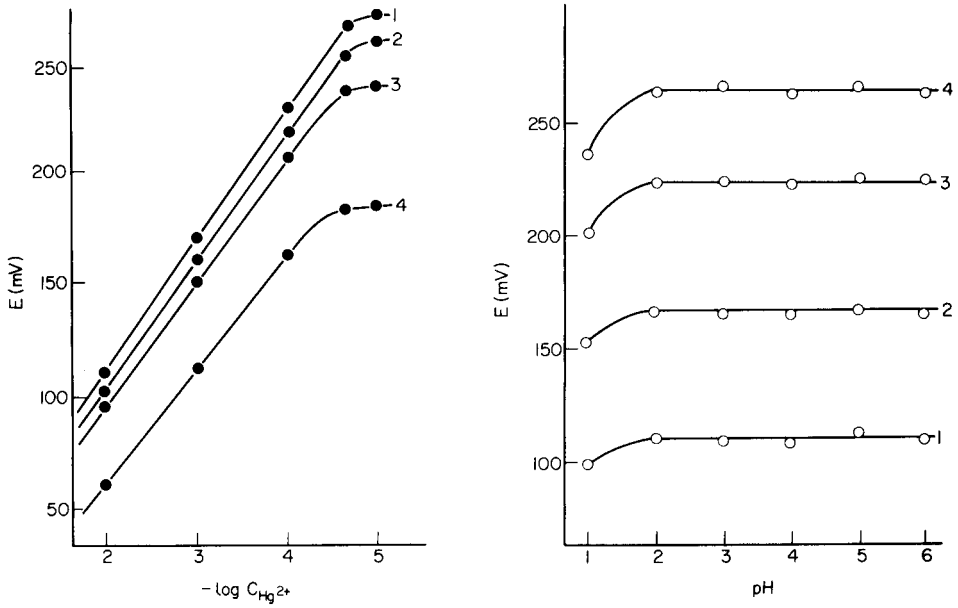

Fig. 2. Calibration curves for membranes with different composition (the numbers refer to Table 1). The solutions contained a constant 0.1 mol dm^{-3} hydrochloric acid concentration.

Fig. 3. The E vs. pH diagrams at different Hg^{2+} concentrations: (1) 10^{-2}; (2) 10^{-3}; (3) 10^{-4}; (4) 5×10^{-5} mol dm^{-3}.

electroactive compound was investigated in hydrochloric acid solutions of different concentration. Far-infrared spectroscopy was used to study the processes that occurred in the membrane containing electroactive material after immersion into a solution of mercury(II) in hydrochloric acid. The spectrum of the $[HgCl_3]^-$-selective membrane was essentially the same as that of the pure salt (Fig. 1, curve a), which indicates that the electroactive material does not undergo any chemical transformation on incorporation into the membrane. There were three characteristic bands in both spectra at 92, 181 and 276 cm^{-1}. The band at 276 cm^{-1} can be assigned to the asymmetric stretching vibration, and the band at 92 cm^{-1} to the bending vibration of the Hg—Cl bond [15]. The tetradecylphosphonium cation present in the salt may give rise to bands from the Hg—P bond. Although no literature data are available on this subject, the band at 181 cm^{-1} may be ascribed to the Hg—P bond, based on data known for other metal—phosphorus bonds [16, 17].

The possibilities of chemical changes in the active material of the electrode were also investigated. Electrode membranes were immersed for 1—3 days in hydrochloric acid solutions of different concentration, ranging from 0.1 to 5 mol dm^{-3}, and containing equal concentrations (0.1 mol dm^{-3})

of mercury(II) chloride. Then the membranes were washed with hydrochloric acid and water to remove any adsorbed species and the infrared spectra were recorded.

The spectra of membranes pretreated in 0.1—3 mol dm^{-3} hydrochloric acid were the same as those of untreated membranes, indicating that the trichloromercurate(II) complex anions remained unchanged even after these treatments. In contrast, the spectra of membranes treated in 4 mol dm^{-3} hydrochloric acid differed significantly from those of the untreated membranes (Fig. 1, curve b). In addition to the band at 276 cm^{-1} characteristic of the $[HgCl_3]^-$ ion, another band of equal intensity appeared at 227 cm^{-1}. This latter band is due to the $[HgCl_4]^{2-}$ ion which can be assumed to be formed in the reaction $[HgCl_3]^- + Cl^- \rightarrow [HgCl_4]^{2-}$. The changes were even more pronounced for membranes treated in 5 mol dm^{-3} hydrochloric acid. In the spectrum of the treated membrane (Fig. 1, curve c), a third band appeared at 378 cm^{-1} in addition to those at 227 and 276 cm^{-1}; according to Poulet and Mathieu [18], this band is characteristic of mercury(II) chloride. Further experiments are needed to elucidate the processes leading to the formation of mercury(II) chloride.

Electrodes made from membranes treated with hydrochloric acid solutions of concentration exceeding 3 mol dm^{-3} did not function, presumably because of changes in the complex equilibria within the membrane. It was also found that the best electrodes were prepared from freshly made PVC membranes.

A calibration curve for $[HgCl_3]^-$ with the electrode at an ionic strength of 0.5 exhibited a near-Nernstian slope of 58 mV/decade down to 5×10^{-6} mol dm^{-3}, but was otherwise similar to curve 1 of Fig. 2. The $[HgCl_3]^-$ activities were calculated from stability constant data [19] at ionic strength 0.5, or at 0.5 mol dm^{-3} free chloride content.

Interferences and pH effects

Interferences by other anions were studied by the mixed solution method. As would be expected, iodide and bromide ions had a strong effect on the electrode potential because of competitive complex formation with the mercury(II) ion. The effect of varying the chloride concentration on the equilibrium $[HgCl_3]^- \rightleftharpoons [HgCl_4]^{2-}$ was mentioned above for hydrochloric acid. In practice, it is advisable to maintain a constant chloride concentration in the test solutions. The selectivity coefficients, K_{ij}, where i is the trichloromercurate(II) ion and j is an interfering anion, were 10^{-2} for nitrate and perchlorate, and 10^{-3} for sulphate and acetate. The cations forming chloro complexes similarly to the Hg^{2+} ion (e.g., Cd^{2+}, Zn^{2+}) can also influence the electrode potential.

The pH dependence was investigated in 2 mol dm^{-3} sodium chloride solutions to avoid changes in the complex equilibrium. With this high background concentration, the chloride ions coming from the hydrochloric acid do not affect the measurements. The potential—pH diagrams obtained

for given mercury(II) ion concentrations (Fig. 3) show that pH changes in the range 1.5—6 do not affect the performance of the electrode for measuring trichloromercurate(II) ions. No measurements were made at pH > 6, because of hydrolysis of the trichloromercurate(II) ions. At values of pH < 1.5, the E^0 of the electrode changed because of changes within the membrane caused by the acid entering the organic phase.

Finally, it must be emphasized that the use of these trichloromercurate(II) ion-selective electrodes depends on careful calibration of the electrodes under the given conditions. The standard addition method is useful for obtaining reliable results for unknown solutions.

REFERENCES

1 I. Nagelberg, C. I. Braddock and G. I. Bardero, Science, 166 (1969) 1403.
2 Yu. I. Urusov, V. V. Sergievskii, A. Ya. Syurchenkov, A. F. Zhukov and A. V. Gordievskii, Zh. Anal. Khim., 30 (1975) 1757.
3 H. B. Herman and G. A. Rechnitz, Anal. Chim. Acta, 76 (1975) 155.
4 U. Fiedler-Linnersund and K. M. Bhatti, Anal. Chim. Acta, 111 (1979) 57.
5 G. Scibona, L. Mantella and R. P. Danesi, Anal. Chem., 42 (1970) 844.
6 R. W. Cattrall and C. P. Pin, Anal. Chem., 48 (1976) 552.
7 A. S. Bychkov, O. M. Petruhin, V. A. Zarinskii and Yu. A. Zolotov, Zh. Anal. Khim., 30 (1975) 2213.
8 A. V. Kopytin, A. F. Zhukov, Yu. I. Urusov and A. V. Gordievskii, Zh. Anal. Khim., 34 (1979) 465.
9 A. V. Gordievskii, Yu. I. Urusov, V. V. Sergievskii, A. F. Zhukov and A. V. Kopytin, Zh. Anal. Khim., 34 (1979) 1252.
10 H. J. James, G. P. Carmack and H. Freiser, Anal. Chem., 44 (1972) 853.
11 E. A. Materova, A. L. Grekovich and N. V. Garbuzova, Zh. Anal. Khim., 20 (1974) 1434.
12 V. M. Tarayan and E. N. Osepyan, Zh. Anal. Khim., 26 (1971) 1627.
13 D. M. Adams, Metal—Ligand and Related Vibrations, Edward Arnold, London, 1967, pp. 55—57.
14 A. Craggs, G. J. Moody and J. D. R. Thomas, J. Chem. Educ., 51 (1974) 541.
15 G. B. Deacon, J. H. S. Green and W. Kynaston, Aust. J. Chem., 19 (1966) 1603.
16 M. Bigorgne, C. R. Acad. Sci. Ser. C, 250 (1960) 3484.
17 D. M. Adams and P. J. Chandler, Chem. Commun., (1966) 68.
18 H. Poulet and J. P. Mathieu, J. Chim. Phys., (1963) 1942.
19 H. Freiser and Q. Fernando, Ionic Equilibria in Analytical Chemistry, Wiley, New York, 1963, p. 310.

Analytica Chimica Acta, 148 (1983) 41—50
Elsevier Science Publishers B.V., Amsterdam — Printed in The Netherlands

DIRECT POTENTIOMETRY AND POTENTIOMETRIC TITRATION OF MERCURY(II) WITH SOLID-STATE ION-SELECTIVE ELECTRODES

G. A. EAST* and I. A. DA SILVA

Departamento de Química, Universidade de Brasília, 70.910-Brasília-DF (Brasil)

(Received 8th July 1982)

SUMMARY

Several mercury(II) chalcogenides and their admixtures with silver(I) chalcogenides or elemental mercury were examined as electroactive materials to obtain sensors responsive to mercury(II) activity. The best characteristics were obtained with HgS (black)/Hg(0), prepared by disproportionation of mercury(I) sulphide, which provided a Nernstian response to mercury(II) ion in the range 10^{-1}—10^{-7} M. Most of the sensors tested proved to be useful for end-point detection in the titration of mercury(II) with EDTA. Studies of interferences of chloride and sulphite ions in direct potentiometry of mercury(II) with the HgS (black)/Hg(0) electrode showed that these sensors respond in a Nernstian manner to both ions within limited ranges of concentration. Chloride, at concentrations of $\leqslant 10^{-3}$ M, does not inferfere in direct potentiometry of mercury(II). Evidence is presented that the electroactive compound in the HgS (black)/Hg(0) electrode is elemental mercury, with HgS (black) acting as an inert matrix.

Differential electrolytic potentiometry is a well established technique [1—5] applicable to end-point detection for most types of titrations and capable of giving extremely precise results. The mercury electrode, initially suggested for titrations by Siggia et al. [6] and studied by Reilley and coworkers [7, 8], has been used extensively as a detector for zero-current and polarized potentiometric titrations with EDTA, the indicator electrode material being mercury or gold amalgam. Both types of electrodes have some unfavourable features. With liquid mercury electrodes, unstable potential readings may be caused by variation of the electrode area during stirring, and careful workmanship is needed in their preparation. Gold amalgam electrodes have fewer problems but gold wire tends to become brittle after amalgamation and breakages may occur on prolonged usage [9]. Because of these drawbacks, a solid-state electrode of the type suggested by Růžička et al. [10] that is responsive to mercury(II) was developed. Some of its relevant features are low cost, sturdiness, ease of construction, and low ohmic resistance.

In describing Selectrodes, Růžička and Lamm [11] outlined some features of an electrode activated by mercury(II) sulphide, but did not give details on the preparation of the electroactive material. This paper reports a study of solid-state electrodes and their evaluation for titrations of mercury(II) with EDTA solutions.

0003-2670/83/$03.00

EXPERIMENTAL

Reagents

Analytical-reagent grade chemicals were used. A home-made, all-borosilicate glass still was used to obtain the doubly-distilled water used throughout. Stock solutions were standardized by appropriate methods. Standard solutions of mercury(II) were prepared by serial dilution (down to 10^{-5} M) or by preparing metal buffers [12] for solutions more dilute than 10^{-5} M. The graphite rods 8 mm thick used to make the electrodes were of spectrographic grade (National Carbon Co., New York). Polyester resin (Ramires e Companhia, São Paulo), silicone grease (Merck) and paraffin wax (BDH Chemicals) were also used.

Resins used to hydrophobize graphite rods. Resin solutions of acrylic and polyurethane were prepared by dissolving bits of the polymer in chloroform. Polyethylene and poly(vinyl chloride) solutions were prepared similarly but with hot xylene and tetrahydrofuran, respectively. Silicone grease was dissolved in carbon tetrachloride.

Electroactive materials. Electroactive materials prepared were: black HgS (metacinnabar), red HgS (cinnabar), HgSe, HgS (black)/Ag_2S, HgS (black)/Hg(0), and HgSe/Ag_2Se. The HgS/Ag_2S and HgS/Hg(0) precipitates were obtained by homogeneous precipitation of the sulphides with thiocetamide in the presence of a 10% excess of EDTA with respect to the mercury(II) content, at pH 4.5 with acetate buffer. A solution equimolar in mercury(II) and silver(I) nitrate was used to prepare the HgS/Ag_2S precipitate and mercury(I) nitrate was used to produce the HgS/Hg(0) precipitate by disproportionation of the mercury(I) sulphide formed. Mercury(II) selenide and HgSe/Ag_2Se were prepared as described earlier [13].

Equipment

Potentials were measured with a Corning Model 12 expanded-scale pH meter or a Corning Model 7 pH meter. Potentiometric titrations were done with a Radiometer Auto-Burette (ABU 1c). Saturated calomel electrodes and glass pH electrodes were from Corning.

Electrode construction. The four steps used in the construction of the mercury(II) sensors were reduction and methylation of the graphite rods, hydrophobization of graphite, electrode assembly, and activation of the exposed surface. Reduction and methylation of graphite were done by refluxing for 24 h with $LiAlH_4$ in dry dioxane and then for 24 h with dimethyl sulphate in dry acetone containing calcined potassium carbonate. For hydrophobization, the graphite rods were immersed in the appropriate resin/solvent system and either refluxed or heated in an oven for 12 h. Then the electrodes were inserted into tightly fitting Tygon tubing; one end of the rod was made flush with the end of the tubing, and this end was dipped into the resin/solvent solution. The open end was then connected to a vacuum pump for 3–4 h. The electrodes used here were assembled in two ways. In the first (Fig. 1A) a

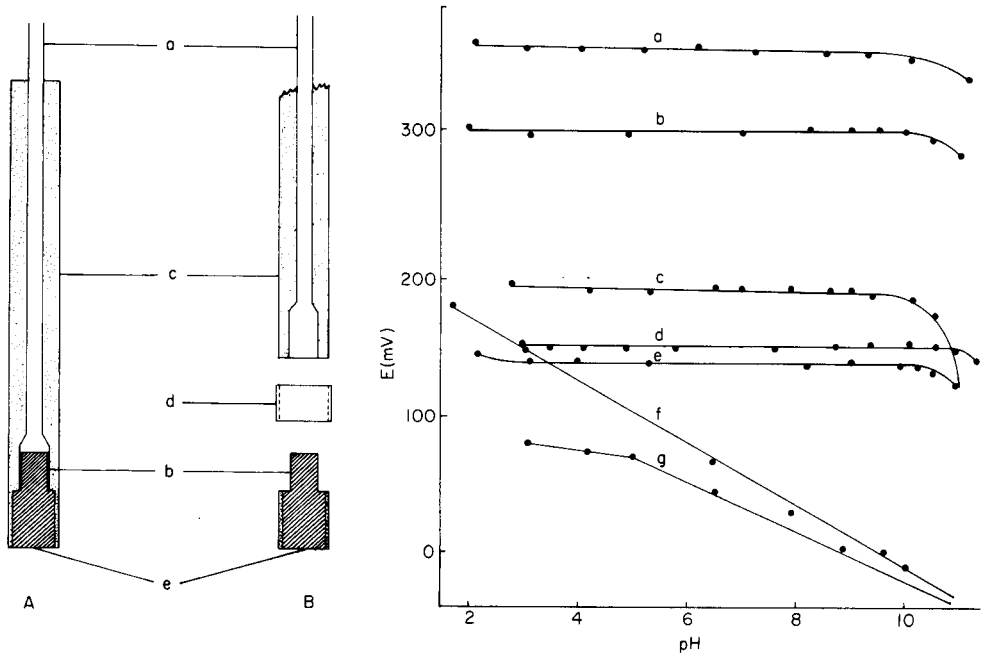

Fig. 1. Electrode construction: A, compact, single-bodied; B, interchangeable-tipped. (a) aluminium stem; (b) hydrophobized graphite rod; (c) polyester resin body; (d) Tygon tubing; (e) sensitive surface.

Fig. 2. Response of graphite to pH: (a) freshly treated (reduced and methylated); (b) as for (a) after 2 days at 100°C, its exposed surface being coated by silicone grease; (c) treated, hydrophobized with paraffin wax, activated with HgS (black)/Hg(0) and conditioned for 16 h in 10^{-3} M EDTA; (d) treated and hydrophobized with polyurethane resin in chloroform; (e) treated and hydrophobized by paraffin wax; (f) untreated graphite, coated with silicone grease; (g) untreated graphite.

compact single-bodied type was obtained by inserting the aluminium stem (a) into a machined collar provided on one end of the graphite rod (b), the other end being impregnated with silicone grease, and then centred in an upright position inside an 11-mm wide test tube. Polyester resin was then poured in to give the desired body length. After a curing period at 70°C, the glass tube was broken and the loose rounded end taken off, exposing the graphite surface to be activated (e). The second type (Fig. 1B) was a modular version, the body being made as described above but with a piece of glass tubing of the same width instead of a test tube. One end was sealed with masking tape and the aluminium stem was then centred inside and the resin poured in. The interchangeable tips were made by using a short piece of test tube bottom as mold and pouring in just enough resin to come level with the rod shoulder. To avoid eventual seepage of the sample solution into the electrode body through the junction of the two pieces, Tygon tubing (d) was inserted

to seal it. For activation, the graphite surface was rubbed with emery paper and then the electroactive material was rubbed into the graphite with a rounded glass rod. The electrode surface was then polished against a sheet of filter paper on a flat glass surface.

All potentials mentioned below are relative to the saturated calomel electrode.

RESULTS AND DISCUSSION

Conditioning of the graphite

Graphite rods used as inert matrix for ion-selective electrodes present two problems, namely pH sensitivity and hysteresis, that must be eliminated by appropriate pretreatment and hydrophobization, respectively, prior to assembly of the sensors. It is well known that free valence electrons at the surface of graphite can be saturated by chemisorbed oxygen; the surface oxides formed change the properties of the graphite surface [14]. Böehm et al. [15] postulated the existence of four different acidic functional groups that included a strongly acidic carboxylic group, a more weakly acidic carboxylic group, a phenolic hydroxyl group and a carbonyl group, each identified by its reaction, or failure to react, with bases of different strengths. These surface oxides are responsible for the pH sensitivity of graphite used as inert matrix in the construction of some ion-selective electrodes (e.g., Selectrodes). Consequently, the spectrographic graphite utilized to make the electrodes was reduced and methylated as described above, to eliminate its pH sensitivity. The procedure proved to be quite effective and rendered the graphite surface pH-independent up to pH 10 (Fig. 2).

The need for hydrophobization of the graphite rods to preclude memory effects was mentioned by Růžička et al. [10]. The method used here resembles the earlier one [11] in that a water-immiscible organic solvent was utilized but, in addition, a resin was dissolved in it. All the solvent/resin systems listed under *Experimental* gave very good results as hydrophobizing agents. The acrylic/chloroform system was preferred throughout the present work.

Choice of electroactive material

The activating material was a mixture of silicone grease with each precipitate in such a proportion that the particles of the precipitate were in contact with one another. This procedure produced sensors with improved qualities over those activated with the precipitate alone.

To find the most suitable activating material, several different precipitates and mixtures of precipitates were tested in direct potentiometry (HgS (black), HgS (red), HgSe, HgS (black or red) with Hg(0) mixed mechanically, HgS (black)/Hg(0) obtained by disproportionation of Hg_2S, HgS (black) with Ag_2S coprecipitated, and HgSe with Ag_2Se mixed mechanically).

The activated sensors were conditioned by immersion in 10^{-3} M Hg(II)

or EDTA solutions. Electrodes activated by mercury(II) chalcogenides and mercury showed increased stability and exhibited slopes very close to 29 mV per decadic concentration change when conditioned with either solution. The same positive effect was obtained when electrodes activated with a mercury(II) chalcogenide alone or mixed with a silver(I) chalcogenide were conditioned in Hg(II) solutions. EDTA solutions were not useful for conditioning in this case. Thus all electrodes were conditioned by immersion in the appropriate solution for at least 16 h before use. When not in use, electrodes were stored in the same solution as used for conditioning. About fifty such electrodes were prepared and tested; the results are summarized in Table 1. All the data in this table were obtained in constantly stirred solutions at pH 1.5 with nitric acid and ionic strength 0.1 M with potassium nitrate. For all the sensors except those activated with HgSe, the potential of a 10^{-3} M mercury(II) solution was in the range 425—445 mV vs. SCE. From Table 1, it can be concluded that electrodes activated with HgS (black)/Hg(0) obtained by disproportionation of mercury(I) sulphide yielded the best electrode of all, with Nernstian response for the pHg range 1—7 and a limit of detection of 5×10^{-8} M. A typical calibration curve is shown in Fig. 3. The detection limits of these electrodes are about two orders of magnitude lower than reported earlier [11]. From Table 1, it can also be inferred that electrodes activated with a single precipitate present narrower Nernstian ranges and so are of limited practical utility.

Mechanism and characteristics of the HgS (black)/Hg(0) electrode

In an effort to gain some insight into the mechanism that governs the HgS (black)/Hg(0) electrode response to mercury(II) ion, two calibration curves were constructed under the same experimental conditions as described above, one for a metallic mercury electrode and the other for a HgS (black)/Hg(0) electrode. Extrapolation of the rectilinear portion of these curves gave intersections at 545 and 549 mV vs. SCE, respectively. These

TABLE 1

Mercury electrodes activated by various materials

Electroactive material	Slope (mV/pHg)	Nernstian range (pHg)	Limit of detection (pHg)	Potential at pHg 3 (mV)
HgS (black)	30.3	1—4	4.3	435
HgS (black)/Hg(0)[a]	28.0	1—4	4.0	442
HgS (black)/Hg(0)[b]	29.6	1—7	7.3	445
HgS (black)/Ag_2S[c]	34.0	2—5	5.2	425
HgS (red)	30.5	1—4	4.6	430
HgS (red)/Hg(0)[a]	29.0	1—5	5.4	440
HgSe	27.5	1—4.5	5.1	540
HgSe/Ag_2S[a]	28.6	1—4	4.4	428

[a]Mechanical mixture. [b]Mercury(I) sulphide disproportionation. [c]Coprecipitated.

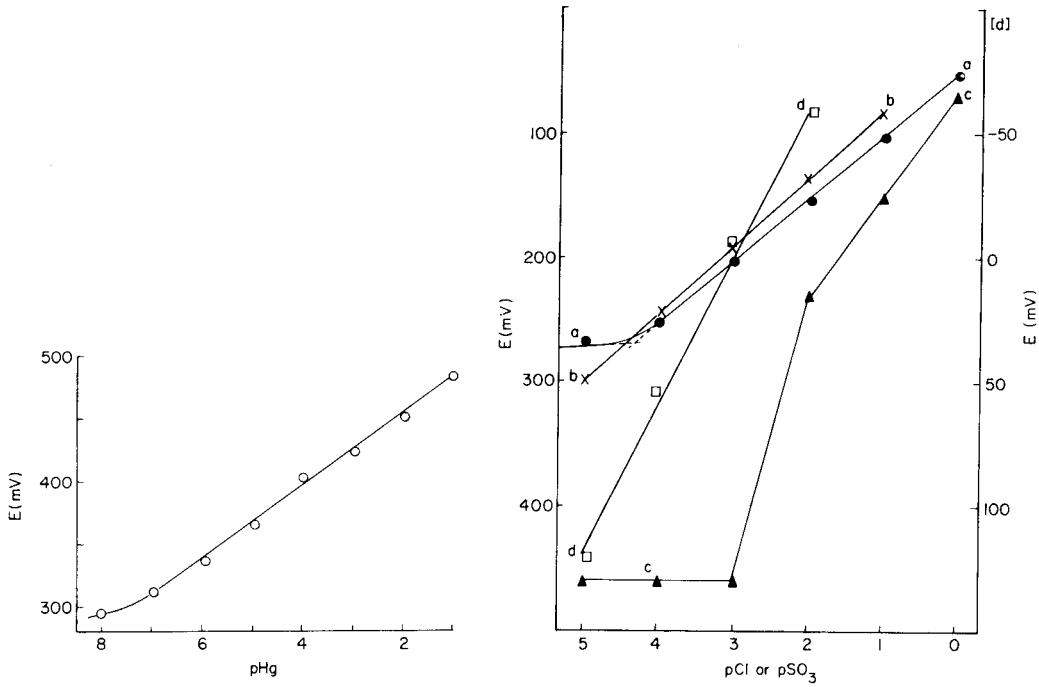

Fig. 3. Calibration curves for the HgS (black)/Hg(0) electrode in stirred solution at pH 1.5 (HNO_3).

Fig. 4. Interference of chloride and sulphite ions: (a) response to chloride of the HgS (black)/Hg(0) electrode; (b) response to chloride of a mercury electrode; (c) as for (a) but all chloride standard solutions were 10^{-3} M in Hg(II); (d) response to sulphite ions of the HgS (black)/Hg(0) electrode. Curves (a—c) were obtained at pH 1.5 with HNO_3; curve (d) was obtained at pH 7.5.

values are too low to correspond to the standard potential of an electrode activated by HgS (black), which from calculations [16] would be between 612 and 851 mV vs. SCE, depending on the minimum and maximum sulphur activities in equilibrium with the neighbouring Hg or S. The standard potential of the Hg(I)/Hg(0) couple is 547 mV vs. SCE, however, and this is very close to the above values, indicating that this system determines the electrode potential. The conclusion must be that Hg(0) is the actual active component while HgS serves simply as a matrix of low solubility and high conductivity [17]. Because electrodes activated with HgS (black)/Hg(0), prepared by disproportionation, were better than others examined, the remainder of this paper is concerned with this type of electrode unless noted otherwise. For these electrodes, the response time was less than 1 min for concentrations above 10^{-5} M but was slower (about 5 min) for lower concentrations. Potentials were quite stable after the conditioning period and in most cases a variation of less than 1 mV in 20 min was noted.

Memory effects and reproducibility were tested as follows. The potentials were recorded for a series of mercury(II) solutions between 10^{-1} and 10^{-9} M; then, after 30 min, the process was repeated in reverse order (10^{-9} to 10^{-1} M), and after another wait of 30 min, the first run was repeated. Results showed that reproducibility was quite good for most of the sensors tested in the concentration range 10^{-1}—10^{-8} M. Electrodes displaying poor reproducibility were discarded. Deterioration, evidenced by irreproducible and sluggish potentials, was noticed after 3—4 weeks of continuous use and electrodes were then reactivated as described above.

Although the electrodes activated with HgS (black)/Hg(0) showed detection limits about 200-fold lower than the HgS-based sensors previously reported, attainment of much lower limits would be expected from the calculated conditional solubility product for HgS ($K_{so} = 10^{-33}$). The limit of detection should be about the same as that found for an electrode activated with copper(II) sulphide ($K_{so} = 10^{-35.2}$) [12]. The poorer detection limit may be due to the mechanisms of the copper-selective and mercury-selective electrodes being quite different.

The interference of chloride ions was investigated because halides generally form insoluble mercury(I) compounds, which may impose a low positive limiting potential. Conclusions drawn for chloride ion interference can be extended to bromide and iodide which form even more insoluble compounds with mercury(I). Standard chloride solutions, 1—10^{-6} M, were prepared by serial dilution in sufficient nitric acid to bring the pH to 1.5, without ionic strength regulation. In the absence of mercury(II), the HgS (black)/Hg(0) electrode showed a Nernstian response (Fig. 4a) over the range 10^{0}—10^{-4} M, with a limit of detection of 4.4×10^{-5} M and a slope of 50 mV per decade change in concentration, in agreement with the value (50—51 mV) reported by Tseng and Gutknecht [18] for a HgS/Hg_2Cl_2-based membrane electrode. Extrapolation of curve (a) to pCl = 0 gave a value of 52 mV vs. SCE, which is closer to the standard potential of the $Hg_2Cl_2/Hg(0)$ couple than to that of the HgS electrode. When a mercury electrode was used (Fig. 4, curve b), the slope was 55 mV per decade but its extrapolation to pCl = 0 gave 26 mV vs. SCE in agreement with the standard potential of the $Hg_2Cl_2/Hg(0)$ couple. Curve (c) was constructed as curve (a) but with 10^{-3} M Hg(II) in each chloride solution; mixed potentials were obtained up to pCl = 3 after which the response became independent of chloride concentration with a potential of 460 mV. The HgS (black)/Hg(0) electrode may be useful for chloride ion measurements. Direct potentiometry of sulphite ion was studied within the concentration range 10^{-2}—10^{-5} M at pH 7.5. The electrode behaved in a strictly Nernstian manner with a mean slope of 60 mV per decade concentration (Fig. 4, curve d). Further studies of these responses are in progress.

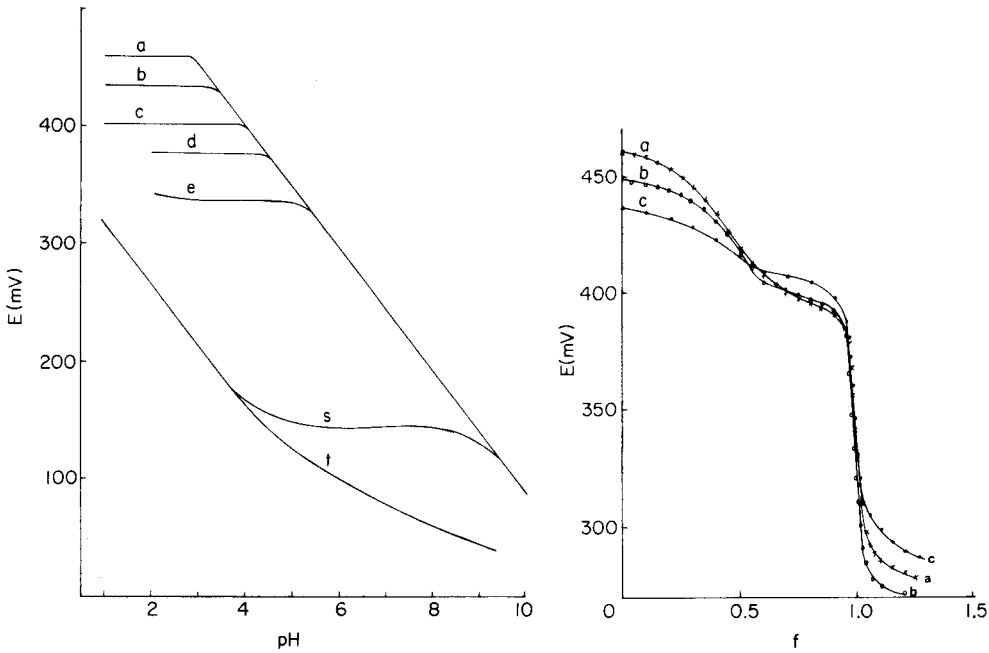

Fig. 5. Potential vs. pH diagram. Curves (a—c) are for pHg 2, 3, and 4, respectively. Curves (d, e, s): [HgY] = [MY] = $[M^{2+}] = 10^{-3}$ M (M = Cu^{2+}, Zn^{2+}, or Ca^{2+}; Y = EDTA). Curve (t): [HgY] = [Y] = 10^{-3} M.

Fig. 6. Potentiometric titration of Hg(II) by EDTA at pH 4.5 in acetate buffer. Curves: (a) HgS (black)/Hg(0) electrode; (b) HgS (red)/Hg(0) electrode; (c) mercury electrode. Initial concentration of the titrand, 6.0×10^{-4} M.

Complexime tric titrations

To determine the best titration conditions, a Reilley—Schmid diagram [7] was constructed (Fig. 5). In this plot, curves (a—c) depict the response of the HgS (black)/Hg(0) electrode to 10^{-2}—10^{-4} M mercury(II) as a function of pH; as expected, the potential changes only when mercury(II) oxide precipitates. In the absence of a complexing agent, precipitation of the oxide sets the upper limit of metal ion that can exist at any given pH and determines the potential of the electrode at the start of the titration. Curve (t) was obtained for a solution that contained equal concentrations of the mercury(II)–EDTA chelate (HgY) and free EDTA (Y), and represents the lower limit of the free metal ion that will be present beyond the end-point. These data indicate that a pH range between 3 and 4 will yield the sharpest potential break. Curves (d), (e), and (s) represent the responses of the same electrode with solutions containing equal concentrations of free Cu(II), Zn(II), or Ca(II), the corresponding metal chelate, and the electrochemical indicator, HgY, respectively.

Figure 6 shows titration curves of a 6×10^{-4} M mercury(II) solution

titrated with 10^{-2} M EDTA in a 9×10^{-2} M acetate buffer of pH 4.5 when three different electroactive materials were used. All the curves present a peculiar shape between $f = 0$ and $f = 0.5$. The potentials at $f = 0$ are higher than those expected from the Reilley diagram in Fig. 5. However, as the titration proceeds, they decrease slowly at the beginning and then rather sharply to fit the upper plateau of the normal potentiometric curves. When these plateaus are extrapolated to $f = 0$ they intersect the ordinate at approximately the same potential value, 425 mV, in reasonable agreement with that predicted by the potential—pH diagram in Fig. 5 for no complexing agent present. This suggests that the acetate buffer accounts for the anomalous shapes of the curves because of the formation of mercury(I) acetate on the electrode surface. This behaviour does not degrade the quality of the end-points obtained for the conditions used here. Several titrations of a 10^{-2} M solution of Hg(II) with EDTA gave an uncertainty of 1.1×10^{-4} M at the 95% confidence level. Problems may be encountered for higher concentrations because erratic end-points have been reported for titrations of 10^{-2} M Hg(II) solutions [19].

Other electrodes (HgS (red), HgS/Ag_2S, HgS (black)/Hg(0), and HgSe) were useful for titrations, with the first three giving uncertainties of 0.9, 0.4 and 1.7×10^{-4} M Hg(II) at the 95% confidence level and the fourth giving an uncertainty of 3.1×10^{-4} M for titrations of 10^{-2} M Hg(II). Gran plots [20] were used to estimate all concentrations. For these titrations, the electrodes activated with HgS/Ag_2S and HgS (red) provided the most precise results. Although no titrations involving Cu(II), Zn(II), or Ca(II) were examined, inspection of the Reilley—Schmid diagram in Fig. 5 indicates that titration curves for Cu(II) and Zn(II) should display sharp breaks at the end-point while Ca(II) would not.

REFERENCES

1 E. Bishop, Mikrochim. Acta, (1956) 619.
2 E. Bishop, Analyst, 83 (1958) 212.
3 E. Bishop and R. G. Dhaneshwar, Analyst, 87 (1962) 207.
4 E. Bishop and G. D. Short, Analyst, 87 (1962) 467.
5 E. Bishop and T. J. N. Webber, Analyst, 98 (1973) 697.
6 S. Siggia, D. W. Eichlin and R. C. Rheinhart, Anal. Chem., 27 (1955) 1745.
7 C. N. Reilley and R. W. Schmid, Anal. Chem., 30 (1958) 947.
8 C. N. Reilley, R. W. Schmid and D. W. Lamson, Anal. Chem., 30 (1958) 953.
9 E. Bishop and P. H. Hitchcock, Analyst, 98 (1973) 465.
10 J. Růžička, C. G. Lamm and Chr. Tjell, Anal. Chim. Acta, 62 (1972) 15.
11 J. Růžička and C. G. Lamm, Anal. Chim. Acta, 53 (1971) 206.
12 E. H. Hansen, C. G. Lamm and J. Růžička, Anal. Chim. Acta, 59 (1972) 403.
13 G. E. Cranton and R. D. Heyding, Can. J. Chem., 43 (1955) 2029.
14 R. W. Coughlin, F. S. Ezra and R. N. Tan, J. Colloid Interface Sci., 28 (1968) 386.
15 H. P. Böehm, E. Diehl, W. Heck and S. Sappok, Angew. Chem. Intern. Ed. Engl., 3 (1964) 669.
16 M. Sato, Electrochim. Acta, 11 (1966) 361.

17 J. F. Lechner and I. Sekerka, J. Electroanal. Chem. Interfacial Electrochem., 57 (1974) 317.
18 P. K. C. Tseng and W. F. Gutknecht, Anal. Chem., 48 (1976) 1996.
19 U. Hannema, G. J. van Rossum and G. den Boef, Fresenius Z. Anal. Chem., 250 (1970) 302.
20 G. Gran, Analyst, 77 (1952) 661.

Analytica Chimica Acta, 148 (1983) 51—57
Elsevier Science Publishers B.V., Amsterdam — Printed in The Netherlands

DETERMINATION OF TRACES OF METALS BY ANODIC STRIPPING VOLTAMMETRY AT A ROTATING GLASSY CARBON RING-DISC ELECTRODE

Part 3. Evaluation of Linear Anodic Stripping Voltammetry with Ring Collection for the Determination of Cadmium, Lead and Copper in Pure Water and High-Purity Sodium Chloride, and of Cadmium, Lead, Copper, Antimony and Bismuth in Sea Water

C. BRIHAYE, G. GILLAIN and G. DUYCKAERTS*

Laboratoire de Chimie Analytique, et Laboratoire d'Océanologie, Université de Liège au Sart Tilman, B6, B-4000 Liège (Belgium)

(Received 26th October 1982)

SUMMARY

A procedure based on linear anodic stripping voltammetry (a.s.v.) with ring collection is described for the determination of cadmium, lead and copper in very pure doubly-distilled water passed through a Millipore Milli-Q purification system and in commercial Suprapur sodium chloride. Concentrations of Cd, Pb and Cu as low as 6, 8 and 5 ng l^{-1}, respectively, were measured in water and 0.12, 0.15 and 0.30 ng g^{-1} in sodium chloride. Results obtained for Cd, Pb, Cu, Sb and Bi in sea water by two different methods (linear a.s.v. with a ring-disc electrode and differential pulse a.s.v. with a hanging mercury drop electrode) were in good agreement for u.v.-irradiated samples; linear a.s.v. with the ring-disc electrode gave systematically higher Cd, Pb and Cu contents because of exchange of mercury(II) ions added to the solution, with the heavy metal non-labile complexes.

In previous parts of this series [1, 2] results on anodic stripping voltammetry (a.s.v.) with collection at a glassy carbon ring-disc electrode mercury-plated in situ were communicated. The first paper was concerned with a study of the parameters of this technique, and in the second paper different variants of the a.s.v. method were compared. This last paper of the series gives results for the measurement, by a.s.v. with collection, of cadmium, lead and copper in high-purity water and in Suprapur sodium chloride and of Cd, Pb, Cu, Sb and Bi in sea-water samples.

Gillain et al. [3] have shown that it is possible to measure Zn, Cd, Pb, Cu, Sb and Bi in sea water by d.p.a.s.v. at a hanging mercury drop electrode, when conditions are such that the total chloride concentration is 2 M, by addition of sodium chloride, and the pH is close to 1.

EXPERIMENTAL

The electrode was as described previously [1].

The high-purity water was produced by a Millipore Milli-Q system and the

0003-2670/83/$03.00

sodium chloride was Suprapur quality (Merck; lot 8602453). The sea-water samples came from the North Sea (Belgian Coast) and were filtered through 0.45-μm filters.

All experiments were done in boxes swept with filtered air. Volumes were measured by weighing. The u.v. irradiation apparatus for the sea-water samples has been described [4].

All potentials are given vs. Ag/AgCl, 0.1 M KCl. Except when specified, the experimental parameters were as follows: rotation speed of the ring-disc electrode ω = 1500 rpm; disc potential scan rate v = 3 V min^{-1}, mercury-(II) concentration [Hg^{2+}] = 1.63 × 10^{-5} M.

RESULTS AND DISCUSSION

Measurement of Cd, Pb and Cu in high-purity water and in sodium chloride

Increasing quantities of sodium chloride were added to a volume of very pure water, and the pH was reduced to 2 by addition of hydrochloric acid (Suprapur, Merck). Each solution was analysed by the method described previously [1]. The concentrations measured were plotted as a function of sodium chloride concentration. Results for cadmium are shown in Fig. 1; the concentration in the water can be deduced from the ordinate at the origin, and the value of the slope gives the content of the metal in the sodium chloride (Table 1).

Measurement of Cd, Pb, Cu, Sb, and Bi in sea water

Choice of medium. Initially, the experimental conditions proposed by Gillain et al. [3] were adopted, but the appearance of an intermetallic compound between copper and antimony was noted, even when the antimony concentration was very low. It was therefore necessary to deposit antimony and bismuth at an electrolysis potential at which copper remained in solution. To achieve this, the influence of the sodium chloride concentration on the potential of appearance of copper deposition was studied by examining

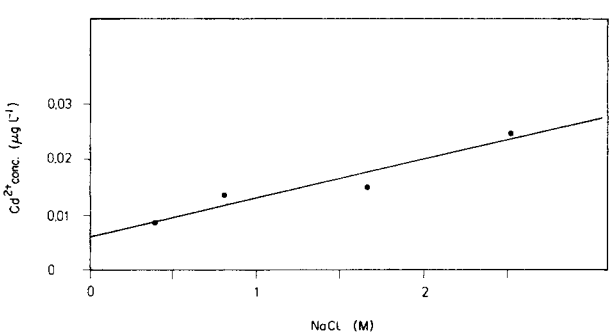

Fig. 1. Cadmium concentration measured by a.s.v. with collection as a function of NaCl concentration. (1.63 × 10^{-5} M Hg^{2+}; ω = 1500 rpm, v = 3 V min^{-1}, t_{dep} = 1 h.)

TABLE 1

Concentration of Cd, Pb and Cu in high-purity water and sodium chloride (1.63×10^{-5} M Hg^{2+}, ω = 1500 rpm, v = 3 V min^{-1}, t_{dep} = 1 h.)

	Cd	Pb	Cu
Water (ng l^{-1})	6	8	5
NaCl (ng g^{-1})	0.12	0.15	0.30

the redissolution peak. Table 2 gives the potentials obtained for different sodium chloride concentrations, for a sea-water sample at pH 1.15 with a copper concentration of 30 μg l^{-1}. These results indicated that the electrolysis of antimony and bismuth would be best done at a potential 150 mV more anodic than the appearance potential of copper deposition.

Figure 2 shows the voltammograms obtained for antimony and bismuth during simultaneous a.s.v. with collection under the conditions E_R = —0.5 V and t_{dep} = 5 min. Comparison of these voltammograms shows that for 1 M sodium chloride, the antimony collection peak is small, probably because the electrolysis potential is not situated in the antimony(III) diffusion plateau, whereas for 1.5 M sodium chloride, the antimony and bismuth collection peaks are clear and well resolved. For 2 M sodium chloride, the antimony and bismuth collection peaks are less well resolved than for 1.5 M sodium chloride. Thus, the most favorable working conditions for simultaneous determinations of these two metals are a 1.5 M sodium chloride medium and an electrolysis potential of —0.4 V. Under these conditions, the peak heights are proportional to the concentration. Up to concentrations of 2 μg l^{-1}, there are no mutual interferences between antimony and bismuth, i.e., the peak height of one is not influenced by the presence of the other.

Reduction of antimony(V) by sulfur dioxide. In 1.5 M sodium chloride at pH 1.15, antimony(V) is not electroactive at a mercury film electrode. Therefore, to measure antimony, it must first be reduced to antimony(III)

TABLE 2

Appearance potential of copper deposition and electrolysis potential of antimony and bismuth as a function of sodium chloride concentration
(Sea water at pH 1.15, 30 μg l^{-1} Cu^{2+}, 1.63×10^{-5} M Hg^{2+}, ω = 1500 rpm, v = 3 V min^{-1}, t_{dep} = 5 min.)

NaCl (M)	Appearance potential of Cu deposition (V)	Electrolysis potential of Sb, Bi (V)
0.5	—0.45	—0.30
1.0	—0.50	—0.35
1.5	—0.55	—0.40
2.0	—0.60	—0.45

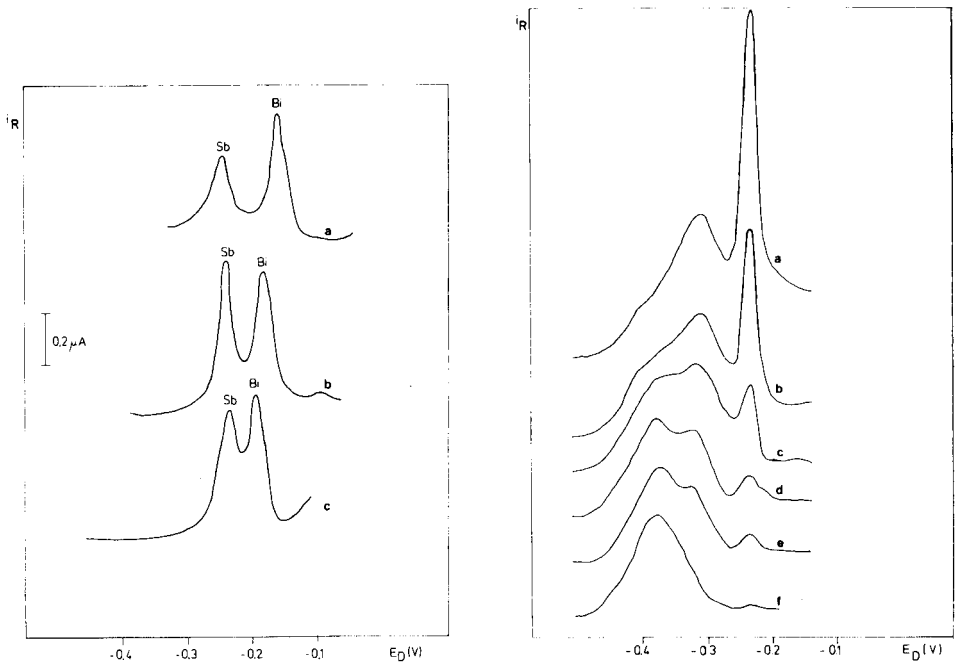

Fig. 2. Voltammograms for sea water doped with antimony and bismuth, by a.s.v. with collection at different NaCl concentrations. Conditions: 1.63×10^{-5} M Hg^{2+}, 0.7 μg l^{-1} Sb^{3+}, 0.7 μg l^{-1} Bi^{3+}, ω = 1500 rpm, v = 3 V min^{-1}, t_{dep} = 5 min, E_R = —0.5 V. (a) 1.0 M NaCl, E_{elec} = —0.35 V; (b) 1.5 M NaCl, E_{elec} = —0.40 V; (c) 2.0 M NaCl, E_{elec} = —0.45 V.

Fig. 3. Voltammograms for copper and antimony by a.s.v. with collection for increasing concentrations of antimony. Conditions: 1.69 μg l^{-1} Cu^{2+}, 1.5 M NaCl, pH 1.15, 1.63×10^{-5} M Hg^{2+}, ω = 1500 rpm, v = 3 V min^{-1}, t_{dep} = 3 min, E_{dep} = —0.65 V, E_R = —0.65 V. Antimony(III) concentration (μg l^{-1}): (a) 2.11, (b) 1.33, (c) 1.00, (d) 0.71, (e) 0.50, (f) 0.33.

by saturating the solution with sulfur dioxide, excess of which is easily eliminated by bubbling nitrogen through the solution at 90°C. The reduction of Sb(V) to Sb(III) is quantitative, and the contribution in heavy metals arising from this treatment is 0.01 μg l^{-1} for cadmium, 0.02 μg l^{-1} for lead and copper and less than 0.005 μg l^{-1} for antimony and bismuth.

Intermetallic Sb—Cu compounds. The simultaneous deposition of copper and antimony at a mercury film electrode causes the formation of an intermetallic Cu—Sb compound, as shown in Fig. 3. The different voltammograms in this figure were obtained from a 1.5 M NaCl solution at pH 1.15. The copper concentration was held at a constant concentration of 1.69 μg l^{-1}, while that of antimony(III) was varied. It can be seen from these voltammograms that the copper collection peak height decreases as the antimony concentration increases. Also, a redissolution peak from an intermetallic Cu—Sb compound appears between the copper and antimony peaks. Even when the copper concentration is higher than that of antimony, the variation

TABLE 3

Variation of peak height for copper (1.69 $\mu g\ l^{-1}$) as a function of antimony concentration

Variation of Cu peak height (%)	−16	−22	−27	−36	−56	−71	−74
Sb conc. ($\mu g\ l^{-1}$)	0.33	0.50	0.71	1.00	1.33	2.11	2.89

in the copper peak height is too large for accurate measurements of this metal. The extent of the interference is shown in Table 3. Application of Stromberg's theory [5], modified to be valid for a mercury film electrode, led to the conclusion that for concentration ratios of copper to antimony in mercury greater than 5, the compound formed is stoichiometrically Cu_3Sb, and for ratios less than 5, the compound formed is CuSb. These results confirm those of Zadharchuk and Zebreva [6].

Oxidation of antimony(III) by u.v. irradiation. The formation of intermetallic compounds between copper and antimony precludes exact measurement of copper when Sb(III) is present. To measure copper, it is therefore imperative to oxidize Sb(III) to the electro-inactive Sb(V). This oxidation can be done by treating the solution with u.v. radiation. Table 4 shows the antimony(III) peak heights obtained from a 1.5 M sodium chloride solution at pH 1.15 as a function of irradiation time.

Comparison between a.s.v. with collection and d.p.a.s.v. with a HMDE for heavy metal measurement in sea water

The concentrations of Cd, Pb, Cu, Sb and Bi were determined in seawater samples by a.s.v. with collection as above and by differential pulse a.s.v. with a hanging mercury drop electrode (HMDE). The experimental conditions for the latter technique were those described by Gillain et al. [3]. During this comparison, it was hoped that information about the speciation of these metals could be obtained, as described earlier [3].

The voltammetric measurements in 1.5 M sodium chloride at pH 1.15 will give the concentrations of free metal and labile metal complexes (antimony being present as Sb(III)). Given that the concentrations of Sb(III) are very low, copper measurements with the rotating ring-disc electrode (RRDE) will be little influenced by the presence of antimony. Cadmium, lead and copper are measured after electrolysis at −0.9 V, and antimony and bismuth

TABLE 4

Antimony peak current as a function of u.v.-irradiation time
(1.5 M NaCl solution, pH 1.15, 1.63×10^{-5} M Hg^{2+}, ω = 1500 rpm v = 3 V min^{-1}, t_{dep} = 5 min, E_{dep} = −0.40 V, 0.55 $\mu g\ l^{-1}$ Sb^{3+}.)

$i_{p,Sb}$ (μA)	0.29	0.09	0.01	0.01
$t_{irr.}$ (min)	0	10	20	30

are measured after electrolysis at —0.4 V; the potentials applied at the ring during the collection are —0.9 and —0.4 V, respectively.

After the treatment with sulfur dioxide, the values obtained for antimony include the sum of the free metal ions and labile ions of Sb(III) and Sb(V) when the electrolysis and collection potentials are —0.4 V.

As u.v. irradiation destroys organic matter [4], the total metal concentrations in the solution are measured when the irradiation is followed by reduction with sulfur dioxide. Under these conditions, the antimony concentration is higher than with measurement at pH 1.15, and direct measurement of copper becomes impossible. It is possible to remedy this situation by taking a part of the solution after u.v. irradiation and measuring cadmium, lead and copper after electrolysis at —0.9 V, while antimony is present as Sb(V). A second aliquot is treated with sulfur dioxide, and this permits measurement of antimony and bismuth after electrolysis at —0.4 V.

Eight samples of sea water were analysed. An example of the results is given in Table 5. If there were no systematic error between the two methods a bilogarithmic plot of all the experimental results should give a straight line with unit slope, passing through the origin. In reality, the plot yields a line parallel to the ideal line, indicating a systematic error (Fig. 4A), the values obtained by a.s.v. with collection are systematically higher. This is due to the mercury(II) ions added to the solution in this method liberating a certain quantity of metals fixed in non-labile complexes. The concentration values found after u.v. irradiation show excellent agreement between the two methods. Figure 4B shows the variation of log C_{HMDE} vs. log C_{RRDE} for the 8 samples after u.v. irradiation. The line passes through the origin with a slope of 1.03, which shows that the presence of mercury(II) ions does not influence measurement by a.s.v. with the RRDE. Finally, Table 5 indicates that a.s.v. with collection has better detection limits than d.p.a.s.v. at the HMDE.

TABLE 5

Concentrations ($\mu g\ l^{-1}$) of Cd, Pb, Cu, Sb and Bi in a sea-water sample measured by d.p.a.s.v. with a HMDE and by a.s.v. with collection, at pH 1.15, after treatment with sulfur dioxide, and after u.v. irradiation followed by treatment with sulfur dioxide (1.63×10^{-5} M Hg^{2+}, ω = 1500 rpm, v = 3 V min^{-1}.)

	Differential pulse/HMDE			Linear/RRDE		
	pH 1.15	$+SO_2$	U.v. $+SO_2$	pH 1.15	$+SO_2$	U.v. $+SO_2$
Cd	0.05	—	0.09	0.06	—	0.09
Pb	0.60	—	0.83	0.69	—	0.79
Cu	1.56	—	2.31	1.72	—	2.22
Sb	0.05	0.11	0.16	0.013	0.092	0.12
Bi	0.05	0.05	0.10	0.011	0.014	0.13

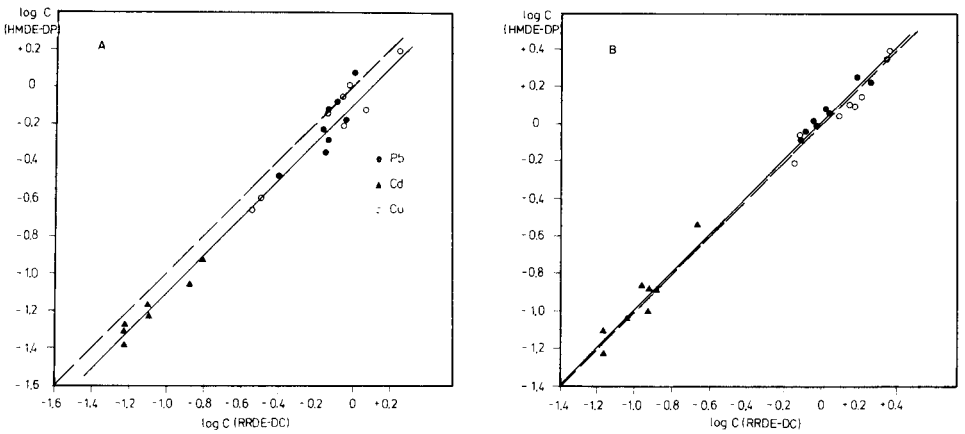

Fig. 4. Variation of log C_{HMDE} as a function of log C_{RRDE} for Cd (▲), Pb (●) and Cu (○) in sea water. (A) Concentrations (μg l^{-1}) were measured at pH 1.15; (B) concentrations were measured at pH 1.15 after u.v. irradiation. Conditions: 1.63 × 10^{-5} M Hg^{2+}, ω = 1500 rpm, v = 3 V min^{-1}.

Conclusions

Anodic stripping with collection applied to heavy metal measurements in various matrices such as high-purity sodium chloride and water, and sea water, gives excellent results from the point of view of detection limits as well as precision. One has to bear in mind, though, the possible liberation of metals from non-labile complexes with organic matter when mercury(II) ion is added. This gives results systematically higher than those obtained at the hanging mercury drop electrode. The effect can be avoided by u.v. irradiation of the solution, which destroys the organic complexes, and provides results in terms of total heavy metal content for cadmium, lead and copper.

REFERENCES

1 C. Brihaye and G. Duyckaerts, Anal. Chim. Acta, 143 (1982) 111.
2 C. Brihaye and G. Duyckaerts, Anal. Chim. Acta, 146 (1983) 37.
3 G. Gillain, G. Duyckaerts and A. Distèche, Anal. Chim. Acta, 106 (1979) 23.
4 G. Duyckaerts and G. Gillain, Essays in Memory of Anders Ringbom, Pergamon, Oxford, 1977.
5 N. A. Mesyats, A. G. Stromberg and M. S. Zakharov, Elektrokhimya, 4 (1968) 987.
6 N. F. Zakharchuk and A. I. Zebreva, Tr. Inst. Khim. Nauk, Akad, Nauk Kaz. SSR, 32 (1971) 31 (Chem. Abstr., 75, 93962b).

Analytica Chimica Acta, 148 (1983) 59—69
Elsevier Science Publishers B.V., Amsterdam — Printed in The Netherlands

DETERMINATION OF SELENIUM, COPPER, LEAD AND CADMIUM IN BIOLOGICAL MATERIALS BY DIFFERENTIAL PULSE STRIPPING VOLTAMMETRY

S. B. ADELOJU and A. M. BOND*

Division of Chemical and Physical Sciences, Deakin University, Waurn Ponds, Victoria 3217 (Australia)

H. C. HUGHES

School of Applied Chemistry, Western Australian Institute of Technology, South Bentley, W.A. 6102 (Australia)

(Received 27th July 1982)

SUMMARY

A simple and rapid stripping voltammetric method is described for the determination of selenium, copper, lead and cadmium in a single sample solution. The method utilizes differential pulse cathodic stripping voltammetry for the determination of selenium and differential pulse anodic stripping voltammetry for the other three elements. The use of a deposition potential of —0.3 V vs. SCE allows the determination of selenium in the presence of interfering ions at 1000-fold concentrations. Subsequent oxidation of the selenium to the electro-inactive selenium(VI) permits direct determination of the other three elements in the same solution. Application of the method to NBS bovine liver and some fish samples proved to be satisfactory. The limits of detection obtained by this method were 0.1 $\mu g\ l^{-1}$ for selenium, 0.5 $\mu g\ l^{-1}$ for copper and 0.01 $\mu g\ l^{-1}$ for lead and cadmium. Determination of the four elements takes about 90 min.

Concern and awareness about the accumulation of heavy metals in the human body have increased considerably over the last decade owing to the toxic or beneficial effects which these elements have been known to cause [1—4]. A thorough understanding of these effects depends largely on the ability to determine the rather low concentrations of heavy metals in various biological materials. This, however, creates a challenging and rather involved task, as the normal concentrations are often near the limits of detection of most instrumental methods. The possibility of sample contamination at these levels is also so enormous that it can easily result in relatively large errors. Various methods have been applied to matrices such as urine, blood, food and various body organs [5—17] but the demand for development and/or improvement of quantitative methods for trace metals is increasing [18—21].

Stripping voltammetric techniques such as anodic stripping voltammetry (a.s.v.) and cathodic stripping voltammetry (c.s.v.) are two of the most sensitive and selective techniques used in quantifying trace metals. To date, a.s.v. has

0003-2670/83/$03.00

been successfully used for the determination of heavy metals such as copper, lead, cadmium and zinc in many matrices [14—17, 22—34] whereas c.s.v. has proved to be most sensitive for selenium, arsenic and tellurium [12, 13, 35—39]. The simplicity and rapidity of these techniques suggest that the concurrent use of both a.s.v. and c.s.v. for multi-element determinations in a single sample solution may reduce the total time needed considerably below that required for individual determinations. However, the possibility of inter-metallic interferences in these techniques [12, 29, 36, 40—45] needs to be considered.

The interferences can sometimes be overcome by selective deposition of the analyte(s) [37] or by appropriate use of masking or oxidizing agents [12]. If this can be achieved, the concurrent use of both techniques for the determination of a number of elements in a single sample solution would be possible. This paper describes a method proposed for the determination of selenium, copper, lead and cadmium in a single sample solution after acid digestion of biological materials.

EXPERIMENTAL

Reagents and standard solutions

All acids used were Aristar grade (BDH Chemicals) while the other reagents were of analytical-grade purity. The magnesium nitrate solution (80% w/v) used as an ashing aid and the acids were further purified by controlled potential electrolysis at —1.2 V for four days to reduce the metallic impurities in the solutions. The metallic impurities in the acids were further reduced by distilling twice before use.

Stock solutions (1 g l^{-1}) of selenium, copper, lead and cadmium were prepared by dissolving their salts in 0.1 M hydrochloric acid, and stored in pre-washed polyethylene bottles. Required standards were made up each day by appropriate dilution of stock with the chosen electrolyte. Doubly-distilled deionized water was used throughout.

Equipment

A Princeton Applied Research (PAR) Model 174 polarographic analyzer connected to a Houston Instrument Omnigraphic X-Y recorder was used to record all stripping voltammograms. A hanging mercury drop electrode (Metrohm E410) was used as the working electrode while a coiled 20-cm length of platinum wire and a saturated calomel electrode (SCE; Koslow Scientific) served as the counter and reference electrodes, respectively. The electrolytic cell was thermostated at (25.0 ± 0.1)°C during the experiments to maintain reproducible conditions for all determinations and the solutions were degassed with highly purified nitrogen at the start of each experiment. A flow of nitrogen over the solution was maintained during the experiment to prevent oxygen interference.

Stirring of the solutions during deposition was achieved with a Metrohm E405 swing-out magnetic stirrer powered by a synchronous motor. Standard solutions of the various metals were added to the electrolytic cell with a variable volume Oxford micropipette with disposable tips.

All glassware was washed in hot (1 + 4) nitric acid, rinsed with deionized water, washed three times with doubly-distilled deionized water and finally steam-washed at least once with doubly-distilled deionized water before use.

Standard reference material and inter-laboratory survey samples

The bovine liver standard reference material was obtained from the U.S. National Bureau of Standards. The fish samples were obtained during an inter-laboratory survey [46]. The liver and fish samples were treated as recommended by the suppliers. Homogenized samples of various freeze-dried marine tissue (shark, flathead, mussel and crayfish) were prepared by the Victorian Ministry for Conservation, Fisheries and Wildlife Laboratories at the Arthur Rylah Institute for Environmental Research, Melbourne. Sets of marine tissue samples provided in powdered form were sent to laboratories undertaking measurement of heavy metals in marine environmental materials. Participating laboratories were requested to analyze each sample by their own routine methods. Specific instructions for sample preparation were provided to participants. The powdered samples had 80% of their original weight removed as moisture and had to be reconstituted strictly as indicated in order to provide wet macerated tissue equivalent to regular field samples. Results reported on a wet-weight sample for the inter-laboratory survey are given in appropriate Tables.

Sample digestion

The bovine liver and fish samples were first digested with nitric acid and 5 ml of 80% (w/v) magnesium nitrate solution and then dry-ashed in an electric Carbolite muffle furnace at 500°C for 30 min, using a method similar to that described by Holak [12]. The ashed material was dissolved by boiling in 10 ml of 6 M hydrochloric acid. The final solution for 1 g of the sample was normally diluted to 1 l with doubly-distilled deionized water and the pH was adjusted to 1 with hydrochloric acid prior to the stripping. For very low concentrations of selenium, solutions were diluted to 100 ml rather than 1 l. The blank values for the four elements were determined by using reagents without sample in the digestion procedure and results were corrected for these blank values. Typically, blank values were 0.00 $\mu g\ l^{-1}$ (Se), 0.10 $\mu g\ l^{-1}$ (Cu), 0.03 $\mu g\ l^{-1}$ (Pb) and 0.02 $\mu g\ l^{-1}$ (Cd). The blank values were so low that very long (60 min) deposition times were required for their determination.

Stripping determinations

An aliquot of the digested sample solution was transferred to an electrolytic cell, degassed for 10 min and maintained under a flow of nitrogen. A fresh drop of mercury of known area was extruded from the micrometer of

the hanging mercury drop electrode (HMDE) and the solution was stirred at constant and reproducible rate without disturbing the mercury drop. The selenium was determined as Se(IV) under the following conditions: differential pulse mode, deposition potential —0.3 V vs. SCE, scan rate —2 mV s^{-1}, duration between pulses 0.5 s, modulation amplitude —25 mV, deposition time 60—180 s (stirred), equilibration period 30 s (unstirred). The d.c. mode was also used during development of the method but not for actual determination of the elements. Conditions for this mode are stated in the text.

Stripping voltammograms for selenium were repeated at least twice before proceeding with the addition of the standard. The solution was stirred and deaerated briefly with nitrogen after each addition and the stripping operation was repeated at least twice before the next addition. The selenium stripping peak, which usually appears at about —0.56 V vs. SCE, was used for the determination. In the presence of metallic interferences, this peak may be shifted to a more negative potential.

To determine the other three elements, drops of mercury were removed from the bottom of the cell and 50 μl of saturated potassium permanganate solution was added to oxidize selenium(IV) to the electrochemically inactive selenium(VI). The solution was then stirred and deaerated for 2 min. Excess of permanganate was removed by adding about 5 mg of hydrazine sulphate, and complete oxidation of the selenium(IV) was confirmed by repeating the c.s.v. operation. When necessary, the oxidation procedure was repeated and a further check was made by c.s.v.

After confirmation of complete oxidation of the selenium(IV) to selenium(VI), the other three elements were determined in the a.s.v. mode; the scan direction and display direction were reversed, electrolysis was done at —0.9 V vs. SCE and the other conditions previously given for the c.s.v. of selenium were maintained. Determinations of copper, lead and cadmium were made by the standard addition method using the peaks appearing at about —0.2 V, —0.5 V and —0.7 V vs. SCE, respectively. The concentrations of the four elements in the samples were estimated from the standard addition experiments.

RESULTS AND DISCUSSION

The cathodic stripping voltammetric determination of selenium(IV) at the selected deposition potential of —0.3 V vs. SCE involves two main reduction processes on a hanging mercury drop electrode [47]. First, mercury(II) selenide is formed during the deposition step: $Se(IV) + Hg + 4e^- \rightarrow HgSe$. Then mercury(II) selenide is reduced during the stripping step: $HgSe + 2H^+ + 2e^- \rightarrow H_2Se + Hg$, with E_p = —0.56 V vs. SCE. The overall reaction, independent of the mercury electrode, can thus be written as $Se(IV) + 2H^+ + 6e^- \rightleftharpoons H_2Se$. The height of the stripping peak increases quantitatively with the amount of selenium present. However, the position and height of the peak may also be influenced by factors such as pH and the presence of other

metal ions [37]. The solution pH (1.0) and acid (HCl) chosen, gave optimum response for the determination of selenium.

In the absence of metallic interferences, the selenium peak appeared at about —0.56 V vs. SCE but was shifted to a more negative potential when large amounts of copper, lead and cadmium were present. An increase in the peak current was also noted, particularly in the presence of copper(II) ions. This increase in the peak current suggests that the other metal ions also contribute to the overall electrode processes. At the selected deposition potential, selenium(IV) may be co-deposited with interfering ions such as copper(II) ions by the reaction

$$M^{n+} + Se^{4+} + Hg + (4 + n)e^- \rightarrow M(Hg)Se$$

The presence of both elements at the surface of the electrode, as an intermetallic compound, may account for the negative shift of the peak potential. However, this electrode process is still useful for quantifying selenium provided that enough of the interfering species is present to maintain the stoichiometry of the intermetallic compound. The calibration curves shown in Fig. 1 indicate that selenium can be determined at concentrations up to 200 $\mu g\ l^{-1}$ in the presence of 5 mg l^{-1} copper(II) ions, but that the linear response region is limited to lower concentrations when copper(II) ions are at a lower concentration of 2.5 mg l^{-1}. Biological samples frequently contain high concentrations of copper. Depending on the sample being investigated, copper

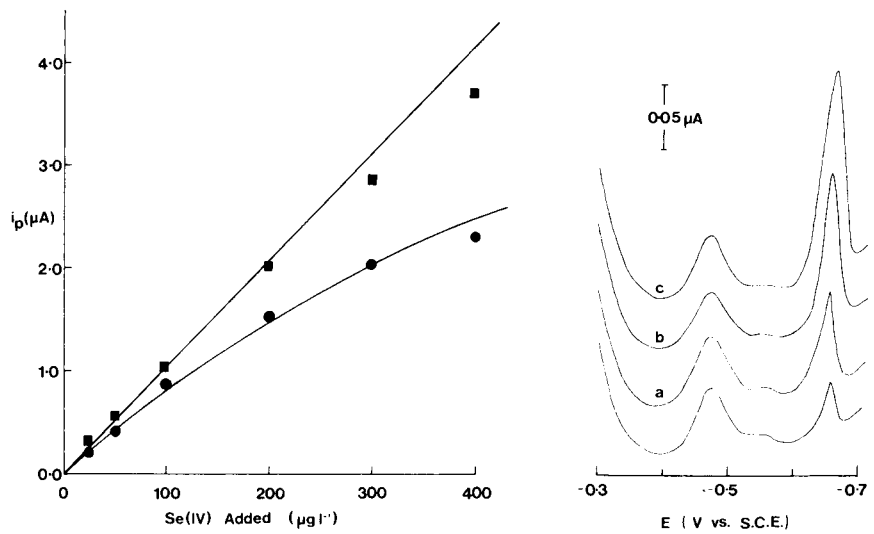

Fig. 1. Calibration curves obtained for selenium(IV) in the presence of (•) 2.5 mg l^{-1} copper(II) and (▪) 5 mg l^{-1} copper(II) ions. Deposition time 90 s, deposition potential —0.3 V vs. SCE, d.c.c.s.v. mode, 0.1 M HCl.

Fig. 2. Stripping voltammograms (d.p.c.s.v.) for determination of selenium in the bovine liver sample by standard addition method: (a) +1 μg Se(IV) l^{-1}; (b) +2 μg Se(IV) l^{-1}; (c) +3 μg Se(IV) l^{-1}. Deposition time 90 s, deposition potential —0.3 V vs. SCE.

may or may not have to be deliberately added to the solution. Selenium concentrations down to 0.1 $\mu g\ l^{-1}$ may be determined this way in the presence of 1000-fold concentrations of metals such as copper, lead and cadmium. It is, however, necessary to ensure that the method of standard addition is applied within the linear response region. If the response is non-linear, then the data cannot be used for the determination. Henze [37] has recently used a similar approach but with a different deposition potential to determine selenium at 0.2 $\mu g\ l^{-1}$ in the presence of 1 mg l^{-1} copper(II) ions in 1 M hydrochloric acid solution, while Ebhardt and Umland [48] used a.c. cathodic stripping voltammetry at a hanging mercury drop electrode to determine selenium at 0.5 $\mu g\ l^{-1}$ in an electrolyte containing copper(II) ions.

Figures 2 and 3 show that the presence of other metal ions results in the formation of additional peaks beside that of the selenium stripping peak. The presence of relatively large amounts of other metals in the bovine liver sample shifted the selenium peak to the more negative potential of about —0.66 V vs. SCE. A similar negative shift in the peak potential was reported by Henze [37], who observed the selenium stripping peak at —0.68 V vs. Ag/AgCl in the presence of 1 mg l^{-1} copper(II) ions. Only a very slight shift in the peak potential was observed for the fish sample (Fig. 3) as interfering

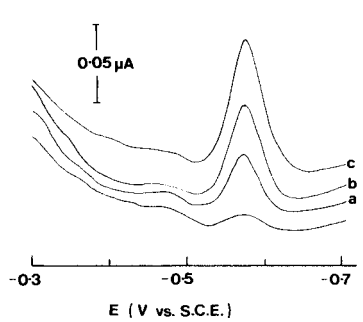

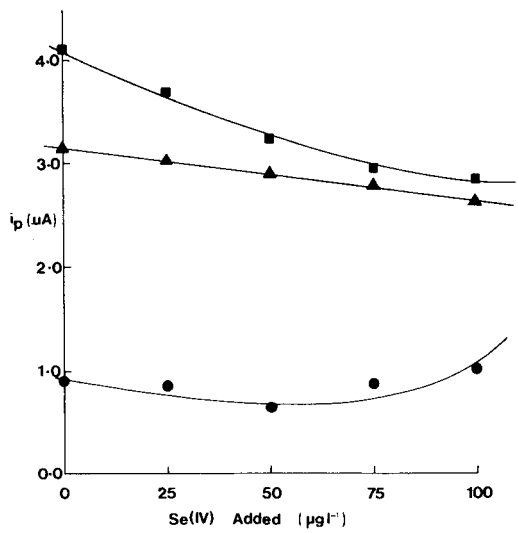

Fig. 3. Stripping voltammograms for determination of selenium in shark fish sample by standard addition method: (a) +0.5 μg Se(IV) l^{-1}; (b) +1.0 μg Se(IV) l^{-1}; (c) +1.5 μg Se(IV) l^{-1}. Conditions as in Fig. 2.

Fig. 4. Influence of selenium(IV) on the d.p.a.s.v. determination of (•) copper, (■) lead and (▲) cadmium. Concentration of analytes 25 $\mu g\ l^{-1}$, supporting electrolyte 0.1 M HCl, deposition time 210 s, deposition potential —0.9 V vs. SCE.

TABLE 1

Concentration of selenium in bovine liver as determined by d.p.c.s.v. with standard additions

Se added (μg)	Total Se found (μg)	Se found in liver ($\mu g\ g^{-1}$)	Certified value ($\mu g\ g^{-1}$)
0	0.98	0.98	
5	6.03	1.03	
10	11.01	1.01	
20	21.06	1.06	
		Av. 1.02 ± 0.03[a]	1.1 ± 0.1[b]

[a]Error is mean deviation for four determinations. [b]Error is standard deviation.

species were present at lower concentrations. Use of the standard addition method was shown to be appropriate for both the liver and fish samples as indicated by the linear response to the increasing concentration of selenium. Tables 1 and 2 indicate that the results obtained for these biological materials agreed satisfactorily with the certified and inter-laboratory survey estimates.

Anodic stripping voltammetric determination of the other three elements is based on the formation of amalgam between the mercury electrode and the respective metal ion and its oxidation during the stripping step, the various elements being identified by their respective peak potentials. The presence of interferants such as selenium in most biological materials may, however, shift the position of the peak and interfere seriously with the determination of these elements. Some results are shown in Fig. 4; they indicate that the presence of selenium(IV) ions may either suppress or enhance the stripping peaks of copper, lead and cadmium depending on the amount present. In most cases, an additional peak was also observed and the voltammograms shown in Fig. 5 indicate that the presence of Se(IV) ions during the deposition of copper at —0.35 V vs. SCE results in both elements being deposited onto the mercury electrode possibly as the intermetallic compound Cu(Hg)Se. The two peaks are such that the first (more negative) peak is the usual stripping peak of copper whilst the second peak, which may be due to the intermetallic compound, increased with increasing concentration of selenium(IV) ions. The observation of the second stripping peak confirms previous suggestions that selenium may be deposited together with other metal ions during the c.s.v. determination.

For copper and lead, the interference from selenium(IV) is quite pronounced, but selenium concentrations greater than 500 $\mu g\ l^{-1}$ are necessary before substantial interference is observed in the cadmium electrode process. For the simultaneous determination of copper, lead and cadmium, selenium(IV) must therefore be removed from solution.

The problem of interference caused by selenium was overcome by oxidizing Se(IV) to the electrochemically inactive Se(VI) form. Holak [12] showed

TABLE 2

Concentrations of selenium, copper, lead and cadmium in inter-laboratory survey fish samples

Sample	Selenium				Copper			
	This work[a]		Inter-lab. Survey[b]		This work		Inter-lab. Survey	
	Mean ($\mu g\ g^{-1}$)	M.d. ($\mu g\ g^{-1}$)	Mean ($\mu g\ g^{-1}$) (n)	S.d. ($\mu g\ g^{-1}$)	Mean ($\mu g\ g^{-1}$)	M.d. ($\mu g\ g^{-1}$)	Mean ($\mu g\ g^{-1}$) (n)	S.d. ($\mu g\ g^{-1}$)
Crayfish	0.17	0.02 (12)	0.16 (44)	0.05 (31)	3.46	0.17 (5)	3.10 (107)	0.60 (19)
Mussel	1.90	0.12 (6)	1.10 (49)	0.33 (30)	2.40	0.12 (5)	2.00 (103)	0.52 (26)
Flathead	0.37	0.03 (8)	0.32 (52)	0.11 (34)	0.39	0.03 (8)	0.39 (90)	0.22 (69)
Shark	0.19	0.03 (16)	0.20 (46)	0.07 (35)	1.01	0.09 (9)	0.70 (105)	0.28 (40)
Sample	Lead				Cadmium			
	This work		Inter-lab. Survey		This work		Inter-lab. Survey	
	Mean ($\mu g\ g^{-1}$)	M.d. ($\mu g\ g^{-1}$)	Mean ($\mu g\ g^{-1}$) (n)	S.d. ($\mu g\ g^{-1}$)	Mean ($\mu g\ g^{-1}$)	M.d. ($\mu g\ g^{-1}$)	Mean ($\mu g\ g^{-1}$) (n)	S.d. ($\mu g\ g^{-1}$)
Crayfish	0.48	0.07 (15)	0.48 (27)	0.32 (67)	0.10	0.02 (20)	0.05 (25)	0.08 (160)
Mussel	5.38	0.35 (7)	5.2 (77)	1.5 (29)	8.55	0.23 (3)	11.0 (94)	1.7 (16)
Flathead	0.92	0.08 (9)	0.42 (29)	0.42 (100)	0.13	0.02 (15)	0.07 (28)	0.07 (100)
Shark	0.57	0.03 (5)	0.44 (47)	0.17 (39)	0.08	0.02 (25)	0.05 (35)	0.04 (80)

[a]M.d. = mean deviation obtained from triplicate determinations; %M.d. is given in parentheses. [b]S.d. = standard deviation obtained from (n) determinations; % relative standard deviation is given in parentheses.

that this oxidation can be achieved with strong oxidizing agents but never applied this approach for multi-element determinations. The voltammograms in Fig. 6 indicate that the selenium(IV) is completely oxidized with relatively small amounts of saturated potassium permanganate solution. No interference was observed from selenium after the oxidation.

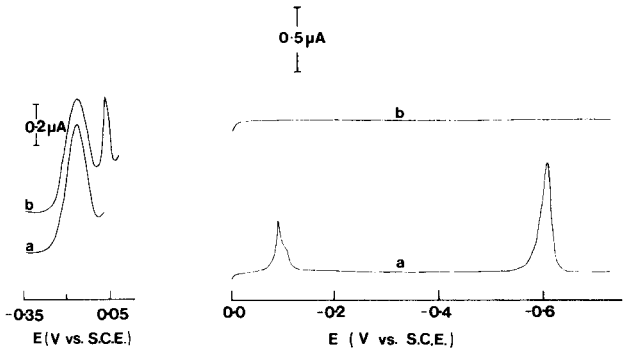

Fig. 5. Formation of intermetallic compound during determination of copper: (a) 25 μg Cu(II) l^{-1}; (b) 25 μg Cu(II) l^{-1} + 100 μg Se(IV) l^{-1}. Deposition potential —0.35 V vs. SCE; other conditions as for Fig. 4.

Fig. 6. Oxidation of selenium(IV) to its electro-inactive selenium(VI) form: (a) 200 μg Se(IV) l^{-1}; (b) 200 μg Se(IV) l^{-1} + 50 μl of saturated $KMnO_4$. Deposition time 90 s, deposition potential 0.0 V vs. SCE, d.c.c.s.v. mode, supporting electrolyte 0.1 M HCl.

The results obtained for copper, lead and cadmium in the fish and bovine liver samples also agreed satisfactorily with the certified and inter-laboratory survey estimates for these samples, as shown in Tables 2 and 3. It does appear, however, that the result obtained for cadmium in bovine liver was higher than the certified value. Repeated determinations gave similar results and the reason for the discrepancy is unknown. Figure 7 shows that selenium did not interfere with the determination of the three elements and that use of the standard addition method again proved satisfactorily. Linear peak height versus concentration responses were always obtained for copper, lead and cadmium.

Conclusion

The proposed method based on stripping voltammetry at a hanging mercury drop electrode provides a simple and suitable approach for the determination of selenium, copper, lead and cadmium in a single sample solution. The

TABLE 3

Concentrations of selenium, copper, lead and cadmium in bovine liver

	Metal found (μg g^{-1})			
	Selenium	Copper	Lead	Cadmium
Present value[a]	1.02 ± 0.03	196 ± 3	0.31 ± 0.03	0.42 ± 0.05
Certified value[b]	1.1 ± 0.1	193 ± 10	0.34 ± 0.08	0.27 ± 0.04

[a]Triplicate determinations, error is mean deviation. [b]Error is standard deviation.

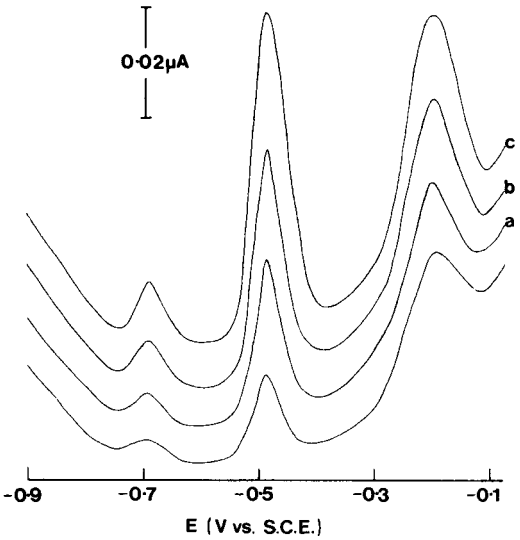

Fig. 7. Stripping voltammograms for simultaneous d.p.a.s.v. determination of copper, lead and cadmium in shark fish sample by standard addition method: (a) + 0.05 μg Cd l^{-1}, 0.5 μg Pb l^{-1} and 0.5 μg Cu l^{-1}; (b) + 0.10 μg Cd l^{-1}, 1.0 μg Pb l^{-1} and 1.0 μg Cu l^{-1}; (c) 0.20 μg Cd l^{-1}, 1.5 μg Pb l^{-1} and 1.5 μg Cu l^{-1}. Deposition time 90 s, deposition potential —0.9 V vs. SCE.

utilization of d.p.c.s.v. at a deposition potential of —0.3 V vs. SCE allowed the determination of selenium down to 0.1 μg l^{-1} in the presence of 1000-fold concentrations of interfering ions such as Cu(II), Pb(II) and Cd(II) without additional pretreatment provided that standard additions could be used in the linear response region. The reproducibility of the method was also most satisfactory with relative standard deviations of 2.5, 2.1, 1.6 and 1.8% for selenium, copper, lead and cadmium, respectively, with 10 samples at the 1 μg l^{-1} level.

For samples containing less than 0.1 μg of selenium and/or producing a non-linear standard addition response, it is recommended that a separation technique such as ion-exchange or solvent extraction be employed prior to the electrochemical determination of the element [13, 49, 50].

The authors thank Mr. B. Kinsella and Mr. K. Manning for help in obtaining the fish and bovine liver samples, respectively. This paper was presented in part at the Fifth Australian Electrochemistry Conference, Perth, August, 1980.

REFERENCES

1 E. J. Underwood, Trace Elements in Human and Animal Nutrition, 4th edn., Academic Press, New York, 1977.
2 R. F. Burk, Trace Elements in Human Health, Vol. 2, Academic Press, New York, 1976, pp. 105—133.

3 E. J. Calabrese, Pollutants and High Risk Groups, Wiley-Interscience, New York, 1978.
4 E. Browning, Toxicity of Industrial Metals, 2nd edn., Butterworths, London, 1969.
5 O. E. Olson, J. Assoc. Off. Anal. Chem., 52 (1969) 627.
6 E. F. Dalton and A. J. Malanoski, At. Absorpt. Newsl., 10 (1971) 92.
7 F. J. Fernandez and D. C. Manning, At. Absorpt. Newsl., 10 (1971) 65.
8 O. J. Kronberg and E. Steinnes, Analyst, 100 (1975) 835.
9 P. N. Vijan and G. R. Wood, Talanta, 22 (1976) 1.
10 Y. Shimoishi, Analyst, 101 (1976) 298.
11 M. W. Blades, J. Dalziel and C. M. Elson, J. Assoc. Off. Anal. Chem., 59 (1976) 1234.
12 W. Holak, J. Assoc. Off. Anal. Chem., 59 (1976) 650.
13 S. Forbes, G. P. Bound and T. S. West, Talanta, 26 (1979) 473.
14 M. J. Pinchin and J. Newham, Anal. Chim. Acta, 90 (1977) 91.
15 H. W. Nurnberg, Sci. Total Environ., 12 (1979) 35.
16 W. Lund and R. Erisken, Anal. Chim. Acta, 107 (1979) 37.
17 G. Chittleborough and B. J. Steel, Anal. Chim. Acta, 119 (1980) 235.
18 J. Versieck and R. Cornelis, Anal. Chim. Acta, 116 (1980) 217.
19 G. V. Iyengar, Elemental Composition of Human and Animal Milk — A Review, International Atomic Energy Agency, Vienna, 1979.
20 L. E. Feinendegen and K. Kasperek, Trace Element Anal. Chem. in Medicine and Biology, Proc. 1st Int. Workshop, Session I, Walter de Gruyter, Berlin, 1980, pp. 1—36.
21 J. Versieck, J. Hoste, F. Barbier, H. Michels and J. D. Rudder, Clin. Chem., 23 (1977) 1301.
22 M. Ariel and U. Eisner, J. Electroanal. Chem., 5 (1963) 362.
23 M. Ariel, U. Eisner and S. Gottesfield, J. Electroanal. Chem., 7 (1964) 307.
24 G. Macchi, J. Electroanal. Chem., 9 (1965) 290.
25 G. C. Whitnack and R. Sasselli, Anal. Chim. Acta, 47 (1969) 267.
26 H. K. Hundley and E. C. Warren, J. Assoc. Off. Anal. Chem., 53 (1970) 705.
27 I. Sinko and J. Dolezal, J. Electroanal. Chem., 25 (1970) 299.
28 T. M. Florence, J. Electroanal. Chem., 27 (1970) 273.
29 L. Luong and F. Vydra, J. Electroanal. Chem., 50 (1974) 379.
30 H. W. Nurnberg, Electrochim. Acta, 22 (1977) 935.
31 P. Valenta, H. Rutzel, H. W. Nurnberg and M. Stoepler, Fresenius Z. Anal. Chem., 285 (1977) 25.
32 M. Oehme, W. Lund and J. Jonsen, Anal. Chim. Acta, 100 (1978) 389.
33 A. M. Sulek, E. R. Elkins and E. W. Zink, J. Assoc. Off. Anal. Chem., 61 (1978) 931.
34 N. I. Ward and D. E. Ryan, Anal. Chim. Acta, 105 (1979) 185.
35 G. D. Christian, J. Electroanal. Chem., 22 (1979) 333.
36 G. P. Bound and S. Forbes, Analyst, 103 (1978) 176.
37 G. Henze, Mikrochim. Acta, 11 (1981) 343.
38 J. Paul and C. Daniel, Trav. Chim. Aliment. Hyg., 72 (1981) 78.
39 F. Vadja, Acta Chim. Acad. Sci. Hung., 63 (1970) 257.
40 B. K. Hovsepian and I. Shain, J. Electroanal. Chem., 14 (1967) 1.
41 R. S. Rodgers and L. Meites, J. Electroanal. Chem., 38 (1972) 359.
42 T. R. Copeland, R. A. Osteryoung and R. K. Skogerboe, Anal. Chem., 46 (1974) 2093.
43 M. S. Shuman and G. P. Woodward, Anal. Chem., 48 (1976) 1979.
44 H. Bloom, B. N. Noller and D. E. Richardson, Anal. Chim. Acta, 109 (1979) 157.
45 G. Gillain, G. Duyckaerts and A. Distèche, Anal. Chim. Acta, 106 (1979) 23.
46 T. R. McKay and B. N. Noller, The Determination of Copper, Zinc, Lead and Cadmium in Marine Tissue. An Australian Collaborative/Interoperator Study. Report prepared by Marine Monitoring Section, Department of Science and the Environment, Canberra, A.C.T. 2606, Australia.
47 G. D. Christian, E. C. Knoblock and W. C. Purdy, Anal. Chem., 35 (1963) 1128.
48 K. B. Ebhardt and F. Umland, Fresenius Z. Anal. Chem., 310 (1982) 406.
49 R. W. Andrews and D. C. Johnson, Anal. Chem., 48 (1976) 1056.
50 A. G. Howard, M. R. Gray, A. J. Waters and A. R. Oromiehie, Anal. Chim. Acta, 118 (1980) 87.

Analytica Chimica Acta, 148 (1983) 71—78
Elsevier Science Publishers B.V., Amsterdam — Printed in The Netherlands

STUDIES ON THE ANODIC STRIPPING VOLTAMMETRY OF LEAD IN POLLUTED ESTUARINE WATERS

SIMON ARRAS ACEBAL and ANGELA DE LUCA REBELLO*
Departmento de Química, Pontifícia Universidade Católica, Rio de Janeiro (Brasil)
(Received 2nd November 1981)

SUMMARY

Lead was determined in polluted tropical sea water by anodic stripping voltammetry in the differential pulse and linear sweep modes. The quantitative implications of heavy metal determinations in polluted sea water and some electrochemical parameters concerning the two voltammetric modes are discussed, as well as the efficiency of the hanging mercury drop mercury film electrodes. Values found for total lead concentration range between 0.07 and 5.4 $\mu g\ kg^{-1}$. Some data are also presented for copper which was shown to interfere at pH $\geqslant$ 2.

Problems related to the determination of heavy metals in water have been widely discussed [1—4], and some highly reliable data on environmental levels are available. However, data concerning heavy metal content in waters from tropical regions are scarce. Little is known, for example, about the physicochemical behavior of those elements in estuarine waters under the more complex conditions resulting from fast weathering processes and high organic enrichments. The absence of data concerning heavy metal levels in Guanabara Bay (Rio de Janeiro) led to a study on the lead determination in surface waters at several points in the bay.

Guanabara Bay represents a complex aquatic system in a tropical climate. Its area of about 400 km^2 is surrounded by the highly populated (7×10^6 inhabitants) and industrialized state of Rio de Janeiro. About 1000 m^3 [5] of fresh water per second runs through the Bay. Rivers carrying industrial and domestic wastes confer a heterogeneous character to the bay waters. Such heterogeneity complicates the application of voltammetric determinations.

This paper discusses the quantitative behavior of lead and copper when voltammetric determinations are done at mercury film electrodes (MFE) and hanging mercury drop electrodes (HMDE). Some electrochemical parameters pertaining to the voltammetry of lead are discussed.

0003-2670/83/$03.00

EXPERIMENTAL

Sample collection and treatment

Sea-water samples were collected in polyethylene bottles previously cleaned as described by Patterson [1], kept filled with dilute nitric acid, and enclosed in polyethylene bags. Samplings were made from an inflatable boat or from a small motor boat moved by rowing against the wind about 50 m from the point where the outboard motor had been stopped and raised. Samples were taken at about 30 cm below the water surface, after the sampling bottles had been emptied and washed several times with the water. The air was never in contact with the interior of the bottles; they were opened and closed under water.

Only a few samples were acidified immediately after collection; usually nitric acid (Suprapur, Merck) was added in the laboratory to adjust the pH to 1.8, 24 h before measurements were made. No differences in concentrations were observed when the acidified sea-water samples were heated at 65°C for 24 h as advised by Patterson [1]. Samples kept at low temperature at the natural pH showed lower lead concentration; the evolution of the adsorption process in a sample stored at room temperature is shown in Fig. 1. Variations in the lead concentration may be caused by biological changes in the plankton fraction or by alterations in the particulates. None of the samples was filtered.

Results obtained for samples acidified 24 h before voltammetric measurement and treated by the method of Patterson et al. [6] were compared with results for samples evaporated under a clean bench; no difference in lead concentration was observed at the 95% significance level.

Equipment

All glassware was cleaned [1] with analytical-grade reagents (Merck) and deionized-distilled water containing 30 ± 5 ng Pb kg^{-1} of water.

Voltammetric measurements were done with a PAR Electrochemical System (Model 174-A) and a saturated calomel reference electrode, a platinum wire auxiliary electrode, and a glassy carbon rod (PAR 0333) coated with a mercury film (MFE) as the working electrode. In some tests, a HMDE (PAR 9323) was used. A pyrex glass cell was used for measurements with the HMDE; either this cell or a teflon cell was used with the MFE. No advantage concerning adsorption or contamination was found when a teflon cell was used for sea water at pH $\leqslant$ 2. Stirring was done magnetically (JKA Combimag-MCH or Metrohm E405). Nitrogen with a maximum oxygen content of 10 ppm was used as purging gas. Mercury(II) nitrate used to form in situ films on the glassy carbon rod was prepared from Merck tridistilled mercury and Suprapur nitric acid.

Experimental parameters used in all the determinations are given in Table 1. Unless otherwise mentioned, all potentials specified are referred to the saturated calomel electrode (SCE).

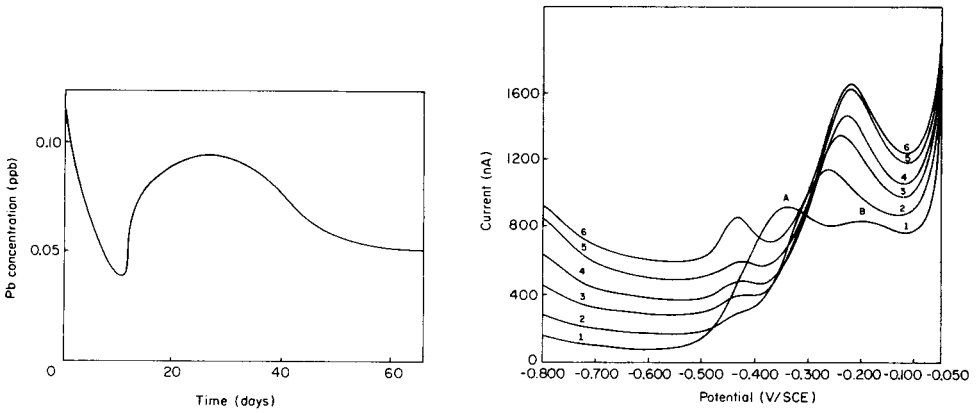

Fig. 1. Variations of lead concentration in sea water stored in polyethylene at room temperature and natural pH.

Fig. 2. Determination of lead in sea water from Guanabara bay by d.p.a.s.v. with the HMDE at different pH values: (1) 2.15; (2) 1.36; (3) 1.32; (4) 1.17; (5) 1.06; (6) 1.06. The lead peak appears at —0.428 V in curves 2—6. Wave A centers at —0.335 V in curve 1. Wave B shifts from —0.260 V at pH 1.36 to —0.215 V at pH 1.06. Curves 1—5: 0.21 μg Pb kg^{-1}, 0.30 μg Cu kg^{-1}. Curve 6: 0.77 μg Pb kg^{-1}.

RESULTS AND DISCUSSION

General experience indicates that voltammetric measurements of lead at the HMDE are less sensitive than at the MFE. However, because the HMDE offers some practical advantages for routine work, it was useful to verify the best conditions of determining lead in estuarine waters by differential pulse anodic stripping voltammetry (d.p.a.s.v.) at the HMDE. The electrochemical parameters used for the tests are summarized in Table 1. Lead and copper were previously determined in the samples by using the MFE, the concentrations found being 0.21 μg Pb kg^{-1} and 0.30 μg Cu kg^{-1} of sea water.

TABLE 1

Experimental conditions used for the voltammetry of lead

Electrode	HMDE	MFE	
Mode	D.p.a.s.v.	L.s.a.s.v.	D.p.a.s.v.
Peak potential (V/SCE)	—0.43	—0.44 to —0.47	—0.52 to —0.56
Stirring speed (rpm)	360	430	430
Mercury drop size (cm^2)	0.022	—	—
Pulse height (mV)	50	—	25—50
Pulse repetition (s)	0.5	—	0.5
Scan rate ($mV\ s^{-1}$)	5	50	5
Electrodeposition time (min)	5—15	5—30	30
Resting time (s)	30	30	30
pH	1.4—1.7	1.4—1.7	1.4—1.7
Mercury concentration	—	(2.2—4.4) X 10^{-5} M	(2.2—4.4) X 10^{-5} M
Electrodeposition potential (V/SCE)	—0.7, —0.9	—0.8	—0.8

Lead is usually determined at pH ≈ 2 with HMDE [7—10]; however, it was found that at those pH values (see Fig. 2) the lead peak was completely masked by a broad double wave (A and B) located between —0.30 and —0.35 V. This masking effect resulted in a drastic increase in the detection limit for lead; Fig. 2 shows how a decrease in pH, by addition of hydrochloric acid or nitric acid, improved the resolution of the lead peak by changing the double wave into a combined wave that appeared at more positive peak potentials (E_p). At pH 1.2, the lead peak was completely resolved. Waves A and B were tested at electrolysis times (t_e) of 5 and 30 min; comparison of the peak currents (i_p) obtained showed that wave B increased more with t_e than wave A, but that the total peak height (A + B) increased almost proportionally with the increase in t_e. Wave A is probably related to copper dissolution with oxidation to $CuCl_2^-$ [11]. The effects of standard addition of copper and increasing t_e at pH 2.1 are shown in Fig. 3. The convergence of waves A and B with decreasing pH may be due to increased reversibility of the oxidation of copper amalgam. These phenomena were observed for all the sea-water samples examined.

To estimate the detection limit and to obtain a suitable quantitative parameter for comparing the influence of different variables, sensitivity was defined as: $S = i_p/Ct_e$ (nA kg μg^{-1} min^{-1}), where i_p is given in nA, C is the concentration (μg kg^{-1}), and t_e is given in min. Table 2 shows the values of S obtained in the determination of lead with the HMDE and MFE. The detection limit was calculated from the expression D.L. = $2.5\,\sigma_B/St_e$ where σ_B is the absolute standard deviation of the blank (in nA) obtained at t_e. The detection limit calculated for the best conditions (pH 1.3, t_e = 15 min, σ_B = 0.3 nA, S = 1.8 (nA kg μg^{-1} min^{-1}) was 0.03 μg kg^{-1}.

The electrochemical reaction of lead at the HMDE with d.p.a.s.v. was characterized by some further studies. To relate i_p to the lead concentration, it was necessary to obtain the limiting diffusion current. The background

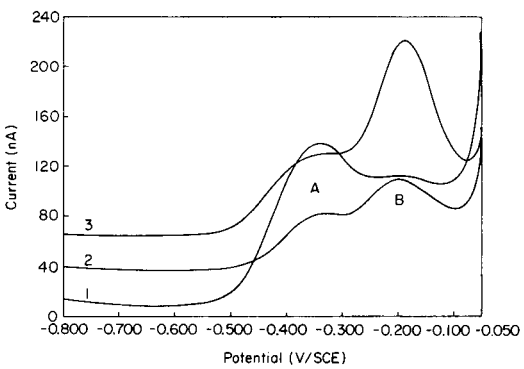

Fig. 3. Influence of copper standard addition on the lead voltammogram at pH 2.1: (1) sea water; (2) sea water with 2.74 μg Cu kg^{-1} added, for electrolysis time 15 min and current scale 200 nA/254 mm; (3) as (2), but electrolysis time 30 min and current scale 500 nA/254 mm.

TABLE 2

Sensitivity parameter for the determination of lead at the HMDE and MFE by d.p.a.s.v. and l.s.a.s.v.

Water	pH	Pb added (μg kg^{-1})	Sensitivity (nA kg μg^{-1} min^{-1})		
			HMDE D.p.a.s.v.	MFE	
				D.p.a.s.v.	L.s.a.s.v.
Distilled	1.5—2.0	—	1.6—1.9	108[a]	—
Sea	2	$\gtrsim$0.25	0.6—0.8	—	—
Sea	2	$\gtrsim$1	1.0—1.2	—	—
Sea	$\lesssim$1.3	—	1.8—2.2	—	—
Sea	1.4—2.2	0.2—10	—	—	51—61
Sea	1.2 $\gtrsim$ 1.8	$\gtrsim$2	—	93[a], 64[b]	—

[a] ΔE = 50 mV. [b] ΔE = 25 mV.

current (i_b) was measured over the pH range 2.2—1.2; nitrogen was bubbled for an hour through 15 g of sea water and the drop size, stirring rate, temperature, and E_d were 0.022 cm^2, 430 rpm, 23 ± 1°C, and —0.80 V, respectively. The relation found between i_b (μA) and [H$^+$] (mol l^{-1}) was i_b = 2.4 [H$^+$]$^{0.3}$, with a correlation coefficient of r^2 = 0.99. The proportionality constant between the background-corrected diffusion current density and lead concentration was $i_d = 1.1 \times 10^6 C_{Pb}$ (μA cm^{-2}). Combining this expression with $S = i_p/Ct_e$ (see above), it can be shown that the relation between peak current and charge is $i_p = 0.26\ Q$ (s^{-1}).

The electrolysis and film formation conditions used in the determination of lead with MFE are given in Table 1. For most determinations, the mercury films were formed in situ from 2.2 × 10^{-5} M or 4.4 × 10^{-5} M mercury(II) solutions, depending on the lead content in the sample. A 25-mV pulse height with a 1-μA current range provided some advantages over the use of 50 mV and 2 μA, as the signals were 35% larger, the sensitivity parameter was more reproducible, and peak resolution was better. Magnetic stirring was always used; stirring rates varying from 70 to 1230 rpm were used to measure the background current, the mercury deposition current, and the lead peak current in sea water at pH 1.5. The measured current values and rotation rates, w, were fitted to the equation $i = aw^k$. Values of k between 0.51 and 0.59 were obtained and the average correlation coefficient was 0.94. Considering the similar hydrodynamic characteristics of magnetic stirring and a rotating electrode, and Levich equation was applied and it was calculated that magnetic stirring was 79% as efficient as a rotating electrode.

From the expression $i_p = 0.26\ Q$ (s^{-1}), and the relation $i_p = (5.51 \pm 0.56) \times 10^5\ C_{Pb}$ for the MFE, the efficiency of the lead accumulation per unit surface area in the HMDE was calculated as double that for the MFE.

The influences of pulse amplitude (ΔE) and mercury film thickness on the lead peak were studied at pH 1.5. As expected from theoretical

considerations [12], the peak potential become more negative with increasing ΔE both in sea water and distilled water. The peak current varied linearly with ΔE between 5 and 50 mV; at higher values the slope decreased. This effect was more pronounced in distilled water. It was observed that as the mercury film thickness (l) was increased, the peak potential (E_p) became more positive. A logarithmic relation between l (in angstrom) and E_p (r^2 = 0.996) was found: $E_p = -0.641 + 0.032 \log_{10} l$. This corresponds to the theoretical equation as defined by Roi and Toni [13]. In the experiments, l varied from 159 to 980 Å within seven 15-min electrolysis cycles, for a pulse amplitude of 25 mV and a lead concentration of 0.25 μg kg^{-1}.

The influence of pH on the d.p.a.s.v. of lead at the MFE was studied in a manner similar to that described for the HMDE. Here again the decrease in pH changed both the width and peak potential of the copper peak, improving markedly the determination of lead.

The average sensitivity for the lead determination by d.p.a.s.v. at the MFE was calculated as before, with the results shown in Table 2. Although the sensitivity obtained for ΔE = 25 mV is 69% of that for ΔE = 50 mV, the relative standard deviation in the first case was smaller by a factor of two.

Copper was also determined in some of the samples, and for ΔE = 25 mV, the sensitivity of 20 nA kg μg^{-1} min^{-1} was about a third that for lead. The detection limit was 0.008 μg Pb kg^{-1} for t_e = 30 min with σ_B = 0.003 μg Pb kg^{-1}.

The differential pulse mode was not applied successfully to samples from the most polluted sites of Guanabara Bay. Figure 4 shows a typical differential pulse voltammogram obtained for those samples with several peaks appearing at potentials more positive than the lead peak. These peaks were all independent of the electrolysis time and are due to organic substances. In such samples, lead could be quantified only by using the linear sweep mode. Figure 5 shows the well defined peaks obtained for lead and copper for a sample similar to that represented in Fig. 4. Unlike the observed effect on d.p.s.a.v., the pH had only a minor influence on the linear sweep voltammograms. The peak current for lead was independent of the deposition potential for values more negative than —0.7 V. For mercury films formed in situ, the $b_{1/2}$ (peak width at half amplitude) of the lead peak was independent of film thickness. The peak potential was constant at —0.47 V for films between 200 and 300 Å, changing to —0.44 V for thicknesses above 1500 Å. The peak current after the second stripping cycle (one cycle includes the electrodeposition and stripping steps) did not change with the film thickness. Copper, however, behaved differently. For film thicknesses of 300—1500 Å, $b_{1/2}$ increased and i_p decreased. At 1500 Å, $b_{1/2}$ reached a maximum ($\approx$2 mV) and i_p a constant value about 50% smaller than initially. In this case, the peak potential was not precisely defined because it became more positive with increasing film thickness. The values found for lead and copper peak parameters with pre-formed film thicknesses of 1500—3000 Å were very similar to those obtained with films formed "in situ" at thicknesses of 200—500 Å.

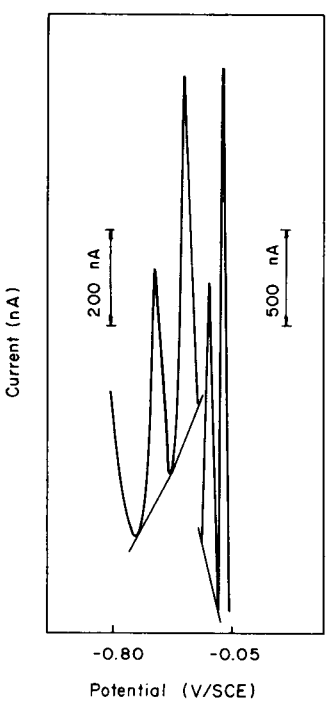

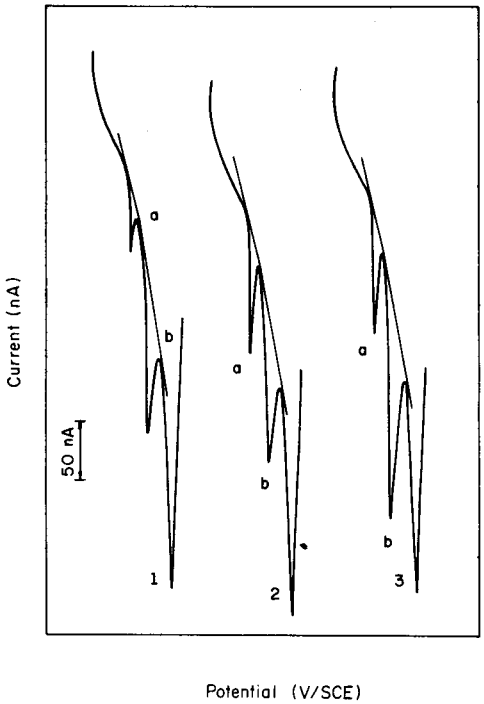

Fig. 4. Differential pulse a.s.v. of a sea-water sample from station 10, with a mercury film electrode.

Fig. 5. Linear sweep voltammograms with a mercury film electrode for sea-water samples from station 11. (Electrodeposition time per cycle, 15 min; potential range, —0.80 to —0.05 V vs. SCE; 0.64 μg Pb kg^{-1} present.) Curves: (1) third cycle (peaks a and b correspond to Pb and Cu, respectively); (2) fourth cycle + 0.64 μg Pb kg^{-1}; (3) fifth cycle + 1.27 μg Cu kg^{-1}.

The sensitivities (nA kg μg^{-1} min^{-1}) calculated from the expression $S = i_p/Ct_e$ for the experimental conditions listed in Table 1 were: 51—61 for lead and 25—30 for copper. There were no significant differences in sensitivity within the pH range 1.4—2.2 and the concentration range 0.2—10 μg kg^{-1}. The sensitivities obtained for lead and copper were found to be in a constant ratio of 0.60 ± 0.05. This allows estimation of the copper concentration after a single standard addition of lead.

The detection limit calculated for t_e = 30 min, σ_B = 0.010 μg kg^{-1} and S = 60 nA kg μg^{-1} min^{-1} was 0.025 μg Pb kg^{-1}. As can be observed from the data, the difference in detection limits for the linear sweep and differential pulse modes is mainly related to the better reproducibility (σ_B) of the latter.

Application to polluted sea water

The above study showed that application of the linear sweep mode at pH 1.5 is a fast and reliable way of dealing with interferences caused by organic

materials in polluted water. The lower sensitivity of this mode limits its use to lead contents exceeding 0.1 $\mu g\ kg^{-1}$, but such levels are commonly reached in polluted waters.

The determination of lead and copper in sea water collected from 14 stations in Guanabara Bay gave values for lead between 0.07 and 5.4 $\mu g\ kg^{-1}$ and values for copper between 0.4 and 5.0 $\mu g\ kg^{-1}$. Results obtained for lead in sea water collected at a station located outside the bay gave an insight into the quality of coastal water in this region. The value of 70 ng kg^{-1} found places those waters in the upper limit for coastal water contamination according to the classification given by Burnet et al. [14].

The authors express their gratitude to Dr. C. D. Patterson for his kind help at the start of this work and to CNPq and FINEP for financial support.

REFERENCES

1 C. D. Patterson and D. M. Settle, in P. D. LaFleur (Ed.), Accuracy in Trace Analysis, N.B.S. Spec. Publ., 000, 1978, p. 1.
2 K. W. Bruland and R. P. Funks, Anal. Chim. Acta, 105 (1979) 233.
3 J. P. Riley and D. Taylor, Anal. Chim. Acta, 10 (1968) 479.
4 H. W. Nürnberg, P. Valenta, L. Mart, B. Raspor and L. Sipos, Fresenius Z. Anal. Chem., 282 (1976) 357.
5 S. Alevato, S. Arras and A. Rebello, Quím. Nova, 4(3) (1981) 70.
6 C. D. Patterson, D. M. Settle and B. Glover, Mar. Chem., 4 (1976) 305, 389.
7 B. E. Batley and T. M. Florence, J. Electroanal. Chem., 55 (1974) 23.
8 T. M. Florence, J. Electroanal. Chem., 27 (1970) 273.
9 P. Valenta, L. Mart and H. Rützel, J. Electroanal. Chem., 82 (1977) 327.
10 H. W. Nürnberg, P. Valenta, L. Mart, B. Raspor and L. Sipos, Fresenius Z. Anal. Chem., 282 (1976) 357.
11 M. J. Pinchin and J. Newhan, Anal. Chim. Acta, 90 (1977) 91.
12 S. R. Arras and S. J. Alevato, Rev. Metal., CENIN, 14(3) (1978) 149.
13 Roi and Toni, cited by E. Barendrecht, in J. Bard (Ed.), Electroanalytical Chemistry, Vol. 2, Dekker, New York, 1967.
14 M. Burnet, D. Settle and C. Patterson, in M. Branica (Ed.), Occurrence, Fate and Pollution in Marine environments, Pergamon Press, Oxford, 1978.

Analytica Chimica Acta, 148 (1983) 79—85
Elsevier Science Publishers B.V., Amsterdam — Printed in The Netherlands

DIFFERENTIAL PULSE VOLTAMMETRY WITH MEDIUM-EXCHANGE FOR ANALYTES STRONGLY ADSORBED ON ELECTRODE SURFACES

JOSEPH WANG* and BASSAM A. FREIHA
Department of Chemistry, New Mexico State University, Las Cruces, NM 88003 (U.S.A.)
(Received 23rd September 1982)

SUMMARY

Differential pulse voltammetry with medium-exchange is employed for selective and sensitive measurements of electroactive species strongly adsorbed on electrode surfaces. In order to minimize interferences resulting from macro solution constituents, the working electrode is transferred into an electrolyte solution possessing ideal background characteristics following the preconcentration/adsorption step. The increased selectivity obtained by making the measurement in the exchanged solution is demonstrated by the determination of the adsorbable species in the presence of 10^3—10^4-fold excess of a solution species with similar redox potential. Illustrative voltammograms of chlorpromazine in blood and urine are presented.

Increasing effort is being directed toward the development of sensitive and selective quantitative techniques based on solid electrodes. Conventional solution-phase potential-pulse techniques suffer from surface background reactions which limit the detectability to the micromolar concentration level [1, 2]. The situation can be improved for analytes that are attached, via adsorption or selective chemical reaction, to solid electrode surfaces (ordinary or modified) [3—5]. Selective preconcentration of these compounds at the electrode surface, followed by measurement of the surface-bound species, has resulted in detection limits down to the nanomolar concentration level [6, 7]. The extent of the preconcentration is proportional to the length of time over which the analyte adsorption or reaction is allowed to occur. This approach is analogous to the technique of stripping voltammetry (s.v.) in which extremely low detection limits can be achieved by electroplating the analyte (usually metal ions) onto the electrode.

An important feature of s.v. is that the stripping step can be done in a solution which has a different (more ideal) composition than the initial sample solution. This approach, known as the medium-exchange method, has been found a useful adjunct to stripping measurements of heavy metals in complex samples [8—10]; interferences resulting from the presence of macro constituents, unsatisfactory resolution, or highly sloped background have been minimized. Based on its similarity to s.v., voltammetry following preconcentration of adsorbable organic species can be coupled with the medium-exchange method to achieve similar advantages. (A transfer of a chemically modified electrode to a blank supporting electrolyte solution is commonly

0003-2670/83/$03.00

used for examining the stability of the modified surface [4], but not for improving the quantitative capability in complex samples.)

This work demonstrates the capability of using differential pulse voltammetry (d.p.v.) in conjunction with the medium-exchange method for the selective and sensitive determination of electroactive analytes that are strongly adsorbed onto the working electrode. After adsorption has proceeded under controlled conditions, the electrode is transferred into a more suitable electrolyte before the measurement step. The characteristics and advantages of this methodology are elucidated by application to the measurement of chlorpromazine and 9,10-phenanthrenequinone at submicromolar concentration levels in the presence of macro amounts of (10^3—10^4-fold excess) solution constituents. Applicability to complex samples, such as blood or urine, is demonstrated.

EXPERIMENTAL

Apparatus

Two 100-ml cells, one containing the sample solution under test and the other containing the electrolytic blank solution of choice, were used. A 0.75-cm diameter home-made carbon paste disk served as the working electrode. The paste was composed of carbon powder thoroughly mixed with mineral oil (37% mineral oil by weight). The electrode was mounted on a rotating disk assembly (Model PIR, Pine Instruments Co.). The working electrode, the Ag/AgCl (3 M NaCl) reference electrode, and the graphite rod auxiliary electrode were placed in the cells through holes in the covers. The blood experiments were done with a 2-ml sample cell, a 4-mm diameter carbon paste disk electrode, and a tiny stirring bar. Differential pulse voltammograms were recorded with a Princeton Applied Research Model 364 Polarographic Analyzer and a Houston Omniscribe strip-chart recorder. The experimental settings employed were: 5 mV s^{-1} scan rate and 50 mV pulse amplitude.

Reagents

All solutions were prepared from deionized water. Supporting electrolytes were 0.1 M phosphate buffer (pH 7.4, prepared from a 1:4 mixture of KH_2PO_4 and K_2HPO_4), and 0.1 M perchloric acid. Millimolar stock solutions of chlorpromazine, 9,10-phenanthrenequinone, dopamine (reagent grade, Sigma Chemical Co.), potassium hexacyanoferrate(II), and ascorbic acid (analytical grade, Baker Chemical Co.) were prepared each day. Aliquots of the stock solution were added to the supporting electrolyte (in the sample cell) to give the desired concentration. Rhesus monkey whole blood samples, preserved in heparin, were stored at 4°C. Human urine samples were used shortly after collection.

Procedure

A fresh working electrode surface was utilized for each experiment. The surface was smoothed with a computer card. The electrode was pretreated

in the supporting electrolyte solution by scanning its potential between −0.5 V and +1.0 V for 5 min. Following this, the various sample constituents were spiked and preconcentration of the adsorbable species was begun. The preconcentration potential (0.0 V for chlorpromazine and −0.2 V for 9,10-phenanthrenequinone) was applied at the electrode for a selected time, determined by the analyte concentration, while the electrode was rotated. At the end of the preconcentration period, the electrode rotation was stopped and the applied potential was disconnected. For medium-exchange, the electrode was removed from the sample solution, rinsed thoroughly with water, and reimmersed in the supporting electrolyte solution of choice. The initial potential (0.0 V or −0.2 V) was then applied, and after the current decay, the voltammogram was recorded by scanning the potential to +1.0 V. Then, the electrode was transferred back to the sample cell, and held at +0.8 V for 4 min to clean it from the remaining adsorbable species.

RESULTS AND DISCUSSION

The exchange of solutions between the preconcentration and measurement steps offers the advantage that the surface-bound species can be measured in a solution that is more favorable than the original sample solution. Oxidation or reduction currents arising from significant concentrations of non-adsorbable sample constituents which would have swamped the required peak current of the surface-bound species are effectively eliminated. To illustrate the improved selectivity achieved by the medium exchange method, 2.5×10^{-7} M chlorpromazine was quantified in a solution containing 5×10^{-4} M ascorbic acid (Fig. 1). When the measurement step is done in the sample solution, the large ascorbic acid oxidation current almost completely masks the chlorpromazine peak current (curves a and b). After exchanging to the blank electrolytic solution, a well-defined peak current for the oxidation of the surface-bound chlorpromazine is observed (curve c). No interference from the 2000-fold excess amount of ascorbic acid in the sample solution is observed (note the significantly different current scales used). The electrode is washed during the transfer to remove the sample solution adhering to the surface. Similar advantages of the medium-exchange method are illustrated in Fig. 2 in which the macro sample constituent is hexacyanoferrate(II). The sought-for d.p.v. peak currents of the adsorbable species, 9,10-phenanthrenequinone (A) and chlorpromazine (B), which are masked in the direct measurement (curve a) by the currents from the 10^3—10^4 excess of hexacyanoferrate(II), are easily evaluated when the medium-exchange method (curve b) is used. Analogous results were obtained in selective measurement of 5×10^{-6} M dopamine in an ethanol solution containing 5×10^{-5} M hexacyanoferrate(II) (conditions: 2 min preconcentration at a Pt electrode, followed by exchange to phosphate buffer and "cleaning" for 2 min at +0.8 V, not shown).

Anodic stripping voltammetry/medium exchange procedures may suffer from errors caused by partial re-oxidation of the metals in the amalgam

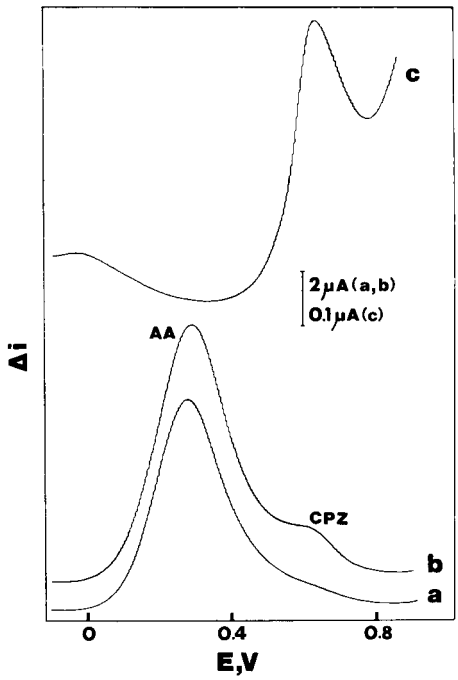

Fig. 1. Differential pulse voltammograms for 2.5×10^{-7} M chlorpromazine and 5×10^{-4} M ascorbic acid: (a) measurement in the sample solution without preconcentration; (b) measurement in the sample solution after 3-min preconcentration with 1600 rpm electrode rotation; (c) preconcentration in sample solution (as in b) with measurement after medium-exchange to the blank solution. Supporting electrolyte, 0.1 M phosphate buffer.

when the circuit is interrupted and the electrode is exposed to the atmosphere [8, 9]. No such losses were experienced in this work. Peak currents recorded after a 2-min preconcentration in a 2×10^{-7} M chlorpromazine solution were reproducible within 5%. Figure 3 presents traces for successive runs for chlorpromazine solutions of different concentrations containing 100—1000-fold amounts of non-adsorbable solution species. The linear response observed for the solutions differing in concentration (Fig. 3A) and the replicate peaks observed for the same sample solution (Fig. 3B) illustrate the absence of losses and carryover effects during the transfer. Least-squares treatment of the calibration data yielded the equation: $I_{(\mathrm{nA})} = (138.4 \pm 4.4)C_{(10^{-7}\ \mathrm{M})} + 79 \pm 15$ with a correlation coefficient of 0.998. Deviations from a linear i_p vs. concentration plot are expected above about 10^{-5} M [6]. The background currents over the 0.2—0.5 V region illustrate the effective elimination of currents arising from non-adsorbable macro sample constituents. Based on the signal and background characteristics of the response shown in Fig. 3A, the detection limit for chlorpromazine with a 3-min preconcentration step would be about 1×10^{-8} M. Lower detectability would be obtainable by using longer preconcentration periods [7] or by utilizing a computerized subtractive mode (in which different preconcentra-

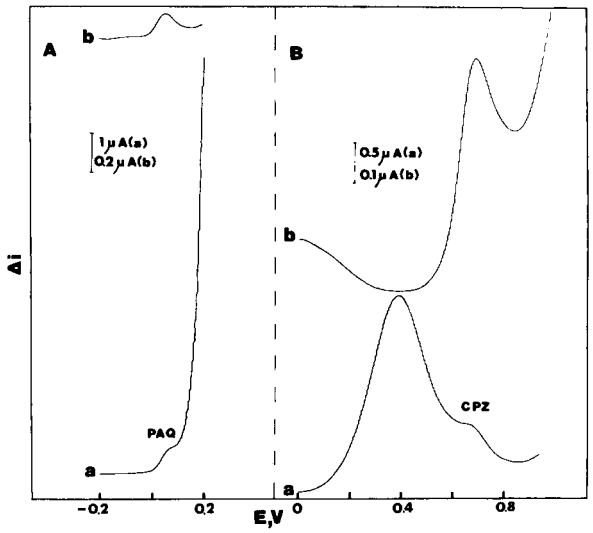

Fig. 2. Differential pulse measurements of 9,10-phenanthrenequinone (A) and chlorpromazine (B) in the presence of hexacyanoferrate(II). (a) Without medium exchange; (b) after medium exchange. Samples: (A) 7×10^{-8} M 9,10-phenanthrenequinone and 1×10^{-3} M hexacyanoferrate(II); (B) 5×10^{-7} M chlorpromazine and 2.5×10^{-4} M hexacyanoferrate(II). Supporting electrolyte: (a) 0.1 M perchloric acid; (b) 0.1 M phosphate buffer. Preconcentration periods: (A) 3 min; (B) 2 min. Rotation speed during preconcentration, 1600 rpm.

tion periods are applied and the resulting current difference is recorded [11]). As expected for such absorptive accumulation, the differential pulse peak current increases in a non-linear fashion with the preconcentration period [6, 7].

In complex samples, such as urine or blood, the advantages of the preconcentration/medium-exchange method are apparent. Such samples contain hundreds of chemicals, some at major component concentration; direct voltammetric measurements of analytes present in such samples at trace levels are often impossible. Figure 4 illustrates the determination of chlor-

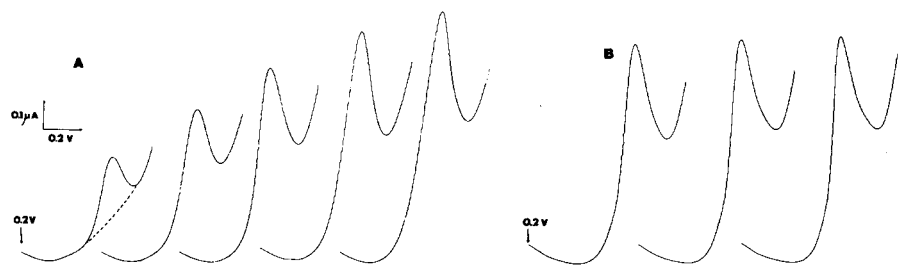

Fig. 3. Differential pulse response for chlorpromazine solutions: (A) 1—5×10^{-7} M; (B) all 5×10^{-7} M. Conditions: preconcentration for 3 min with 1600 rpm rotation, 0.1 M phosphate buffer. Sample solutions also contained 1×10^{-3} hexacyanoferrate(II) (A) and 5×10^{-4} M ascorbic acid (B). The dotted line represents the blank solution.

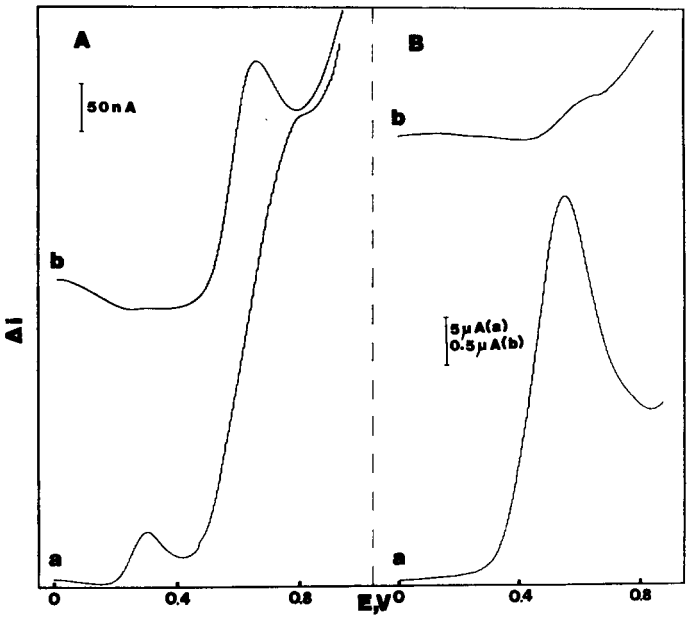

Fig. 4. Differential pulse voltammograms for chlorpromazine in blood (A) and urine (B): (a) without medium-exchange; (b) after medium-exchange (0.1 M phosphate buffer). Samples: (A) rhesus monkey whole blood spiked with 5×10^{-5} M chlorpromazine; (B) human urine diluted 1 + 3 and spiked with 7.5×10^{-6} M chlorpromazine. Preconcentration periods: (A) 4 min; (B) 3 min. Stirring rate (A) 450 rpm. Rotation speed (B) 1600 rpm.

promazine in blood and urine samples with the medium-exchange method. The rhesus monkey whole blood voltammogram (A, curve a) is characterized by an unidentified peak near +0.3 V and a large current near +0.5 V which limits the useful potential range; this latter current and the chlorpromazine peak (after 3-min preconcentration) virtually coalesce and chlorpromazine cannot be quantified. In contrast, after medium-exchange to a phosphate buffer solution (A, curve b), the chlorpromazine peak is well resolved and measurable; also, the peak near +0.3 V disappears after the exchange. The human urine sample (Fig. 4B) is characterized by a very large d.p.v. response over the +0.3 to +0.8 V potential region (curve a) that is related at least in part to the oxidation of uric acid. This current masks completely the chlorpromazine peak. After exchanging to the phosphate buffer solution (curve b), no response from the urine constituents is observed and the chlorpromazine peak (near +0.6 V) can be detected. The flat baseline over the 0 to +0.4 V region (Fig. 4B, curve b), indicates the absence of oxidizable adsorbing species among the urine constituents. The presence of additional adsorbing species may lower the peak current of the species of interest by their effect on the surface coverage.

In conclusion, the data presented above suggest many possibilities for extensions and elaboration. Applicability of the method to determinations of other groups of adsorbable organic compounds and with other modes of

attaching analytes to electrode surfaces seems clear. Adaptation of the method to a flow system would provide additional selectivity to on-line electrochemical detection. Finally, in adsorption studies, medium-exchange to an adsorbent-free solution may provide new insights into adsorption processes. Work in this laboratory is continuing in these directions.

REFERENCES

1 P. Söderhjelm, J. Electroanal. Chem., 71 (1976) 109.
2 J. W. Dieker, W. E. van der Linden and H. Poppe, Talanta, 25 (1978) 151.
3 J. F. Price and R. P. Baldwin, Anal. Chem., 52 (1980) 1940.
4 A. B. Brown, C. Koval and F. C. Anson, J. Electroanal. Chem., 72 (1976) 379.
5 L. Gorton and G. Johansson, J. Electroanal. Chem., 113 (1980) 151.
6 H. Y. Cheng, L. Falat and R. L. Li, Anal. Chem., 54 (1982) 1384.
7 T. R. Jarbawi and W. R. Heineman, Anal. Chim. Acta, 135 (1982) 359.
8 S. L. Phillip and I. Shain, Anal. Chem., 34 (1962) 262.
9 G. Koster and M. Ariel, J. Electroanal. Chem., 33 (1971) 339.
10 E. Desimoni, F. Palmisano and L. Sabbatini, Anal. Chem., 52 (1980) 1889.
11 J. Wang and B. G. Greene, Anal. Chim. Acta, 144 (1982) 137.

Analytica Chimica Acta, 148 (1983) 87—101
Elsevier Science Publishers B.V., Amsterdam — Printed in The Netherlands

THE VIBRATING WIRE ELECTRODE AS AN AMPEROMETRIC DETECTOR FOR FLOW-INJECTION SYSTEMS

KENNETH W. PRATT, Jr.[a] and DENNIS C. JOHNSON*
Department of Chemistry, Iowa State University, Ames, IA 50011 (U.S.A.)
(Received 13th September 1982)

SUMMARY

The application of vibrating wire electrodes for amperometric detection in flow-injection systems is reported. Equations of response for these electrodes in a flow-through cell are derived and verified experimentally. The applicability of the equations for other convective detectors in flow-through cells is discussed. A detection limit of 5×10^{-10} M iodide and a linear dynamic range of 6.3 decades were obtained for a platinum vibrating wire electrode.

In a previous publication [1], details of the design and construction of miniature vibrating wire electrodes (VWE) were presented. These electrodes are characterized by large rates of mass transport, typically equivalent to those that would be attained at a rotating disc electrode (RDE) of equal area under conditions of laminar flow at 25,000 rev. min^{-1}, and by correspondingly high sensitivities in voltammetric and amperometric measurements.

The high sensitivity of the VWE, which results from the turbulent, forced convection induced by the vibration, can be advantageously applied for flow injection systems at ultratrace levels. Furthermore, the small cell volume required by the VWE facilitates its application to flow-injection systems of customary dimensions (e.g., 0.9-mm i.d. tubing, flow rate ca. 1.0 ml min^{-1}). When employed in this manner, the VWE provides an example of the use of supplementary forced convection, induced independently from the flowing stream, to provide increased sensitivity in amperometric flow-through detection. This principle was first employed by Johansson [2] in a detector for liquid chromatography which utilized a rotating platimum gauze electrode, as well as by Blaedel and Schieffer [3] in the turbulent tubular electrode. More recent applications include several flow-through systems employing the RDE [4—8]. Passwaters [9] studied mass transport to a vibrating Pt disc in a flowing stream of 0.01 M hexacyanoferrate(II); however, application of the electrode to flow injection systems was not attempted.

Here we describe the first application of vibrating electrodes to flow injection systems and demonstrate the increased sensitivity of this detector relative to

[a]Present address: Chemistry A-225, National Bureau of Standards, Washington, DC 20234 (U.S.A.).

0003-2670/83/$03.00

other flow-through or flow-by electrodes. Practical utility of the method is demonstrated by the determination of iodide in iodized table salt. Also, the fundamental equations describing the response of the VWE in flow-injection systems are derived and experimentally evaluated. The extension of applicability of these equations to the use of an RDE in flow-injection systems is discussed.

EXPERIMENTAL

Instrumentation

The experimental studies were conducted with a VWE constructed from 28-gauge Pt wire, sealed into a 5-μl micropipet. The measured length and diameter of the exposed section of wire were 5.193 mm and 0.305 mm, respectively. The electrode was vibrated at a frequency of 240.0 Hz and a peak-to-peak amplitude of 0.481 mm. Details of construction and calibration of the electrode and associated equipment, including electronic circuitry, have been presented [1, 10]. Current—time recordings were obtained using a Leeds-Northrup Speedomax XL-680 strip chart recorder. A dual-function circuit comprising a d.c. recorder offset (0—85 mV) and first-order low-pass filter (time constant 0.2 s) was connected between the current output of the potentiostat and the recorder input. This circuit [10] permitted simultaneous cancellation of background currents and reduction of high-frequency noise generated by the potentiostat.

The flow-through cell for the VWE was constructed at the Chemistry Machine Shop, Iowa State University. The main body of the cell was machined from a single block of silica-loaded teflon and consisted of a thin (2.5 mm) central portion, depicted in Fig. 1, surrounded on the sides and bottom by a thicker (40 mm) rim. This outer rim, not shown in Fig. 1, served to stabilize the entire cell assembly and provided sufficient space for the reference and counter electrode chambers, as well as the inlet and outlet connections. During operation, the VWE was situated as shown in Fig. 1. The plane of vibration was parallel to the plane of the central portion of the cell body.

The front and rear walls of the flow-through cell were made from 25 × 35-mm microscope slides. A sheet of transparent teflon tape (coated on the inside surface with silicone stopcock grease) was sandwiched between the cell body and each glass plate to eliminate leakage of electrolyte from the cell. The glass plates and teflon tape were clamped to the cell body by means of two U-shaped metal plates and six screws. The existence of the transparent sides of the cell permitted in situ observation of the VWE during operation. When assembled in this manner, the compartment containing the VWE had a cross-section of 4.0 × 2.4 mm and an effective height of 17.5 mm, measured from the inlet to the outlet channel. The volume of the compartment, as calculated from these dimensions and verified by direct volumetric measurement, was 165 ± 5 μl when empty and 155 μl with the VWE in place. The outlet channel of the flow-through cell was connected to an airtight waste bottle, which in turn was connected to an aspirator.

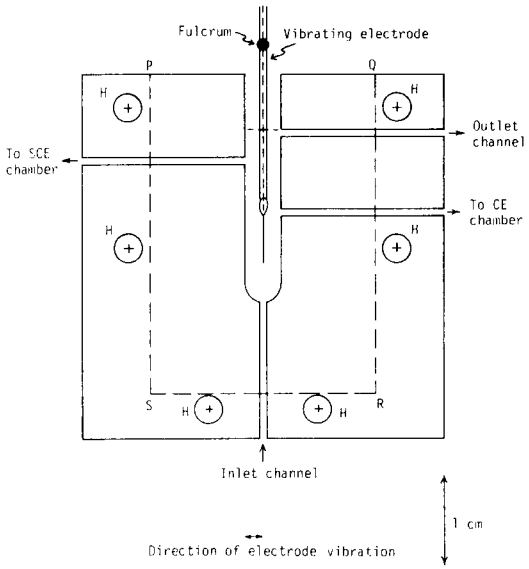

Fig. 1. Cross-section of the central portion of the flow-through cell showing the vibrating electrode. Body material, silica-loaded teflon; thickness of central portion of cell, 2.5 mm; rectangle PQRS is covered by teflon tape and glass plate. H, six holes for screws used to mount U-shaped clamp; CE, counter electrode; SCE, saturated calomel reference electrode. See Fig. 1 of [1] for diagram of mounting.

The flow-through cell was mounted on a miniature lab jack (Precision Scientific, Chicago, IL). This lab jack permitted precise vertical positioning of the flow-through cell without alteration of the horizontal position of the cell. The VWE was inserted into the central compartment of the flow-through cell by vertically raising the cell until the electrode was positioned in the center of the compartment. In its final position, the tip of the VWE was situated 4 mm above the end of the inlet channel. The tubing connected to the inlet of the flow-through cell passed through a hole in the upper platform of the lab jack.

A significant advantage of the design presented here is that experiments are readily performed, using the same VWE under otherwise identical conditions, both in the flow-through cell and in conventional voltammetric cells of larger volume. This feature permits comparison of the hydrodynamic properties of the VWE in cells of limited volume with those prevailing in "batch" cells of semi-infinite volume. Furthermore, electrochemical parameters can be optimized in a conventional cell, followed by direct application to flow-injection systems. This latter strategy simplifies development of electroanalytical methods for flow injection systems.

Procedures

The gravity flow system employed in these studies consisted of four basic components: a source bottle, which maintained a constant head of pressure on the system; a 4-way, pneumatically actuated sample-injection valve (Laboratory Data Controls SVA8031, Riviera Beach, FL); the flow cell with VWE described above; and the waste bottle. All interconnections were made with 0.9-mm i.d. teflon tubing and Cheminert fittings (Laboratory Data Controls). The flow-through cell and sample-injection valve were both enclosed in a single Faraday cage and an electrical solenoid valve located external to the cage was used to control sample injection. The source bottle was similarly shielded and the 1.5-m length of tubing connecting the source bottle to the injection valve was wrapped in aluminum foil. All shielding was directly connected to a water-pipe ground.

The volume of the sample loop used with the injection valve was 0.955 ml [11]. Dispersion of the injected sample plug was minimized by utilizing a minimal length of tubing, 11 cm, to connect the injection valve to the flow-through cell.

The value of volume flow rate (v_f) for the flow system was governed by the head of pressure of the solution in the source bottle. In this work, flow rates in the range 0.632—2.85 ml min^{-1} were employed, corresponding to pressure heads of 37.7—133.5 cm. Calibration of v_f was effected by recording the time required for a known volume of solution to accumulate in a 10-ml buret. The flow rate was directly proportional to the head of pressure in the range studied. Uncertainties in the value of v_f were ± 2% maximum. Use of gravity feed in the flow system obviated the need for a pulse dampener and significantly decreased the observed noise level of the detector.

A miniature SCE (No. 476017, Corning Scientific Instrum., Medfield, MA) and platinum wire served as the reference and counter electrodes, respectively, in both the batch [1] and flow-through cells. Electrode potentials (reported in V vs. SCE) were indicated on a digital multimeter (Model 461, Simpson Electric Co., Elgin, IL) connected to the output of the reference follower of the potentiostat.

Except as noted, experiments were done with 0.020 M HCl as the supporting electrolyte. Standard solutions of potassium iodide in deaerated 0.020 M HCl were prepared by serial dilution from a stock solution of 0.1000 M potassium iodide in water. Solutions below 0.5 mM in iodide were prepared immediately prior to use, and all dilutions were done with pyrex volumetric ware. These precautions precluded air oxidation and surface adsorption of iodide from the standard solutions.

Voltammetric measurements were done at a potential of +0.800 V, corresponding to a value on the limiting plateau for the mass-transport controlled oxidation of iodide to iodine [12]. The VWE was "iodized" and preconditioned by repeated cycling of the electrode between the potential limits of 0.0 V and 1.0 V, with the electrode immersed in a 0.5 mM solution of iodide in 0.020 M hydrochloric acid. The response of the VWE to injections of

0.500 mM iodide remained constant within ±0.5% with daily pretreatment.

All chemicals were reagent grade and water was triply distilled with demineralization after the first distillation and the second distillation from alkaline permanganate. The potassium iodide was ground in a mortar, dried at 110°C for 3 h, and stored in a desiccator prior to weighing.

Reported uncertainties are all calculated at the 90% confidence interval.

THEORY

The flow-injection system described above is modeled as a VWE contained in a cell of constant volume, V_{cell}. This cell is provided with one inlet and one outlet, through which all flow occurs. A sample plug of volume V_s containing electroactive species at a concentration C_0 is injected into the inlet channel. The theoretical derivation which follows is based on seven basic assumptions regarding the behavior of this system: (i) the volume flow rate, v_f, is constant; (ii) the concentration of analyte in the supporting electrolyte is zero; (iii) no dispersion of the sample plug occurs in the inlet channel of the cell, and the "length" of the sample plug expressed in units of time is $\tau = V_s/v_f$; (iv) the time $t = 0$ is defined as the point in time at which the leading edge of the sample plug enters the cell; (v) instantaneous complete mixing of the contents of the cell results from the stirring induced by the VWE, and mixing effects do not extend beyond the boundaries of the cell; (vi) the rate of reaction of analyte at the VWE is limited by mass transport, and the VWE is operated at a potential on the limiting plateau for reaction of the analyte; (vii) the mass transport coefficient, k_m, for the VWE is independent of the value of v_f, i.e., the thickness δ of the diffusion layer at the VWE is governed solely by the vibration of the electrode and is unaffected by the flowing stream. (For convenience, symbols are summarized in Table 1.)

The total flux of analyte to the VWE based on assumption (vi) is described by Fick's law:

$$(dN/dt)_{elec} = ADC(t)/\delta = Ak_mC(t) \quad (1)$$

where $C(t)$ represents the time-dependent bulk concentration of analyte in the cell and $k_m = D/\delta$. The time-dependent limiting current for the VWE, $I_l(t)$, is thus given by

$$I_l(t) = nFADC(t)/\delta = nFAk_mC(t) \quad (2)$$

The fundamental equations describing the response of the VWE in flow-injection systems are readily derived by application of the principle of material balance [13]. For a given increment of time, dt, the incremental quantity of analyte accumulating in the cell equals the quantity entering the cell minus the sum of the quantities leaving the cell through the outlet channel or reacting (being consumed) at the electrode:

$$dN_{cell} = dN_{in} - (dN_{out} + dN_{elec}) \quad (3)$$

TABLE 1

List of symbols

A	Surface area (cm^2)
a_{pp}	Amplitude of vibration, peak—peak (cm)
$C(t)$	Time-dependent concentration of analyte (mol l^{-1})
C_{init}	Initial concentration of analyte in bulk electrolysis (mol l^{-1})
C_0	Concentration of analyte in sample plug (mol l^{-1})
C_{ss}	Steady-state concentration (in flow-injection systems) (mol l^{-1})
D	Diffusion coefficient (cm^2 s^{-1})
F	Faraday constant (96,487 C eq^{-1})
$I_l(t)$	Time-dependent limiting current (A)
$I_{l,ss}$	Steady-state limiting current (A)
I_p	Peak current in a flow-injection system (A)
k_m	Mass transfer coefficient (cm s^{-1})
N	Quantity of analyte (mol)
n	Number of electrons in reaction (eq mol^{-1})
Q_p	Peak area in a flow-injection system (C)
R	Relative, time-dependent limiting current, $I_l(t)/I_{l,ss}$ (dimensionless)
Re_v	Vibrational Reynolds number (dimensionless)
t	Time (s)
V_{cell}	Volume of cell (ml)
V_s	Volume of injected sample (ml)
v_f	Volume flow rate (ml s^{-1})
δ	Thickness of diffusion layer (cm)
ϵ	Fractional conversion (dimensionless)
τ	Length of sample plug in time units (s)
ω	Rotation speed of RDE (rev s^{-1})

These incremental molar quantities can be expressed in terms of incremental volumes and concentrations by utilizing the basic relationship between quantity, volume and concentration. For the period from $t = 0$ to $t = \tau$, corresponding to the inflow of analyte into the cell for the total sample, the expression of material balance is given by

$$V_{cell}dC = C_0\,dV - [C(t)dV + dN_{elec}] \tag{4}$$

Division of both members of Eqn. (4) by dt, followed by substitution of Eqn. (1) for $(dN/dt)_{elec}$ and v_f for dV/dt, yields the differential equation defining $C(t)$ from $t = 0$ to $t = \tau$:

$$dC/dt + [(v_f + Ak_m)/V_{cell}]C(t) = C_0 v_f/V_{cell} \tag{5}$$

At the point when the leading edge of the sample plug enters the cell, the concentration of analyte in the cell is zero:

$$C(t) = 0 \text{ when } t = 0 \tag{6}$$

Equations (5) and (6) define an initial value problem [14], the solution to which describes $C(t)$ for the period from $t = 0$ to $t = \tau$:

$$C(t) = [C_0 v_f/(v_f + Ak_m)][1 - \exp\{-[(v_f + Ak_m)/V_{cell}]t\}] \tag{7}$$

The equation defining $C(t)$ for $t > \tau$ is derived in similar fashion. In this

case, the quantity dN_{in} in Eqn. (3) is zero, because analyte is no longer entering the cell. All other terms remain the same as in Eqn. (4). Simplification and rearrangement yield a second differential equation:

$$dC/dt + [(v_f + Ak_m)/V_{cell}]C(t) = 0 \tag{8}$$

The initial condition applicable in this instance is

$$C(t) = C(\tau) \text{ at } t = \tau \tag{9}$$

The solution to the initial value problem formed by Eqns. (8) and (9) defines $C(t)$ for all times $t > \tau$:

$$C(t) = C(\tau) \exp\{-[(v_f + Ak_m)/V_{cell}](t - \tau)\} \tag{10}$$

where $C(\tau)$ is given by Eqn. (7) for $t = \tau$.

Substitution of $C(t)$ from Eqns. (7) or (10) into Eqn. (2) yields the current response for the VWE. Of analytical importance is the result that $I_l(t)$ is directly proportional to C_0, the concentration of analyte in the sample. Equations (7) and (10) reduce to various limiting forms in cases where $t \to \infty$, $v_f \gg Ak_m$, $Ak_m \gg v_f$, and $v_f = 0$. For $t \to \infty$, Eqn. (7) reduces to

$$C_{ss} = v_f C_0/(v_f + Ak_m) \tag{11}$$

where C_{ss} represents the steady-state concentration of analyte in the cell for a sample plug of infinite length. The fractional conversion, ϵ, for the amperometric electrode is given by the ratio of the flux of analyte to the electrode, $Ak_m C_{ss}$, to the total influx of analyte into the cell, $v_f C_0$. Substitution of Eqn. (11) for C_{ss} yields

$$\epsilon = Ak_m/(v_f + Ak_m) \tag{12}$$

Equations corresponding to Eqns. (11) and (12) were cited by Pickett [13] in his treatment of the continuously stirred tank electrochemical reactor. However, equations describing the time dependence of $C(t)$ and $I_l(t)$ were not discussed, because this dependence is not of primary interest in chemical engineering.

In the case for which $v_f \gg Ak_m$, Eqns. (11) and (12) approach $C_{ss} = C_0$ and $\epsilon = 0$, respectively, indicating that depletion of analyte at the electrode is negligible. Equations (7) and (10) reduce to forms previously derived by Pungor and coworkers [15, 16] for flow-injection systems employing a mixing chamber between the point of injection and a potentiometric detector. For $Ak_m \gg v_f$, Eqns. (7) and (12) approach $C(t) = 0$ and $\epsilon = 1$, respectively. These trivial results indicate that the electrode in this hypothetical system functions as a quasi-coulometric detector. Quantitative, coulometric detection is obtained only for $Ak_m \to \infty$ for a flowing stream (i.e., $v_f > 0$).

If the concentration in the cell is $C(t) = C_{init}$ and the flow of solution through the cell is stopped at $t = 0$, $C(t)$ decays exponentially according to Eqn. (10) where $v_f = 0$ and $C(\tau) = C_{init}$, i.e.,

$$C(t) = C_{init} \exp\{-(Ak_m/V_{cell})t\} \tag{13}$$

This is the well-known equation describing $C(t)$ for the bulk electrolysis of the contents of an electrolytic cell in controlled-potential coulometry, where $Ak_m/V_{cell} = AD/V_{cell}\delta$, the cell constant.

From the above discussion, it is evident that the equations derived for the VWE comprise a generalization of previously known relations which apply to several unrelated techniques. Each of the four limiting cases treated here exemplifies the relationship of the VWE to one of these techniques.

Calculation of the areas under the $C(t)$ and $I_l(t)$ curves provides further information of quantitative significance. The area under the $C(t) - t$ curve is given by the sum of the definite integrals from $t = 0$ to $t = \tau$ for Eqn. (7) and $t = \tau$ to $t = \infty$ for Eqn. (10). Evaluation yields the result

$$\int_0^\infty C(t)\mathrm{d}t = C_0 v_f \tau/(v_f + Ak_m) \tag{14}$$

Substitution of Eqn. (11) simplifies this to

$$\int_0^\infty C(t)\mathrm{d}t = C_{ss}\tau \tag{15}$$

It is evident from this equation that the area under the $C(t)-t$ curve is equal to that which would occur in the same system if exponential tailing were not present. Furthermore, this result demonstrates that the area under the $C(t) - t$ curve is independent of the cell volume.

The area under the $I_l(t)$ curve is calculated in similar fashion, following removal from the integral of the proportionality constant $nFAk_m$ which relates $I_l(t)$ and $C(t)$. The result in this case represents Q_p, the peak area for quantitative work:

$$Q_p = \int_0^\infty I_l(t)\mathrm{d}t = nFAk_m C_0 v_f \tau/(v_f + Ak_m) \tag{16}$$

Substitution of the definition of τ and Eqn. (12) yields

$$Q_p = \epsilon nFC_0 V_s \tag{17}$$

Equation (17) states that the area under the peak is equal to the coulometric area for the injected sample times the fractional conversion at the electrode. As noted for $I_l(t)$, Q_p is directly proportional to C_0. The other conclusions noted above for $\int C(t)\mathrm{d}t$ apply as well to Q_p.

The equations developed here should also apply to flow-injection systems employing the rotating disc electrode [4—8], provided that the assumptions of instantaneous, perfect mixing in the cell and independence of k_m and v_f are satisfied. The theory should also apply to the turbulent tubular electrode [3], although the definition of V_{cell} for this system is vague. However, the equations are not valid in cases such as the packed bed [17] and reticulated vitreous carbon [18] electrodes, in which the foregoing assumptions are not satisfied. Applicability in other cases can be judged by the degree to which the basic assumptions set forth above apply to the system under study.

RESULTS AND DISCUSSION

Verification of theory

Measured values of the limiting steady-state current, $I_{l,\,ss}$, obtained at the VWE for v_f = 0.632 to 2.85 ml min^{-1} are presented in Table 2. A 0.500 mM standard solution of potassium iodide replaced the blank supporting electrolyte in the source bottle, simulating a sample plug of infinite length. Experimental values of ϵ were calculated as

$$\epsilon = I_{l,\,ss}/nFv_fC_0 \tag{18}$$

Each tabulated value for Ak_m was obtained from the corresponding ϵ and v_f using Eqn. (12). When expressed in equivalent units (cm^3 s^{-1} and ml s^{-1}), Ak_m and v_f represent the relative amounts of analyte reacting at the VWE and leaving the cell, respectively. Division by the area of the VWE (0.0505 cm^2) and application of the definition of k_m yielded the values for k_m and δ.

The experimental values of k_m and δ are constant within 3% over the range of v_f studied, showing that the assumption of independence of k_m and v_f is valid for the electrode in this flow system. The fractional conversions tabulated for the VWE compare with values of 0.0093 at v_f = 2.0 ml min^{-1} [19] and 0.0035 at v_f = 3.15 ml min^{-1} [20] calculated for tubular electrodes of similar area.

Calculation of k_m for the VWE in similar experiments at v_f = 0.632 and 1.69 ml min^{-1}, as well as for the same electrode under identical conditions in a batch cell, yielded experimental values of 0.0414, 0.0402, and 0.0410 cm s^{-1}, respectively. The value of k_m for the VWE in the batch cell was calculated from Eqn. (2) for I_l = 100 μA and $C(t)$ = 0.500 mM. The increase of ca. 10% in k_m in this second series of experiments is attributed to the elimination of partial fouling of the electrode caused by the silicone grease used as a sealant for the window of the flow-through cell. Periodic cleaning of the VWE in an ethanolic solution of potassium hydroxide eliminated this problem.

TABLE 2

Study of vibrating electrodes in flow system under steady-state conditions

Volume flow rate (ml min^{-1})	$I_{l,\,ss}$ (μA)	nFv_fC_0 (μA)	ϵ	Ak_m (10^{-3} cm^3 s^{-1})	k_m (10^{-2} cm s^{-1})	δ (μm)
0.632	79.0	508	0.156	1.94	3.84	4.06
0.800	80.9	644	0.126	1.92	3.80	4.10
1.09	82.8	878	0.0944	1.90	3.76	4.15
1.38	84.2	1107	0.0761	1.89	3.74	4.17
1.69	85.2	1357	0.0628	1.88	3.72	4.19
2.09	86.3	1679	0.0514	1.89	3.74	4.17
2.32	86.5	1862	0.0465	1.88	3.72	4.19
2.85	87.9	2293	0.0383	1.90	3.76	4.15

The k_m value for the VWE in the 28-ml batch cell is within 3% of values obtained for the same electrode in the 155-μl flow-through cell. This indicates that the hydrodynamic conditions prevailing at the electrode in these two cells are similar. The decreased values of $I_{l,\,ss}$ in the flow-through cell (84.3 μA at v_f = 0.632 ml min^{-1} and 91.2 μA at 1.69 ml min^{-1} vs. 100.0 μA in the batch cell) resulted not from a decreased value of k_m, but rather from the depletion of analyte in the flow-through cell. The average value calculated for k_m in this experiment is equal to that attained at a RDE rotating at 23,400 rev. min^{-1}.

Substitution of Eqns. (11) and (2) into Eqns. (7) and (10), followed by rearrangement and removal of the exponentials, yields the equivalent forms

$$\ln (1 - R) = -[(v_f + Ak_m)/V_{\text{cell}}]\,t \tag{19}$$

for the rising portion of the $I_l(t)$ peak and

$$\ln R = -[(v_f + Ak_m)/V_{\text{cell}}]\,(t - \tau) \tag{20}$$

for the falling portion of the peak. In these equations, R represents the ratio $I_l(t)/I_{l,\,ss}$ and $I_l(\tau)$ is assumed equal to $I_{l,\,ss}$ (valid for $\tau \to \infty$). Based on Eqns. (19) and (20), the time-dependent portions of Eqns. (7) and (10) were verified by graphical evaluation of experimental $I_l(t)$ peaks obtained for injections of 0.500 mM potassium iodide at v_f = 0.632 ml min^{-1}. Experimental data are presented in Figs. 2 and 3. Values of R were calculated from measured

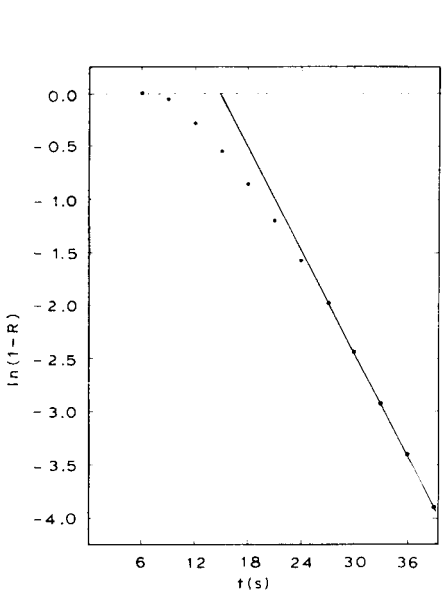

Fig. 2. Plot of ln(1 — R) vs. time for the rising portion of current response. See text for conditions.

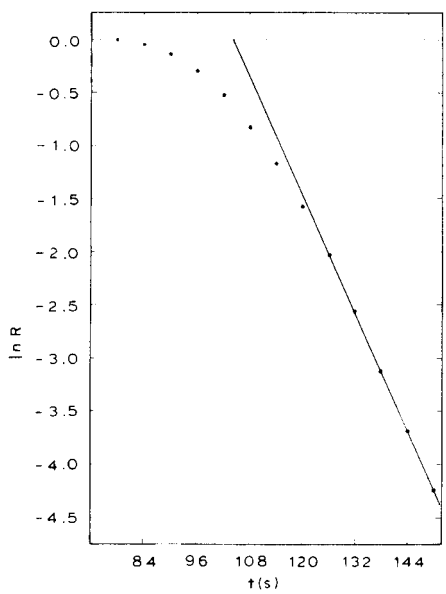

Fig. 3. Plot of ln(R) vs. time for the falling portion of current response. See text for conditions.

$I_l(t)$ by using $I_{l,\,ss}$ = 84.3 μA at v_f = 0.632 ml min^{-1}. The point t = 0 was defined as the time at which the sample loop was switched into the flow stream. Values of V_s and v_f were chosen such that the maximum value of $I_l(t)$ was experimentally indistinguishable from $I_{l,\,ss}$ at a point prior to $t = \tau$. From Eqns. (19) and (20) it is evident that the slope of each graph is $-[(v_f + Ak_m)/V_{cell}]$. An effective V_{cell} for the observed limiting slope of each graph was calculated by using the measured values of v_f and Ak_m from the steady-state experiments. The results of these calculations are summarized in Table 3. In each case, the effective V_{cell} is significantly smaller than 155 μl, the actual cell volume, indicating that mixing effects do not extend instantaneously over the entire cell. Similar results were obtained from evaluation of data obtained for other values of v_f.

The ca. 73% variance between the values of V_{cell} for the rising and falling portions of the $I_l(t)$ peak is attributed to dispersion of the trailing edge of the sample plug, which passes through a 1.5-m length of tubing before reaching the cell inlet. Dispersion of the leading edge of the plug is negligible. Hence, V_{cell} for the rising portion of the peak is considered more representative of the actual mixing conditions prevailing in the cell.

Observation of the VWE compartment during injection of a sample plug containing 0.05% potassium permanganate verified that instantaneous mixing did not extend to the upper portion of the compartment. However, mixing in the lower half of the cell was substantially instantaneous, and the composition of the region surrounding the VWE, as estimated visually from the depth of color in the solution, was homogeneous. Significant dispersion of the trailing edge of the sample plug was also noted.

In conclusion, the assumption of instantaneous, perfect mixing is substantially valid for the lower half of the VWE compartment, but not for the entire cell volume. Although the assumption of zero dispersion is reasonable for the leading edge of the sample plug, significant dispersion takes place for the trailing edge, as expected.

The effect of non-instantaneous mixing on the $I_l(t)$ curves was not investigated. However, back-mixing of analyte from the upper to the lower half of the VWE compartment likely occurs during the falling portion of the peak and contributes to the observed increase in V_{cell}. The deviations from linearity in Figs. 2 and 3 may also arise from this non-ideal behavior.

TABLE 3

Summary of graphical evaluation of $I_l(t)$ peaks

Volume flow rate (v_f)	0.632 ml min^{-1}	1.69 ml min^{-1}
Rising portion of peak	Slope -0.161 s^{-1}	-0.395 s^{-1}
	V_{cell} 78.5 μl	76.3 μl
Falling portion of peak	Slope -0.0924 s^{-1}	-0.230 s^{-1}
	V_{cell} 137 μl	131 μl

Applicability to rotating disc electrode in flow-injection systems

Data presented by Brunt et al. [7] for the RDE in flow-injection systems permit evaluation of the dependence of Ak_m on v_f for their system. Values of Ak_m were calculated from quoted values of ϵ (Fig. 3 of [7]) at v_f = 0.42, 1.08, and 2.01 ml min^{-1} for ω = 17, 29, and 41 rev. s^{-1}. Referred to k_m at v_f = 0.42 ml min^{-1}, k_m decreased slightly (2.7%, 9.6%, and 11.3% at 17, 29, and 41 rev. s^{-1}, respectively) with increasing v_f, in contrast to the behavior expected and predicted by the authors. This effect is noted to a lesser extent with the VWE, as is evident in Table 1. A probable explanation is that the flowing stream tends to disrupt the hydrodynamic flow patterns induced by the RDE or VWE. Conversely, Ak_m for the same system at 0 rev. s^{-1} (i.e., a wall-jet configuration) increased 40% at 1.08 ml min^{-1} and 57.5% at 2.01 ml min^{-1}, as is expected for an electrode in which the hydrodynamic conditions are determined solely by a flowing stream.

Quantitative application

Figure 4 illustrates the increased sensitivity of the VWE in the flow system. Voltammograms (I—E) are presented for the platinum electrode in iodide-free, air-saturated 0.010 M sulfuric acid at v_f = 0.800 ml min^{-1}. Mass-transport limited current for the reduction of oxygen is attained at $E < +0.1$ V, with surface-controlled background currents observed at $E > +0.65$ V. Vibration of the electrode effects a 13-fold increase in the sensitivity at the VWE for the reduction of oxygen without producing a significant increase in the surface-controlled background currents. Hence, the detection limit is lowered by a factor of 13. Similar experiments with 0.500 mM iodide yielded enhancement factors of 12 at v_f = 0.632 ml min^{-1} and 8.3 at 1.69 ml min^{-1}.

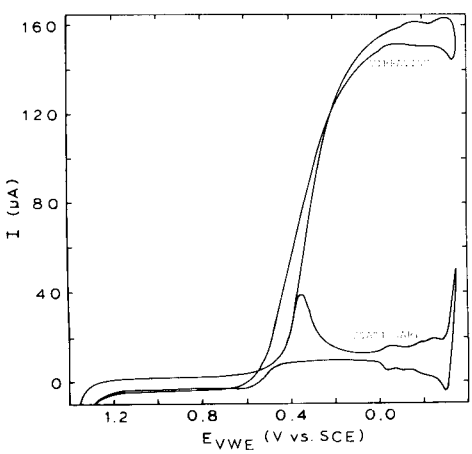

Fig. 4. Effect of vibration of the electrode on the voltammetric signal. Conditions: scan rate 5.0 V min^{-1}; frequency 240.0 Hz; Re_v 66.5; a_{pp} = 0.481 mm; v_f = 0.800 ml min^{-1}; solution, air-saturated 0.010 M sulfuric acid.

These values for the VWE in the flow-injection system compare with analogous increases in sensitivity of 5.2 [3], 3—4 [4,5], 3—3.6 [6], 2—3 [7], and 3—10 [8] for the various other systems noted in the introductory section.

A calibration curve was prepared for the amperometric response of the VWE to injections of iodide at v_f = 0.632 ml min^{-1}. The concentrations of iodide in the sample injected ranged from 5.00×10^{-10} to 1.00×10^{-3} M, and the corresponding peak currents, I_p, ranged from 138 pA to 159 μA. The experimental results were obtained over a period of 5 days, and triplicate injections were performed at each concentration level. Long-term variations in the response of the VWE to injections of 5.00×10^{-4} M iodide over this period were less than 1% relative. The response of the VWE after removal and re-insertion into the cell was reproducible within 1%. At all concentrations, the observed current peaks were similar in form to those evaluated in Figs. 2 and 3. The values of I_p for triplicate injections were within 1% at each concentration above 5.00×10^{-9} M iodide; variations of 5% and 15% were noted for 1.00×10^{-9} M and 5.00×10^{-10} M iodide, respectively. Representative peaks are depicted in Fig. 5 with emphasis placed on peaks recorded at concentrations of iodide at or near the detection limit. The response of the VWE to an injection of supporting electrolyte containing no added iodide is also shown. The log—log plot of $|I_p|$(C s^{-1}) vs. C_{I^-} (mol l^{-1}) was linear and is described by $\log|I_p| = (0.878 \pm 0.071) + (0.956 \pm 0.011) \log C_{I^-}$ with $s_{y/x}$ = 0.0518 and r = 0.9997, as determined by linear regression. The uncertainties shown were calculated at the 90% confidence level.

The detection limit for iodide at the VWE, estimated from the data of Fig. 5, is 5×10^{-10} M for a S/N ratio of 2. Based on results of the calibration studies, the dynamic range of the VWE in this application is 2000000 to 1, or 6.3 decades. These results represent both the lowest detection limit and largest dynamic range reported to date for a flow-injection system with electrochemical detection, and constitute a 20-fold improvement over values cited for the tubular electrode [19, 20].

The slope of the log—log calibration curve cited above is less than 1.0 indicating that the response of the VWE exhibits slight nonlinearity, in contrast to theory. Similar behavior has also been noted for Pt VWE's in batch cells in this and earlier [21, 22] work. Thus, the nonlinearity is a function of the design of the VWE and is not related to its application to flow-injection systems.

The VWE was also applied to the determination of iodide in commercial iodized table salt by the method of standard additions. Morton iodized salt was dried for 3 h at 110°C and stored in a desiccator. A 2.4565-g sample of the dried salt was dissolved in 0.020 M hydrochloric acid and diluted to 100.00 ml. From this stock solution, five 5.00-ml aliquots were transferred to separate 100-ml volumetric flasks, and 5.00-ml, 10.00-ml, 15.00-ml, and 20.00-ml aliquots of a 10.55 μM iodide solution in 0.020 M hydrochloric acid were added to four of these five flasks, respectively. All five flasks were then diluted to volume with 0.020 M hydrochloric acid. Iodide was then

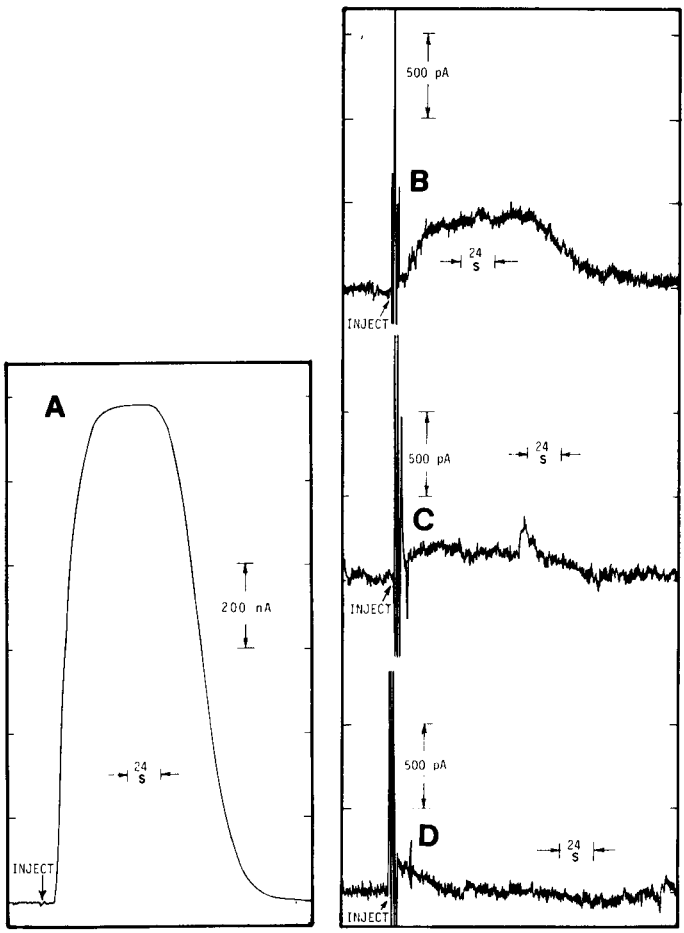

Fig. 5. Observed response of Electrode B to injected samples of iodide. Conditions: frequency 240.0 Hz; Re_v = 66.5; a_{pp} = 0.481 mm; v_f = 0.632 ml min^{-1}; V_s = 0.995 ml; E = +0.800 V vs. SCE. Curves: A, $C_0 = 5.00 \times 10^{-6}$ M I^- in 0.020 M HCl; B, $C_0 = 1.00 \times 10^{-9}$ M I^- in 0.020 M HCl; C, $C_0 = 5.00 \times 10^{-10}$ M I^- in 0.020 M HCl; D, C_0 = 0 (i.e., blank, 0.020 M HCl).

quantified for triplicate injections of the five solutions using the flow-injection system. The plot of $|I_p|$ (C s^{-1}) vs. concentration of added iodide (mol l^{-1}) was linear as described by $|I_p| = (1.09 \pm 0.18)10^{-7} + (0.243 \pm 0.014)$-$C_{\text{added } I^-}$ with $s_{yx} = 7.4 \times 10^{-9}$ and $r = 0.9995$. The unknown concentration of iodide was determined from the x-intercept to be $(1.09 \pm 0.18)10^{-7}/(0.243 \pm 0.014) = (4.52 \pm 0.66)10^{-7}$ M which corresponds to 150 ± 22 μg of potassium iodide in the 2.4565-g sample, or 61.1 ± 9.0 ppm potassium iodide. The comparatively large values for the uncertainties are a direct result of the nonlinearity in the electrode response, which was noted previously. The

final result compares to the value of 85 ppm potassium iodide quoted in a private communication from the manufacturer.

REFERENCES

1 K. W. Pratt and D. C. Johnson, Electrochim. Acta, 27 (1982) 1013.
2 G. Johansson, Talanta, 12 (1965) 163.
3 W. J. Blaedel and G. W. Schieffer, Anal. Chem., 46 (1974) 1564.
4 J. Wang and M. Ariel, Anal. Chim. Acta, 99 (1978) 89.
5 J. Wang and M. Ariel, Anal. Chim. Acta, 101 (1978) 1.
6 B. Oosterhuis, K. Brunt, B. H. C. Westerink and D. A. Doornbos, Anal. Chem., 52 (1980) 203.
7 K. Brunt, C. H. P. Bruins, D. A. Doornbos and B. Oosterhuis, Anal. Chim. Acta, 114 (1980) 257.
8 W. J. Blaedel and J. Wang, Anal. Chim. Acta, 116 (1980) 315.
9 W. R. Passwaters, Ph.D. Dissertation, University of West Virginia, Morgantown, WV, 1978.
10 K. W. Pratt, Ph.D. Dissertation, Iowa State University, Ames, IA, 1981.
11 P. L. Meschi and D. C. Johnson, Anal. Chim. Acta, 124 (1981) 303.
12 D. C. Johnson, J. Electrochem. Soc., 119 (1972) 331.
13 D. J. Pickett, Electrochemical Reactor Design, 2nd edn., Elsevier, Amsterdam, 1979, pp. 263—290.
14 W. E. Boyce and R. C. DiPrima, Introduction to Differential Equations, Wiley, New York, 1970, pp. 7—17.
15 G. Nagy, Zs. Fehér and E. Pungor, Anal. Chim. Acta, 52 (1970) 47.
16 Zs. Fehér, G. Nagy, K. Tóth and E. Pungor, Anal. Chim. Acta, 98 (1978) 193.
17 D. C. Johnson and J. H. Larochelle, Talanta, 20 (1973) 959.
18 W. J. Blaedel and J. Wang, Anal. Chem., 51 (1979) 799.
19 W. J. Blaedel, C. L. Olson and L. R. Sharma, Anal. Chem., 35 (1963) 2100.
20 W. J. Blaedel and S. L. Boyer, Anal. Chem., 43 (1971) 1538.
21 E. D. Harris and A. J. Lindsey, Analyst, 76 (1951) 647; 76 (1951) 650.
22 H. Küster, Ber. Dtsch. Bot. Ges., 68 (1955) 183.

Analytica Chimica Acta, 148 (1983) 103—109
Elsevier Science Publishers B.V., Amsterdam — Printed in The Netherlands

AMPEROMETRIC DETERMINATION OF METAL IONS IN A FLOW-INJECTION SYSTEM WITH A COPPER-AMALGAM ELECTRODE

PETER W. ALEXANDER* and UMAPORN AKAPONGKUL

Department of Analytical Chemistry, University of New South Wales, P.O. Box 1, Kensington, 2033 N.S.W. (Australia)

(Received 4th October 1982)

SUMMARY

The direct electroreduction of metal ions in an ammoniacal buffer as complexing carrier stream is demonstrated at a copper amalgam working electrode in a flow-injection system. Injection of 0.02—80 μg of cadmium(II) in volumes of 1—40 μl gave sharp response peaks; the relative standard deviation for peak-height measurements was 0.6% and the response time was 12 s for baseline resolution. After deaeration of the ammoniacal buffer and sample solutions, detection limits of 2—3 ng were obtained for copper, cadmium, and zinc at working potentials of −0.60 V, −1.00 V and −1.40 V (vs. SCE), respectively.

The amperometric determination of metal ions has been done traditionally by titrations with the dropping mercury electrode (DME) as indicator electrode [1], the electrode having the advantage of a regularly renewed surface. In the study described here, a flow-through cell utilizing a stationary copper amalgam wire electrode was developed for amperometric determination of metal ions in a flow-injection system. The advantages of a solid electrode like this over the more unwieldy DME [1] and static drop mercury electrode (SMDE) recently developed at Princeton Applied Research (E.G. & G.) are the miniature cell design, the ease of electrode conditioning, the very low dead volume, and the elimination of the need to handle mercury.

There have been many reports on amperometric detection in flow-injection systems and in liquid chromatography, as recently reviewed [2, 3]. Previous flow studies have been concerned, for example, with organic oxidations [3] or reductions [3, 4], metal—organic reductions [5, 6], metal ion oxidations [7], metal ion reductions at the DME [8, 9], SMDE [10], mercury pool electrodes [11, 12], and platinum electrodes [13], and metal complex oxidations [14, 15]. In this study, the novel use of the miniature copper amalgam wire electrode is shown to allow direct reductive determination of metal ions without serious electrode poisoning. The applications of this type of electrode in flow analysis and liquid chromatography are discussed.

0003-2670/83/$03.00

EXPERIMENTAL

Apparatus

The flow-injection system consisted of a peristaltic pump (Desaga, Type 131900) fitted with a single PVC pump tube (Elkay), with 0.63-mm bore, and connected via PVC tubing (0.5-mm bore) to a liquid chromatographic system injector [16]. The outlet of the injector was connected to a flow-through electrochemical cell via a coil of PVC tubing (0.5 mm bore, 190 cm long). The cell was coupled to a Princeton Applied Research Polarograph, Model 174A, and the output was recorded with a Houston Omniscribe strip-chart recorder. Figure 1 shows a diagram of the complete system. Samples were injected into the carrier stream with micro-syringes (SGE, Parkville, Australia) graduated to either 5-μl or 100-μl volumes.

Flow cell. A flow cell was constructed of perspex, as shown in Fig. 2, consisting of a 2-electrode configuration with a third electrode, a saturated calomel reference electrode, placed downstream from the cell in a separate flow cap. The two electrodes were metal wires, one of copper (1.0-mm diameter) as the working electrode and the second of platinum (0.6-mm diameter) as the auxiliary electrode with a 1.0-mm flow path separating the two. The wires were sealed into the perspex with epoxy, and Omnifit connectors were used to interconnect the cell with the flow tubing. The length of tubing separating the flow cell from the reference electrode was 25.0 cm.

Reagents and solutions

Metal salts and buffer components used were analytical-reagent grade. The ammoniacal buffer composition was 0.2 M ammonium chloride, 0.2 M ammonia, and 8.0×10^{-3} M sodium sulphite, added in order to reduce oxygen as recommended previously [1]. Stock metal ion solutions (1.0×10^{-2} M) were prepared from copper nitrate, cadmium chloride and zinc nitrate, and diluted freshly just before use to the working concentrations in the range $0.01—1.0 \times 10^{-2}$ M with sodium sulphite (8.0×10^{-3} M) added to each sample.

Procedures

Electrode preparation. The copper wire electrode was amalgamated with mercury by pumping a solution of mercury(II) nitrate (0.01 M) in 1% nitric acid through the flow cell and depositing mercury by electrolysis at —0.5 V

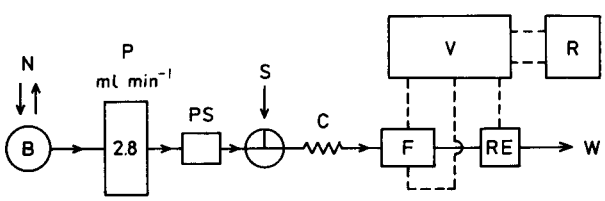

Fig. 1. Diagram of the flow-injection system. N, nitrogen; B, buffer solution; P, pump; PS, pulse suppressor; S, sample injection port; C, mixing coil (100 cm); F, flow-cell; RE, reference electrode; W, waste; V, voltammeter; R, recorder.

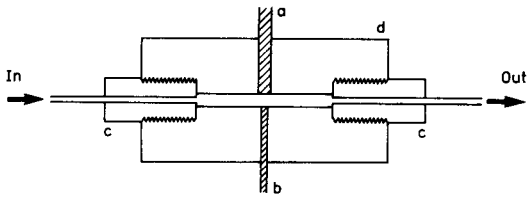

Fig. 2. Flow cell constructed of perspex: (a) copper-amalgam electrode; (b) platinum auxiliary electrode; (c) Omnifit connectors (0.5 mm i.d.); (d) cylindrical perspex body (1.0 mm i.d., 2.5 cm length, 1.2 cm diameter).

vs. SCE for 5 min. A shiny mercury surface resulted and the cell was then washed out with distilled water. The cell has been operated for 2 months without the need to replace the wire electrodes. When not in use, the electrodes were stored in contact with 0.2 M ammonia buffer. The copper electrode was recoated with mercury after 2 weeks by repeating a 5-min deposition step; this had no effect on the baseline current. Accumulated metal ion reduction products were removed when necessary by anodic stripping at −0.4 V during a wash with buffer.

Determination of metals. Hydrodynamic voltammetric recordings were made while a test solution was pumped continuously through the flow cell. The voltage scan was initiated from the PAR 174A instrument and recorded from −0.5 to −1.7 V, all potentials with reference to the SCE. The scan rate was set at 5 mV s^{-1} in the d.c. operational mode, with current sensitivity 0.02–2.0 μA, low pass filter 0–3.0 s as required, recorder input 10 V, and chart speed 5.0 cm min^{-1}. The solution flow rate was kept constant at 2.8 ml min^{-1} throughout this study with the pump speed controller set at maximum speed. When necessary, oxygen was removed from the test solution by bubbling nitrogen saturated with ammonia through the solution for 30 min before measurement.

The half-wave potentials for Cd(II) and Zn(II) were established, and voltages were set at −0.60, −1.00 and −1.40 V for the amperometric detection of Cu, Cd and Zn, respectively. Solutions of metal ions with concentrations in the range 0.1–2.0 × 10^{-2} M were injected into the 0.2 M ammoniacal buffer as the carrier stream after the latter had been deaerated. Injection volumes were varied between 1 and 40 μl and the current response of the Cu/Hg electrode at the working voltage was recorded continuously at appropriate current sensitivity and chart speeds as described under Results. The samples were not deaerated before injection, but contained sodium sulphite (8.0 × 10^{-3} M) to reduce oxygen.

RESULTS

An ammoniacal buffer was chosen as the carrier stream for two reasons: (1) to maintain high pH and hence give a wider cathodic working range, and (2) to provide a background complexing capacity for the metal ions tested.

Obviously, other buffers could be used to give different working rang metal complexing capacity, but the ammonia used here serves as an ex of what is possible with this approach to the development of ele detectors for flow analysis.

In this study, the features considered were the effect of oxygen, the lity and drift characteristics, the working voltage range, response tim sensitivity of the Cu/Hg electrode in a flow-injection system of the described by Růžička and Hansen [17]. The cell was designed in or obtain low hold-up volume, miniature size, easily manipulated perform and rapid response. The design shown in Fig. 1 gave a dead-volume of 0.8 μl, considerably lower than thin-layer and static mercury drop elec previously reported [4, 10]. The cell is also much simpler to fab The small size allowed very rapid response times to be obtained in injection analysis with amperometric operation.

Effect of oxygen on the hydrodynamic voltammetry

In 0.2 M ammoniacal buffer as carrier stream, the presence of oxyge found to have a marked effect on the voltammetric curves at the Cu/H trode. Figure 3 shows the d.c. voltammetric recordings from —0.5 to —

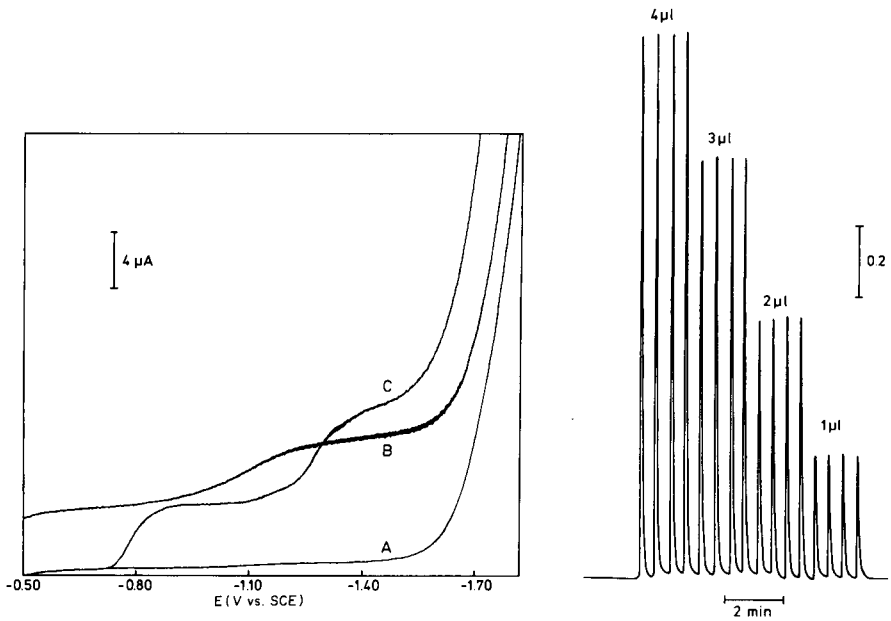

Fig. 3. Hydrodynamic voltammograms recorded with the copper-amalgam electro 0.2 M ammoniacal buffer after deaeration; (B) solution A before deaeration; (C) Zn (0.5×10^{-3} M) in 0.2 M ammonia buffer after deaeration.

Fig. 4. Effect of injection volume on sample peak heights for injection of a ca sample (1.0×10^{-2} M) of fixed concentration.

both before and after deaeration of the carrier stream. The working voltage range and current sensitivity were clearly dependent on the oxygen content. By removing oxygen, a range from −0.5 to −1.6 V was obtainable in ammoniacal buffer. It is also possible to use the electrode in the presence of oxygen for some applications by employing high current densities where the high background level is not important, but of course sensitivity is severely limited in such a situation.

Metal ions forming soluble complexes with ammonia gave well-defined voltammograms at the Cu/Hg electrode in the flowing ammoniacal carrier stream. Figure 3 shows a voltammetric recording for a solution containing 0.5×10^{-3} M Cd^{2+} and Zn^{2+} in 0.2 M ammoniacal buffer, when pumped continuously through the flow cell. Well-defined limiting current regions were obtained for each metal ion with half-wave potentials at −0.79 and −1.28 V, respectively. These values agree closely with the $E_{1/2}$ values reported [1] for the DME, as shown in Table 1. The possibility of operating with amperometric detection combined with flow-injection analysis [17] is therefore clear from Fig. 3, if oxygen is removed.

Amperometric flow-injection system

The voltage was set on the limiting current region for cadmium(II) at −1.00 V, and samples were injected into the ammoniacal buffer stream. A steady baseline current was obtained when the ammonia was kept deaerated and when the cadmium(II) sample solutions were deoxygenated by adding sodium sulphite. Injection of low volumes (1—4 μl) gave zero blanks when the blank ammonia was injected, because so little oxygen was introduced. Injection of 4 μl of cadmium solutions ($0.4—2.0 \times 10^{-2}$ M) gave sharp peaks, with heights in linear relationship to the cadmium concentrations. Similarly, injection of a fixed concentration of cadmium(II) (1.0×10^{-2} M) using aliquots of 1—4 μl gave peak heights linear with injection volume as shown in Fig. 4. Linear regression analysis of the two calibration plots showed a correlation coefficient of 0.9981 and a slope of 0.40 μA μg^{-1} injected. A linear working range was obtained for injections of 0.02—80 μg of cadmium which

TABLE 1

Hydrodynamic electrochemical characteristics at a copper-amalgam electrode in 0.2 M ammonia buffer

Metal	$E_{1/2}$ (V)	Sensitivity (μA μg^{-1})	Detection limit (ng)
Cu	—[a] (−0.53)[b]	0.43	2.7
Cd	−0.79 (−0.81)	0.40	3.2
Zn	−1.28 (−1.33)	0.51	3.3

[a]Not measurable because of anodic decomposition of the electrode. [b]$E_{1/2}$ values in parentheses are for the DME [1].

gave reproducible peak heights with no effect on baseline. The Cu/Hg electrode sensitivity is shown in Table 1 for the particular electrode area used here (0.008 cm^2).

Precision, carry-over and detection limit

Cadmium samples were injected at the rate of two per minute as shown in Figs. 4 and 5. Figure 5B shows a peak width of 12 s, i.e., the time required for the current reading to return to baseline, so that there was no carry-over between samples. The precision (relative standard deviation) obtained for replicate 3-μl injections of the same sample (1.0×10^{-2} M) was 0.6% as shown in Fig. 5A. The effect on baselines given in Figs. 4 and 5 was negligible and peak heights remained constant after injection of 26 samples over a period of 15 min.

Hence, the use of a solid amalgam electrode has been shown to be reproducible despite the accumulation of solid metal deposit in the amalgam. The reaction occurring at the electrode is a 2-electron reduction of $[Cd(NH_3)_4]^{2+}$ to Cd^0 (amalgam). The absence of drift and the peak precision obtained is indicative of many possible applications of the flow cell described here in the reductive mode of operation, including use as a liquid chromatographic detector. However, baseline drift was observed when maximum current sensitivity was used over a period of 20 min with injection of 80 ng of cadmium. The drift was about 0.3 nA min^{-1}, with a noise level of about 0.5 nA when the low pass filter was set on the 1.0 s time constant.

The presence of oxygen and the high noise level of the pump used in this flow system prevented the attainment of very low limits of detection for cadmium. The noise level was approximately 0.5 nA after deaeration of the

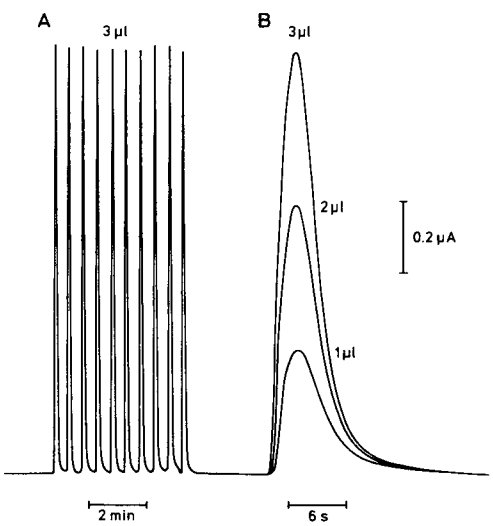

Fig. 5. Precision (A) and response speed (B) for flow-injection determination of a cadmium sample (1.0×10^{-2} M), recorded at different chart speeds: (A) 1.0; (B) 20 cm min^{-1}.

carrier buffer solution, but the presence of traces of oxygen increased the noise level, drift and baseline current. The detection limits for metal ion samples prepared in sodium sulphite to reduce oxygen content were determined by injecting 12 replicates of 80 ng; calculated as 3σ, the values obtained were 2.7, 3.2 and 3.3 ng for Cu, Cd, and Zn, respectively (Table 1). These are higher than those found by Bratin and Kissinger [4] who used thin-layer glassy carbon electrodes for determination of reducible organic molecules, and by Bond and Wallace [14] for metal complex oxidations under h.p.l.c. conditions. The detection limits in this work could obviously be improved by use of a pump with lower pulsing rate with high pressure flow in order to obtain a lower noise level, and also by more rigorous exclusion of oxygen. However, no attempt was made to do this, as the main purpose of this study was to show that even with injections of relatively large quantities of metal ion, the Cu/Hg electrode functions with a reproducible response.

Conclusions

The copper amalgam electrode operated in a miniature flow-cell has been shown to respond reproducibly to metal ion reductions in a complexing medium. The applications of this electrode configuration are feasible in many areas where the DME, SMDE, and mercury-pool electrode have been used previously, but without their clumsy electrode configurations. Gold could obviously be used in a similar way, but it dissolves in the mercury, and hence has a limited lifetime, and the hydrogen overvoltage is lower than on copper [18]. The advantage of gold/amalgam electrodes [4, 6] is the wider anodic range possible, but copper has the advantages of low cost and ready availability.

REFERENCES

1 I. M. Kolthoff and J. J. Lingane, Polarography, Vols. I and II, Interscience, New York, 1952, pp. 887—953.
Application Notes, No. ABT2, E.G. & G. Princeton Applied Research, Princeton, NJ, U.S.A.
2 K. Toth, G. Nagy, Z. Feher, G. Horvai and E. Pungor, Anal. Chim. Acta, 114 (1980) 45.
3 A. Ivaska and W. F. Smythe, Anal. Chim. Acta, 114 (1980) 283.
4 K. Bratin and P. T. Kissinger, Talanta, 29 (1982) 365.
5 W. A. MacCrehan, Anal. Chem., 53 (1981) 74.
6 W. A. MacCrehan and R. A. Durst, Anal. Chem., 50 (1978) 2108.
7 J. A. Lown and D. C. Johnson, Anal. Chim. Acta, 116 (1980) 41.
8 W. J. Blaedel and J. H. Strohl, Anal. Chem., 36 (1964) 445.
9 P. W. Alexander and H. Marpaung, Talanta, 29 (1982) 213.
10 P. Maitoza and D. C. Johnson, Anal. Chim. Acta, 118 (1980) 233.
11 P. W. Alexander and S. H. Qureshi, J. Electroanal. Chem., 71 (1976) 235.
12 J. Janata and J. Růžička, Anal. Chim. Acta, 139 (1982) 105.
13 K. Stulik and V. Hora, J. Electroanal. Chem., 70 (1976) 253.
14 A. M. Bond and G. G. Wallace, Anal. Chem., 54 (1982) 1706.
15 A. M. Bond and G. G. Wallace, Anal. Chem., 53 (1981) 1209.
16 P. W. Alexander, R. J. Finlayson, L. E. Smythe and A. Thalib, Analyst, 107, in press.
17 J. Růžička and E. H. Hansen, Flow Injection Analysis, Wiley, New York, 1981.
18 J. O'M. Bockris and S. U. M. Khan, Quantum Electrochemistry, Plenum Press, New York, 1979, p. 321.

Analytica Chimica Acta, 148 (1983) 111—125
Elsevier Science Publishers B.V., Amsterdam — Printed in The Netherlands

SELECTIVITY IN FLOW INJECTION ANALYSIS

E. H. HANSEN* and J. RŮŽIČKA

Chemistry Department A, The Technical University of Denmark, DK-2800 Lyngby (Denmark)

F. J. KRUG and E. A. G. ZAGATTO

Centro de Energia Nuclear na Agricultura (CENA), C.P. 96, 13.400 Piracicaba, S.P. (Brasil)

(Received 18th October 1982)

SUMMARY

A generalized method for assessing the extent of interference of foreign species on a given chemical assay is proposed. The interference can be quantified by a parameter termed selectivity coefficient. The method is based on injecting the analyte and the interfering species simultaneously, and then letting them merge either synchronously or asynchronously; the analytical readout is taken from that element of fluid where the dispersion of the two species is identical. It is shown that this makes the accompanying calculations simple, because the selectivity coefficient can be related directly to the originally injected concentrations. The general interference method is demonstrated for a spectrophotometric procedure for the determination of manganese with formaldoxime, and the selectivity coefficients for various metal ions are determined. The applicability of three different f.i.a. manifold configurations is discussed.

No chemical method used analytically is completely interference-free, yet the ability of any assay to provide a result unbiased by the presence of foreign species is crucial to its practical application. Interference may be caused either by individual species, or by the collective influence of many species which may arise from not only chemical but also physical phenomena such as ionic strength or viscosity, which latter are usually termed matrix effects. The mechanisms of interference may vary: the interference may be caused by a substance providing a signal by a mechanism similar to that of the analyte (SM interference), or to an interference in which the analytical signal is influenced by a different mechanism than the analyte (DM interference) [1]; the extent of interference may also be subject to kinetic factors. Furthermore, the degree of an interference is not necessarily proportional to the concentration of the content of the interfering species in a sample, and the effect of the presence of several interferents may not always be additive. Synergic as well as compensating effects may occur. But, whatever the source or mechanism of an interference, the information essential to the practising analyst is the (overall) effect of particular concentrations of other substances on particular concentrations of the analyte under the experimental conditions required by the analytical method.

0003-2670/83/$03.00

Despite the abundant literature on the subject, there is no universally accepted definition of the term interference. Wilson [2] has proposed the following definition: "An interfering substance for an analytical method is one that causes systematic error (of any magnitude) in the analytical result for at least one concentration of the determinand within the range of the method". This definition has been adopted as the basis for defining the selectivity coefficient in potentiometry and has met with general acceptance. Yet in spectrophotometry it is still normal to give only qualitative statements indicating the levels of interfering ions that can be tolerated for certain levels of the primary ion. This may seem surprising insofar as photometry is a classical analytical technique which still accounts for more than 50% of all chemical assays performed today. The lack of a more quantitative statement of interfering effects can probably be attributed to the complexity of the sources of interference, which make it virtually hopeless to try to reproduce exactly the experimental conditions between individual sets of experiments and between separate laboratories. In order to quantify the extent of interferences, it is essential to be able to conduct all measurements at precisely defined and reproducibly maintained conditions so that the interfering species are treated, physically and chemically, in exactly the same manner as the substance to be determined (analyte).

Such identical treatment can be achieved in flow injection analysis (f.i.a.) where all experimental parameters such as sample volume, residence time, dispersion, temperature and time of exposure of sample and/or interferent(s) to the reagent(s) can be rigidly controlled and reproducibly maintained. With these conditions met, it makes sense to attempt to express the selectivity of a method for species A of concentration C_A, towards an interfering species B of concentration C_B, by a numerical value. As any interfering species always will appear as positive or negative "pseudo A", it is suggested that this interference parameter can be expressed quantitatively as the selectivity coefficient k_{AB}, defined for any f.i.a. method, similarly to the approach adopted in potentiometry, by the equation

$$C'_A = C_A + k_{AB}C_B \tag{1}$$

where C'_A is the total concentration of A measured. While the combined effects of several interfering species as mentioned above may not necessarily be additive, the k_{AB} value can be perceived as a conditional selectivity coefficient for a particular matrix of fixed composition. Such conditional coefficients should prove to be reasonably reproducible in other laboratories even under slightly different experimental conditions for a particular procedure.

The concentrations C_A and C_B in Eqn. (1) are, of course, the concentrations as measured by the detector. In f.i.a., these concentrations are related to the originally injected concentrations C^0_A and C^0_B through the dispersion coefficients D_A and D_B where $D_A = C^0_A/C_A$ and $D_B = C^0_B/C_B$. [In accordance with IUPAC nomenclature, it is suggested that the term dispersion be used

for the physical dilution process of the injected sample taking place in the f.i.a. system, while the term dispersion coefficient is reserved for numerical expression of the extent of the dispersion process in a particular segment of fluid of the dispersed sample zone. Thus if the analytical readout is taken at peak maximum the dispersion coefficient D_{max} will be given by C^0/C^{max} while the dispersion coefficient D for any other point on the peak is C^0/C, where C is the concentration in that particular segment of the injected and dispersed sample zone which constitutes the basis for the analytical readout, thus corresponding to a point on the f.i.a. gradient curve, for which $D \geqslant D_{max}$.] Provided that the system and detector used gives a linear response to the concentration of A and B then the recorded signal H will be given by $H = k\ C'_A$, where k is a constant. For the A species alone, this yields $H_1 = k\ C_A = k\ C^0_A/D_A$, but for a mixture of A and B, the equation becomes

$$H_2 = k\ (C_A + k_{AB}C_B) = k\ [(C^0_A/D_A) + k_{AB}\ (C^0_B/D_B)] \tag{2}$$

Identical treatment of the primary species A and the secondary species (interferent) B implies that whatever experimental conditions (manifolds) are used, the actual measurements must always be made of the point(s) where the dispersion coefficients for A and B are identical. Thus for $D_A = D_B = D$, the expressions for H_1 and H_2 yield

$$D = (k/H_1)\ C^0_A = (k/H_2)\ (C^0_A + k_{AB}C^0_B) \tag{3}$$

$$\text{or } k_{AB} = [(H_2/H_1) - 1]\ C^0_A/C^0_B \tag{4}$$

Thus, the higher the k_{AB} value, the more secondary species B will interfere in the measurement of the primary species A, and this interfering effect may be either positive (more species A found than actually present), or negative (depression of signal generated by A in the presence of B). Accordingly, the selectivity coefficient may have a positive or a negative value.

Equation (4) may be rearranged to

$$H_2 = (k_{AB}H_1\ C^0_B/C^0_A) + H_1 \tag{5}$$

which shows that for a fixed concentration of C^0_A, and hence a fixed value of H_1, a graphical representation of H_2 against C^0_B will yield a line where the k_{AB} value can be calculated from the slope for any concentration of C^0_B within the interference range covered. If k_{AB} is constant, a straight line will be obtained (the sign of the slope indicating if k_{AB} is positive or negative) while if k_{AB} varies with different levels of C^0_B, the line will bend; for increasing values of C^0_B it will bend upward with increasing value of k_{AB}, and downward with decreasing value of k_{AB}.

In trace analysis, it is often convenient to express concentration levels in ppm (μg ml^{-1}) or ppb (ng ml^{-1}). If all concentrations are given in the same units (say ppm as represented by c_i), Eqns. (4) and (5) become

$$k_{AB} = [(H_2/H_1) - 1]\ (c^0_A m_B/c^0_B m_A) \tag{6}$$

and $H_2 = (k_{AB}H_1 m_A\, c_B/c_A^0 m_B) + H_1$ (7)

where m_A and m_B are the molecular weights of species A and B, respectively.

When a flow injection system is designed for selectivity measurement, two provisions must be kept in mind: (a) the manifold must be similar to that used for the actual routine measurement of A so that all conditions remain constant with or without the presence of interferent B; and (b) measurements must be made on that segment of fluid where $D_A = D_B$.

In this paper three different manifold designs will be discussed in detail. The first design, Fig. 1(a), uses the premixed solution technique, i.e., where A and B have to be premixed prior to injection; the other two designs allow the use of individual solutions of A and B which are mixed in the flow injection system by the merging zone technique, either synchronously (Fig. 1b) or asynchronously (Fig. 1c), i.e., the zones merge either totally or partially. Advantages and disadvantages of each approach are discussed below. It is, however, useful to point out here that all the flow injection techniques described below offer particular advantages when used for determining the k_{AB} values. Thus all selectivity measurements are made under conditions similar to those of actual determinations, and the only concentrations which need to be known are the originally injected concentrations C_A^0 and C_B^0.

To compare the merits of these three approaches, the same spectrophotometric procedure was investigated, employing the colour-forming reaction

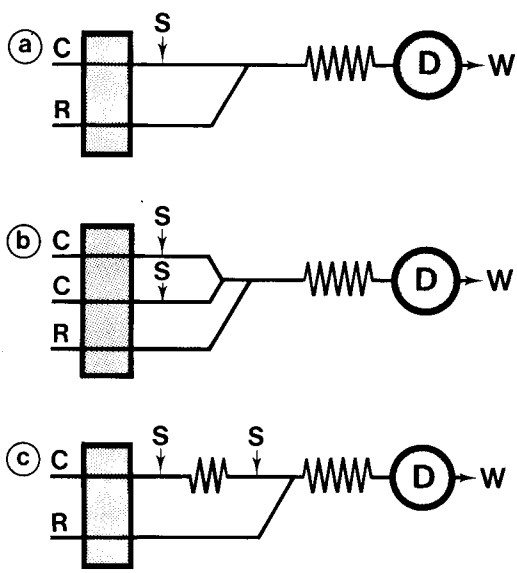

Fig. 1. Schematic drawings of f.i.a. manifolds used for interference measurements by: (a) premixed solution method; (b) two-line system for synchronous or asynchronous merging of the injected samples A and B; and (c) one-line system for asynchronous merging of samples of primary and secondary species. C, carrier stream; R, reagent stream; S, sample inject position; D, detector; W, waste. For details see also Figs. 2—5.

between manganese and formaldoxime. In alkaline medium, these two components initially form a colourless manganese(II) complex which on oxidation by atmospheric oxygen is converted instantaneously to an orange-red complex of manganese(IV), the absorbance of which can be measured at 455 nm [3]. This reaction has been applied in a flow injection method for manganese in waters and plant digests [4]. Irrespective of the reagent used for pH adjustment and the excess of formaldoxime, only one coloured complex is formed in the solution. The Mn:CH_2NOH ratio in this complex is 1:6, corresponding to $[Mn(CH_2NO)_6]^{2-}$. Formaldoxime, however, forms coloured complexes with metals having chromophoric properties, such as Ni(II), Co(II), Fe(III) and Cu(II); as these complexes all exhibit pronounced absorption at 455 nm, these metal ions interfere with the manganese determination, and the interferences are quantitatively evaluated.

EXPERIMENTAL

Apparatus and materials

All experiments were done with a BIFOK-TECATOR FIA-5020 Flow Injection Analyzer equipped with a two-channel rotary injection valve of fixed sample volume (30 μl). Optical measurements were made with a Bausch & Lomb Mini 20 spectrophotometer adjusted to 455 nm and equipped with a FIAstar tubular flow cell [5]. The transmittance signal from the spectrophotometer was fed to a logarithmic converter and then simultaneously to the microprocessor of the FIA-5020 via the detector input terminal and to a recorder (Radiometer Servograph REC-61 furnished with a REA-112 high-sensitivity unit). Results were digitally displayed on the FIA-5020 and written out on an attached printer (Alphacom, Sprinter 40). For peak-maximum measurements, the peak-height program of the FIA-5020 was used; for peak-height measurements of other delay times, the gradient program was used for for the selected and preprogrammed delay time.

Microline tubing (0.5 mm i.d.) was used throughout for construction of manifolds (for coil lengths used in the various manifolds, see Results). The peristaltic pump 1 of the FIA-5020 unit was used for pumping carrier and reagent streams, while pump 2 was used for aspirating sample materials. The automated sequential operation of the pumps was controlled by the microprocessor of the FIA-5020.

Reagents

All reagents were of analytical-reagent grade. Distilled and degassed water was used throughout.

The carrier stream (Figs. 2, 3 and 5) in all experiments consisted of distilled water to which was added 0.01% Brij-35.

The reagent solution (R, Figs. 2, 3 and 5) was a 1:1 mixture of formaldoxime and 2.8 M ammonia solution. The formaldoxime solution was prepared by dissolving 25.0 g of paraformaldehyde and 58.75 g of hydroxylammonium

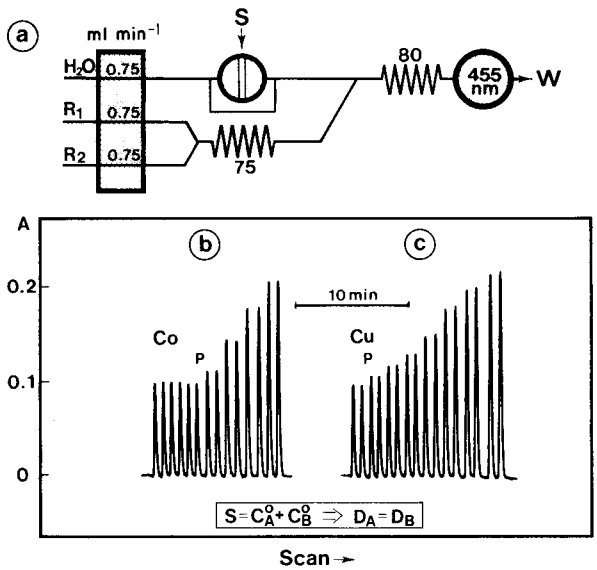

Fig. 2. (a) Manifold for interference studies by the premixed solution method. Reagents R_1 (formaldoxime) and R_2 (ammonia) are premixed in the 75-cm coil before being merged with the carrier stream (H_2O) into which the samples are injected; mixing with the reagent solution occurs in the 80-cm coil. (b) Injection of premixed samples, each containing C^0_{Mn} = 6 ppm and increasing levels of Co(II) (from left to right): 0, 5, 10, 25, 50, 75 and 100 ppm, each sample injected in duplicate. P denotes the position where interference starts to occur. (c) Injection of premixed samples, each containing C^0_{Mn} = 6 ppm and increasing levels of Cu(II): 0, 6.25, 12.5, 25, 50, 75, and 100 ppm, each sample injected in duplicate.

sulphate in 350 ml of water with gentle heating (50—60°C), and diluting with water to 500 ml. The ammonia solution (2.8 M) was made by diluting 190 ml of 25% ammonia solution (d = 0.88) to 500 ml. The 1:1 mixture of these reagents is stable only for a couple of days as it gradually turns yellow in time. Thus, either the mixture should be prepared fresh daily, or mixing can be done directly in the flow injection manifold prior to merging with the carrier stream (cf. manifold Fig. 2a, where R_1 and R_2 denote the formaldoxime and ammonia reagent lines).

Standard solutions of Mn(II), Ni(II), Co(II), Fe(III) and Cu(II) were made by suitable dilutions of 1000 ppm stock solutions prepared from $MnSO_4 \cdot H_2O$, $Ni(NH_4)_2(SO_4)_2 \cdot 6H_2O$, $CoSO_4 \cdot 7H_2O$, $Fe(NH_4)(SO_4)_2 \cdot 12H_2O$, and $CuSO_4 \cdot 5H_2O$, respectively. All standards were prepared in 0.005 M sulphuric acid to prevent hydrolysis. Hence, all injected blank solutions consisted of 0.005 M sulphuric acid.

RESULTS

Mixed solution method

This approach requires the manual preparation of a series of mixtures, containing a fixed level of the primary species A and increasing concentra-

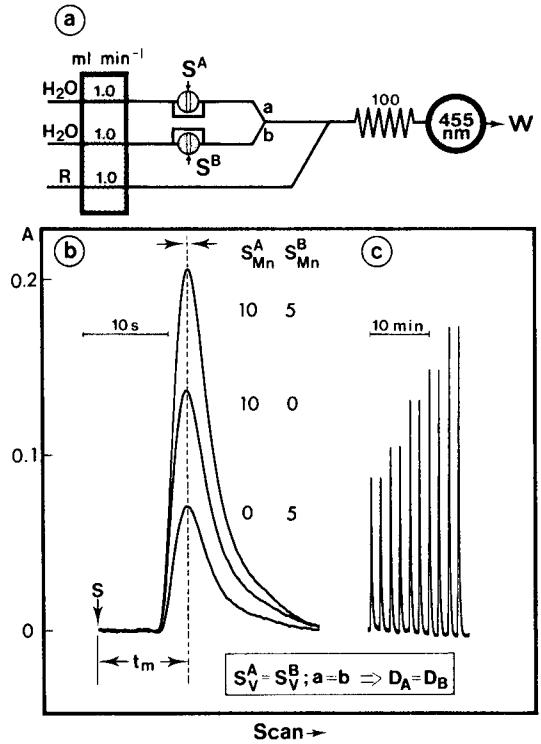

Fig. 3. Synchronous merging of samples S^A and S^B injected simultaneously into two separate carrier streams (water). (a) Manifold with identical lengths of a and b (13 cm); R is the premixed formaldoxime—ammonia solution. (b) Test of synchronization, where identical sample volumes of manganese(II) ($S_V^A = S_V^B$) are injected by means of valves A and B; the concentrations of C_{Mn}^A and C_{Mn}^B are (from the top) 10 and 5 ppm, 10 and 0 ppm, and 0 and 5 ppm, respectively; t_m is the delay time at which the peak heights were recorded for quantitative evaluation (corresponding to the peak maximum). (c) Interference of Ni(II) on manganese, where C_{Mn}^A = 6 ppm and C_{Ni}^B = 0, 2, 5, 7, and 10 ppm, respectively; each level run in duplicate.

tions of the secondary species B, which are then injected into the flow system. As examples, the interferences of cobalt and copper on the determination of Mn(II), in the manifold depicted in Fig. 2(a), are shown in Fig. 2(b) and (c); the reagent streams of formaldoxime and ammonia are premixed in the 75-cm coil. The C_{Mn}^0 was fixed in all injected solutions at 6 ppm while the concentrations of the interfering ion (Co or Cu) covered the range 0—100 ppm. An increase in the peak height thus indicated the interference of species B on Mn, and k_{MnB} values were evaluated from the position of the break point P, situated between injections producing no apparent interference and those where the level of B influenced the peak height. A comparison of Fig. 2(b) and (c) shows that cobalt interferes less than copper with the measurement of manganese. Precise k_{MnB} values were computed from the individual peak heights according to Eqn. (6) (cf. Table 1). If the interference

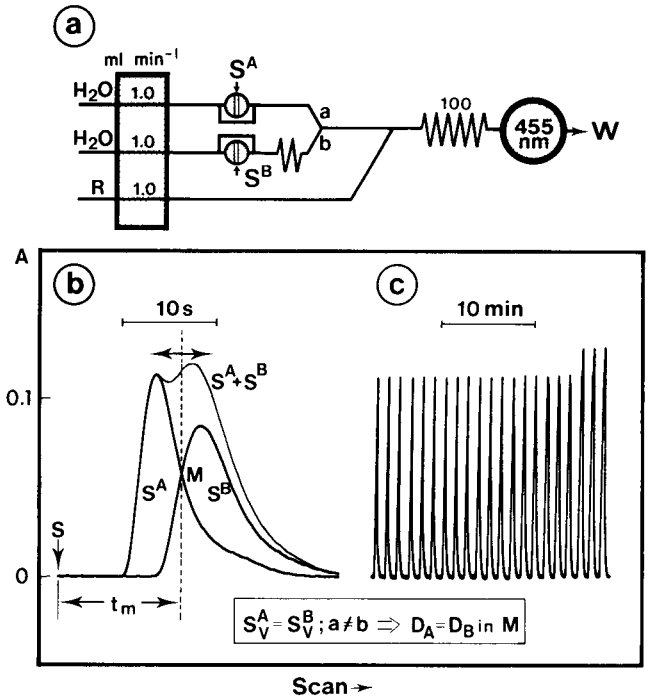

Fig. 4. Asynchronous merging of samples S^A and S^B injected into two separate carrier streams (water). (a) Manifold with a ≠ b (a = 13 cm; b = 48 cm). (b) S^A and S^B are the outputs obtained by injecting samples of identical volume and concentration of manganese(II) (6 ppm) alternately into valves A and B; the composite curve $S^A + S^B$ is obtained by injecting the samples simultaneously. Quantitative evaluation is done at delay t_m corresponding to M where $D_A = D_B$. (c) Interference of Co(II) on manganese, where C^A_{Mn} = 6 ppm and C^B_{Co} = 0, 5, 10, 25, 50, 75, and 100 ppm; all samples injected in triplicate.

is proportional to the concentration of the interfering species, the k_{MnB} value may also be obtained by extrapolation to that signal level which is twice as high as that of manganese alone, in which case Eqn. (4) simplifies to $k_{AB} = C^0_A/C^0_B$. It is of interest that this provision is obviously valid for nickel as interferent (Table 1) throughout the concentration range, but not for cobalt and copper for which the k_{MnB} values progressively increase and decrease, respectively, with increasing concentration of the interferent.

The significant advantage of the mixed solution method is that the interference measurements are made in the manifold used for the actual assay without any alterations or modifications whatsoever. Furthermore, as A and B are injected simultaneously by the same valve cavity the dispersion for both the primary and secondary species are identical at every segment of the dispersed sample zone, i.e., the quantitative evaluation of the interference can be done at any point of the recorded signal. For convenience, it is, of course, preferable to measure the peak maximum heights. The drawback of this approach is that all the injected solutions must be premixed,

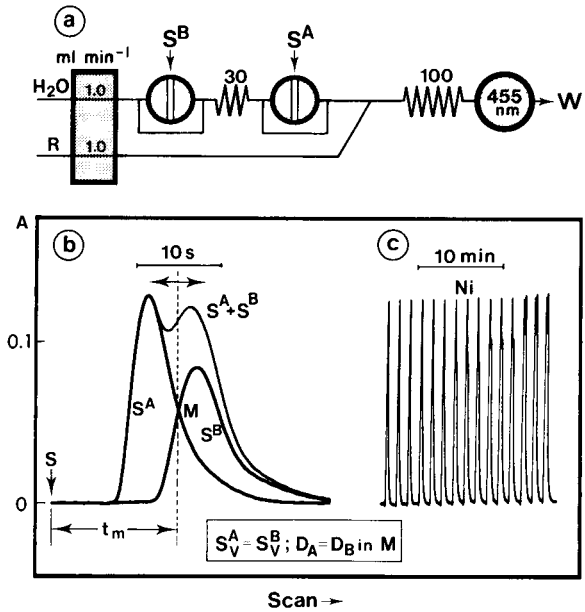

Fig. 5. Asynchronous merging of identical volumes of samples S^A and S^B injected simultaneously into a one-line carrier system (water) by two separate valves (A and B). (a) Manifold with a 30-cm coil between A and B which delays sample B relative to sample A before both samples are merged with the reagent stream. (b) Injection of manganese(II) (6 ppm) alternately by valves A and B (curves S^A and S^B), and then simultaneously (composite curve $S^A + S^B$). At point M, corresponding to delay time t_m, the dispersion for both curves is identical. (c) Interference measurements for nickel, where $C^A_{Mn} = 6$ ppm and $C^B_{Ni} = 0, 2, 5, 7$ and 10 ppm, with each sample level injected in triplicate.

making the procedure tedious as separate series of solutions must be prepared for each secondary species B and each concentration level of primary species A. Hence, it would be preferable to inject individual solutions of the primary and secondary species separately and mix them in the desired ratios automatically in the channel of the flow injection system.

Separate solution methods

In these methods, the primary and secondary species are injected separately by means of a double valve (Fig. 1b) or by two valves connnected in series (Fig. 1c) and then merged prior to mixing with the reagent R. The simultaneous injection of A and B into two separate lines may result in synchronous or asynchronous merging, (Figs. 3 and 4), while the use of a single-line system with two valves only allows asynchronous merging of the two zones (Fig. 5). It should be recalled that, regardless of the flow design used, the signals must be obtained from those segments of fluid where the condition $D_A = D_B$ holds.

Method I. Injection into separate lines with synchronous merging. Details of the manifold used for the interference measurement of various cations on

TABLE 1

Comparison of k_{MnB} values found by different methods[a] and calculated by Eqn. (6)

B	C_B^0 (ppm)	Mixed solution method	Separate solutions methods			
			Synchronous merging 2-line b	Synchronous merging 2-line c	Asynchronous merging 1-line	Asynchronous merging 2-line
	2	0.72	0.69	0.62	0.63	0.67
	5	0.74	0.69	0.62	0.63	0.67
Ni(II)	7	0.74	0.68	0.62	0.63	0.69
	10	0.74	0.68	0.62	0.61	0.67
	5	−0.016	−0.13	−0.091	0.024	−0.024
	10	−0.016	−0.049	−0.038	0.048	0.023
Co(II)	25	0.031	0.033	0.012	0.068	0.056
	50	0.061	0.061	0.034	0.068	0.065
	75	0.069	0.068	0.040	0.068	0.064
	100	0.070	0.068	0.042	0.067	0.063
	6.25	0.22	0.29	0.21	0.27	0.21
	12.5	0.17	0.21	0.15	0.19	0.17
Cu(II)	25	0.15	0.17	0.12	0.15	0.16
	50	0.12	0.14	0.09	0.12	0.15
	75	0.09	0.12	0.07	0.10	0.14
	100	0.08	0.10	0.06	0.09	0.13
	12.5	0.010	0.012	0.014	0.018	0.017
	25	0.011	0.012	0.011	0.022	0.017
Fe(III)	50	0.014	0.015	0.013	0.022	0.015
	75	0.018	0.016	0.016	0.027	0.017
	100	0.021	0.018	0.017	0.028	0.019
t_m (s)		11	10	16	14	12
D_m^d		5	9.4	10.6	12.9	18.5

[a]All measurements done at C_{Mn}^0 = 6 ppm. [b]Manifold Fig. 3(a). [c]Manifold Fig. 3(a), where each of the two carrier solutions was pumped at a rate of 0.53 ml min^{-1} while the pumping rate of the reagent solution was unaltered. [d]Measured by means of dye of known concentration [4].

the manganese procedure are given in Fig. 3(a). The synchronous merging is achieved by pumping the injected zones of equal volumes of A and B through equally long lines (a = b) in which the pumping rates are identical. This synchronization is conveniently checked by injecting zones of A (Mn) alternately by both valves and by recording the peaks at high chart rate. Figure 3(b) shows this check of synchronization of the two zones, and Fig. 3(c) shows the actual signal output for a series of injections of increasing concentrations of nickel (2, 3, 7 and 10 ppm Ni) for a fixed level (6 ppm) of

manganese (cf. Table 1). When exact synchronization of the two injected zones is achieved, the dispersion of both species in the merged zone is identical along the whole merged gradient and therefore quantitative evaluation may be applied, as in the previous method, at any point of the recorded signal (Fig. 3b). Yet it is most practical to measure peak maximum heights and to calculate the k_{MnB} value as in the premixed solution method.

Method II. Injection into separate lines with asynchronous merging. The asynchronous merging in a two-line system may be done either by pumping the carrier solution of the two lines at different rates, or by making the lines between the injection valve and the merging point of different lengths (i.e., $a \neq b$ in Fig. 4a). Advantage is then taken of the fact that within that region where the two zones overlap there is always a segment of fluid, characterized by a certain delay time t_m (Fig. 4b), where the dispersion for both sample zones is equal ($D_A = D_B$). This delay time t_m is easily identified by injecting identical sample concentrations into each loop in two separate experiments, and by recording the resulting peaks from the same starting point. Thus curves S^A and S^B in Fig. 4(b) were recorded by injecting 6 ppm Mn alone by sample loop A and B, respectively, from the same starting point (S). The composite curve $S^A + S^B$ was obtained by simultaneous injection of 6 ppm Mn from both sample loops. As the sum of a set of linear processes will yield a linear response, the signal recorded at any composite curve $S^A + S^B$ at delay time t_m (point M where the dispersions for S^A and S^B are identical) will be, for a fixed level of A, a function of the concentration of B injected into loop B. Once determined, this delay time, t_m, may be programmed into the microcomputer of the FIA-5020; then by using the "gradient read-out mode" of the analyzer, all readouts (Fig. 4c) can be done at this particular delay time, thus facilitating the evaluation.

The practical advantage of the separate solutions methods is that only a few solutions have to be prepared: essentially only a single solution of A and a few solutions of B. The method has, however, a serious drawback: it is essential that the flow rates in both channels be maintained absolutely constant throughout all experiments. The injected zones must merge strictly reproducibly at all times, otherwise the requirement that all measurements be made at $D_A = D_B$ is no longer met. For both synchronous and asynchronous merging, the precision is critically dependent on maintaining not only the ratio of the two pumping rates, which is generally quite easy to do with a peristaltic pump, but also their absolute values, which is significantly more difficult. Thus, a more practical flow system would allow the two species to be injected separately without particular attention to keeping the pumping rates in both lines absolutely constant. Method III is such a system.

Method III. Injection into a single line with asynchronous merging. This procedure is similar to the above asynchronous merging approach, but the two zones A and B are injected by means of a double valve into a single carrier line, and the two injection zones are separated by a suitable length of delay coil (Fig. 5a). Again advantage is taken of the fact that the over-

lapping part of the two zones contains an element of fluid where the dispersions D_A and D_B are equal at a definite delay time t_m; once determined as described above, t_m can be programmed into the FIA-5020 (Fig. 5b). As B has to travel through a longer path than A, injection of identical concentrations in the two valves will result in peaks of different heights. There is only one carrier line, and any change in the pumping rate will influence the delay time t_m corresponding to point M, but not as seriously as a change in a pumping ratio between two lines. Once M and t_m have been determined, they can readily be rechecked by injecting a fixed concentration of A alternately by each valve: if M has remained unchanged, the peak height measurements for each injection should be identical.

A series of measurements for the determination of the interference of nickel on the manganese procedure is shown in Fig. 5(c). The 30-cm delay coil placed between the valves (Fig. 5a) disperses zone B to an extent such that the signal recorded at point M corresponds to approximately half the peak maximum recorded for zone A (Fig. 5b). Consequently, the peak maximum height of the manganese peak itself will not be affected by increasing concentrations of nickel, because the segment of fluid corresponding to the peak maximum contains no nickel, yet at any longer delay time t_m, the recorded signal will increase with increasing concentrations of the interfering species. This is observed at higher concentrations of nickel where double peaks are formed (Fig. 5c).

DISCUSSION

Comparison of the values of the selectivity coefficients summarized in Table 1 shows that all four methods give valuable information on the interfering effects of various secondary ions on the spectrophotometric determination of manganese. A closer look reveals differences between individual methods as well as between k_{MnB} values found with increasing levels of the interfering species. While the k_{MnNi} value is constant over the range studied by any of the proposed methods, thus indicating a true selectivity constant, the k_{MnCo} values increase and tend to level off at higher concentrations of cobalt(II). In contrast, the k_{MnCu} values tend to decrease with increasing concentrations of copper(II). As all the values of "pseudo Mn", equivalent to $k_{MnB}C_B$, fall within the linear range of the manganese calibration, these deviations are certainly not due to reagent deficiency. Yet, as mentioned in the introduction, the reasons for deviation from linearity may be quite complex, including kinetic factors; what is observed and measured by the proposed methods are, indeed, the collective influences exerted by all factors associated with the presence of the foreign species. Therefore, in the rigorously controlled conditions of f.i.a., the k_{AB} values yield useful information, even with changing levels of interfering species, about the maximum permissible level of secondary ion at which no interfering effect is observed. The values also serve as a quantitative guide to the levels at which potential interferences actually require to be corrected for.

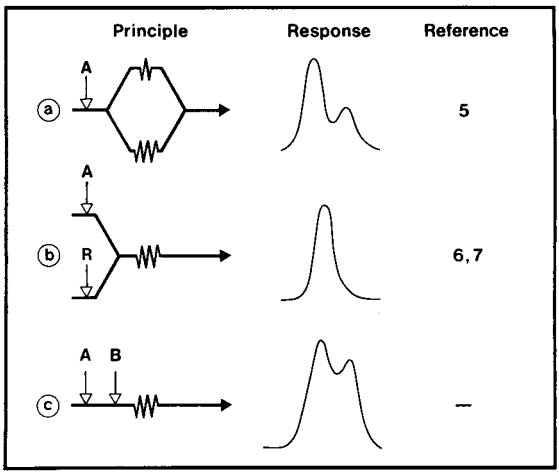

Fig. 6. Development of merging-zone techniques. A, analyte; R, reagent; B, interfering species.

Comparison of the values of the selectivity coefficients for each species B obtained by different methods outlined above, shows that the differences between the k_{MnB} values are remarkably small. Seen from a practical viewpoint of estimating the maximum permissible level of interfering species, the information obtained by all methods used is the same. Closer examination reveals, however, that the conditions for colour formation differ in the different experimental setups. In all cases, precautions were taken to mix the manganese with B prior to contact with the reagent stream (cf. flow diagrams in Figs. 1, 2, 3 and 5), but there are still differences in the t_m and D values between individual methods. This means that there are slight differences between the individual methods with respect to the reaction times of metal ions with formaldoxime, and the reagent excess over the metal ions present. While these differences in reaction conditions are not significant for interference studies with Ni, Co and Fe, the value of k_{MnCu} is lower for high concentrations of copper in the method with low D and t_m. Thus a lower interference of copper with increasing concentration is found, which contrasts with what would be expected intuitively. Yet, this observation should be treated with reservation as the differences are rather small.

From the practical viewpoint of obtaining rapid reliable information on the selectivity of a particular f.i.a. procedure, the choice of method is straightforward: the mixed solution method (Fig. 1a) and the asynchronous one-line merging approach (Fig. 1c) are the best techniques as they require the simplest manifolds and least experimental skill, and are closest to the conditions of an actual assay.

There is nothing simpler than to inject into a flow injection system a mixture of A plus B, rather than A alone in order to estimate the interfering effect. For more comprehensive studies, however, a double-barrelled valve

and a coil seem to be a good replacement for a single valve; this will allow more flexibility in testing a number of interfering species, and in further development of a method, should the composition of the reagent stream be modified by adding masking agents in order to increase selectivity. The speed of the f.i.a. method will thus allow rapid screening of a number of experimental variables (pH, reagent concentration, masking agents) which will allow the selectivity of the method to be enhanced. Though such optimization studies will always begin with conditions described in the literature and obtained by batch methods and equilibrium methods, the dynamic f.i.a. conditions will necessarily yield different selectivities than conventional methods as soon as kinetic factors (reaction rates) become significant. Whether or not these differences will play into the hands of the practising analyst will probably depend on the chemistry of the method used, but it is obvious that f.i.a. offers a reliable approach for very rapid detection of whether an interference occurs and for quantitative estimation of the selectivity of the method.

CONCLUSION

The new approach to selectivity measurements described above is not limited to spectrophotometric measurements. Obviously the selectivity of any other f.i.a. method can be evaluated in the same manner, regardless of the detector employed. Both SM and DM interferences can be detected and their magnitude described by a number which, because of the reproducibility of all processes within the f.i.a. system, precisely describes the extent of the influence of a foreign species on the analytical result.

Once detected, the interference may be easier to eliminate, either by masking procedures or by modification of the detector. For this purpose, the proposed method is an excellent diagnostic tool. By changing the environment for the chemical reactions involved (pH, reagent concentration, etc.) the search for less interference-prone conditions may be carried out effectively and with relative ease compared to manual procedures.

Another aspect of the present approach is its use as a vehicle for the standard addition technique. If species A is regarded as the unknown sample, known additions of the same analyte in concentrations bracketing the unknown level present in A can be injected as "pseudo species B". This will allow corrections to be made for (moderate) interfering contributions of unknown foreign species. Because at least two (but preferably several) standard additions will be needed, the one-line asynchronous merging method, with a readout at delay t_m, will be most practical to use (cf. Fig. 5).

In conclusion, a short review of existing f.i.a. methods based on zone merging and zone splitting (Fig. 6) places the above-described approaches into a wider perspective and suggests some future trends. The purpose of the first f.i.a. paper on zone splitting and merging [6] (Fig. 6a), was to accommodate the peak height within the span of the recorder chart in the

spectrophotometric assay of water samples from the Amazone estuary containing chloride at widely varying concentrations. For this purpose, each sample zone was split and merged again in asynchronous mode yielding a set of double peaks, the twin peak maxima having a fixed ratio. The next step, the merging zone approach (Fig. 6b), developed independently in Brasil [7] and in Denmark [8], allowed synchronous merging of sample and reagent zones with the aim of reducing reagent consumption [7] and asynchronous merging with the aim of reducing the peak height (in cases where the concentration of analyte was too high [8]). The present work follows the concept of zone merging to another variant, zone penetration (Fig. 6c). While this may be viewed as the development of yet another f.i.a. technique, it is important to appreciate that its exploitation for selectivity studies is possible only through the concept of controlled dispersion. The segment of fluid, within which the dispersion coefficients of the primary and secondary species are equal ($D_A = D_B$), carries unique information and this allows the technique of merging zones to be fully exploited for interference studies. There is no doubt that closer examination of dispersion coefficients of individual, merging or penetrating zones will reveal further possibilities which the gradient flow injection methods [9] offer as new tools for instrumental analyses.

The authors express their appreciation to J. Janata for enlightening discussions; to Inge Marie Johansen for conscientious technical assistance, and to the Danish International Development Agency (DANIDA) for financial support which made the cooperation between our two Institutes possible.

REFERENCES

1 IUPAC Anal. Div., Comm. on Analytical Reactions and Reagents, (G. den Boef and A. Hulanicki), Recommendations for the Usage of Selective, Selectivity and Related Terms in Analytical Chemistry.
2 A. L. Wilson, Talanta, 21 (1974) 1109.
3 Z. Marczenko, Spectrophotometric Determination of Elements, Ellis Horwood, Chichester, 1976, p. 342.
4 M. F. Giné, E. A. G. Zagatto and H. Bergamin F°, Analyst, 104 (1979) 371.
5 J. Růžička, E. H. Hansen and A. U. Ramsing, Anal. Chim. Acta, 134 (1982) 55.
6 J. Růžička, J. W. B. Stewart and E. A. G. Zagatto, Anal. Chim. Acta, 81 (1976) 387.
7 H. Bergamin F°, E. A. G. Zagatto, F. J. Krug and B. F. Reis, Anal. Chim. Acta, 101 (1978) 17.
8 J. Mindegaard, Anal. Chim. Acta, 104 (1979) 185.
9 J. Růžička, Phil. Trans. R. Soc. Lond. A, 305 (1982) 645.

Analytica Chimica Acta, 148 (1983) 127—133
Elsevier Science Publishers B.V., Amsterdam — Printed in The Netherlands

DUAL WORKING-ELECTRODE ELECTROCHEMICAL DETECTOR FOR LIQUID CHROMATOGRAPHY

SAM A. McCLINTOCK and WILLIAM C. PURDY*

Department of Chemistry, McGill University, 801, Sherbrooke St. W., Montreal, Quebec H3A 2K6 (Canada)

(Received 19th July 1982)

SUMMARY

The construction and characterization of a dual working-electrode electrochemical detector are described. A comparison of this cell in the dual working-electrode mode and the single working-electrode mode for reversible and quasireversible couples shows a 6-fold improvement in the signal-to-noise ratio. The electrodes are made from low-temperature isotropic carbon. Hexacyanoferrate(II), norepinephrine, epinephrine and 3,4-dihydroxybenzylamine were used as test substances.

Electrochemical cells have proven to be both sensitive and selective detectors for h.p.l.c. [1]. Recent work, based on an earlier paper by Blank [2], has shown that both the sensitivity and selectivity of these devices can be improved by using more than one working electrode [3–6]. In the commonest arrangement, these cells include an upstream electrode to remove interfering species and a second electrode for the actual measurement. In this same configuration, the products of one electrode reaction are detected at another electrode in the manner of the ring-disk systems.

In this laboratory, work has been directed toward lowering the detection limits of electrochemical detectors by locating two working electrodes on opposite walls of a thin-layer cell [7]. Reilley and coworkers [8—11] first developed this concept for stationary solutions and more recently Fenn et al. [12] extended it to flowing streams with only limited success. For this technique to be successful, the species being determined must be part of a reversible or quasireversible redox couple, the working electrodes must be close to each other, and their potentials must be independent of one another. In the simplest case, one electrode is held at a potential at which oxidation takes place and the second electrode at a potential at which this oxidized form is reduced back to the starting material. The current will increase in proportion to the number of conversions that take place at each working electrode.

To achieve this cycling process, the two working electrodes must be close to one another so that the oxidized and reduced forms can make their way to the appropriate electrode for further electrochemical conversion during

0003-2670/83/$03.00

the residence time in the cell. Further, there must be no contact between the working electrodes. The practical difficulties of electrode placement have been overcome by employing an electrode material which is both very hard and flat. This material, low-temperature isotropic carbon (LTIC, a gift from Carbomedics, Austin, TX) has been shown to have the desired physical characteristics and to be an acceptable alternative to other types of carbon electrode [13].

Dual working electrode detectors produce not only an increase in faradaic current but also an increase in the system noise. This problem has been reduced by employing a current sampling technique developed by Weber and Purdy [14], who showed that the noise in a dual working electrode detector can be reduced by sampling the current at a given frequency and duty cycle.

EXPERIMENTAL

Cell and equipment

The thin-layer cell (see Fig. 1) is a modification of the design used in this laboratory for some time [15]. Two LTIC plates, 2 × 6 cm, were glued with

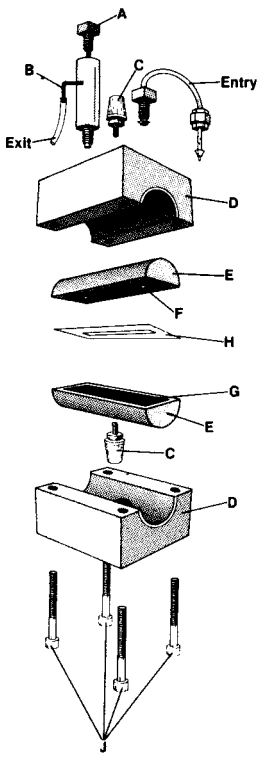

Fig. 1. Cell, exploded view. A, Ag/AgCl reference electrode; B, auxiliary electrode; C, electrical connectors to working electrodes; D, yokes machined from polyvinyl chloride; E, upper and lower cell halves machined from Kel-F; F and G, LTIC plate electrodes; H, teflon spacer.

epoxy resin to two hemicylinders of Kel-F. Exit and entrance ports were then drilled through both the upper Kel-F block, and the electrode was glued to it. The area and thickness of the cell is determined by the channel cut from a thin teflon spacer. This design has the disadvantage of reducing one electrode area relative to the other (because of the presence of the entrance and exit ports) and of preventing the development of laminar flow before the stream reaches the electrode surface. However, these disadvantages are balanced by the achievement of a thin cell which did not leak and one in which the electrodes did not make contact with one another. To attain an acceptable electrode area (about 0.4 cm^2) and still meet the above criteria, the most efficient channel shape was a rectangle 4 cm long and 1 mm wide. This would yield a cell volume of 1 μl if 25-μm thick teflon were used or 0.5 μl if 12-μm thick teflon were used. Teflon thicknesses are from manufacturer's specifications.

The circuitry used for independent control of the potentials of the two working electrodes has been described elsewhere [16]. To this bipotentiostat was added a difference circuit to obtain the sum of the oxidation and reduction currents. The signal is then filtered with a low pass filter with a variable time constant to reduce unwanted noise frequencies generated in the subtraction process. The difference circuit was constructed from three TL-071 operational amplifiers (Texas Instuments Inc., Dallas, TX) and the current-sampling circuit was constructed from an analog switch (AD-7512) controlled by a 555 timer. The frequency and duty cycle of the timer was established with external resistors and capacitors.

The flow system was constructed from an M6000-A pump (Waters Associates, Milford, MA) or a Varian 4100 pump (Varian Associates, Palo Alto, CA), an injection valve (Valco Instrument Co., Houston, TX) with a 10-μl sample loop for sample introduction and three Heath-Schlumberger Model SR-204 recorders (Heath Co., Mississauga, ON, Canada). For chromatography, a 15-cm column was packed with 5-μm Spherisorb (CSC Inc., Town of Mount Royal, PQ, Canada).

Chemicals

Phosphate buffer solutions, 0.07 M, pH 3.0 and 7.4, were made from reagent-grade chemicals dissolved in distilled water. The chromatographic mobile phase was a 9:1 mixture of pH 3.0 phosphate buffer and methanol (HPLC grade; BDH Chemicals) containing 90 mg of octanesulfonic acid, sodium salt, and 30 mg of EDTA. Norepinephrine and epinephrine (both from Sigma Chemical Co.) and 3,4-dihydroxybenzylamine (Aldrich Chemical Co.) were used as received.

RESULTS AND DISCUSSION

Weber and Purdy [17] have developed an expression for current in a thin-layer electrochemical cell. This expression relates cell geometry, flow rate

and analyte concentration to the current produced in rectangular channel cells operating under laminar-flow conditions with the working electrode at "infinite" potential. For the three-electrode system, electrode E1 forms the floor of the channel, with length (L), width (W) and height (b) determined by the teflon spacer. While conducting three-electrode experiments the upper electrode, E2, is disconnected. For the amperometric conditions used throughout these studies, the expression derived by Weber and Purdy reduces to:

$$i = 1.467\, nFC\, (DLW/b)^{2/3}\, U^{1/3} \qquad (1)$$

where i is the current in amperes, n is the number of Faradays per mole, F is Faraday's constant, C is the concentration in mol ml^{-1}, D is the diffusion coefficient in $cm^2\ s^{-1}$, U is the flow rate in ml s^{-1} and the cell dimensions are in cm.

The cell was evaluated in both the single and dual working-electrode mode by pumping a 0.5×10^{-6} M solution of potassium hexacyanoferrate(II) in pH 7.4 phosphate buffer through the cell and comparing the current obtained with that predicted from the theoretical expression. In the single working-electrode mode the hydrodynamic voltammogram for the oxidation of potassium hexacyanoferrate(II) gives a well-defined wave and plateau region (see Fig. 2). The dependence of the limiting current on flow rate is shown in Fig. 3 and is in good agreement with the theoretical expression. This log i vs. log (UA^2/b^2) plot gives a slope of 0.34 ± 0.05 with a correlation coefficient of 0.983 and an intercept that is within 3% of the calculated value.

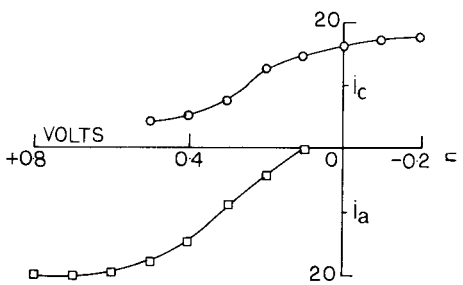

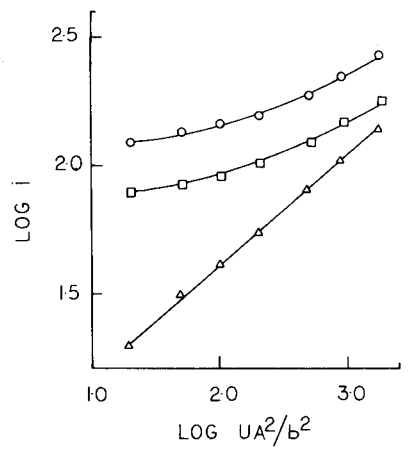

Fig. 2. Hydrodynamic voltammograms for 4 ng of potassium hexacyanoferrate(II) injected into a pH 7.4 phosphate stream: (□) anodic wave at electrode E1; (○) cathodic wave at electrode E2 when electrode E1 is held at 0.7 V vs. Ag/AgCl and the potential of electrode E2 is varied.

Fig. 3. Logarithmic plot of current as a function of flow rate. (△) Response for the single working-electrode mode; (□) cathodic and (○) anodic response for the dual working-electrode mode for a 0.5×10^{-6} M potassium hexacyanoferrate(II) solution pumped continuously through the detector.

To evaluate operation in the dual working-electrode mode, electrode E1 was held at 0.7 V vs. Ag/AgCl and electrode E2 was made more negative until a cathodic current plateau was reached (see Fig. 2). With electrode E1 at 0.7 V and electrode E2 at −0.1 V vs. Ag/AgCl the current/flow rate dependence of the dual working-electrode mode was evaluated (see Fig. 3). The anodic and cathodic currents produced do not have a linear dependence on flow rate. This is to be expected, as at slower flow rates the residence time in the cell is longer and the number of electrochemical conversions should be greater. Thus the effective concentration of each half of the redox couple is increased, giving a current which is dependent on both concentration and flow rate.

A comparison of the data collected with a 25-μm and a 12-μm spacer shows the multiplying effect to be greater with the thinner spacer. At a flow rate of 1.0 ml min^{-1}, the 25-μm spacer increases the current 3.5-fold relative to a single electrode. If the anodic and cathodic currents and their sum are compared at various flow rates (see Fig. 4), the advantage of the dual working-electrode mode can be appreciated. It is seen that a 10-fold magnification of the faradaic current can be realized.

To demonstrate the effectiveness of this cell as a detector for h.p.l.c., a test mixture of norepinephrine, epinephrine and 3,4-dihydroxybenzylamine was separated and quantified. Hydrodynamic voltammograms were run on these three compounds to determine the potential settings for the working electrodes. With E1 at 0.7 V and E2 at −0.15 V vs. Ag/AgCl, a comparison

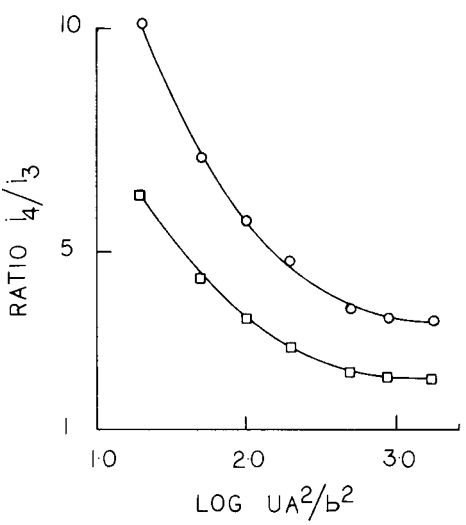

Fig. 4. Plot of the ratios of currents produced in the dual working-electrode (i_4) and single working-electrode (i_3) modes as a function of flow rate. (□) Ratio of anodic currents; (○) ratio of total current for a 0.5 × 10^{-6} M potassium hexacyanoferrate(II) solution pumped continuously through the detector.

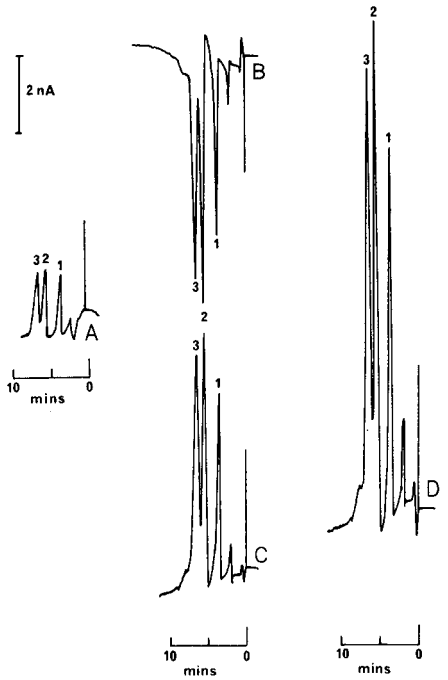

Fig. 5. Chromatograms of a test mixture of 0.5 ng of norepinephrine (1), 1 ng of epinephrine (2) and 1 ng of 3,4-dihydroxybenzylamine (3). A, Anodic current in the single working-electrode mode; B, cathodic current in the dual working-electrode mode; C, anodic current in the dual working-electrode mode; D, total current in the dual working-electrode mode.

was made of currents obtained in the single working-electrode mode and of the anodic, cathodic and total currents in the dual working-electrode mode (Fig. 5). Based on the hexacyanoferrate(II) data, the increase in current is expected to be about a factor of 4 for a flow rate of 1.0 ml min^{-1}. However, at pH 3.0, more than one product is formed in the initial oxidation [18] so that several species are involved in the cycling process. This increases the response of the detector.

As can be seen from Table 1, the detection limit has been reduced by a factor of two for the dual working-electrode mode with direct current monitoring and by a factor of six when the current is sampled at a frequency of 200 Hz with a 2% duty cycle.

The electrochemical detector is expected to lower the detection limits of all electrochemically reversible and quasireversible couples that can be separated by h.p.l.c. The anodic and cathodic currents produced in the dual working-electrode mode show an advantage over the single working-electrode mode at all flow rates tested. An increased advantage is achieved when the electrochemical process is more complex than a simple one-electron transfer and more than one species takes part in the cycling process. Work is

TABLE 1

Signal and noise data for norepinephrine

Variable	Single working electrode	Dual working electrode					
		Direct current mode			Sampled current mode		
		Oxidation peak	Reduction peak	Total	Oxidation peak	Reduction peak	Total
Peak current (nA)[a]	1.6	6.0	6.0	12.0	5.2	5.2	10.0
P.p. noise (nA)[b]	0.1	0.3	0.3	0.4	0.08	0.06	0.1
S/N	16	20	20	30	65	87	100

[a]Peak current for injection of 500 pg of norepinephrine. [b]Peak-to-peak baseline current measured for 2 min with a time constant of 2 s. [c]Current sampled at a frequency of 200 Hz with a 2% duty cycle.

continuing to exploit the advantage of this system as a detector for microbore chromatography. The cell can be modified easily to give an electrode area of 0.1 cm^2 and a cell volume of 0.1 μl. As the cycling process shows increased advantage at low flow rate, it probably can be used to reduce the higher detection limits [19] presently encountered in electrochemical detectors for capillary h.p.l.c.

The authors are grateful to the Natural Sciences and Engineering Research Council of Canada for support of this work and to William Bastian for his help in constructing the cell.

REFERENCES

1 R. E. Shoup (Ed.), Bibliography of Recent Reports on Electrochemical Detection, BAS Press, W. Lafayette, IN, 1981.
2 C. L. Blank, J. Chromatogr., 117 (1976) 35.
3 G. W. Schieffer, Anal. Chem., 52 (1980) 1944.
4 W. A. MacCrehan and R. A. Durst, Anal. Chem., 53 (1981) 1700.
5 D. A. Roston and P. T. Kissinger, Anal. Chem., 54 (1982) 429.
6 M. Goto, T. Nakamura and D. Ishii, J. Chromatogr., 226 (1981) 33.
7 S. G. Weber, Ph.D. Thesis, McGill University, Montreal, 1979.
8 L. B. Anderson and C. N. Reilley, J. Electroanal. Chem., 10 (1965) 295.
9 L. B. Anderson and C. N. Reilley, J. Electroanal. Chem., 10 (1965) 538.
10 L. B. Anderson, B. McDuffie and C. N. Reilley, J. Electroanal. Chem., 12 (1966) 477.
11 C. N. Reilley, Pure Appl. Chem., 18 (1968) 137.
12 R. J. Fenn, S. Siggia and D. J. Curran, Anal. Chem., 50 (1978) 1067.
13 B. R. Hepler, S. G. Weber and W. C. Purdy, Anal. Chim. Acta, 102 (1978) 41.
14 S. G. Weber and W. C. Purdy, Anal. Chem., 54 (1982) 1751.
15 B. R. Hepler and W. C. Purdy, Anal. Chim. Acta, 113 (1980) 269.
16 S. A. McClintock and W. C. Purdy, Anal. Lett., 14 (1981) 791.
17 S. G. Weber and W. C. Purdy, Anal. Chim. Acta, 100 (1978) 531.
18 M. D. Hawely, S. V. Tatawawadi, S. Piekarski and R. N. Adams, J. Am. Chem. Soc., 89 (1967) 447.
19 Y. Hirata, P. T. Lin, M. Novotny and R. M. Wightman, J. Chromatogr., 181 (1980) 287.

Analytica Chimica Acta, 148 (1983) 135—157
Elsevier Science Publishers B.V., Amsterdam — Printed in The Netherlands

DETERMINATION OF PLATINUM METALS BY X-RAY FLUORESCENCE, ATOMIC EMISSION AND ATOMIC ABSORPTION SPECTROMETRY AFTER PRECONCENTRATION WITH A POLYMERIC THIOETHER

YU. A. ZOLOTOV*, O. M. PETRUKHIN, G. I. MALOFEEVA and E. V. MARCHEVA

V.I. Vernadsky Institute of Geochemistry and Analytical Chemistry, Academy of Sciences of the U.S.S.R., Moscow (U.S.S.R.)

O. A. SHIRYAEVA, V. A. SHESTAKOV and V. G. MISKAR'YANTS

State Research and Designing Institute of Rare Metal Industry, Moscow (U.S.S.R.)

V. I. NEFEDOV

N. S. Kurnakov Institute of General and Inorganic Chemistry, Academy of Sciences of the U.S.S.R., Moscow (U.S.S.R.)

YU. I. MURINOV and YU. E. NIKITIN

Institute of Chemistry, Bashkir Branch, Academy of Sciences of the U.S.S.R., Ufa (U.S.S.R.)

(Received 4th August 1982)

SUMMARY

A method for preconcentration of platinum metals based on their sorption by a polymeric thioether $(-CH_2-S-)_n$ is reported. The method is characterized by selectivity, high recovery and simplicity, and is suitable for a wide range of platinum metal concentrations; light non-ferrous metals do not interfere. The concentrate can be analyzed either directly or after rapid dissolution. The sorbent has a high capacity for platinum metals. X-ray fluorescence is suitable for determination of the metals in the concentrate after it has been compressed. This method provides a high precision in the determination of platinum metals (s_r = 0.02—0.04 for 250 $\mu g\ g^{-1}$). Electrothermal atomic absorption spectrometric methods can be applied to the concentrates with or without prior dissolution; these allow the determination of platinum metals even at the 1 ng ml^{-1} level in technical logical solutions and at the 0.1 ng g^{-1} level in solid products (s_r = 0.18). The concentrate can be also subjected to atomic emission spectrometry either with the inductively-coupled plasma after dissolution or with an arc discharge without dissolution. These methods allow the determination of platinum metals (0.1—100 $\mu g\ ml^{-1}$) in technical solutions; the precision (s_r) is 0.01—0.04 when the plasma method is used.

The determination of small amounts of platinum metals is of great importance in the analysis of ores, minerals, and various technical materials. For this purpose, x-ray fluorescence (x.r.f.), atomic absorption (a.a.s.) and atomic emission (a.e.s.) spectrometric methods can be applied. However, direct measurements do not always provide the required limit of detection, thus necessitating preconcentration of the element being determined.

0003-2670/83/$03.00

The application of the x.r.f. method for the determination of platinum metals in complex materials is often encumbered by matrix effects. Furthermore, this method, like the other methods which were used here, employs small samples, and uneven distribution of platinum metals in most materials makes preconcentration from a relatively large sample desirable. Another imporant problem arises in connection with the availability of standard reference materials. Preconcentration and preparation of concentrates on a standard selected matrix considerably helps to solve this problem. Therefore, the x.r.f. determination of platinum metals in matrices of complex composition is often based on a preliminary chemical preparation of the samples aimed at separating interfering elements and obtaining the concentrate of platinum metals on a uniform matrix, irrespective of the composition of the original samples. To obtain the concentrate, ion-exchange membranes [1—3], coprecipitation with organic and inorganic coprecipitating agents [4—6], and extraction with readily melting agents [7] have been used prior to the x.r.f. determination. These methods of preconcentration are not group techniques and do not allow the separation of platinum metals from interfering metals.

Appropriately low detection limits are attained by direct a.a.s. determination of platinum metals in powdered samples with graphite atomizers [8—11]. However, in these cases, special arrangements are necessary to eliminate nonselective interferences [9—11]. Special techniques are required for measuring the signals and for calibration. The application of preconcentration techniques can widen the possibilities for the a.a.s. determination. Similarly to x.r.f., preconcentration allows a single "matrix" to be obtained in the course of analyses of different objects, which again helps to compensate for the absence of standard reference samples. Replacement of the interfering matrix by a proper collector, which can be of less mass, makes it possible to standardize the a.a.s. conditions for samples of very different compositions.

Atomic emission spectrometry is widely used for the determination of platinum metals in ores and concentrates. This method often involves introduction of the powdered sample to the end-face of the graphite electrode or injection of the powdered sample into the arc. The application of high-frequency inductively-coupled plasma (i.c.p.) as a source of spectral agitation appears to be very promising. However, the composition of the samples can influence the results of the analysis by both procedures because of the spectral overlapping and the processes which occur in the plasma discharge. In both cases, the most efficient means of reducing these effects is again a preliminary separation of the test sample components and the matrix. For the group concentration of platinum metals from solutions obtained in the analysis of products of ores and of non-ferrous metals the following procedures have been used: precipitation by thiourea [12], coprecipitation by copper sulfide and mercaptobenzothiazole [13, 14], liquid—liquid extraction of platinum metals with di-2-ethylhexyldithiophosphoric acid [15] and *n*-alkylaniline [16], and sorption on chelating sorbents on the basis of polystyrene and azorhodanine [17] or with PMBM sorbents [18].

An experimental examination of several known methods of preconcentration of platinum metals from various technological solutions allowed a comparison of these methods. The selectivity of the liquid—liquid extraction methods is rather high. However, the stability of the conditions for excitation is often disturbed when organic extracts are put directly into an inductively-coupled plasma. Moreover, upon atomizing the extracts, such spectral interferences as intensification of the background, appearance of cyanogen bands, etc., occur. Upon coprecipitation in the presence of thioacetamide and mercaptobenzothiazole, copper behaves as a collector, and quite a large amount of copper passes into the concentrate. Therefore, it is necessary to prepare standard reference samples with a given copper concentration. Precipitation of platinum metals by thiourea from sulfate solutions of complex salt composition requires reprecipitation of the residue in order to obtain a concentrate of the required purity. Chelating sorbents based on polystyrene and azorhodanine as well as the PMBM sorbent provide proper selectivity for the isolation of platinum metals; however, it is practically impossible to desorb the elements to be determined and is rather difficult to dissolve the concentrate. Therefore, the determination in solution is found to be complicated.

Thus, a search for new techniques for platinum metal concentration was very desirable. The above short review of the known methods indicates that sulfur-containing reagents are often employed for platinum metal separations; among them, mention should be made of such neutral extractants [19] as sulfides, thiourea derivatives and others. Coprecipitation in the systems with sulfur-containing compounds and sorption on chelating resins with active groups containing sulfur atoms [20] have also be utilized. Inorganic sulfides have been used [20] for isolation of platinum metals. It was, therefore, considered that an investigation of a polymeric thioether $(-CH_2-S-)_n$ as a sorbent would be of interest. It was found that the sorbent affords complete and selective separation of small amounts of platinum metals from solutions of complex composition. The concentrate is readily compressed, which is suitable for x.r.f. measurements, and can be used for direct electrothermal a.a.s. and a.e.s. determinations of platinum metals. The concentrate also dissolves readily and the solutions obtained are also suitable for the a.a.s. and a.e.s. methods (with the inductively-coupled plasma). The present paper deals with the results of the work done in this field.

EXPERIMENTAL

Reagents and solutions

All stock solutions of platinum metals were prepared by dissolving the respective salts obtained by chlorination of the metals in a potassium chloride melt (iridium, ruthenium and rhodium) or by dissolving the metal in aqua regia and evaporating the solution so obtained with hydrochloric acid (palladium and platinum). The solution concentrations were determined

by standard methods [12]. Stock solutions of the platinum metals contained 1 mg ml^{-1} of the metal and were prepared as described earlier [12]. The working solutions were 1 M with respect to hydrochloric acid.

To study the sorption of platinum metals in the presence of interfering elements, series of solutions were prepared containing each platinum metal at the 0.001, 0.005, 0.02 and 2.0 μg ml^{-1} levels as well as variable amounts of nickel, cobalt, iron and copper (0.1, 1 and 10 mg ml^{-1}), selenium and tellurium (1, 5 and 10 mg ml^{-1}). All the solutions were 3 M in hydrochloric acid. The reagents were of analytical-reagent grade.

Synthesis and properties of the sorbent

The sorbent used is a linear polymeric thioether $(-CH_2-S-)_n$. It was obtained by condensation of formaldehyde with hydrogen sulfide in alkaline medium or by condensation of formaldehyde with sodium sulfide [21]. The synthesis is simple and is based on readily available reagents. The preparation was identified by means of elemental analysis, melting point and the values of the maximum capacity with respect to platinum and silver. The sorbent was a white finely divided powder, practically insoluble in water and organic solvents. The average molecular mass of the sorbent was 1000, and the sulfur content was higher than 60% (theoretically 69.6%); the melting point was in the range 115—140°C. (Elemental composition: 25.0% C, 5.1% H, 60.7% S, 2.2% ash.)

Heating in aqueous solutions and in dilute solutions of sulfuric acid, the polymer is stable, whereas on heating in hydrochloric acid, it dissolves slowly. When heated in a mixture of hydrochloric and nitric acids, the sorbent dissolves quickly and sulfate ions appear in the solution. A brief contact of the sorbent with nitric acid (e.g., during washing with nitric acid) results in the appearance of oxidized sulfur on the surface (this was shown by the ionization energy of the 2*p* electron from e.s.c.a. data). In such case, the sorption properties of thioether with respect to platinum metals deteriorated markedly.

The determination of the ionization energy of the sulfur atom 2*p* electron showed that, as could be predicted, the oxidation state of sulfur in the sorbent corresponds to the oxidation state of sulfur in monomeric dialkylsulfides. The sorbent may apparently be classed as a soft electron-donor reagent.

Procedure for concentration

Sorption was done by the batch technique. Prior to the x.r.f. determination, 50—500 ml of a solution, 3 M with respect to hydrochloric acid, was heated to boiling, 1 g of the sorbent was added, and 3 M HCl was added periodically during boiling to keep the volume constant. After boiling for 1 h, the residue was filtered off and washed with 3 M HCl, acetone and ether (3 times with each). The air-dried concentrate was then pressed into tablets.

Prior to the a.e.s. determination, 0.1—0.5 g of the sorbent was added to 10—100 ml of the test solution, 3 M in hydrochloric acid, and the solution

was boiled for 2 h. The concentrate was then filtered off and washed with 1 M HCl on the filter not less than 5 times. When the solutions were examined by means of the i.c.p. or a.a.s. method, the washed concentrate was dissolved in nitric acid or in a mixture of nitric and hydrochloric acids and the solution thus obtained was transferred to a calibrated flask, the solution being diluted to the mark by means of 2 M hydrochloric acid solution. Before the a.e.s. determination by means of the powder injection method, or the electrothermal a.a.s. determination, the concentrate was washed additionally with acetone and ether (3 times) after it had been filtered and washed with 1 M hydrochloric acid. The air-dried concentrate was weighed for the spectrometric determination.

X-ray fluorescence spectrometry

The samples for all x.r.f. measurements were prepared by compressing the concentrate into tablets in the cuvettes of the x.r.f. spectrometer under a pressure of 1 ton. The diameter of the tablets was 30 mm. All x.r.f. measurements were done with a Philips PW-1410 semi-automatic spectrometer. A tungsten anode x-ray tube (FA-100/2) operated at 50 kV and 25 mA; the analyzing crystal was LiF 200, and the detector was a scintillation counter employing a NaI(Tl) crystal.

Atomic absorption spectrometry

Absorbances were measured with a two-channel spectrometer (Model C-2500; Giredmet Institute), using a graphite atomizer and a program-controlled process. For determinations, 5—10 mg of the air-dried concentrate mixed with a graphite powder of special-grade purity was placed in the graphite atomizer by means of a special insertion device for solid samples. The presence of the graphite powder makes it possible to avoid non-selective absorption. It also facilitated insertion of the sample because in the absence of the graphite powder the collector became considerably electrified. Non-selective absorption is likely to be due to condensation of the sorbent vapours on cool parts of the atomizer and their subsequent evaporation on heating to the temperatres relevant to the atomization of the element being determined. The presence of the graphite powder seems to change the kinetics of matrix evaporation. The atomizers (length 53 mm, i.d. 8.5 mm) were cleaned by calcination. Powdered samples were atomized in an argon atmosphere at a gas flow rate of 1 l min^{-1}. Concentrations were determined by integration of absorbance values.

The reference samples were prepared by sorption of platinum metals under the conditions described above. The air-dried concentrate was mixed with the graphite powder to prepare a series of reference samples containing the platinum metals (0.05—5 μg each).

Atomic emission spectrometry

An inductively-coupled plasma torch (Model IY-38; Jobin-Yvon, France) was used; the output power of the high-frequency generator was up to 2.5

kW h and the frequency was 27.12 MHz; the HP-1000 monochromator had a holographic grating of 2400 lines/mm and the reverse linear dispersion was 0.4 nm in the range 200—750 nm. Argon was used as the nebulizing (0.65—0.75 l min^{-1}) and cooling (13—15 l min^{-1}) gas. For injection of the solution into the plasma, a pneumatic concentric nebulizer with a solution delivery speed of 2 ml min^{-1} was used. The overall concentration of the salts in the solutions did not exceed 5 mg ml^{-1}. The analytical lines used for the platinum metals are given in Table 1. The observation zone was situated 12 mm over the upper coil of the induction coil. For determination with the plasma, the sample solutions and reference solutions were sprayed into plasma alternately. The arithmetic mean of two measurements on separate aliquots of the solutions was taken as the result.

When the powder injection technique was used, the powdered samples were introduced into an arc discharge in an AI-3 semi-automatic instrument. An a.c. arc of 15 A was employed. The sample weighed 50 mg. The spectra were taken on a DFS-8 spectrograph with a grating of 600 lines/mm on plates (Model W 4-2; ORWO Co.). The main reference sample containing 0.01% (mass) of platinum metals was prepared under the optimal conditions of sorption. Samples with lower contents of the platinum metals were prepared by diluting the main reference sample with graphite powder (or a sorbent). The reference elements, titanium and cerium, were introduced into all reference samples in the form of solutions, and then the samples were dried at 70°C.

Investigation by x-ray electron spectroscopy

The x-ray electron spectra were taken by using a VIEE-15 spectrometer with a magnesium anode in vacuum (1.3×10^{-4} Pa). The substances were spread over the adhesive side of a strip of polyethylene film. The spectra were calibrated with respect to the carbon of a hydrocarbon layer settled on the surface of the samples in the spectrometer. Reproducibility of the binding energy was ±0.1 eV.

TABLE 1

Analytical lines for the platinum metals

Metal	Analytical line (nm)	
	IY-38 instrument	AI-3 instrument
Palladium	360.955	324.270
Platinum	265.945	306.470
Rhodium	343.489	349.675
Ruthenium	372.803	343.674
Iridium	380.012	322.078

PRECONCENTRATION BY SORPTION

Survey of metal behaviour

Sorption of many elements was studied in relation to the acidity of the medium (Fig. 1). Solutions of the highest acidity allow the separation of platinum metals, gold, selenium, tellurium, mercury, arsenic and copper; sorption of cobalt, nickel and iron(III) is attained in solutions at pH > 2.

Preconcentration of platinum metals

To identify the conditions for simultaneous concentration of platinum metals, the effects of the hydrochloric acid concentration, the duration of sorption and the temperature were studied.

Figure 2 shows the recovery of platinum metals from hydrochloric solutions. Palladium, rhodium, ruthenium and platinum are completely isolated from 1—10 M HCl. The recovery of iridium and osmium decreases with an increase in the solution acidity; 1—3 M can be taken as the optimal concentration of hydrochloric acid for sorption of these metals. With the concentrations in solution of >0.001 $\mu g\ ml^{-1}$, platinum, palladium, rhodium and ruthenium are completely sorbed with the use of 50 mg of the sorbent from a volume of 50 ml. The sorption of iridium is 80%. Preliminary treatment of the test solution with tin(II) chloride allows iridium to be completely sorbed, and the separation of the other platinum metals is quantitatively preserved. In this case, tin is practically not adsorbed. The recovery of platinum metals decreases with an increase in the volume of the solution from which the platinum metals are separated.

In real samples of materials, the contents of platinum and palladium often exceed the contents of iridium, rhodium and ruthenium. Therefore, the sorption of the last three metals was studied in the presence of variable amounts of palladium and platinum. As shown in Table 2, a 500-fold excess of platinum and palladium does not significantly affect the recovery of iridium, rhodium and ruthenium (conditions of sorption: 10 ml of solution, 100 mg of the sorbent, and 2-h sorption time). These results prove that polymeric thio-

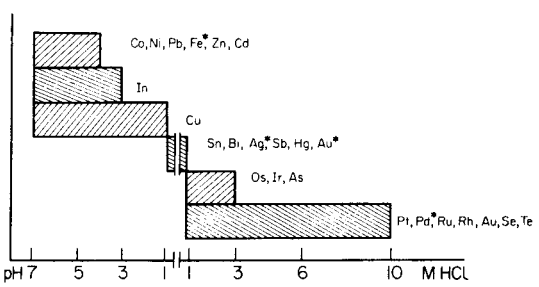

Fig. 1. Sorption of various metals by polymeric thioether depending on acidity of the medium. Elements marked by asterisks can be isolated without heating.

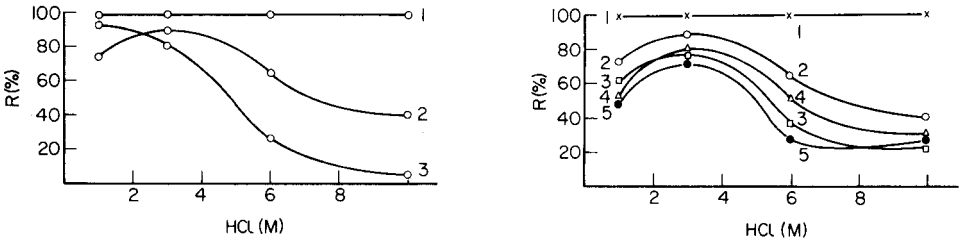

Fig. 2. Recovery of platinum metals (R, %) from hydrochloric acid solutions. Each metal was present at 250 μg/50 ml. (1) Pd, Rh, Ru, Pt; (2) Ir; (3) Os.

Fig. 3. Recovery of platinum metals (1 mg/50 ml each) in the presence of other elements: (1) Pd, Pt, Rh, Ru in the presence of Co, Cu or Fe(III) (10 mg ml^{-1}); (2) Ir in the presence of Co or Ni (10 mg ml^{-1}); (3) Ir in the presence of Cu (2 mg ml^{-1}); (4) Ir in the presence of Cu, Co, Fe(III) and Ni (25 mg of each); (5) Ir in the presence of Fe(III) (2 mg ml^{-1}).

ether can be successfully used for separation of trace amounts of platinum metals.

Experiments on desorption of platinum metals showed that sorption of these metals is irreversible. For example, when 1 g of the sorbent containing 250 μg of each platinum metal was shaken at room temperature with 50 ml of 0.1 or 1 M hydrochloric acid and then boiled for 1 h, the concentration of the platinum metals in the sorbent did not change (except for palladium, the concentration of which decreased by 26%). After these sorptions of metals, the sorbents were studied by x-ray electron spectroscopy (see below).

Separation of platinum metals from solutions containing other metals, especially non-ferrous metals and iron(III), is of practical interest. Figure 3 shows the recovery of platinum metals in the presence of copper, nickel, cobalt and iron. The presence of 10 mg ml^{-1} each of these metals does not affect the sorption of palladium, rhodium, ruthenium and platinum. Increasing contents of cobalt and nickel do not markedly affect the recovery of platinum metals, whereas increased copper or iron contents somewhat decrease the recovery of ruthenium and rhodium. The sorption of iridium is unaffected by 10 mg ml^{-1} cobalt and nickel whereas 2 mg ml^{-1} copper and iron somewhat decrease the extent of separation. Osmium behaves similarly to iridium.

TABLE 2

Recovery (%) of iridium, rhodium and ruthenium (μg ml^{-1}) in the presence of platinum and palladium

Concentration of Pt and Pd (mg ml^{-1})	Recovery (%)		
	Iridium	Rhodium	Ruthenium
0.1	87	100	112
0.5	82	98	103
1.0	76	102	96

Table 3 gives some additional data on the effects of other metals. The results obtained show that palladium, rhodium, ruthenium and platinum can be almost quantitatively separated from 1—10 M HCl with practically any content of nickel and cobalt as well as with contents of copper and iron up to 10 mg ml^{-1}. Iridium and osmium can be isolated from 1—3 M HCl solutions containing 2 mg ml^{-1} copper and iron. The recoveries of small amounts of platinum and iridium (fractions of a microgram) were 90% and 80%, respectively. This high selectivity of the proposed method allows the concentrates thus obtained to be used without any additional purification.

Nature of sorption

The main objective of this part of the work was to identify the forms of the platinum metals present in the sorbent. The nature of palladium sorption was studied in detail. Analysis of the concentrate for platinum metals and chlorine showed (Table 4) that after sorption at room temperature the ratio of metal to chlorine is 1:2 for Pd, 1:4 for Pt, and 1:3 for Au. When sorption is done with heating, the ratio of metal to chlorine is much less and decreases with increased heating times. In the case of palladium, the ratio is 1:0.4 after sorption at boiling temperatures during 8 h.

TABLE 3

Recovery (%) of platinum metals in the presence of varying amounts of other elements

Other metal	Conc. ($\mu g\ ml^{-1}$)	Recovery (%) of									
		Ir		Pt		Ru		Rh		Pd	
		I[a]	II[b]	I	II	I	II	I	II	I	II
Cu	0.1	88	77	100	—	80	—	80	—	—	—
	1	82	—	98	94	86	90	90	96	—	—
	10	88	72	98	80	76	79	71	75	98	95
Fe	0.1	74	72	93	86	79	90	81	—	78	—
	1	79	—	91	93	79	85	93	88	—	89
	10	64	62	86	98	79	98	75	85	88	86
Ni	1	—	—	—	96	—	98	95	—	—	—
	10	—	67	—	—	—	—	96	—	—	—
Se	0.04	85	80	96	93	88	85	96	95	96	94
	0.4	67	65	91	89	64	66	83	85	91	90
	10	31	—	80	—	60	—	80	—	80	—
Te	0.4	82	80	95	93	84	85	94	91	95	95
	10	77	75	—	—	71	—	90	—	91	—

[a] 2 $\mu g\ ml^{-1}$, 10 ml of solution. [b] 0.02 $\mu g\ ml^{-1}$, 100 ml of solution.

TABLE 4

Results of elemental analysis of sorbent and palladium concentrate (Solution volume 50 ml, 3 M HCl, sorbent mass 250 mg, boiling temperature)

Sample	Sorption time (h)	Content (%)			Cl:Me
		S	Cl	Pd	
Initial sorbent	—	60.64	<0.1	—	—
Sorbent after 1-h boiling	—	69.83	0.0	—	—
Pd concentrate	1	64.37	0.64	4.00	0.74
	2	64.33	0.74	5.19	0.61
	4	64.95	0.61	4.66	0.51
	6	65.40	0.66	4.93	0.40
	8	64.20	0.64	4.93	0.39

These results, in conjunction with the nature of the dependence of sorption on the conditions of acidity, time and temperature, as well as the correlation of the recovery with the kinetic inertness of platinum metal complexes, all indicate that the initial sorption step involves formation of the following coordinately solvated complexes:

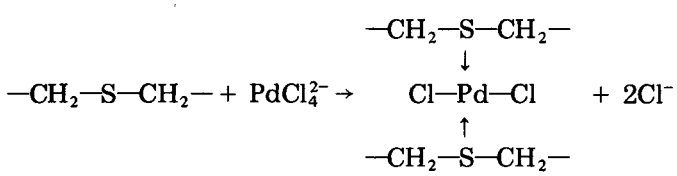

Similarly to liquid—liquid extraction, the greater the inertness of the complexes of the metal being sorbed, the slower will be the sorption of the elements.

Heating seems to cause homolytic breakage of the S—C bond to form a surface polymeric mercaptide. This was proved both by a relatively small amount of chlorine found in the concentrate and by the binding energy of the palladium electron, $3d_{3/2}$, in the surface compound (337.4 eV) compared with the ionization potential in palladium transdiphosphinediiodide (Table 5). The investigation of the electron spectra of the surface complex of palladium and of model complexes of this element with sulfur-containing ligands, and comparison with the electron spectrum of palladium sulfide, showed that the coordination number of palladium remains constant and is equal to four for all the compounds studied. This means that the coordination sphere of palladium in the mercaptide is supplemented by the formation of donor—acceptor bonds with the sulfur atoms in the neighbouring molecules [22]:

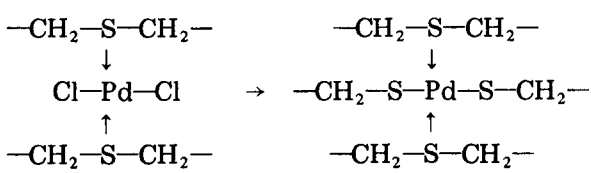

TABLE 5

Binding energies of sulfur in the sorbent and of platinum metals in the sorbed complexes and in some model compounds of these elements

Electron	Compound	Binding energy (eV)	Electron	Compound	Binding energy (eV)
S 2*p*	Sorbent	163.3	Os $4f_{7/2}$	Osmium concentrate	51.3
	$(C_6H_5CH_2-)_2S$	163.5		$OsCl_2$(DPThio)	51.8
	$(C_6H_5CH_2)_2SO$	166.1		$OsCl_3$(DPThio)$_2$	52.7
	$(C_6H_4NH_2)SO_2$	168.1	Ir $4f_{7/2}$	Iridium concentrate	61.4
	Diphenylthiourea	162.2		$Ir(C_2Ph_2)(PPh_3)_2Cl$	61.4
Pd $3d_{3/2}$	Palladium concentrate	337.4		$Ir(PPh_3)_2(CS)Cl$	61.2
	K_2PdCl_4	338.4	Rd $3d_{5/2}$	Rhodium concentrate	308.8
	$[Pd(NH_2)_2(CS)]Cl_2$	338.0		RhI_3	308.8
	trans-$PdI_2(PPh_3)_2$	337.7		$Rh(Thio)_3Cl_3$	309.8
Pt $4f_{7/2}$	Platinum concentrate	72.5		$[Rh(Thio)_6Cl(NO_3)_2]$	309.8
	$PtPh_2(PPh_3)_2$	72.6			
	$Pt(C_2H_4)(PPh_3)_2$	72.4			
	trans-$PtCl_2Py_2$	72.9			

This corresponds to the coordination chemistry of monomeric palladium mercaptides $Pd(RS)_2$ (where R stands for ethyl, *n*-propyl, *n*-butyl, *n*-amyl) which also associate in solution, although they are polymeric in the solid state, the adjoining atoms of palladium being bound by bridging sulfur atoms [23].

The results of elemental analysis done after saturation of the sorbent with palladium showed that there was no breakage of the second bond (sulfur—carbon) to form an inorganic sulfide. The atomic mass ratio of carbon to hydrogen remained practically the same as in the initial polymeric thioether. Comparison of the electron spectra of the surface-sorbed complex and palladium sulfide confirmed this conclusion [22].

Other platinum metals appear to form mercaptide-like compounds or at least compounds with covalent metal—sulfur bonds; otherwise, it is difficult to explain the high ionization energies of the inner electrons in their sorbed complexes (Table 5). The binding energies of inner electrons of the platinum metals in the sorbed complexes are compared with the binding energies of inner electrons of platinum metals in complexes of known structure in Table 5. This comparison leads to the conclusion that the platinum metals in the sorbed complexes are in very low oxidation states: Ir(I), Os(II), Pt(II).

The relationship between coordinately solvated compounds and mercaptides in the sorbent seems to depend on the nature of the metal (its kinetic inertness to substitution reactions) and the conditions of sorption (temperature and duration of heating).

The x-ray electron spectroscopic data and the results of elemental analysis of the concentrate made it possible to determine the degree of enrichment of the sorbent surface of platinum metals in relation to the volume. The data

obtained show that an increase in the concentration of platinum metals in the concentrate results in a decrease of the ratio of the metal to sulfur in the surface layer (Table 6). This appears to be quite natural because metals are sorbed primarily by the surface layer of the sorbent. A more unexpected result is that the metals are sorbed not only on the surface but also in the bulk of the sorbent surface layer (Fig. 4). The degree of enrichment of the sorbent surface in relation to the bulk depends on the nature of the metal and decreases in the following sequences: Os > Ir > Pt and Ru > Rh > Pd. These sequences seem to correspond to the sorption rate. In fact, the rapidly sorbed metals are held in the sorbent surface, while the metals being sorbed more slowly (because of the kinetic inertness of platinum metals to substitution reactions) have a longer period of solution contact with the entire mass of the sorbent. This results in a more uniform distribution of the metal between the surface and the bulk of the sorbent.

Thus, the formation of the coordinately solvated compounds correlates with the formation of similar compounds in liquid—liquid extraction with monomeric sulfides. However, under the sorption conditions, polymeric mercaptides are further formed. With selenium and tellurium, the reaction proceeds up to the formation of the elemental forms. In extraction systems with sulfur-containing reagents with strong electron-donating substituents, reduction of gold to metal is also observed.

X-RAY FLUORESCENCE DETERMINATIONS

Interelement effects

As is known, the analytical line intensity of the element to be determined is greatly affected by the matrix or the specimen filler [24]. Calibration graphs for determining the elements remain linear only over limited ranges of concentration. Therefore, it is necessary to know the maximum possible concentrations of each element up to which one need not consider interelement effects if the magnitude of the error is established beforehand. In this case, reference samples can be prepared from platinum metal solutions

TABLE 6

Atomic ratio of S/Me on the concentrate surface from x-ray electron spectroscopic data and bulk contents of metal from elemental analysis data

Metal	Bulk content of metal (%)	S/Me	Metal	Bulk content of metal (%)	S/Me
Pd	1.0	71.5	Pt	1.0	56.5
	1.5	68.3		1.5	56.5
	2.0	27.7		2.0	43.0
	3.0	28.4		3.0	29.0
	4.0	18.0			

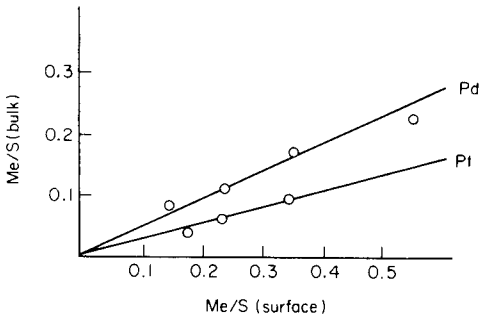

Fig. 4. Bulk and surface ratio Me/S for the concentrates of palladium and platinum.

by the same procedure as that used to prepare the actual samples. The contents of the elements can be calculated by using linear calibration relationships.

To estimate the possible mutual effects of platinum metals in the polymeric thioether, the following calculations were done. For simplification reasons, the criterion of estimation was expressed as the ratio of the line intensity of element A in the presence of interfering element (I_A^x) to the intensity of the same analytical line in the absence of interfering element (I_A^o). In the general case, this ratio is a function of the sample composition and cannot always be taken as a criterion for evaluation of all possible inter-element effects. However, in this particular case, we consider the determination of small amounts of the element contained in a known filler and, therefore, the proposed approach is justified.

According to Losev [24], and assuming that the exciting radiation is monochromatic, the saturated layer can be expressed as

$$I_A^x = K\, C_A/[C_A\alpha_A + (1 - C_A)\alpha_F] \tag{1}$$

where C_A is the concentration of element A, and α_A and α_F are the absorption parameters of element A and the filler, respectively. For a sample which does not contain any interfering element B and has the same concentration, C_A, of element A,

$$I_A^o = K\, C_A/[C_A\alpha_A + (1 - C_A)\,\alpha_T] \tag{2}$$

where α_T is the absorption parameter of the polymeric thioether. The mass absorption coefficient of the element A line by the filler containing interfering element B (μ^F) can be expressed by

$$\mu^F = C_B/(1 - C_A) = \mu^B + [1 - C_B/(1 - C_A)]\,\mu^T \tag{3}$$

where μ^B and μ^T are the mass absorption coefficients of the element A line by element B and the polymeric thioether, respectively; C_B is the concentration of B. The mass absorption coefficient of the primary radiation μ_p^F can be expressed in the same way. Given expression (3), and the analogous expression for the μ_p^F absorption parameter, $\alpha_F\mathrm{F} = [(\mu_p^F/\sin\phi) + (\mu^F/\sin\psi)]$, where ϕ and ψ are the angles of incidence and of selected radiation, can be expressed by the equation:

$$\alpha_F = \alpha_B C_B(1 - C_A) + \alpha_T[1 - C_B(1 - C_A)] \quad (4)$$

where α_B is the absorption parameter of primary and secondary radiation for interfering element B.

The ratio I_A^x/I_A^o for the line intensities can be expressed by the equation (cf. Eqn. (4) which was first transformed):

$$I_A^x/I_A^o = 1/[1 + C_B(C_A M + N)] \quad (5)$$

where $M = (\alpha_A + \alpha_T)/(\alpha_B + \alpha_T)$ and $N = \alpha_T/(\alpha_B - \alpha_T)$.

Calculations made by using Eqn. (5) permit the evaluation of a probable effect of platinum metals on the intensities of the analytical lines. Figure 5 shows the change in the relative intensities of the ruthenium and iridium lines at a concentration of 0.04% (400 μg g^{-1} of sorbent) depending on the contents of palladium and platinum in the sample. The values of the effective wavelength of the primary radiation λ_1 were determined from a published nomogram [24]. For iridium, it was 0.095 Å; for ruthenium, it was 0.410 Å. The values of mass absorption coefficients were calculated from the data given by Leroax [25] (angle $\varphi = 60°$ and $\psi = 40°$).

In the general case, noble metals may be divided into two groups. As a rule, silver, palladium, rhodium and ruthenium are determined via lines of the K-series, while gold, platinum, iridium and osmium are determined via characteristic lines of the L-series. If the osmium L_{α_1} line, overlapped by the copper K_{β_1} line, is neglected, it is possible to conclude that the analytical lines of ruthenium and iridium, each in its arbitrary group, are situated at the long wave side compared to the lines of other platinum metals. Calculations made by Eqn. (5) show that the line intensities of these elements are somewhat less subject to the effect of other platinum metals than, for example, the lines of metals adjoining them in the periodic system of elements. However, iridium and ruthenium are normally present in the samples in relatively small concentrations and, therefore, are usually determined on

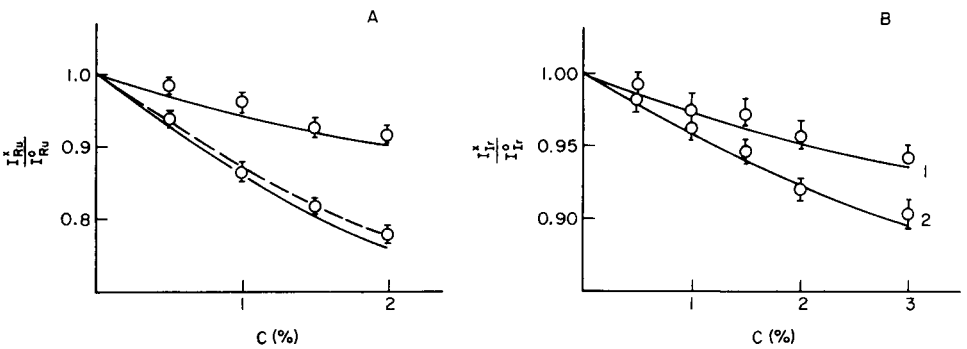

Fig. 5. Dependence of the changes in relative intensity of the analytical lines of (A) ruthenium I_{Ru}^x/I_{Ru}^o, and (B) iridium I_{Ir}^x/I_{Ir}^o, on the contents of an interfering element in the sorbent ($C_{Ir} = C_{Ru} = 0.04\%$). (1) In the presence of palladium; (2) in the presence of platinum.

the background of considerably greater concentrations of other platinum metals (especially palladium and platinum). Accordingly, the possible mutual effects given in Fig. 5 should be considered as limiting. Calculations by means of Eqn. (5) prove this.

It should be noted that with a change in the concentration of the element to be determined, the change in the relative intensity of its analytical line caused by a mutual interference between the elements is not very great. This results from the small value of parameter M in Eqn. (5). According to calculations of the effect of palladium metals on, for example, the intensity of ruthenium lines, the values of M range from 0.335 (with osmium as the interfering element) to 0.866 (with palladium as the interfering element). In the case of iridium, the values of M range from 0.951 to 1.879 for platinum and ruthenium as the interfering elements, respectively.

The proximity of the value of parameter M to unity is due to the relative proximity of the absorption parameters of platinum metals provided that account is taken of the fact that the absorption parameter of the sorbent, α_T, is much less than the values of α_A or α_B with respect to the absolute value. Hence, for the contents of element A considered in the present work, the main change in intensity of its analytical line will depend on the value of N or on the ratio of the line absorption parameters by the sorbent and the interfering element. For instance, the absorption parameter of the ruthenium line by sorbent (α_T) is 10.3 $cm^2\ g^{-1}$, whereas the absorption parameters α_B by the interfering elements, palladium and platinum, are 70.5 and 179.0 $cm^2\ g^{-1}$, respectively.

Thus, it appears that the data given in Fig. 5 allow the determination of concentration levels of each element such that mutual effects can be neglected within acceptable errors. The contents of osmium, iridium, platinum and gold in the sample should be considered first, because those elements can markedly affect both the line intensities for palladium, rhodium and ruthenium, and the line intensities of each other.

Equation (5) was verified experimentally by using samples containing 400 μg of ruthenium or iridium and various amounts of palladium and platinum. Figure 5 shows the experimental relative line intensities for these elements at confidence intervals corresponding to 65% probability. The correlation between the experimental and calculated data is quite satisfactory. Some deviation of the experimental dependence of ruthenium line intensity in the presence of platinum (the dotted line) can be considered negligible.

Analytical characteristics of the procedure

The detection limits for platinum metals, the lower limits of determination for the elements, and the precision of the results were evaluated on samples containing various amounts of the elements (50—1500 μg). Table 7 lists the values for the detection limits, $C_{min,P}$, at a confidence probability P of 0.99. The values of $C_{min,P}$ were calculated according to 3 σ-criterion: $C_{min,0.99} = 3\ I_B^{1/2}/S$, where I_B is the background intensity at the line, and S is the sensi-

tivity coefficient of the calibration plot. Table 7 shows that detection limits of platinum metals are in the $\mu g\ g^{-1}$ range in the sorbent. It was verified that the proposed procedure for the sorption of platinum metals is applicable to solutions with volumes up to 400—500 ml. Recalculated for volume, the detection limits are in the range 9×10^{-3}—$3 \times 10^{-2}\ \mu g\ ml^{-1}$.

The precision of the determinations was estimated for samples which contained 250 or 1000 μg of each platinum metal. Table 8 lists the relative standard deviations, s_r, calculated from the results obtained in the parallel analysis of 8 samples. The average s_r value is 0.02—0.03. These s_r values characterize the total precision of the method, including sorption concentration and x.r.f. measurements. Most of the error arises from the preconcentration; the s_r values for measuring the line intensities evaluated from counting statistics and from instrumental instability do not exceed 0.01 at the given contents of the elements; the error arising from preparation of the tablets by pressing is insignificant.

The lower limits of determination of the platinum metals are about 80 μg for rhodium, ruthenium and palladium, and 100 μg for platinum, iridium and osmium. The corresponding s_r values range from 0.04 to 0.05.

The completeness of the platinum metal preconcentration and the high degree of their separation from other metals allow the preparation of reference samples from standard solutions of platinum metals by using the same procedure as that applied for treatment of the samples. As has been noted above, a maximum possible content of each element in the sorbent is of great importance. Calculations by means of Eqn. (5) and the data given in Fig. 5 lead to the following conclusion: if the admissible error arising from matrix effects is 2—3%, then the total content of platinum metals in the sorbent should not exceed 8—10 mg. More rigid requirements should be applied in determining ruthenium and rhodium; e.g., the contents of platinum, iridium or osmium should not exceed 2 $mg\ g^{-1}$ of sorbent in determining ruthenium with the given error. When somewhat larger amounts of platinum metals are determined, the reference samples should take account of the

TABLE 7

Limits of detection for the platinum metals by the x.r.f. method ($P = 0.99$)

Element	Analytical line	Detection limit	
		$\mu g\ g^{-1}$ in sorbent	$\mu g\ ml^{-1}$ in solution
Palladium	K_α	4.2	1.0×10^{-2}
Rhodium	K_α	3.6	9.0×10^{-3}
Ruthenium	K_α	3.5	8.8×10^{-3}
Platinum	L_{β_1}	12.9	3.2×10^{-2}
Iridium	L_{α_1}	12.8	3.2×10^{-2}
Osmium	L_{β_1}	11.6	2.9×10^{-2}

TABLE 8

Relative standard deviations (s_r) of the results obtained for platinum metals by x.r.f. spectrometry (n = 8)

Element content (μg ml^{-1})	Relative standard deviation					
	Pd	Rh	Ru	Pt	Ir	Os
5	0.031	0.032	0.019	0.019	0.030	0.033
20	0.028	0.031	0.018	0.036	0.034	0.040

ratio of platinum metals in the sample in order to minimize errors caused by the interrelation of the metals. It may be added that calibration graphs for each particular element are linear for contents up to 10—12 mg g^{-1} of the sorbent.

The selectivity of this separation of platinum metals allows the described procedure to be applied to various materials. The procedure was applied to several industrial solutions containing various amounts of elements along with platinum metals. The results are compared with the data from a.a.s. determinations in Table 9. The agreement of the results is reasonably good.

ATOMIC ABSORPTION SPECTROMETRIC DETERMINATIO N

The conditions for the electrothermal a.a.s. determination of the platinum metals in the sorbent are given in Table 10. If the content of metals exceeded the upper limits stated, the concentrate was further diluted with graphite powder. It is possible to determine platinum metals down to 1 ng ml^{-1} in solution or 0.1 ng g^{-1} in the solid. Measurements on the solid concentrate ensure the determination of all platinum metals including ruthenium and osmium. If the concentration of platinum metals in the concentrate exceeds $n \times 10^{-3}$%, it is feasible to determine the metals after dissolving the concentrate in nitric acid (20-μl aliquots were used). Some losses of ruthenium and osmium result from getting the concentrate into solution.

Table 11 shows the results obtained for the platinum metals in technical solutions by the above method and by measurements of concentrate solutions obtained after separation of platinum metals with thiourea [26]. The contents of other elements in these test solutions were: up to 25% iron, up to 10% nickel, up to 10% cobalt, up to 10% copper, and up to 1% silicon.

ATOMIC EMISSION SPECTROMETRIC DETERMINATION

Inductively-coupled plasma emission spectrometry (i.c.p.e.s.)

As has been shown [27], the lower limits of determination of platinum, palladium, ruthenium, rhodium and iridium by i.c.p.e.s. are about 0.1 μg ml^{-1}. Calibration graphs are linear over 2—3 orders of magnitude above that limit

TABLE 9

Results of the determination of platinum metals by x.r.f. and flame a.a.s.
(Results are given as g l^{-1} with $P = 0.95$; $n = 3$)

Solution analyzed	Solution volume (ml)	Palladium		Rhodium		Ruthenium		Platinum	
		X.r.f.	A.a.s.	X.r.f.	A.a.s.	X.r.f.	A.a.s.	X.r.f.	A.a.s.
Chloride melt solution	100	0.046 ± 0.004	0.045 ± 0.004	0.023 ± 0.005	0.27 ± 0.003	0.002 ± 0.00	0.002 ± 0.001	0.04 ± 0.01	0.030 ± 0.003
	10	0.57 ± 0.03	0.58 ± 0.06	0.015 ± 0.003	0.018 ± 0.002	0.010 ± 0.001	0.009 ± 0.001	0.11 ± 0.01	0.097 ± 0.010
Raffinate solution	2	3.30 ± 0.014	2.50 ± 0.17	0.92 ± 0.05	1.00 ± 0.07	0.26 ± 0.003	0.002 ± 0.02	0.13 ± 0.01	0.12 ± 0.01
Research solution	2	0.39 ± 0.03	0.40 ± 0.04	0.18 ± 0.02	0.20 ± 0.02	—	—	0.38 ± 0.03	0.40 ± 0.04
Alloy solution	1	3.58 ± 0.15	3.50 ± 0.24	1.22 ± 0.08	1.30 ± 9.10	—	—	5.30 ± 0.20	5.10 ± 0.35
Concentrate solution	25	0.005 ± 0.001	0.005 ± 0.001	—	—	—	—	—	—

TABLE 11

Results of a.a.s. determinations of platinum metals (μg ml^{-1}) in technical solutions after preconcentration with polymeric thioether (I) and thiourea (II)

Solution analyzed	Rhodium		Iridium		Ruthenium		Platinum	
	I	II	I	II	I	II	I	II
3 M H_2SO_4	3.5 ± 0.6	3.8 ± 0.8	0.6 ± 0.02	—	1.0 ± 0.3	1.2 ± 0.4	0.5 ± 0.1	0.4 ± 0.1
1—2 M NaOH	0.1 ± 0.2	0.12 ± 0.03	0.1 ± 0.04	0.07 ± 0.03	0.1 ± 0.02	0.1 ± 0.03	0.5 ± 0.1	0.34 ± 0.1
3 M HCl	12 ± 2.2	13 ± 2.7	2.1 ± 0.8	2.0 ± 0.8	2.8 ± 0.8	3.0 ± 0.9	—	—

TABLE 10

Conditions for electrothermal a.a.s. determination of platinum metals in the powdered concentrate

Element	Wavelength (nm)	Ashing temperature[a]	Range of tested contents (μg)	s_r
Pd[b]	247.6	120—1200	4×10^{-3}—10^{-1}	0.10
Pt	266.0	120—1200	5×10^{-3}—10^{-1}	0.13
Ir	264.0	120—1400	4×10^{-3}—10^{-1}	0.18
Rh	343.5	120—1400	4×10^{-3}—10^{-1}	0.08
Ru	349.9	120—1400	1×10^{-2}—10^{-1}	0.13
Os	290.0	120—1400	$n \times 10^{-3}$—10^{-1}	0.18

[a]In all cases, the drying temperature was 120°C for 30 s, the ashing ramp took 90 s and the atomization temperature was 2700°C for 50 s. The tubes were then cleaned at 3000°C for 10 s. [b]If samples contain considerable copper concentrations the 340.4-nm line should be used.

for individual platinum metals in solution. Direct determinations of platinum metals are hindered by elements which produce multiline spectra (nickel, iron, cobalt). Separation of the platinum metals with the polymeric thioether ensures complete separation from these elements. Selenium and tellurium get into the concentrate, and selenium exerts a strong interference but it can be removed from the concentrate by distillation [28]. Tellurium does not markedly affect the results at concentrations up to 5 mg ml^{-1}. Experiments showed that there are no mutual interferences between the platinum metals. Results obtained by i.c.p.e.s. of solutions show good precision (Table 12). Comparison of results for industrial samples after preconcentration on the polymeric thioether or by means of thiourea is given in Table 13; the agreement is good.

Measurements on the solid concentrate

The solid concentrate was tested by using the powder injection method. It was mixed with graphite powder in the ratio 1:1 to provide better condi-

TABLE 12

Relative standard deviations (n = 8) of atomic emission methods for the determination of platinum metals each present at 250 μg g^{-1} in the concentrate

Metal	I.c.p.e.s.	Arc, evaporation from electrode crater	Arc, powder injection
Platinum	0.03	0.11	0.07
Palladium	0.03	0.16	0.11
Rhodium	0.04	0.14	0.05
Iridium	0.01	0.09	0.09
Ruthenium	—	0.11	0.07

TABLE 13

Results obtained for platinum metals ($\mu g\ ml^{-1}$) by i.c.p.e.s. after their sorption on polymeric thioether(I) and precipitation with thiourea(II) in products from copper—nickel slurries[a]

Platinum		Palladium		Rhodium		Iridium	
I	II	I	II	I	II	I	II
36.1	34.6	130.6	120.7	19.4	18.8	4.0	4.1
8.6	8.6	30.1	28.4	5.3	5.2	0.9	0.9
9.6	7.9	30.9	26.5	5.6	5.5	1.1	1.3
10.0	9.4	32.0	29.8	5.7	5.5	1.3	1.3
8.6	8.7	27.5	26.0	5.3	5.3	1.1	1.1

[a]Contents: copper 40—45%; nickel 11—12%; cobalt 10%; iron 4—5%.

tions for blowing the sample into the arc discharge. When the sorbent was diluted with graphite powder, the lower limits for the platinum metals were practically unchanged from the lower limits obtained for graphite reference samples. When the reference samples were prepared on the basis of the sorbent, the lower limit of determination increased (Table 14). The platinum metals in the concentrate can also be determined by the common technique, i.e., by evaporating the concentrate from the electrode crater but the precision of the results is then somewhat worse (Table 12).

The results for some industrial samples after preconcentration of platinum metals on polymeric thioether are compared in Table 15. The data obtained by different methods are in good agreement.

Comparison of a.e.s. methods

The methods developed allow platinum metals to be determined in the concentration range 0.1—100 mg l^{-1} in products from treatment of copper—nickel slimes. The i.c.p.e.s. method provides good precision. Powder injection ensures the determination of osmium and ruthenium because it excludes possible losses during dissolution of the concentrate.

TABLE 14

Lower limits of determination for the platinum metals against various reference samples

Metal	Limit of determination (% mass)		
	Graphite powder	Sorbent + graphite powder	Sorbent
Platinum	1×10^{-4}	1×10^{-4}	2×10^{-4}
Palladium	1×10^{-4}	2×10^{-4}	5×10^{-4}
Rhodium	5×10^{-4}	5×10^{-4}	1×10^{-3}
Iridium	1×10^{-3}	1×10^{-3}	2×10^{-3}
Ruthenium	2×10^{-4}	5×10^{-4}	1×10^{-3}

TABLE 15

Results ($\mu g\ ml^{-1}$) obtained for the platinum metals in products from copper–nickel slurries[a] by the a.e.s. method with powder injection (PI) and by atomic absorption spectrometry (a.a.s.)

Platinum		Iridium		Rhodium		Palladium		Ruthenium	
PI	A.a.s.	PI	A.a.s.	PI	A.a.s.	PI	A.a.s.	PI	A.a.s.
0.2	0.2	0.2	0.2	1.4	1.6	0.2	0.18	0.02	0.02
0.2	0.2	0.6	0.55	6.0	5.9	0.2	0.19	0.16	0.15
0.6	0.45	0.4	0.5	10	10	0.2	0.17	0.14	0.13
0.2	0.2	0.2	0.2	0.2	0.2	0.2	0.19	0.02	0.02
0.2	0.4	0.6	0.8	1.6	1.3	0.2	0.18	0.08	0.1
0.2	0.3	0.2	—	0.6	0.5	0.2	0.19	0.06	0.05

[a]Contents, mg ml^{-1}: copper up to 45, nickel 5, cobalt 15, iron 3.

DISCUSSION

Comparison of the conditions for sorption of platinum metals and their accompanying elements (i.e., copper, nickel, cobalt and iron) on the polymeric thioether with the conditions for their sorption on inorganic sulfides and for liquid–liquid extraction by sulfur-containing extractants indicates the similarity of the nature of separation. The acidity range for metal sorption approximately coincides with the acidity ranges for liquid–liquid extractions and precipitation of sulfides. The interaction of the polymeric thioether and the metals can be considered in terms of hard and soft acids and bases.

The kinetic behaviour is of some interest. Among the noble metals, only palladium and gold are completely sorbed at room temperature; platinum is less sorbed. For complete sorption of other platinum metals which are more resistant to substitution reactions, the solution must be heated in the presence of the sorbent by batchwise techniques.

The proposed method of preconcentration can be used for isolation of platinum metals from samples containing these metals at concentrations of 1 ng ml^{-1} or 0.1 ng g^{-1} or higher.

For comparison of all the procedures developed, and for intercorrelation of the results obtained by the application of these procedures, some materials were analyzed by each procedure. As shown in Table 16, the agreement of the results obtained was generally good.

Various sorbents have been proposed for the concentration of the platinum metals, gold and silver; chelating sorbents (i.e., sorbents with chelating groups grafted to a polymeric matrix) have been widely used. The sorbent proposed here is of a new type in which the electron-donating element is contained in the matrix. This gives certain advantages, the most important one being the high capacity achieved; for example, the capacity is 4.0 g g^{-1} for gold(III), and 1.2 g g^{-1} for palladium. Comparison of the sorption properties of

TABLE 16

Results obtained for platinum metals in various materials

Sample	Metal	Metal found ($\mu g\ g^{-1}$)				
		X.r.f.	Flame a.a.s.	Electrothermal a.a.s.	I.c.p.e.s.	A.e.s. (powder injection)
Chalcogenide concentrate[a]	Pt	6.2 ± 0.3	6.2 ± 0.9	—	6.6 ± 0.4	—
	Pd	30.9 ± 1.8	30.7 ± 3.9	—	30.1 ± 1.8	—
	Rh	—	1.2 ± 0.1	—	1.16 ± 0.05	—
Raffinate solution	Pt	0.13 ± 0.01	0.12 ± 0.02	—	—	—
	Pd	3.3 ± 0.2	2.5 ± 0.01	—	—	—
	Rh	0.92 ± 0.06	1.0 ± 0.08	—	—	—
Chloride melt solution	Pt	—	74 ± 18	—	79 ± 6.6	—
	Pd	—	180 ± 23	—	176 ± 11	—
	Rh	—	13.1 ± 0.1	—	12.6 ± 0.3	—
	Ir	—	—	4.5 ± 0.2	4.7 ± 0.1	—
Technical solution	Pt	—	—	0.4 ± 0.1	—	0.4 ± 0.1
	Pd	—	—	0.3 ± 0.1	—	0.2 ± 0.1
	Rh	—	—	0.1 ± 0.02	—	0.09 ± 0.03
	Ru	—	—	1.6 ± 0.5	—	1.5 ± 0.6
	Ir	—	—	0.1 ± 0.03	—	0.11 ± 0.04

[a] All results for this sample are given as %.

the described sorbent $(-CH_2-S-)_n$ with the properties of the sorbent $(-CH_2-CH_2-S-)_n$ containing 50% less sulfur has shown that the latter sorbent is less active.

The preconcentration of metals over wide concentration ranges (from fractions of a microgram to tens of milligrams) because of the high capacity of the sorbent, the high distribution coefficients, and the good selectivity, make it possible to widen the list of the materials that can be analyzed. Furthermore, investigations along similar directions can contribute to the solution of some problems of general chemical interest. For example, there is an opportunity to compare the chemical activity of the same donor atom after the transition from monomer to polymer and to compare the composition of the compounds which are formed with the monomer on the surface of the polymer. Thus it becomes possible to observe when and where surface phenomena start to acquire a leading role. Finally, it becomes possible to compare the kinetics of interaction between homogeneous reaction in the one case and heterogeneous reactions in the other.

REFERENCES

1 W. J. Campbell, E. F. Spano and T. E. Green, Anal. Chem., 38 (1966) 987.
2 M. G. Bapat and F. E. Beamish, Anal. Lett., 7 (1969) 387.
3 H. Taylor and F. E. Beamish, Talanta, 15 (1968) 497.
4 C. L. Luke, Anal. Chim. Acta, 41 (1968) 237.
5 C. W. Fuller, G. Himsworth and J. Whitehead, Analyst, 96 (1971) 177.
6 P. N. Gerrard and N. Westwood, J. S. Afr. Chem. Inst., 25 (1972) 285.

7 F. I. Lobanov, S. E. Sorokin and I. M. Gibalo, in: Improvement of effectiveness and quality of the control of chemical composition of materials, Znanie, Moscow, 1978, p. 60 (in Russian).
8 D. A. Katzkov, L. P. Kruglikova and B. V. L'vov, Zh. Anal. Khim., 30 (1975) 238.
9 D. A. Katzkov, I. L. Greenstein and L. P. Kruglikova, Zh. Prikl. Spektrosk., 32 (1980) 536.
10 L. P. Kruglikova, Ph.D. Thesis, Leningrad, 1975, p. 12.
11 E. D. Pruknikov, in Abstracts of papers for XI All-Union Meeting on Chemistry, Analysis and Technology of Platinum Metals, Nauka, Moscow, 1979, p. 53 (in Russian).
12 S. I. Ginzburg, K. A. Gladishevskaya, N. A. Ezerskaya, O. M. Ivoina, I. L. Prokof'eva, N. V. Fedorenko and A. N. Fedorova, Handbook on Chemical Analysis of Platinum Metals and Gold, Nauka, Moscow, 1965 (in Russian).
13 G. V. Myasoedova, G. I. Malofeeva, O. P. Shvoeva, E. V. Illarionova, S. B. Savvin and Yu. A. Zolotov, Zh. Anal. Khim., 32 (1977) 645.
14 L. N. Kolonina, O. A. Shiryaeva, G. I. Malofeeva and E. V. Marcheva, Zh. Anal. Khim., 35 (1980) 92.
15 N. A. Bortsch, Yu. A. Zolotov, L. N. Kolonina, O. M. Petrukhin, V. N. Shevchenko and O. A. Shiryaeva, Zh. Anal. Khim., 35 (1980) 2369.
16 L. M. Gindin, A. P. Sokolov, V. I. Bushmakina, N. A. Tkacheva, V. N. Andrievskii, L. I. Kotlyarevskii, E. N. Gilbert, G. V. Verevkin and G. N. Chernousova, Izv. Sib. Otd. Akad. Nauk. SSSR, Ser. Khim., No 7, 3 (1977) 137.
17 N. N. Basargin, Yu. T. Rozovskii, V. G. Khitrov and G. E. Belousov, in Optical methods for the control of chemical composition of materials, MDNTP, Moscow, 1974, p. 138 (in Russian).
18 I. I. Antokol'skaya, G. V. Myasoedova, L. I. Bol'shakova, M. G. Ezernitskaya, M. P. Volinetz, A. V. Karyakin and S.B. Savvin, Zh. Anal. Khim., 31 (1976) 742.
19 N. G. Vanifatova, I. V. Seryakova and Yu. A. Zolotov, Extraction of Metals with Neutral Sulfur-containing Compounds, Nauka, Moscow, 1980 (in Russian).
20 G. V. Myasoedova and G. I. Malofeeva, Zh. Anal. Khim., 34 (1979) 1626.
21 E. Dachself, Thioplaste, Leipzig, 1971, S. 42, 67.
22 N. N. Kazanova, O. M. Petrukhin, I. I. Antipova-Karataeva and G. I. Malofeeva, Coord. Chem., 8 (1982) 1510.
23 S. Livingston, Chemistry of Ruthenium, Rhodium, Palladium, Osmium, Iridium, Platinum, Mir, Moscow, 1978, p. 212 (in Russian).
24 N. F. Losev, Quantitative X-Ray Fluorescence Analysis, Nauka, Moscow, 1969, p. 28, 330 (in Russian).
25 J. Leroax, Adv. X-Ray Anal., 5 (1962) 153.
26 S. I. Ginzburg, N. A. Ezerskaya, I. V. Prokof'eva, N. V. Fedorenko, V. I. Shlenskaya and N. K. Bel'skii, Analytical Chemistry of Platinum Metals, Nauka, Moscow, 1972 (in Russian).
27 V. P. Baluda, G. I. Ermolina, L. N. Kolonina, S. A. Somashevich, V. P. Khvostova and D. Ya. Choporov, Zh. Anal. Khim., 35 (1980) 713.
28 I. I. Nazarenko and A. N. Ermakov, Analytical Chemistry of Selenium and Tellurium, Nauka, Moscow, 1971, p. 184 (in Russian).

Analytica Chimica Acta, 148 (1983) 159—170
Elsevier Science Publishers B.V., Amsterdam — Printed in The Netherlands

A DIALOGUE COMPUTER PROGRAM SYSTEM FOR STRUCTURE RECOGNITION OF COMPLEX MOLECULES BY SPECTROSCOPIC METHODS

L. A. GRIBOV*, M. E. ELYASHBERG, V. N. KOLDASHOV and I. V. PLETNJOV

V. I. Vernadsky Institute of Geochemistry and Analytical Chemistry, USSR Academy of Sciences, Vorobyovskoye Shosse 47a, Moscow V-334 (U.S.S.R.)

(Received 15th April 1982)

SUMMARY

A dialogue computer program system for structure recognition by infrared, proton magnetic resonance and carbon-13 nuclear magnetic resonance spectra is described. The results of the application of this system to identify organophosphorus compounds are examined.

The new trend in analytical spectrochemistry based on utilization of artificial intelligence, has been intensely developed in recent years. The first studies in which artificial intelligence was used for spectroscopic recognition of molecular structure appeared in late 60's and early 70's. Since then, the annual output of original articles has increased greatly (see, e.g., [1—7]) and reviews [8, 9] and a monograph [10] have appeared.

Experience accumulated in this area indicates that any system of artificial intelligence designed for the recognition of molecular structure, must include the three following basic blocks: A, structural group analysis (s.g.a.) based on spectrum—structure correlations; B, mathematical synthesis of structures from atoms, chosen as a result of s.g.a. fragments when the overall formula is given; C, checking of each synthesized structure for correspondence with given experimental spectra. The presence of these system components, irrespective of the mathematical algorithms introduced, allows quite successful identification of compounds belonging to different classes. Attempts to recognize large molecular structures containing a variety of functional groups and/or polyatomic fragments without any sharp characteristic signals are very difficult. The reason is that in such situations a large number of fragments and free atoms of the skeleton (which belong to unrecognized structural elements) must go into the mathematical synthesis.

As the real number of discrete structural units from which most structures can be synthesized during a reasonable time with the help of modern computers is not greater than 7—10, it is evident that the synthesis stage is the bottle-neck in all recognition systems. It seems unlikely that extremely fast programs for structure generation will appear in the near future, thus the

0003-2670/83/$03.00

generation block will probably remain the most conservative part of recognition systems. Accordingly, further development will depend on improvement of the first and last stages of recognition (s.g.a. and evaluation of possible structures).

As has been shown [11], increased effectiveness of the artificial intelligence system is achieved at the expense of increasing the dimensions of the fragments used in the synthesis. All accessible kinds of spectra should be used in the process of s.g.a., spectral parameters of lines and signals should be taken into consideration, and there should be active human participation at all stages in the solution of the identification problem. In this paper, such an approach is examined within the limits of the STREC-2 system of artificial intelligence. Application of this system in the identification of organophosphorus compounds is described.

THE STREC-2 SYSTEM

When the STREC-2 system was developed, the main effort was directed to increasing the molecular dimensions to 30—40 atoms in the skeleton. This demanded changes in the algorithms, programs and fragment libraries described earlier [10, 12] to provide the possibility of working with large structural units. A large fragment involving many skeleton atoms can join a structural unit under definite conditions, if there is significant electron interaction. Working like discrete structural units, such fragments allow the molecule to be represented as the sum of quasi-independent structural units, and that fulfils the condition of additivity, which is basic to the concept of characteristic spectral signals. For example, with the compound CH_2=$CHCH_2CH_2CH_2COCH_3$, if vinyl and ketone groups have own characteristic signals (frequencies in i.r. spectra, chemical shifts in n.m.r.), then fragment CH_2=$CHCOCH_2$ already possesses individual signals in the structure CH_2=$CHCOCH_2CH_2CH_2CH_3$. However, the creation of a library of large fragments is complex, because the construction of tables of spectral signals for such fragments demands a great deal of human effort, being difficult to automate. Expenditure on such libraries can be worthwhile only for specialised purposes, e.g., for recognition of definite classes of chemical compounds. Accordingly, the optimal variant of the system is one based on library storage of both large and small fragments which are of interest to the particular team of investigators.

The s.g.a. block of the STREC system [12] and the typical fragment library (TFL) used in this system have been completely reconstructed. Large fragments were added to the s.g.a. library collected before (the maximum size of fragments provided for in the program is 15 atoms in the skeleton), and separate molecules could be used as fragments. To increase the discriminatory power of the system, intervals of characteristic spectral signals in i.r., p.m.r. and ^{13}C-n.m.r. spectra are compared for each fragment, apart from its valency and overall formula. If fragment signals are not

characteristic in some spectrum, they are not introduced into the library. Because of this approach, it is no longer necessary to have a special library for s.g.a. of i.r., p.m.r. and ^{13}C-n.m.r. spectra separately. Simultaneously, the probability of unique selection of a fragment increases (selection is done by a large number of signals).

Intervals of changing of frequencies and band halfwidths and intensities in accordance with five-point scales are introduced as signals in i.r. spectra. Intervals of changing of chemical shifts and coupling constants of corresponding nuclei for n.m.r. spectrum are also included. In cases for which multiplicities of signals can be predicted beforehand, their values are also placed in the TFL. As the geometry of groups in large fragments having characteristic signals is completely defined, these signal intervals can be made narrower than standard values. A descriptor is compared with each fragment, and shows the possibility of connecting hydrogen atoms or heteroatoms to the free bonds. In addition, the relation of the fragment to the cycle (enter, do not enter, does not matter) and the possibility of constructing multiple bonds via free valences is noted. Descriptors enable each fragment and its allowed position in the molecule to be described with adequate strictness; that can be used to choose the most probable structures. Intervals of characteristic signals were established from listings in the literature [13—16], as well as calculations based on additivity rules and on spectra for reference compounds.

As an example, two large fragments with their characteristic signals are shown in Table 1. The experimental spectra are represented by the set of corresponding signals. If any parameter of the spectrum cannot be measured (e.g., $\Delta\nu_{1/2}$, J) or if a multiplet cannot be described as a first-order spectrum, it is noted by conditional symbols. The possible results of comparing experimental infrared intensities with those given in the library are determined by a comparison matrix:

		Experiment				
		1	2	3	4	5
From	1	+	+	+	+	+
the	2	+	+	+	+	+
TFL	3	+	+	+	+	+
	4	—	—	+	+	+
	5	—	—	+	+	+

where + means a positive comparison and — means a negative result.

It can be seen that comparison of band intensities in an i.r. spectrum gives a negative result only when the TFL indicates that a strong band is expected at some frequency interval whereas a weak line appears in the experiment. In the opposite situation (where a weak band is expected and a strong band is observed), the comparison of intensities gives a positive result, as consideration is given to the fact that a weak band can be overlapped by a strong band arising from the absorption of some other fragment. In cases for which

TABLE 1

Large fragments with their characteristic signals

—$CH_2CH_2O\overset{\overset{O}{\|}}{C}CH_2\ CH_2\overset{\overset{O}{\|}}{C}OCH_2CH_2$—			
I.r.: $\nu(cm^{-1})$	1730—1740	1200—1260	1100—1170
$\Delta\nu_{1/2}(cm^{-1})$	20—50	30—100	20—80
I	5	5	5
P.m.r.: δ(ppm)	2.20—2.70	3.90—4.30	
J(Hz)	0—0	6—9	
M	1	3	
^{13}C-n.m.r.: δ(ppm)	166—217	25—40	45—72
J(Hz)	0—0	126—132	138—150
M	1	3	3
—$CH_2\ CH_2\ O\overset{\overset{O}{\|}}{C}O\ CH_2\ CH_2$—			
I.r.: $\nu(cm^{-1})$	1735—1745	1200—1260	
$\Delta\nu_{1/2}(cm^{-1})$	20—50	30—100	
I	5	5	
P.m.r.: δ(ppm)	4.10—4.40		
J(Hz)	6—9		
M	3		
^{13}C-n.m.r.: δ(ppm)	151—162	62—72	
J(Hz)	0—0	135—145	
M	1	3	

the frequency is not characteristic by intensity or when a band of medium intensity is observed in the spectrum, the intensity is estimated by the amount $I = 3$. Because of careful discrimination by the intensity signal, erroneous action of this criterion is excluded. The aim of estimating the band halfwidths is to distinguish between wide and narrow bands observing in the same frequency intervals. Because of this, i.r. bands of ν_s(≡C—H) and ν_s(—OH), observed in the region 3300—3400 cm^{-1}, for example, will be correlated with different fragments according to the different values of $\Delta\nu_{1/2}$. Consequently, when both groups are present in the molecule, this can be established unambiguously; instead of the logical function $\nu \rightarrow$ (C≡C—H) ν_s (OH), the program will give two implications $\nu \rightarrow$ (C≡C—H) and $\nu \rightarrow$ (OH).

INTERACTION WITH THE COMPUTER

The system of artificial intelligence will be able to solve intricate problems encountered in practice only when a close interactive dialogue with the specialist is possible. Such a regime makes it possible to exploit fully the capability of the man—computer partnership. To make this dialogue possible, the specialist must use certain techniques, transmitting to the computer all the relevant information accumulated during the study, as well as hypotheses based on the specialist's experience and intuition.

These demands were considered in developing the dialogue regime for the STREC-2 system. The interactive exchanges are achieved by means of electronic displays. The program questions the chemist, explaining simultaneously in what form the answer should be given. Accordingly, the operator does not need technical knowledge, but simply presses display keys to produce the necessary figures and words in normal language.

Initially, the program requests information on the types of spectra and spectral parameters available. After introducing all the spectral information (frequencies, chemical shifts, parameters) and the empirical formula of the substance, the operator indicates the regime to be used for decision on the implications (i.e., logical correlations of the $\omega_j \rightarrow A_1$ vs. A_2 vs.... vs. A_n type, which show that if there is a feature ω_j in the spectrum, the molecule has at least one of fragments $A_1, A_2 \ldots A_n$ [17]). Seven regimes of implication listing are envisaged:

	1	2	3	4	5	6	7
I.r.	+	−	+	−	+	−	+
P.m.r.	−	+	+	−	−	+	+
^{13}C-n.m.r.	−	−	−	+	+	+	+

The positive sign means that implications must be constructed in accordance with frequencies (chemical shifts) of the corresponding spectrum; the negative sign shows that the particular spectrum simply confirms the possibility of the presence of the selected fragments or it is not put into the computer at all. The freedom of choice of regime makes it possible, for each particular problem, both to choose the most informative types of spectra to form the initial system of hypotheses and to examine the dependence of the final result on the type of spectrum used to build the "reasoning" of the computer.

When automatic construction of implications is over, the operator can make any changes thought necessary, e.g., exclusion or addition of some library fragments or of some implications. While doing so, the specialist can rely on the validity of the correlations generating each implication. This validity rests primarily on the singular logical relations of the $\omega_j \rightarrow A_i$ type. For example, if ω_j = 3635 cm^{-1} and $A_i \equiv (CH_2OH)$, the accuracy of the expression $\omega_j \rightarrow A_i$ is beyond doubt, whereas in the case of ω_j = 1040 cm^{-1} and the same fragment, this expression must be regarded with suspicion because the 1000—1100 cm^{-1} region of an i.r. spectrum almost always contains absorption bands and cannot be correlated unambiguously with an alcohol group.

When consistent logical equations have been solved, sets of fragments are displayed. Each set has its display line containing a certain number of atoms of chemical elements corresponding to subtraction of the elemental composition of the set from the empirical formula of the molecule. According to the operator's instructions, either sets which do not exceed the

empirical formula of the substance, or the whole collection of sets forming the solution of logical equations, can be produced. Knowledge of the complete solution of logical equations can become necessary in cases of s.g.a. of a mixture for which the approximate elemental composition is known, or to elucidate the causes of any contradictions between the molecule empirical formula and all possible sets of fragments.

The produced sets of fragments are scanned and analysed by the specialist, who can change any set or completely cancel it. Changes include the transposition of the set numbers (the order of their arrival for synthesis), exclusion or addition of library fragments, and introduction of new fragments which are not included in the TFL, or discrete structural units with given valence and structure represented by connection tables. This is the end of the s.g.a.

Then the program asks the operator questions concerning the requirements of synthesis and filtration of structures. At this stage, forbidden fragments and fragments which must be present in every structure can also be introduced; any such fragments must not be discrete structural units, but will allow overlapping of atoms in the library fragments and in any new fragments introduced by the specialist. The introduction of such fragments makes it possible to connect up discrete structural units selected at the s.g.a. stage. Cyclic structures of different dimensions can act as forbidden or necessary fragments; this helps to exclude structures containing, for example, three- or four-membered rings (as a rule, compounds with strained rings demand the use of special methods of synthesis, so that any probability of their presence in the sample can be estimated with sufficient surety). If, having given the spectra and the type of fragments chosen for synthesis, the specialist can establish the maximum multiplicity of bonds constructed in the process of generation, he can show the maximum possible multiplicity of the bond (m_{max}). This makes it possible to suppress the mathematical synthesis of structures containing $m > m_{max}$, providing an obvious gain in computer time. If there are no signs of multiple bonds in the spectra and if the empirical formula shows the existence of rings in the molecule under consideration, then given $m_{max} = 1$, only cyclic compounds will be obtained in the output. The operator can also indicate the regime of output for structural formulae. Usually only those structural formulae are printed which have been confirmed in the process of filtration. However, it may happen that for some reason (e.g., because of some experimental signal exceeding the interval indicated in the TFL) all synthesized structures become defective. In this case, all the structures should be printed out, with an indication of the causes for their failure to pass the filter.

Thus the dialogue regime of the STREC-2 system offers wide possibilities for coordinating human experience and intuition with the ability of the computer to complete fast searches and to make complex logical and combinatorial calculations.

The filter system

To achieve the last stage of recognition (filtration of structures), new algorithms and programs have been developed, which provide for elucidation of the total atom structure of molecules containing about 40 atoms in the skeleton, and also for establishing the existence or absence in this structure of large (about 15 skeleton atoms) fragments from the filter library. The filter library, as before [12], preserves its block structure. It contains libraries of i.r., p.m.r., m.s. and u.v. filters worked out at earlier stages, and also the new TFL used in the STREC-2 system at the s.g.a. stage. It allows additional checks to be made on structures for their correspondence to u.v. and mass spectra (if such data are available) and permits utilization of fragments with signals of low information content, that were not used in s.g.a.

RESULTS OF EXPLOITATION OF THE SYSTEM

In order to check the functional capacity of the STREC-2 system, identification of 20 sufficiently large molecules containing no aromatic rings was examined. The program was provided with i.r., p.m.r. and ^{13}C-n.m.r. spectra of these compounds. The parameters of the i.r. bands and the n.m.r. signals were given if they could be measured. Table 2 shows some recognized structures.

TABLE 2

Examples of recognized structures

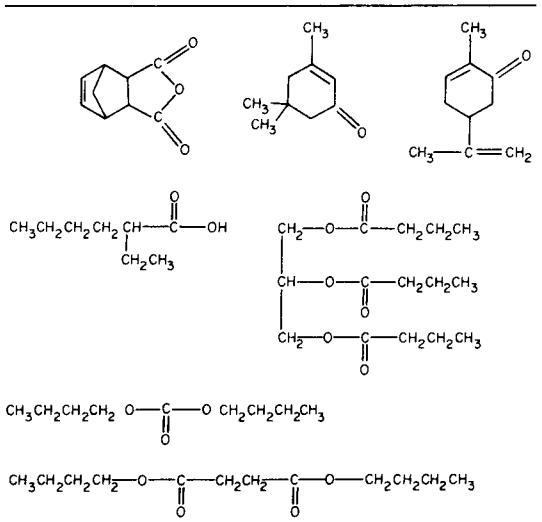

Recognition of organophosphorus compounds

The expansion of the possibilities of the system is connected not only with the recognition of larger molecules but also with the increased number and variety of chemical elements that can be dealt with. Obviously, the creation of the TFL becomes more complete with the increased number of different heteroatoms, as the number of possible atom combinations increases sharply.

An attempt was made to construct a TFL for identification of organophosphorus compounds based on their i.r. spectra. Information about the characteristic frequencies of organophosphorus compounds is available in monographs [18, 19]. Fifty fragments which are most commonly found in organophosphorus compounds were chosen from these sources and added to the system library [12]. Some examples of the fragments and the corresponding intervals of characteristic frequencies are given in Table 3. Evaluation of the TFL for phosphorus-containing fragments showed that: (a) their characteristic intervals are mainly in the "finger-print" region where there are many absorption bands of different nature; (b) frequency intervals are usually wide and their number is usually small; (c) frequency intervals of different fragments often overlap each other. Therefore, it was expected that the recognition of organophosphorus substances would be done under difficult conditions, characterized by a high degree of informational noise.

More than 70 problems were chosen for study, either from the atlas [20] or on suggestions from researchers. Apart from trivalent or pentavalent

TABLE 3

Examples of organophosphorus fragments

Fragments	Frequency intervals (cm^{-1})	Fragments	Frequency intervals (cm^{-1})
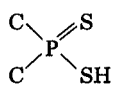	450—480, 470—500, 580—620, 730—785, 2350—2450	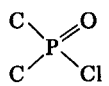	455—550, 1215—1270
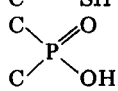	450—540, 940—1010, 1085—1205, 1600—1740, 2080—2350, 2525—2725	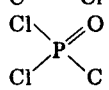	480—515, 530—575, 1230—1300
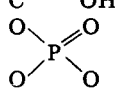	1210—1315	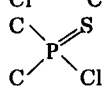	440—485, 475—515, 590—700, 730—820
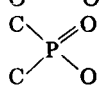	1150—1240	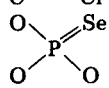	500—535, 555—600
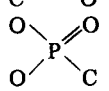	1150—1290	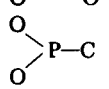	860—870, 1270—1285
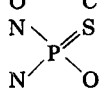	645—700, 775—835		

phosphorus, the molecules contained other heteroatoms such as O, N, S, Se and halogens. Problems were divided into two categories, A and B. Molecules consisting of not more than 10 discrete structural units (except for skeleton atoms, aromatic rings are discrete structural units) belong to class A (40 compounds; examples are given in Table 4). Large structures with fragments known to the investigator and provided, were consigned to class B. Large fragments were added to the library fragment sets found by the system. Obviously, the truth of such assumptions about fragments must be checked during the filtration stage, and if the experimental spectrum is found to contradict the filter library, then the structural formula with a fragment introduced on a priori information must be rejected. It was found that 40% of the problems from class A could be solved without specialist help, but in the other cases help was necessary at the dialogue stage. The commonest cause of difficulties in the program was contradiction between the chosen sets of fragments and the empirical (overall) formula of the substance. The contradictions usually appeared in the computer output about the simultaneous presence of some phosphorus fragments in a structure with one phosphorus atom, and could usually be attributed to fragments with low information content in the TFL, e.g.,

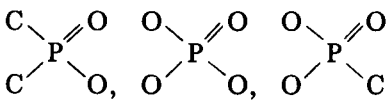

all of which show absorption in the same frequency interval.

TABLE 4

Examples of recognized organophosphorus compounds belonging to class A

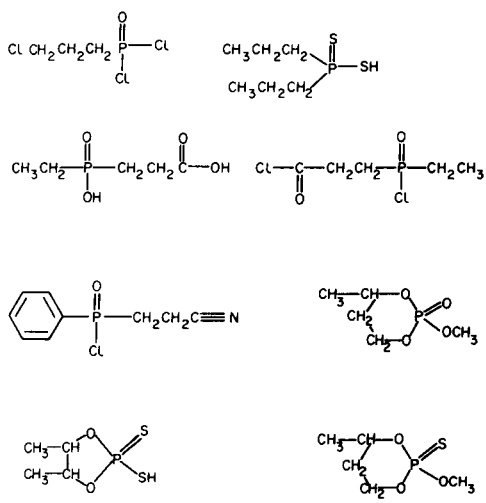

Such contradictions were resolved by distribution of the competing fragments according to the probability of their presence. The fragment probability was determined by the number of its characteristic intervals, by the presence of signals in the functional group region (1400—3700 cm^{-1}) where the reliability of identification increased, and also by chemical considerations. For example, when the molecule

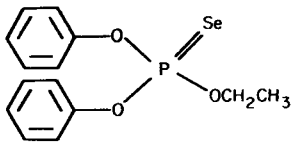

was identified, the logical correlation system constructed by the program was of the following type:

502 cm^{-1} → |17|
525 cm^{-1} → |17|
595 cm^{-1} → 17
690 cm^{-1} → 51
770 cm^{-1} → 51 vs. 52 vs. 54
1165 cm^{-1} → |14| vs. |15| vs. |19|
1190 cm^{-1} → |14| vs. |15| vs. |19|
1290 cm^{-1} → |15|
1490 cm^{-1}
1598 cm^{-1} } → 51 vs. 52 vs. 54
3030 cm^{-1}

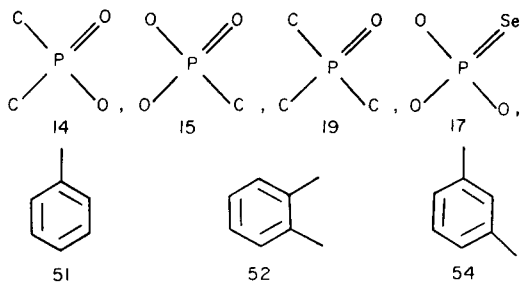

The numbers of competing fragments are enumerated here to the right of the implications; fragments appearing because of some experimental frequencies in the same intervals are placed in columns. It can be seen that fragments 14, 15, 19 possess one characteristic interval (1150—1240, 1150—1290, 1130—1200 cm^{-1}, respectively); therefore the probability of their presence is less than for fragment 17 represented by two narrow intervals (500—525 and 595—600 cm^{-1}). As fragment 51 is established simply from the band at 690 cm^{-1}, it is clear that the most probable set must consist of fragments 17 and 51 which give two solutions:

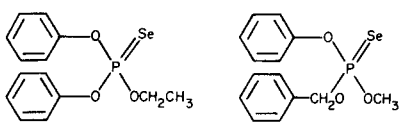

Recording of the p.m.r. spectrum should then immediately allow identification of the true structure.

Experience with identification of the class B compounds showed that, because of the dialogue regime, complete compounds could be identified, even when they possessed up to 25—30 skeleton atoms. The isomers found differed mainly through transposition of alkyl radicals. Examples of class B compounds are given in Table 5. It is worth noting that the recognition of rather large and complex molecules by the STREC-2 system appears to be possible only when the presence of large fragments is indicated from prior

TABLE 5

Examples of complex organophosphorus compounds identified

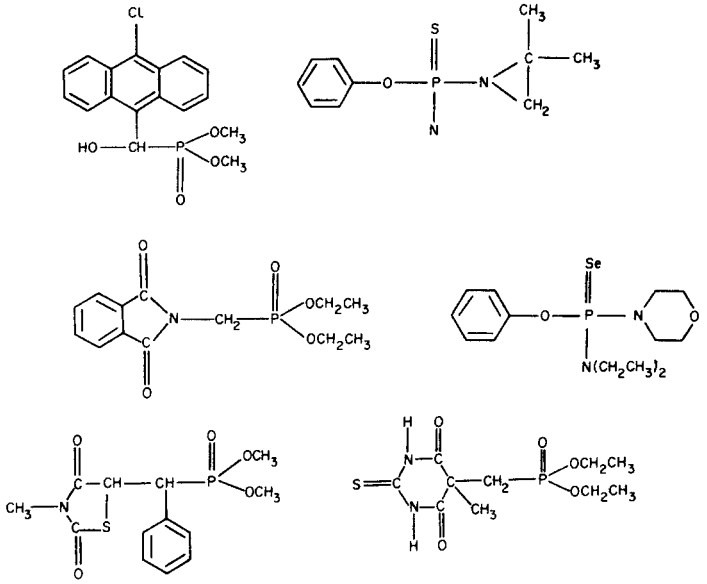

information. For instance, for the appropriate structures in Table 5, the following fragments were given a priori: If the number of competing frag-

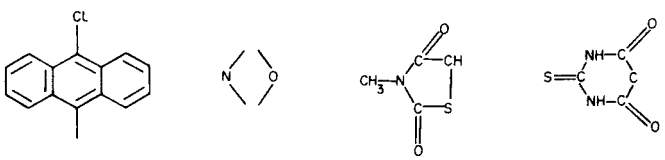

ments is large, and all the fragments have roughly the same probabilities, then the number of possible sets of fragments and, consequently, of possible structures, becomes too large to have practical value.

As the maximum effect from the use of computerized identification systems can be achieved when they are specialized, a more complete fragments library for organophosphorus chemistry with the use of correlations in i.r., p.m.r. and ^{13}C-n.m.r. spectra will be developed. This will allow the range of solved problems to be expanded and the selectivity of the system to be improved. In conclusion, all system programs are written in Fortran-IV, and part of dialogue regime is written in PL/1.

REFERENCES

1 S. Sasaki, I. Fujiwara, H. Abe and T. Yamasaki, Anal. Chim. Acta, 122 (1980) 87.
2 T. Oshima, Y. Ishida, K. Saito and S. Sasaki, Anal. Chim. Acta, 122 (1980) 95.

3 M. Vida, Anal. Chim. Acta, 122 (1980) 41.
4 B. Debska, J. Duliban, B. Guzowska-Swider and Z. Hippe, Anal. Chim. Acta, 133 (1981) 303.
5 M. Farkas, J. Markos, P. Szepesvary, I. Bartha, G. Szalontai and Z. Simon, Anal. Chim. Acta, 133 (1981) 19.
6 G. Szalontai, Z. Simon, Z. Csapo, M. Farkas and Gy. Pfeifer, Anal. Chim. Acta, 133 (1981) 31.
7 D. Smith, N. A. B. Gray, J. G. Nourse and C. W. Crandell, Anal. Chim. Acta, 133 (1981) 471.
8 L. A. Gribov and M. E. Elyashberg, Crit. Rev. Anal. Chem., 8 (1979) 111.
9 Z. Hippe and R. Hippe, Appl. Spectrosc. Rev., 16 (1980) 134.
10 M. E. Elyashberg, L. A. Gribov and V. V. Serov, Molecular Spectral Analysis and Computers, Nauka, Moscow, 1980 (in Russian).
11 M. E. Elyashberg, in Application of Computers in Molecular Spectroscopy and Chemical Research, 5th All-Union Conference, September, 1981, Novosibirsk, U.S.S.R. (in Russian).
12 L. A. Gribov, M. E. Elyashberg and V. V. Serov, Anal. Chim. Acta, 95 (1977) 75.
13 L. S. Bellamy, The Infrared Spectra of Complex Molecules, Methuen, London, 1963.
14 A. J. Gordon and R. A. Ford, The Chemist's Companion, Wiley, New York, 1972.
15 D. E. Leyden and R. H. Cox, Analytical Applications of Nuclear Magnetic Resonance, Wiley, New York, 1977.
16 F. W. Wehrli and T. Wirthlin, Interpretation of Carbon-13 NMR Spectra, Heyden, London, 1976.
17 L. A. Gribov, M. E. Elyashberg and L. A. Moscovkina, J. Mol. Struct., 9 (1971) 357.
18 L. C. Thomas, The Identification of Functional Groups in Organophosphorus Compounds, Academic Press, London, 1974.
19 L. C. Thomas, Interpretation of the Infrared Spectra of Organophosphorus Compounds, Heyden, London, 1974.
20 R. R. Shagidullin, F. S. Mukhametov, R. B. Nigmatullina, V. S. Vinogradova and A. V. Tshernova, Atlas of Infrared Spectra of Organophosphorus Compounds, Nauka, Moscow, 1977 (in Russian).

Analytica Chimica Acta, 148 (1983) 171—180
Elsevier Science Publishers B.V., Amsterdam — Printed in The Netherlands

THE ATOMIC EMISSION SPECTROMETRIC DETERMINATION OF NON-CONDUCTING MATERIALS WITH A BOOSTED-OUTPUT GLOW-DISCHARGE SOURCE

G. S. LOMDAHL and R. McPHERSON

Department of Materials Engineering, Monash University, Clayton, Victoria 3168 (Australia)

J. V. SULLIVAN*

CSIRO Division of Chemical Physics, PO Box 160, Clayton, Victoria 3168 (Australia)

(Received 20th October 1982)

SUMMARY

Factors influencing the determination of non-conducting materials (nickel, copper and iron oxides) by emission spectroscopy with a boosted-output glow-discharge source are discussed. The sample is pressed with a conducting binder (copper, iron or nickel) and is made the cathode of the excitation source. Good precision (1—2%) may only be achieved if the powders eventually forming the cathode are properly mixed and adequately outgassed. The binder element is chosen so that the spectral interference is minimal. The detection limits are 0.002% NiO and 0.0015% CuO, in a Cu and Ni binder, respectively.

The potential of the Grimm lamp [1,2] as an excitation source for emission spectrochemistry of metallic samples has been investigated by several workers [3—6]. Its application to the analysis of non-conducting materials pressed into pellets with a conducting binder has been reported by several authors [7—11], who used the Grimm source for the determination of major elements in rocks and other geological samples. The samples were pulverized and mixed with metal or graphite powder, and the mixture was pressed into conducting discs to be used as cathodes. Copper was found to be a more satisfactory binder than graphite because it provided the pellet with good mechanical strength and high thermal conductivity, and made it easier to outgas.

In the boosted-output glow-discharge lamp [12], the metal sample, which forms the cathode for the glow discharge, is atomized by cathodic sputtering and the vapour thus formed is excited by a secondary low-voltage, high-current discharge, which tends to enhance the resonance lines relative to the other lines in the spectrum. The boosted-output lamp has been used as an excitation source for the analysis of metallic samples [13] but has not hitherto been applied to the analysis of non-conducting materials. The usefulness of this type of source in the simultaneous, multi-element analysis of natural materials could not be assessed until the factors influencing the

0003-2670/83/$03.00

precision and accuracy of the technique have been investigated. This the present work attempts to do.

EXPERIMENTAL

Samples

The non-conducting materials used were oxides of copper (CuO), nickel (NiO), and iron (Fe_2O_3), and the conducting binders were copper, nickel and iron powders. Table 1 shows the particle sizes of the materials used. The metal powders were used as supplied, whereas the oxides had a wide range of particle sizes and were dry-sieved to the sizes indicated. The table also gives the concentrations of some impurities in the materials; these values were obtained by flame atomic absorption spectrometry.

Figure 1 shows the sample divider used to prepare homogeneous mixtures of oxide and metal powder. It is constructed of glass, consists of a main body and two side arms, and is rotated about a horizontal axis at 20 rpm. During each revolution, the mixture is divided into approximately equal masses which are then recombined. Mixing in this manner for 30 min resulted in a homogeneity better than could be achieved using a vibratory ball mill.

Cathodes were pressed from 3 g of mixture, by using the punch and die shown in Fig. 2(a), the shape and dimensions of the pellet thus produced being shown in Fig. 2(b). This design of punch and die minimizes wear on the surfaces in contact with the powders because there is little or no movement of the powders over the surfaces. The sloping sides of the pellet allow it to be removed easily from the die. More than 250 pellets have been pressed with one punch and die, and their diameters have remained constant. Pellet thickness is not critical because of the design of the pellet holder described below.

Instrumentation

Figure 3 shows the boosted-output glow-discharge source, and Fig. 4 shows the cathode (sample) holder. The holder, made of brass, takes the place of

TABLE 1

Specifications and particle sizes of materials, with concentrations of some impurities

Material	Particle size (μm)	Impurity concentrations (wt. %)		
		Cu	Ni	Fe
CuO (Hopkin and Williams 3340)	<36	—	nil	0.17
NiO (Lab. Reagents 29325)	<36	0.0001	—	0.0060
Fe_2O_3 (Merck 3924)	<36	0.0027	0.0037	—
Cu (Merck 2703)	53	—	nil	0.0022
Ni (Cerac N1023)	10	0.0006	—	0.0259
Fe (Merck 3819)	44	0.0008	0.0021	—

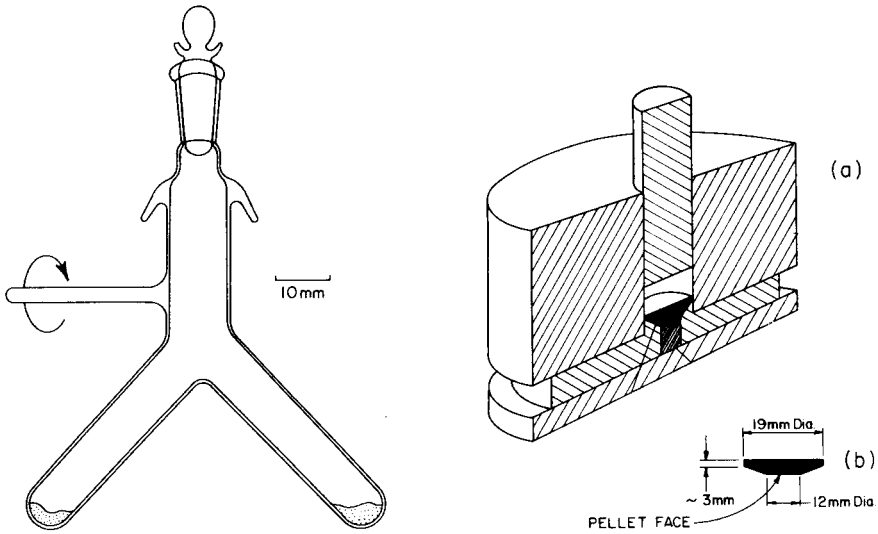

Fig. 1. Sample divider for mixing powders.

Fig. 2. (a) Punch and die used to press powders; (b) shape and dimensions of the pressed cathode.

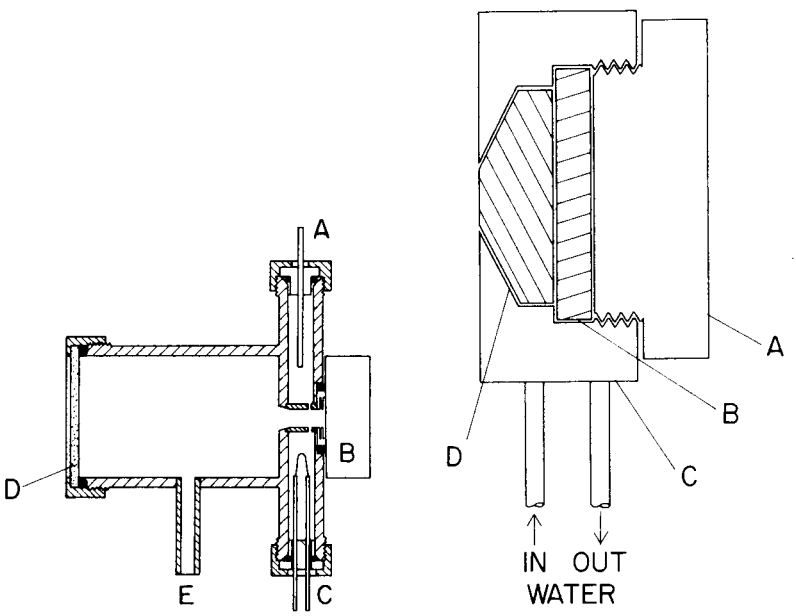

Fig. 3. Boosted-output glow-discharge source: (A) anode; (B) sample (cathode) holder; (C) filament (cathode); (D) exit window; (E) pumping port.

Fig. 4. Schematic diagram of sample holder: (A) nut; (B) viton plug; (C) water-cooled body; (D) pellet.

the solid sample and is held in position against the evacuated lamp body via an O-ring seal by atmospheric pressure. The pellet is held snugly in the holder by the nut A, which screws against a viton plug B to ensure a good vacuum seal. The water-cooled body C houses the pellet D. The holder has the advantage that the pellet thickness in not critical because of the flexibility of the viton. When the sample is in position, the surface on which the sputtering takes place lies in the plane of the front of the holder or just below that plane. It is essential that the distance between the faces of the pellet and the holder be as small and as constant as possible in order to ensure proper and reproducible flow of argon carrier gas across the surface of the specimen. Measurements made on 200 pellets have shown that the mean of this distance is 12.5 μm, with a standard deviation of 5 μm.

The power supplies for the source have been described elsewhere [13]. The supplies were operated in the d.c. mode in order to ensure that the highest possible sputtering current (40 mA) could be used without significant interaction between the discharges, and that current regulation could be maintained under these conditions. The boosting current was 500 mA. The flow of pure argon through the source was maintained at 0.2—0.3 l min^{-1} and the pressure at ca. 400 Pa using the gas-control unit described by Larkins [14]. The gas was directed across the surface of the specimen by means of an arrester, the details of which have been described by Gough [15].

Figure 5 shows a schematic diagram of the two-channel spectrometer used to isolate the analytical lines of the sample and binder. The light emitted from the source was modulated by a mechanical chopper at 285 Hz and passed to a half-silvered quartz plate which split the beam into two, each of which passed to a 0.5-m grating monochromator (Varian Techtron., Springvale, Victoria) equipped with an R106 photomultiplier tube. The intensities of the analytical lines were measured by using amplifiers (Varian Techtron AA4) tuned to the frequency of modulation. Two channels were used in order to determine whether a line in the spectrum of the metal powder could be used for the purpose of internal standardization.

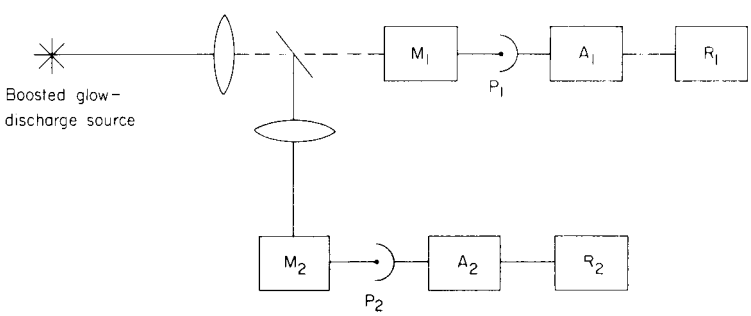

Fig. 5. Diagram of two-channel spectrometer for simultaneous measurement of the intensities of analytical and reference lines. M_1, M_2, monochromators; P_1, P_2, photomultiplier tubes; A_1, A_2, amplifiers tuned to frequency of modulation; R_1, R_2, chart recorders.

Limits of detection

Limits of detection were obtained by making a series of ten repetitive measurements on a pellet containing a very low concentration (0.01% w/w) of the oxide in the appropriate metal powder. The discharge was allowed to operate for 30 s and the emission intensity of the analytical line was measured before the discharge was switched off for 10 s. The sample was not removed from the system between successive measurements. The limit of detection was calculated by using the IUPAC definition [16], viz., the concentration of analyte for which the signal has a value equal to three times the standard deviation of a series of readings made on a sample whose concentration is just above this limit.

RESULTS AND DISCUSSION

Preparation of cathodes

Proper preparation of cathodes is extremely important if precision and accuracy are to be achieved in the determinations and if the time for each analysis is to be kept to a minimum. El Alfy [11] prepared cathodes by pulverizing the sample material to give a grain size of 25—50 μm, drying the powder at 300°C for 1 h in air, and mixing it with four times its weight of copper powder. Cathodes prepared in this way were tried in the boosted-output source, but the time taken for the emission intensity of the analytical line to reach a constant value was always greater than 20 min and sometimes as long as 40 min. The shorter time of 4—5 min found by El Alfy [11] to be required with the Grimm source probably results from the higher powers (600 W cm^{-2}) used during the pre-burn period to outgas the surface layers of the specimen cathode. This power is very much greater than the 85 W cm^{-2} used in the sputtering discharge of the boosted-output source. In addition to long equilibration times, poor precision (10—15% r.s.d.) was found when cathodes prepared by El Alfy's method were used in the boosted-output source.

The relatively low power normally available for use with the boosted-output source necessitated an investigation of alternative procedures for the preparation of cathodes. The problem of long equilibration times was overcome by outgassing the cathodes in vacuo for 30 min at 300°C; this resulted in equilibration times of 3—4 min after the discharge had been switched on. Further improvement was achieved when means were developed for obtaining homogeneous mixtures of sample and binder.

The homogeneity of mixing was determined by measuring the concentration of oxide in ten 50-mg samples collected at random from a mixture of the oxide and metal powder which had been shaken in the divider. The concentration of the metal of the oxide was determined by dissolving each sample in dilute hydrochloric acid and making flame atomic absorption measurements. Table 2 shows the relative standard deviations (r.s.d.) obtained in this way at two concentration levels for copper oxide in iron,

TABLE 2

Homogeneity of mixing of oxides with binders

Oxide	Concentration (wt. %)	Binding metal	R.s.d.[a] (%)
CuO	0.1	Fe	2.0
CuO	5.0	Fe	1.8
NiO	0.1	Cu	1.8
NiO	5.0	Cu	1.2
Fe_2O_3	0.1	Ni	1.8
Fe_2O_3	5.0	Ni	2.0

[a]10 samples.

nickel oxide in copper, and iron oxide in nickel as binder. These values are taken as a measure of the homogeneity achieved. It was found that an r.s.d. of 2% indicated that good precision could be expected in the spectrochemical emission determination. The values in Table 2 seem to indicate that slightly better mixing was achieved at the higher concentrations of copper and nickel oxides, but not for mixtures containing iron oxide, which tended to cling to the inner surface of the divider. The relative standard deviations obviously depend on the mass of the sample chosen: the larger the mass, the lower will be the variation of the measured concentration from the mean concentration. Thus, while this method of measuring homogeneity cannot give an absolute indication of the degree of mixing, it should be semi-quantitative at least.

Choice of binder

Any overlapping of the analytical line by lines from the metal binder or from the carrier gas constitutes spectral interference which may lower the sensitivity of the determination. Figure 6A shows spectra from pellets with a copper binder recorded in the neighbourhood of the iron line at 371.994 nm. The traces were obtained for a spectral dispersion of 1.6 nm mm^{-1}, a scanning rate of 0.5 nm min^{-1}, and a chart speed of 25 mm min^{-1}. It can be seen that the iron present as impurity in the copper powder constitutes a weak signal. Figure 6A indicates that spectral interference is not a serious problem when the combination of iron oxide and copper powder is used and measurements of intensity are made at Fe 371.994 nm. Figure 6B likewise shows the spectra from pellets with a nickel binder, recorded in the neighbourhood of the iron line at 371.994 nm. It can be seen that spectral interference from nickel is minimal. Figure 7 shows spectra from pellets with nickel or iron binder in the neighbourhood of the copper line at 324.754 nm. Figure 7(a) shows the copper line as a small shoulder on the nickel line at 324.846 nm, the copper being an impurity in the nickel powder. Figure 7(b) shows the copper line from a pellet containing 0.01% of copper oxide in a nickel binder and illustrates the difficulty of using the copper

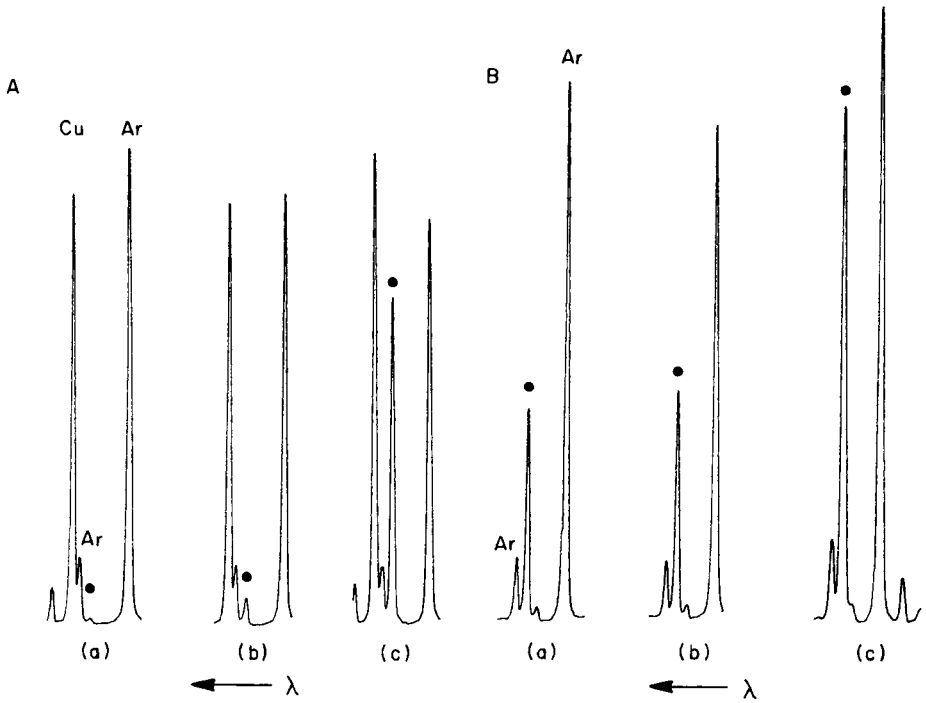

Fig. 6. Recorder traces showing the extent of spectral interference on the iron line at 371.994 nm. A, Interference from copper: (a) "pure" copper (0.0022% Fe); (b) 0.01% Fe_2O_3 in copper; (c) 0.1% Fe_2O_3 in copper. B, Interference from nickel: (a) "pure" nickel (0.026% Fe); (b) 0.01% Fe_2O_3 in nickel; (c) 0.1% Fe_2O_3 in nickel. ((•) Fe 371.994 nm; Cu 372.077 nm; Ar 371.821 and 372.043 nm.)

324.754-nm line as the analytical line when nickel is used as the binder. Figure 7(c) shows the spectrum from a pellet of iron powder containing only a trace of copper as impurity. Figure 7(d) shows the severity of the interference on added copper, the copper line being incompletely resolved from the neighbouring iron lines. Similar types of recorder trace show that nickel may be determined with a copper binder without spectral interference at the nickel 351.505-nm line and that copper oxide may be determined with an iron binder if the copper line at 327.396 nm is used.

Precision, accuracy and limits of detection

The precision with which determinations of metal oxides may be made when the boosted-output source is used was found by measuring the standard deviation of a set of measurements of emission intensity using ten electrodes each containing the same amount of oxide. Table 3 shows the results of such measurements done with copper, nickel and iron oxides. The precision was assessed for two concentrations of oxide, and ranged from 1.5 to 2.1%. In general, the precision obtained was of the same order as that reported by earlier workers with the Grimm source [7—11].

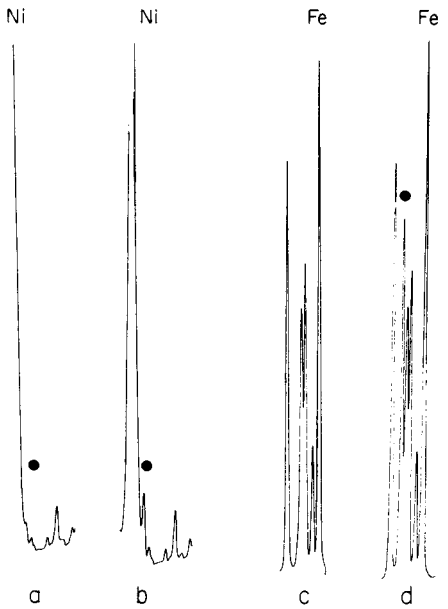

Fig. 7. Recorder traces showing the extent of spectral interference from nickel or iron on copper at 324.754 nm: (a) "pure" nickel (0.0006% Cu); (b) 0.01% CuO in nickel; (c) "pure" iron (0.0008% Cu); (d) 0.01% CuO in iron. ((•) Cu 324.754 nm; Ni 324.846 nm; Fe 324.598 nm.)

The presence of impurities in the metal powders made some assessments of detection limits difficult. However, nickel oxide in a copper binder could be examined, because the copper powder was free from nickel; the detection limit was 0.002% for nickel oxide. Similarly, it was possible to establish a detection limit of 0.0015% for copper in a nickel binder, taking into account the impurity level of copper in the nickel.

TABLE 3

Reproducibility of determination of metal oxides

Oxide	Concentration of analyte oxide in binder (wt. %)	Binder	R.s.d.[a] (%)
CuO	0.10	Fe	2.1
CuO	5.0	Fe	1.5
NiO	0.10	Cu	1.6
NiO	5.0	Cu	1.6
Fe_2O_3	0.10	Ni	1.6
Fe_2O_3	5.0	Ni	1.5

[a]For 10 electrodes.

The calibration graphs for nickel, iron and copper oxides in the various binders were linear up to at least 5% (w/w). Determination of oxide concentration may be made with a precision of ±1% relative.

The most precise and accurate results were obtained when the sputtering discharge was operated at constant power. With constant current already provided by the power supply, it was necessary only to maintain constant voltage, which could be done by altering the pressure. The intensities of spectral lines emitted by the source are thus subject to variation not only because of changes in the discharge parameters but also because of inhomogeneity in the mixing of the oxide and metal powder. Such variations tend to lower the precision of measurement, and so attempts were made to improve the precision by using internal standardization. The measured intensities of the analyte line were normalized to the average value of the intensity of a chosen line of the metal comprising the binder. The intensities of the analyte and reference lines (Ni 351.505 nm and Cu 327.396 nm, respectively) obtained from a set of ten measurements on samples containing 0.1% nickel oxide in a copper binder were measured. The relative standard deviation of the nickel intensities was 1.6%, but after normalization to the average copper intensity value (which had an r.s.d. of 1.8%) the r.s.d. became 2.3%. Thus, where the intensities of analyte and reference line vary independently, normalization gives no improvement in precision.

In the Jäger method of internal standardization [17] the raw data are normalized with respect to the integrated sputtering, S, which may be defined as $S = \Sigma_j^n a_j I_j$ $(1 \leqslant j \leqslant n)$, where n represents all the elements in the sample, I_j is the intensity of the analytical line of element j, and a_j is a normalizing constant obtained by dividing the concentration of the element by emission intensity obtained from measurement of standard samples. The normalized intensities, J, may be written $J_i = a_i I_i/S$, which is plotted against concentration. The Jäger method could not be used in the present work because it was not possible to measure simultaneously the intensities of a line of oxygen (from the oxide), an analytical line and a line of the binder metal. Other workers have not, however, found Jäger's method particularly successful in improving the precision of spectrometric analysis for gold [17], copper-base alloys [18] or silver [19]. It is thus doubtful if its application to the present measurements with powdered samples would be any more successful. This situation arises because the fundamental problem with Jäger's method is that the integrated sputtering which is used as a reference is related to bulk concentrations of the atoms rather than to the concentrations actually present in the sputtered layers, which are depleted of lighter elements once equilibrium has been established [20].

Conclusions

Satisfactory precision and accuracy (2% relative for both) may be obtained for the determination of non-conducting materials with the boosted output source if the procedures outlined here for the preparation of sample cathodes

are applied. The choice of conducting powder is largely determined by the need to minimize spectral interference and is not critical if the Fe 371.994-nm, Ni 351.505-nm and Cu 327.396-nm lines are used. Methods of internal standardization are unlikely to improve precision because the signals from the analyte and reference elements do not vary proportionally to each other. This may be due to the presence of reactive oxygen atoms produced by the sputtering of the cathode.

The authors thank Dr. J. B. Willis for much helpful advice and criticism. One of us (GSL) thanks the Directors of Labtest (Southeast Asia) Pty. Ltd., for a grant to carry on this work.

REFERENCES

1 W. Grimm, Naturwissenschaften, 54 (1967) 586.
2 W. Grimm, Spectrochim. Acta, Part B, 23 (1968) 443.
3 W. Grimm, H. Pfundt and H. Ritzl, Proc. XV Colloq. Spectrosc. Int., Madrid, 1969, Vol. 4, Adam Hilger, London, 1971, p. 433.
4 M. Dogan, K. Laqua and H. Massmann, Proc. XV Colloq. Spectrosc. Int., Madrid, 1969, Vol. 4, Adam Hilger, London, 1971, p. 385.
5 H. Jäger, Anal. Chim. Acta, 60 (1972) 303.
6 K. Laqua, Pure Appl. Chem., 49 (1977) 1595.
7 M. E. Ropert, XVI Colloq. Spectrosc. Int., Heidelberg, 1971, Preprints Vol. 2, Adam Hilger, London, 1971, p. 214.
8 J. Y. Moal and G. Brossier, XVI Colloq. Spectrosc. Int., Heidelberg, 1971, Preprints Vol. 2, Adam Hilger, London, 1971, p.219.
9 M. Dogan, K. Laqua and H. Massmann, Spectrochim. Acta, 27B (1972) 65.
10 S. El Alfy, K. Laqua and H. Massmann, Fresenius Z. Anal. Chem., 263 (1973) 1.
11 S. El Alfy, Thesis, Dortmund, 1978.
12 R. M. Lowe, Spectrochim. Acta, Part B, 31 (1976) 257.
13 D. S. Gough and J. V. Sullivan, Analyst, 103 (1978) 887.
14 P. L. Larkins, Anal. Chim. Acta, 132 (1981) 119.
15 D. S. Gough, Anal. Chem., 48 (1976) 1926.
16 IUPAC Comission on Spectrochemical and other Optical Procedures for Analysis, Spectrochim. Acta, Part B, (1978) 242.
17 H. Jäger, Anal. Chim. Acta, 58 (1972) 57.
18 R. A. Kruger, L. R. P. Butler, C. J. Liebenberg and R. G. Bohmer, Analyst, 102 (1977) 949.
19 N. P. Ferreira and L. R. P. Butler, Analyst, 103 (1978) 607.
20 N. Andersen and P. Sigmund, K. Dan. Vidensk. Selsk. Mat. Fys. Medd. 39 (1974) No. 3.

Analytica Chimica Acta, 148 (1983) 181—192
Elsevier Science Publishers B.V., Amsterdam — Printed in The Netherlands

MICRODROP SAMPLE APPLICATION IN ELECTROTHERMAL ATOMIZATION FOR ATOMIC ABSORPTION SPECTROMETRY

J. G. SHABUSHNIG and G. M. HIEFTJE*
Department of Chemistry, Indiana University, Bloomington, IN 47405 (U.S.A.)
(Received 11th July 1982)

SUMMARY

The application of liquid samples in the form of microdrops, approximately 150 μm in diameter, to an electrothermal atomizer has been evaluated. This technique offers improved precision (1—2% RSD), microsampling capabilities, and simplified calibration with a single concentration standard. Examination of dried samples after deposition indicates reduced spreading and crystal size for microdrop and aerosol deposition compared with manual micropipetting methods. Crystal size and deposit spreading were found to correlate with the degree of suppression of lead signals by chloride and of gold signals by sulfate.

Electrothermal atomization in atomic absorption spectrometry (a.a.s.) has remained a valuable tool for element determinations, despite the recent introduction of the inductively coupled plasma. This value is due primarily to efficient sample use and the superior sensitivity achieved, typically 2—3 orders of magnitude better than that obtained by flame atomic absorption or plasma emission spectrometry [1].

Unfortunately, electrothermal atomization produces not just improved sensitivity but also an increase in interferences and a decrease in precision in a.a.s. determinations. This imprecision has been attributed, in part, to a lack of reproducibility in the sample application procedure [2]. In these procedures, two significant problems appear to exist: irreproducible transfer of solution from the dispenser to the atomizer surface [2—4], and spreading and absorption (by the atomizer surface) of the solution once deposited [2, 5]. Attempts to overcome these difficulties have included the construction of accurate positioning devices for syringe-based dispensers [6—8] and the deposition of sample as an aerosol onto a preheated atomizer surface [9—11]. The latter method has also been reported to reduce occlusion-based interference effects.

Sampling errors have also been reduced by measuring the volume of solution after its deposition, instead of before. This measurement has been accomplished by incorporating into the sample solution a small amount of organic solvent as an internal standard [4]. Absorbance at a wavelength appropriate for the particular solvent is then monitored during the drying

0003-2670/83/$03.00

stage, and is proportional to the volume of solution originally deposited. Changes in resistance in a tungsten loop atomizer [12] have also been used to signal the end of sample evaporation. The volume initially applied can then be determined from the duration of this drying step.

In the present study, a device was developed which is capable of reproducibly and repetitively dispensing aqueous samples in the form of microdrops, approximately 150 μm in diameter. This microdrop generator has been described previously [13] and was applied to the study of sample application in electrothermal atomization with minor modification. The characteristics of the generator are summarized in Table 1.

For instrumental convenience, microdrops are produced approximately 2 cm above the atomizer unit, and fall freely into it; consequently, any problems associated with solution transfer are eliminated. Sample spreading and absorption also are reduced by introducing microdrops into a preheated atomizer, as is ordinarily done in aerosol deposition [9—11]. This procedure results in immediate desolvation of the sample upon contact with the graphite surface.

In this investigation, it was determined that the microdrop generator is highly efficient in sample utilization and results in lower imprecision (1—2% RSD) than that obtained from manual pipetting methods. Moreover, because the dispensed volume can be varied conveniently and, if desired, automatically, calibration curves can be generated by using a single standard. The sample introduction system will be compared with other methods of application (micropipette and aerosol deposition) with regard to sample spreading and crystal size in the dried sample as well as such practical considerations as efficiency of sample use, compatibility with organic solvents and ease of operation.

Other researchers [14, 15] have suggested that some atomization interferences are linked in part to occlusion of the analyte within the sample matrix. Differences in crystal size in the dried sample should then alter the incidence of occlusion and thus result in a change in the amount of suppression observed. Based on these comparisons, the new sample dispenser should offer a greater degree of freedom from occlusion-based interferences than manual pipetting. Two model interference systems, chloride on lead and sulfate on gold, were

TABLE 1

Microdrop generator operating characteristics

Microdrop size	150 μm diameter (typical)
Microdrop production rate	160 s^{-1}
Solution deposition rate	18 μl min^{-1}
Bimorph driving voltage	100 V(p—p)
Minimium bulk sample volume	100 μl
Deposition volume range (without air jet deflection system [13])	200 nl and up

examined in the present study under controlled sample deposition conditions to evaluate the importance of this occlusion effect.

EXPERIMENTAL

Instrumentation

The microdrop generator described previously [13] was modified slightly and coupled to a controlled-temperature graphite-furnace atomizer (model 655, Instrumentation Laboratory, Inc., Wilmington, MA). Both peak and integrated absorbance values were recorded with an automated atomic absorption spectrometer (model 951, Instrumentation Laboratory) equipped with single-element hollow-cathode lamps (Visimax, Instrumentation Laboratory). These lamps were run at the current recommended by the manufacturer [16]. All measurements were made with deuterium-arc background correction. Aerosol deposition was accomplished with a concentric pneumatic nebulizer, spray chamber, and appropriate manifold system (model 254 FASTAC, Instrumentation Laboratory).

For these experiments, the microdrop generator was fitted with a modified reservoir system to accommodate smaller bulk sample volumes (100 μl), and to afford easier sample change. This modified reservoir is shown schematically with the rest of the generating apparatus in Fig. 1. The reservoir consists of a section of 3-mm i.d. glass tubing with a right angle bend. A 1.6 mm (1/16-inch) wide delivery slot is cut into the forward portion of the tube. To initiate a dispensing cycle, a peristaltic pump transfers an aliquot of solu-

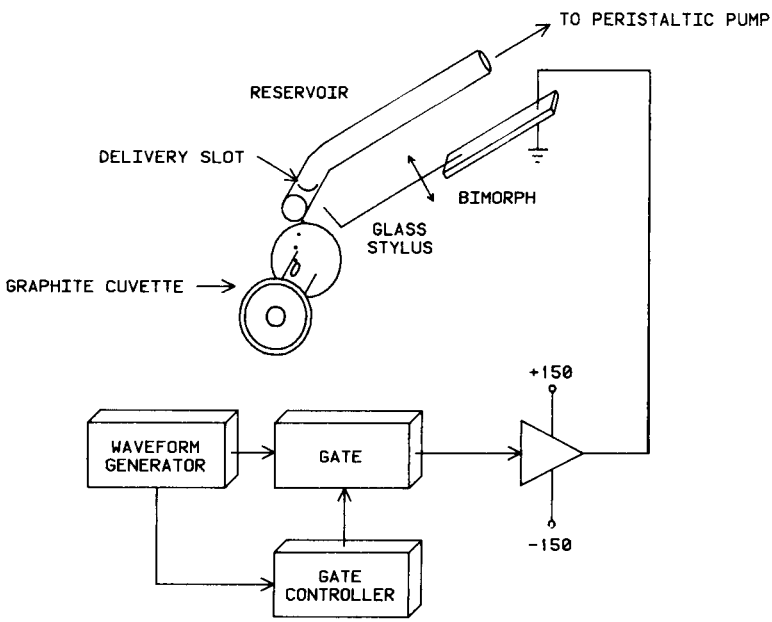

Fig. 1. Schematic diagram of microdrop generator sample deposition system.

tion into position above this slot, the solution being held in the slot by surface tension. Ordinarily, the solution is pumped slightly past the slot and then moved back in place by reversing the pump to provide a consistent sample location and solution level in the slot. Once the sample is in position, a bimorph-driven drawn-glass stylus (approximately 120 μm in diameter) reaches through the slot in the reservoir to withdraw and dispense microdroplets from the bulk aliquot. Conveniently, undispensed solution can be recovered by reversing the peristaltic pump.

In the current study, the reservoir was always rinsed with deionized water between samples. However, it would also be possible to alternate sample and wash water "plugs" in an air-segmented stream to reduce sample change-over time. Two 200-μl aliquots of deionized water were found to be adequate for rinsing of the reservoir.

Other modifications to the microdrop generating system are shown in Fig. 2. These include a screw-adjustable plexiglas mounting seat for the bimorph to allow accurate positioning of the stylus with respect to the delivery slot and a horizontal translator to accurately position the entire assembly over the furnace cuvette for sample deposition. This translator was firmly attached to an adaptor plate to facilitate mounting the generator to the graphite atomizer housing.

Operation of the microdrop generator

In operation, the furnace power supply is placed in the manual mode and allowed to reach the temperature selected for sample deposition. This temperature is measured using a tungsten resistance thermometer. The generator is then slid forward against an adjustable stop to position it accurately above the cuvette. With the sample in place in the reservoir, the gate controller is

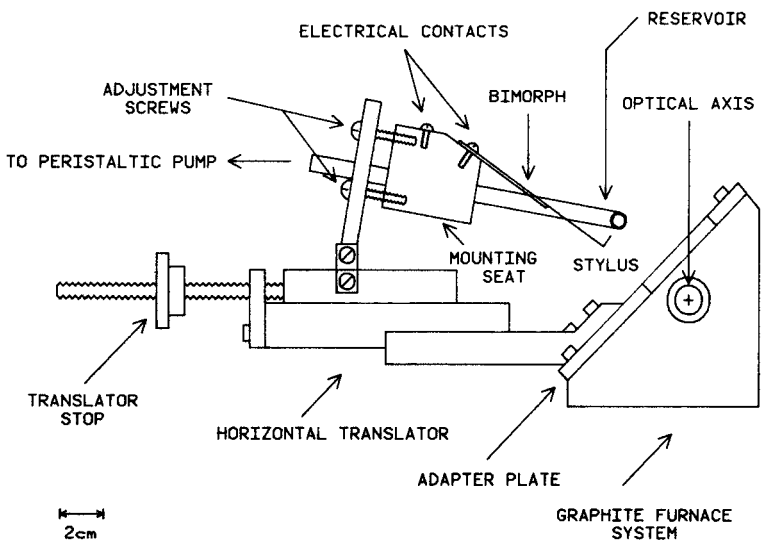

Fig. 2. Interface between microdroplet generator and graphite furnace.

activated and a preset number of microdrops are dispensed into the furnace. The generator is then manually withdrawn from above the atomizer and a cover plate placed over the opening in the adapter plate. Finally, the atomizer is placed in the automatic mode and allowed to execute the remainder of the preset temperature program (i.e., ash and atomize). Operating conditions used for individual elements are summarized in Table 2.

Because cleaning and filling of the generating apparatus can be automated and can occur during the normal atomizer ash, atomization, and cool-down period, only the actual sample deposition time affects the speed of a determination. Typical deposition times for the microdrop generator are 45 s, compared to 30 s for aerosol sampling and 5—10 s for manual pipetting. Understandably, the time required for the former two methods will depend on the desired sample volume, whereas the latter technique will depend on the skill and dexterity of the operator.

Argon was used to purge the atomizer during all experiments; the flow rate was reduced from the manufacturer's recommended 30 SCFH to 10 SCFH in order to avoid perturbations in the trajectory of the microdrop stream. This reduction in purge gas flow rate was found not to affect the analytical performance or lifetime of the graphite atomizer.

Conventional graphite atomizer cuvettes coated with pyrolytic graphite were used exclusively. However, the sample introduction opening in the cuvette was enlarged to 3.0 mm (0.120 inch) to facilitate microdroplet introduction.

Examination of dried sample deposit

Sample spreading and crystal size were evaluated by photographing the residue left after deposition of 10-μl aliquots of 10% NaCl solution. For this study, a 12.7 × 4.8 mm (1/2 × 3/16-inch) section was removed from the center of each graphite cuvette before sample deposition to simplify observation and photographic recording. The results demonstrated here were duplicated in unaltered cuvettes to insure the validity of the results reported. No significant differences were observed.

Interference studies

The magnitude of a given interference is expressed in terms of percent suppression. These values were determined by calculating the percent change

TABLE 2

Atomizer operating conditions

	Cu	Mg	Mn	Pb	Au
Wavelength (nm)	324.7	285.2	279.5	217.0	242.8
Bandpass (nm)	1.0	1.0	0.5	1.0	1.0
Integration period (s)	5	5	5	5	5
Atomization temp (°C)	2000	2100	2200	1800	1800

in signal intensity with and without interferent present. Sample deposition conditions were duplicated from the previous studies allowing microscopic observation of deposited material. A general comparison could then be made between crystal size in the deposited material and the degree to which suppression occurred.

Reagents

All sample solutions were prepared daily by dilution of 1000 μg ml^{-1} standard stock solutions (Alfa Products, Thiokol/Ventron Division, Danvers, MA). Deionized water was used for all dilutions and nitric acid was added to all samples to achieve a final acid concentration of 1%.

RESULTS AND DISCUSSION

Optimization of deposition temperature

Figure 3 indicates the effect on the absorption signal (area) of furnace temperature during microdrop deposition. For all elements, the recorded peak area remains constant until about 100°C, the boiling point of the solvent, above which a distinct loss in signal occurs. Presumably, the deposited sample boils violently upon contact with the heated atomizer at these higher temperatures (>100°C), resulting in expulsion of a portion of the analyte.

Not surprisingly, the precision of these determinations is also dependent on furnace temperature during deposition, as demonstrated in Fig. 4. As before, the boiling point of the solvent divides two distinct performance regions. Below 100°C the imprecision remains relatively constant at 0.8–2.5% RSD for the elements studied. Above this temperature, precision degrades rapidly. Although precision is always worse at these higher deposition temperatures, specific precision values are not significant and a comparison among the curves for elements listed in Fig. 4 would not be valid.

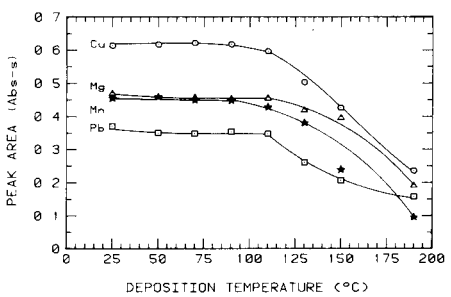

Fig. 3. Effect of deposition temperature (graphite cuvette wall temperature) on atomic absorption peak area: (○) Cu, 5.4 μl at 100 μg ml^{-1}; (△) Mg, 3.6 μl at 100 μg ml^{-1}; (★) Mn, 4.5 μl at 5 μg ml^{-1}; (□) Pb, 9.0 μl at 100 μg ml^{-1}.

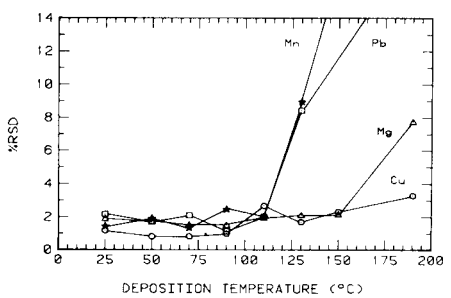

Fig. 4. Effect of deposition temperature on measurement precision (relative standard deviation based on 5 replicate samples). Symbols as in Fig. 3.

From these preliminary experiments, the deposition temperature was selected to be 90°C for all subsequent studies. At this temperature, the imprecision falls between 1 and 2% RSD for five replicate samples, superior to that obtained with a 10-μl manual micropipette (3—4% RSD) and comparable to that achieved in this laboratory with a commercial aerosol deposition system (1—2% RSD).

Single standard calibration

Electrothermal atomization is inherently a mass-sensitive rather than concentration-sensitive technique. Consequently, it should be possible to calibrate instrument response in terms of volume (with a constant concentration) rather than concentration (with a constant volume) as is conventionally done. Such a procedure would simplify calibration because only a single standard solution would be required.

Previous attempts to calibrate electrothermal atomization devices in this manner have suffered from poor precision and nonlinearity [5]. Problems of this type, however, can be significantly reduced by using microdrop sample deposition. Precision was maintained at 1—2% RSD for the aqueous copper solutions examined. This improvement is attributed to the reproducible deposition and reduction in spreading of a liquid sample when it is applied as microdrops to a preheated atomizer surface. In this manner, differences in deposit size and character between large and small volume samples are minimized.

A family of curves illustrating single-standard calibration for copper is shown in Fig. 5. In this experiment, the dispensed volume ranged from 0.6μl to 20 μl for each of three copper solutions, having concentrations of 20, 50 and 100 μg l^{-1}, respectively. Bending observable in the 100 μg l^{-1} curve is the result of nonlinearity in absorption measurements made at magnitudes greater than 1.0. These same data are plotted in a more analytically useful

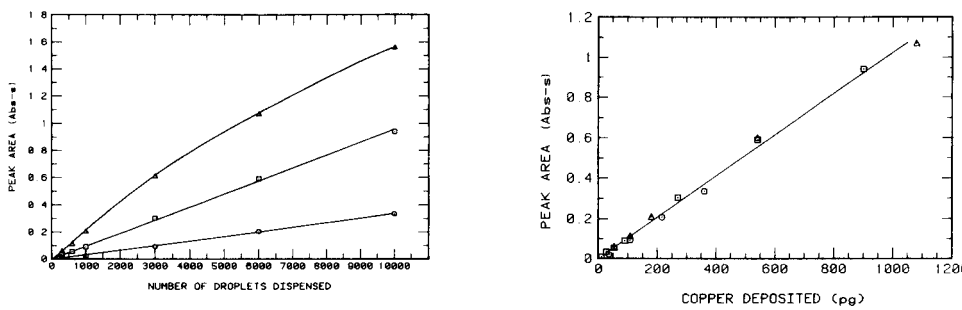

Fig. 5. Example of single-standard calibration curves with three copper solutions: (△) 100 μg l^{-1}; (□) 50 μg l^{-1}; (○) 20 μg l^{-1}.

Fig. 6. Single standard calibration data from Fig. 5 normalized for mass of copper deposited. Data points: (○) taken from standards at 20 μg l^{-1}; (□) obtained with a 50 μg l^{-1} standard; (△) obtained with a 100 μg l^{-1} standard solution.

form in Fig. 6. Values in Fig. 6 are plotted on the basis of the mass of copper deposited and should define a single calibration line which is independent of the individual concentration or volume of each sample. Curvature apparent above 900 pg copper is a result of customary nonlinearity observed in high absorbance measurements.

Morphology of dried sample

In the previous section, the practical importance of controlling the spreading of liquid samples at the atomizer surface was emphasized. Such spreading, as well as absorption of the sample solution into the atomizer, is significantly reduced when the sample is applied to a preheated atomizer. To facilitate application at elevated temperature, samples should be applied in the form of microdrops or an aerosol, procedures which enable rapid desolvation without spattering-induced sample losses.

Figure 7(A—C) indicates typical dried sample deposits obtained after micropipette, microdrop, and aerosol deposition, respectively. Samples from both microdrops and aerosol were deposited at elevated temperatures, 90° and 130°C, respectively, and dried instantly upon contact with the atomizer surface. Deposition in this manner produces a noticeably more uniform and compact distribution of dried sample on the atomizer surface than that produced by micropipette application. The micropipetted samples were added to the atomizer at room temperature, followed by a 20-s ramp to 70°C and 20 s at 100°C.

Figure 8(A—C) shows small sections of dried sample from Fig. 7 under equal magnification. It is obvious that aerosol deposition (Fig. 8C) produces the smallest crystals, appearing like a frost on the atomizer surface. Microdrops, by comparison, yield a fine crystalline structure (Fig. 8B) in the dried sample but one which is noticeably coarser than that produced by the aerosol. Sample deposited with a micropipette (Fig. 8A) results in the largest crystals

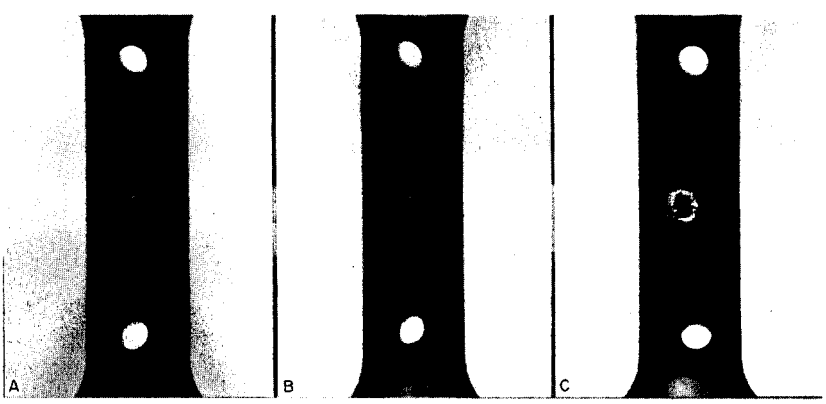

Fig. 7. Photographs of sample within graphite cuvette after deposition of 10 μl of 10% NaCl solution: (A) with a micropipette; (B) as microdrops; (C) as an aerosol.

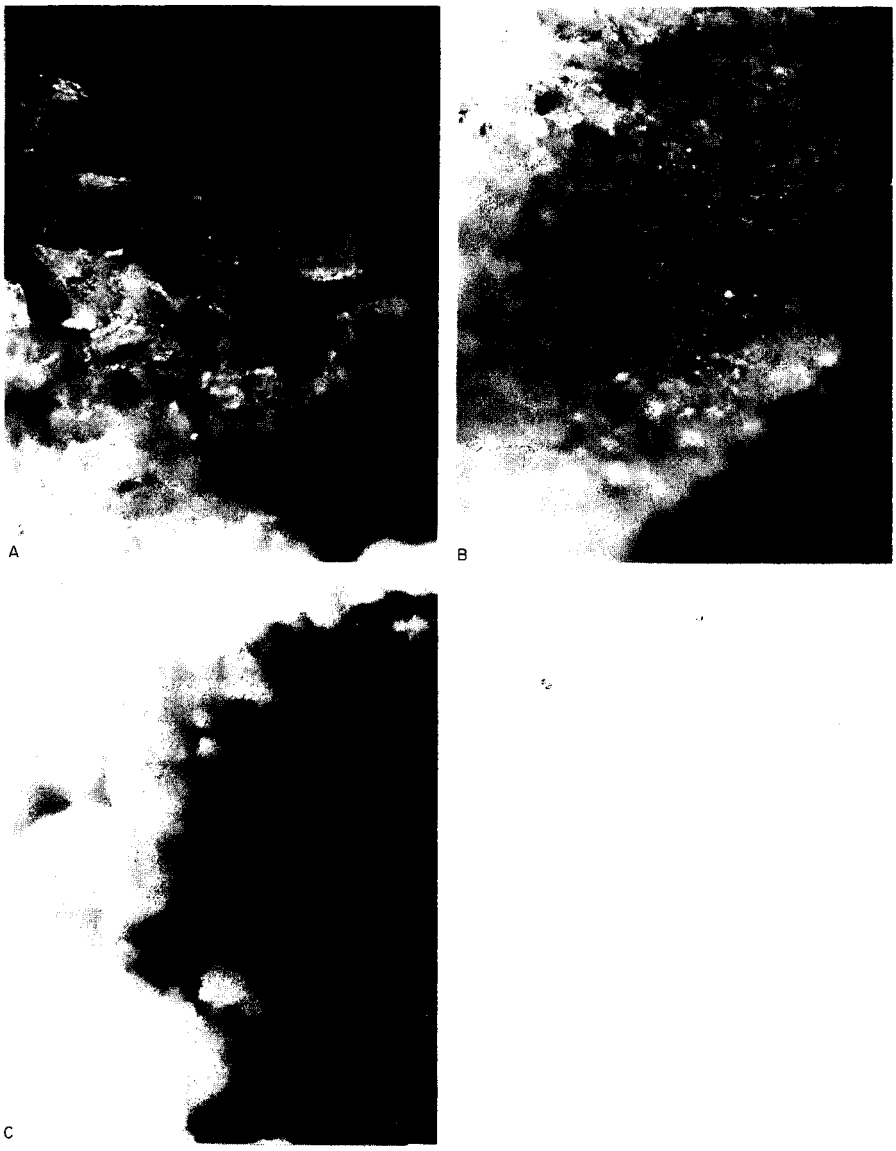

Fig. 8. Photomicrographs of dried NaCl deposits corresponding to A—C in Fig. 7.

of the three deposition techniques studied. This large crystal size is most likely a result of the slow drying rate necessitated by micropipette application.

Interference reduction

As shown in Fig. 8, the crystal size found in dried sample varies with the method of deposition in the following manner: micropipette > microdrop

> aerosol deposition. From the data presented in Table 3, it seems clear that the greatest degree of signal suppression, and thus of interference, occurs when sample is applied with a micropipette, and thus resides in the form of larger crystals at the atomizer surface. The decrease in suppression found with microdrop and aerosol deposition appear also to follow this trend in crystal size.

In general, a decrease in crystal size results in a decrease in the magnitude of suppression observed. This trend would support an occlusion-based mechanism for the particular interferences studied.

Practical considerations

Several other factors besides those already discussed are important in the selection of an appropriate method of sample application for electrothermal atomization. The volume of sample available, the importance of conserving the sample, convenience, and compatibility with a given solvent must all be considered.

Microdrops are dispensed directly from a bulk volume of 100—200 μl in the reservoir, from which several aliquots can be taken. Moreover, the only limitation to the number of such aliquots is that at least 25 μl must remain in the reservoir for stable microdrop generation. Conveniently, even this undispensed portion can easily be recovered by reversing the peristaltic pump, (cf. Fig. 1), making the microdrop generator highly efficient in its use of sample. In comparison, a micropipette can be operated with a bulk sample volume only slightly greater than the calibrated volume of the pipette. It then dispenses all of its contents.

Both a micropipette and the microdrop generator use sample more efficiently than aerosol deposition. Using a pneumatic nebulizer to generate the aerosol requires that more than a milliliter of solution be available to deposit a 10—20 μl volume in the atomizer. Most of the solution remains behind in the nebulizer spray chamber and is often not easily recovered.

TABLE 3

Effect of deposition method on occlusion-based atomization interferences

Deposition method	Interference of Na_2SO_4 on Au determination (% suppression)[a]		Interferences of NaCl on Pb determination (% suppression)[a]	
	A	B	C	D
Micropipette	90	65	9	42
Microdrop	85	—	3	—
Aerosol	71	45	9	0

[a]Percent suppression based on integrated peak areas. (A) 10 μl; 25 μg l^{-1} Au, 0.1% Na_2SO_4. (B) 25 μl; 10 μg l^{-1} Au, 0.1% Na_2SO_4 (from ref. 17). (C) 10 μl; 100 μg l^{-1} Pb, 0.5% NaCl. (D) 10 μl; 100 μg l^{-1} Pb, 0.5% NaCl (from ref. 17).

Although the microdrop generator and aerosol deposition are instrumentally more complex than a micropipette, once adjusted they provide high precision with little operator intervention. In contrast, a micropipette is a relatively simple device yet requires a skilled operator to achieve optimal performance with it. With additional automation, the microdrop generator has the potential to provide unattended highly precise sample deposition.

Lastly, solvent compatibility with each device must be considered. Both micropipette and aerosol deposition of organic solvent is possible. The microdrop generator is at present not capable of dispensing solutions prepared with an organic solvent, principally because of the reservoir system which is now being used. The relatively low surface tension of organic solvents results in a tendency for solutions made from them to creep through the slot in the reservoir, making reproducible microdrop formation impossible.

Importantly, working with aqueous and organic solvent mixtures (up to 25% methanol) is possible with the microdrop generator. Moreover, altering the design of the reservoir and the material from which it is constructed might make the use of undiluted organic solvents feasible in the future.

Conclusion

Depositing liquid samples in the form of microdrops has been found to be advantageous in several aspects of electrothermal atomization. In routine use, better precision is obtained than is possible with a conventional micropipette. Most likely, precision is improved because of the absence of transfer problems and reduced spreading and absorption of the sample at the atomizer surface.

The convenience of electronic control of the dispensed volume allows simplified calibration with a single concentration of standard solution. Lastly, reduced crystal size in the dried analyte results in reduced atomization interferences which are believed to be caused by occlusion of the analyte within the dried sample matrix.

This paper was presented in part at the Federation of Analytical Chemistry and Spectroscopy Societies Meeting, Philadelphia, PA, September, 1981. The work was supported in part by the Office of Naval Research and by the National Science Foundation through grant CHE 79-18073. We thank Instrumentation Laboratory, Inc., for providing the graphite furnace and spectrometer system as well as for partial support of this project.

REFERENCES

1 J. D. Winefordner, in G. F. Kirkbright and R. M. Dagnall (Eds.), Atomic Absoprtion Spectroscopy, Butterworth, London, 1971, p. 37.
2 F. J. M. J. Maessen, F. D. Posma and J. Balke, Anal. Chem., 46 (1974) 1445.
3 C. F. Emanuel, Anal. Chem., 45 (1973) 1568.
4 G. F. Kirkbright and R. D. Snook, At. Absorpt. Newsl., 16 (1977) 108.
5 K. G. Brodie and J. P. Matousek, Anal. Chem., 43 (1971) 1557.
6 K. R. Millar, F. Cookson and F. M. Gibb, Lab. Pract., 28 (1979) 752.
7 V. Sacchetti, G. Tessari and G. Torsi, Anal. Chem., 48 (1976) 1175.

8 E. H. Pals, D. N. Baxter, E. P. Johnson and S. R. Crouch, Chem. Biomed. Environ. Instrum., 9 (1979) 71.
9 J. P. Matousek, Talanta, 24 (1977) 315.
10 R. Woodriff and G. Ramelow, Spectrochim. Acta, Part B, 23 (1968) 665.
11 M. Chamsaz, B. L. Sharp and T. S. West, Talanta, 27 (1980) 867.
12 L. R. Layman and G. M. Hieftje, Anal. Chem., 46 (1974) 322.
13 J. G. Shabushnig and G. M. Hieftje, Anal. Chim. Acta, 126 (1981) 167.
14 L. R. Hageman, J. A. Nichols, P. Viswanadham and R. Woodriff, Anal. Chem., 51 (1979) 1407.
15 J. A. Krasowski and T. R. Copeland, Anal. Chem., 51 (1979) 1843.
16 R. H. Emmel, M. Fogg Bancroft, S. B. Smith, Jr., J. J. Sotera and T. L. Corum, Atomic Absorption Methods Manual, Vol. 2, Flameless Operations, Instrumentation Laboratory, Inc., 1976.
17 H. L. Kahn, M. K. Conley and J. J. Sotera, Am. Lab., 12 (Aug., 1980) 72.

Analytica Chimica Acta, 148 (1983) 193—201
Elsevier Science Publishers B.V., Amsterdam — Printed in The Netherlands

DETERMINATION OF TRACE METALS IN SILICEOUS STANDARD REFERENCE MATERIALS BY ELECTROTHERMAL ATOMIC ABSORPTION SPECTROMETRY AFTER LITHIUM TETRABORATE FUSION

M. BETTINELLI
ENEL DCO Central Laboratory, I-29100 Piacenza (Italy)
(Received 8th April 1982)

SUMMARY

Trace elements (Fe, As, Cd, Co, Cr, Cu, Mn, Ni, Pb, V, Zn) in the standard reference materials N.B.S. 1633 and 1633a (coal fly ash), N.B.S. 1645 (river sediment), N.B.S. 1648 (urban particulate matter), Eurostandards 877-1 (furnace dust) and 680-1, and 681-1 (iron ore), are determined by graphite-furnace atomic absorption spectrometry after lithium tetraborate fusion. In all the determinations, the precision and accuracy are similar to those obtained for acid digestion, but the time needed is considerably less. The results show good recoveries, with coefficients of variation for many elements below 8%.

Metals in geological or siliceous samples can be determined by acid dissolution or by fusion with different salts before the measurement step. Hydrochloric, nitric, perchloric and hydrofluoric acids are commonly used [1—4]; sulphuric acid is avoided because it leads to the formation of insoluble sulphates with low recoveries, especially for lead [5, 6]. Although many authors have successfully adopted this method of decomposing sediments, rocks, coal ash, particulate matter and various other siliceous materials, the use of acid mixtures can have disadvantages, such as loss of chromium through volatilization of chromyl chloride [6], incomplete recovery of some elements such as iron and chromium [7, 8], and incomplete destruction of organic matter present in some samples [9, 10]. Such disadvantages require the use of special equipment such as a teflon bomb [2, 11—15], but in some cases a black residue which is hard to remove from the walls of the bomb may be formed [7, 8].

Fusion of the sample can be achieved by various salts, such as Na_2CO_3 [16], Na_2O_2 + NaOH [17], $Sr(BO_2)_2$ [18], $LiBO_2$ [19—21], $Na_2B_4O_7$ [22] and $Li_2B_4O_7$ [21—24]. The use of the fusion method, in spite of its adoption in the determination of the principal constituents of siliceous materials, has never been satisfactory for trace element determinations. The main problems are the blank level in the tetraborate, possible loss of some elements by volatilization, and higher background levels because of the high salt concentration in solution. This laboratory has long used such a method for the dissolution of soil samples, refractory materials, coal ash and slags.

0003-2670/83/$03.00

The elements which are routinely determined by atomic absorption spectrometry (a.a.s.) in flames are Si, Fe, Al, Ca, Mg, Na, K and Mn, while in the same fusion solution Ti and P are determined spectrophotometrically. Recently, the use of graphite-furnace a.a.s. for determining trace elements in N.B.S. 1633 fly ash after fusion was reported [25]. The present paper shows the results obtained by extending this fusion method to four different reference standards.

EXPERIMENTAL

Instrumentation

For the determination of As, Cd, Co, Cr, Cu, Mn, Ni, Pb, V and Zn, the Perkin-Elmer model 503 atomic absorption spectrometer used was fitted with a deuterium background corrector, a HGA-500 furnace and a model 56 chart recorder. Background correction was used for all measurements at less than 320 nm. Hollow-cathode lamps were used except for arsenic, for which an electrodeless discharge lamp was employed.

The optimum conditions used are shown in Table 1. Particularly for arsenic, in order to reduce its volatility during ashing and to reduce the influence of matrix elements, matrix modification was used [26]. The optimum program for this element (20 μl of sample injected with 100 $\mu g\,ml^{-1}$ nickel as stabilizer in 0.15 M nitric acid) was: drying for 45 s at 110°C, ashing for 30 s at 1000°C, atomization for 5 s at 2700°C, cleaning for 3 s at 2800°C.

TABLE 1

Recommended conditions for the spectrometry of trace elements in the lithium tetraborate solution[a]

Element	λ (nm)	Slit-width (nm)	Ash (°C)	Atomize (°C)	Clean (°C)
As	193.7	0.7	1000	2700	2800
Cd	228.8	0.7	500	2000	2500
Cr	357.9	0.7	1200	2700	2800
Cu	324.7	0.7	1000	2500	2800
Co[b]	240.7	0.2	1000	2700	2800
Mn	279.5	0.2	1100	2700	2800
Ni[b]	232.0	0.2	1000	2700	2800
Pb	283.3	0.7	1000	2500	2800
V[b]	318.4	0.2	1500	2700	2800
Zn	213.9	0.7	700	2300	2500

[a]Optimal instrument operating parameters held constant: drying temperature 110°C; drying time 45 s; ashing time 60 s; atomization time 5 s; cleaning time 5 s; argon purge gas; continuous gas flow mode; volume injected 20 µl. [b]Pyrolytic graphite-coated tubes.

The determinations of iron (in N.B.S. 1633 and N.B.S. 1648), iron and chromium (in N.B.S. 1645), and iron lead and zinc (in Eurostandards 877-1, 680-1 and 681-1) were done with a Perkin-Elmer model 5000 atomic absorption spectrometer, fitted with a standard air—acetylene burner, a PRS-10 printer and single hollow-cathode lamps. The instrumental conditions conformed to those given in the instrument manual.

Reagents

All solutions were prepared with deionized water obtained from a Millipore Milli-Q system. All the glassware had previously been washed with 20% (v/v) nitric acid and rinsed with deionized water. The hydrochloric, nitric and phosphoric acids used were Merck Suprapur and the lithium tetraborate was analytical-reagent grade. Standard solutions for atomic absorption (BDH) were used to prepare the working standards by diluting the concentrated chloride or nitrate solutions with lithium tetraborate solution (6 g l^{-1} in 1% hydrochloric acid), so as to have the same salt concentration in the samples and standards. For arsenic, working standards and samples were prepared in 0.15 M nitric acid in the presence of 100 μg ml^{-1} nickel (as nitrate).

Procedure

About 0.3 g of sample (accurately weighed), 1.5 g of lithium tetraborate and 78 mg of nickel nitrate (only for arsenic determinations) were placed in a 50-ml platinum crucible and thoroughly mixed. The crucible was heated in a muffle furnace at 1000°C for 1 h. When the fusion was complete, the cooled crucible was placed in a 100-ml beaker, a small teflon-coated stirrer was inserted and 50 ml of 5% hydrochloric acid was added. The solution was heated for 15 min at 50—60°C on a magnetic stirrer, and transferred to a 250-ml polyethylene flask. This procedure was repeated with a second aliquot of hydrochloric acid and when dissolution was complete, the contents of the flask were adjusted to volume with deionized water. The working blank was obtained by taking the same quantity of lithium tetraborate through the entire procedure.

RESULTS AND DISCUSSION

It is well known that the presence of an acid or salt introduced during a chemical procedure can influence the instrumental response of the required analyte, both by altering the chemical equilibria in solution, and by affecting the reactions which lead to atomization [27]. Such an effect is particularly important for the more volatile elements for which interferences may occur in the condensed phase. In this work, with the specific purpose of establishing such phenomena, the effects of ashing and atomization temperatures were determined for all elements in the fusion solution.

As an example, Fig. 1 shows the effect of ashing and atomization tem-

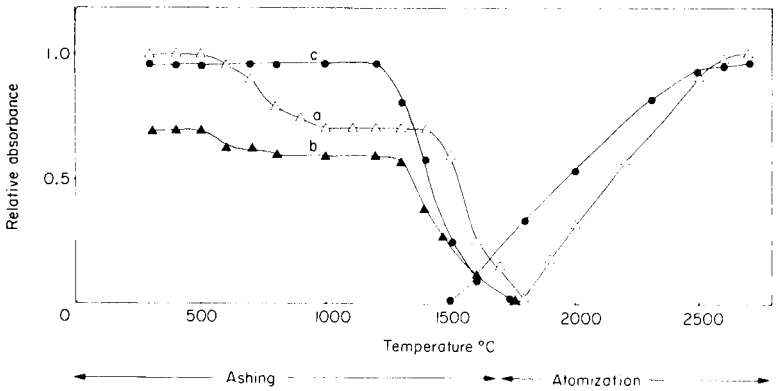

Fig. 1. Effect of ashing temperature (2700°C atomization) and atomization temperature (1000°C ashing) on the signal from arsenic (20 μl of 25 μg l^{-1}): (△) in 1% HNO_3; (▲) in $Li_2B_4O_7$ solution; (●) with 100 mg Ni l^{-1} in $Li_2B_4O_7$ solution.

peratures on the response from arsenic (as $AsCl_3$) in aqueous 1% nitric acid, and in lithium tetraborate solution with and without nickel. From the ashing curves (a) and (b), it appears that part of the arsenic volatilizes at about 600°C while from 800 to 1300°C there is no further loss. In the presence of nickel, a stable metal—arsenic compound is formed so that the ashing temperature can be raised to 1200—1300°C without losses of arsenic (curve c). The presence of nickel also greatly reduces the depressive effect of the lithium tetraborate.

Figure 2 shows similar curves for cadmium (as chloride) in various solutions. These curves show that cadmium atomization takes place by different mechanisms. When hydrochloric acid is present, it takes place via the salt or

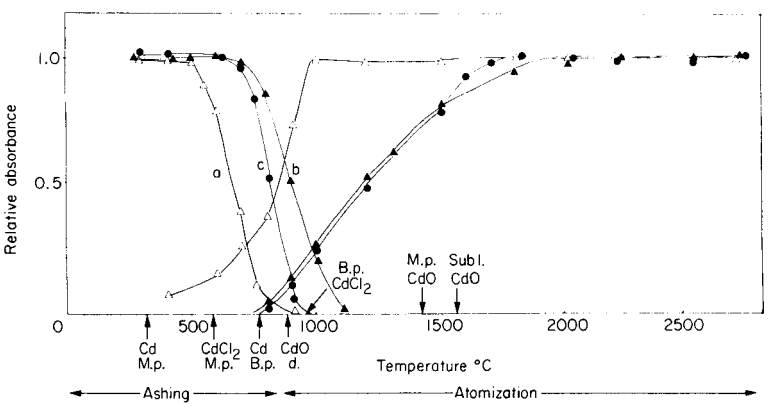

Fig. 2. Effect of ashing temperature (2000°C atomization) and atomization temperature (500°C ashing) on the signal from cadmium (20 μl of 20 μg l^{-1}) in: (△) 1% HCl; (▲) 1% HNO_3; (●) $Li_2B_4O_7$ soln. (d. = decomposition).

the metal, while from the nitric acid or lithium tetraborate solutions, it occurs via the oxide.

The effect of the type of acid is less pronounced for lead than for cadmium, and lithium tetraborate exhibits the major depressive effect. Compared with the 1% nitric acid solution, an average 70% reduction in sensitivity was recorded for lead. However, matrix modification by addition of 1% phosphoric acid allows the ashing temperature to be raised to 1000°C. This considerably reduces the interference of lithium tetraborate, and the loss of sensitivity is reduced to about 30% with an accuracy comparable to that in aqueous solution.

For less volatile elements (Cr, Cu, Ni, Fe, Mn), the presence of the flux in solution does not alter noticeably the atomization mechanism and consequently the optimum ashing temperature is less critical. Figure 3, for example, shows the ashing and atomization curves for chromium (as $Cr(NO_3)_3$) in various solutions. The other elements noted above behaved similarly.

Application to samples

The fused mass of the four standards analyzed dissolved completely in 5% hydrochloric acid to give clear solutions. This implies satisfactory destruction of carbonaceous materials and of the chromite, ilmenite or chlorite minerals, which are particularly resistant to acid dissolution.

The blank levels in the tetraborate were determined for four different sources of material (Merck, BDH, C.Erba and Hoechst). The trace element concentrations, which in some cases were significantly different, ranged as follows: 0.8—2.4 μg As g^{-1}, 0.05—0.15 μg Cd g^{-1}, 0.2—1.5 μg Mn g^{-1}, 0.2—0.5 μg Co g^{-1}, 0.30—1.0 μg Cr g^{-1}, 0.7—1.8 μg Cu g^{-1}, 0.6—2.5 μg Ni g^{-1}, 0.8—2.5 μg Pb g^{-1}, 0.7—2.6 μg V g^{-1} and 1.5—3.6 μg Zn g^{-1}. When the

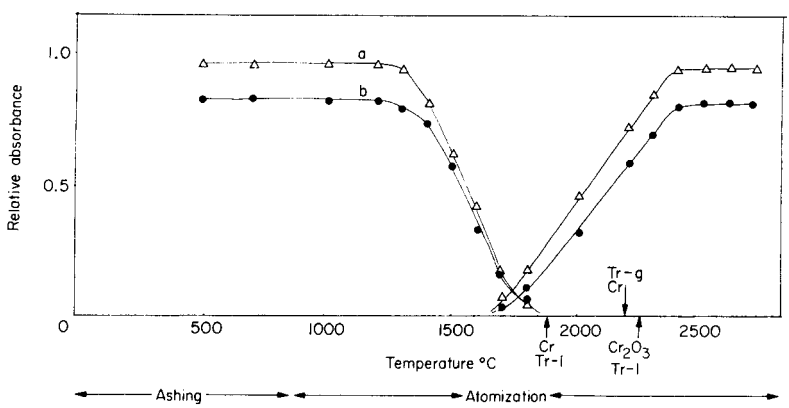

Fig. 3. Effect of ashing temperature (2700°C atomization) and atomization temperature (1200°C ashing) on the signal from chromium (20 μl of 100 μg l^{-1} as $Cr(NO_3)_3$) in: (△) 1% HNO_3; (•) $Li_2B_4O_7$ soln. (Tr-l = solid—liquid transition, Tr-g = liquid—gas transition).

purest salt was used with the instrumental conditions reported in Table 1, the detection limits (in $\mu g\ l^{-1}$) were: 2.0 (As), 0.20 (Cd), 0.60 (Co), 0.55 (Cr), 0.70 (Cu), 0.70 (Mn), 1.0 (Ni), 1.30 (Pb), 1.0 (V) and 1.70 (Zn). Tables 2–5 give the precision and accuracy obtained for the analysis of N.B.S. 1645, 1633, 1648 and Eurostandard 877-1, respectively, compared with the certified values. The results obtained, in nearly all cases, are within the certified tolerance limits and comparable with those recently reported by Gladney [28]. The coefficients of variation are on average less than

TABLE 2

Results for N.B.S. River Sediment (SRM-1645)

Element	Metal found[a] ($\mu g\ g^{-1}$)	Certified value	Average recovery (%)
Fe	11.5% ± 0.5	11.3% ± 1.2	102
As	81 ± 8	(66)[b]	123
Cd	9.1 ± 0.8	10.2 ± 1.5	89
Co	7.8 ± 0.4	(8)[b]	97
Cr	2.82% ± 0.14	2.96% ± 0.28	95
Cu	106 ± 15	109 ± 19	97
Mn	791 ± 12	785 ± 97	101
Ni	43.8 ± 7.0	45.8 ± 2.9	96
Pb	699 ± 48	714 ± 28	98
V	27.7 ± 2.0	23.5 ± 6.9	118
Zn	1659 ± 123	1720 ± 169	97

[a]Mean of 4 results with 95% tolerance limit. Results are given as $\mu g\ g^{-1}$ except where indicated. [b]Values reported but not certified by N.B.S.

TABLE 3

Results for N.B.S. Fly Ash (SRM-1633)

Element	Metal found[a] ($\mu g\ g^{-1}$)	Certified value	Average recovery (%)
Fe	6.19% ± 0.10	(6.20% ± 0.4)[b]	100
As	57 ± 5	61 ± 6	93
Cd	1.50 ± 0.15	1.45 ± 0.06	103
Cr	135 ± 9	131 ± 2	103
Co	37 ± 3	(38)[c]	97
Cu	123 ± 14	128 ± 5	96
Mn	502 ± 14	493 ± 7	102
Ni	98 ± 3	98 ± 3	100
Pb	72 ± 10	70 ± 4	103
V	231 ± 5	214 ± 8	108
Zn	208 ± 20	210 ± 20	99

[a]See footnote to Table 2. [b]Value reported by Gladney [28]. [c]Value reported but not certified by N.B.S.

TABLE 4

Results for N.B.S. Urban Particulate Matter (SRM-1648)

Element	Metal found[a] ($\mu g\ g^{-1}$)	Certified value	Average recovery (%)
Fe	4.02% ± 0.2	3.91% ± 0.20	103
As	110 ± 20	115 ± 10	96
Cd	70 ± 6	75 ± 7	93
Cr	421 ± 40	403 ± 12	104
Co	17 ± 2	(18)[b]	94
Cu	602 ± 30	609 ± 27	99
Mn	865 ± 70	(860)[b]	101
Ni	85 ± 6	82 ± 3	104
Pb	6600 ± 150	6550 ± 80	101
V	125 ± 5	(130)[b]	96
Zn	4805 ± 150	4760 ± 140	101

[a]See footnote to Table 2. [b]Values reported but not certified.

TABLE 5

Results for Eurostandard 877-1 Furnace Dust

Element	Metal found[a] (%)	Certified value	Average recovery (%)
Fe	61.52 ± 0.74	62.07 ± 0.35	99
As	0.013 ± 0.002	0.014 ± 0.002	93
Cd	0.0028 ± 0.0008	(0.0029)[b]	97
Cr	0.017 ± 0.002	0.017 ± 0.001	100
Cu	0.024 ± 0.002	0.025 ± 0.001	96
Mn	1.33 ± 0.04	1.37 ± 0.02	97
Ni	0.010 ± 0.002	0.010 ± 0.001	100
Pb	1.000 ± 0.03	1.000 ± 0.03	100
Zn	1.16 ± 0.02	1.16 ± 0.04	100

[a]Mean of 4 results with 95% tolerance limit. [b]Value reported but not certified.

5—8% except those for nickel and cadmium (respectively 12 and 14% for Eurostandard 877-1). The recoveries for all the elements are between 93 and 103%; only for N.B.S. 1645 arsenic and vandadium show significantly high recovery and cadmium only 89% recovery.

The Eurostandards 680-1 and 681-1 (analyzed only for arsenic, lead and zinc) were used to evaluate the fusion method on materials of widely different chemical composition (Fe = 59.98 and 33.21%, respectively) and to verify the recovery of more volatile elements present at high concentrations. Duplicate analyses gave the following results: for Eurostandard 680-1, Pb found 3081, 3124 $\mu g\ g^{-1}$ (certified, 3166 ± 80), Zn found 1632, 1629 $\mu g\ g^{-1}$ (certified 1652 ± 38); Eurostandard 681-1 Pb found 69 and 71 $\mu g\ g^{-1}$

(reported 72). The values for lead agree with those reported by Nuhfer and Romanosky [29] and Pella et al. [23]. They show that loss of lead by volatilization may be prevented by simply keeping the fusion temperature below 1100°C.

Contrary to the report of Sinex et al. [4], the data for chromium indicate complete fusion of the samples and excellent recovery at the high chromium level in the N.B.S. 1645 river sediment. Recovery data for arsenic are much higher than those reported by Owens and Gladney [20] after fusion of N.B.S. 1633. A possible explanation might be the improvements brought about by matrix modification. Yet, the anomalous value for N.B.S. 1645 might also signify the presence of compensating errors, i.e., losses during fusion and positive errors arising in other parts of the system. To clarify this point, for fusion in the presence of nickel nitrate, the arsenic contents of N.B.S. 1633a fly ash, Eurostandard 680-1 and 681-1 iron ore were determined. Duplicate analyses gave the results reported in Table 6. The results show that the arsenic recovery is quantitative (99—105%), and there are no measurable losses of the element by volatilization during fusion.

The correlation coefficients (calculated by the least-squares method) between the concentrations of Cd, Cr, Cu, Mn, Ni, Pb, V and Zn measured in this work (and in N.B.S. 1632a and N.B.S. 1635 (for which data are not published here)) and the concentration certified, are in all cases above 0.995 (value for vanadium). These results confirm the possibility of using the fusion method for trace element determinations. Generally speaking, this method does not seem to suffer any particular effects associated with differences in the matrices studied. Probably this is the result of a uniform high content of lithium tetraborate which acts as a spectrochemical buffer to minimize other interference effects [30]. The advantages of using a lithium tetraborate fusion instead of acid attack are that it is faster, it needs no special equipment and it readily dissolves refractory minerals which are particularly resistant to acid mixtures.

TABLE 6

Arsenic concentrations ($\mu g\ g^{-1}$) in environmental standard reference materials

Standard	Certified value	This work
N.B.S. 1633a	145 ± 15	156, 149
Eurost. 681-1	(109)[a]	110, 106
Eurost. 680-1	571 ± 26	596, 574

[a] Value reported but not certified.

REFERENCES

1 H. Agemian and A. S. Y. Chau, Analyst, 101 (1976) 761.
2 H. Agemian and A. S. Y. Chau, Anal. Chim. Acta, 80 (1975) 61.
3 K. Scott, Analyst, 103 (1978) 745.
4 S. A. Sinex, A. Y. Cantillo and G. R. Helz, Anal. Chem., 52 (1980) 2342.
5 J. A. Maxwell, Rock and Mineral Analysis, Interscience, New York, 1968.
6 T. T. Gorsuch, Analyst, 84 (1959) 135.
7 J. G. Farmer and M. J. Gibson, At. Spectrosc., 2 (1981) 176.
8 J. W. McLaren, S. S. Berman, V. J. Boyko and D. S. Russell, Anal. Chem., 53 (1981) 1802.
9 J. W. Owens and E. S. Gladney, At. Absorpt. Newsl., 14 (1975) 76.
10 E. N. Pollock, in S. Babu (Ed.), Trace Elements in Fuel, Am. Chem. Soc., Washington, DC, 1975, p. 23.
11 Y. Talmi, Anal. Chem., 46 (1974) 1005.
12 R. J. Guidoboni, in C. Karr (Ed.), Analytical Methods for Coal and Coal Products, Vol. 1, Academic Press, New York, 1978, p. 421.
13 R. A. Nadkarni, Anal. Chem., 52 (1980) 1210.
14 H. Uchida, T. Uchida and C. Iida, Anal. Chim. Acta, 116 (1980) 433.
15 W. J. Price and P. J. Whiteside, Analyst, 102 (1977) 664.
16 J. K. Kaakinen and R. M. Jorden, in W. Fulkerson (Ed.), Proc. 1st Ann. NSF Trace Contam. Conf., 1974, p. 165.
17 E. S. Gladney, Ph.D. Thesis, University of Maryland, 1974.
18 E. Jeanroy, Analysis, 2 (1973) 703.
19 P. L. Boar and L. K. Ingram, Analyst, 95 (1970) 95.
20 J. W. Owens and E. S. Gladney, At. Absorpt. Newsl., 25 (1976) 95.
21 A. Boix, M. Draignaud and J. Debras-Guedon, Bull. Soc. Fr. Ceram., 106 (1975) 69.
22 H. Bennett, in A. W. Nicol (Ed.), Physicochemical Methods of Mineralogical Analysis, Plenum Press, New York, 1975, p. 451.
23 P. A. Pella, K. E. Lorber and K. F. J. Heinrich, Anal. Chem., 50 (1978) 1268.
24 W. M. Wise and S. D. Solsky, Anal. Lett., 9 (1976) 1047.
25 M. Bettinelli, La Rivista Dei Combustibili, 35 (1981) 446.
26 D. Chakraborti, W. De Jonghe and F. Adams, Anal. Chim. Acta, 119 (1980) 331.
27 M. Pinta, Modern Methods for Trace Element Analysis, Ann Arbor Science, Ann Arbor, MI, 1978, p. 203.
28 E. S. Gladney, Anal. Chim. Acta, 118 (1980) 385.
29 E. B. Nuhfer and R. R. Romanosky, At. Absorpt. Newsl., 18 (1979) 8.
30 A. A. Verbeek, M. C. Mitchell and A. M. Ure, Anal. Chim. Acta, 135 (1982) 215.

Analytica Chimica Acta, 148 (1983) 203—210
Elsevier Science Publishers B.V., Amsterdam — Printed in The Netherlands

EVALUATION OF A METHOD FOR DETERMINATION OF INDIUM AND THALLIUM IN FOODSTUFFS

W. H. EVANS*, P. J. BROOKE and BRENDA E. LUCAS

Department of Industry, Laboratory of the Government Chemist, Cornwall House, Stamford Street, London SE1 9NQ (Gt. Britain)

(Received 25th June 1982)

SUMMARY

For the determination of total indium and thallium (0.05—0.4 mg kg^{-1}) in foodstuffs, organic matter is destroyed by wet oxidation and both elements are concentrated by chelation with ammonium pyrrolidinedithiocarbamate and extraction into 4-methylpentan-2-one prior to measurement by flame atomic absorption spectrometry. Probable ionic interferences in foodstuffs are outlined. The accuracy of the method is assessed by recovery of indium and thallium from foodstuff homogenates. The method is not sufficiently sensitive to determine normal levels of indium in foodstuffs, but values for thallium in spinach, orchard leaves, bovine liver and Bowen's kale are given. The detection limits for indium and thallium are 0.04 and 0.06 mg kg^{-1}, respectively.

Indium and thallium are rare elements in nature, but are associated in ores with more abundant metals of industrial importance. During the processing of such ores, thallium may be emitted from copper, zinc and lead smelters while indium may be emitted from zinc (and tin) smelters. Such emissions may contaminate the surrounding biosphere and so enter the food chain.

Apart from radiochemical analysis for indium, relatively few methods have been described for determination of these two elements in solution. These involve liquid—liquid extraction, often after chelation, followed by spectrophotometry, atomic absorption spectrometry (a.a.s.) or atomic emission spectrometry (a.e.s.). These methods have been summarized [1, 2]. Their few applications have been directed to inorganic matrices [3, 4]. It is generally considered that a.e.s. is more sensitive than a.a.s. for indium. Detailed examination of measurements by each technique with various fuel—oxidant combinations on acid and organic solvent solutions during the investigation indicated that measurement by a.a.s. was to be preferred, because of excessive base-line continuum noise with a.e.s. measurements. The present investigation describes findings on a method for determining low levels of each element in foodstuffs after wet oxidation using chelation and extraction, with measurement by a.a.s.

0003-2670/83/$03.00

EXPERIMENTAL

Reagents and apparatus

Reagents were of analytical grade or the grade indicated. Solutions were prepared with distilled water. Sulphuric acid, nitric acid and ammonia solution were of BDH Aristar of Hopkin and Williams Ultrar grade. A pH 4.6 buffer solution was prepared from 30 g of anhydrous sodium acetate and 21 ml of acetic acid in 500 ml of water. The ammonium pyrrolidinedithiocarbamate (APDC) solution was prepared daily by dissolving 3 g in 100 ml of water to give a clear solution.

Commercially-prepared stock 1000 mg l^{-1} solutions of indium and of thallium were diluted to give a solution containing 0.5 mg l^{-1} of both elements in 5% (v/v) sulphuric acid. Working standard solutions of 0.000, 0.005, 0.01, 0.015, 0.02 and 0.04 mg l^{-1} of both elements were prepared in 5% (v/v) sulphuric acid.

All glassware was kept in or full of 1 M nitric acid.

An Instrumentation Laboratories IL453 atomic absorption spectrometer fitted with a 100-mm triple-slot burner and a Counter Flo-Jet nebulizer was used. The wavelengths were 303.9 and 276.8 nm for indium and thallium, respectively; single-element hollow-cathode lamps were used as sources. Measurement was made at burner heights of 15 and 10 mm for indium and thallium, respectively, without background correction, and responses were chart-recorded.

Procedure

Destroy organic matter in 5—50 g of foodstuff (depending on the nature of the foodstuff) with nitric and sulphuric acids as described previously [5]. The resulting 100 ml of digest in nominally 5% sulphuric acid should be colourless and free from suspended solids. Prepare at the same time two reagent blank solutions from the same volumes of acid as used in the sample oxidation. To 70 ± 1 ml of the digest in 150-ml beakers, add 5 ± 0.2 ml of buffer solution and ⩾ 7 ml of concentrated ammonia. Cool and adjust to pH 4 ± 0.1 with ammonia solution. Transfer immediately to a 100-ml separating funnel, add 5 ml of APDC solution, shake strongly for 30 s and stand for 3 min. Extract the chelates into 10 ml of 4-methylpentan-2-one (MIBK) by shaking strongly for 30 s. After 6 min, separate the organic phase and filter through silicone-treated phase-separating paper into a clean, dry receiver. Similarly treat 70 ± 1 ml of the working standard solutions. Using a non-luminous flame to reduce background noise and drift, obtain a steady baseline by aspirating water-saturated MIBK. Arrange the sample, blank and working standard extracts in random order but with a reagent blank in each half of the sequence. Measure the extracts on the day of preparation by a.a.s., using the conditions described above, and returning to water-saturated MIBK between each measurement to obtain a steady baseline.

RESULTS AND DISCUSSION

Chelation and extraction

It has been reported that indium and thallium are stable in chloride solution up to pH 3.0 and 6.5, respectively [6]. No losses would be expected from digests or standards prepared in 5% sulphuric acid as indium(III) is present. Thallium in standard solutions would exist as thallium(I). Thallium(III) would initially be present in digests, but this would revert rapidly to thallium(I) on standing. In the presence of APDC, any thallium(III) would be reduced to thallium(I).

Investigations were made into the amount of APDC required, the pH dependence, and shaking and standing times during the chelation and extraction stages. The ratio of responses from solutions containing both indium and thallium (0.014 and 0.029 mg l^{-1}), after chelation with 5 ml of 1, 2 or 3% APDC solution, was constant for indium but increased by 25 and 32% for thallium as the APDC concentration increased. Thus the highest reagent strength was selected for further use. The pH dependence of responses at the above levels are shown in Table 1. A pH of 4 is recommended for chelation.

Responses obtained after different shaking and standing times are shown in Table 2 for solutions containing 0.04 mg l^{-1} of both elements. None of the

TABLE 1

Relative responses after extraction at different pH values

pH	1.0	3.0	3.5	4.0[a]	4.5	5.0
Indium	0.85	1.02	0.98	1.00	1.10	1.04
Thallium	0.00	0.60	0.99	1.00	1.03	0.97

[a]Recommended condition.

TABLE 2

Dependence of relative responses on duration of chelation and extraction steps

Shaking time (s)						
with reagent	15	15	30[a]	15	15	
with solvent	15	30	30[a]	45	60	
Indium	0.97	0.94	1.00	0.98	0.98	
Thallium	1.00	0.97	1.00	0.98	0.98	
Standing time (min)						
after reagent addition	3[a]	5	10	3	3	3
after extraction	6[a]	6	6	3	9	18
Indium	1.00	1.03	1.07	0.92	0.98	0.99
Thallium	1.00	0.94	1.07	1.06	1.00	1.03

[a]Recommended conditions.

deviations exceeded the 95% confidence limits calculated from the repeatabilities at 0.04 mg l^{-1} for each element (Table 3).

Comparison of the responses from chelates of the working standard solution after storage for 24 h at 4°C with those freshly prepared indicated a 14% decrease in response for indium. It was therefore necessary to measure all extracts on the day of preparation.

Calibration

Fifteen series of working standards were measured by three analysts over a period of ten months. For each series of standards, the average net response for 5 μg l^{-1} increments was calculated. The range and relative standard deviation (r.s.d.) are shown in Table 3. Also given are the ratio of the mean of the reagent blanks (taken through the whole procedure) to that of the zero standard, together with the r.s.d. of their difference, and the ratio of the responses at each standard concentration to the average response, for all 15 calibrations, and the reproducibility (r.s.d.), s, of their differences. Finally the standard deviation obtained within a series of 6 extractions and measurement of standards on one occasion by one analyst, the repeatability s_0, is listed.

The reagent blank is only slightly above the zero standard blank, and consistency is indicated by the small range of the average responses. Calibration linearity is assured because deviations from unity for the ratio of individual standard responses to the average responses are well within the 95% confidence limits required by the relevant r.s.d. values. A constant r.s.d. is obtained at higher concentrations of each element, but for thallium the lowest standard is in the region of the limit of detection (5 μg l^{-1}) for the procedure. If s_0 and s are compared for the same concentrations by an F-test, the ratios for 15 and 5 degrees of freedom should lie within 95% confidence limits

TABLE 3

Calibration data[a]

Element	Indium	Thallium
Range of average response (%)	75—125	78—119
R.s.d. of average response (%)	15	13
Ratio of reagent blank to zero standard ± r.s.d.	1.13 ± 0.20	1.08 ± 0.15
Ratio of standard to average response ± r.s.d.		
at 0.005 mg l^{-1}	0.99 ± 0.15	1.00 ± 0.35
at 0.010 mg l^{-1}	1.02 ± 0.09	0.95 ± 0.15
at 0.015 mg l^{-1}	1.01 ± 0.08	0.97 ± 0.11
at 0.020 mg l^{-1}	0.97 ± 0.07	1.02 ± 0.07
at 0.040 mg l^{-1}	0.99 ± 0.07	0.99 ± 0.07
Repeatability at 0.010 mg l^{-1}, ±r.s.d.	±0.043	±0.091
Repeatability at 0.040 mg l^{-1}, ±r.s.d.	±0.035	±0.050

[a]For explanation of terms, see text.

of 0.39 and 1.89 to reflect an absence of between-series contributions from chelation and measurement by different analysts [7]. This test is satisfied for thallium, but exceeded slightly for indium, which reflects previous comments on the detrimental influence of indirect interferences on routine measurements [8].

Interferences

Direct interferences from other ionic species were assessed. Standard solutions containing 0.00, 0.01 and 0.04 mg l^{-1} of indium and thallium were tested for the ions listed in Table 4, at the maximum levels which could be encountered in foodstuff digests prepared by the above procedure. The higher of the zero standard plus ionic species or zero standard alone was used to obtain the net response for solutions containing added ions only, and this was taken into account when estimating interference effects. The 95% confidence limits were calculated from s_0 at the equivalent levels (Table 3), but are restrictive because they do not include the contribution to the variation from the blank or from solution preparation.

For thallium, molybdate at levels greater than 2.8 mg kg^{-1} interfered, but this is unlikely to be exceeded in foodstuffs. Also, manganese(II) interfered at levels greater than 14 mg kg^{-1} which may invalidate the method for application to tea leaves, some cereals (but not bread or flour) and some herbs [9]. For cadmium, occasionally present at 0.28 mg kg^{-1} in offal or shellfish, similar invalidation could occur. This surprising interference for such low levels of cadmium has been noted in a similar procedure for lead [10]. Only tin interfered with determination of indium (as would be found in canned foodstuffs). Interference increased when mixtures of tin and indium were left to stand for several h, and in the absence of acetate buffer at pH 4 no response for indium was obtained. It was concluded that this interference occurs before chelation because of the scavenging effect of hydrolysed tin on indium at pH 4; this effect was enhanced at higher pH values.

Application to foodstuffs

No information exists on possible losses of either element during the proposed destruction of organic matter. An assessment of the accuracy and variation of the total procedure was therefore made by measuring the recovery of each element, added as its sulphate, to nine food homogenate groups (50 g of beverages, 20 g of milk, 5 g of fats and 10 g of cereals, meat, fish, root vegetables or green vegetables). Amounts of 0.5, 1.0 and 2.0 μg of each element were recovered in duplicate, the base levels being determined within the same series of determinations. The accuracy of the method may be assessed from the results summarised in Tables 5 and 6. To test whether any of the recoveries were abnormal, each duplicate mean was tested for 95% confidence intervals of $\pm\, ts2^{1/2}$ from the overall mean at each particular level. Only one of the 54 means in the exercise was exceeded, that for the fats homogenate, giving statistical significance for the recovery of 0.5 μg

TABLE 4

Interference effects

Added ion	Amount[a] (mg)	Relative difference on result for In or Tl[b]			
		Indium ($mg\ l^{-1}$)		Thallium ($mg\ l^{-1}$)	
		0.01 (±0.12)	0.04 (±0.09)	0.01 (±0.23)	0.04 (±0.13)
Ag^{+}	0.02	−0.11	−0.03	[−0.07]	[−0.08]
Al^{3+}	0.5	−0.10	+0.03	+0.01	+0.05
Ca^{2+}	40	−0.10	−0.01	−0.16	−0.04
Cd^{2+}	0.02	−0.09	+0.06	[+0.11][c]	[−0.11][c]
	0.01	—	—	−0.07[c]	−0.14[c]
	0.002	—	—	+0.06	0.00
Cl^{-}	500	−0.11	+0.01	+0.05	+0.02
Co^{2+}	0.1	+0.13	−0.01	−0.03	−0.01
CrO_4^{2-}	0.1	0.00	0.00	−0.03	+0.06
Cu^{2+}	0.5	−0.02	+0.03	−0.09	−0.04
Fe^{3+}	2.0	−0.21	+0.04	+0.05	+0.03
Hg^{2+}	0.02	−0.13	−0.05	−0.10	−0.09
K^{+}	500	0.00	+0.01	+0.04	0.00
Mg^{2+}	50	+0.12	+0.08	+0.15	+0.05
Mn^{2+}	0.5	−0.05	+0.01	[−0.17][c]	[+0.35][c]
	0.1	—	—	+0.02	−0.09
MoO_4^{2-}	0.1	+0.07	+0.06	[−0.20][c]	[+0.20][c]
	0.02	—	—	−0.13	−0.05
Na^{+}	500	0.00	−0.07	+0.16	+0.05
Ni^{2+}	0.1	−0.18	+0.06	0.00	0.00
NO_3^{-}	500	−0.09	+0.06	−0.15	+0.02
Pb^{2+}	0.1	+0.09	0.00	−0.17	−0.05
$P(PO_4)^{3-}$	200	−0.05	+0.04	−0.12	−0.04
Sn(IV)	0.5	−0.44[c]	−0.43[c]	0.00	−0.02
	0.25	−0.31[c]	−0.38[c]	+0.07	+0.08
	0.1	−0.05	−0.11	+0.20	+0.02
Sr^{2+}	1.0	−0.02	−0.03	+0.09	−0.05
Zn^{2+}	1.0	+0.12	+0.04	[+0.14]	[+0.08]
Ca^{2+}	40				
Mg^{2+}	50	+0.01	+0.01	0.00	−0.09
$P(PO_4)^{3-}$	200				
Average of non-significant differences		−0.03	+0.02	0.00	−0.01

[a]For 100 ml of digest prepared from 10 g of foodstuff, the concentration of interfering species as $mg\ kg^{-1}$ may be obtained by multiplying by 140.

[b]Relative difference compared to a signal of 1.00 in the absence of the added ion. Two levels of indium or thallium were tested; the numbers in parentheses are the 95% confidence levels. The numbers in square brackets are duplicate readings, in which case 95% confidence limits are reduced by $1/2^{1/2}$.

[c]<5% significance.

thallium. This in turn was caused by a single result and in total 3 out of 108 results exceeded the 95% confidence intervals for individual results.

The values for s_0 and s, as defined above, are shown in Table 6. Inspection of the ratio of s from the recovery experiments to that from the calibration solutions at the same levels shows that 95% confidence limits (0.60—1.65) are not exceeded, indicating little contribution from the digestion procedure as carried out by different analysts. A similar comparison of s_0 (≡0.01 mg

TABLE 5

Average of six recoveries of indium and thallium added to homogenates

Food homogenate	Average recovery (%)[a]		Food homogenate	Average recovery (%)[a]	
	In	Tl		In	Tl
Cereals	96	87	Root veg.	100	83
Meat	90	94	Other veg.	105	93
Fish	109	108	Beverages	88	103
Fats	96	117	Milk	94	97
Fruit	93	101	Overall average	97	98

[a]Average content of homogenates was 3.2 ng for indium and 80 ng for thallium.

TABLE 6

Recovery of indium and thallium[a]

Element	Amount added (μg)	Mean recovery (%)	Range (%)	s_0		s		95% CI[b] (mg kg^{-1})
				(%)	(μg)	(%)	(μg)	
Indium	0.5	92	48—127	22	0.11	23	0.11	0.025/0.024
	1.0	100	72—115	13	0.13	14	0.14	0.029/0.030
	2.0	99	80—114	11	0.21	11	0.22	0.047/0.046
Thallium	0.5	97	47—173[c]	20	0.10	27	0.14	0.022/0.029
	1.0	95	58—130	15	0.16	19	0.19	0.035/0.040
	2.0	103	91—120	8.0	0.16	8.0	0.16	0.033/0.033

[a]Each row represents 18 results obtained by 3 analysts, comprising duplicates on 9 foodstuff homogenates.
[b]These 95% confidence intervals are for a single result, the first value derived from s_0, the second from s. Concentrations are based on 10 g samples.
[c]<5% significance from different foodstuffs.

l^{-1}) is indicated for thallium, but disagreement for indium gives further evidence for the presence of indirect interferences in the measurement of this element [8].

The accuracy of the method as applied to foodstuffs should be established by obtaining agreement with authenticated levels in standard reference materials. None is certified for these two elements, but for thallium uncertified levels of 0.03 and 0.05 mg kg^{-1} are suggested for N.B.S. spinach and N.B.S. bovine liver, respectively, and 0.15 mg kg^{-1} for Bowen's kale [11]. These standard reference materials, together with N.B.S. orchard leaves (2-g samples) and samples of flour, mushrooms, cooked cabbage and cooked leeks (10-g samples) were analysed in duplicate by three analysts. For indium, the mean levels for these samples were so low that they were not considered significant in relation to the detection limit for the mean of six results. For thallium, means (corrected for moisture content) of 0.02, 0.03,

0.09 and 0.66 mg kg^{-1} were obtained for spinach, bovine liver, orchard leaves and kale, respectively. No further information could be obtained from the first three sets of results because of skewed distributions of results, but for Bowen's kale the following data were derived: mean, 0.66 mg kg^{-1}; range, 0.56—0.74 mg kg^{-1}; amount, 1.33 μg; s_0 and s, 11% and 0.14 μg; 95% confidence interval ±0.19 mg kg^{-1}. The low levels of both elements in these samples are similar to those found in uncontaminated foodstuffs.

The derivation of a practical limit of detection can be based on the formula $t_{0.005}\, s$ [7]. The limit of detection (10-g samples) derived from recovery of 0.5 and 1.0 μg of each element is 0.036 and 0.048 mg kg^{-1} for indium and thallium, respectively. The value from Bowen's kale for thallium is 0.058 mg kg^{-1}; 95% confidence intervals for results up to 0.2 mg kg^{-1} appear constant and of the order of 0.05 mg kg^{-1} for either element.

This paper is published with the permission of the Government Chemist.

REFERENCES

1 M. S. Cresser, Solvent Extraction in Flame Spectroscopic Analysis, Butterworths, London, 1978.
2 S. D. Shete and V. M. Shinde, Analyst, 107 (1982) 225.
3 A. J. Aller, Anal. Chim. Acta, 134 (1982) 293.
4 C. M. Elson and C. A. R. Albuquerque, Anal. Chim. Acta, 134 (1982) 393.
5 Analytical Methods Committee, Analyst, 85 (1960) 643, Method 1C.
6 A. E. Smith, Analyst, 98 (1973) 209.
7 W. H. Evans, Analyst, 103 (1978) 452.
8 W. H. Evans, D. Dellar, B. E. Lucas, F. J. Jackson and J. I. Read, Analyst, 105 (1980) 529.
9 R. W. Wenlock, D. H. Buss and E. J. Dixon, Br. J. Nutr., 41 (1979) 253.
10 W. H. Evans, J. I. Read and B. E. Lucas, Analyst, 103 (1978) 580.
11 H. J. M. Bowen, J. Radioanal. Chem., 19 (1974) 215.

Analytica Chimica Acta, 148 (1983) 211—223
Elsevier Science Publishers B.V., Amsterdam — Printed in The Netherlands

ELECTROCHEMICAL SEPARATION AND ISOTOPIC DETERMINATION OF THALLIUM AT THE NANOGRAM LEVEL BY SURFACE IONISATION MASS SPECTROMETRY

JOHN W. ARDEN

Department of Geology and Mineralogy, University of Oxford, Parks Road, Oxford OX1 3PR (Gt. Britain)

(Received 19th October 1982)

SUMMARY

A rapid low-blank procedure is described for the co-separation of thallium and lead by sequential cathodic and anodic electrodeposition from natural samples, especially complex natural silicates, for subsequent mass spectrometry. A micro anion-exchange procedure is also described for the separation of thallium and lead. Ion currents of 10^{-10} A can be obtained from 1 ng of thallium. The isotopic composition of 1 ng of thallium can be measured on a Faraday detector with a precision of 0.05—0.1%. The total procedural blank is 3 pg. By using stable isotope dilution, 0.2 ng of thallium can be measured with a precision of 0.6% with only a 2% blank correction. This allows the accurate determination of thallium in natural samples down to concentration levels of about 50 pg g^{-1}. The detection limit is 50 fg. This procedure has been applied to meteorites and terrestrial rocks. The stable isotope dilution technique is suitable for geochemical, environmental and toxicological studies requiring a highly sensitive, accurate and precise method for the determination of thallium.

Thallium, a heavy volatile element with two stable isotopes, ^{203}Tl and ^{205}Tl, is of considerable cosmochemical interest. The now extinct *s*-process nuclide ^{205}Pb ($t_{1/2} = 1.4 \times 10^7$ y) and its decay product ^{205}Tl, are in principle a potential chronometer for early solar system events [1]. Evidence for the presence of ^{205}Pb in meteorites at the time of their solidification would be revealed in the $^{205}Tl/^{203}Tl$ ratio as a function of the Pb/Tl ratio. Recent theoretical studies [2], however, indicate that ^{205}Pb may have decayed prior to incorporation into solar system material. Precise isotopic composition and abundance studies of thallium and lead in meteoritic samples should provide insight into both the termination of *s*-process nucleosynthesis, and the problem of the apparent primordial lead composition in meteorites. Abundance studies of thallium and lead in meteoritic phases may reveal how the pattern of volatile elements was established: by direct condensation from the early solar nebula [3] or by the evaporation of primitive dust [4].

A basic requirement in geochemical, environmental and toxicological studies of thallium is for a highly sensitive, accurate and precise analytical method. Electrodeposition is, in principle, a rapid, efficient and low blank technique

0003-2670/83/$03.00

for the separation of lead and thallium from complex matrices. The principal interferences that can occur, and result in a low yield, are complexing of the electroactive species in solution and the occurrence of undesired redox reactions at the electrode/solution interface. For rapid electrodeposition at the optimum electrode potential, it is essential that transport of the desired electroactive species (i.e., aquated Tl(I), Pb(II) ions) and not electrochemical reduction, is the rate-determining step.

For lead, these interferences have been studied experimentally and the optimum conditions for rapid electrodeposition determined [5]. For thallium, the effect of complex formation in chloride media is particularly important. The chloro complexes exert a complex effect on the homogeneous Tl(I)—Tl(III) rate of exchange; thallium(I) is only weakly complexed whereas thallium(III) can form stable chloro species. For increasing chloride concentration, the observed second-order rate constants for Tl(III)—Tl(I) exchange first decrease to a minimum ($k \approx 10^{-6}$ l mol^{-1} s^{-1}) and then increase [6] to reach a value of 0.6 l mol^{-1} s^{-1} at about 1.5 M HCl [7]. The rate constant is minimal when the species $TlCl_2^+$, which exists over a wide range of chloride concentrations, is maximal, which provides evidence for its relative inertness [6]. Further, the rate of exchange at low chloride concentrations (<0.01 M) is considerably below its value in the absence of chloride [7], indicating that the $TlCl_2^+$ ion has a much lower exchange rate with the aquated thallium(I) ion than does uncomplexed Tl(III). The catalytic effect of high chloride concentrations (>0.1 M) on the homogeneous exchange reaction is thought to be due to faster exchange between complexes of thallium in both oxidation states [6]. Equilibration of thallium species in a sample, and between sample and spike (for isotope dilution mass spectrometry, i.d.m.s.) can therefore be obtained in a high chloride concentration where the dominant species is $TlCl_4^-$.

Interferences with the deposition of thallium and lead are caused mainly by preferential reduction and co-deposition at the cathode. The principal interfering major element in geological samples is iron, with some chondritic meteorites containing up to ~30%. Preferential reduction of iron(III) at the electrode/solution interface inhibits thallium and lead deposition and the reduction of iron(II) can result in the co-deposition of iron. These effects are minimised by reduction of iron(III) with hydrazine and control of solution conditions during cathodic deposition. Formal potential measurements of iron(III) showed that the decrease in the rate of lead deposition with increasing total iron concentration is proportional to the iron(III) remaining in the solution (after partial reduction with the hydrazinium ion) prior to electrolysis [5]. This interference of iron(III) depends on both the total iron concentration and the position of the final iron(II)—iron(III) equilibrium. The latter is a function of the hydrazinium and particularly the hydrogen ion concentrations as expected from the reaction $N_2H_5^+ + Fe(III) \rightarrow NH_4^+ + 1/2\ N_2 + Fe(II) + H^+$ in acidic solution, and confirmed by formal potential measurements of the iron(III) remaining in solution for various H^+ and $N_2H_5^+$ ion concentrations [5]. The residual iron(III) is minimised when the reduc-

tion is done in acidic solution with a final overall hydrazinium ion excess (>0.1 M) and a low hydrogen ion concentration (0.05—0.1 M).

At the high cathode potential required for the deposition of thallium, the co-deposition of iron becomes particularly important from solutions with high iron concentrations. The deposition rate of iron, on an iron electrode, in acidic solution has been shown to be proportional to both the hydroxyl ion and the square of the iron(II) activity [8]. The hydroxyl ion interaction is dependent on the activity at the electrode/solution interface. The discharge of hydrogen ions is another reaction that can interfere with deposition at the trace level. If the cell current is high, blocking of sites by preferential hydrogen ion reduction and hydrogen bubble formation can reduce the effective electrode area available for deposition. This interference, which is potentially serious at the high cathodic potential required for thallium deposition, is minimised by control of the solution pH and thus the cell current during electrolysis.

Prior to separation by electrodeposition, thallium is required as thallium(I). The Tl(III)—hydrazine reaction which proceeds rapidly in acidic media with a stoichiometry of 4, involves a 2-electron transfer in a single step [9]. The presence of iron(II) in a sample should enhance the Tl(III)—Tl(I) reduction compared to that in the absence of iron. The iron(II)—thallium(III) exchange reaction appears to proceed by a succession of 1-electron transfers [10]. The rate of reaction depends on the inverse hydrogen-ion concentration and increases up to a chloride ion concentration of 1.5—2 M [11]. In summary, the optimum conditions for holding thallium as thallium(I) and for minimising the iron(III) interference are high concentrations of both the chloride and hydrazinium ions, and a low H^+ ion concentration.

EXPERIMENTAL

Reagents

The reagents used were prepared by sub-boiling distillation, first in quartz (except hydrofluoric acid) and then in teflon FEP; the blanks are given in Table 1. Perchloric acid and hydrogen peroxide were the only reagents not purified in this laboratory. The ^{203}-Tl-enriched spike was calibrated

TABLE 1

Thallium and lead contents of reagents

Reagent	Tl (10^{-15} g ml^{-1})	Pb (10^{-12} g ml^{-1})
H_2O	1.7	2.4
HCl 6 M	1.1	5
HF 27 M	5.4	5.6
HNO_3 16 M	<30	6
$HClO_4$	390	390

with a highly-purity thallium standard. The 0.25 M phosphoric acid was prepared from Ultrex grade phosphorus pentoxide. The silica gel was prepared by controlled hydrolysis of high-purity silicon tetrachloride. The resultant silica gel was washed with water until neutral and then dispersed by ultrasonic excitation, and the solution was calibrated.

Apparatus

The electrodeposition cells are as previously described [5], but with a fused quartz microjunction for the saturated calomel electrode (SCE). Micro ion-exchange columns (1.5 cm long, 0.15 cm i.d.) were fabricated from 4:1 shrink PTFE tubing. Each column had a 1-ml reservoir at the top and a porous polyethylene disc at the tip. The anion-exchange resin (BioRad AG1-X8, 100—200 mesh) was washed, batchwise in a quartz column, by cyclic gradient elution in hydrochloric acid and then stored under 6 M hydrochloric acid in an FEP bottle. The resin was slurried, in 6 M hydrochloric acid, to form a column 1.5 × 0.15 cm and equilibrated with 10 M hydrochloric acid immediately before use. All other apparatus was constructed of FEP or PTFE. PTFE tubing (0.5 mm i.d.) coupled via a hypodermic needle to a Hamilton microsyringe was used for small reagent additions (1 μl $\approx$ 0.5 cm) and loading of rhenium filaments. Dissolution of samples was done in PTFE autoclaves and solutions were evaporated in PTFE evaporation vessels, fitted with PTFE sheet windows ($\approx$0.03 mm thick), in a stream of highly purified air under infrared lamps [5]. The teflon apparatus (except ion-exchange columns) was cleaned initially by heating for at least a day in 16 M nitric acid and then 6 M hydrochloric acid. The PTFE autoclaves were then heated at about 130°C for 12 h with 5 ml of 6 M hydrochloric acid, followed four times with (5 ml HF + 0.5 ml HNO_3).

Cathodic deposition of thallium

Optimum deposition potential. The critical deposition curves for lead [5] and thallium are given in Fig. 1. Thallium was determined by i.d.m.s. by using a standard thallium solution. The measurements were made with a platinum cathode, copper-plated in situ (—0.4 V vs. SCE for 10 min) immediately prior to the deposition of thallium. Table 2 presents a comparison between the critical deposition potentials obtained from the graph, with potentials calculated from the original Nernst equation (on the assumption that the thermodynamic activity of the cathode is unity) for the reactions: (i) $Tl^+ + e^- \rightarrow Tl^0$ ($E^0 = -0.582$ V) and (ii) $TlCl + e^- \rightarrow Tl^0 + Cl^-$ (1 M HCl; $E^0 = -0.803$ V vs. SCE) [12].

Complexing of thallium(I) by the chloride ion can modify the deposition potential with a shift to more cathodic potentials. The chloride ion concentration of electrodeposition solutions will vary with sample size and composition, and will lie in the range of $\approx$0.3 M for blank solutions to the region of 2 M for 1 g of chondrite. From the stability constants, K_1 and K_2, of the first two chloro complexes of thallium(I) [13], the increase in potential

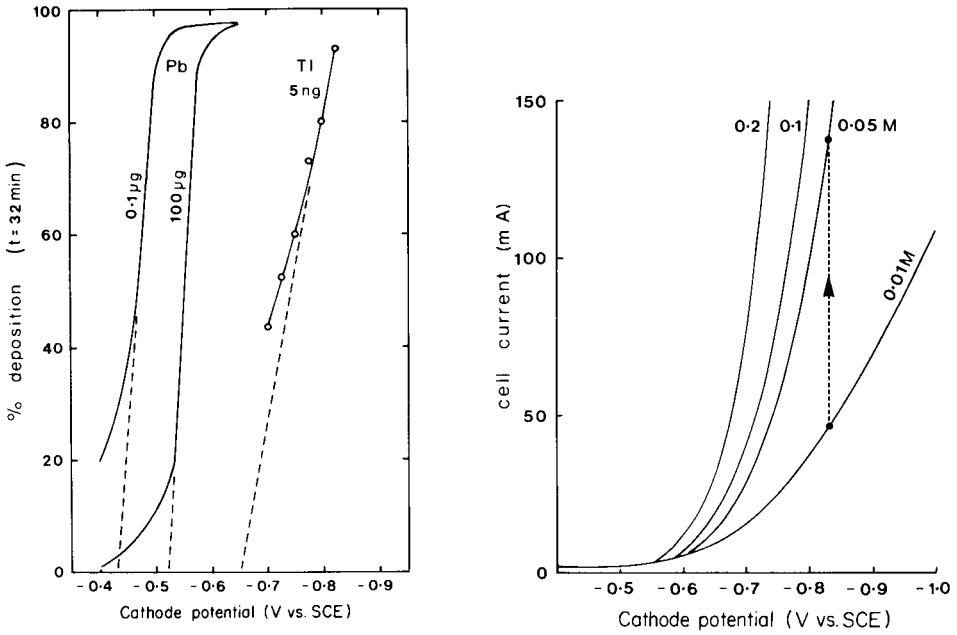

Fig. 1. Critical deposition curves for thallium and lead. The solution and cell conditions are as given in Table 2. The lead data [5] are given for comparison.

Fig. 2. Current—potential curves determined in the electrodeposition cell, for solutions containing 0.01—0.2 M H^+ ion and 0.05 M $N_2H_5^+$ ion. Other conditions are given in Table 2. The increase in cell current for a solution initially 0.01 M in hydrogen ion with a copper-plated Pt cathode (in situ copper deposition at —0.4 V for 10 min), at a potential of —0.83 V and electrolysis period of 30 min is shown by the broken line.

required to compensate for complexing with an increase in the chloride ion from 0.3 M to 3 M is about 0.05 V.

The critical deposition curves (Fig. 1) indicate that cathode potentials of —0.65 V and —0.83 V (vs. SCE) are required for the efficient deposition of lead and thallium, respectively, for the solution and cell conditions given in Table 2. For solutions of high chloride ion concentration, the optimum potential for thallium deposition should be increased to —0.88 V (vs. SCE).

Hydrazinium ion concentration. As thallium is deposited at a higher cathode potential than lead, a large hydrazinium ion excess is used. This is to ensure a decrease in the iron(III) remaining after reduction and to increase the efficiency of anodic depolarisation, thereby minimising iron(II) oxidation during electrolysis.

Hydrogen ion concentration. Because of the more cathodic potential required for the deposition of thallium, pH control is particularly important. For solutions containing high iron concentrations (>15 mg Fe ml^{-1}), the reduction of iron(II) resulting in co-deposition of iron, and oxidation of iron(II) to an orange hydrous iron(III) oxide species, can occur in the region of

TABLE 2

Critical deposition potential for thallium[a]

Tl	Deposition potential (V)		Undervoltage (V)
	Critical[b]	Calculated[c]	
5 ng, 1.4×10^{-9} M	−0.65	(i) −1.11	0.46
		(ii) −1.33	0.68

[a] Solution: 0.05 M H^+ ion, 0.18 M $N_2H_5^+$ ion, 0.3 M Cl^- ion; volume 18 ml; cathode area 7.6 cm^2; deposition time 32 min. [b] See Fig. 1. [c] See text for couples.

a high pH at the electrode/solution interface. To minimise these effects, a low solution pH should be maintained (pH ≈ 1). However, at low pH the active surface area of the cathode available for deposition may be reduced by blocking of sites (see above). During the electrolysis the net hydrogen ion concentration (from $N_2H_5^+$ ion oxidation and H^+ ion reduction) increases. Current–potential curves, measured with the deposition cell for several initial hydrogen ion concentrations, are shown in Fig. 2. The increase in cell current from about 50 mA to 140 mA during electrolysis of a solution 0.01 M in hydrogen ion and 0.05 M in hydrazinium ion with a Pt(Cu) cathode at a potential of −0.83 V (vs. SCE) for 30 min, is shown by the broken line. For solutions of higher ionic strength, the rate of current increase is much lower. During the deposition of thallium and lead, the cell current is easily maintained in the region 50–150 mA by the dropwise addition of dilute hydrazine hydrate solution.

The conditions for the cathodic deposition of thallium which differ from those required for lead [5] are an increased hydrazinium ion excess (over that required for iron(III) reduction), control of pH to 1–2 and a cathode potential of −0.83 V (vs. SCE). For solutions of high iron concentration, the procedure is modified to include a second cathodic separation. At the potential required for thallium deposition, a small amount of iron may be co-deposited. Also, as the cathode cannot be rinsed without some loss of deposited species [5], and as iron interferes with the anodic deposition of lead and thallium, it is often necessary to separate the latter, by dilution, from iron in the occluded sample solution. A second cathodic deposition is done after the Cu, Pb, Tl (and Fe) have been stripped from the cathode. Because of the increased chloro complexing as a result of the higher sample concentration, a cathode potential of −0.88 V is used for the first deposition, and −0.83 V (vs. SCE) for the second.

Anodic deposition of thallium

In extending the method for lead [5] to co-separate thallium by anodic deposition, minor changes are required. Residual chloride ion in the solution of deposited material from the cathodic deposition, sufficient to complex

thallium, may persist even after evaporation with nitric acid and cause low and variable yields in the anodic deposition. The thallium is partly complexed, presumably as $TlCl_2^+$, rather than as the aquated thallium(I) ion. To obtain a high and reproducible yield in the anodic deposition, the nitric acid evaporation is followed by an evaporation with 1—2 drops of nitric acid and 1—2 μl of perchloric acid to destroy any chloro complexes.

The effect of pH on the oxidation and deposition of thallium (Tl(I) → Tl_2O_3) at a platinum anode in nitric acid is more critical than for lead. Table 3 summarises the effect of nitric acid concentration on the anodic deposition yield. These yields are only relative, as the dissolution of deposited Tl_2O_3 in hydrochloric acid is incomplete even at trace levels. Quantitative removal of Tl_2O_3 and PbO_2 is obtained by reduction with H_2O_2—HNO_3, as shown in Table 3.

Procedure

Dissolution. To the sample in a cleaned PTFE autoclave bomb, add about 5 ml of hydrofluoric acid (and 0.5 ml of nitric acid for meteorites and other samples containing oxidisable material) and heat in an oven at about 150°C. These amounts of reagents are suitable for a 1-g sample of meteorite. The decomposition time depends on the type, weight and particle size of sample; for some powdered samples, only 2—3 h is required, but with gram-sized lump samples of meteorites, 1—2 days is usually allowed. Allow the autoclave to cool, and transfer the PTFE autoclave vessel to a PTFE evaporation vessel, where the solution is evaporated in a flow of highly purified air under an infrared lamp. Evaporate the residue to dryness with a further 1—2 ml of hydrofluoric acid. Add 6 M hydrochloric acid (about 5 ml for $\leqslant$0.5 g samples, and about 10 ml for 1—2 g samples) to the residue and reheat the autoclave at 120—150°C for several hours or overnight. Transfer the solution to a tared FEP beaker and heat any residue again with a further similar volume of 6 M hydrochloric acid. Combine the two leachates and aliquot by weight into two parts; to one, add lead and thallium tracer for concentration determination by i.d.m.s. and process the other unspiked for thallium and lead isotopic composition determination. Evaporate each aliquot to 1—2 ml.

Preparation of solution for electrodeposition. Dilute the evaporated solutions to about 10 ml and heat the FEP beaker in an evaporation vessel

TABLE 3

Effect of nitric acid concentration on anodic deposition yield[a]

HNO_3 (M)	10^{-2}	10^{-3}	10^{-4}	10^{-5}
Yield (%)				
HCl	24	46	74	82
HNO_3/H_2O_2			96	

[a]Volume 1 ml; deposition time 20 min.

under an infrared lamp for about 10 min. Add dilute hydrazine hydrate solution dropwise to the hot solution, with stirring, until the acidity is reduced to about pH 1. Return the beaker to the evaporation vessel and continue heating for about 20 min to allow the iron(III) reduction to proceed. Readjust the solution to about pH 1, if necessary, by addition of hydrazine hydrate or hydrochloric acid and allow to cool to room temperature. Add 1 ml of copper solution (~250 μg Cu ml^{-1}), dilute to ~20 ml with water and transfer to the electrolysis cell. The required volumes of hydrazine hydrate and hydrochloric acid can be calculated as reported earlier [5], with the added constraint that the solution should be at least 0.3 M in chloride and stricter control of pH is required in the thallium deposition.

Cathodic deposition of thallium and lead. Insert the electrode assembly into the solution which is stirred at 1800 rpm and adjust the cathode-stirrer clearance to 0.5—1 mm. Maintain the cathode potential at —0.4 V (vs. SCE) for 10 min to deposit the copper and then at —0.83 V (or —0.88 V for solutions of high iron concentration) for 35 min to deposit the thallium and lead. Adjust the cell current, if necessary, to 50—150 mA by dropwise addition of dilute hydrazine hydrate during the course of the electrolysis. Withdraw the electrode assembly, remove the cathode with its adhering liquid and dissolve the deposited material off the cathode with a few drops of nitric acid into the FEP beaker, rinse with water and evaporate to dryness. If the residue is not a blue or blue-green colour, a second cathodic separation is necessary as follows: add 1 ml of 6 M hydrochloric acid to the residue, dilute to about 10 ml and continue as described above for the preparation of solution for electrodeposition and cathodic deposition but without further copper addition. To the residue after nitric acid evaporation, add 2 drops of nitric acid and 1—2 μl of perchloric acid and evaporate the solution to dryness.

Anodic deposition of thallium and lead. Dissolve the residue from the cathodic deposition in about 1 μl of 0.1 M nitric acid and 1 ml of water and transfer the solution to the anodic cell. Electrodeposit the thallium, lead and copper from the stirred solution at 1.8 V for 20 min. Rinse the anode with a drop of water and dissolve the Tl_2O_3 and PbO_2 in 1—2 ml of warm 6 M nitric acid and about 1 μl of hydrogen peroxide, rinse the anode wire with a few drops of water, and evaporate the solution gently to incipient dryness. Add 1—2 drops of 0.1 M nitric acid and slowly evaporate to 1—2 μl immediately prior to mounting the thallium and lead with silica gel—phosphoric acid on an outgassed rhenium filament (see below).

Anion-exchange separation of thallium and lead. Thallium and lead can be readily separated and further purified by anion exchange should this be required. Evaporate the HNO_3—H_2O_2 solution containing the separated thallium and lead from the anodic deposition to a small drop, add 1 drop of 10 M hydrochloric acid and warm to oxidise Tl(I) to Tl(III). Repeat with a further drop of 10 M hydrochloric acid (or until the nitric acid is destroyed). Add 3 drops of 10 M hydrochloric acid to the sample and transfer to a

prepared and equilibrated column. Wash the column with 3 × 6 drops of 10 M hydrochloric acid and collect the eluate for lead. Elute thallium with 2 × 3 drops and then 2 × 6 drops of 0.1 M HCl saturated with sulphur dioxide (because of the slow aerial oxidation of SO_2 this solution should not be kept for extended periods). Evaporate the lead and thallium fractions carefully to incipient dryness, followed by two evaporations with 1—2 drops of 6 M nitric acid. Finally add 1—2 drops of 0.1 M nitric acid.

Procedural blanks and chemical yields. Procedural blanks determined for various stages of the co-separation of thallium and lead are given in Table 4. Chemical yields for various stages in the co-separation of thallium and lead are summarised in Table 5.

Filament loading and mass spectrometry. Filament loading is done with the aid of a Hamilton microsyringe coupled via a hypodermic needle to a 2—3 cm length of PTFE tubing (i.d. 0.5 mm). The tubing is cleaned in hot nitric acid. Silica gel (0.5—1 mm, i.e., 0.1—0.2 μl) is drawn into the PTFE tubing and then placed in the centre of an outgassed rhenium filament. The gel is gently dried by passing a low current (0.2—0.4 A) through the filament. A further 5 × 1 mm of silica gel is similarly loaded to form a deposit about 1.5 mm^2 in the centre of the filament. The sample solution, in 1 drop of 0.1 M nitric acid, is evaporated to 0.5—1 μl and loaded in 0.5-mm aliquots on top of the silica gel and evaporated as above. Finally 2 × 0.5 mm of 0.25 M phosphoric acid is added to the deposit and evaporated to dryness. The sample is bonded to the filament by slowly increasing the current to, and then holding at, 1—1.5 A for 5 s.

The single focusing mass spectrometer used in this work is equipped with both Faraday and electron multiplier collectors and controlled on-line by computer [14]. Data are accumulated in a "peak-hopping" mode in which different masses are automatically selected by stepping the magnetic field intensity in a sequence set by program and counted for preselected times.

RESULTS

Concentration measurements

Sample solutions for concentration measurements were aliquoted in 6 M hydrochloric acid and then spiked with ^{203}Tl before being passed through the combined electrodeposition procedure. To demonstrate the suitability of 6 M hydrochloric acid as a medium for equilibration of thallium between sample and spike, aliquots were taken over a period of 14 days from the same solution of the Allende meteorite, spiked and then processed. The results (Table 6) indicate the precision of the concentration measurements and the aliquoting. The thallium concentration obtained for the standard rock BCR-1 was 277 ± 2 ng g^{-1} (2σ precision); this agrees well with the value 295 ± 60 ng g^{-1} obtained by radiochemical neutron activation analysis (n = 27) [15] and the value 260 ± 56 ng g^{-1} obtained by differential pulse anodic stripping voltammetry (n = 3) [16].

TABLE 4

Procedural and loading blanks

Blank	Tl (pg)	Pb (ng)
Complete separation	3.5, 3.1, 3.7 mean = 3.4 ± 0.3	1.33, 1.26, 1.14, 1.46, 1.19, 1.10 mean = 1.25 ± 0.13
Decomposition	0.29	0.11
Tl—Pb column separation	0.5	0.08
Loading	0.21, 0.32	0.005, 0.007

Isotopic measurements

As thallium has only two stable isotopes, ^{203}Tl and ^{205}Tl, high-precision isotopic measurements of the ratio $^{205}Tl/^{203}Tl$ are subject to mass-dependent fractionation which cannot be internally corrected. The observed ratio changes with time, becoming progressively enriched in the heavy isotope. The rate of this change and the fractionation law obeyed, which probably depends on many factors (e.g., sample loading, temperature, filament material), result in the measured ratio differing from the true ratio by an unknown amount.

The extent of this fractionation was demonstrated by using a thallium(I) chloride standard (Ultrapure, Ventron). Isotopic measurements on samples and standards were made under identical conditions which included a filament temperature—time schedule. The filament was heated by a manually controlled power supply and its temperature was measured with an optical pyrometer. The filament temperature was first increased to 150°C (~0.5 A) in 1 min, then incrementally at a rate of 40°C/5 min to 600°C and finally at 10°C/3 min to 690°C. Focussing of the beam and monitoring of the growth and decay of background peaks were started at about 350°C by using the electron multiplier. At about 600°C, data were obtained by using the Faraday collector. At about 690°C and when the $^{205}Tl/^{203}Tl$ ratio had approached a plateau, data acquisition was started and at least 20 data sets

TABLE 5

Yields for various stages in the separation of thallium

	Sample	Tl yield (%)	Pb yield[a] (%)
Cathodic deposition	5 ng Tl	93	97.8
Anodic deposition	5 ng Tl	96	98.6
Complete separation	0.5 g chondrite	80	86
Tl—Pb column separation	15 ng Tl	99	100

[a]Yields for lead, except for column separation, are from ref. 5.

TABLE 6

Precision of concentration measurements and aliquoting

Sample[a]	Aliquot weight (mg)	Interval	Thallium found (ng g^{-1} ± 2σ)
1	81.63	0	62.63 ± 0.37
2	83.93	11 days	63.26 ± 0.33
3	87.65	14 days	62.93 ± 0.44

[a]Solution of the Allende meteorite in 6 M HCl.

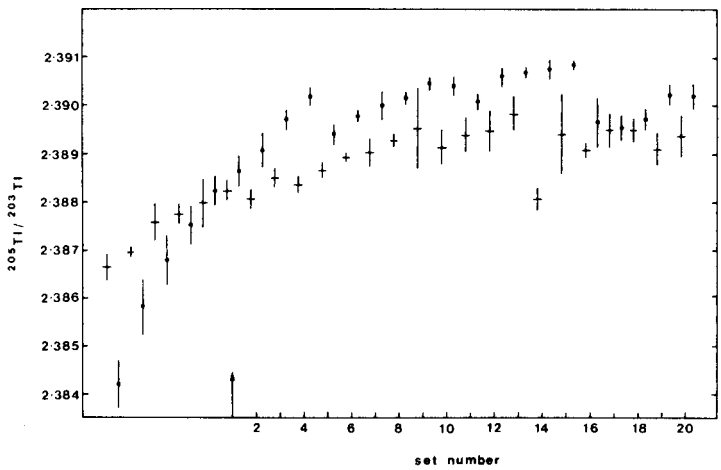

Fig. 3. Fractionation behaviour of two thallium standards at 690—710°C. The start of data acquisition is indicated by the arrow. Each data set (indicated by • and +) represents the mean of 5 ratios ± $2\sigma_m$. The time interval for acquisition of 20 data sets is about 40 min.

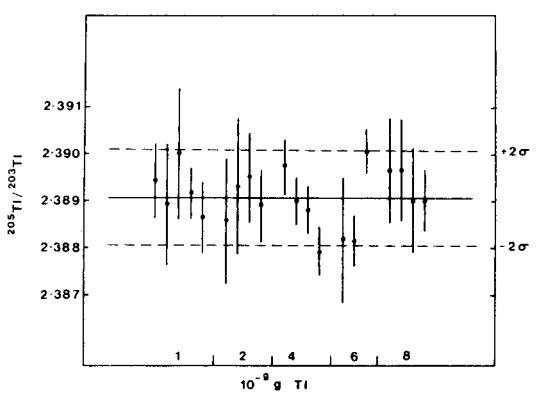

Fig. 4. Isotopic measurements on a thallium standard in the range 1—8 ng Tl. Each data point represents the mean $^{205}Tl/^{203}Tl$ ± 1σ for each set of measurements. The overall mean, for the 20 data sets, is 2.38907 ± 0.00102 (2σ).

(i.e., 100 ratios) were collected. Typical ion beam currents of 4×10^{-10}—3×10^{-11} A were obtained for a few ng of thallium. The $^{205}Tl/^{203}Tl$ ratios reported in Figs. 3 and 4 are raw uncorrected data. In Fig. 3 the fractionation behaviour of two standards is shown. The mean $^{205}Tl/^{203}Tl$ ratios were 2.39008 ± 100 and 2.38897 ± 108 for the two standards. The uncertainty in the mean value for each measured sample is given as 2σ and not $2\sigma_m$ as quoted in previous thallium measurements [17]. This is probably a realistic estimate of the precision of the thallium isotopic composition measurements, because of the inability to initiate data acquisition for all samples at the same point on the fractionation curve.

Replicate isotopic analyses of the thallium standard in the range 1—8 ng Tl are shown in Fig. 4. The mean of 20 analyses is 2.38907 ± 0.00102 (2σ) and represents, when compared to the work of Huey and Kohman [17], an increase in the precision of replicate measurements from ±0.15% to ±0.04%. Measurement of the isotopic composition and abundance of thallium in a few terrestrial and meteoritic samples are summarised in Table 7.

At the end of thallium data acquisition, the filament temperature is slowly increased to 1050—1150°C for the measurement of the lead isotopic composition. No spectral interference from lead emission was observed during thallium isotopic measurements at 690—710°C. This was demonstrated in two ways. The first was by monitoring the ^{206}Pb peak intensity, with the electron multiplier, during the thallium measurements. The ion beam current

TABLE 7

Summary of thallium isotopic and concentration measurements

Sample	Sample weight[a] (mg)	$^{205}Tl/^{203}Tl$ (±2σ)	Tl (±2σ) (ng g^{-1})
Terrestrial			
Tl reagent standards (20)		2.38907 ± 0.00102	
Mantle nodules[b]: BD2501	464	2.38962 ± 0.00142	16.24 ± 0.05
EJ B4	464	2.38969 ± 0.00124	36.05 ± 0.12
USGS standard BCR-1	65.7	2.38851 ± 0.00134	277 ± 2
Allende C3V Meteorite[c]			
Bulk	149	2.38837 ± 0.00212	67.79 ± 0.36
Matrix fractions[d]: No. 21	120	2.38944 ± 0.00224	85.73 ± 0.20
23	172	2.38818 ± 0.00308	32.69 ± 0.18
25	74.6		96.14 ± 0.22
Ca—Al inclusions:			
Coarse grained	112		1.56 ± 0.01
Fine grained	14.0		10.82 ± 0.14
Chondrule	37.9		1.43 ± 0.06

[a]For concentration measurement. [b]Mantle nodules from South African kimberlite pipes. [c]Smithsonian Institution No. USNM 3576. [d]Sieved matrix fractions.

at mass 206 was found to be 10^{-15}—10^{-16} A. The second way was to add about 60 ng of lead (NBS 982 standard) to several of the thallium standards before processing. No relation between fractionation and sample size was observed in the data, as shown in Fig. 4.

I am grateful to R. S. Clarke for the sample of Allende, and to J. B. Dawson and E. Butler for the mantle nodules. This work was supported by the Natural Environment Research Council.

REFERENCES

1 T. P. Kohman, Ann. N.Y. Acad. Sci., 62 (1956) 503.
2 J. B. Blake and D. N. Schramm, Astrophys. J., 197 (1975) 615.
3 J. W. Larimer, Geochim. Cosmochim. Acta, 31 (1967) 1215.
4 J. A. Wood, Earth Planet. Sci. Lett., 56 (1981) 32.
5 J. W. Arden and N. H. Gale, Anal. Chem., 46 (1974) 2.
6 G. Nord-Waind, in M. T. Beck (Ed.), Proc. Symp. Coord. Chem., Tihany, Hungary, 1964, p. 437.
7 G. Harbottle and R. W. Dodson, J. Am. Chem. Soc., 73 (1951) 2442.
8 T. Hurlen, Acta Chem. Scand., 14 (1960) 1533.
9 W. C. E. Higginson, D. Sutton and P. Wright, J. Chem. Soc., (1953) 1380.
10 K. G. Ashurst and W. C. E. Higginson, J. Chem. Soc., (1953) 3044.
11 F. R. Duke and B. Bornong, J. Phys. Chem., 60 (1956) 1015.
12 W. M. Latimer, The Oxidation States of the Elements and their Potentials in Aqueous Solutions, 2nd. edn., Prentice-Hall, Englewood Cliffs, NJ, 1952, p. 163.
13 L. G. Sillèn and A. E. Martell (Eds.), Stability Constants of Metal—Ion Complexes. Spec. publ. No. 17, Chemical Society, London, 1964.
14 J. W. Arden and N. H. Gale, Anal. Chem., 46 (1974) 687.
15 R. R. Keays, R. Ganapathy, J. C. Laul, U. Krähenbühl and J. W. Morgan, Anal. Chim. Acta, 72 (1974) 1.
16 G. Calderoni and T. Ferri, Talanta, 29 (1982) 371.
17 J. M. Huey and T. P. Kohman, Earth Planet. Sci. Lett., 16 (1972) 401.

Analytica Chimica Acta, 148 (1983) 225—235
Elsevier Science Publishers B.V., Amsterdam — Printed in The Netherlands

DETERMINATION OF GOLD IN NATURAL WATERS BY NEUTRON ACTIVATION—γ-SPECTROMETRY AFTER PRECONCENTRATION ON ACTIVATED CHARCOAL

T. W. HAMILTON and J. ELLIS*

Chemistry Department, University of Wollongong, P.O. Box 1144, Wollongong, N.S.W. 2500 (Australia)

T. M. FLORENCE

C.S.I.R.O. Division of Energy Chemistry, Lucas Heights Research Laboratories, Lucas Heights, N.S.W. 2234 (Australia)

(Received 13th July, 1982)

SUMMARY

A method for the determination of gold at very low levels in waters is presented. The method involves batchwise pre-concentration of gold from 1 l of water at pH 3—4 onto 0.1 g of activated charcoal by shaking for 5 min and subsequent treatment of the activated charcoal by instrumental neutron activation—γ-spectrometry. Activated charcoal quantitatively adsorbs ionic and colloidal gold from solutions prepared with distilled water and also from natural surface waters spiked and equilibrated with these two forms of gold. Three ion-exchange resins were evaluated for pre-concentration purposes; ionic gold removal was quantitative but colloidal gold removal was incomplete. Electrodeposition at a carbon fibre electrode gave similar results. The charcoal pre-concentration technique was tested on solutions containing ^{198}Au tracer and a total gold concentration of 1 μg l^{-1}. The limit of detection of total gold (ionic and colloidal) for the carbon adsorption/neutron activation—γ-spectrometry procedure is 0.3 ng l^{-1}. The method was used to determine gold in surface waters from auriferous regions.

Hydrogeochemical prospecting for gold by determining the gold content of surface waters has received attention from few workers, despite the appearance of several relevant methods in the literature over the past 15 years. Direct hydrogeochemical prospecting with gold as an indicator of its deposits has met with varying degrees of success: Goleva et al. [1], Schiller et al. [2] and Lemne [3] showed that the gold content of surface waters can be used as a specific means of prospecting for gold-bearing deposits but Gosling et al. [4] concluded that such prospecting was unpromising.

The paucity of studies into the viability of direct hydrogeochemical prospecting for gold, and thus the uncertainty of whether such prospecting gives useful results, may reflect the fact that present methods for the determination of gold in fresh waters have inadequate limits of detection, are insensitive to some of the species of gold in fresh waters, or are unsuitable for monitoring large numbers of samples.

0003-2670/83/$03.00

In streams and rivers, gold concentrations generally range upwards from one part in 10^{12} (1 ng l^{-1}) [5]. This concentration is too low for direct application of current instrumental methods, and so almost all methods reported have included a preconcentration step prior to the final measurements.

Methods for the determination of gold in rock and other solid samples are not directly applicable in the analysis of waters because, after dissolution of a rock sample, all the gold present is converted to ionic species and can then be concentrated in this form and measured. In waters, gold may be present in other than ionic forms, and so may not be concentrated by the methods used for ionic gold. Published methods for determining gold in sea water are likewise not necessarily applicable, because speciation of gold is different in the presence of the high chloride concentration of sea water [6].

The extremely small concentration of gold in fresh waters makes the problem of determination of the speciation of the element most difficult. Thermodynamic data have been used by Baes and Mesmer [7] to produce a Pourbaix phase diagram for the speciation of gold as a function of pH and chloride concentration. However, gold released into water flowing over an ore body would not necessarily be converted immediately into the most thermodynamically stable species, and as yet none of the available analytical techniques have both sufficient sensitivity and a capacity to discriminate between different possible forms of gold in natural waters. Dissolved organic acids probably play an important role in gold speciation in fresh waters. Ong and Swanson [8] found that in slightly acidic to basic waters (i.e., in the general pH range of natural waters), the only form in which gold can be transported is as colloids less than 10 μm in diameter. The organic acids stabilise gold sols formed by abrasion of gold particles with grains of silica, by surrounding the colloid-size particles with protective coatings that inhibit their further growth and precipitation. Because organic acid solutions have the capacity to reduce gold chloro complexes to negatively charged colloids of gold metal, it seems unlikely that any significant proportion of gold can exist as the chloro complex in fresh surface waters.

Fisher et al. [9] found that humic and fulvic acids interact with gold chloro complexes to form stable, soluble auriferous humate and fulvate complexes. Other authors have proposed that gold species such as thiosulphate, cyanide, thiocyanate, sulphide and various other inorganic complexes exist under certain conditions in fresh waters. Finally, gold may also be adsorbed on various humic complexes, suspended particulate matter, and various free swimming and floating microorganisms and plants [6].

This uncertainty concerning gold speciation in fresh water means that great care should be taken in evaluating any new method. Testing a new procedure using only ionic gold, as many authors have done, is inadequate. Furthermore, methods which involve addition of relatively large quantities of reagents to water samples which may contain as little as 1 ng l^{-1} gold inevitably lead to contamination problems and high blanks.

Chao [10] and Gosling et al. [4] determined gold in fresh waters with pre-concentration on AG-1 anion-exchange resin. To evaluate the method, Chao spiked samples with standard ionic gold solution just before preconcentration. The present work confirmed the observations of Schiller and Cook [11], who found anion-exchange resins to be inefficient collectors of colloidal gold. A pre-concentration method for gold in fresh waters by means of a chelating resin was reported by Zlatkis et al. [12]. The method involved the addition of more than 50 ml of concentrated reagents to each litre of sample, and necessitated a lengthy sample preparation step.

Four methods have been reported which use evaporative pre-concentration of gold in natural water samples. Lemne [3] evaporated a 1-l sample down to 50 ml and irradiated 0.2 ml of the concentrated solution as part of a radiochemical neutron activation (r.n.a.) method. He separated the gold on a strong basic ion-exchange resin after dissolution of the irradiated residue in aqua regia. Abdullaev et al. [13] and Battiston and Moauro [14] reported similar methods involving evaporation followed by r.n.a. Kolpakova et al. [15] followed an evaporative pre-concentration step with an anodic stripping voltammetric determination.

Liquid—liquid extraction of gold directly from fresh water samples was reported by Kulmatov et al. [16] and Brooks et al. [17]. These methods, too, were not tested against any other methods or even with synthetic colloidal gold solutions.

Schiller and Cook [11] co-precipitated gold with lead sulphide and polyurethane foam and tested the method with tap water containing added gold tracer (^{198}Au) in ionised, colloidal, and very fine precipitated forms. However, the technique was not applied to natural waters. The method involved adding more than 100 ml of concentrated hydrochloric acid and sufficient lead in solution to give more than 10 g of precipitant in each litre of water sample. Stepanov and Artem'ev [18] published a similar method utilising co-precipitation with lead sulphide after addition of about half of the quantities of the same reagents described for the previous method. Borovitskii et al. [19] used co-precipitation with calomel, and Musha and Takahashi [20] used coagulation with soybean protein for pre-concentrating gold from natural water samples.

Activated charcoal was used for pre-concentrating ionic gold from natural waters by Plyusnin et al. [21]. These authors used activated charcoal (0.25 g) to adsorb gold from 1-l water samples at pH < 1 and used only anionic gold to test the method. A similar method was reported almost simultaneously by Pogrebnyak [22] but appears not to have been tested at all. Finally, Salbu et al. [23] determined gold directly in natural waters by instrumental neutron activation (i.n.a.) by direct irradiation and counting of a 5-ml aliquot of water. They claimed a theoretical limit of determination for gold in water of 2.0 ng l^{-1}.

Very few techniques are suitable for completing a determination of gold in natural waters because of the requirement for very high sensitivity. Of the

published methods, more than half employ neutron activation, because of its very high sensitivity for gold and freedom from interferences. Both instrumental [16, 22, 23] and radiochemical [3, 24] neutron activation procedures have been reported. Instrumental methods are usually preceded by concentration of the gold in the sample before irradiation. Other methods reported include atomic absorption spectrometry [10, 12], stripping voltammetry [15], spectrophotometry with Brilliant Green [25], and spectrography [21], but none are as sensitive as neutron activation methods.

In choosing a pre-concentration method that would concentrate all forms of gold in fresh natural waters, comparison of the published methods proved to be very difficult because most had not been adequately evaluated. An ideal scheme should have a limit of detection for gold in water below 1 ng l^{-1} and require minimum addition of reagents and operator time. A pre-concentration system which could be used in the field would minimise the time between sample collection and pre-concentration and so avoid the problems associated with sample storage [26].

Evaporative methods, although potentially the most accurate, were considered too lengthy and not suited to field work. Of the other possibilities, concentration of gold onto resins, carbon fibre or activated charcoal showed most promise because these materials can be obtained in high purity and carbon is not significantly activated by thermal neutron irradiation.

EXPERIMENTAL

Apparatus and reagents

Filtrations were done with a Millipore 25-mm vacuum filtration unit; this glass unit did not cause significant adsorption. Filter discs were Sartorius 25-mm cellulose acetate discs (0.45-μm and 1.2-μm pore size).

All water samples were stored in 1-l polythene bottles which were previously soaked for 24 h in 5 M nitric acid and then washed thoroughly with distilled water. Immediately before sampling, the bottles were rinsed well with the natural water being sampled.

All gold and gold tracer solutions were prepared by dissolving gold metal (Fluka; 99.9995%) in a minimum of aqua regia and diluting to 40 mg l^{-1} with 0.5 M HNO_3. Anionic gold standards were prepared daily by diluting this stock solution with distilled water. These Au(III) solutions were found to be at pH 6—7. Colloidal gold standards were prepared by adjusting the 40 mg l^{-1} standard solution to pH 7 and then adding just sufficient humic or tannic acid to produce a red sol which was diluted to give the working solutions required. The initial red sol took some time to form, and at least two hours was required for the colour to develop fully.

Tracer solutions contained ^{198}Au and varied in activity from 1 to 40 Bq ml^{-1} per μg l^{-1} total gold. Counting was done on a 1-ml aliquot of solution which was evaporated onto a stainless steel planchet and counted for 10—30 min in a well-type sodium iodide detector which had been pre-calibrated for efficiency.

Activated charcoal was of analytical grade (Merck) and all acids were Merck Suprapur grade. Water was distilled and redistilled twice from quartz.

Preparation of equilibrated gold solution. An aliquot of anionic gold solution at pH 7 containing ^{198}Au tracer was added to 1-l sample of a typical "clean" river water (pre-filtered through a 0.45-μm filter) to give a final concentration of 1 $\mu g\ l^{-1}$ gold. The gold was allowed to equilibrate with the water for 5—15 days before use. The resulting gold speciation was assumed to be that present in natural waters.

Recommended procedures

Preconcentration. As soon as possible after sampling, the 1-l water sample was filtered through a 1.2-μm filter to remove particulate matter. The residue was dried and irradiated without further treatment. The pH of the filtrate was adjusted to between 3 and 4, then 0.1 g of activated charcoal was added and the mixture was shaken for 5 min. The suspension was filtered on a 1.2-μm filter at not more than 20 ml min^{-1}, and the filtrate was discarded. The filtrate has a pH of 6.2—6.5. The filter disc with the activated charcoal residue was folded into a plastic pill pack and dried in a desiccator before irradiation.

Instrumental neutron activation. Each of the Millipore filters containing the activated carbon was packaged into pre-washed (nitric acid, demineralised water, air-dried) polyethylene vials (8 mm internal diameter, 27 mm depth) and heat-sealed. These vials were irradiated for 24 h in the X-6 tube of HIFAR, a 15-MW Dido-type system located at Lucas Heights Research Laboratories at a thermal-neutron flux of 5×10^{12} n $cm^{-2}\ s^{-1}$.

Activity measurements and data reduction. The samples were subjected to high-resolution γ-spectrometry, four days after the irradiation, with a coaxial lithium-drifted germanium detector having a resolution of 1.8 keV for the 1332-keV peak of ^{60}Co and a relative efficiency of 20%, and coupled to a 4096-channel pulse-height analyser. Subsequent elucidation of the γ-spectra for gold via the 412-MeV peak of ^{198}Au was done via a series of FORTRAN programs on an IBM 370 computer. Blank measurements on the filters, activated carbon and pre-washed polyethylene vials were similarly determined and appropriate corrections were applied where necessary.

RESULTS AND DISCUSSION

Preliminary experiments

Several separation schemes were investigated for pre-concentrating "dissolved" gold (i.e., particles small enough to pass through a 0.45-μm filter) in fresh waters. These included the use of ion-exchange and chelating resins, a carbon-fibre reactor and activated charcoal. The early work was done at gold concentrations of 1 mg l^{-1} (with final measurements by flame atomic absorption spectrometry), and the later work at concentrations of 0.5—5 $\mu g\ l^{-1}$ (^{198}Au tracer and γ-counting). Three forms of gold were used in the concen-

tration work: anionic, colloidal (stabilised with humic acid) and colloidal (stabilised with tannic acid). In all cases, the results for the two colloidal gold species were within 5% of one another and so only results for humic acid-stabilised sol will be reported. An "equilibrated" gold solution was used in some of the later work.

Srafion-NMRR chelating resin has been used for the separation of anionic gold from aqueous solution in the pH range 0.5—2.5 [27, 28, 29], and the effectiveness of this resin was verified in the present experiments. It was also found that 78—90% of colloidal gold (1 mg l^{-1}) was held on a column of this resin at pH 1, and 60—70% at pH 2. Chelex-100 was also found to hold anionic gold (1 μg l^{-1}) quantitatively at pH 6. However, only 10—20% of colloidal gold (1 μg l^{-1}) was adsorbed by this resin. Later experiments with equilibrated gold solutions indicated a mean adsorption efficiency of 13% at pH 4 for colloidal gold. The anion-exchange IRA-400 resin was found to remove anionic gold (1 μg l^{-1}) completely from solution at pH 2 and 6, but separation of colloidal gold (1 μg l^{-1}) was only 50—70% efficient at these pH values. Adsorptions of gold from "equilibrated" solutions at various pH values are shown in Table 1. This and other work with ion-exchange and chelating resins appeared to suggest that while ionic gold was chemically bound to the resins, colloidal gold was simply mechanically trapped in the resin voids as evidenced by increased adsorption efficiency with increase in resin pore size. Further (approximately equal) proportions of colloidal gold were retained when the column eluate was repeatedly re-run through the resin column.

The next approach to the pre-concentration problem was electrochemical and involved the use of a carbon fibre reactor. This reactor consisted of 1 g of unsized carbon fibre (0.5-μm diameter) packed into a cylindrical plastic tube (slightly tapered; 7 × 20 mm). The main attraction of such a reactor was the very large surface area of the packed carbon fibres [30]. A flow rate of 1—2 ml min^{-1} through the reactor was maintained throughout the testing. A potentiostat was connected to the reactor by a platinum wire wound tightly around the carbon fibres inside the plastic sleeve. Solutions of pH 2 were made 0.01 M in potassium nitrate to increase ionic strength. The gold concentrations of all test solutions were 1 mg l^{-1}.

At pH 1, anionic gold was quantitatively collected on the reactor at applied potentials of +0.5 to −0.5 V (vs. SCE), and also with open circuit. Colloidal gold was collected at the reactor to the extent of 90—92% at

TABLE 1

Adsorption of "equilibrated" gold (1 μg l^{-1}) onto IRA-400 versus pH (adjusted with hydrochloric acid)

pH	6.5	5.0	4.0	3.1	2.1
Adsorption (%)	84	66	46	48	88

potentials of +0.5, 0 and −0.5 V and with open circuit. At pH 5, collection of anionic gold was about 95–97% at all potentials (+0.5 to −1.0 V). Colloidal gold collection reached a maximum of 55% with open circuit, but dropped as increasingly negative potentials were applied to the electrode being only 15% at −1.0 V. At higher pH values, adsorption efficiency for ionic and colloidal gold decreased further. Next, mercury (0.4 mg) was electroplated onto the carbon fibre reactor at −0.2 V and then gold was electrodeposited as before. Collection of gold on the mercury-coated reactor was at a maximum with open circuit and pH 1.5, but only 88–94% of the colloidal gold was removed from solution on one pass through the reactor. On passing the eluent through the electrode a second time, removal of gold was increased to above 98%. Anionic gold was quantitatively removed from solution under the conditions described. Absorption of colloidal gold was greatest at low pH values because at these values, the organic coating on the colloidal particles is at least partially desorbed, allowing the gold to react with the mercury droplets.

Pre-concentration with activated charcoal

The adsorptive properties of activated charcoal are related to the porous nature and high specific surface area of the charcoal, though the detailed mechanism of adsorption remains rather speculative [31]. It has been proposed [32] that activated charcoal behaves like a gas (oxygen) electrode in which irreversibly fixed molecular oxygen reacts with the surface of the charcoal to form a surface complex or functional group that is sufficiently active to cause the oxidation of water as follows: $C_xO + H_2O \rightarrow C_x^{2+} + 2OH^-$. The presence of such charged sites on the charcoal surface, together with the nature of the surrounding electrical double layer does explain, at least qualitatively, many of the observed influences affecting the adsorption of certain charged ions. The relative affinity of different organic molecules for the carbon surface is also considered to be a function of their hydrophobic/hydrophilic character and of their functional groups [33]. This provides a basis for interpreting the behaviour of synthetic gold colloids stabilised with adsorbed tannic or humic acids and may also be relevant to colloidal gold in natural waters.

Preliminary experiments showed that activated charcoal was the only medium which quantitatively removed colloidal gold from water samples on a single pass, and did so at pH values close to natural, thus avoiding the need to add large amounts of acid to the sample.

A column of activated charcoal (1.5 × 1.5 cm) quantitatively removed anionic and colloidal gold (1 $\mu g\ l^{-1}$) at pH 2.5, 6 and 10 but the flow rate through such a column was very slow. To hasten matters, the activated charcoal was thoroughly dispersed in the water sample and separated by sedimentation, centrifugation or filtration. Sedimentation suffered from very fine particles of charcoal remaining in suspension after 24 h. These particles were found to have adsorbed a disproportionately high fraction of anionic

and colloidal gold. Centrifugation was much quicker than gravity sedimentation but also left some of the finer material in suspension. Flocculation of the charcoal was attempted with a variety of flocculants, but was unsuccessful, possibly because of the relatively large particle size of the charcoal or the very low cation concentration.

Filtration through a 1.2-μm filter offered two advantages over the previous approaches. It separated all of the activated charcoal from suspension into a form which was easily available for further manipulation. Secondly, filtration boosted adsorption efficiency by increasing the opportunity for contact between the charcoal and gold as the gold-containing water filtered through the charcoal bed which formed on top of the filter disk. The concentration of activated charcoal required for quantitative adsorption of colloidal gold (1 μg l^{-1}) was 0.1% (w/v) for centrifugal separation (with mixing for 10 min and equilibration for 2 h before centrifugation), and only 0.01% (w/v) for filtration (mixing for 5 min and no standing).

Table 2 shows how the adsorption of anionic and colloidal gold varies with charcoal concentration for suspensions filtered at 20 ml min^{-1} through a 1.2-μm filter. The results given for 0% charcoal represent the proportion of gold which did not pass through a 1.2-μm filter. These data were obtained at pH 7, although variations of 2 pH units either side of this value were found to have little effect on the adsorption efficiency.

As a suitable compromise between maximum adsorption of gold on the one hand and a minimum blank level on the other, an activated charcoal concentration of 0.01% is recommended. Also, as shown in Table 2, anionic gold was found to be adsorbed more readily than the organic acid-stabilised colloids.

As a further check on the efficiency of the activated charcoal pre-concentration method, it was tested at various pH values using an "equilibrated" gold solution (15 days equilibration). The results (Table 3) show that the adsorption efficiency is less than 100% at natural pH levels, but 100% at pH 3—4. Suggested reasons for these results, which differ from those shown for 0.01% activated charcoal in Table 2, are: (a) a difference in colloidal particle size between the synthetic and naturally occurring colloids, or (b) at

TABLE 2

Efficiency of gold adsorption at different charcoal concentrations

Activated charcoal (% w/v)	% Adsorption of gold (pH 7)	
	Anionic gold	Colloidal gold
0.03	100	100
0.01	100	99
0.003	98	91
0.001	88	71
0.000	2	3.7

TABLE 3

Adsorption efficiency of 1 $\mu g\ l^{-1}$ gold ("equilibrated" solution) onto 0.01% activated charcoal vs. pH (pH adjusted with hydrochloric acid)

pH	6.5	5.0	4.0	3.1	2.1
Adsorption (%)	85	95	100	100	97

least a portion of the gold being in a physicochemical form other than anionic or colloidal. These discrepancies highlight the need to allow for the uncertainty in gold speciation when a method is tested for pre-concentrating gold from natural water.

In sampling, the question of losses of gold from the sample by adsorption on the container walls must be considered. Chao et al. [26] found that at pH 6, gold was adsorbed from a 5 $\mu g\ l^{-1}$ solution onto the walls of a 1-l polythene container at an approximately constant rate of 2.5% per 24 hours over 21 days. Our experiments with 1 $\mu g\ l^{-1}$ gold in an "equilibrated" solution (solution was equilibrated for 5 days and then transferred to a cleaned container and monitored for 8 days), agreed with Chao's results within a 20% error.

Neutron activation—γ-spectrometry

This determination of gold relies on the nuclear reaction: $^{197}Au\ (n, \gamma)^{198}Au$ which for thermal neutrons has a cross-section of 96 barns, giving the ^{198}Au isotope with a half-life of 65 h and a γ-ray energy of 0.412 MeV. (Native gold is monoisotopic, consisting wholly of ^{197}Au.) The sensitivity of the method is limited by the blank gold levels of materials used in the analysis. Table 4 shows the gold content of all materials present during irradiation. The limit of detection of the method, calculated as $(2 \times 2^{1/2})$ times the standard deviation of the blank, is 0.3 ng l^{-1} total gold.

The analytical method has been applied to the determination of gold concentrations in surface waters flowing across auriferous regions where the locations of gold lodes are well defined. Some typical results are given in

TABLE 4

Gold content of materials used in the method

Material	Gold content (ng)[a]
Polyethylene vial (1 g)	0.9 ± 0.1
Millipore filter disk (25 mg)	0.3 ± 0.05
Activated charcoal (100 mg)	1.0 ± 0.1
Combined blank (1 vial, One filter disk and 100 mg activated charcoal)	2.2 ± 0.1

[a]Equivalent to ng l^{-1} in water samples.

TABLE 5

Gold concentrations found in rivers traversing auriferous regions

Sample[a]	Gold found (ng l^{-1})	
	Dissolved	Particulate
A	2.2	—
B	11.5	—
C	2.0	—
D	75	14
E	130	6

[a]Samples are from Glen Wills Creek taken upstream (A), within (B) and 2 km downstream (C) from the Glen Wills goldfield. Samples D and E were collected from Copeland Creek, within the Barrington goldfield.

Table 5, and are means of duplicate (A, B, C) or triplicate (D, E) samples. A more detailed investigation of the use of this method as a hydrogeochemical prospecting procedure will be reported elsewhere [34].

This research was conducted with financial support from the Australian Institute of Nuclear Science and Engineering in the form of a Research Fellowship to one of the authors (T.H.).

REFERENCES

1 G. A. Goleva, V. A. Krivenkov and Z. G. Gutz, Geochem. Int., 7 (1970) 518.
2 P. Schiller, G. B. Cook and C. K. Beswick, Mikrochim. Acta, (1971) 420.
3 M. Lemne, Int. Atomic Energy Agency Report No. 1020-F, 1973.
4 A. W. Gosling, E. A. Jenne and T. T. Chao, Econ. Geol., 66 (1971) 309.
5 K. H. Wedepohl (Ed.), Handbook of Geochemistry, Springer-Verlag, Berlin, 1978, Vol. II/5, p. 79-I-3.
6 R. W. Boyle, Geological Survey of Canada, Bulletin 280: The Geochemistry of Gold and Its Deposits, 1979, pp. 57—79.
7 C. F. Baes, Jr. and R. E. Mesmer, The Hydrolysis of Cations, Wiley-Interscience, New York, 1976, p. 282.
8 H. L. Ong and V. E. Swanson, Q. Colo. Sch. Mines, 64 (1969) 395.
9 E. I. Fisher, V. L. Fisher and A. D. Miller, Sov. Geol., (1974) 142.
10 T. T. Chao, Econ. Geol., 64 (1969) 287.
11 P. Schiller and G. B. Cook, Anal. Chim. Acta, 54 (1971) 364.
12 A. Zlatkis, W. Bruening and E. Bayer, Anal. Chem., 41 (1969) 1692.
13 A. A. Abdullaev, A. Sch. Zakhidov, P. Kh. Nishanov and Yu. F. Korshunov, Neitronoaktivatsionnyi Analiz, (1971) 116.
14 U. Battiston and A. Moauro, Com. Naz. Energ. Nucl., (1974) 74.
15 N. A. Kolpakova, A. G. Stromberg and N. I. Belousova, Izv. Tomsk. Politekh. Inst., 238 (1977) 128.
16 R. A. Kulmatov, A. A. Kist and I. I. Karimov, J. Anal. Chem. USSR., 35 (1979) 161.
17 R. B. Brooks, A. K. Chatterjee and D. E. Ryan, Chem. Geol., 33 (1981) 163.
18 V. M. Stepanov and O. I. Artem'ev, Izv. Akad. Nauk. Kaz. SSR. Ser. Fiz-Mat, 15 (1977) 64.

19 V. P. Borovitskii, A. D. Miller and V. N. Shemyakin, Geochem. Int., 3 (1966) 371.
20 S. Musha and Y. Takahashi, Jpn. Anal., 24 (1975) 365.
21 A. M. Plyusnin, Yu. F. Pogrebnyak and E. M. Tatyankina, J. Anal. Chem. USSR., 34 (1979) 311.
22 Yu. F. Pogrebnyak, J. Anal. Chem. USSR., 34 (1979) 70.
23 B. Salbu, E. Steinnes and A. C. Pappas, Anal. Chem., 47 (1975) 1011.
24 K. Jorstad and B. Salbu, Anal. Chem., 52 (1980) 672.
25 V. G. Skripchuk, L. N. Dzyubo and O. K. Zakharova, Ind. Lab., 42 (1976) 1029.
26 T. T. Chao, E. A. Jenne and L. M. Heppting, US Geol. Surv. Prof. Paper 600-D, (1968) 16.
27 T. E. Green, S. L. Law and W. J. Campbell, Anal. Chem., 42 (1970) 1749.
28 R. A. Nadkarni and G. H. Morrison, Anal. Chem., 46 (1974) 232.
29 L. L. Sundberg, Anal. Chem., 47 (1975) 2037.
30 B. Fleet and S. D. Gupta, Nature, 263 (1976) 122.
31 R. J. Davidson, J. S. Afr. Inst. Min. Metall., 75 (1974) 67.
32 J. S. Mattson and H. B. Mark, Activated Charcoal, Dekker, New York, 1971.
33 G. Belfort, Environ. Sci. Technol., 14 (1980) 1037.
34 T. W. Hamilton, J. Ellis, T. M. Florence and J. J. Fardy, Econ. Geol., in press.

Analytica Chimica Acta, 148 (1983) 237—244
Elsevier Science Publishers B.V., Amsterdam — Printed in The Netherlands

WEIGHTING SCHEME FOR REGRESSION ANALYSIS USING pH DATA FROM ACID—BASE TITRATIONS

ALEX AVDEEF

Department of Chemistry, Syracuse University, Syracuse, NY 13210 (U.S.A.)

(Received 20th September 1982)

SUMMARY

A general weighting scheme is proposed for use in least-squares fits of pH data. The scheme assigns lower weights to pH measurements in end-point regions and in regions of pH <3 and pH >11 than for buffer and intermediate regions. The weighting scheme is evaluated with nearly 1200 pH measurements (pH 1.6—12.4), in 16 separate acid—base titrations of ethylenediamine done with a computerized titrator. The weighting scheme yields near-random distributions of residuals, and the slope (0.96) and intercept (—0.05) of an Abrahams—Keve normal probability plot approach the expected values of 1.0 and 0.00.

It is generally recognized that measurements of pH in unbuffered solutions are less precise than measurements in buffered solutions. Furthermore, special problems arise when the pH of a very basic or very acidic solution is measured with a glass electrode. It follows that regression analysis based on pH measurements as dependent variables should not ascribe equal importance to all measurements in a broad pH range. Earlier reports have described studies of the reactions of transition metal ions with ligands having pK_a values higher than 12 (e.g., catechols [1]), and as low as 1.2 (e.g., penicillamine disulphide [2]). It was possible to compensate for the inherent difficulties in obtaining reliable data for pH <2 and pH >11 by averaging data from multiple titrations. The procedure yielded more precisely determined equilibrium constants and also the means to assess errors in pH measurements in these regions.

Even in neutral solutions, the accuracy of pH measurements is seldom better than 0.02 [3]. Time-dependent effects and other systematic errors in pH measurements can frustrate efforts to acquire highly precise pH data. Consideration of such errors can be of paramount importance, both in work with extreme-region pH data, and in studies of polynuclear complexes formed between cadmium and sulfhydryl ligands [4].

During these studies, a comprehensive computer program, STBLTY [5], was developed; this program refines the equilibrium constants by non-linear regression methods. In STBLTY, the function minimized by regression is

$$S = \sum^{N} (pH^{obs} - pH^{calc})^2/\sigma^2(pH) \quad (1)$$

0003-2670/83/$03.00

where N is the number of pH measurements, pH^{calc} is calculated as a function of equilibrium constants and total reactant concentrations, and $\sigma^2(pH)$ is the variance assigned to each pH measurement. The slope-dependent weighting scheme [1]

$$\sigma^2(pH) = \sigma_c^2 + (\sigma_v \, dpH/dV)^2 = (weight)^{-1} \quad (2)$$

was used in all of these refinements based on pH data. The volume of titrant is denoted by V, and typically, $\sigma_c = 0.02$ and $\sigma_v = 0.001$ ml. It appears to be a common practice to assume unit weights in regression fits based on potentiometric data. Notable exceptions are the studies of Schaefer [6] and Lansbury et al. [7].

This paper presents the experimental basis for the weighting scheme used, supported by the analysis of variance [8] of sixteen acid—base titrations of ethylenediamine (en). The thrust of the present study is to characterize the functional dependence of errors in pH measurements for the purpose of devising a general weighting scheme for use in regression fits of pH data.

EXPERIMENTAL

The experimental procedures used in the pH titrations of ethylenediamine were as described elsewhere [1, 9]. Nearly 1200 pH measurements (pH 1.6—12.4), in 16 separate titrations, were acquired at 25°C by using a computerized titrator. Total concentrations of ethylenediamine dihydrochloride were 5—19 mM; the solutions were initially acidified with nitric acid (18—59 mM). Potassium nitrate (0.148—0.168 M) was used as an auxiliary electrolyte to maintain the total ionic strength at 0.2 M. Imprecision is reported as one standard deviation unit (s).

A Beckman 39501 combination glass electrode was used. Before each titration, the pH meter was adjusted in the usual manner, by using commercial pH 7 and pH 4 buffers. Meter readings were converted to the conventional pH scale based on concentration of hydrogen ions, according to the equations

$$pH_{meter} = \Delta + S\,pH + j_H[H^+] + j_{OH}[OH^-] \quad (3)$$

$$pH_{meter} = -\log \gamma_{\pm} + pH \quad (4)$$

where $pH = -\log [H^+]$. Equation (3) is associated with an empirical procedure based on the universal buffer method and is described elsewhere [9]. In the present study, $\Delta = 0.071$ ($s = 0.007$), $S = 1.0052$ ($s = 0.0015$), $j_H = 1.3$ ($s = 0.3$) and $j_{OH} = -0.8$ ($s = 0.3$). The j_H and j_{OH} parameters account for non-linear electrode responses in the extreme pH regions. The hydroxide ion concentration was calculated as $[OH^-] = 10^{-13.75 + pH}$ [10]. Equation (4) incorporates the experimental activity coefficients of hydrochloric acid and potassium hydroxide (in KCl ionic medium): $\log \gamma_{\pm} = (\log \gamma_{HCl} + \log \gamma_{KOH})/2$. The extensive functions of Pitzer et al. [11, 12] were coded into STBLTY for the evaluation of $\gamma_{\pm}$; at 25°C, pH 7, and ionic strength 0.2 M, $-\log \gamma_{\pm} = 0.133$.

Equation (4) implicitly assumes that the pH meter detects solely the activity of hydrogen ions. Changes in the reference electrode junction potential and changes in the glass electrode asymmetry potential are not taken into account.

RESULTS AND DISCUSSION

Glass electrode calibration

A preliminary assessment of errors came from examination of the differences between pH_{meter} values and pH values calculated from Eqn. (3). The differences, $\Delta pH = pH_{meter} - pH$, are listed in Table 1 for pH values corresponding to critical features in titration curves such as that in Fig. 1 (endpoints at pH 4.8, 8.6, and 11; buffer regions at pH 7.2 (pK_{a1}), 10.0 (pK_{a2}), <3, and >11). At the critical pH values, the mean differences, $\overline{\Delta pH}$, vary from 0.096 (pH 2) to 0.152 (pH 8.6) and have the overall average value 0.123 (s = 0.017), which is 0.01 less than $-\log \gamma_{\pm}$ calculated from the Pitzer formulas.

Of further interest are the standard deviations resulting from averaging

TABLE 1

Selected values[a] of $\Delta pH = pH_{meter} - pH$

Expt. No.	pH							
	1.7	2.0	4.8	7.2	8.6	10.0	12.0	12.4
1	0.096	0.084	0.208	0.093	0.096	0.076	0.094	0.077
2	0.093	0.084	0.277	0.095	0.105	0.082	0.100	0.081
3	0.101	0.095	0.200	0.103	0.109	0.101	0.109	0.093
4	0.115	0.096	0.316	0.127	0.120	0.109	0.136	0.087
5	0.093	0.078	0.356	0.126	0.186	0.162	0.182	0.168
6	0.098	0.079	−0.217	0.113	0.137	0.114	0.127	0.112
7	0.104	0.093	−0.201	0.117	0.158	0.137	0.126	0.097
8	0.099	0.084	0.101	0.115	0.171	0.128	0.131	0.113
9	0.111	0.089	−0.107	0.113	0.133	0.133	0.150	0.132
10	0.112	0.086	−0.179	0.127	0.162	0.155	0.172	0.150
11	0.150	0.122	0.120	0.118	0.161	0.135	0.117	0.098
12	0.152	0.124	0.110	0.122	0.170	0.145	0.119	0.100
13	0.104	0.092	0.077	0.120	0.146	0.129	0.150	0.150
14	0.092	0.083	0.147	0.134	0.162	0.153	0.172	0.171
15	0.145	0.126	0.303	0.138	0.206	0.164	0.149	0.129
16	0.145	0.128	0.382	0.141	0.209	0.170	0.140	0.124
$\overline{dpH/d\ V}$[b]	0.9	1.4	274.4	6.5	20.4	5.9	1.0	0.5
$\overline{\Delta pH}$	0.113	0.096	0.118	0.119	0.152	0.131	0.136	0.118
$s(\Delta pH)$	0.022	0.018	0.199	0.015	0.034	0.028	0.026	0.030

[a]Equation (3) was used to determine pH = −log $[H^+]$. [b]Average titration curve slope, in units of ml^{-1}.

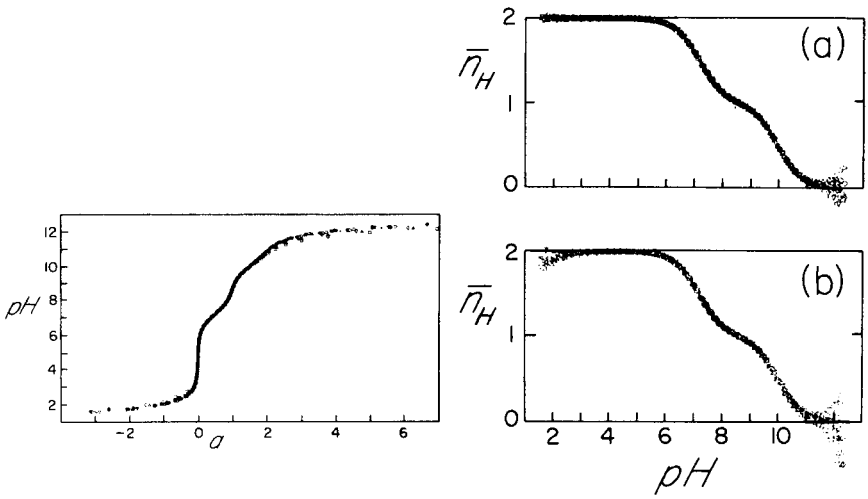

Fig. 1. Titration curves for ethylenediamine. The number of moles of KOH added per mole of en is denoted by a. Negative values of a correspond to conditions of excess of mineral acid.

Fig. 2. Bjerrum formation plots for ethylenediamine: (a) Eqn. (3) used to convert pH_{meter} to pH; (b) Eqn. (4) used to convert pH_{meter} to pH.

ΔpH at each critical pH. These values (Table 1) vary from s = 0.015 to s = 0.199, and tend to be smaller in the buffer regions and larger in the end-point regions. Imprecision in low pH regions (s = 0.022 at pH 1.7) seems to be slightly lower than imprecision in high pH regions (s =0.030 at pH 12.4). The initial value of the slope factor σ_v (Eqn. 2) was estimated from the fit of $(\Delta pH - \overline{\Delta pH})^2$ vs. $\sigma_c^2 + \sigma_v^2(dpH/dV)^2$. When the 128 values of ΔpH (Table 1) were used and σ_c = 0.015 (the minimum s in Table 1) was taken, the value σ_v = 0.00057 (s = 0.00003) ml was found. This value closely approximates the 0.02% imprecision of the Gilmont glass-piston buret used to dispense the titrant.

Errors in the "extreme" pH regions

Figure 2 shows the Bjerrum formation curves for ethylenediamine. These are plots of the number of bound dissociable protons per ethylenediamine ($\bar{n}_H$) as a function of pH, and have been described in detail elsewhere [13]. Figure 2(a) represents pH data based on Eqn. (3); Fig. 2(b) represents data based on Eqn. (4). Of interest are the dispersions in the extreme pH regions. Figure 2(b) indicates that the dispersions are significant for pH <3 and pH >11. This is not surprising, because Eqn. (4) does not take into account non-linear electrode responses. One can see that the dispersions systematically underestimate $\bar{n}_H$ values in Fig. 2(b); pH <3 and pH >11 dispersions are not symmetric about $\bar{n}_H$ = 2 and 0, respectively. Because Eqn. (3) accounts for non-linear electrode effects (j_H and j_{OH}), it is not surprising to see improvements

in the formation curves in Fig. 2(a). Not only are the dispersions smaller, but they are symmetrically disposed in the extreme regions. In Fig. 2(a), $\bar{n}_H$ = 2.006 (s = 0.023) at pH 1.6 and $\bar{n}_H$ = 0.03 (s = 0.12) at pH 12.3.

Refinement of equilibrium constants.

The weighting scheme suggested by the electrode calibration study described above (σ_c = 0.015 and σ_v =0.0006) was used in refining the two pK_a values by non-linear least-squares (eqn. 1), by means of data in the pH 1.6—12.4 range.

Data treated according to Eqn. (4) yielded pK_a values of 7.173 (s = 0.003) and 9.996 (s = 0.003). The refinement converged at a goodness-of-fit of $[S/(N-2)]^{1/2}$ = 1.73. The expected value is unity, provided that systematic errors are absent and the weighting scheme properly describes the random errors. The average value of $(pH^{obs} - pH^{calc})/\sigma(pH) = -0.5$ indicates the presence of systematic errors.

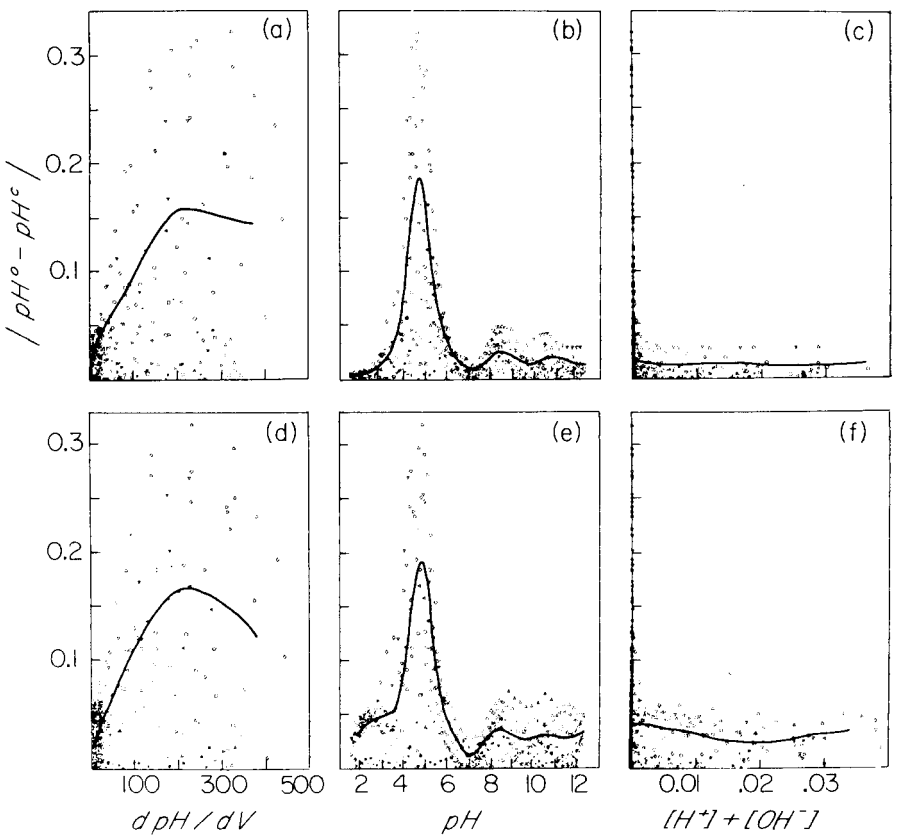

Fig. 3. Deviations between observed pH values and pH values calculated in least-squares refinement of pK_a values. (a)—(c) correspond to pH values computed with Eqn. (3); (d)—(e) correspond to the use of Eqn. (4). The solid lines are sequential averages taken every 25 points.

The refinement using pH data treated with Eqn. (3) converged at a goodness-of-fit of 1.01, and the mean value of $(pH^{obs} - pH^{calc})/\sigma(pH) = -0.05$, which is close to the expected value of zero. The refined pK_a values are 7.188 (s = 0.002) and 9.989 (s =0.002). The difference between the two estimates of pK_{a1} is of the order of the difference between the overall average value of $\overline{\Delta pH}$ (vide supra) and $-\log \gamma_{\pm}$ deduced from the Pitzer equations.

Statistics for analysis of variance

The values of $(pH^{obs} - pH^{calc})/\sigma(pH)$ $(=\delta)$ calculated in the least-squares refinements served as statistics for the analysis of variance. STBLTY is coded to test the dependence of $|\delta|$ on (i) volume of titrant, (ii) ionic strength, (iii) titration curve slopes, (iv) pH, and (v) $([OH^+] + [OH^-])$, which is only sizeable in the extreme pH region.

Figure 3 shows the distribution of $|pH^{obs} - pH^{calc}|$ values as functions of the last three test variables. Figure 3(a—c) depicts the distributions in data processed with Eqn. (3); Fig. 3(d—f) depicts the distributions in the data processed with Eqn. (4). The deviations $|pH^{obs} - pH^{calc}|$ clearly depend on the slopes of the titration curves. This is dramatically evident in Fig. 3(b and e), where the largest deviations occur at pH values corresponding to the three end-points (pH 4.8, 8.6, and 11.0). The deviations appear to be noticeably larger when Eqn. (4) is used than when Eqn. (3) is used, particularly in the "extreme" regions (pH 2 and 12 in Fig. 3b vs. 3e or Fig. 3c vs. 3f).

Figure 4 shows the effect of the weighting scheme. The weighted deviations $|\delta|$ approximate a random distribution as a function of the three variables tested for effect.

Figure 5 shows an Abrahams—Keve [14] normal probability plot. This is a comparison of the ordered distribution of weighted statistics to that expected from a normal, Gaussian distribution of the same sample size. If the weighting scheme is proper, such a plot should have a well-defined slope of unity and an intercept of zero. In Fig. 5, the slope is 0.96 (s = 0.03) and the intercept is —0.05 (s = 0.03).

Use of δ statistics to remove dependence of errors on a tested variable

Figures 3 and 4 illustrate the effects of a weighting scheme on minimizing the systematic dependences of statistics on tested variables. An iterative method can be applied to achieve similar reductions. Consider a weighting scheme, characterized by the individual variances $\sigma^2(pH)_{old}$, which produces a set of statistics, δ, by least-square refinement. For a tested variable P, such as dpH/dV, the linear fit of δ^2 versus $[P/\sigma(pH)_{old}]^2$ produces intercept a and slope b. A new weighting scheme can be constructed in the following manner:

$$\sigma^2(pH)_{new} = \sigma^2(pH)_{old}[a + b\,P^2/\sigma^2(pH)_{old}] = a\sigma^2(pH)_{old} + b\,P^2 \qquad (5)$$

The object of this operation is to approximate $(pH_{obs} - pH_{calc})^2$ with $\sigma^2(pH)_{new}$, so that the weighted statistics randomly distribute about unity.

As an example, for $\sigma^2(pH)_{old}$ constructed with $\sigma_c = 1$ and $\sigma_v = 0$, according

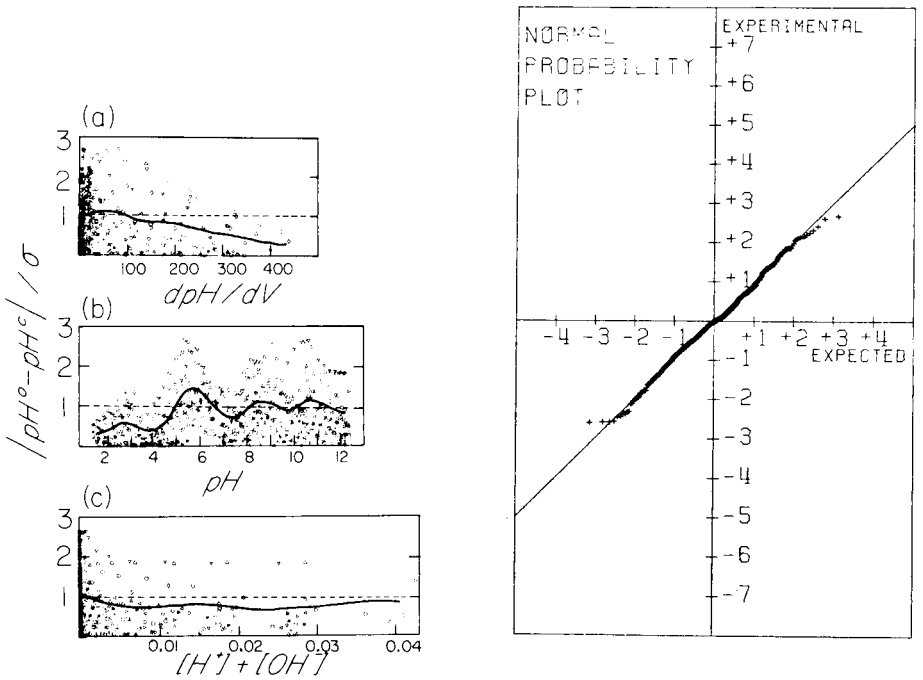

Fig. 4. Weighted deviations calculated in least-squares refinement of pK_a values: the observed pH values were computed with Eqn. (3). The dashed lines correspond to the statistically expected value of unity for the weighted deviations. The solid lines correspond to 25-point sequentially averaged weighted deviations.

Fig. 5. Abrahams—Keve normal probability plot [14].

to Eqn. (2), the plot of $(pH^{obs} - pH^{calc})^2$ vs. $(dpH/dV)^2/\sigma^2(pH)_{old}$ produces $a = 0.00163$ and $b = 2 \times 10^{-7}$ (for data processed with Eqn. 3):

$$\sigma^2(pH)_{new} = [(1)^2 + (0\ dpH/dV)^2](0.00163) + 2 \times 10^{-7}(dpH/dV)^2$$
$$= (0.040)^2 + (0.0005\ dpH/dV)^2 \quad (6)$$

After four cycles of such calculations, the weighting scheme reaches self-consistency with the parameters $\sigma_c = 0.013$ and $\sigma_v = 0.00086$.

When the above iterative procedure was used, it was found that the variances in the data processed by Eqn. (4) can be satisfactorily described by the expression

$$\sigma^2(pH) = \sigma_c^2 + (\sigma_v dpH/dV)^2 + (\sigma_H[H^+] + \sigma_{OH}[OH^-])^2 \quad (7)$$

with $\sigma_c = 0.028$, $\sigma_v = 0.00082$, $\sigma_H = \sigma_{OH} = 0.54$. The last term ascribes less weight to data in the extreme pH regions, as is reasonable from preceding considerations.

Conclusion

This study suggests that a general weighting scheme constructed from variances described by Eqn. (7) properly treats pH errors in regression analysis. Additional terms can be added as further variance effects are discovered. If the conversion pH_{meter} to pH is implemented with Eqn. (3), use of the parameters $\sigma_c = 0.02$, $\sigma_v = 0.001$, and $\sigma_H = \sigma_{OH} = 0$ is recommended. If Eqn. (4) is used, then we suggest the values $\sigma_c = 0.03$, $\sigma_v = 0.001$, and $\sigma_H = \sigma_{OH} = 1$. If the titrant buret is less precise than a Gilmont glass-piston buret, higher values of σ_v would be justified. The methods described above have been in use for about seven years and it has been found that refinements of pK_a values normally converge at goodness-of-fit values of 0.5—1.2. Higher goodness-of-fit values usually indicate systematic errors. In refinements of metal—ligand binding constants, the goodness-of-fit is usually 1—3, depending on the complexity of the equilibrium model and the imprecision of the pH data.

This research was funded by The Petroleum Research Fund (Grant 11609, Type G) administered by the American Chemical Society, and by BRSG Grant S07 RR07068-14 awarded by the Biomedical Research Support Grant Program, Division of Research Resources, NIH. I thank Hans H. Stuting and Diane L. Kearney for technical assistance.

REFERENCES

1 A. Avdeef, S. R. Sofen, T. L. Bregante and K. N. Raymond, J. Am. Chem. Soc., 100 (1978) 5362.
2 S. H. Laurie, E. S. Mohammed and D. M. Prime, Inorg. Chim. Acta, 56 (1981) 135.
3 W. H. Beck, A. E. Bottom and A. K. Covington, Anal. Chem., 40 (1968) 501.
4 A. Avdeef and D. L. Kearney, J. Am. Chem. Soc., 104 (1982) 7212.
5 A. Avdeef, in D. J. Leggett (Ed.), Computational Methods for the Determination of Stability Constants, Plenum, New York, 1983.
6 W. P. Schaefer, Inorg. Chem., 4 (1965) 642.
7 R. C. Lansbury, V. E. Prince and A. A. Smeeth, J. Chem. Soc., (1965) 1896.
8 W. C. Hamilton, Statistics in Physical Sciences, Ronald Press, New York, 1964, Ch. 3.
9 A. Avdeef and J. J. Bucher, Anal. Chem., 50 (1978) 2137.
10 F. H. Sweeton, R. E. Mesmer and C. F. Baes, Jr., J. Solution Chem., 3 (1974) 191.
11 K. S. Pitzer and G. Mayorga, J. Phys. Chem., 77 (1973) 2300.
12 K. S. Pitzer and J. J. Kim, J. Am. Chem. Soc., 96 (1974) 5701.
13 H. M. N. H. Irving and H. S. Rossotti, J. Chem. Soc., (1954) 2904.
14 S. C. Abrahams and E. T. Keve, Acta Crystallogr., Sect. A, 27 (1971) 157.

Analytica Chimica Acta, 148 (1983) 245—254
Elsevier Science Publishers B.V., Amsterdam — Printed in The Netherlands

SOME PYRAZOLINES AND ISOXAZOLINES AS FLUORIMETRIC REAGENTS. KINETIC—FLUORIMETRIC DETERMINATION OF VANADIUM

F. GRASES* and C. GENESTAR

Department of Analytical Chemistry, Faculty of Sciences, University of Palma de Mallorca (Spain)

F. SALINAS

Department of Analytical Chemistry, Faculty of Sciences, University of Extremadura, Badajoz (Spain)

(Received 4th August 1982)

SUMMARY

A study of the analytical use of a series of pyrazolines and isoxazolines as new fluorescent reagents is reported. A kinetic—fluorimetric method for the determination of vanadium(V) (0.03—0.15 $\mu g\ ml^{-1}$) is described, based on its oxidation of 1,3,5-triphenyl-Δ^2-pyrazoline. The product formed is shown to be the corresponding pyrazole.

Fluorimetric determination of many transition metals with organic reagents is difficult because of the slight tendency shown by these paramagnetic metal ions to form fluorescent chelates. However, an investigation has been started for ions which have several oxidation states and so can participate in redox reactions where fluorescent organic products are also involved. This allows fluorimetric methods based on these reactions to be established. However, these reactions are usually slow, so that kinetic—fluorimetric methods become possible for determining metal ions.

The following family of reagents is described in the present paper: 1,3,5-triphenyl-Δ^2-pyrazoline (TPP, I), 1,5-diphenyl-3-(2-styryl)-Δ^2-pyrazoline (DPEP, II), 2,3-diphenyl-hexahydro-Δ[1,7a]-isoindazole (DPHHI, III), 3,5-diphenyl-Δ^2-isoxazoline (DPI, IV), 5-phenyl-3-(2-styryl)-Δ^2-isoxazoline (PEI, V) and 3-phenyl-hexahydro-Δ[1,7a]-anthranil (FHHA, VI). Compound I has been mentioned [1] as a fluorescent product capable of being oxidized during a catalytic dehydrogenation used in organic synthesis. The synthesis of TPP, DPEP, DPI and PEI has been described [2—5]; TPP and DPEP have been the object of numerous physicochemical studies [6—16] and have been used as organic photoconductors [17—19], as additives in plastic scintillators [20] and in the production of electrochemiluminescence [21—23]. To date, none of these compounds has been used analytically. On the basis of the investigation of the metal ion reactions of these reagents, a method has been developed for the kinetic—fluorimetric determination of

0003-2670/83/$03.00

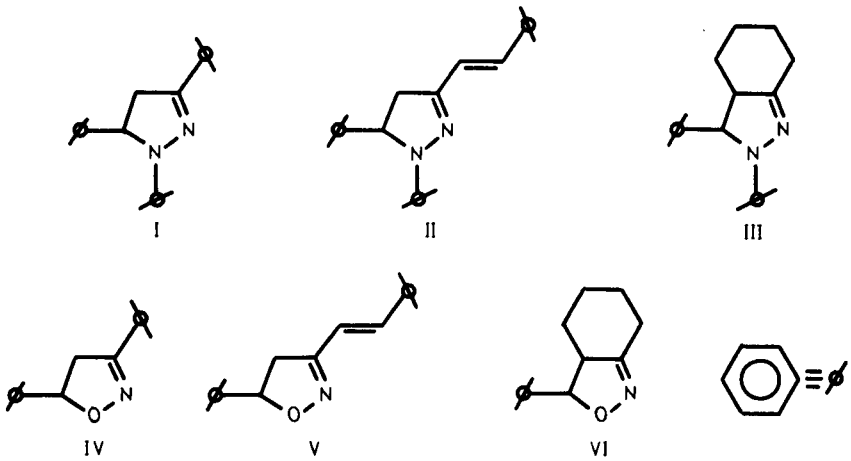

vanadium(V) based on its reaction with TPP. Only three methods have previously been described for the kinetic—fluorimetric determination of vanadium(V), all based on its reaction with anthraquinone derivatives [24—26].

EXPERIMENTAL

Synthesis of reagents

The appropriate enone was mixed in an aqueous alkaline solution either with phenylhydrazinium chloride (pyrazoline series), or with hydroxylammonium chloride (isoxazoline series). In all cases, the solid obtained was recrystallized from ethanol. (Calculated for $C_{21}H_{18}N_2$ (TPP), 84.5% C, 6.1% H, 9.4% N; found, 84.6% C, 6.1% H, 9.4% N. Calculated for $C_{23}H_{20}N_2$ (DPEP), 85.2% C, 6.2% H, 8.6% N; found 85.2% C, 6.1% H, 8.7% N. Calculated for $C_{19}H_{20}N_2$ (DPHHI) 82.6% C, 7.3% H, 10.1% N; found 82.6% C, 7.2% H, 10.2% N. Calculated for $C_{15}H_{13}NO$ (DPI), 80.7% C, 5.8% H, 6.3% N; found 80.8% C, 5.9% H, 6.4% N. Calculated for $C_{17}H_{15}NO$ (PEI), 81.9% C, 6.0% H, 5.6% N; found 82.0% C, 6.1% H, 5.6% N. Calculated for $C_{13}H_{15}NO$ (FHHA) 77.6% C, 7.5% H, 7.0% N; found 77.6% C, 7.4% H, 6.9% N.)

Solutions and equipment

TPP and related reagents were dissolved in ethanol to give 0.1 g l^{-1} solutions. An 8×10^{-3} M solution of vanadium(V) was prepared from ammonium vanadate (Merck) and standardized gravimetrically [27].

All spectrofluorimetric measurements were done with a Fika model 55, MK II fluorescence spectrophotometer. The fluorescence intensity—time curves were obtained by fixing the excitation and emission wavelengths (see below) and using a constant movement of the chart paper (60 s cm^{-1}). A Crison digital pH meter with combined electrode, a Perkin-Elmer 577 i.r. spectrometer and a Varian Mat-711 mass spectrometer were also used.

Procedure for determination of vanadium(V) (0.3—1.5 μg)

In a 10-ml volumetric flask were placed 2 ml of TPP (0.01 g l^{-1}), 2 ml of (1 + 1) hydrochloric acid and the volume of cation solution necessary for the final concentration of vanadium(V) to be between 0.03 and 0.15 μg ml^{-1}. The final volume was adjusted to 10 ml by addition of deionized water before the acid. All solutions had been thermostated at 20°C. After 30 s had elapsed from the addition of vanadium(V), the fluorescence intensity—time curve was recorded for 7 min ($\lambda_{(ex)}$ = 360 nm, $\lambda_{(em)}$ = 465 nm), and the rate of reaction was calculated therefrom by the initial rate (tangent) method (see below).

Isolation of the reaction product

The TPP reagent (1.5 g) was dissolved in 200 ml of an ethanol—benzene mixture (3:2) and 20 ml of concentrated hydrochloric acid and 1.5 g of ammonium vanadate were added. The mixture was then shaken for 2 h. Afterwards, the solution was neutralized with concentrated ammonia, and the intensely red benzene layer of the precipitate was removed by filtration. It was concentrated by evaporation nearly to dryness, and the oily mass that resulted was recrystallized from ethanol, the final product being an orange solid.

RESULTS AND DISCUSSION

Study of the reagents

The spectrofluorimetric behaviour of the reagents and their stability were studied in different media. As can be seen in Fig. 1, the pyrazoline series shows maximum fluorescence intensity in neutral and alkaline media but decreasing intensity in acidic media, whereas the isoxazoline series shows maximum fluorescence intensity in neutral media, this intensity diminishing in acidic or alkaline media. In all cases, the fluorescence of the pyrazoline series is more intense than that of the isoxazoline series. In the pyrazoline series, TPP and DPEP showed a much more intense fluorescence, at a given pH, than DPHHI. In the isoxazoline series, DPI and PEI showed, at a given pH, a fluorescence more intense than that of FHHA. These observations can be explained by considering the existence of rigid resonating structures in those species with higher fluorescence intensity.

All the reagents are soluble in ethanol and slightly soluble in alcohol—water mixtures. Components of the pyrazoline series are stable in ethanolic solution (a 0.01 g l^{-1} solution of TPP in ethanol is stable for at least one month). Reagents of the isoxazoline series are only moderately stable in ethanol, and in such a medium they decompose under u.v. irradiation. The pyrazoline series is oxidized by air in alcohol—water solutions, a process that is favoured by decreasing pH and increasing water content, and leads to formation of the respective aromatic compound. Oxidation of the isoxazoline reagents by atmospheric oxygen or other oxidizing agents leads to the corresponding

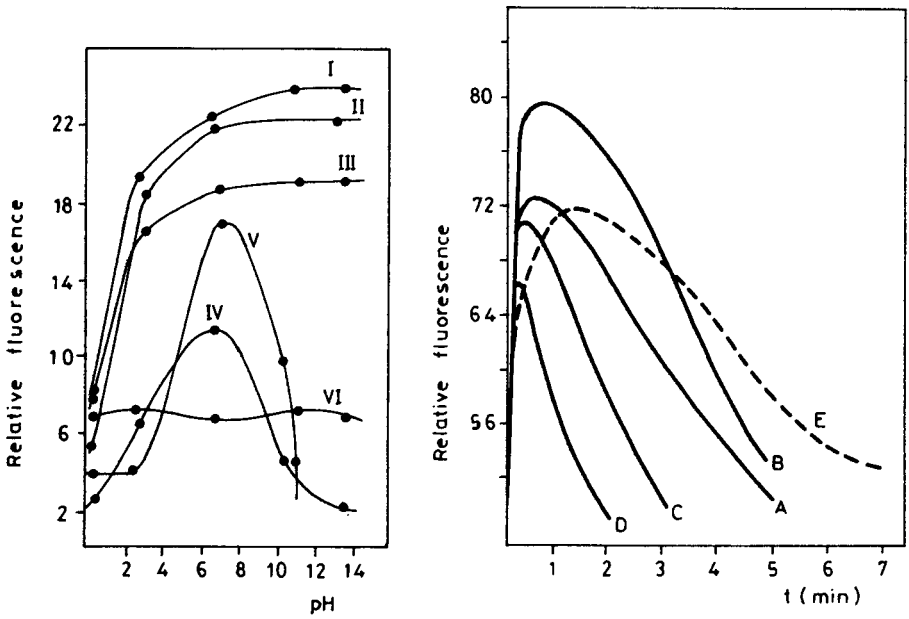

Fig. 1. Influence of pH on the fluorescence of the reagents (10^{-4} M): (I) TPP, sensitivity $\times 1$, $\lambda_{(ex)}$ = 325 nm, $\lambda_{(em)}$ = 465 nm; (II) DPEP, sensitivity $\times 1$, $\lambda_{(ex)}$ = 330 nm, $\lambda_{(em)}$ = 510 nm; (III) DPHHI, sensitivity $\times 10$, $\lambda_{(ex)}$ = 363 nm, $\lambda_{(em)}$ = 535 nm; (IV) DPI, sensitivity $\times 20$, $\lambda_{(ex)}$ = 360 nm, $\lambda_{(em)}$ = 463 nm; (V) PEI, sensitivity $\times 100$, $\lambda_{(ex)}$ = 363 nm, $\lambda_{(em)}$ = 533 nm; (VI) FHHA, sensitivity $\times 100$, $\lambda_{(ex)}$ = 363 nm, $\lambda_{(em)}$ = 520 nm.

Fig. 2. Fluorescence intensity—time curves for various vanadium concentrations (μg ml^{-1}); (A) 0.05; (B) 0.1; (C) 0.15; (D) 0.4; (E) reagent blank. The recommended procedure was used.

aromatic product ($\lambda_{(ex)}$ = 310 nm, $\lambda_{(em)}$ = 360 nm), and entails a decrease in the fluorescence intensity of the system because the maximum emission wavelength of the product obtained is very close to the excitation wavelength of the initial product (inner-filter effect). However, members of this series also undergo photochemical oxidation reactions under u.v. irradiation, yielding intermediate products which show a more intense fluorescence ($\lambda_{(ex)}$ = 360 nm, $\lambda_{(em)}$ = 460 nm).

The characteristics of the excitation spectra depend notably on the concentrations of the reagents, as can be seen in the results summarized in Table 1; this implies that these substances have a marked tendency to form molecular associations.

Reactions with metal ions

The reactions of the six reagents with 30 ionic species were examined by observation of any changes in fluorescence that appeared when the excitation was at 360 nm. The data obtained are shown in Table 2, which shows

TABLE 1

Fluorescence spectral characteristics of pyrazolines and isoxazolines

Reagent	λ(max)[a] (nm)		λ(max)[b] (nm)	
	Excitation	Emission	Excitation	Emission
TPP	325 360	465	360 250	465
DPEP	320	510	360 270	510
DPHHI	300 360	535	360 270	520
DPI	360 315	465	360 295 255	465
PEI	360 260	530	360 310 250	460
FHHA	360	520	360 260	460

[a]Reagent concentration 10^{-4} M. [b]Reagent concentration 5×10^{-6} M.

that all the reagents reacted with V(V), Ce(IV), Fe(III) and Au(III), with the exception of FHHA, which did not yield any appreciable change in fluorescence with any of these ions. Some other metal ions reacted under certain conditions, but they were not general for the group, and the reactions were usually less sensitive. The greatest sensitivities were obtained for reactions with TPP in hydrochloric acid solutions: TPP—V(V), pD = 8; TPP—Ce(IV), pD = 7.7; TPP—Au(III), pD = 7.3; TPP—Fe(III) pD = 7.3, where D is the detection limit. Maximum sensitivity was obtained with V(V) and Ce(IV). The TPP—V(V) system was therefore chosen to establish a kinetic-fluorimetric method for the determination of vanadium.

Kinetic studies

The reaction substrate TPP produced a blue-green fluorescence ($\lambda_{(ex)}$ = 360 nm, $\lambda_{(em)}$ = 465 nm) in neutral and acidic media, while the product obtained in the presence of vanadium(V) had a violet fluorescence ($\lambda_{(ex)}$ = 260 nm, $\lambda_{(em)}$ = 370 nm) in both media, remaining undetected when there was an excess of reagent in the medium (inner-filter effect). For this reason, the excitation and emission wavelengths chosen were 360 and 465 nm, respectively, so that a decrease in fluorescence was observed in the intensity—time curves, as shown in Fig. 2.

To establish the optimum conditions for the determination of vanadium(V), the influence of the acidity, ethanol concentration and reagent concentration on the reaction rate were studied. The reaction proceeded only in acidic

TABLE 2

Reactions of pyrazolines and isoxazolines (10^{-5} M) with metal ions (10 μg ml^{-1}) in different media ($\lambda_{(ex)}$ = 360 nm)

Reagent	1 M HCl	0.5 M CH_3COOH	0.5 M NH_3	0.5 M NaOH
TPP	Au(III) Fe(III) Ce(IV) V(V)	Au(III) Fe(III) Ce(IV) V(V)	Au(III) Fe(III) Ce(IV)	Fe(III) Ce(IV)
DPEP	Au(III) Fe(III) Ce(IV) V(V) Pt(IV) Mo(VI) Tl(III)	Au(III) Fe(III) Ce(IV) V(V)	Au(III) Fe(III) Mn(II)	Au(III) Fe(III) Ce(IV) Mn(II)
DPHHI	Au(III) Fe(III) Ce(IV) V(V)	Au(III) Fe(III) V(V) Hg(II)	Fe(III)	Fe(III) Hg(II)
DPI			V(V) Ce(IV) Fe(III)	V(V) Ce(IV) Fe(III) Au(III)
PEI	Au(III) Fe(III) Ce(IV) Hg(II)	Au(III) Ce(IV) V(V) Pt(IV)	Au(III) Fe(III)	Au(III) Fe(III) Ce(IV) V(V) Hg(II) Pt(II)

media, being extremely slow when hydrochloric acid concentrations were lower than 0.6 M and therefore unsuitable for kinetic measurements. Above 1.8 M hydrochloric acid the reaction occurred rapidly in the absence of vanadium. Thus, the optimum concentration was taken as 1.2 M.

As shown in Fig. 3, changes in fluorescence intensity depended on the ethanol concentration. The reaction rate was practically zero at high ethanol concentrations. As the ethanol concentration was diminished, the rates of the reactions in the presence and absence of vanadium increased and a maximum difference between the two rates was reached in 10% ethanol. At lower ethanol concentrations, both rates decreased. For further work the ethanol concentration chosen was 20% (v/v), because it gave better precision than at the more sensitive 10%.

The effect of TPP concentration is shown in Fig. 4. The plateau in the reaction rate vs. concentration plot is convenient because small variations in reagent concentrations in the plateau region do not influence the results. For

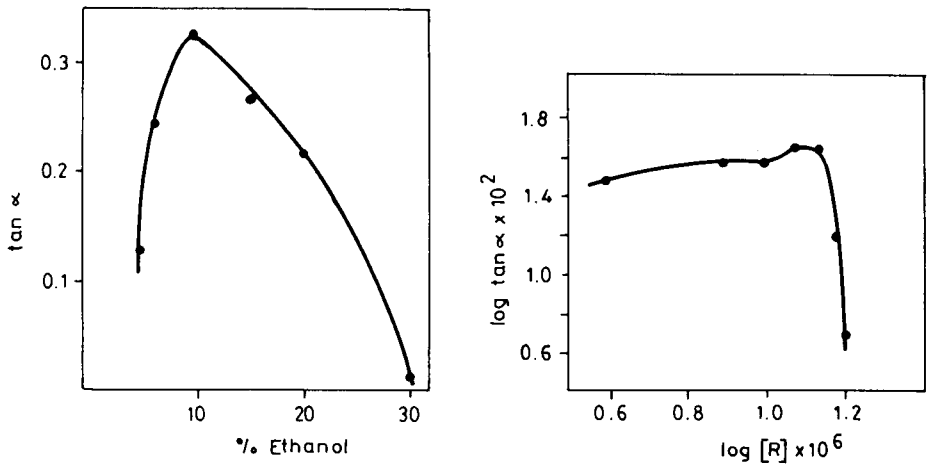

Fig. 3. Effect of ethanol concentration (vol. %) on the initial rate of the net vanadium reaction. 6.7×10^{-6} M TPP, 1.2 M HCl, 0.1 μg ml^{-1} V(V); $\lambda_{(ex)}$ = 360 nm; $\lambda_{(em)}$ = 465 nm.

Fig. 4. Effect of TPP concentration on the initial rate of the net vanadium reaction. 20% (v/v) ethanol, 1.2 M HCl, 0.1 μg ml^{-1} V(V), $\lambda_{(ex)}$ = 360 nm; $\lambda_{(em)}$ = 465 nm.

this reason, a final TPP concentration of 6.7×10^{-6} M was chosen for the determination of vanadium(V).

Under these optimum conditions, there was a linear relationship between the initial reaction rate and the vanadium concentration in the range 0.03—0.15 μg ml^{-1} in the final solution (Fig. 5).

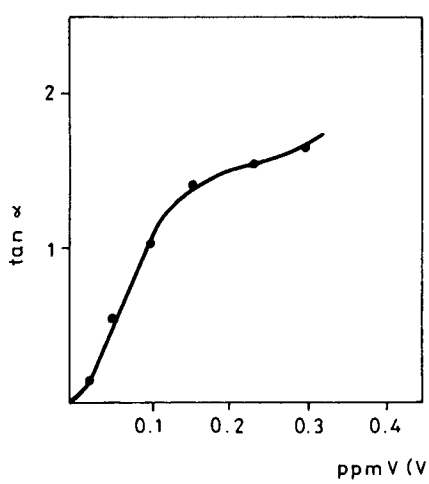

Fig. 5. Dependence of the initial rate of the net vanadium reaction on the vanadium concentration, when the recommended procedure was used.

Characteristics of the analytical method

The fluorescence—time curves were recorded at the maximum excitation and emission wavelengths (360 and 465 nm, respectively) for different amounts of vanadium(V) (Fig. 2), for the optimum pH values and concentrations of ethanol and reagent. Owing to the shape of these curves, the tangent method was the only one applied for preparing the calibration graph. The calibration graph was linear for 0.03—0.15 μg ml^{-1} vanadium(V) and the relative standard deviation was 4.3% (n = 11, α = 0.05).

The selectivity of the method was tested by obtaining the intensity—time curves in the presence of 0.1 ppm of V(V) and several other ions under the recommended conditions. A 100-fold amount of Ca, Sr, Ba, Mg, Zn, Cd, Be, Ni, Mn(II), Co(II), Hg(II), Ga, Al, Zr, Ti(IV), Mo(VI), F^-, SO_4^{2-}, $H_2PO_4^-$ or acetate and twice the amount of Ce(IV) did not interfere. Only 0.02 ppm of Pd, Fe(III), Au(III), Tl(III) and Pt(IV) could be tolerated.

Nature of the reaction and the product obtained

Further study of the reaction of vanadium(V) with TPP was undertaken in order to clarify the nature of the reaction and the product formed. It was found that products formed in the reaction of TPP with V(V), Ce(IV), Fe(III) and Au(III) showed spectral characteristics identical to those of the product resulting from oxidation of TPP in acidic media in the absence of vanadium and in the presence of water. This observation, together with the poor complexing ability derived from the structure of TPP, the marked paramagnetism of these ions which prevents the formation of fluorescent chelates, and their well-known oxidizing ability, led to the conclusion that the process involves oxidation of TPP, where the final product shows fluorescent characteristics different from those of the initial product. It was also shown that when an inert atmosphere was used, so as to eliminate dissolved oxygen, no reaction occurred in the absence of vanadium in an acidic medium, and in the presence of vanadium it proceeded only to a smaller extent, thus proving that the reaction involved oxidation of the reagent. The product of the reaction was isolated and characterized by mass spectrometry and analysis for carbon, hydrogen and nitrogen. It was deduced that the product was 1,3,5-triphenylpyrazole resulting from the reaction

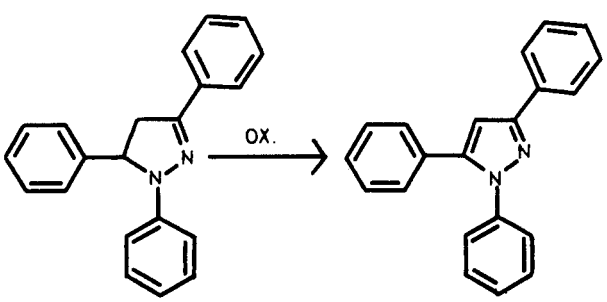

Results for the elements in the product were 84.9% C, 5.3% H, 9.3% N (calculated for $C_{21}N_2H_{16}$, 85.1% C, 9.4% N, 5.4% H). The mass spectrum showed a molecular ion at m/z = 294, compared with the one at m/z = 296 for TPP itself, which indicates loss of two hydrogen atoms to produce the corresponding aromatic compound.

It is of interest that fluorescence of the product can be detected only when it is in higher concentration than that of the initial reagent, because the emission wavelength of the product (370 nm) coincides with the excitation wavelength of the initial reagent (360 nm). Hence, a clear inner-filter effect appears when both substances are present. The special shape of the fluorescence intensity—time curves may be ascribed to the formation of an intermediate product with higher fluorescence than the initial reagent and which yields the aromatic product through subsequent transformation.

REFERENCES

1 J. N. Shah and C. K. Shah, J. Org. Chem., 43(6) (1978) 1266.
2 V. F. Lavrushin, S. V. Tsukerman, E. G. Buryakov-Skaya and Yu. M. Vinetskaya, Prom. Khim. React. Osobo Chist. Veshchestv., 8 (1967) 77.
3 B. M. Krasovitskii and G. F. Slezko, USSR Pat. 239, 344 (Cl. CO7d, CO9d) 18 Mar., 1969.
4 G. F. Slezko and B. M. Krasovitskii, Monokrist. Stsintill. Org. Lyuminofory, 5 (1969) 115.
5 V. Jaeger, V. Buss and W. Schwab, Tetrahedron, 34 (1978) 3133.
6 E. G. Buryakovskaya, S. V. Tsukerman and V. F. Lavrushin, Zh. Fiz. Khim., 43(4) (1969) 863.
7 Yu. V. Naboikin, L. A. Ogurtsova, A. P. Podgornyi and F. S. Pokrovskaya, Opt. Spektrosk., 27(2) (1969) 307.
8 M. M. Agrest, E. A. Andreeschev, S. E. Kilin, M. M. Rikenglaz and I. M. Rozman, Izv. Akad. Nauk. SSSR Ser. Fiz., 34(3) (1970) 625.
9 L. Ya. Kheifets, D. M. Aleksandrova, L. I. Kolotora, N. P. Shomans-Kaya and L. I. Dimitrierskaya, Zh. Anal. Khim., 25(5) (1970) 1004.
10 L. M. Kutsyna, Opt. Issled. Mol. Dvizheniya Mezhnol. Vzaimodsstv. Zhidk. Rastuorakh., (1965) 98.
11 E. Lutskii, A. V. Shepel and E. M. Obukhora, Khim. Geterotsikl. Soedin., (1967) 248.
12 R. N. Nurmukhametov and V. G. Tishchenko, Opt. Spektrosk., 23(1) (1967) 838.
13 L. M. Kutsyma and O. I. Andryushchenko, Zh. Prikl. Spektrosk., 24(3) (1976) 470.
14 I. F. Ogorodneuchvk, A. I. Bykh, V. P. Leonov, Yu. K. Khudenskii, A. V. Kukoga and A. V. Kerimbekov, Vopr. Fiz. Elekrolyumin., (1975) 198.
15 E. G. Buryakovskaya, S. V. Tsukerman and V. F. Lavrushin, Zh. Fiz. Khim., 49(4) (1975) 909.
16 F. Spurny, Proc. Tihany. Symp. Radiat. Chem., 3rd (1971) (Pub. 1972) 1, 59.
17 H. Hogel, US Pat. 3,287,122 (Cl. 96-1, 5) Nov. 22, 1966.
18 F. Bolleta and P. G. Di Marco, Atti. Ist. Veneto Sci. Lett. Arti Cl. Sci. Mat. Nat., 125 (1967) 69.
19 G. A. Reynolds, C. V. Wilson and B. C. Cossar (Eastman Kodak Co.) Germ. Pat. 1,807,359 (Cl GO3g, CO7d) 19 Jun. 1969.
20 S. V. Tsukerman, E. G. Buryakovskaya, O. A. Gunder, V. F. Lavrushin and I. K. Petsova, Zh. Prikl. Spectrosk., 8(1) (1968) 135.
21 N. N. Rozhitskii, Yu. K. Klsudensku and A. I. Bykh, Prikl. Bioneki, 16 (1976) 84.
22 V. A. Zhivnov and I. Yu. Rumyantsev, Spectrosc. Lett., 11(12) (1978) 969.

23 V. P. Leonov, A. I. Bykh and Yu. K. Khudenskii, Zh. Prikl. Spektrosk., 22(5) (1975) 837.
24 F. Salinas, F. Garcia-Sanchez, F. Grases and C. Genestar, Anal. Lett., 13(A6) (1980) 473.
25 F. Garcia-Sanchez, A. Navas, M. Santiago and F. Grases, Talanta, 23 (1981) 833.
26 A. Navas, M. Santiago, F. Grases, J. J. Laserna and F. Garcia-Sanchez, Talanta, 29 (1982) 615.
27 A. I. Vogel, A Text-book of Quantitative Inorganic Analysis, Longman, London, 1961. p. 538.

Analytica Chimica Acta, 148 (1983) 255—262
Elsevier Science Publishers B.V., Amsterdam — Printed in The Netherlands

ORANGE-I LAURATE, A NEW CHROMOGENIC SUBSTRATE FOR THE ASSAY OF LIPASE IN BLOOD

SHINICHI KAMACHI and KIYOSHIGE WAKABAYASHI

New Drug Research Laboratories, Chugai Pharmaceutical Co., Ltd., Takada, Toshima-ku, Tokyo 171 (Japan)

MASATOSHI YAMAGUCHI and YOSUKE OHKURA*

Faculty of Pharmaceutical Sciences, Kyushu University 62, Maidashi, Higashi-ku, Fukuoka 812 (Japan)

(Received 13th October 1982)

SUMMARY

Eight long-chain fatty acid esters (laurates, myristates, palmitates and stearates) of sodium *m*- or *p*-(4-hydroxy-1-naphthylazo)-benzenesulfonate were synthesized and assessed as chromogenic substrates for the assay of lipase. All are hydrolyzed in the presence of lipase, the laurates most rapidly. Orange-I laurate (the *p*-compound) was selected for detailed study. A very selective assay of lipase in the presence of other esterases was achieved by adding sodium dodecylbenzenesulfate and protamine sulfate as inhibitors. Orange-I laurate could be used as a substrate for lipase in serum.

Lipase (glycerol-ester hydrolase, EC 3.1.1.3) catalyzes the hydrolysis of triglycerides. An increase in activity of lipase in serum has been observed in pancreatic diseases. Because this increase is more directly diagnostic of pancreatic diseases than an increase in activity of amylase in serum, the assay of lipase activity in serum is of clinical importance [1—4].

For the assay of lipase, olive oil has been used as a natural substrate [2—8], and the laurates of phenols (β-naphthyl laurate [9], phenyl laurate [10], *p*-nitrophenyl laurate [11] and fluorescein dilaurate [12]) and dimercaptopropan-1-ol tributyrate [13] have served as synthetic substrates. The assay with olive oil requires much time and is insensitive. The assays with the synthetic substrates are simple and in general are fairly sensitive, though those with β-naphthyl laurate, phenyl laurate and dimercaptopropan-1-ol tributyrate require a further chromogenic reaction for detection of the reaction products (β-naphthol, phenol and dimercaptopropan-1-ol).

To develop suitable chromogenic substrates with fairly high molar absorptivities, long-chain fatty acid esters of phenolic naphthylazo compounds with a sulfonic acid group were synthesized. These were the laurates, myristates, palmitates and stearates of *p*-(4-hydroxy-1-naphthylazo)-benzenesulfonic acid (sodium salt; Orange-I) and the *m*-isomer (HNB). Of these, the laurates of Orange-I and HNB were found to be most rapidly hydrolyzed in a lipase-

0003-2670/83/$03.00

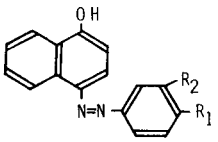

$R_1 = SO_3Na$, $R_2 = H$: Orange-I
$R_1 = H$, $R_2 = SO_3Na$: HNB

catalyzed reaction. Of the two, Orange-I laurate was more easily available and so its selectivity for lipase was studied by using bovine serum albumin (BSA), human serum and purified enzyme preparations.

EXPERIMENTAL

Materials

All chemicals were of reagent grade, unless otherwise noted. Orange-I was obtained from Wako Pure Chemicals (Japan) and HNB was synthesized as described by Muller et al. [14]. Lipase (from hog pancreas, 51100 U mg^{-1} protein, lyophilized powder), carboxyl esterase (from porcine liver, ca. 100 U mg^{-1} protein, suspension in 3.2 M ammonium sulfate), cholesterol esterase (from bovine pancreas, 2000—4000 U mg^{-1} protein, lyophilized powder), cholinesterase (from human serum, 3—9 U mg^{-1} protein, lyophilized powder) and BSA (fraction V) were obtained from Sigma Chemical Co., and lipoprotein lipase (from micro-organisms, 1300 U mg^{-1} protein, lyophilized powder) was from Iatron Co. (Japan). Aryl esterase was separated from human serum and purified by the method of Kurooka et al. [13] (ca. 30 U mg^{-1} protein). Human sera were supplied from Kyushu University Hospital.

Syntheses of esters of Orange-I and HNB

Orange-I or HNB (25 mmol) was dissolved in 100 ml of dimethylformamide; 10 ml of pyridine and 50 mmol of lauric anhydride, myristic anhydride, palmitic anhydride or stearic anhydride dissolved in 50 ml of acetone were added, and the mixture was heated at 70—90°C for 1 h. The precipitate which formed on cooling was filtered off and recrystallized from a dimethylformamide—acetone mixture. All the esters obtained were pale yellow crystalline powders [yield 70—75%; m.p.>250°C (dec.)].

Apparatus

Infra-red spectra were measured in potassium bromide pellets with a Hitachi 260-30 grating infrared spectrophotometer, and ultraviolet and visible absorption spectra and absorbances were obtained with a Hitachi 124 spectrophotometer and 10-mm quartz cells. pH was measured with a Hitachi-Horiba M-7 pH meter at 20°C.

Procedures

Standard procedure for testing esters. A synthesized ester solution (20 mM, 1.0 ml) in dimethylformamide was added to a mixture of 8.0 ml of 0.1 M barbital buffer (pH 8.6) and 4.0 ml of 1% polyvinyl alcohol (degree of polymerization, 2000) solution, and emulsified. The emulsion was diluted

with water to a total volume of 20 ml. The resulting emulsion could be used for 3 days when stored at 4° C. To 5.0 ml of the emulsion, 50 μl of enzyme solution, BSA solution or human serum was added. The mixture was incubated at 37° C for 30 min, 1.0 ml of 1.8 M trichloroacetic acid was added and the mixture was centrifuged at 1000 *g* for 10 min. To 4.0 ml of the supernatant liquid, 3.0 ml of 0.47 M sodium carbonate was added, to bring the pH to 9. The absorbance was measured at 475 nm against a blank. For the blank, the order of addition of enzyme and trichloroacetic acid was reversed and the same procedure as above was carried out.

When enzyme inhibitor (or activator) was used, 50 μl of the enzyme preparation was added to 100 μl of the inhibitor (or activator) solution which was prepared so as to give the indicated concentration in the enzyme reaction mixture (see Figs. 1—3 and Table 5); 5.0 ml of the emulsion of the ester was added after pre-incubation for 10 min, and the mixture was treated as above.

When *p*-nitrophenyl laurate was used in place of an ester of Orange-I or HNB for comparison, 1.0 ml of 20 mM *p*-nitrophenyl laurate in acetone replaced the 1.0 ml of synthesized ester solution. It was treated as described above and the absorbance was measured at 405 nm.

Procedure for gel permeation chromatography. To a column (60 × 1 cm i.d.) of Sephadex G-200, which was equilibrated with 0.05 M Tris-hydrochloric acid buffer containing 0.1 M potassium chloride (pH 8.0) for 12 h, 0.25 ml of human serum, aryl esterase or carboxyl esterase solution was added and eluted with the same buffer. The eluate was collected in fractions

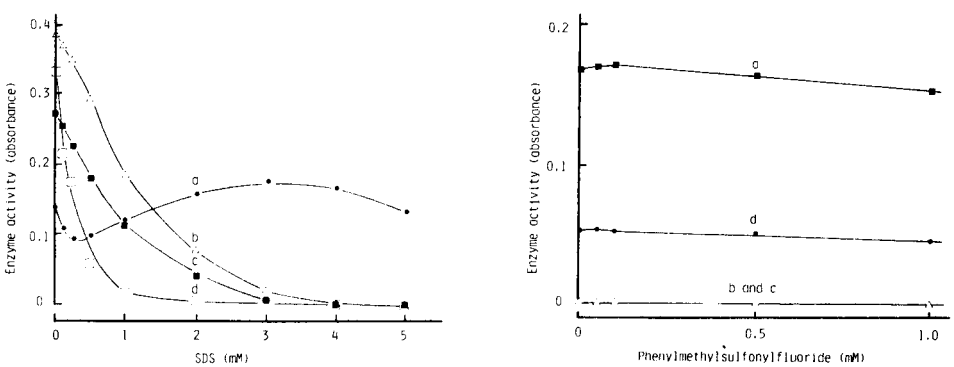

Fig. 1. Effect of the concentration of sodium dodecylbenzenesulfonate (SDS) on the hydrolysis of Orange-I laurate by: (a) lipase (2450 U ml^{-1}); (b) carboxyl esterase (0.24 U ml^{-1}); (c) aryl esterase (3 U ml^{-1}); (d) BSA (50 mg ml^{-1}). (50 μl of enzyme or BSA solution treated as in the standard procedure with Orange-I laurate.)

Fig. 2. Effect of the concentration of phenylmethylsulfonyl fluoride on hydrolysis of Orange-I laurate in the presence of 4 mM SDS by: (a) lipase (2450 U ml^{-1}); (b) carboxyl esterase (0.24 U ml^{-1}); (c) aryl esterase (3 U ml^{-1}); (d) normal human serum. (50 μl of enzyme preparation or normal human serum treated as in the standard procedure with Orange-I laurate.)

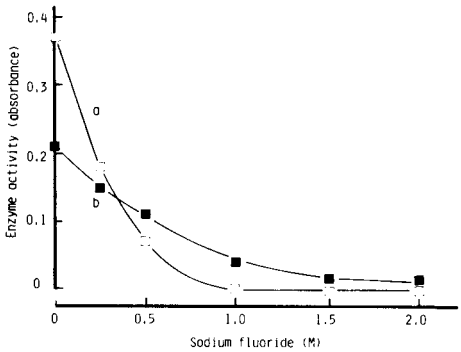

Fig. 3. Effect of sodium fluoride concentration on the activities of: (a) lipase (6150 U ml^{-1}); (b) human serum from a patient with pancreatitis. (Procedure as Fig. 2.)

of 30 drops (ca. 1.4 ml) in a fraction collector. The enzyme activity of each fraction was measured by the standard procedure with Orange-I laurate as substrate in the absence of enzyme inhibitors, and by the method of MacDonald and LeFave with olive oil as substrate [4]. The absorbance of each fraction was also monitored at 280 nm.

RESULTS AND DISCUSSION

All the synthesized substances show infra-red absorption caused by carbonyl stretching around 1750 cm^{-1}, stretching of methylene and methyl groups of the fatty acid moiety around 2950 cm^{-1} and 2850 cm^{-1}, and methylene and methyl deformations around 1460 cm^{-1} and 1380 cm^{-1}. The ultraviolet and visible absorption spectra of all the esters of Orange-I in dimethylformamide have their maxima at 383 nm and those of HNB at 377 nm, though the maxima for Orange-I and HNB are at longer wavelengths (Table 1). These results and the elemental data (Table 2) indicate that the synthesized substances are the esters of the corresponding phenolic naphthylazo compounds.

TABLE 1

Absorption maxima and molar absorptivities (ϵ, 1 mol^{-1} cm^{-1}) of Orange-I and HNB and their esters in dimethylformamide

Compound		Absorption maximum (nm)	log ϵ	Compound		Absorption maximum (nm)	log ϵ
Orange-I		417	4.17	HNB		412	4.25
	laurate	383	4.25		laurate	377	4.19
	myristate	383	4.17		myristate	377	4.20
	palmitate	383	4.20		palmitate	377	4.20
	stearate	383	4.20		stearate	377	4.19

TABLE 2

Elemental data for the esters of Orange-I and HNB

		Formula	C(%)		H(%)		N(%)	
			Calc.	Found	Calc.	Found	Calc.	Found
Orange-I	laurate	$C_{28}H_{33}O_5N_2SNa$	63.1	62.9	6.2	6.5	5.3	5.5
	myristate	$C_{30}H_{37}O_5N_2SNa$	64.3	64.1	6.65	6.6	5.0	4.8
	palmitate	$C_{32}H_{41}O_5N_2SNa$	65.3	65.0	7.0	7.5	4.8	4.8
	stearate	$C_{34}H_{45}O_5N_2SNa$	66.2	66.1	7.35	7.2	4.5	4.5
HNB	laurate	$C_{28}H_{33}O_5N_2SNa$	63.1	63.0	6.2	6.3	5.3	5.5
	myristate	$C_{30}H_{37}O_5N_2SNa$	64.3	64.3	6.65	6.5	5.0	5.0
	palmitate	$C_{32}H_{41}O_5N_2SNa$	65.3	65.3	7.0	7.2	4.8	5.0
	stearate	$C_{34}H_{45}O_5N_2SNa$	66.2	66.3	7.35	7.4	4.5	4.4

All the esters were insoluble in water, as was the laurate used in the previously reported assays for lipase. Thus these esters were used as emulsions prepared by dissolving them in dimethylformamide and then mixing with a mixture of barbital buffer and polyvinyl alcohol solution, as was done for *p*-nitrophenyl laurate, which has been widely used as a chromogenic lipase substrate.

For testing these esters as substrates for lipase, the conditions of the enzyme reaction and the procedure for the deproteinization of the enzyme reaction mixture in the assay method with *p*-nitrophenyl laurate were conveniently employed, with some modifications as described in the standard procedure.

The esters did not hydrolyze in the absence of enzyme under the conditions of the standard procedure. Changes in absorbance caused by lipase-catalyzed hydrolysis of the esters are shown in Table 3. *p*-Nitrophenyl laurate was also examined for comparison. All the esters were hydrolyzed under the conditions of the standard procedure. In particular, the laurates of Orange-I

TABLE 3

Hydrolysis of esters by lipase[a]

Ester		Absorbance (lipase activity)	Ester		Absorbance (lipase activity)
Orange-I	laurate	0.154	HNB	laurate	0.148
	myristate	0.039		myristate	0.050
	palmitate	0.012		palmitate	0.015
	stearate	0.013		stearate	0.013
			p-Nitrophenyl laurate		0.051

[a] 50 μl of 2560 U ml^{-1} lipase solution were treated as in the standard procedure.

TABLE 4

Hydrolysis of Orange-I laurate by esterase preparations and BSA[a]

	Absorbance (enzyme activity)
Lipoprotein lipase (13 U ml^{-1})	0.256
Carboxyl esterase (0.2 U ml^{-1})	0.326
Aryl esterase (3 U ml^{-1})	0.283
Cholinesterase (5 U ml^{-1})	0.000
Cholesterol esterase (300 U ml^{-1})	0.000
BSA (50 mg ml^{-1})	0.327

[a]50 μl of enzyme or BSA solution was treated according to the standard procedure.

and HNB were most rapidly hydrolyzed, more so than *p*-nitrophenyl laurate. The molar absorptivities of Orange-I and HNB, the enzyme reaction products, in the final mixture in the procedure are 27200 and 28100 l mol^{-1} cm^{-1}, respectively, being greater than that of *p*-nitrophenol (18000 l mol^{-1} cm^{-1} at the absorption maximum of 405 nm). This provides a basis for a sensitive spectrophotometric assay of lipase activity by using the laurates of Orange-I and HNB as substrates. Orange-I is commercially available and therefore its laurate was chosen for further study.

As shown in Table 4, Orange-I laurate was hydrolyzed by lipoprotein lipase, carboxyl esterase, aryl esterase and BSA. It is known that albumin has an esterase-like activity [15, 16]. Cholinesterase and cholesterol esterase were without effect.

Sodium dodecylsulfate, an inhibitor of some esterases [13], completely inhibited carboxyl esterase, aryl esterase and the esterase-like activity of BSA at a concentration of 4 mM, but activated lipase most effectively at the same concentration (Fig. 1). The effect of phenylmethylsulfonyl fluoride, an inhibitor of carboxyl esterase and aryl esterase [13], together with 4 mM sodium dodecylsulfate was investigated on lipase and on the enzymes in human serum, as well as carboxyl esterase and aryl esterase. The inhibitor had only a slight effect on lipase and on the enzyme activity of human serum at concentrations less than 1 mM (Fig. 2).

A little lipoprotein lipase is present in normal human serum. The activity increases when heparin is administered intravenously, but remarkably decreases in patients with arteriosclerosis of the brain or coronary sclerosis [17]. Protamine sulfate, an inhibitor of lipoprotein lipase [18], inhibited the activities of lipase (2560 U ml^{-1}) and enzymes in normal human serum only by 5% and 7%, respectively, at a concentration of 0.2 mg ml^{-1} in the reaction mixture.

Calcium ions at low concentrations activate lipase, but inhibit the enzyme at high concentrations [4, 19]. When the effect of calcium was tested on the hydrolysis of Orange-I laurate, the activities of lipase and human serum were most strongly activated at 5×10^{-4}—1×10^{-3} M calcium and inhibited at more than 5×10^{-3} M (Table 5). Sodium fluoride inhibits lipase [18]. Lipase

TABLE 5

Effect of calcium chloride concentration on hydrolysis of Orange-I laurate by lipase and normal human serum[a]

$CaCl_2$ conc. (M)	Absorbance (lipase activity)	Absorbance (activity of human serum)
0	0.092	0.082
1×10^{-4}	0.115	0.103
5×10^{-4}	0.131	0.158
1×10^{-3}	0.138	0.174
5×10^{-3}	0.092	0.098
1×10^{-2}	0.042	0.055
5×10^{-2}	0.007	0.008

[a](50 μl) of 160 U ml^{-1} lipase solution or normal human serum was treated as in the standard procedure with Orange-I laurate.

was completely inhibited at fluoride concentrations of 1 M or greater, and the activity of human serum was decreased by 96% at 1.5 M fluoride or greater (Fig. 3).

The above observations indicate that lipase activity in human serum may be assayed without any influence from carboxyl esterase, aryl esterase, lipoprotein lipase and the esterase-like activity of albumin when Orange-I laurate is used as substrate in the presence of sodium dodecylbenzenesulfate and protamine sulfate.

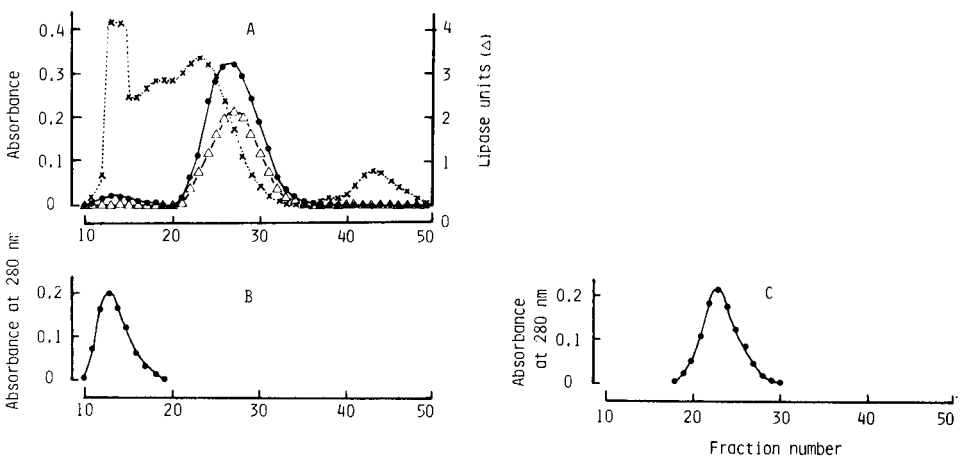

Fig. 4. Gel permeation chromatograms of 0.25-ml samples of human serum and preparations of aryl esterase and carboxyl esterase: (A) serum from a patient with pancreatitis; (B) aryl esterase (20 mg protein ml^{-1}); (C) carboxyl esterase (20 mg protein ml^{-1}). (•) Absorbance obtained by standard procedure, indicating enzyme activity; (×) absorbance at 280 nm; (△) lipase units obtained by the method of MacDonald and LeFave [4]. In parts B and C, only the absorbances at 280 nm are shown.

A human serum sample was fractionated by gel permeation chromatography on Sephadex G-200. The preparations of aryl esterase and carboxyl esterase were also subjected to chromatography for comparison. As shown in Fig. 4A, lipase activity was observed in fractions 21—33 by both the standard procedure and the method of MacDonald and LeFave, and the peaks on the chromatogram were consistent. A small peak was also observed at fractions 11—18 when enzyme activities were monitored by the standard procedure. This peak was ascribed to aryl esterase because the preparation of aryl esterase was separated in the same fractions (Fig. 4B). Carboxyl esterase was at fractions 18—28 (Fig. 4C). This suggested that carboxyl esterase, which acts on Orange-I laurate, is hardly present in the serum, though a peak ascribable to the enzyme is observed around fraction 23 when the fractions are monitored by u.v. absorption at 280 nm (Fig. 4A). These observations indicate that Orange-I laurate is hydrolyzed by lipase in serum fairly selectively even in the absence of sodium dodecylsulfate and protamine sulfate.

We are grateful to the Central Clinical Laboratory of Kyushu University Hospital for the supply of sera.

REFERENCES

1 P. D. Webster and L. Zieve, N. Engl. J. Med., 267 (1962) 604.
2 L. S. Cherry and L. A. Crandall, Am. J. Physiol., 100 (1932) 266.
3 N. W. Tietz and E. A. Frierck, Clin. Chim. Acta, 13 (1966) 356.
4 R. P. MacDonald and R. O. LeFave, Clin. Chem., 8 (1962) 509.
5 B. Borgstron, Scand. J. Clin. Lab. Invest., 9 (1957) 226.
6 C. W. Vogel and L. Zieve, Clin. Chem., 9 (1963) 168.
7 P. H. Dirstine, C. Sobel and R. J. Henry, Clin. Chem., 14 (1968) 1097.
8 Y. Suzuki, T. Irino, H. Fujita and E. Maehata, Rinsho Byori, 23 (1975) 466.
9 A. M. Seigman and M. M. Nachlas, J. Clin. Invest., 29 (1950) 31.
10 H. J. Raderechts and H. Moskau, Clin. Chim., Acta, 4 (1959) 221.
11 K. Furuya and S. Furuya, Seikagaku, 33 (1961) 615.
12 J. G. Meyer-Bertenrath and H. Kaffarnik, Hoppe Seyler's Z. Physiol. Chem., 349 (1968) 1071.
13 S. Kurooka, S. Okamoto and M. Hashimoto, J. Biochem., 81 (1977) 361.
14 J. B. Muller, L. Blangey and H. E. Fiertz-David, Helv. Chim. Acta, 35 (1952) 2579.
15 J. T. Tildon and J. W. Ogilvie, J. Biol. Chem., 247 (1972) 1265.
16 C. E. Wilde and R. G. O. Kekwick, Biochem. J., 91 (1964) 297.
17 T. Matsuo, Y. Ushihama and K. Niimi, Rinsho Byori, 23 (1975) 419.
18 C. Hollet and H. C. Meng, Am. J. Physiol., 184 (1956) 428.
19 G. Benzonena, Biochim. Biophys. Acta, 151 (1968) 137.

Analytica Chimica Acta, 148 (1983) 263—269
Elsevier Science Publishers B.V., Amsterdam — Printed in The Netherlands

FLUORIMETRIC DETERMINATION OF SELENIUM(IV) AND TOTAL SELENIUM IN NATURAL WATERS

KAZUFUMI TAKAYANAGI* and GEORGE T. F. WONG
Department of Oceanography, Old Dominion University, Norfolk, VA 23508 (U.S.A.)
(Received 16th July 1982)

SUMMARY

A fluorimetric method for the determination of selenium(IV) in natural waters is described. Selenium(IV) is preconcentrated by extracting its complex with ammonium 1-pyrrolidinedithiocarbamate into chloroform, and back-extracting the selenium into nitric acid. The preconcentrated selenium is complexed with 2,3-diaminonaphthalene to form 4,5-benzopiazselenol, which is determined fluorimetrically. The optimal conditions for the fluorimetric determination of dissolved total selenium in natural waters were re-examined. The required volume of sample can be reduced from 5 l to 1 l. The detection limit is about 20 pM for a 1-l sample. The imprecision is about 2% between 275 and 600 pM and 8% at 131 pM.

Selenium is one of the elements which exist in more than one oxidation state in sea water. Although selenium(VI) should be the only detectable species in oxygenated sea water [1], the presence of both selenium(IV) and selenium(VI) has been reported [2—6]. The concentration of total selenium ranges from about 0.3 nM in surface sea water to 2.0 nM in the deep oceans, while the concentration of selenium(IV) ranges from undetectable to 0.7 nM [2, 4, 5]. In coastal and estuarine waters, higher values of total selenium and selenium(IV) have been reported [3, 6, 7].

In order to study the marine geochemistry of selenium, it is essential to have a quantitative method which not only has an adequate detection limit, but is also capable of distinguishing between the different oxidation states. Furthermore, it would be convenient if the required sample volume could be reasonably small. Because few existing methods [2, 3, 6, 8—10] meet these criteria, a re-investigation of the fluorimetric determination of dissolved selenium in natural waters was undertaken.

Fluorimetric methods have been used extensively for the determination of selenium in biological materials [11—14], soils and sediments [15, 16], and polluted [17] and unpolluted waters [2, 8, 18]. The chemistry involved in the fluorimetric determination of selenium has been thoroughly investigated [19, 20]. Selenium(IV) reacts with 2,3-diaminonaphthalene to form 4,5-benzopiazselenol, which emits a lime-green fluorescence on excitation. Other forms of selenium can be determined if they are first converted to selenium(IV). Sugimura and Suzuki [8] and Hiraki and co-workers [21, 22]

0003-2670/83/$03.00

have evaluated modifications of this method for determinations of selenium-(IV) and (VI) in sea water; however, the methods required 5 l of sample and detection limits were too high to be useful for sea water.

This paper describes the optimization and application of the fluorimetric method for the determination of selenium(IV) and total selenium in natural waters. Selenium(IV) is preconcentrated by extracting its complex with ammonium 1-pyrrolidinedithiocarbamate (APDC) into chloroform, and then back-extracting the selenium into nitric acid.

EXPERIMENTAL

Reagents and apparatus

Spectrograde cyclohexane and glass-distilled chloroform were used. Hydrochloric acid, ammonia liquor, nitric acid, perchloric acid, and hydrazine sulfate were reagent-grade chemicals.

DAN solution (0.5%). Dissolve 0.1 g of 2,3-diaminonaphthalene (DAN) and 0.5 g of hydroxylamine hydrochloride in sufficient 0.1 M hydrochloric acid to make 200 ml. Heat the solution in a water bath at 50°C for 20 min. Extract the solution with three 15-ml of cyclohexane. Prepare this solution daily.

APDC solution (2%). Dissolve 10 g of ammonium 1-pyrrolidinedithiocarbamate (APDC) in deionized water and dilute to 500 ml. Purify the solution by extracting with three 25-ml portions of chloroform.

Ammonium acetate buffer. Dissolve 170 g of ammonium acetate in deionized water and dilute to 500 ml.

Tellurium carrier solution (1000 ppm). Dissolve 0.868 g of sodium tellurite in sufficient 1 M hydrochloric acid to make 500 ml. Purify the solution by adding 5 ml of APDC solution and extracting with three 25-ml portions of chloroform.

Selenium(IV) and selenium(VI) standards. Prepare 1 mM stock solutions from sodium selenite and sodium selenate. Prepare working standards by serial dilution with deionized water.

Apparatus. A Perkin-Elmer 650-10S fluorescence spectrophotometer equipped with a chart recorder and a digital display was used.

Procedures

Preconcentration of selenium(IV). Transfer 1 l of a filtered sample to a 1 l separatory funnel. Adjust the pH to 4.2 by adding 2.5 ml of 6 M hydrochloric acid and 5.2 ml of ammonium acetate buffer. Add 10 ml of APDC solution and mix the solution thoroughly. Add 20 ml of chloroform and shake the mixture vigorously for 2 min. Transfer the organic phase to a 125-ml separatory funnel which contains 23 ml of 8 M nitric acid. Extract the aqueous phase with another 15 ml of chloroform and combine it with the first extract. Allow the chloroform—nitric acid mixture to stand for at least 8 h, shaking the mixture occasionally. Transfer the aqueous phase to a

50-ml beaker and add 3 ml of 70% perchloric acid. Evaporate the acid mixture to near dryness.

Preconcentration of total selenium. Add 6 ml of tellurium carrier, 4 g of hydrazine sulfate, and 300 ml of concentrated hydrochloric acid to 1 l of filtered sample. Slowly bring the solution to boiling and boil for about 15 min. Allow to cool to room temperature. Filter through a Gelman A/E glass-fiber filter. Dissolve the precipitate in 10 ml of concentrated nitric acid and 3 ml of 70% perchloric acid. Evaporate the acid mixture to near dryness.

Fluorimetric procedure. Add 10 ml of 6 M hydrochloric acid to the preconcentrated sample and boil for 5 min. Adjust to pH 1.0 with 7.5 M ammonia solution, add 0.5 ml of 0.1 M EDTA (disodium salt) solution and 10 ml of DAN solution, and adjust the volume to 50 ml with 0.1 M hydrochloric acid. Heat the sample in a water bath at 50°C for 20 min. Allow to cool to room temperature, transfer to a 125-ml separatory funnel and add 5 ml of cyclohexane. Shake the solution vigorously for 2 min. Centrifuge the organic phase at 2500 rpm for 15 min and measure the fluorescence intensity at 520 nm with excitation at 380 nm.

Calibration graphs. Known amounts of selenium(IV) were added to 1-l aliquots of a sea-water sample and the samples were processed as described above to obtain calibration graphs for selenium(IV) and total selenium.

RESULTS AND DISCUSSION

Preconcentration of selenium(IV)

Although the exact molecular structure of the complex is not well understood, APDC readily forms a complex with selenium(IV) in weakly acidic solutions [23, 24]. That APDC reacts with selenium(IV) and not with selenium(VI) was confirmed at the selected pH of 4.2 [25] by determining the amount of selenium recovered from standard selenium(IV) and selenium(VI) solutions. The results are presented in Table 1. Selenium(IV) was quantitatively recovered (100.3 ± 8.8%), while no selenium was detected when only selenium(VI) was present. In mixtures, only the selenium(IV) was detected.

TABLE 1

APDC as a complexing agent for selenium(IV) in the presence of selenium(VI)

Se(IV) added (nM)	Se found (nM)	Recovery (%)	Se(IV) added (nM)	Se(VI) added (nM)	Se found (nm)	Recovery (%)
0.020	0.024	120.0	1.60	6.40	1.60	100.0
0.050	0.046	92.0	3.20	6.40	3.20	100.0
0.100	0.092	92.0	0	3.20	0	—
3.20	3.26	101.9	0	6.40	0	—
3.20	3.16	98.8				
4.80	4.70	97.9				

In all this study, recoveries were computed by comparing calibration slopes or concentrations for samples that had been processed as described above, with similar data for solutions prepared to have the same final concentrations without preconcentration [26]. Figure 1 shows the effect of APDC concentration on the recovery of selenium(IV). Recovery increases with increasing amount of added APDC up to 10 ml of 2% APDC solution for each liter of sample but then stays approximately constant at 93% with larger volumes of APDC; 10 ml of APDC solution was therefore added to each liter of sample in further work.

In the back-extraction of selenium from chloroform into nitric acid, the selenium—APDC complex decomposes under the strongly acidic conditions, and inorganic selenium is back-extracted. Thus, the efficiency of this back-extraction depends on the rate of decomposition of the selenium—APDC complex. The optimal conditions were studied by extracting the complexes from 1 l of a 3.2 nM selenium(IV) solution into chloroform. The chloroform extracts were transferred to separatory funnels containing 8 M nitric acid. The samples were vigorously shaken for 2 min, and then left for various periods of time with occasional shaking during the first hour. The results obtained for the concentration of selenium in each sample are shown in Fig. 2. After 8 h, the recovery of selenium(IV) was between 97% and 102%.

Although most of the experimental conditions described earlier [8] were found to be acceptable, there were crucial steps that deserve special attention. Even though only 1 l of sample was used for the present procedure, it was found that 6 ml of 1000 ppm tellurium carrier [8] was still necessary for the quantitative recovery of selenium. Furthermore, the sample must be brought to boiling slowly to avoid fine precipitates which cannot be recovered quantitatively by filtration through a glass fibre filter. The average recovery

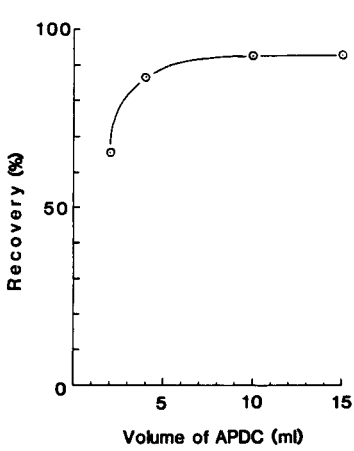

Fig. 1. Recovery of selenium(IV) by complexation with APDC.

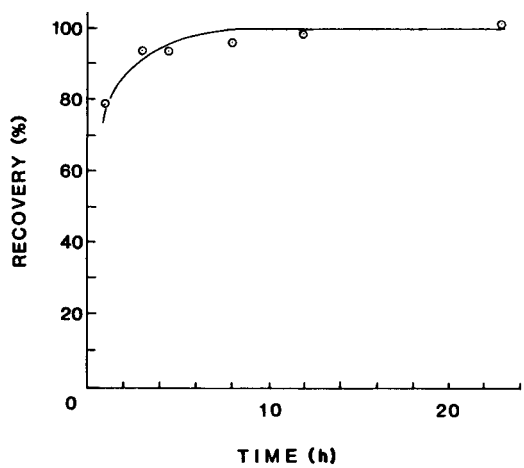

Fig. 2. Effect of time on the back-extraction of selenium from chloroform into nitric acid.

TABLE 2

Recovery of selenium(IV) and selenium(VI) by coprecipitation with tellurium

Se(IV) (pM)	Se(VI) (pM)	Se found (pM)	Recovery (%)	Se(IV) (pM)	Se(VI) (pM)	Se found (pM)	Recovery (%)
100	0	97	97.0	400	0	393	98.3
200	0	179	89.5	200	200	409	102.3
100	100	196	97.5	0	400	426	106.5
0	200	212	106.0				

for seven samples containing 0.1—0.4 nM selenium was 99.6% with a relative standard deviation of 5.9% (Table 2). The recovery of both selenium(IV) and selenium(VI) were considered to be quantitative.

Application to sea water and estuarine water

Plots of fluorescence intensity vs. selenium(IV) and total selenium concentration added to sea water were linear. By comparing the slopes of the lines relating fluorescence intensities to the concentrations of added selenium for the samples and the standards, the average recovery of selenium(IV) and total selenium were calculated to be 92% (Table 3).

The detection limit, calculated as the concentration which produces a signal-to-noise ratio of two, was observed to be about 20 pM for both selenium(IV) and total selenium with a 1-l sample. The precision of the method was evaluated with subsamples of sea water and estuarine waters. The relative standard deviations were about 2% at concentrations above 274 pM and 8% at 131 pM.

The vertical profiles of selenium(IV) and total selenium in the Sargasso Sea at 28°18'N and 63°00'W are shown in Fig. 3. The selenium—APDC complexes were extracted at pH 2 because the samples were preserved at that pH. The shapes of the profiles and the concentrations observed are similar to those reported previously for other parts of the Atlantic Ocean [4].

TABLE 3

Recovery of selenium added to sea waters and estuarine waters

Sample	Salinity (‰)	Species determined	Slope for samples by std. additions	Slope for standards	Recovery (%)
Sea	31.8	Total Se	5.80	6.13	94.6
Estuarine	27.4	Total Se	5.63	6.15	91.5
Estuarine	13.5	Total Se	5.56	6.14	90.6
					Ave. 92.2 ± 2.1
Sea	31.8	Se(IV)	20.9	22.5	93.0
Sea[a]	31.2	Se(IV)	21.4	23.4	91.5
					Ave. 92.3 ± 1.1

[a]The selenium—APDC complex was extracted at pH 2.

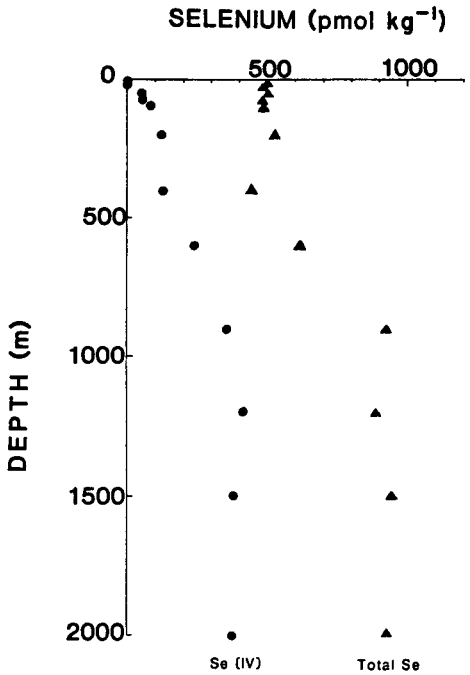

Fig. 3. Vertical profiles of selenium(IV) and total selenium in the Sargasso Sea at 28°18'N and 63°00'W.

Applications to other waters

When this method was applied to river waters with low salinities, the recoveries of both selenium(IV) and total selenium were somewhat lower than with highly saline samples (Table 4). River waters have higher concentrations of dissolved organic carbon than estuarine and sea waters [27, 28]. In the preconcentration of total selenium from river waters containing >5 mg l^{-1} dissolved organic carbon, finer precipitates are formed. Therefore, evaluation by standard additions is recommended for each sample. In the determination of selenium(IV), chloroform may extract selenium associated with fatty acids, hydrocarbons, lipids, and some humic substance, so that the concentration of selenium measured includes selenium(IV) and some of the organic

TABLE 4

The recovery of selenium added to river waters

Salinity (‰)	Species determined	Slope for samples by std. additions	Slope for standards	Recovery (%)
0	Total Se	4.88	5.89	82.9
0.07	Total Se	5.30	6.14	86.3
4.65	Total Se	5.38	6.14	87.6
0	Se(IV)	10.3	12.8	80.5

selenium in a sample. The amount of chloroform-extractable organic selenium was found to be negligible in open ocean water where the dissolved organic carbon content was low. In river waters, this fraction may be quantitatively significant. This problem can be circumvented by extracting the sample with chloroform at pH 4.2 before the preconcentration procedure. However, even in the absence of APDC, part of the selenium(IV) was found to be extracted with chloroform in the presence of acetate; thus, the pH should be adjusted with hydrochloric acid alone. Such a solution has small buffering capacity, but precise pH control in the sample is not really necessary, because selenium(IV) complexes preferentially with APDC in the pH range 1.0—5.0 [25].

We thank R. Lacouture and D. Velinsky for collecting some of the samples and one of us (K. T.) thanks Old Dominion University for a student research grant. The Sargasso Sea samples were collected aboard USNS Lynch 710-82 with the assistance of Drs. David Reid and Denis Wiesenberg of NORDA. This work forms a part of the doctoral dissertation of K. Takayanagi which was submitted to the Department of Oceanography, Old Dominion University.

REFERENCES

1 L. G. Sillen, in M. Sears (Ed.), Oceanography, Washington, D.C., 1961, p. 549.
2 Y. Sugimura, Y. Suzuki and Y. Miyake, J. Oceanogr. Soc. Jpn., 32 (1976) 235.
3 G. A. Cutter, Anal. Chim. Acta, 98 (1978) 59.
4 C. I. Measures and J. D. Burton, Earth Planet. Sci. Lett., 46 (1980) 385.
5 C. I. Measures, R. E. McDuff and J. M. Edmond, Earth Planet. Sci. Lett., 49 (1980) 102.
6 H. Uchida, Y. Shimoishi and K. Toei, Environ. Sci. Technol., 14 (1980) 541.
7 C. I. Measures and J. D. Burton, Nature, 273 (1978) 293.
8 Y. Sugimura and Y. Suzuki, J. Oceanogr. Soc. Japan, 33 (1977) 23.
9 H. J. Robberecht and R. E. Van Grieken, Anal. Chem., 52 (1980) 449.
10 C. I. Measures and J. D. Burton, Anal. Chim. Acta, 120 (1980) 177.
11 P. F. Lott, P. Cukor, G. Moriber and J. Solga, Anal. Chem., 35 (1963) 1159.
12 P. Cukor, J. Walzcyk and P. F. Lott, Anal. Chim. Acta, 30 (1964) 473.
13 W. H. Allaway and E. E. Cary, Anal. Chem., 36 (1964) 1359.
14 R. J. Hall and P. L. Gupta, Analyst, 94 (1969) 292.
15 W. R. T. Hemsted, M. Sina and S. Cekicer, Analyst, 97 (1972) 383.
16 Y. Tamari, Ph.D. Dissertation, Kinki University, Japan, 1978, p. 51.
17 J. A. Raihle, Environ. Sci. Technol., 6 (1972) 621.
18 J. M. Rankin, Environ. Sci. Technol., 7 (1973) 823.
19 C. A. Parker and L. G. Harvey, Analyst, 87 (1962) 558.
20 P. Cukor and P. F. Lott, J. Phys. Chem., 69 (1965) 3232.
21 K. Hiraki, O. Yoshii, H. Hirayama, Y. Nishikawa and T. Shigematsu, Analyst (Japan), 22 (1973) 712.
22 O. Yoshii, K. Hiraki, Y. Nishikawa and T. Shigematsu, Bunseki Kagaku, 26 (1977) 91.
23 O. Foss, Inorg. Synth., 4 (1953) 91.
24 A. Hulanicki, Talanta, 14 (1967) 1371.
25 T. Kamada, T. Shiraishi and Y. Yamamoto, Talanta, 25 (1978) 15.
26 L.-G. Danielsson, B. Magnusson and S. Westerlund, Anal. Chim. Acta, 98 (1978) 47.
27 J. P. Riley and R. Chester, Introduction to Marine Chemistry, Academic Press, New York, 1971, p. 465.
28 R. A. Duce and E. K. Duursma, Mar. Chem., 5 (1977) 319.

Analytica Chimica Acta, 148 (1983) 271—275
Elsevier Science Publishers B.V., Amsterdam — Printed in The Netherlands

Short Communication

ANALYSE QUANTITATIVE DE LA TRANSFORMATION SPIROPYRANNE—MEROCYANINE PAR SPECTROSCOPIE INFRAROUGE DE REFLEXION

E. DAVIN, M. GUILIANO, H. REYMOND, G. MILLE* et J. KISTER

Centre de Spectroscopie Moléculaire et L.A. 126 de chimie moléculaire et de pétroléochimie, Faculté des Sciences et Techniques, Rue Henri Poincaré, 13397 Marseille, Cedex 13 (France)

(Reçu le 8 juillet 1982)

Summary. (Quantitative measurement of the spiropyran—merocyanin transformation by infrared reflectance spectrometry.) Infrared multiple internal reflection spectrometry of the spiropyran—merocyanin transformation is utilized. Quantitative measurements are made directly with spiropyran layers on solid supports (polyester film) with polymeric resins (rhodopas or ethylcellulose) under the conditions of photographic utilization. The accuracy of the method is about 10%.

Résumé. Une méthode de dosage de la transformation spiropyranne—mérocyanine par spectroscopie infrarouge de réflexion est présentée. Les dosages sont effectués directement sur des couchages de spiropyranne sur supports solides (plan film type polyester) en présence d'un liant polymérique (rhodopas ou éthylcellulose) dans les conditions d'une utilisation photographique. Les résultats sont obtenus avec une précision de l'ordre de 10%.

Cette étude entre dans le cadre de la mise au point d'un procédé photographique non-argentique, à haute résolution et à développement à sec [1, 2]. Ce procédé fait intervenir dans sa phase initiale, une étape photochimique utilisant comme substrats photochromes des composés de type spiropyrannes et mérocyanines azahétérocycliques [3]:

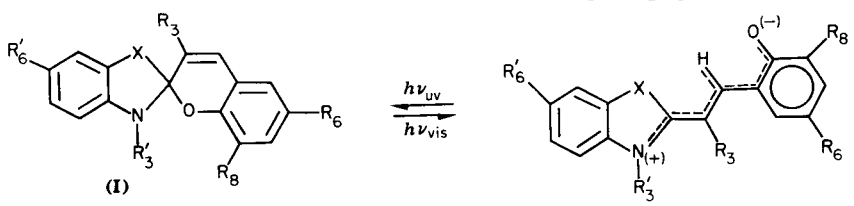

La phase d'amplification de ce signal photonique primaire est une réaction de réarrangement SR ⇌ NR autocatalytique ionique et contrôlable thermiquement [1, 2, 4].

Les substrats impliqués dans les deux étapes du procédé sont déposés sur un support solide en présence d'un semiconducteur et d'un liant. Le rôle du semiconducteur est de stabiliser par adsorption la photomérocyanine obtenue

0003-2670/83/$03.00

par irradiation du spiropyranne. Les semiconducteurs utilisés sont du type oxyde de titane, de zinc, d'aluminium et de silicium. Le liant est un polymère réticulable dont le rôle est de fixer l'ensemble des substrats sur le support solide (plan film type polyester) assurant ainsi la rigidité du couchage et éventuellement d'assurer une stabilisation chimique de la photomérocyanine [5].

Le but de ce travail est de doser quantitativement la transformation spiropyranne—mérocyanine et ceci directement dans les conditions technologiques du procédé, c'est-à-dire à l'état solide et en présence de semiconducteur et de liant (directement sur la pellicule ou le papier photo).

En solution, le contrôle physicochimique des réactions du procédé s'est heurté déjà à une première difficulté, due à l'insolubilité totale des mérocyanines dans les solvants usuels. Ainsi les techniques de résonance magnétique nucléaire (r.m.n.) et u.v. ont été abandonnées au profit de l'infrarouge de transmission. La spectroscopie infrarouge classique permet l'étude des composés directement à l'état solide [6, 7] et constitue ainsi un bon moyen de contrôle réactionnel de la phase photochrome par l'identification rapide des structures intermédiaires et finales (spiropyranne ou mérocyanine) et par le contrôle de la pureté des composés (spiropyranne dans mérocyanine et vice-versa, produit de départ résiduel et produit de dégradation) [7]. Elle permet en outre de suivre la stabilité thermique des spiropyrannes et mérocyanines directement en phase adsorbée sur semiconducteurs à la tempe'rature du procédé, soit environ 140°C [8].

Par contre, lorsqu'on veut une étude du procédé rigoureusement "dans l'état", la technique infrarouge classique de transmission devient à son tour inutilisable en raison de l'opacité de l'ensemble constitué par le support solide et le liant. A ce niveau, nous avons dû faire appel à la technique de spectroscopie infrarouge par réflexion interne multiple (m.i.r.).

Partie expérimentale

Les spectres infrarouges ont été enregistrés sur des spectrographes Perkin-Elmer 125 ou 225 au moyen de deux accessoires m.i.r. Wilks (modèle 9) et de cristaux de KRS_5 (environ 25 réflexions) utilisés sous une incidence de 45°.

La préparation des échantillons est la suivante: la quantité désirée de spiropyranne (60—600 mg) est dissouté dans le liant polymérique déjà lui-même en solution à 12% dans le chloroforme. Les couchages sont faits sur le support solide à l'aide d'une règle de Meyer qui donne un film humide de 100 μm.

Choix des substrats. Les composés spiropyranniques optima du procédé sont du type benzothiazoliniques (I: X = S; $R_3 = OC_6H_5$; $R_6 = NO_2$; $R_8 = OCH_3$; $R'_3 = CH_3$ avec $R'_6 = OCH_3$ pour le composé 1 et $R'_6 = SCH_3$ pour le composé 2) [2]. Leur synthèse est particulièrement délicate: 12 à 14 étapes avec un rendement global voisin de 1% [2, 3]. En conséquence nous avons choisi pour la mise au point de la méthode d'analyse un composé dont nous

disposions en quantité plus importante. Celui-ci est du type indolénique (I: X = $C(CH_3)_2$; R_3 = H; R_6 = NO_2; R_8 = OCH_3; R'_3 = *i*-Pr et R'_6 = H, composé 3).

Une analyse spectrale m.i.r. a été réalisée de façon systématique sur une gamme importante de liants afin de déterminer ceux présentant la zone de transparence la plus intéressante pour la suite de l'étude. Compte tenu du fait que la région spectrale la plus caractéristique des spiropyrannes et mérocyanines est 1700—1200 cm^{-1} [7], nous avons sélectionné deux liants: le rhodopas AXCM3 (copolymère de chlorure de vinyle et d'acide maléique) et l'éthyl cellulose N_4.

Résultats

Plusieurs couchages du spiropyranne 3 à différentes concentrations ont été réalisés dans le rhodopas et l'éthylcellulose. L'allure des empreintes spectrales obtenues entre 1800 et 1200 cm^{-1} est réprésentée sur la Fig. 1. Sur cette figure sont indiquées les bandes i.r. correspondant au spiropyranne et au liant, respectivement par les lettres SP et L. Nous avons sélectionné dans chaque cas une bande caractéristique du spiropyranne et une autre spécifique du liant (indiquée par un astérisque dans la figure). Ce choix doit obéir à deux impératifs: premièrement, les bandes doivent être d'intensité suffisante, et, deuxièmement, il ne doit pas y avoir de chevauchement important de la bande du spiropyranne avec d'une part celle du liant et d'autre part avec une absorption de la mérocyanine correspondante. Nous avons vu dans une précédente étude [7] qu'il existait dans le spectre du spiropyranne une bande disparaissant lors de l'ouverture de ce composé. Il s'agit du sommet $\nu_s(NO_2)$ vers 1335 cm^{-1} dans le spectre du spiropyranne qui glisse à 1290 cm^{-1}

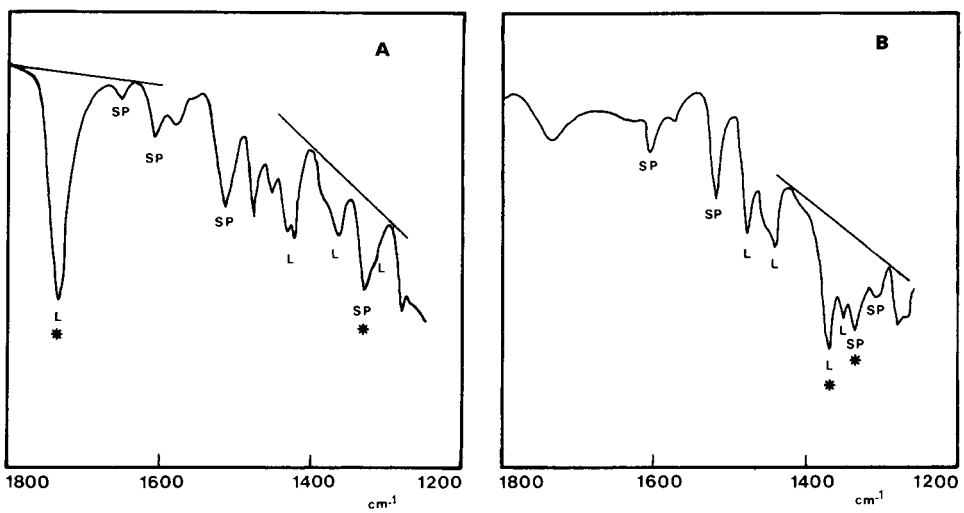

Fig. 1. Allures du spectre i.r. de réflexion d'un couchage de spiropyranne 3: (A) dans le rhodopas AXCM 3; (B) dans l'éthylcellulose N_4.

lors de la transformation en mérocyanine. En conséquence nous avons choisi pour les dosages les bandes infrarouges caractéristiques suivantes:

couchage dans le rhodopas: SP 1335 cm^{-1}, L 1735 cm^{-1}

couchage dans l'éthylcellulose: SP 1335 cm^{-1}, L 1370 cm^{-1}.

Les intensités de ces bandes ont été mesurées à chaque concentration, compte tenu du choix de la ligne de base qui est indiqué sur la Fig. 1. Les résultats de ces différentes mesures sont rassemblés dans le Tableau 1. Les rapports des intensités des bandes d'absorption retenues pour le spiropyranne et le liant ont été portés en fonction de la concentration du spiropyranne (% en poids). Les équations (méthode des moindres carrés) des courbes d'étalonnage ainsi obtenues sont de la forme suivante:

rhodopas: $I_{1335}/I_{1735} = 1.4 \times 10^{-2}$ (% spiro) + 0.15

ethylcellulose: $I_{1335}/I_{1370} = 4.8 \times 10^{-2}$ (% spiro) + 0.11

Discussion

Les bonnes valeurs des coefficients de corrélation, respectivement 0.9939 et 0.9975 justifient la validité d'un tel dosage.

Dans le cas du composé dans le rhodopas, il se produit un léger chevauchement entre la bande à 1335 cm^{-1} du spiropyranne et une absorption du liant. Ceci explique que l'ordonnée à l'origine de la courbe d'étalonnage soit assez différente de zéro.

Pour tester la validité de ce dosage, nous avons utilisé ces deux courbes d'étalonnage pour des couchages des spiropyrannes 1 et 2. Ces divers couchages ont tous été réalisés à 15% en poids de spiropyranne par rapport au liant sec. Les valeurs trouvées au moyen des courbes d'étalonnages sont comprises entre 13 et 16% (Tableau 2).

TABLEAU 1

Données spectroscopiques expérimentales relatives à des couchages étalons du spiropyranne 3 dans le rhodopas et l'éthylcellulose

Spiropyranne 3 par rapport au liant sec (% poids)		0	5	10	15	20	30	40	50
Rhodopas	I 1335	4,5	7	14	15	16			
	I 1735	29	36	49,5	41	38			
	$\frac{I\ 1335}{I\ 1735}$	0,15	0,22	0,28	0,38	0,42			
Ethylcellulose	I 1335	1	6	15,5	15	11,5	13,5	15,5	17,5
	I 1370	15,5	15	23	20,3	10,5	9	7,5	7
	$\frac{I\ 1335}{I\ 1735}$	0,06	0,40	0,67	0,74	1,10	1,50	2,07	2,50

TABLEAU 2

Validité de la méthode de dosage. Détermination spectroscopique du pourcentage de spiropyrannes dans divers couchages (à 15%) de composés 1 et 2

Composés	Liant	I_L	I_{1335}	$\frac{I_{1335}}{I_L}$	% spiro trouvé
Spiro 1	Rhodopas	47	16	0,34	14
Spiro 1	Rhodopas	32,5	12	0,37	16
Spiro 1	Ethylcellulose	13	9	0,70	13
Spiro 2	Rhodopas	68	23	0,34	14
Spiro 2	Rhodopas	40	14	0,35	14,8
Spiro 2	Ethylcellulose	26	21	0,80	15
Spiro 2	Ethylcellulose	10	8	0,80	15

Ces résultats montrent que la méthode décrite est applicable à l'ensemble des dérivés spiropyranniques, à condition toutefois que ceux-ci possèdent un groupement nitro, compte tenu du choix de la bande infrarouge servant au dosage ($\nu_s NO_2$). Mais il est bien connu que l'absence de groupement nitro en position 6 entraîne une perte du caractère photochrome du spiropyranne correspondant [2].

La mise au point du dosage spiropyranne—mérocyanine par spectroscopie infrarouge de réflexion présente un intérêt général. Dans le cadre d'un procédé photographique complexe [1], cette étude permet de suivre les phénomènes photochromiques qui interviennent dans la phase initiale. Dans le cas de procédés reversibles [2] où l'étape photochromique est l'étape centrale, le dosage spiropyranne—mérocyanine par infrarouge permet de vérifier les études de colorimétrie. Cette méthode est aussi utilisable pour l'étude de spiropyrannes thermochromes [9]. Enfin l'étude des dégradations et interactions dans le cadre de procédés complexes est rendue possible in situ [8].

BIBLIOGRAPHIE

1 J. Metzger, Brevet français No. 7328538, 1973.
2 J. Kister, Thèse Sciences, Marseille, 1977.
3 J. Kister, A. Blanc, E. Davin et J. Metzger, Bull. Soc. Chim. Fr., (1975) 2297.
4 J. Kister, G. Assef, G. Mille et J. Metzger, Can. J. Chem., 57 (1979) 813; 57 (1979) 822.
5 J. Fayard, Diplome d'Etudes Superieures Marseille, 1980.
6 M. Guiliano, E. Davin, G. Mille, J. Chouteau et R. Guglielmetti, Helv. Chim. Acta, 61 (1978) 1072.
7 M. Guiliano, G. Mille, J. Chouteau, J. Kister et J. Metzger, Anal. Chim. Acta, 93 (1977) 33.
8 J. Kister, E. Davin, M. Guiliano et G. Mille, Analusis, à paraître.
9 R. Guglielmetti, Brevets français No. 7418018 et 7418079, 1974.

Analytica Chimica Acta, 148 (1983) 277—283
Elsevier Science Publishers B.V., Amsterdam — Printed in The Netherlands

Short Communication

THE S_2 CALIBRATION CURVE OBTAINED BY USING MOLECULAR EMISSION CAVITY ANALYSIS

A. C. CALOKERINOS* and T. P. HADJIIOANNOU
Laboratory of Analytical Chemistry, University of Athens, Athens (Greece)

(Received 25th October 1982)

Summary. The effect of various experimental parameters on the slope and the deviations from linearity of the S_2 calibration graph for thiourea when the S_2 excited species are generated on a m.e.c.a. cavity are studied. Previous explanations for the negative deviations at high concentrations are investigated and the formation of a stable sulphur allotrope is proposed to explain this effect.

Molecular emission cavity analysis (m.e.c.a.) has been extensively used for the determination of sulphur compounds in a wide variety of samples [1, 2]. In all applications, the characteristic sigmoidal calibration curve has been observed; this is partly due to the following relationship between the S_2 emission intensity (I) and the sulphur concentration, [S] [3, 4]: $I = K\,[S]^n$, where K is a constant and depends on the experimental conditions and sulphur compound used. The theoretical value of n is 2 because two sulphur species produce one excited S_2 molecule in the rate-determining step. In practice, n can take any value between 1 and 2 and is calculated from the slope of the log I—log [S] curve (abbreviated as log—log curve): $\log I = \log K + n \log [S]$. The n-value has been found to be critically dependent on the flame conditions [4, 5] and sulphur compound [3, 6, 7] when hydrogen—air flames are used in a flame photometric detector. The log—log graph shows a deviation from linearity towards the concentration axis at high sulphur concentrations. Many explanations have been suggested for this, such as photomultiplier saturation [8], self-absorption [9] and the formation of SO [6]. All information available about the variations of the n-value and the negative deviation of the calibration graph with experimental conditions originates from flame photometric detectors connected to gas chromatographic columns or permeation tubes.

The work described in this communication was undertaken to investigate the effect of various experimental parameters on the n-value and the upper curvature of the log—log graph when the excited S_2 molecules are generated near the cool surface of a cavity within a hydrogen diffusion flame.

Experimental

Analytical-grade reagents and deionized-distilled water were used throughout.

0003-2670/83/$03.00

The apparatus consisted of a spectrometric unit and a cavity-burner unit. The components of the spectrometric unit are summarized in Table 1. The cavity-burner unit (Fig. 1) consisted of a nitrous oxide burner head, as used in a Perkin-Elmer model 403 atomic absorption spectrometer. Hydrogen and nitrogen were supplied to the burner through the fuel and nebulizer inlets, respectively. Oxygen, when required, was introduced into the burner through the auxiliary inlet. All gas flows were controlled with Matheson model 603 flow meters. The burner was positioned perpendicularly to the optical axis of the monochromator, 80 mm from the entrance slit. A water-cooled aluminium cavity (8 mm deep, 5 mm diameter) was used, situated at the centre of the flame, 10 mm above the burner head. The cavity was pitched 7° downwards from the horizontal and cooling water was supplied at 200 ml min^{-1}. All measurements were made at 384 nm with an 0.8-mm slit-width, unless otherwise stated.

Results and discussion

The m.e.c.a. variant introduced by Pourreza [10] was further developed and used: an aqueous solution of the sulphur compound was aspirated into the hydrogen diffusion flame and the molecular emission generated on the surface of a cavity, continuously situated within the flame, was measured by the detector. Sulphur at low concentrations generated S_2 emission only on the surface of the cavity, because of the Salet phenomenon (the increased intensity caused by a cold environment) [11, 12]. The advantage of the method is that the S_2 emission from compounds otherwise difficult to introduce reproducibly into the cavity, can be generated and measured. The precision of the measurement is improved because the emission intensity can be recorded as long as the solution is aspirated into the flame.

A series of aqueous thiourea solutions (100—1900 ppm S) was aspirated into the flame and the effect of various experimental parameters on the

TABLE 1

Items of spectrometric unit

Item	Model	Characteristics
Monochromator	Heath EU-700	0.35-m Czerny-Turner optical system with grating (1180 G mm^{-1}) blazed at 250 nm; dispersion 2 nm mm^{-1}
Photomultiplier	EMI 6256B	End-window type, S11 response, fused silica window
Power supply	Kepco	0—1000 V, 0—20 mA
Photometric readout	Heath EU-703-31	Maximum output 0.1 V at each current range (10^{-6}, 10^{-7}, 10^{-8}, 10^{-9} A)[a]
Recorder	Sargent-Welch XKR	

[a]For comparison of measurements taken at different ranges, the outputs were divided by 10 when the range was reduced by one decade.

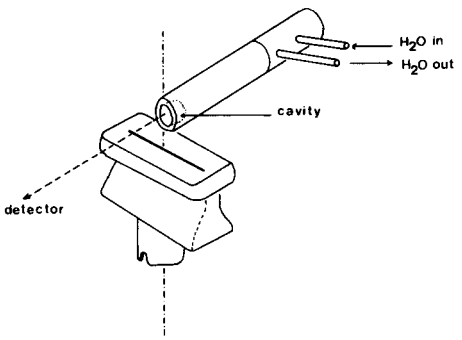

Fig. 1. The cavity-burner unit.

n-value and the negative deviations of the log—log graph were investigated. The n-value was always calculated by the least-squares method using the above logarithmic equation.

The effect of photomultiplier voltage. Detector saturation has been proposed to explain the negative deviations of the log—log graph at high sulphur concentrations [8] but this effect has not been reported for other molecular emissions. With the m.e.c.a. system described, the n-value and the negative deviations were found to increase with photomultiplier tube (PMT) voltage (Fig. 2). The linearity of the log—log plot extended to higher concentrations when low PMT voltages were used but this was due to the decreased sensitivity of the detector. All further studies were done with 1000 V supplied to the PMT.

The effect of slit-width and wavelength. The n-value increased with slit-width, thus showing the effect of a wider wavelength range entering the detector (Fig. 3). The n-value was independent of the wavelength of maximum emission (Fig. 3) because the same excitation mechanism is responsible for all the emission peaks in the S_2 band.

The effect of flame composition and cavity position. Variation of the flows of hydrogen and nitrogen supplied to the burner alter the concentration of flame radicals as well as the flame temperature and size. The concentration and distribution of hydrogen radicals within the flame depend on the amount of air diffusing into the flame and the dilution of hydrogen by the total flow of flame gases. This dilution of hydrogen can be expressed by the dilution function D, defined as $D = F_r(H_2)/[F_r(H_2) + F_r(N_2)]\,(0 < D \leqslant 1)$, where F_r denotes the flow rate.

The effect of D on the emission intensity from 300 ppm S as thiourea is shown in Fig. 4. As D increases, more hydrogen is present in the flame and the temperature increases; decreased emissions are thus obtained because of the decrease in the Salet effect [11, 12]. Small D values are best for greatest intensities. High nitrogen flows are also required for increased aspiration rates.

Slight variations of the flows of the flame gases severely affect the n-value and the log—log graph [4, 5]. This was again verified experimentally in the

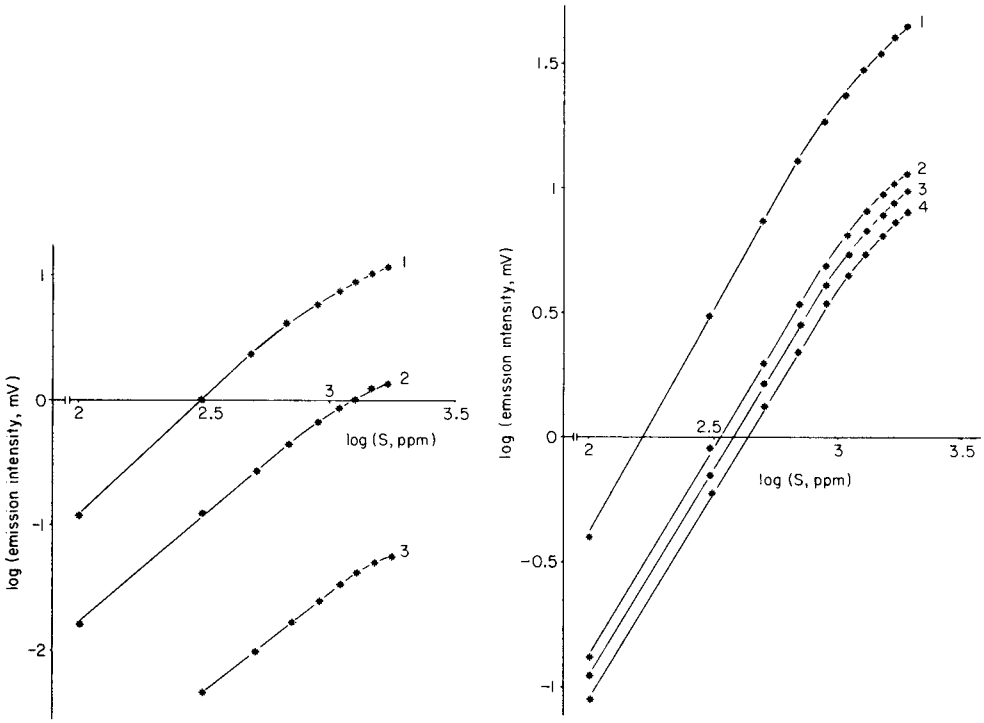

Fig. 2. The effect of photomultiplier voltage on the S_2 log—log calibration graph: (1) 1000 V (n = 1.83); (2) 800 V (n = 1.74); (3) 600 V (n = 1.55).

Fig. 3. The effect of wavelength on the S_2 log—log calibration graph: (1) 384 nm (n = 1.80); (2) 384 nm (n = 1.68); (3) 364 nm (n = 1.67); and (4) 404 nm (n = 1.68). Slit widths: (1) 2 mm; (2—4) 0.8 mm.

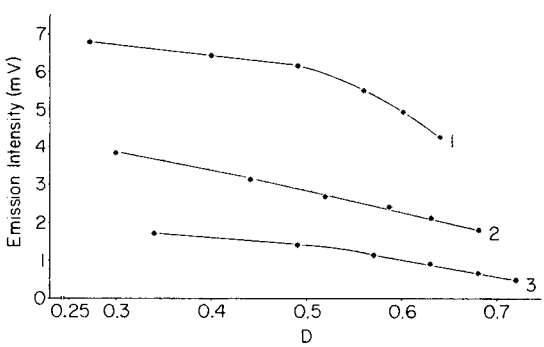

Fig. 4. The effect of the hydrogen dilution function D on the S_2 emission intensity from 300 ppm S as thiourea at: (1) 2.64; (2) 2.30; (3) 1.90 l N_2 min^{-1}.

present studies. The results are shown in Table 2. As D increases, the n-value increases although the corresponding sulphur response decreases. The same observation was made by Sugiyama et al. [13] who introduced benzo(b)-thiophene in the eluent from a gas chromatographic column into a flame photometric detector. Other workers [5, 6] introduced gaseous sulphur compounds (SO_2, H_2S, CH_3SH) into the flame photometric detector from permeation tubes and found that the maximum n-values occurred at or near the hydrogen flow rate which gave maximum sensitivity, whereas they decreased at other flow rates. The procedure of sample introduction into the flame and the nature of the compound undoubtedly affect the dependence of the n-value on the flame composition.

The observation that the n-value increases with flame temperature was further verified by calculating the n-value with the cavity positioned at the centre and the edge of the flame for a given flame composition. The edge is hotter than the centre of the flame because of the larger amounts of diffusing air at the edge. For D = 0.494, the values of n at the edge and centre, respectively, were 1.48 and 1.39. For D = 0.608, the corresponding n-values were 1.59 and 1.44.

The effect of oxygen. Formation of SO has also been proposed to explain the negative deviation of the S_2 calibration graph [6]. Thus, oxygen introduction into the hydrogen diffusion flame was expected to enhance the upper curvature of the log—log plot, but this was not found experimentally (Fig. 5). The introduction of oxygen into the hydrogen flame reduced the sensitivity because of the higher temperature, but the general range of the plot was unchanged. Competitive reactions might also occur which could remove sulphur atoms. Scanning the spectrum of the generated molecular emissions from different concentrations of thiourea did not reveal any SO emission heads at the expected wavelengths [14].

The effect of quenching and self-absorbance. The S_2 emission is severely quenched by organic compounds when present in the hydrogen flame, probably due to formation of the thermodynamically stable gaseous carbon—

TABLE 2

The effect of the hydrogen dilution function D on the n-value and the S_2 emission intensity from 300 ppm S as thiourea

D	n	Emission intensity (mV)
0.648	1.63	1.0
0.604	1.50	1.9
0.548	1.48	2.1
0.533	1.47	2.3
0.511	1.42	3.0
0.494	1.40	4.3

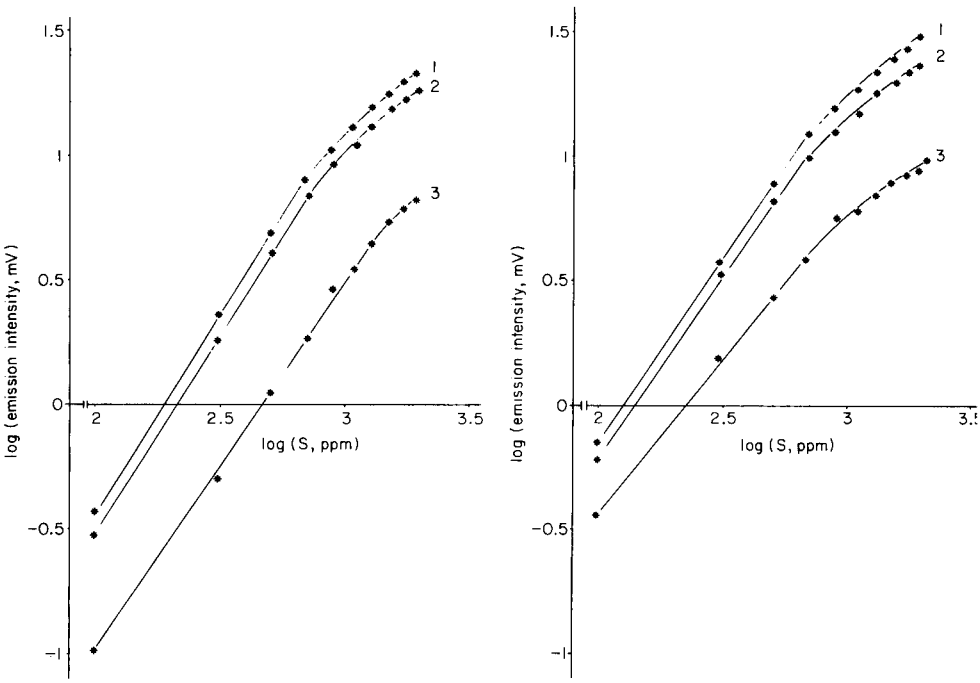

Fig. 5. The effect of oxygen on the S_2 log—log calibration graph for thiourea. Oxygen supply: (1) 0; (2) 88; (3) 760 ml min^{-1} to the hydrogen diffusion flame.

Fig. 6. The effect of additives on the S_2 log—log calibration graph for thiourea: (1) no additive; (2) ethanol; (3) isopropanol (both 1%, v/v).

sulphur species [15]. The effect of quenching by ethanol and isopropanol on the S_2 calibration graph is shown in Fig. 6. In all cases the upper curvature begins at the same sulphur concentration, which indicates that quenching is probably not responsible for the negative deviations.

An attempt to correct the log—log curve by using the equation for self-absorbance given by Greer and Bydalek [9] did not give a straight line at high sulphur concentrations. The same observation was made by Everett et al. [16] who suggested that self-quenching is responsible for the negative deviations of the log—log graph.

Conclusions

The critical dependence of the slope of the log—log graph on a variety of experimental parameters requires frequent calculations of the *n*-value when the S_2 calibration curve is linearized by taking the *n*-th root of the response [17].

Sulphur exists in three stable allotropic forms, S_π (π = 4), S_μ (μ = 6) and S_λ (λ = 8) which are in equilibrium. λ-Sulphur is the stable solid allotrope [18]. Large amounts of a sulphur compound introduced into the hydrogen

flame generate high concentrations of sulphur atoms which might form the stable S_λ allotrope on the surface of the cavity. Therefore, the concentration of the excited S_2 molecules and the emission intensity will be decreased and the calibration graph will show negative deviations at high sulphur concentrations. Formation of S_λ also explains the sulphur deposit on the cavity surface previously observed [12]. The deposit may be responsible for the enhancement of the S_2 emission on a cool surface (Salet phenomenon) and for this reason treatment of the cavity with sulphur prior to analyzing standards and unknowns is desirable [17]. Work is still in progress to establish the formation of the S_λ allotrope and the nature of the solid deposit on the surface of the cavity.

REFERENCES

1 S. L. Bogdanski, M. Burguera and A. Townshend, CRC Crit. Rev. Anal. Chem., 10 (1981) 185.
2 A. C. Calokerinos and A. Townshend, Prog. Anal. Atom. Spectrosc., 5 (1982) 63.
3 T. Sugiyama, Y. Suzuki and T. Takeuchi, J. Chromatogr. Sci., 11 (1973) 639.
4 T. Sugiyama, Y. Suzuki and T. Takeuchi, J. Chromatogr., 85 (1973) 45.
5 J. G. Eckhardt, M. B. Denton and J. L. Moyers, J. Chromatogr. Sci., 13 (1975) 133.
6 C. H. Burnett, D. F. Adams and S. O. Farwell, J. Chromatogr. Sci., 16 (1978) 68.
7 D. A. Ferguson and L. A. Luke, Chromatographia, 12 (1979) 197.
8 F. P. Scaringelli and K. A. Rehme, Anal. Chem., 41 (1969) 707.
9 D. G. Greer and T. J. Bydalek, Environ. Sci. Technol., 7 (1973) 153.
10 N. Pourreza, Ph. D. Thesis, Birmingham University, 1981.
11 C. Veillon and J. Y. Park, Anal. Chim. Acta, 60 (1972) 293.
12 S. L. Bogdanski, A. C. Calokerinos and A. Townshend, Can. J. Spectrosc., in press.
13 T. Sugiyama, Y. Suzuki and T. Takeuchi, J. Chromatogr., 77 (1973) 309.
14 R. W. B. Pearse and A. G. Gaydon, The Identification of Molecular Spectra, 4th edn., Chapman and Hall, London, 1976.
15 S.-A. Fredriksson and A. Cedergren, Anal. Chim. Acta, 100 (1978) 429.
16 G. L. Everett, T. S. West and R. W. Williams, Anal. Chim. Acta, 68 (1974) 387.
17 A. C. Calokerinos and A. Townshend, Fresenius Z. Anal. Chem., 311 (1982) 214.
18 B. J. Heinrich, M. D. Grimes and J. E. Puckett, in I. M. Kolthoff and P. J. Elving (Eds.), Treatise in Analytical Chemistry, Part II, Vol. 7, Interscience, New York, 1961.

Analytica Chimica Acta, 148 (1983) 285—291
Elsevier Science Publishers B.V., Amsterdam — Printed in The Netherlands

Short Communication

EVALUATION OF INTERFERENCE SUPPRESSORS IN ELECTROTHERMAL ATOMIC ABSORPTION SPECTROMETRY

MAMORU TOMINAGA* and YOSHIMI UMEZAKI

National Research Institute for Pollution and Resources, Yatabe, Tsukuba-gun, Ibaraki 305 (Japan)

(Received 9th September 1982)

Summary. Suppression of interferences from iron(III) chloride and sodium chloride by the addition of ascorbic acid, formic acid and carbon dioxide is investigated for the determination of Pb, Sn, Mn, V, Mo, Co, Cu, Ni and Al. The addition of ascorbic acid was most effective for Pb, Sn, Mn, V and Mo.

Interferences of foreign metals, especially chlorides, in graphite-furnace atomic absorption spectrometry are complicated [1—7], and several workers have reported that matrix modification is effective for suppression of these interferences for several elements. Modifiers investigated include ammonium peroxodisulfate [8], ammonium nitrate [9], nitric acid [10], EDTA [11], thiourea [12], and L-ascorbic acid [13]. In previous papers [14, 15], matrix modification with ascorbic acid was reported for the determination of lead, tin, manganese, vanadium and molybdenum. The mechanism of matrix modification with ascorbic acid and other organic compounds was investigated, as a result of which it was suggested that carbon monoxide or carbon dioxide generated by pyrolysis of these compounds might have a role in the suppression of interferences, and that as the number of carbon atoms in a carboxylic acid increased, both the sensitivity and the suppressive effect became poorer. Best interference suppression achieved by carboxylic acid addition was obtained with formic or acetic acid. The exact mechanism, however, has not been elucidated. This report describes the interferences of sodium chloride and iron(III) chloride on several elements, and the effect of ascorbic acid, formic acid and carbon dioxide for suppression of these interferences.

Experimental

Apparatus and reagents. A Perkin-Elmer graphite furnace (HGA-2100) was used in conjunction with a Perkin-Elmer 403 atomic absorption spectrometer and a Hitachi 056 recorder. The light sources were Hamamatsu TV single-element hollow-cathode lamps. A deuterium lamp was used for background correction. Sample solutions were injected into the graphite tube

0003-2670/83/$03.00

by an autosampler (Perkin-Elmer AS-1). Suppressors were injected from a micropipette (Rainin Co. P-20). The absorption signal in the atomization step was evaluated by using a transient memory (Tokyo Kagaku TM-706) and the above recorder. Gases generated by ascorbic acid during the char step were examined by gas chromatography (Shimazu GC-6AM), with a 3-mm i.d. × 3 m stainless column containing Unibeads C (60—80 mesh).

The preparation of stock solutions for lead, tin, manganese, vanadium and molybdenum was as described previously [15]. Cobalt(II) chloride (2.20 g), copper nitrate trihydrate (3.80 g), nickel nitrate hexahydrate (4.95 g) and aluminum nitrate nonahydrate (13.9 g) were dissolved in the minimum amount of concentrated hydrochloric acid and diluted to 1 l with distilled water. These solutions were diluted as necessary with (1 + 9) hydrochloric acid. All acids used were of super-special grade (Wako Pure Chemicals). L-Ascorbic acid and other reagents were of analytical-reagent grade.

General procedure. Instrumental parameters for lead, tin, manganese, vanadium and molybdenum were as described previously [15]. Those for cobalt, copper, nickel and aluminum are summarized in Table 1. A 20-μl portion of suppressor solution was injected into the graphite tube, followed by the sample solution (20—40 μl) from the autosampler. Argon was used as sheath gas at 80 ml min^{-1}. The peak height was recorded. Background correction with a deuterium lamp was used when necessary. In the study of signal—time profiles, some elements were atomized at a lower than optimal temperature because it was difficult to record the profiles obtained at rapid temperature rises. The atomization temperatures used were 1600°C for lead, 2200°C for tin and 2000°C for manganese, cobalt, copper, nickel and aluminum. The signals from the atomization step were introduced into a transient memory with an input time of 50 ms and recorded at an output time of 10 s. The gases generated from ascorbic acid in the char step were trapped and the volume ratio of carbon monoxide and carbon dioxide was measured. A 100-ml quartz trap with a stopcock at both ends was used. One end was attached to the injection port of the furnace and the other end was sucked at the argon flow rate. The generated white fumes

TABLE 1

Instrumental parameters

Element	Co	Cu	Ni	Al
Lamp current (mA)	15	10	12	10
Wavelength (nm)[a]	240.7	324.7	232.7	309.2
Char (°C)[b]	900	800	1000	1500
Atomize (s)[c]	10	6	10	10

[a]Slit-width 0.7 nm. [b]For 40 s after drying at 100°C for 40 s. [c]At 2500°C.

were trapped from the beginning of the char step. Sample injections were 20 μl of metal solution and 20 μl of ascorbic acid.

Results and discussion

The effect of suppressors on chloride interference in the determination of the metals is shown in Table 2. A 20-μl portion of 5% ascorbic acid or concentrated formic acid was injected into the graphite tube to mix with the 20 μl of sample solution, previously injected, before the dry, char and atomization steps. Carbon dioxide was added at 0.5 l min^{-1} in the dry and char steps with the argon sheath gas.

Interference of sodium chloride in the determination of lead, manganese and vanadium was almost suppressed by the addition of ascorbic acid, and tin and molybdenum gave a recovery of $\geqslant$110%. Interference in manganese and lead determinations was suppressed by the addition of formic acid or carbon dioxide, respectively. For tin, vanadium and molybdenum, interference was not suppressed so effectively by formic acid or carbon dioxide. For cobalt and copper, the suppressors had little effect, but for nickel and aluminum, formic acid or carbon dioxide removed the suppressive effect. The effect of iron(III) chloride was suppressed by all three sup-

TABLE 2

Suppression of interferences of sodium chloride[a] and iron(III)[a] chloride by matrix modification

Metal (mg l^{-1})	Interferent	Recovery (%)			
		Without suppressor	CO_2[b]	HCOOH[c]	Ascorbic acid[d]
Pb	NaCl	46	98	89	93
(0.2)	$FeCl_3$	72	70	101	103
Sn	NaCl	72	83	53	110
(0.5)	$FeCl_3$	32	36	49	101
Mn	NaCl	44	52	92	100
(0.02)	$FeCl_3$	92	99	106	101
V	NaCl	91	91	80	103
(5)	$FeCl_3$	77	97	108	106
Mo	NaCl	102	—	92	112
(2)	$FeCl_3$	40	46	90	106
Co	NaCl	61	55	72	75
(0.2)	$FeCl_3$	152	129	155	139
Cu	NaCl	54	48	70	75
(0.5)	$FeCl_3$	106	93	106	79
Ni	NaCl	85	102	105	86
(0.5)	$FeCl_3$	123	87	118	120
Al	NaCl	88	95	96	19
(0.1)	$FeCl_3$	74	98	83	44

[a]Presence of Na or Fe in 1000-fold amount for each metal. [b]0.5 l min^{-1}. [c]Concentrated solution. [d]Aqueous 5% (w/v) solution.

pressors for lead, manganese and vanadium. For tin, ascorbic acid addition suppressed the interference, and for molybdenum ascorbic acid and, less effectively, formic acid were satisfactory suppressors. For cobalt, copper, nickel and aluminum, suppression of the interference was less effective, and interference increased for some elements. With carbon dioxide addition, the lifetime of the graphite tube was shorter for the other two suppressors. Carbon dioxide was detected during the atomization step. Carbon dioxide would be less effective as a suppressor in the char step. Carbon dioxide might also react with the graphite tube and generate carbon monoxide during atomization.

The atomic absorption—time profile during atomization was investigated for several elements, after addition of ascorbic acid, formic acid or carbon dioxide. Figure 1 shows the lead profile with suppressors. The lead peak appeared earlier when carbon dioxide had been introduced, and earlier still in the presence of ascorbic acid. Formic acid delayed the peak. Figures 2 and 3 show the effect of interference suppressors on manganese and cobalt, respectively. The manganese peak appeared later with each suppressor, but ascorbic acid gave the greatest delay. The cobalt peak appeared later when carbon dioxide had been introduced, but the other compounds had little effect. For copper, the three suppressors had little effect on the peak time, but ascorbic acid in particular increased the peak height. The changes in peak time on addition of the interference suppressors are listed in Table 3; the effect of suppressors on peak height is also shown. In most instances, only ascorbic acid increased the signal.

Hydes [13] and McLaren and Wheeler [16] suggested that the addition of ascorbic acid and oxalic acid would convert chlorides to oxides in the dry and char steps. The later appearance of the lead peak with formic acid would therefore correspond to the formation of lead oxide. If lead chloride is the dominant compound during the char step, ascorbic acid would convert lead chloride to elemental lead, and the change in peak time would correspond to the consequent faster atomization of lead.

The tin peak appeared earlier with formic acid and carbon dioxide, but the peak height was depressed. Ascorbic acid, however, enhanced the peak height, without affecting the peak time. This suggests that the depressive interference resulted from the enhanced formation of volatile tin compounds with the matrix during the char step, and that this occurred to at least a lesser extent in the presence of ascorbic acid. Tin oxide would be a dominant compound produced during charring, but carbon dioxide could increase the co-volatilization of tin chloride.

For manganese, vanadium and molybdenum, the peak tended to be delayed by the interference suppressors, especially ascorbic acid. For these elements, a dominant compound produced during charring would be the oxide or oxide chloride. These compounds would be reduced to metal by the suppressor. Table 4 shows the effect of suppressors in the presence of interferences on the peak time for lead, manganese and cobalt. Peak

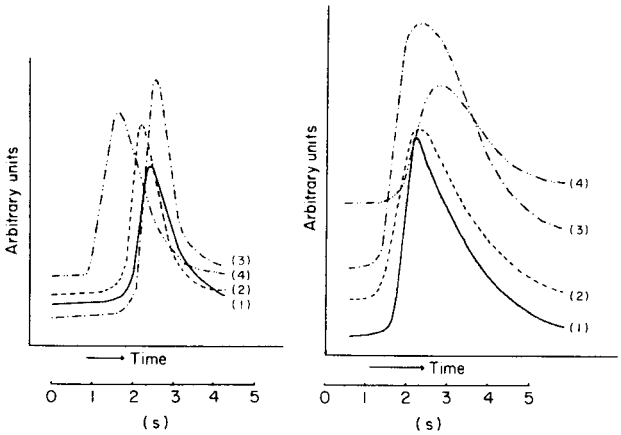

Fig. 1. Atomic absorption—time profile of lead (0.2 mg l^{-1}): (1) in the absence of suppressor; (2) with CO_2 (0.5 l min^{-1}); (3) with formic acid (concentrated solution); (4) with ascorbic acid (5% w/v) solution.

Fig. 2. Atomic absorption—time profile of manganese (0.02 mg l^{-1}): (1—4) as in Fig. 1.

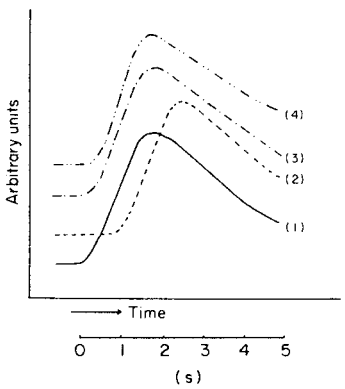

Fig. 3. Atomic absorption—time profile of cobalt (0.2 mg l^{-1}): (1—4) as in Fig. 1.

time would be dependent on the analyte compound produced during charring. In Table 4, the peak times of lead and manganese under suppression of interference show a similar variation to that with ascorbic acid in the absence of interferent. In the presence of interferent, atomization of lead or manganese would differ from that in the absence of interference. But these atomization processes would become the same on addition of a suppressor.

Table 5 shows the contents of carbon monoxide and dioxide generated by ascorbic acid in the graphite furnace during the char step. The volume ratio of carbon monoxide was lower in the presence of lead, tin, manganese and molybdenum, in which interferences were suppressed by ascorbic acid,

TABLE 3

Peak ratio and change of peak time obtained by matrix modification

Metal ($mg\ l^{-1}$)	Conc.	Peak ratio[a]			Change of peak time[e]		
		CO_2[b]	HCOOH[c]	Ascorbic acid[d]	CO_2[b]	HCOOH[c]	Ascorbic acid[d]
Pb	0.2	1.00	1.00	1.29	−0.2	+0.2	−0.7
Sn	0.5	0.59	0.87	1.23	−0.4	−0.2	0.0
Mn	0.02	0.87	0.95	1.13	0.0	+0.2	+0.5
V	5	0.70	1.00	0.80	0.0	0.0	+0.2
Mo	2	0.61	1.17	0.84	+0.4	+0.1	+0.6
Co	0.2	1.00	1.00	0.79	+0.6	0.0	+0.1
Cu	0.5	1.06	1.52	1.53	0.0	+0.2	0.0
Ni	0.5	1.18	1.00	0.95	−0.6	−0.3	−0.3
Al	0.1	0.47	1.00	0.92	+0.8	+0.2	+0.1

[a]To peak height in the absence of interference suppressor. [b]0.5 l min^{-1}. [c]Concentrated solution. [d]Aqueous 5% (w/v) solution. [e]+ = delayed peak.

TABLE 4

Change of lead (0.2 $mg\ l^{-1}$), manganese (0.02 $mg\ l^{-1}$) and cobalt (0.2 $mg\ l^{-1}$) peak times on matrix modification in the presence of iron(III) chloride (200 mg Fe l^{-1}) or sodium chloride (200 mg Na l^{-1})

	Change of peak time[a] (s)			
	Without suppressor	CO_2[b]	HCOOH[c]	Ascorbic acid[d]
$PbCl_2$	0.0	−0.2	+0.2	−0.7
$PbCl_2 + FeCl_3$	−0.2	+0.3	+0.4	−0.7
$PbCl_2$ + NaCl	−0.3	−0.4	−0.4	−0.7
$MnCl_2$	0.0	0.0	+0.2	+0.5
$MnCl_2 + FeCl_3$	−0.8	−0.4	−0.6	−0.2
$MnCl_2$ + NaCl	+0.2	−0.6	−0.1	+0.6
$CoCl_2$	0.0	+0.6	0.0	+0.1
$CoCl_2 + FeCl_3$	+0.2	+0.4	+0.2	0.0
$CoCl_2$ + NaCl	+0.8	+0.3	+0.3	+0.1

[a]+ = delayed peak. [b–d]As Table 3.

TABLE 5

Gases generated in the char step with addition of ascorbic acid[a]

Element[b]	None	Pb	Sn	Mn	V	Co	Cu	Al
CO (%)	12	3	7	3	6	7	11	13
CO_2 (%)	88	97	93	97	94	93	89	87

[a]Aqueous 20% (w/v) solution. [b]1% metal solution.

than in the absence of the metal. This suggests that ascorbic acid would reduce these metal compounds during the char step, especially if the compound is a chloride. These conclusions were not valid for other metals. Further investigations are still required before all the processes are completely elucidated.

REFERENCES

1 D. A. Segar and J. G. Gonzalez, Anal. Chim. Acta, 58 (1972) 7.
2 W. Frech and A. Cedergren, Anal. Chim. Acta, 88 (1977) 57.
3 S. Yasuda and H. Kakiyama, Anal. Chim. Acta, 89 (1977) 369.
4 R. D. Ediger, G. E. Peterson and J. D. Kerber, At. Absorpt. Newsl., 10 (1971) 65.
5 W. C. Campbell and J. M. Ottaway, Analyst, 102 (1977) 495.
6 M. Tominaga, A. Kimura, A. Miyazaki and Y. Umezaki, Bunseki Kagaku, 24 (1975) 61.
7 M. Tominaga and Y. Umezaki, Bunseki Kagaku, 28 (1976) 347.
8 K. R. Sperling, Fresenius Z. Anal. Chem., 287 (1977) 23.
9 J. R. Montgomery and G. N. Peterson, Anal. Chim. Acta, 117 (1980) 397.
10 V. B. Stein, E. Canelli and A. H. Richard, Int. J. Environ. Anal. Chem., 8 (1981) 99.
11 R. Guevremont, Anal. Chim. Acta, 115 (1980) 163.
12 M. Suzuki, K. Ohta and T. Yamakita, Anal. Chem., 53 (1981) 9.
13 D. J. Hydes, Anal. Chem., 52 (1980) 959.
14 M. Tominaga and Y. Umezaki, Nippon Kagaku Kaishi, (1981) 7; Anal. Chim. Acta, 110 (1979) 55.
15 M. Tominaga and Y. Umezaki, Anal. Chim. Acta, 139 (1982) 279.
16 J. W. McLaren and R. C. Wheeler, Analyst, 102 (1977) 542.

Analytica Chimica Acta, 148 (1983) 293—298
Elsevier Science Publishers B.V., Amsterdam — Printed in The Netherlands

Short Communication

THE RECOVERY OF SILVER AFTER LEAD COLLECTION AND PERCHLORIC ACID PARTING

A. DIAMANTATOS
Rand Refinery, Ltd., Germiston (South Africa)

(Received 27th August 1982)

Summary. A method is described for determination of silver, which eliminates cupellation. The sample is fused with lead flux and the resulting lead assay button is parted with perchloric acid after heating at ca. 180° C. Complete precipitation of silver chloride is attained by dilution and overnight standing. After filtration and dissolution of the precipitate in ammonia, silver is determined by atomic absorption spectrometry. Results on samples of varying nature and composition are higher than those obtained by the classical lead-cupellation method.

The classical fire-assay is the oldest and commonest method for the determination of silver in natural and metallurgical products and has been critically evaluated by several workers [1—3]. The overall conclusions were that the silver results tend to be low by 2—30%, and that the cupellation process is the main cause of the reduced silver values. Faye and Inman [2], using silver-110, showed that the extent of silver losses depends on the temperature and duration of cupellation, the quantity of silver present in the lead button, the silver—gold ratio, and the composition of the cupel. They concluded that the silver loss is usually 5—10% and even under ideal conditions is never less than 2%. In an earlier radiochemical study, Nakamura and Fukami [3] showed that the losses of silver to the cupel could vary from 5 to 30% for samples containing 2 to 0.1 mg of silver, respectively.

The efficiency of collectors other than lead has also been examined. Moloughney and Graham [4] applied the tin-collection scheme [5] for silver in ores and metallurgical concentrates. After dissolution of the tin button with hydrochloric acid, silver was precipitated by reduction with tin powder; recoveries were similar to those obtained by classical cupellation. Robert et al. [6], however, found low and inconsistent results because of incomplete precipitation of silver by the tin powder. The efficiency of nickel sulphide collection was investigated by Kuznetsov et al. [7]; the loss of silver into the slag was found to be about 6% and, when the nickel sulphide button was parted with hydrochloric acid, silver as H $[AgCl_2]$ passed into the nickel chloride solution to the extent of 92—97%. Radio-isotopic tests [8] showed that the first nickel sulphide button collected about 89.3% of silver and that another 7.3% could be recovered by re-fusing the slag of the first fusion.

0003-2670/83/$03.00

When the button was dissolved with hydrochloric acid, about 91.6% of silver was dissolved but could not be measured directly by atomic absorption spectrometry (a.a.s.) in that medium.

Numerous procedures involving direct acid decomposition of silver-bearing materials followed by a.a.s. determination of silver, have been recorded. Rubeska et al. [9] determined silver in minerals such as galenites, sphalerites, tetraedrites and antimonites by a.a.s. after digestion of 0.1—0.3 g of the mineral with nitric acid, and addition of tartaric acid to mask antimony. Purushottam et al. [10] digested sulphide ores (0.1—0.2 g) with aqua regia, masked silver with ammonia, precipitated most of the other metal ions as hydroxides, and determined silver by a.a.s. Decomposition of galena, sphalerite and pyrites (0.1—0.2 g) with hydrochloric acid alone or with nitric acid, and EDTA and thiosulphate for complexing silver and lead, respectively, was recommended by Ng [11]. Walton [12] found extremely low results for silver during an examination of several dissolution procedures reported in the literature. He recommended the use of a mixture of hydrofluoric, hydrochloric, nitric and perchloric acids for effective dissolution of oxide and sulphide ores, but stressed that further treatment of the residue was needed to recover an additional 5.7% of silver. Chowdhury et al. [13] decomposed sulphide ores in a nitric—perchloric acid mixture, added ammonium citrate and ammonia to eliminate chloride interferences, filtered and measured silver in the filtrate by a.a.s. Recently, Brooks et al. [14] proposed an aqua regia—bromine mixture for the decomposition of sulphide ores after proving the inadequacy of the nitric acid attack. All these wet procedures were claimed to be superior to the classical fire assay, with 1—10% higher recoveries, but these claims should be regarded with strong reservations. Apart from the conflicting reports on the sample treatment, the acid attack procedures were applied to specific silver-bearing samples. The major problem encountered in acid dissolution is the completeness of silver dissolution, and results on unknown samples must be regarded as dubious. Other serious disadvantages of these wet methods are the use of small samples (0.1—0.2 g), which may not be representative, and the possibility of silica causing some absorption of the noble metal.

Surprisingly, no method which combines lead collection of silver with subsequent wet treatment of the complete lead assay button, appears to have been reported despite the advantages of eliminating the cupellation. Two integrated schemes were reported earlier [15] for determining the six platinum metals and gold after parting the lead—noble metals button with perchloric acid. The present communication records the extension of this parting technique to silver.

Experimental

Equipment and solutions. A fire-assay electric furnace with a silicon carbide element, fireclay crucibles, and cast iron conical moulds (150-ml capacity) were used for the lead fusion. A Techtron A-375 atomic absorption spectrometer was used.

The assay lead flux contained (parts by weight) litharge 50, borax 20, soda ash 60, silica 20, flour 5—6. A 1000 mg l^{-1} stock silver solution was prepared by dissolving 1.3287 g of silver chloride (analytical grade) in 1 l of 1:1 ammonia. A secondary stock solution (100 ppm) was prepared by dilution and used to make the working standard solutions containing 0.2—10 ppm of silver in (1 + 1) ammonia.

Recommended procedure. Mix thoroughly 1—50 g of sample (roast if necessary) with 150—180 g of lead flux and transfer to a No. 2 fire-clay crucible. Fuse at 1200° C for 1 h and pour the melt into a conical iron mould. After cooling, detach the lead button from the slag by tapping, place it in 100 ml of a 30% (w/v) sodium hydroxide solution and boil to remove completely any adhering slag. Place the button in a 1-l squat beaker and add 300 ml of perchloric acid (70%) and 30 ml of anhydrous acetic acid. Cover the beaker, heat to 185° C initially, remove the heat source for a time and then maintain the mixture at 180 ± 5° C until all the lead has dissolved. Continue heating for another 20 min at 150° C to ensure complete dissolution of any platinum, palladium and rhodium present. Allow to cool to about 100° C and dilute the solution slowly with 200 ml of water while stirring. Boil the diluted solution for 2—3 min and then cool in water. After 15 min, stir again and leave the solution overnight in a dark place.

Filter the solution through a Millipore filter apparatus using a Millipore filter disc (0.45 μm) and wash 3—4 times with small portions of water. Place the filter disc with the retained precipitate in a 250-ml beaker, add 5 ml of concentrated hydrochloric acid and heat for 2—3 min. Cool completely, add carefully ca. 50 ml of concentrated ammonia solution (32% minimum), cover and heat gently for 5—6 min to ensure complete dissolution of the silver chloride. Cool, transfer to an appropriate volumetric flask (concentration should be 1—5 ppm Ag) and dilute to volume to yield a (1 + 1) ammonia solution. Aspirate this solution into the air—acetylene flame and measure at 328.1 nm, consecutively with similarly prepared standards.

Results

For convenience, the investigation began with a silver-rich material, a gold refinery borax slag, having a known silver content of 13.27 mg g^{-1}. The sample (2 g) was fire-assayed with ca. 160 g of the lead flux and the resultant lead button (38 g), cleaned as described above, was parted with perchloric acid and acetic acid (as above) at 175—185° C until the button dissolved and effervescence of hydrogen ceased. The hot clear lead perchlorate solution was then split quickly, and almost equally, into six 250-ml beakers, using a measuring cylinder. While hot, each aliquot (ca. 50 ml) containing approximately 4 mg of silver, was carefully diluted to 100 ml with water and mixed. The solutions immediately became turbid, indicating precipitation of silver. The first three solutions were cooled in water for 15 min, stirred for 1 min, and left overnight in the dark. The other three solutions were boiled gently

for 3 min, which dissolved the white precipitate, and then cooled in water for 15 min, during which time the turbidity re-appeared. The solutions were then stirred for 1 min, and left overnight in the dark. The observations next day were interesting. In all six solutions, a silver chloride precipitate had settled and the supernatant liquid was water-clear. However, it was obvious from the last three mixtures that the 3-min boiling period had had an advantageous effect on the coagulation of the precipitate.

The easy dissolution of silver chloride in ammonia and the advantages described by Walton [12] in measuring silver by atomic absorption spectrometry in a strong ammoniacal solution (stability of sample solution, no depression on silver signal, a straight-line calibration graph etc.), were confirmed. Filtration through the Millipore system described above was quite fast and the filtrates were clear. The retained precipitate was readily dissolved in 50 ml of the ammonia liquor by heating gently for 5 min, but the upper side of the filter remained slightly mauve, indicating some photochemical reaction. Analysis of the filter paper showed that about 1.2% of the silver had remained unattacked by the ammonia treatment. To overcome this drawback, the filter with the precipitate was first heated gently with a little concentrated hydrochloric acid and then, after complete cooling, 50 ml of the ammonia liquor was added and re-heated for 5 min. This procedure proved entirely successful; not even traces of silver were found on the filter after this treatment. These dissolution conditions were, therefore, adopted for further work.

Effect of perchloric acid concentration on the precipitation. Three lead buttons, each obtained by fusing 37.8 mg of solid silver nitrate with 150 g of lead flux, were parted with 300 ml of perchloric acid and 30 ml of acetic acid as before. The resulting solutions were diluted with different volumes of water (200, 300 and 500 ml), and the determinations were completed as before. No differences were observed in the speed of precipitation or the coagulation of the precipitate. The perchlorate parting solutions were therefore diluted with equal volumes of water.

Accuracy and precision. The accuracy of the method was evaluated as follows: lead fluxes were salted with known amounts of silver nitrate, added as solid or in solution. After fusion, silver was determined by the recommended procedure. The results given in Table 1 indicate satisfactory accuracy.

A platiniferous sample of known composition was also analysed for silver, in triplicate. The sample was a Rustenburg converter matte containing 81 ppm Ag, a total of 1883 ppm of platinum group metals and gold, 48.2% Ni, 28.9% Cu, 1.4% Fe, 22.4% S, etc. The "standard" matte (1 g) was roasted over a thin silica bed at 800°C for 1 h to remove sulphur and fused with

TABLE 1

Recovery of silver from synthetic samples

Ag added (mg)	0.200, 0.500, 1.00, 5.00, 10.00, 20.00
Ag found (mg)	0.205, 0.492, 1.01, 5.03, 9.93, 20.06

160 g of the lead flux, and the lead—noble metals button was taken through the recommended procedure. This time, together with the silver chloride precipitate, there were tiny black particles of iridium, ruthenium and osmium metals which had remained unattacked by the parting acid [16]. These metals were easily separated from silver by filtration of the final ammoniacal silver solution. The amounts of silver found were 79.5, 79.5 and 81 ppm, respectively, thus confirming the high accuracy and precision and applicability of the proposed procedure to samples containing silver together with other precious metals and base metals.

Application to various silver-bearing materials and comparison with the classical lead cupellation. Various widely different samples were analysed for silver by the proposed method and by classical lead cupellation. A comparison of the results (Table 2) demonstrates the improved recovery of silver by the proposed method.

Discussion

The lead fusion—perchloric acid parting technique is applicable to the determination of silver in a wide variety of materials irrespective of the presence of other noble metals in large or small amounts. The method is easily integrated in the previously published schemes [15] for the determination of the six platinum metals and gold after lead fusion and perchloric acid parting. An agreeable feature of this procedure is that silver can be isolated at an early stage in the wet analysis of the lead—noble metals button, and so will not pose procedural difficulties in the subsequent determination of the platinum metals.

The method is simple and more accurate than the classical fire-assay because of the deletion of the cupellation step. It provides a simple and reliable means for estimating the magnitude of the silver losses occurring in cupellation. It seems to be the first scheme for recovering silver directly by wet chemical attack of the complete lead collector.

TABLE 2

Comparison of lead/wet chemical and lead/cupellation assays with a.a.s. measurements

Sample	Sample size (g)	Silver found ($\mu g\ g^{-1}$)[a]	
		Wet method	Cuppellation
Platinum ore (South Africa)	30	0.69	0.58
Rustenburg converter matte	1	80	71
Rustenburg filter concentrate	30	9.8	8.1
Crude matte	1	6989	6530
Refinery borax slag	5	3108	2876
Refinery borax slag	2	13238	12315
Crude speiss	1	4820	3970
Gold refinery sweeps	0.5	54646	49860

[a] Average of 3 determinations.

The author gratefully acknowledges the assistance of Mr. I. J. Leibbrandt with the preparations of many lead assay buttons. He is also greatly indebted to Mr. E. F. Statham, General Manager of Rand Refinery, for support and permission to publish this investigation.

REFERENCES

1 V. S. Dillon, Assay practice on the Witwatersrand, Parow, Cape Times, 1952.
2 G. H. Faye and W. R. Inman, Anal. Chem., 31 (1959) 1072.
3 Y. Nakamura and K. Fukami, Jpn. Analyst, 6 (1957) 687.
4 P. E. Moloughney and J. A. Graham, Talanta, 18 (1971) 475.
5 G. H. Faye, Mines Branch Research Report R-154. The Queen's Printer, Ottawa, Canada, 1965.
6 R. V. D. Robert, E. Van Wyk and K. Dixon, Nat. Inst. Metall., Repub. S. Afr., Rep. No. 1580, 1973.
7 A. P. Kuznetzov, Y. N. Kukushkin and D. F. Makarov, Zh. Anal. Khim., 29 (1974) 2155.
8 K. Dixon, E. A. Jones, S. Rasmussen and R. V. D. Robert, Nat. Inst. Metall., Repub. S. Afr., Rep. No. 1714, 1975.
9 I. Rubeska, Z. Sulcek and B. Moldan, Anal. Chim. Acta, 37 (1967) 27.
10 A. Purushottam, S. S. Lal and P. P. Naidu, Talanta, 19 (1972) 208.
11 W. K. Ng, Anal. Chim. Acta, 63 (1973) 469.
12 G. Walton, Analyst, 98 (1973) 335.
13 A. N. Chowdhury, A. K. Das and T. N. Das, Fresenius Z. Anal. Chem., 269 (1974) 284.
14 R. R. Brooks, J. Holzbecher, D. E. Ryan, H. F. Zhang and A. K. Chatterjee, At. Spectrosc., 2 (1981) 151.
15 A. Diamantatos, Anal. Chim. Acta, 94 (1977) 49; 98 (1978) 315.
16 A. Diamantatos, Anal. Chim. Acta, 90 (1977) 179; 91 (1977) 281.

Analytica Chimica Acta, 148 (1983) 299—303
Elsevier Science Publishers B.V., Amsterdam — Printed in The Netherlands

Short Communication

DETERMINATION OF CHLORIDE IN GEOLOGICAL SAMPLES BY ION CHROMATOGRAPHY

STEPHEN A.WILSON* and CAROL A. GENT

U.S. Geological Survey, Analytical Laboratories, DFC, Box 25046, MS 928, Denver, CO 80225 (U.S.A.)

(Received 19th July 1982)

Summary. Samples of silicate rocks are prepared by sodium carbonate fusion and then treated by ion chromatography. The method was tested for geological standards with chloride concentrations between 0.003 and 3%. Observed chloride concentrations compared favorably with literature values. The relative standard deviation and detection limit for the method were 8% and 7 ppm, respectively. Up to 30 determinations per 24-hour period were possible.

The determination of chloride in geological samples is considered important geochemically because chloride is associated with numerous transition metals. It is believed that this association involves the creation of metal—chloro complexes which are important in the formation of ore deposits [1, 2]. Thus chloride is often used as a geochemical indicator for the location of ore deposits containing metals such as tungsten, zinc, molybdenum, lead, and manganese [3—7].

Because of the variability of chloride concentrations in geological samples, techniques are required which can accurately determine chloride concentrations varying over several orders of magnitude. In the past, potentiometric, titrimetric, and spectroscopic techniques were used to quantify chloride in geological materials [8—14]. Recent advances in the field of ion chromatography provide an alternative to these techniques. Ion chromatography has been used successfully for samples from geothermal wells, oil shales, and soil extracts [15—17]. The use of ion chromatography for quantifying total chloride in solid samples has received only limited attention, however, because of the difficulty in extracting chloride from the matrix. The need for rapid chloride determinations can be satisfied by a method which utilizes a sodium carbonate fusion followed by ion chromatography. The procedure developed initially for fluoride [18] was modified for the direct determination of chloride in geological samples.

Experimental

Apparatus. A Dionex Model 12S ion chromatograph was used. Initial studies were conducted using a 3 × 50 mm S-3 precolumn, 3 × 250 mm S-3 anion

0003-2670/83/$03.00

separator and a 6 × 250 mm anion suppressor column; a solution containing 3mM $NaHCO_3$ and 2.4 mM Na_2CO_3 served as the eluent. Later studies used a 3 × 50 mm S-2 precolumn, 3 × 250 mm S-2 separator column and a 6 × 250 mm anion suppressor column; a solution containing 3 mM Na_2CO_3 and 1.5 mM NaOH served as the eluent. Other system parameters were: 138 ml h^{-1} flow rate, 0.1 ml sample injection loop, 1 V recorder input, and a 0.5 cm min^{-1} chart speed. Conductance measurements for standards and samples ranged between 1 and 100 microsiemens (μS). Measurements at the 1 μS level required the use of a Dionex pulse dampener. The Dionex 12S ion chromatograph is equipped with a microprocessor which controls the operations during the chromatographic process. The program developed for this study uses a 3-min loading step followed by a 25-min recording interval. The program was later expanded to include suppressor regeneration and equilibration steps which facilitate round the clock operation.

Sample preparation. U.S. Geological Survey standards used in the study were ground to pass a 200-mesh sieve. A 100-mg sample and 200 mg of anhydrous sodium carbonate were mixed in a 35-ml platinum crucible. The crucible was covered and heated over a Meker burner at red heat for 5 min. The crucible was then allowed to cool to room temperature. Approximately 10 ml of water was added to the crucible to dissolve partially the fusion cake. After 30 min, the contents of the crucible were broken up with a glass rod and transferred to a 50-ml volumetric flask. Approximately 10 ml of the solution was removed with a syringe, filtered through a 0.45-μm filter, and transferred to a 20 × 150-mm glass test tube. Samples and standards were placed in the sample carousel and the chromatographic separation was initiated. The chloride standards used were prepared in a carbonate matrix, with fused sodium carbonate. Aliquots of a chloride standard were added to the sodium carbonate solution to produce the desired standards.

In studies involving the determination of chloride with the S-3 separator column, a pretreatment process was devised to remove the sodium interference on chloride. Sodium ions were removed from the solutions by using Bio-Rad AG-50W-X12 resin in the hydrogen form: about 3 ml of resin conditioned overnight in deionized water was added to a test tube containing 10 ml of solution. The contents were mixed on a mechanical shaker for 4 h, and then an aliquot was removed for chloride quantitation.

Results and discussion

Although it was shown that chloride could be quantified with an S-3 column after removal of sodium from the fusion step [18] with an ion-exchange column (see Fig. 1A), the S-3 column was considered inappropriate for routine use because of the time required for the ion-exchange step. An alternative procedure was developed which quantified chloride directly with S-2 separator columns. A combination of the S-2 anion separator column and an eluent of sodium carbonate and sodium hydroxide provided good resolution of the chloride and carbonate peaks (Fig. 1B). This resolution was noted for all

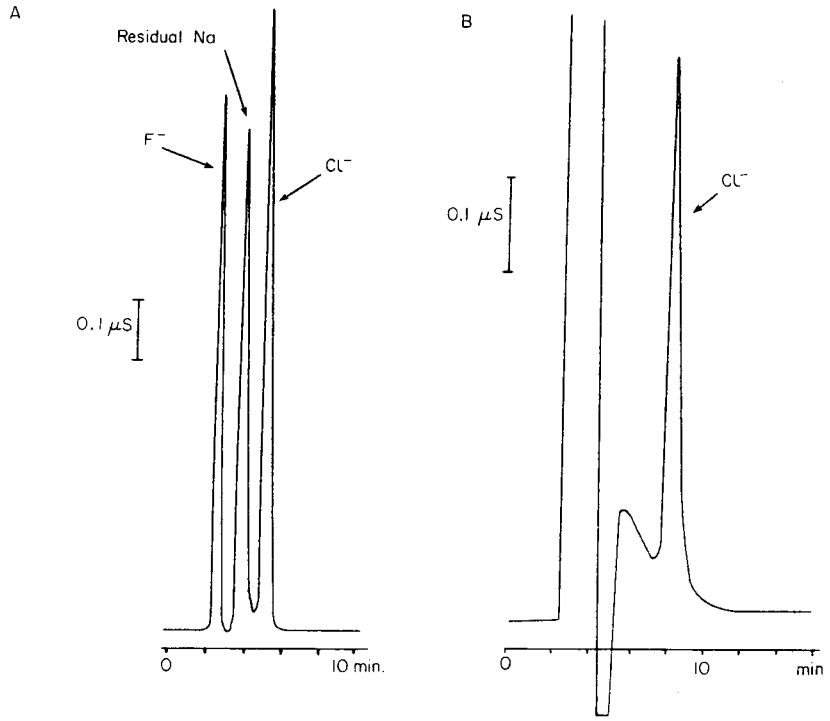

Fig. 1. Anion chromatograms for U.S. Geological Survey Standards after sodium carbonate fusion: (A) standard W-1 with prior ion-exchange treatment and an S-3 column; (B) standard GSP-1 with an S-2 anion separator column.

samples, even those with low chloride concentration, which required the use of a 1-μS, full-scale setting. Based on the separation of chloride and carbonate peaks, chloride could be quantified by using peak heights.

Because of the separation characteristics of the S-2 column, concern developed over the presence of nitrate in the final solution. If nitrate were present in the final solution, it would be necessary to extend the chromatographic step to 40 min for complete elution of the nitrate peak. To test for the effects of nitrate, samples were doped with magnesium nitrate and fused by the standard procedure. Soil samples known to contain nitrate were also subjected to the proposed technique. Nitrate was not detected in any of these solutions. On the basis of these observations, it was assumed that nitrate was removed during the fusion procedure, probably volatilizing as oxides of nitrogen. Because nitrate was removed from consideration, the 28-min period required for the ion chromatography was considered appropriate. Based on the time required for the sample preparation and ion chromatography, up to 30 determinations were possible over a 24-h interval. Because of the automated capabilities of the Dionex 12S ion chromatograph, the chromatography was done overnight without operator assistance.

Chloride concentrations in various geological standards were determined by

TABLE 1

Chloride concentration in geological samples

Sample	Type	Chloride content ($\mu g\ g^{-1}$)		
		Found[a]	Literature value	Ref.
G-2	Granite	81 ± 6(5)	100	20
BHVO-1	Basalt	98 ± 6(6)	94?	21
BCR-1	Basalt	110 ± 7(7)	58?	20
AGV-1	Andesite	170 ± 10(6)	185	20
PCC-1	Peridotite	120 ± 8(4)	80?	20
W-1	Diabase	240 ± 16(4)	200?	20
GSP-1	Granodiorite	330 ± 20(27)	340	20
STM-1	Syenite	480 ± 16(7)	450?	21
RGM-1	Rhyolite	550 ± 31(9)	540	21
NOD P-1	Manganese nodule	1 200 ± 50(4)	1 200	22
NOD A-1	Manganese nodule	4 800 ± 50(4)	4 300	22
MESS-1	Marine sediment	7 000 ± 280(4)	8 200	23
BCSS-1	Marine sediment	11 300 ± 550(4)	11 200	23
MAG-1	Marine sediment	29 300 ± 930(4)	30 900	21
AMH-1	Andesite	87 ± 6(5)	—[b]	
BIR-1	Basalt	24 ± 1(5)	—	
COQ-1	Carbonatite	54 ± 2(4)	—	
DNC-1	Diabase	49 ± 7(5)	—	
DTS-1	Dunite	32 ± 3(6)	—	
GSM-1	Gabbro	230 ± 14(4)	—	
TLM-1	Tonalite	250 ± 12(4)	—	

[a]With standard deviation and, in parentheses, the number of determinations.
[b]Not available.

the proposed technique. The results in Table 1 represent replicate determinations done over several days. Reasonable agreement with reported chloride values was observed. The imprecision of the method was estimated from the standard deviations of the samples tested. Relative standard deviation was better than 8% for all the samples tested, except DTS-1 and DNC-1.

The detection limit for the method was established from studies conducted over several days at the 1-μS full-scale setting with chloride standards in a sodium carbonate matrix. A regression analysis of chloride concentration ($\mu g\ g^{-1}$) versus chloride peak height (μS) showed a correlation coefficient of 0.995, a slope of 0.62 $\mu S\ \mu g^{-1}$ g and a standard error of regression equal to 2.8×10^{-3} μS. Based on this information and established statistical procedures [19], the detection limit for the method was 7 $\mu g\ g^{-1}$ chloride in the rock at the 90% confidence level.

REFERENCES

1 K. B. Krauskopf, Introduction to Geochemistry, McGraw-Hill, New York, 1967, p. 48.
2 H. D. Holland, Econ. Geol., 67 (1972) 281.
3 I. I. Ginzburg, Principles of Geochemical Prospecting, Pergamon Press, Oxford, 1960, p. 311.
4 L. M. Lebedev, Geochem. Int., 9 (1972) 485.
5 R. W. Boyle, Geol. Surv. Can. Pap., 74-75 (1974) 35.
6 G. Stollery, M. Borcsik and H. D. Holland, Econ. Geol., 66 (1971) 361.
7 J. P. Lalonde, Geol. Surv. Can. Pap., 73-28 (1973) 1.
8 B. Mason, U.S. Geol. Surv. Pap. 440-B-1, 25, 26 (1979) 37.
9 R. O. Rye and J. Haffty, Econ. Geol., 64 (1969) 629.
10 W. T. Parry, Econ. Geol., 67 (1972) 972.
11 E. J. Duff and J. L. Stuart, Analyst, 100 (1975) 739.
12 L. C. Peck and E. J. Tomasi, Anal. Chem., 31 (1959) 2024.
13 W. H. Huang and W. D. Johns, Anal. Chim. Acta, 37 (1967) 508.
14 G. Troll and A. Farzaneh, Geostd. Newsl., 4 (1980) 37.
15 F. J. Trujillo, M. M. Miller, R. K. Skogerboe, H. E. Taylor and C. L. Grant, Anal. Chem., 53 (1981) 1944.
16 R. D. Lash and O. J. Hill, Anal. Chim. Acta, 108 (1979) 405.
17 W. A. Dick and M. A. Tabatabai, J. Soil Sci. Am., 43 (1979) 899.
18 S. A. Wilson and C. A. Gent, Anal. Lett., 15 (1982) 851.
19 R. K. Skogerboe and C. L. Grant, Spectrosc. Lett., 3 (1970) 215.
20 S. Abbey, Geol. Surv. Can., 80-14, part 6 (1979).
21 S. Abbey, Geostd. Newsl., 6 (1982) 47.
22 F. J. Flanagan and D. Gottfried, U.S. Geol. Surv. Prof. Pap. 1155 (1980).
23 Mar. Anal. Chem. Stds. Prog. Natl. Res. Counc. Can., (1981).

Analytica Chimica Acta, 148 (1983) 305—309
Elsevier Science Publishers B.V., Amsterdam — Printed in The Netherlands

Short Communication

PRECONCENTRATION OF TRACE HEAVY METALS IN LARGE AQUEOUS SAMPLES BY COPRECIPITATION—FLOTATION IN A FLOW SYSTEM

ATSUSHI MIZUIKE*, MASATAKA HIRAIDE and KIYOSHI MIZUNO
Faculty of Engineering, Nagoya University, Chikusa-ku, Nagoya 464 (Japan)

(Received 27th September 1982)

Summary. In a stream (0.5 l min^{-1}) of sample solution, trace heavy metals are quantitatively coprecipitated with indium hydroxide and floated with sodium oleate and nitrogen bubbles. Indium and the surfactant are removed by solvent extraction. Cadmium at the ng l^{-1} level in 20 l of water is concentrated 2000-fold with recoveries of greater than 93%.

Generally, flame atomic absorption spectrometry and inductively-coupled plasma atomic emission spectrometry are not directly applicable to the determination of trace heavy metals at the nanogram per liter level in aqueous solutions because of lack of intrinsic detectability. Therefore, preconcentration techniques are always necessary. For example, to achieve ca. 1000-fold concentrations, 10 l of original sample is reduced to ca. 10 ml, the minimal volume required for multi-element determinations. Conventional enrichment techniques, including solvent extraction, ion exchange, coprecipitation and evaporation, are inconvenient or time-consuming for such large samples. The coprecipitation—flotation technique using indium hydroxide collector precipitates and surfactants has been developed for simultaneous preconcentration of trace heavy metals in fresh and sea waters [1, 2]. It was difficult, however, to construct efficient flotation cells having capacities of greater than 5 l. The present communication describes a new coprecipitation—flotation technique using a flow system, which is suitable for treating large aqueous samples. As an example, 1—10 μg of cadmium in 20 l of water is concentrated 2000-fold with recoveries of better than 93%.

Experimental

Apparatus. In the apparatus shown in Fig. 1, the sample flow rate is kept constant at 0.5 l min^{-1}. Reaction vessels (Fig. 2) are four 50-ml polyethylene bottles attached to a vibrator (ca. 25 Hz). A pyrex glass flotation cell consists of two compartments, connected with flanges with ground surfaces, for facilitating collection of the foam—precipitate layer. The sample inlet is extended obliquely upward along the walls of the flotation cell, so that the flotation is not disturbed by the sample stream. All tubes through which the sample flows are 10 mm i.d. polyethylene tubing.

0003-2670/83/$03.00

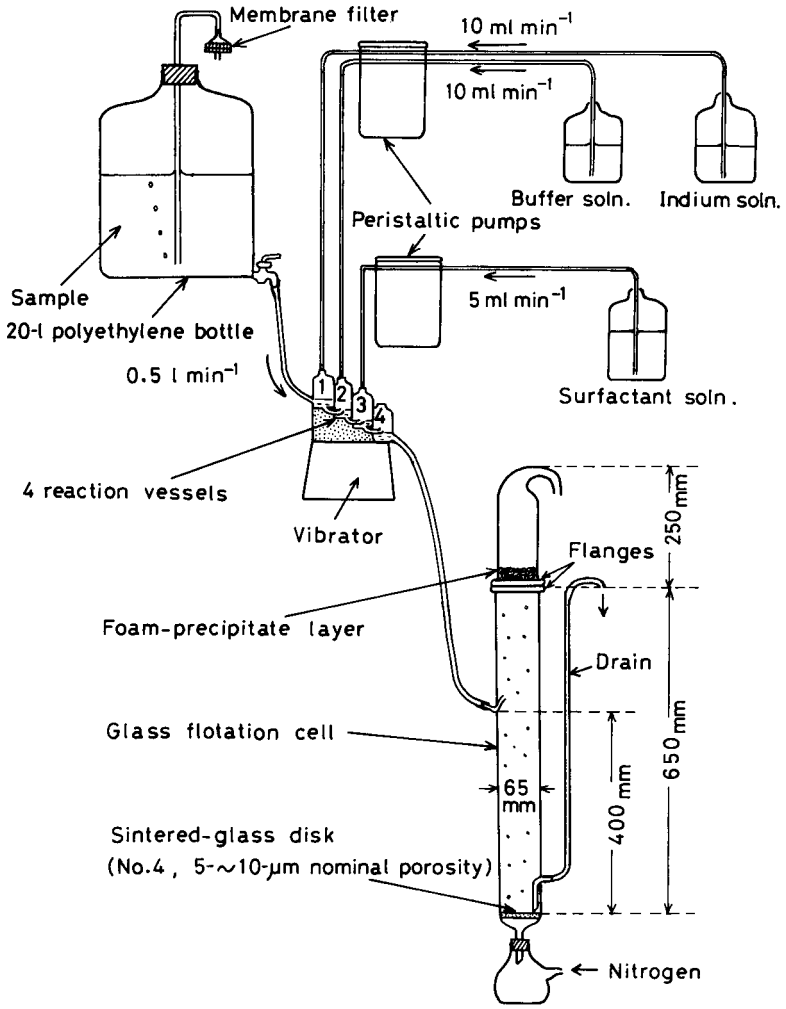

Fig. 1. Apparatus.

Reagents. For the indium solution (5 g l^{-1}), dissolve 50.0 g of indium metal (99.9999% purity) in 200 ml of 14 M nitric acid and dilute to 10 l with water. For the buffer solution, dissolve 500 g of sodium hydrogencarbonate and 425 g of sodium carbonate in water and dilute to 10 l. For the surfactant solution (0.2 g l^{-1}) dissolve sodium oleate (Extra Pure, Nakarai Chemicals) in 70% ethanol. Water was purified by distillation and ion-exchange. All reagents were of reagent grade, unless otherwise stated.

Procedure. Place 20 l of sample in the 20-l polyethylene bottle. To the lower compartment of the flotation cell, add 2 l of purified water, 30 ml of buffer solution and 10 ml of ethanol, and pass nitrogen at a flow rate of ca. 1 ml cm^{-2} min^{-1} through the sintered-glass disk. Set the upper compartment

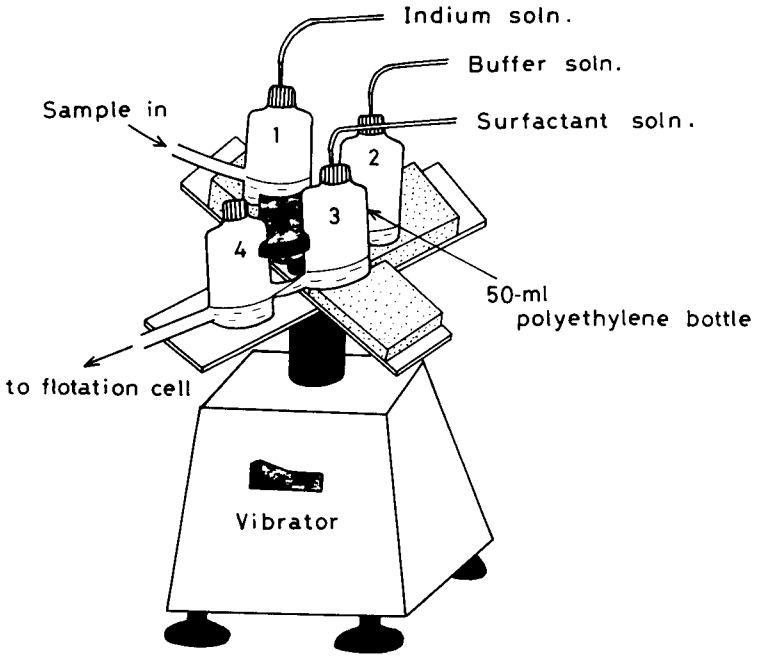

Fig. 2. Detail of reaction vessels.

of the flotation cell, and place the tip of a polyethylene drain near the flanges of the flotation cell. Switch on the vibrator, start the peristaltic pumps to inject indium, buffer and surfactant solutions into the reaction vessels at flow rates of 10, 10 and 5 ml min^{-1}, respectively, and open the stopcock of the 20-l polyethylene bottle to feed the sample at a flow rate of 0.5 l min^{-1}. Coprecipitation of trace heavy metals with indium hydroxide at pH 9.5 and flotation of the precipitate continue for 40 min.

Immediately before completion of the sample feeding, adjust the bottom of the foam—precipitate layer (10 cm or less in height) to the upper flange of the flotation cell by changing the height of the drain tip. Switch off the pumps and the vibrator. Rapidly slide the upper compartment of the flotation cell and collect the foam—precipitate layer in a 300-ml beaker.

Add 60—70 ml of 8.5 M hydrobromic acid to dissolve the precipitates and rupture the foam, and dilute the solution to 100 ml with water. Transfer the solution and 100 ml of diisopropyl ether into a 300-ml separatory funnel, and shake for 2 min to extract indium and the surfactant. Discard the organic phase, and repeat the extraction twice more with 100 ml each of diisopropyl ether. Evaporate the aqueous solution to dryness, dissolve the residue in 3 ml of 8.5 M hydrobromic acid and ca. 5 ml of water, and dilute to 10 ml with water.

Tracer experiments. Cadmium recoveries were determined by γ-activity measurements of ^{115m}Cd, with coefficients of variation of 1—2%.

Results and discussion

Experimental conditions for coprecipitation—flotation, such as reagents and their quantities, pH of the solution and bubble generation, were based on previous work [1, 2].

Vibrating polyethylene bottles in series are essential for the quantitative precipitation of indium hydroxide. The solution levels in the bottles were kept less than half the bottle height, so that the solution was vigorously mixed. With vibrating polyethylene tubing (10 mm i.d. × 4 m) instead of the bottles, mixing was insufficient. The dimensions of the flotation cell were minimized. When the diameter of the flotation cell was reduced to 40 mm, the sample stream disturbed the flotation. The height of the cell and the position of the sample inlet were determined in order that both the loss of the precipitates through a drain and the redispersion of the floated precipitates into the bulk solution did not occur.

Table 1 shows satisfactory recoveries of 1—10 μg of ^{115m}Cd-labeled cadmium through the whole procedure. Recoveries in each step are also given. Most of the loss of cadmium occurred in the collection of the foam—precipitate layer; small amounts of precipitates remained near the flange of the lower compartment of the flotation cell.

The foam—precipitate layer contained 2 g of indium and appreciable amounts of sodium oleate. Indium remaining after the repeated bromide extractions was less than 5 mg and did not interfere with the trace determination. The surfactant, which formed an emulsion in hydrobromic acid solutions, was also removed by the extraction.

The whole procedure required ca. 2.5 h (40 min for coprecipitation—flotation, 20 min for extraction and 90 min for evaporation).

The proposed technique can be applied to simultaneous enrichment of trace heavy metals such as Cd, Co, Cr(III), Cu, Mn(II), Ni and Pb, because these elements are known to behave similarly to cadmium in the coprecipitation—flotation [1] and in the bromide extraction [3]. Although the blank value for cadmium through the whole procedure was less than 0.2 μg (lower detection limit of flame atomic absorption spectrometry) in the present work, contamination should be carefully controlled for ubiquitous

TABLE 1

Cadmium recoveries (%)

Labeled Cd added (μg)	1.0	5.0	10.0
Coprecipitation and flotation	97	96, 94[a]	95
Extraction	99	99	98, 99
Evaporation	98	98	97
Extraction and evaporation	97, 97	98	97, 98
Through the whole procedure	95	93	93

[a] 2 mg each of Fe(III) and Al added.

elements. The technique is directly applicable in the analysis of fresh waters. Minor modifications may be required for sea-water samples as described in a previous paper [1]: pH adjustment with sodium hydroxide and buffer solutions and combined use of two surfactants, sodium dodecyl sulfate and sodium oleate.

REFERENCES

1 M. Hiraide, T. Ito, M. Baba, H. Kawaguchi and A. Mizuike, Anal. Chem., 52 (1980) 804.
2 M. Hiraide, J. Mizutani and A. Mizuike, J. Chem. Soc. Jpn., 1981 (1981) 161.
3 F. A. Pohl and W. Bonsels, Fresenius Z. Anal. Chem., 161 (1958) 108.

Analytica Chimica Acta, 148 (1983) 311—314
Elsevier Science Publishers B.V., Amsterdam — Printed in The Netherlands

Short Communication

DETERMINATION OF TOTAL FLUORINE IN BLOOD BY AN OPEN ASHING TECHNIQUE

J. ALARY*, P. BOURBON and C. BALSA

Institut National de la Santé et de la Recherche Médicale, B.P. 14, 31320 Vigoulet Auzil (France)

(Received 8th October 1982)

Summary. A simple method for the determination of total fluorine in blood plasma and serum (0.5—1 ml) is described. The method involves fixation of fluorine with low-fluoride magnesium acetate, ashing in a platinum crucible at 270°C and 650°C, and direct determination of fluoride in the dissolved ash with a fluoride-selective electrode. The blank value is 0.05 μg of fluoride. The relative accuracy of the method is about 15% for total fluorine contents in the range 0—0.5 μg.

Several methods for the determination of covalently bound fluorine in biological materials such as plasma and serum have been proposed [1—5]. For total fluorine determinations, open ashing techniques [2] or combustion of samples in an oxygen bomb [3, 4] have been followed by the separation of fluoride and measurement. A method for the determination of fluorine in urine and blood serum by aluminium monofluoride molecular absorption spectrometry has also been reported [5]. These methods are time-consuming or require specialized equipment. Determination of low levels of fluorine in numerous small samples of blood plasma requires a simple, rapid method with a low fluoride blank.

The method described has been applied to the determination of fluorine from several organic fluorine compounds and of fluoride in plasma samples spiked with organic fluorine compounds.

Experimental

Apparatus. A combination fluoride electrode (Orion model 96.09) was used with a Philips PW-9409 digital pH meter.

Reagent. Low-fluoride magnesium acetate was used as fixative. The fixative was prepared as follows. In a platinum crucible, place 35 ml of distilled water and 14.5 ml of anhydrous acetic acid. Weigh 3 g of magnesium ribbon (99.5%) and add the magnesium little by little. Complete the reaction by heating gently until the pH is strongly alkaline. Cool and make up to 100 ml with distilled water. This solution is stored in polythene bottles.

Determination of free fluoride. Measure the free fluoride directly with the electrode in a 1-ml plasma sample after addition of 0.1 ml of total ionic

0003-2670/83/$03.00

strength adjustment buffer (TISAB-III; Orion formulation) using the single known addition method.

Total fluorine determination. In a 5-ml platinum crucible, place 0.5 or 1 ml of plasma. Add 0.1 ml of fixative solution and homogenise. Evaporate to dryness under a 500 W infrared lamp (30 mn). Place the crucible on a pipe-clay triangle above a Hoffmann electric furnace and heat at 270°C for 10 min. Then lower the triangle to just above the furnace and keep at 650°C for 30 min. Stir the ash occasionally with a spatula to hasten mineralisation. Cool the crucible and add 1 ml of 10% (v/v) acetic acid and 0.1 ml of TISAB-III. Determine the fluoride concentration after a 10-min equilibration period by a single known addition. Protein-bound fluorine is determined by subtracting ionic fluoride from total fluorine. Mineralisation and measurements must be done in a room without extraneous fluorine contamination.

Results and discussion

Earlier observations have shown that ashing of serum without fixative leads to important losses of fluoride [6]. Several fixatives have been used, e.g., magnesium oxide [6], magnesium chloride [1] or calcium phosphate [2], but the preparation of low-fluoride fixatives is difficult from calcium or magnesium salts. From magnesium, the preparation of the fixative solution is easy and the fluoride blank value (0.05 μg) is suitable for the determination of 0.1—0.2 μg of F^- in 1-ml plasma samples.

The amount of the MgO fixative is 5 mg per sample when 0.1 ml of fixative solution is used. The fluoride blank value was determined by adding 0.2 μg F^- (NaF) and ashing. The use of more fixative (10 mg MgO) increased the fluoride blank without significantly increasing the fluoride recovery.

To avoid losses by volatilisation during combustion, mineralisation was done in two stages (270°C for 10 min and 650°C for 30 min). As an open furnace was used, temperatures in the crucible were calibrated by the melting point method. The two positions of the pipe-clay triangles were fixed above the furnace; the temperature of roughly 270°C was established from the melting points of phenolphthalein (261°C) and sulphanilic acid (288°C), and the temperature of 650°C was taken from the melting point of silver sulphate (652°C). Tests showed that above 800°C losses of fluoride occurred and that below 500°C mineralisation was very slow. The use of a muffle furnace was avoided for fear of fluoride contamination [7].

Fluoride measurements were done by the single known addition method, because comparative trials showed that results obtained from a calibration graph lacked accuracy. The known addition (20 μl) must lead to a ΔE between 20 and 30 mV corresponding to 2—3 times the original fluoride content. As the total ionic strength in the sample is very high, the equilibration time of the electrode is about 10 min.

Fluorine recovery from organic fluorine compounds. The fluorine recovery in the range 0.2—1 μg F^- was studied for several organic fluorine compounds. The results obtained (Table 1) show that the recovery was

TABLE 1

Percentage recovery of fluorine from organic fluorine compounds

Compound	Fluorine taken (μg)	Fluoride found (μg)				Average recovery (%)
		n	Max.	Min.	Av.	
NaF	0.20	5	0.22	0.20	0.21	105
	0.50	3	0.5	0.48	0.49	98
	1.0	4	1.05	0.90	1.01	100
Trifluoromethyl-3-phenylamino-2-nicotinic acid	0.20	3	0.2	0.19	0.195	98
	0.50	3	0.51	0.47	0.48	96
	1.0	3	0.11	0.90	0.93	93
5-Fluorouracil	0.20	3	0.22	0.20	0.21	105
	0.50	6	0.49	0.47	0.48	96
	1.0	6	1.0	0.9	0.95	95
Sodium fluoropyruvate	0.2	3	0.2	0.18	0.19	95
	0.5	5	0.5	0.45	0.47	94
	1.0	3	0.86	0.82	0.84	84
Sodium monofluoro-acetate	0.2	3	0.21	0.19	0.20	100
	0.5	3	0.48	0.45	0.46	92
	1.0	3	0.90	0.85	0.88	88
2-Fluorobenzoic acid	0.2	2	0.21	0.19	0.20	100
	0.5	3	0.45	0.50	0.47	94
	1.0	3	0.90	0.70	0.80	80

better than 90% for all the tested compounds in the range 0.2—0.5 μg F^- in the sample. At the 1-μg level, organic fluorine was lost but this is not very important because the total fluorine levels in blood are less than 1 μg in a 0.5- or 1-ml sample. Although open ashing techniques can be subject to errors arising from loss of organic fluorine during ashing [8] and contamination with extraneous fluoride, this type of problem was not significant in the present work.

Fluorine recovery from plasma spiked with organic fluorine compounds. Samples (1 ml) of horse plasma were analysed repeatedly and the total fluoride content was 0.18 ± 0.03 μg ml^{-1}. Samples were also spiked with various amounts of fluorine compounds; Table 2 gives the results. These results confirm the previous tests (Table 1); recoveries are quite good though there is a lack of precision.

The method was applied to the determination of total fluorine of animal and human sera. The levels found were generally in the range 0.1—0.3 μg ml^{-1} whereas ionic fluoride lay in the range 0.02—0.06 μg ml^{-1}. The total fluorine content was also determined in numerous blood plasmas from pathological cases associated with bone structure disturbances, in which inorganic fluoride (sodium fluoride) was used as a medical treatment. In these cases the content of free fluoride increased sharply (0.5—1 μg ml^{-1}) but the level of protein-bound fluorine did not increase.

TABLE 2

Recovery of fluoride added to horse plasma with an original fluorine content of 0.18 ± 0.03 $\mu g\ ml^{-1}$

Added compound	F^- (μg)	Theoretical value[a] (μg)	Found (μg)
Fluorobenzoic acid	0.2	0.38	0.40
	1.0	1.18	0.92
NaF	0.4	0.58	0.55
	1.0	0.18	1.06
Fluoroacetic acid	0.2	0.38	0.40
	1.0	1.18	1.08
5-Fluorouracil	0.5	0.68	0.64
	0.2	0.38	0.41
Fluoropyruvic acid	0.2	0.38	0.35
	1	1.18	1.0

[a]With a standard deviation of 0.03 μg in all cases.

In conclusion, the proposed method is simple and comparatively rapid, requiring no specialized skills while providing acceptable accuracy.

REFERENCES

1 D. R. Taves, Nature, 217 (1968) 1050.
2 L. Singer and R. H. Ophaug, Anal. Chem., 49 (1977) 38.
3 P. Venkateswarlu, Anal. Biochem., 68 (1975) 512.
4 J. Belisle and D. F. Hagen, Anal. Biochem., 87 (1978) 545.
5 K. Chiba, K. Tsumoda, H. Maraguchi and K. Fuwa, Anal. Chem., 52 (1980) 1582.
6 L. Singer and W. D. Armstrong, Anal. Chem., 31 (1959) 105.
7 W. Oelschläger and M. Kirchgessner, Landwirtsch. Forsch., 13 (1960) 64.
8 W. S. Guy, D. R. Taves and W. S. Brey, Biochemistry Involving Carbon—Fluorine bonds, ACS, Washington, DC, 1976, pp. 117—134.

Analytica Chimica Acta, 148 (1983) 315—320
Elsevier Science Publishers B.V., Amsterdam — Printed in The Netherlands

Short Communication

A HIGHLY SENSITIVE SPECTROPHOTOMETRIC DETERMINATION OF URANIUM WITH CHROMAL BLUE G IN THE PRESENCE OF CETYLTRIMETHYLAMMONIUM CHLORIDE

KATSUYA UESUGI* and TOHRU NAGAHIRO
Laboratory of Chemistry, Himeji Institute of Technology, Shosha, Himeji (Japan)
MITSUO MIYAWAKI
Laboratory of Applied Chemistry, Kobe Technical College, Tarumi, Kobe (Japan)

(Received 26th August 1982)

Summary. The ternary complex between uranium chromal blue G (Color Index 43835) and cetyltrimethylammonium chloride in aqueous solution has maximal absorbance at pH 4.0—6.2, and 648 nm. Beer's law is obeyed over the range 0.2—2.0 mg l^{-1} uranium, with a molar absorptivity of 1.32×10^5 l mol^{-1} cm^{-1} and a sandell sensitivity of 1.8×10^{-3} μg U cm^{-2}. Only aluminum and beryllium interfere when calcium-1,2-cyclohexanediaminetetraacetic acid is used as masking agent.

The most commonly used methods for the spectrophotometric determination of uranium are based on reactions with hydrogen peroxide [1], arsenazo-I [2, 3], arsenazo-III [4, 5], and 8-quinolinol [6]. More recently, procedures based on the formation of ternary uranium complexes with pyrogallol red and cationic surfactants have been suggested [7, 8]. Chromal blue G (sodium-2''-chloro-4''-nitro-4-hydroxy-3,3'-dimethylfuchsone-5,5'-dicarboxylate; C.I. 43835), a triphenylmethane dye, has been used as a spectrophotometric reagent for beryllium [9], scandium [10], palladium [11] and gallium [12]. It has also been found that microgram amounts of uranium react very sensitively with chromal blue G in the presence of a cationic surfactant. This communication describes a highly sensitive method for the determination of uranium based on the formation of a colored complex with chromal blue G in the presence of cetyltrimethylammonium chloride (CTMA).

Experimental

Reagents. A 1×10^{-3} M uranium solution was prepared by dissolving 0.5021 g of uranyl nitrate hexahydrate in distilled water, adding 10 ml of concentrated nitric acid and diluting to 1 l. This solution was diluted further as required. Chromal blue G (Geigy Co., New York) was purified by recrystallization from ethanol, and an aqueous 0.1% (w/v) solution (2.13×10^{-3} M) was prepared. The CTMA (Tokyo Kasei Kogyo Co.) solution (3.0×10^{-3} M) was prepared by dissolving 0.960 g of the product in 1 l of distilled water. The pH 5.0 buffer solution was prepared by mixing 0.2 M sodium hydroxide

0003-2670/83/$03.00

and 0.2 M potassium hydrogenphthalate. A calcium—cyclohexane-1,2-diaminetetraacetic acid (Ca—CyDTA) solution was prepared by mixing equal volumes of 0.02 M calcium chloride and 0.02 M CyDTA. All other chemicals were of analytical-reagent grade.

Apparatus. Absorbances were measured with a Hitachi model 624 automatic recording digitial spectrophotometer and 1.00-cm matched quartz cells. The pH values were measured with a Hitachi-Horiba model F-7LC digital pH-meter.

Standard procedure. Transfer the sample solution containing 5—50 μg of uranium(VI) to a 50-ml Erlenmeyer flask, and add 2.5 ml of CTMA solution, 1.5 ml of chromal blue G solution, and 2.5 ml of phthalate buffer solution (if the pH of the resulting solution is not 4.0—6.2, preneutralize the sample solution with hydrochloric acid or sodium hydroxide). Add a little water to make the volume about 20 ml, and heat in a water-bath at 60—65° C for 10 min. After cooling to room temperature, transfer to a 25-ml volumetric flask, dilute to the mark with distilled water, and measure the absorbance at 648 nm against a reference solution containing the same amounts of reagents.

Results and discussion

Spectral characteristics. The absorption spectra of chromal blue G have been reported [10, 11]. Maximal absorption of chromal blue G in the presence of CTMA occurs at 510 nm below pH 3.0, at 430 nm at pH 3.5—10.0 and at 640 nm above pH 10.5. Figure 1 (curves A and B) shows the absorption spectra of chromal blue G and its uranium complex at pH 5.0, and the effect of CTMA (curves C and D). The formation of the uranium complex in the presence of CTMA is accompanied by a marked increase in the absorbance and a bathochromic shift of the wavelength of maximum absorption of the complex from 608 nm to 648 nm compared to the situation in the absence of CTMA. The spectral changes on varying the pH in the presence of CTMA are shown in Fig. 2. The maximum absorbance of the uranium complex occurs at 540 nm above pH 9.5; between pH 3.6 and 9.0, two absorbance maxima occur, at 648 nm and 670 nm; below pH 2.8, maximum absorbance occurs at about 620 nm.

Effect of experimental variables. The effect of pH on the absorbance of the complex at 648 nm is shown in Fig. 3. The absorbance of the ternary complex is greatest and nearly constant at pH 4.0—6.2. Phthalate—sodium hydroxide buffer (pH 5.0) was satisfactory, and the amount of buffer solution added had no effect on the absorbance measured by the standard procedure over the range 2—5 ml.

The effect of varying the concentration of chromal blue G on the absorbance of the ternary complex at pH 5.0 was examined for solutions containing constant concentrations of uranium and CTMA. The optimal amount of chromal blue G is 1.5 ml of a 0.1% solution for less than 50 μg of uranium. The effect of changes in CTMA concentrations was similarly measured. The

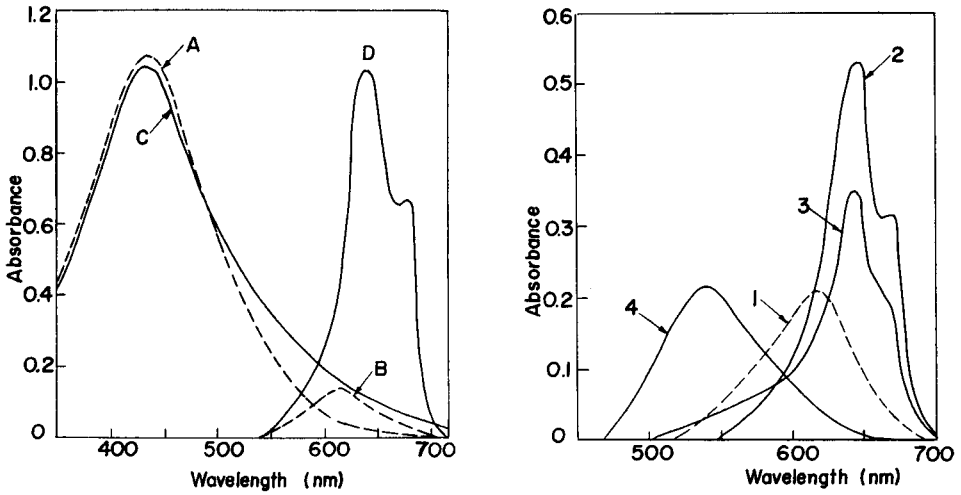

Fig. 1. Absorption spectra of chromal blue G (1.3×10^{-4} M) and its uranium complex at pH 5.0: (A) alone; (B) with 2.4×10^{-5} M U; (C) with 3.0×10^{-4} M CTMA; (D) with 8.0×10^{-6} M U and 3.0×10^{-4} M CTMA.

Fig. 2. Absorption spectra of the ternary uranium complex at various pH values: (1) 2.6, (2) 5.1, (3) 8.0, (4) 10.6. (1.3×10^{-4} M chromal blue G, 4.0×10^{-6} M U, 3.0×10^{-4} M CTMA; measured against reagent blank.)

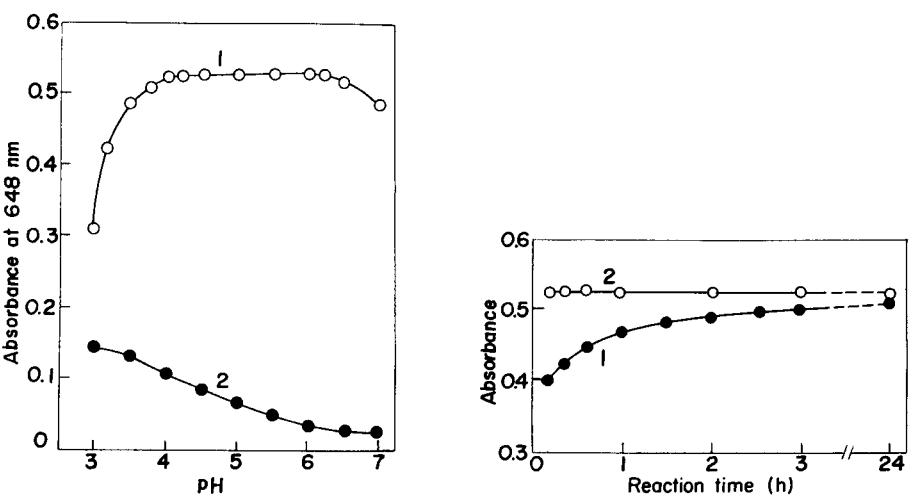

Fig. 3. Effect of pH on absorbance of: (1) uranium complex (4.0×10^{-6} M U, 1.3×10^{-4} M chromal blue G, 3.0×10^{-4} M CTMA) vs. reagent blank; (2) reagent blank vs. water.

Fig. 4. Effect of reaction time for: (1) unheated solution, (2) solution at 60—65°C. (Concentrations as in Fig. 3.)

greatest absorbance is obtained over the range 2.0×10^{-4}—4.5×10^{-4} M CTMA; there is a gradual decrease with more than 5×10^{-4} M CTMA. The optimal amount of CTMA is 2.5 ml of a 3×10^{-3} M solution in a final volume of 25 ml.

Figure 4 shows the absorbances for heated and unheated solutions of the ternary complex. At room temperature (20—23°C), the absorbance gradually increased and maximum absorbance was not obtained after 24 h. When a prepared solution was heated in a water-bath at 60—65°C, however, the reaction was greatly accelerated and maximum color development was obtained in 10 min. The absorbance is stable for at least 24 h.

Calibration, sensitivity and precision. Calibration graphs for uranium were prepared by use of the standard procedure. Beer's law is obeyed over the range 0.2—2.0 mg l^{-1}. The molar absorptivity (ϵ) is 1.32×10^5 l mol^{-1} cm^{-1} at 648 nm, and the spectrophotometric sensitivity is 1.8×10^{-3} μg U cm^{-2}.

The proposed method is very sensitive, more so than the methods based on arsenazo-I ($\epsilon = 2.29 \times 10^4$) [2], chlorophosphonazo-I ($\epsilon = 2.31 \times 10^4$) [13], chlorophosphonazo-III ($\epsilon = 7.36 \times 10^4$) [14], crystal violet ($\epsilon = 4.28 \times 10^4$) [15], eriochrome cyanine R with CTMA ($\epsilon = 9 \times 10^4$) [16], chromazurol S with cetylpyridinium bromide ($\epsilon = 9.9 \times 10^4$) [17] and anthranilic acid with rhodamine 6G ($\epsilon = 6.25 \times 10^4$ l mol^{-1} cm^{-1}) [18].

A solution containing 23.8 μg of uranium was analyzed 10 times by the standard procedure. The average absorbance was 0.528 with a standard deviation of 0.002.

Effect of diverse ions. Aluminum, Be, Cu(II), Ga, Fe(III), Ni, Sc, Y, and the lanthanides also form colored complexes with chromal blue G in weakly acidic solutions [9, 10, 12]. These ions were therefore included in a study of possible interference in the determination of uranium. The ions were added individually to a solution containing 23.8 μg of uranium, and their effects were examined under the conditions of the standard procedure. The results are summarized in Table 1. It can be seen that some cations, especially Al, Be, Cu(II), Ga, Fe(III), Th(IV) and Sc interfere seriously. Nickel, yttrium and lanthanides do not give colors in the presence of CTMA. Chloride, sulfate and nitrate are without effect even in large amounts. EDTA, fluoride, phosphate and citrate prevent the formation of the uranium complex.

Strelow and Van Der Walt [19] recommended diethylenetriaminepentaacetic acid for masking interferences in the determination of uranium. The calcium—cyclohexane-1,2-diaminetetraacetic acid complex (Ca—CyDTA) was investigated here as a masking agent for the more seriously interfering ions. As shown in Table 2, copper(II), gallium, iron(III), scandium and thorium(IV) are effectively masked, but not aluminum and beryllium.

Complex stoichiometry. The method of continuous variations was employed to establish the stoichiometry of the uranium complex in the presence of CTMA. The constant concentration of CTMA was 3.0×10^{-4} M, and measurements were made at pH 5.0 and 648 nm. The results indicated that a 1:2 uranium:chromal blue G complex is formed in the presence of CTMA,

TABLE 1

Effect of diverse ions on the determination of 23.8 μg of uranium

Ion	Added (μg)	U found (μg)	Ion	Added (μg)	U found (μg)
Al(III)	5	64.5	Pb(II)	100	23.8
Au(III)	100	23.9	Sc(III)	10	39.4
Ba(II)	250	23.8	Sr(II)	250	23.6
Be(II)	10	54.0	Y(III)	100	23.7
Ca(II)	250	23.5	Zn(II)	100	23.8
Co(II)	100	23.6	La(III)	100	23.5
Cu(II)	100	29.2	Ce(III)	100	23.5
Fe(III)	10	45.2	Nd(II)	100	23.2
Ga(III)	10	50.7	Gd(III)	100	23.4
Th(IV)	10	27.4	Dy(III)	100	23.3
Mg(II)	250	23.7	Er(III)	100	23.5
Mn(II)	100	23.5	Cl^-	1000	23.5
Mo(VI)	100	23.2	NO_3^-	1000	23.7
Ni(II)	100	23.6	SO_4^{2-}	1000	23.6

TABLE 2

Effect of Ca—CyDTA as a masking agent on the determination of 23.8 μg of uranium (1 ml of 0.01 M Ca—CyDTA added)

Ion	Added (μg)	U found (μg)	Error (μg)
Al(III)	50	37.5	+13.7
Be(II)	10	76.1	+52.3
Cu(II)	250	23.4	—0.4
Fe(III)	250	23.6	—0.2
Ga(III)	250	24.0	+0.2
Th(IV)	250	23.2	—0.6
Cu(II)	100		
Fe(III)	100	23.4	—0.4
Ga(III)	100		
Sc(III)	100	24.0	+0.2
Th(IV)	100		

and a 1:1 complex in its absence. These results were confirmed by the mole ratio method.

REFERENCES

1 E. B. Sandell, Colorimetric Determination of Traces of Metals, 3rd edn., Interscience, New York, 1959, p. 915.
2 J. S. Fritz and M. J. Richard, Anal. Chim. Acta, 28 (1959) 167.
3 H. P. Holcomb and J. H. Yoe, Anal. Chem., 32 (1960) 612.
4 S. B. Savvin, Talanta, 8 (1961) 673.

5 T. Taketatsu, M. Kaneko and N. Kono, Talanta, 21 (1974) 87.
6 K. Motojima, H. Yoshida and K. Izawa, Anal. Chem., 32 (1960) 1083.
7 Om Prakash, S. Kumar and S. P. Mushran, Talanta, 26 (1979) 1167.
8 S. Kumar, Om Prakash and S. P. Mushran, Analyst, 105 (1980) 474.
9 K. Uesugi, Bull. Chem. Soc. Jpn., 42 (1969) 2998.
10 K. Uesugi, Bull. Chem. Soc. Jpn., 42 (1969) 2051.
11 K. Uesugi and T. Shigematsu, Anal. Chim. Acta, 84 (1976) 377.
12 K. Uesugi and M. Miyawaki, Microchem. J., 26 (1981) 288.
13 A. A. Nemodruk, Yu P. Novikov, A. M. Lukin and I. D. Kalinina, Zh. Anal. Khim., 16 (1961) 180.
14 A. A. Nemodruk, Yu P. Novikov, A. M. Lukim and I. D. Kalinina, Zh. Anal. Khim., 16 (1961) 292.
15 N. S. B. Singh, S. V. Mohan and G. R. Balasubramanian, J. Radioanal. Chem., 52 (1979) 319.
16 M. Otomo and K. Kodama, Jpn. Analyst, 20 (1971) 1531.
17 C. L. Leong, Anal. Chem., 45 (1973) 201.
18 T. V. Ramakrishna and R. S. S. Murthy, Talanta, 27 (1980) 442.
19 F. W. E. Strelow and T. N. Van Der Walt, Talanta, 26 (1979) 537.

Analytica Chimica Acta, 148 (1983) 321—325
Elsevier Science Publishers B.V., Amsterdam — Printed in The Netherlands

Short Communication

BISOXALATO AND BISMALONATO COMPLEXES OF CHROMIUM(III) AS ACID—BASE INDICATORS

ALICJA ŁODZIŃSKA* and FATHY AHMED EL-SEIFY
Institute of Chemistry, N. Copernicus University, Toruń (Poland)

(Received 24th August 1982)

Summary. The anionic complexes diaquobis(oxalato)chromium(III) and diaquobis(malonato)chromium(III) are suggested as acid—base indicators for accurate titrations of various strong and weak acids. The apparent acidity constants are pK_a = 7.508 (10°C) and pK_a = 7.73 (24°C), respectively. Reversibility is excellent, indicator blanks are low, and solutions are stable for about a month. Colour changes are from violet to green.

The commonly used indicators in acid—base titrations are generally weak organic acids or bases; metal complexes have received little attention for this purpose. Hirsch [1] used the formation and extraction of the red lead dithizonate to indicate the end-point of aqueous acid—base titrations. Schilt [2] used complexes of dicyanobis(1,10-phenanthroline)Fe(II) and dicyanobis(2,2-bipyridine)Fe(II) as indicators for titrations of weak organic bases in nonaqueous solvents. Metal complexes of pyridine-2-aldehyde-2-pyridylhydrazone [3] and of some metallochromic indicators [4—6] have been suggested as acid—base indicators, as have metal complexes of hydroxyl derivatives of pyridine [7, 8] and pyrimidine [9].

Complex ions, particularly those containing water and amine ligands, are frequently acids of measurable strength and the corresponding hydroxo complexes are then weak bases. The change from the diaquo to aquohydroxo complexes can be accompanied by remarkable changes in colour, depending on the pH of the solutions. Such complexes should be useful as acid—base indicators. In this communication anionic complexes of Cr(III), *cis*$[Cr(L)_2(H_2O)_2]^-$, where L is oxalate or malonate, are examined as acid—base indicators. The complexes deprotonate in alkaline medium to give the aquohydroxo complexes which are different in colour from the diaquo complexes:

$$cis[Cr(L)_2(H_2O)_2]^- + H_2O \rightleftharpoons cis[Cr(L)_2(OH)(H_2O)]^{2-} + H_3O^+$$

The colour changes from red-violet for the oxalate complex (or blue-violet for the malonate complex) to green for both the hydroxo complexes.

0003-2670/83/$03.00

Experimental

Preparation of the complexes. Potassium *cis*-diaquo-bis(oxalato)chromate(III) dihydrate was prepared in a manner similar to that described by Kauffman and Faoro [10], by allowing potassium dichromate and oxalic acid to react with only minimal water present. Potassium *cis*-diaquobis-(malonato)chromate(III) trihydrate was prepared by the method of Chang [11]: aqueous malonic acid and potassium dichromate solutions were boiled together and evaporated to a quarter of the original volume, and the complex was precipitated by addition of ethanol on cooling. For purification, the complexes were dissolved in water (10^{-2}—10^{-3} M) and washed into a column of Dowex 1-X8 (100—200 mesh) anion-exchange resin with 10^{-3} M HNO_3; about 2 l of 0.2 M sodium nitrate was used to separate the sorbed species. The pure complexes thus isolated have two characteristic peaks in the visible region 416 nm (ϵ = 69.4) and 562 nm (ϵ = 47.8) [10] for $[Cr(Ox)_2(H_2O)_2]^-$, and 417 nm (ϵ = 41.4) and 566 nm (ϵ = 49.9) for $[Cr(Mal)_2(H_2O)_2]^-$ [12].

Buffer solutions. Buffer solutions of tris(hydroxymethyl)aminomethane (Tris) were prepared by adjusting 100 ml of a solution 0.1 M in Tris and 0.1 M in acetic acid, with suitable amount of Tris (or acetic acid) to the required pH value using a pH meter (type N-5122).

Determination of apparent indicator constants. Solutions for pK determinations were prepared by mixing 5 ml of a 0.0136 M solution of the oxalato complex or 5 ml of a 0.0345 M solution of the malonato complex with 20 ml of a buffer and diluting to 50 ml in a volumetric flask with redistilled water; the ionic strength was maintained at 0.2 with sodium nitrate. The spectra were recorded (Spekord UV-Vis) over the range 400—700 nm. The absorption spectra of the oxalato complexes at different pH (Fig. 1) show four isosbestic points at 406, 422, 518 and 586 nm and

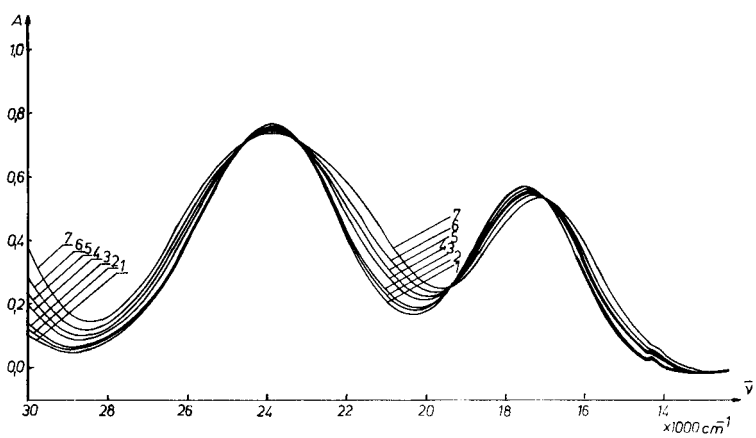

Fig. 1. Visible absorption spectra of the $[Cr(Ox)_2(H_2O)_2]^-$ complex in aqueous solution at different pH values: (1) 6.6, (2) 6.8, (3) 7.0, (4) 7.2, (5) 7.4, (6) 7.6, (7) 7.85.

those for malonato complexes (Fig. 2) show two isosbestic points at 518 and 584 nm. The acidity constants were calculated by a nonlinear least-squares method from the equation:

$$(A_{OH} - A_i)/(A_i - A_H) = K_a/[H^+]$$

where A_i is the absorbance at $[H^+]_i$, A_H and A_{OH} are the absorbances of the acidic and basic forms of the complexes, and K_a is the acidity constant. A_i was measured for $[Cr(Ox)_2(H_2O)_2]^-$ and $[Cr(Mal)_2(H_2O)_2]^-$ at 470 nm. The values of A_{OH}, A_H and A_i were treated as unknown quantities.

The results obtained were $K = 3.1 \times 10^{-8}$, $pK = 7.508$ ($T = 10°C$) for the oxalato complex and $K = 1.86 \times 10^{-8}$, $pK = 7.73$ ($T = 24°C$) for the malonato complex.

Application as acid—base indicators

Indicator concentration and reversibility. Hydrochloric acid solutions were titrated with standard sodium hydroxide solutions in the presence of different concentrations of indicators (1×10^{-3}—10^{-2} M); volumes were about 120 ml at the end-point. These indicator concentrations sufficed to give sharp changes of colour at the end-points. The recommended quantities of indicator are about 0.5 ml of 10^{-2} M solution in a total volume of about 100 ml.

The reversibility of the indicators was satisfactory; one drop of 0.1 M alkali or acid gave the colour change from green to violet or vice versa.

Precision and accuracy. Precision and accuracy were calculated [13] from the results of a large number of titrations with each indicator using acid or base as titrant. The typical results given in Table 1 show that the proposed indicators have nearly the same accuracy and precision in most cases as phenolphthalein. In some cases (e.g., acetic, tartaric, *o*-phthalic

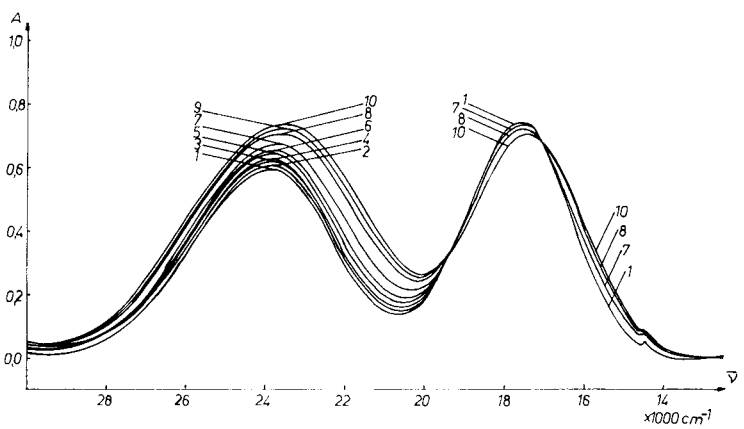

Fig. 2. Visible absorption spectra of the $[Cr(Mal)_2(H_2O)_2]^-$ complex in aqueous solution at different pH values: (1) 5, (2) 6.12, (3) 6.32, (4) 6.60, (5) 6.88, (6) 7.02, (7) 7.28, (8) 7.55, (9) 7.82, (10) 8.00.

TABLE 1

Comparison of results for titrations of different weak acids with 0.2 M sodium hydroxide in the presence of the oxalato (ox.) and malonato (mal.) complexes and phenolphthalein (phph.)[a]

Acid	Acetic 0.2 N			Oxalic 0.2 N		
Indicator	Ox.	Mal.	Phph.	Ox.	Mal.	Phph.
$\bar{x} \pm t_{0.95} \cdot s_{\bar{x}}$	21.52 ± 0.02	21.67 ± 0.02	21.71 ± 0.19	21.52 ± 0.05	21.67 ± 0.05	21.71 ± 0.05
s	0.02	0.02	0.15	0.04	0.04	0.04
Relative average deviation from mean	0.12	0.12	0.56	0.20	0.10	0.16
Relative maximum deviation from mean	0.15	0.15	0.95	0.25	0.25	0.30
Acid	**Malonic 0.2 N**			**Benzoic 0.1 N**		
Indicator	Ox.	Mal.	Phph.	Ox.	Mal.	Phph.
$\bar{x} \pm t_{0.95} \cdot s_{\bar{x}}$	20.29 ± 0.05	20.55 ± 0.05	20.49 ± 0.05	10.20 ± 0.05	10.20 ± 0.01	10.11 ± 0.05
s	0.04	0.04	0.04	0.04	0.01	0.04
Relative average deviation from mean	0.16	0.10	0.16	0.20	—	0.32
Relative maximum deviation from mean	0.30	0.25	0.30	0.50	—	0.60
Acid	***o*-Phthalic 0.2 N**			**Tartaric 0.2 N**		
Indicator	Ox.	Mal.	Phph.	Ox.	Mal.	Phph.
$\bar{x} \pm t_{0.95} \cdot s_{\bar{x}}$	20.69 ± 0.05	20.95 ± 0.05	20.88 ± 0.08	20.54 ± 0.05	20.63 ± 0.03	20.51 ± 0.05
s	0.04	0.04	0.06	0.02	0.02	0.04
Relative average deviation from mean	0.16	0.10	0.22	0.16	0.12	0.16
Relative maximum deviation from mean	0.30	0.25	0.40	0.30	0.15	0.30

[a]Each titration was done 5 times. The mean result, $\bar{x}$, is given with probability 0.95 ($\pm t_{0.95} s_{\bar{x}}$; $t_{0.95} = 2.776$ for $n = 5$, and $s_x = s/n^{1/2}$, s being the standard deviation).

and benzoic acids), the malonato and oxalato complexes are more precise. In general, the malonato complex gave more precise results than the oxalato complex.

To investigate the clarity of the end-point for titrations with acidic solutions, five titrations were done for each indicator at each of several different hydrochloric acid concentrations between 0.95 and 0.095 M. The colour change was from green to violet and the results obtained were very close to those obtained when phenolphthalein, methyl orange and bromothymol blue were used. Analogous results were obtained when hydrochloric acid solutions were titrated with different concentrations of sodium hydroxide between 1.12 and 0.112 M. However, sharp end-points are obtained only when the concentration of alkali is $\geqslant 0.1$ M.

As the indicators change colour in slightly basic medium, they are suitable for titrations of many weak acids with sodium hydroxide; oxalic, acetic, malonic and tartaric acids were titrated in water and phthalic and benzoic acids in aqueous ethanol (cf. Table 1). Borax can also be titrated in presence of these indicators.

Indicator errors. The indicator solutions were prepared from the com-

plexes in their acidic forms. To convert 2 ml of a 10^{-2} M solution of the indicators to the fully deprotonated forms would theoretically require ca. 0.024 ml of 0.1 M sodium hydroxide. With the recommended quantities of indicators, the indicator error should not exceed 0.02 ml of 0.1 M solution. These small indicator errors were confirmed experimentally.

Effect of carbon dioxide. Indicators which show colour changes above about pH 4.5 are inevitably affected by carbon dioxide introduced either from the reagents or from the atmosphere. To check this effect on the proposed indicators, hydrochloric acid was titrated with 0.1 M sodium hydroxide to within 0.1—0.2 ml of the end-point; the solution was then boiled to remove carbon dioxide, immediately cooled in an ice-bath, and titrated to the end-point. The results were 0.05—0.10 ml lower than those obtained without boiling.

Stability of stock indicator solutions. Freshly prepared aqueous stock solutions of the indicators (ca. 10^{-2} M) were stored for several weeks in clear glass bottles exposed to diffused daylight and artificial light but not to direct sunlight. The visible absorption spectra recorded immediately, and after storage for 3, 7, 10, 14 and 21 days, were exactly the same except that the absorbances of the oxalato complex solutions after 21 days were slightly less than those of the fresh solution; this would not affect the efficiency of the indicator. The malonato complex was more stable. In practice, the indicator solutions could be stored for at least a month.

REFERENCES

1 W. Hirsch, Analyst, 73 (1948) 160.
2 A. A. Schilt, Anal. Chim. Acta, 26 (1962) 134.
3 A. J. Cameron and N. A. Gibson, Anal. Chim. Acta, 51 (1970) 249.
4 R. A. Chalmers and F. I. Miller, Analyst, 96 (1971) 97.
5 L. Legradi, Talanta, 19 (1972) 1470.
6 F. Bosch-Serrat, Inf. Quim. Anal. pura apl. Ind., 23(2) (1969) 36.
7 K. Veena, M. Katyal and R. P. Singh, Talanta, 21 (1974) 763.
8 Y. K. Bhoon, K. B. Pandeya and R. P. Singh, J. Ind. Chem. Soc., 51 (1974) 960.
9 M. Katyal, S. K. Kundra and R. P. Singh, Mikrochim. Acta, (1974) 973.
10 G. B. Kauffman and D. Faoro, Inorganic Synthesis, Vol. 17, McGraw-Hill, New York, 1977, p. 147.
11 J. C. Chang, Inorganic Synthesis, Vol. 16, McGraw-Hill, New York, 1976, p.81.
12 J. C. Chang, J. Inorg. Nucl. Chem., 30 (1968) 945.
13 K. Eckschlager, Errors, Measurement and Results in Chemical Analysis, Van Nostrand, London, 1969.

Analytica Chimica Acta, 148 (1983) 327—330
Elsevier Science Publishers B.V., Amsterdam — Printed in The Netherlands

Short Communication

DETERMINATION OF EXTRACTION CONSTANT FOR POLONIUM DIETHYLDITHIOCARBAMATE BY SUBSTOICHIOMETRIC EXTRACTION

J. M. LO and C. M. WAI*

Department of Chemistry, University of Idaho, Moscow, Idaho 83843 (U.S.A.)

(Received 22nd September 1982)

Summary. The extraction constant of polonium diethyldithiocarbamate, $Po(DDTC)_4$, is shown to be 2.75×10^{56}. The value of $1/4 \log K_{Po(DDTC)_4}$ (= 14.1) is slightly greater than $1/3 \log K_{Bi(DDTC)_3}$ (= 13.8) and much greater than $1/2 \log K_{Pb(DDTC)_2}$ (= 9.49). Because of these differences, ^{210}Po and ^{210}Bi may be separated from ^{210}Pb in Ra-DEF by extraction with a metal—DDTC complex such as $Cu(DDTC)_2$ or $Bi(DDTC)_3$.

Diethyldithiocarbamate (DDTC) forms chelates with many metal ions that can be extracted with organic solvents [1]. Extraction constants for different elements vary by many orders of magnitude, and the reagent can be used for the selective extraction of trace metals [1—4]. Polonium can also be extracted by DDTC [5]. The extraction constant of $Po(DDTC)_4$ determined by the substoichiometric extraction technique is reported in this communication. From a quantitative point of view, this value is important for predicting selective extraction of polonium by using metal—DDTC complexes as extracting agents. This is important because polonium is one of the important radioactive elements present in the environment [6, 7].

Data treatment

The extraction constant of $Po(DDTC)_4$ was determined by reacting a Ra-DEF (^{210}Pb, ^{210}Bi, and ^{210}Po) solution with substoichiometric amounts of $Cu(DDTC)_2$ in chloroform. The decay scheme of Ra-DEF is

$$^{210}Pb \xrightarrow[22\ y]{0.061\ MeV\ \beta^-} {}^{210}Bi \xrightarrow[5\ d]{1.17\ MeV\ \beta^-} {}^{210}Po \xrightarrow[138\ d]{5.3\ MeV\ \alpha} {}^{206}Pb\ (stable)$$

The predominant form of each metal ion in the nitric acid solution should be Pb^{2+}, Bi^{3+}, and Po^{4+}, respectively [8—10]. For Bi^{3+} and Po^{4+} in the aqueous phase reacting with $Cu(DDTC)_2$ in the organic phase, it can be shown that

$$[Po^{4+}]_w^{1/2}\,[Bi(DDTC)_3]_o^{2/3}/[Bi^{3+}]_w^{2/3}\,[Po(DDTC)_4]_o^{1/2} = (K_{Bi(DDTC)_3})^{2/3}/(K_{Po(DDTC)_4})^{1/2} \quad (1)$$

where the extraction constants are defined as $K_{M(DDTC)m} = [M(DDTC)_m]_o/[M^{m+}][DDTC^-]^m$, with m being the charge on the metal ion.

0003-2670/83/$03.00

The concentrations of bismuth and polonium in Eqn. (1) can be expressed in terms of distribution ratios ($D_M = C_{M(o)}/C_{M(w)}$) and Ringbom coefficients (α):

$$[(D_{Bi})^{2/3}/(D_{Po})^{1/2}]\,[\alpha_{Bi^{3+}}/\alpha_{Bi(DDTC)_3}]^{2/3}[\alpha_{Po(DDTC)_4}/\alpha_{Po^{4+}}]^{1/2} = (K_{Bi(DDTC)_3})^{2/3}/(K_{Po(DDTC)_4})^{1/2} \quad (2)$$

The Ringbom coefficients [11] are defined as

$$\alpha_{M^{m+}} = C_{M(w)}/[M^{m+}] = \{[M^{m+}] + \Sigma[MX_n^{n-m}]\}/[M^{m+}] \quad (3)$$

$$\alpha_{M(DDTC)_m} = C_{M(o)}/[M(DDTC)_m]_o = \{[M(DDTC)_m]_o + \Sigma[M(DDTC)_{m-n}X_n]_o\}/[M(DDTC)_m]_o \quad (4)$$

where X^- represents other complexing anions (OH^- and NO_3^-) in the system.

Experimentally, D_{Bi} and D_{Po} can be obtained by the substoichiometric extraction technique combined with radiometry [12]. The activities of ^{210}Bi and ^{210}Po in each phase can be measured with a β-counter and an α-counter, respectively. The α values can be estimated by changing the concentration of nitric acid or diethyldithiocarbamate in the experiments. Because $K_{Bi(DDTC)_3}$ is available in the literature, $K_{Po(DDTC)_4}$ can be calculated from the experimental data by using Eqn. (2).

Experimental

Reagents. A Ra-DEF solution in 3 M nitric acid was purchased from Amersham. Chloroform (Baker analyzed reagent; J. T. Baker Co.), nitric acid (ultra-pure grade; Ultrex Baker Co.) and sodium diethyldithiocarbamate (Fisher Scientific Co.) were used as received. The $Cu(DDTC)_2$ complex was synthesized by adding excess of copper(II) ions to a sodium diethyldithiocarbamate solution, as described by Wyttenbach and Bajo [2]. All containers used for the extraction experiments were new Beckman polyvials which were washed with (1 + 9) nitric acid and rinsed with demineralized water before use.

Procedure. About 10 μCi of ^{210}Pb in equilibrium with ^{210}Bi and ^{210}Po were used in each experiment. A portion (1 μl) of the Ra-DEF source in 0.38 M nitric acid was placed in a 5-ml Beckman polyvial with a fast turn cap. After that, 1 ml of $Cu(DDTC)_2$ in chloroform was added. The concentration of the $Cu(DDTC)_2$ in chloroform was adjusted beforehand so that only part of the bismuth and polonium were extracted. The mixture was shaken vigorously for 3 min to reach equilibrium. After another 3 min to allow phase separation, 25 μl of each phase was pipetted into a separate stainless steel planchet. The samples were dried in a hood before counting. The ^{210}Po activities were counted with an α-scintillation counter (ZnS; Model PAS-8; Technical Associates). The β-activities from ^{210}Bi were measured with a Geiger-Müller counter. A thin aluminum absorber (12 mg cm^{-2}) was placed between the planchet and the GM window to remove α-particles from ^{210}Po.

Results and discussion

Table 1 shows the distribution ratios, D_{Bi} and D_{Po}, obtained from the extraction of Ra-DEF in 0.38 M nitric acid by a series of substoichiometric $Cu(DDTC)_2$ solutions in chloroform. A significant observation is that the ratio $(D_{Bi})^{2/3}/(D_{Po})^{1/2}$ for this series of experiments appears to be constant near 0.24 ± 0.02. Because $(D_{Bi})^{2/3}/(D_{Po})^{1/2}$ is independent of DDTC concentration, this implies that both $\alpha_{Bi(DDTC)_3}$ and $\alpha_{Po(DDTC)_4}$ are probably close to unity.

Table 2 shows the distribution ratios in the extraction of Ra-DEF in different nitric acid concentrations by 5×10^{-6} M $Cu(DDTC)_2$ in chloroform. In the nitric acid concentration range from 0.72 to 0.07 M, the $(D_{Bi})^{2/3}/(D_{Po})^{1/2}$ ratio was found to be 0.23 ± 0.02. However, at 1.06 M and 0.03 M nitric acid, lower values were observed. The results seem to indicate that both $\alpha_{Bi^{3+}}$ and $\alpha_{Po^{4+}}$ are also close to unity in 0.72—0.07 M nitric acid. This means that polonium in its tetravalent state predominates in these solutions; which agrees with the report of Koch and Schmidt [10]. At 1.06 M HNO_3, diethyldithiocarbamate is likely to undergo decomposition and so cause lower distribution ratios for bismuth and polonium. At 0.03 M HNO_3, the chemical species of polonium must have changed and the value of $(D_{Bi})^{2/3}/(D_{Po})^{1/2}$ is no longer a constant.

Hataye et al. [13] reported that $Po(OH)_3^+$ should be the predominant species in the nitric acid range 0.01—0.4 M. If the following equation involving $Po(OH)_3^+$ is valid

$$2\,Po(OH)_3^+ + Cu(DDTC)_{2(o)} \rightleftharpoons 2\,Po(OH)_3DDTC_{(o)} + Cu^{2+} \qquad (5)$$

then the equation obtained after combination with the reaction of ionic Bi^{3+} with $Cu(DDTC)_2$ would be

$$(D_{Bi})^{2/3}/(D_{Po})^2 = [\alpha_{Po(OH)_3^+}/\alpha_{Po(OH)_3DDTC}]^2[\alpha_{Bi(DDTC)_3}/\alpha_{Bi^{3+}}]^{2/3}$$
$$[(K_{Bi(DDTC)_3})^{2/3}/(K_{Po(OH)_3DDTC})^2] \qquad (6)$$

It is interesting to note that, in this case, the experimental data for D_{Bi} and D_{Po} shown in Tables 1 and 2 do not give consistent $(D_{Bi})^{2/3}/(D_{Po})^2$ values. The present data do not seem to support the presence of $Po(OH)_3^+$ as the predominant species in the acid range reported by Hataye et al. [13].

TABLE 1

Substoichiometric extraction of Ra-DEF in 0.38 M HNO_3 by $Cu(DDTC)_2$ in chloroform

$[Cu(DDTC)_2]_o$ (M)	D_{Bi}	D_{Po}	$(D_{Bi})^{2/3}/(D_{Po})^{1/2}$
1×10^{-5}	0.80	12.3	0.25
5×10^{-6}	0.50	6.44	0.25
4×10^{-6}	0.39	6.09	0.21
2×10^{-6}	0.30	3.28	0.25
1.5×10^{-6}	0.22	2.51	0.23

TABLE 2

Substoichiometric extraction of Ra-DEF in different concentrations of nitric acid by 5×10^{-6} M $Cu(DDTC)_2$ in chloroform

HNO_3 (M)	D_{Bi}	D_{Po}	$(D_{Bi})^{2/3}/(D_{Po})^{1/2}$
1.06	0.02	1.25	0.06
0.72	0.21	2.86	0.21
0.38	0.50	6.44	0.25
0.16	0.40	6.31	0.22
0.07	0.17	1.89	0.23
0.03	0.02	1.50	0.05

The value of $K_{Bi(DDTC)_3}$ is known to be 2.51×10^{41} [3]. Taking $(D_{Bi})^{2/3}/(D_{Po})^{1/2}$ to be 0.24 and assuming all α values to be 1, $K_{Po(DDTC)_4}$ calculated from Eqn. (2) is 2.75×10^{56}, or 1/4 log $K_{Po(DDTC)_4}$ = 14.1. This value is greater than 1/3 log $K_{Bi(DDTC)_3}$ (= 13.8) and much greater than 1/2 log $K_{Pb(DDTC)_2}$ (= 9.49) [3, 4]. Therefore, it should be possible to separate ^{210}Po and ^{210}Bi from ^{210}Pb in Ra-DEF using $Bi(DDTC)_3$ or other metal—DDTC complexes with extraction constants between those of $Pb(DDTC)_2$ and $Bi(DDTC)_3$ (e.g., $Cu(DDTC)_2$). Among uranium and its daughters, only lead, bismuth, and polonium isotopes can be efficiently extracted by DDTC in acidic solutions. Application of this extraction method for separating and concentrating Ra-DEF from environmental samples is under investigation.

REFERENCES

1 See, e.g., K. Kodama, Methods of Quantitative Inorganic Analysis, Interscience, New York, 1963, p. 69 ff.
2 A. Wyttenbach and S. Bajo, Anal. Chem., 47 (1975) 1813.
3 S. J. Yeh, J. M. Lo and L. H. Shen, Anal. Chem., 52 (1981) 528.
4 L. H. Shen, S. J. Yeh and J. M. Lo, Anal. Chem., 52 (1981) 1882.
5 C. M. Wai and J. M. Lo, Radiochem. Radioanal. Lett., 50 (1982) 293.
6 C. R. Hill, Nature, 208 (1965) 423.
7 E. P. Radford and V. Hunt, Science, 143 (1964) 247.
8 J. Inczedy, Analytical Applications of Complex Equilibria, Ellis Horwood, Chichester, 1976.
9 E. Hogfeldt, Stability Constants of Metal—Ion Complexes, Part A, Inorganic Ligands, IUPAC Chemical Data Series No. 21, Pergamon, Oxford, 1979.
10 V. H. Koch and H. Schmidt, Z. Naturforsch., Teil B, 18 (1963) 936.
11 A. Ringbom, Complexation in Analytical Chemistry, Interscience, New York, 1963.
12 J. Růžička and J. Stary, Substoichiometry in Radiochemical Analysis, Pergamon, Oxford, 1968.
13 I. Hataye, H. Suganuma, M. Sakata and Y. Nagame, J. Inorg. Nucl. Chem., 43 (1981) 2575.

ANALYTICA CHIMICA ACTA, VOL. 148 (1983)

AUTHOR INDEX

Acebal, S. A.
— and de Luca Rebello, A.
Studies on the anodic stripping voltammetry of lead in polluted estuarine waters 71
Adeloju, S. B.
—, Bond, A. M. and Hughes, H. C.
Determination of selenium, copper, lead and cadmium in biological materials by differential pulse stripping voltammetry 59
Akapongkul, U., see Alexander, P. W. 103
Alary, J.
—, Bourbon, P. and Balsa, C.
Determination of total fluorine in blood by an open ashing technique 311
Alexander, P. W.
— and Akapongkul, U.
Amperometric determination of metal ions in a flow-injection system with a copper-amalgam electrode 103
Arden, J. W.
Electrochemical separation and isotopic determination of thallium at the nanogram level by surface ionisation mass spectrometry 211
Avdeef, A.
Weighting scheme for regression analysis using pH data from acid–base titrations 237

Balsa, C., see Alary, J. 311
Bettinelli, M.
Determination of trace metals in siliceous standard reference materials by electrothermal atomic absorption spectrometry after lithium tetraborate fusion 193
Bond, A. M., see Adeloju, S. B. 59
Bourbon, P., see Alary, J. 311
Brihaye, C.
—, Gillain, G. and Duyckaerts, G.
Determination of traces of metals by anodic stripping voltammetry at a rotating glassy carbon ring-disc electrode. Part 3. Evaluation of linear anodic stripping voltammetry with ring collection for the determination of cadmium, lead and copper in pure water and high-purity sodium chloride, and of cadmium, lead, copper, antimony and bismuth in sea water 51
Brooke, P. J., see Evans, W. H. 203

Calokerinos, A. C.
— Hadjiioannou, T. P.
The S_2 calibration curve obtained by using molecular emission cavity analysis 277

Da Silva, I. A., see East, G. A. 41
Davin, E.
—, Guiliano, M., Reymond, H., Mille, G. et Kister, J.
Analyse quantitative de la transformation spiropyranne—mérocyanine par spectroscopie infrarouge de réflexion 271
de Luca Rebello, A., see Acebal, S. A. 71
Di Paolantonio, C. L.
— and Rechnitz, G. A.
Stabilized bacteria-based potentiometric electrode for pyruvate 1
Diamantatos, A.
The recovery of silver after lead collection and perchloric acid parting 293
Duyckaerts, G., see Brihaye, C. 51

East, G. A.
— and Da Silva, I. A.
Direct potentiometry and potentiometric titration of mercury(II) with solid-state ion-selective electrodes 41
Ellis, J., see Hamilton, T. W. 225
El-Seify, F. A., see Łodzińska, A. 321
Elyashberg, M. E., see Gribov, L. A. 159
Evans, W. H.
—, Brooke, P. J. and Lucas, B. E.
Evaluation of a method for determination of indium and thallium in foodstuffs 203

Florence, T. M., see Hamilton, T. W. 225
Freiha, B. A., see Wang, J. 79

Gábor-Klatsmányi, P., see Kopytin, A. V. 35
Genestar, C., see Grases, F. 245
Gent, C. A., see Wilson, S. A. 299
Gillain, G., see Brihaye, C. 51
Grases, F.
—, Genestar, C. and Salinas, F.
Some pyrazolines and isoxazolines as fluorimetric reagents. Kinetic—fluorimetric determination of vanadium 245
Gribov, L. A.
—, Elyashberg, M. E., Koldashov, V. N. and Pletnjov, I. V.
A dialogue computer program system for structure recognition of complex molecules by spectroscopic methods 159
Guiliano, M., see Davin, E. 271
Gureviciene, V. V., see Kulys, J. J. 13

Hadjiioannou, T. P., see Calokerinos, A. C. 277
Hamilton, T. W.
—, Ellis, J. and Florence, T. M.
Determination of gold in natural waters by neutron activation—γ-spectrometry after preconcentration on activated charcoal 225
Hansen, E. H.
—, Růžička, J., Krug, F. J. and Zagatto, E. A. G.
Selectivity in flow injection analysis 111
Hieftje, G. M., see Shabushnig, J. G. 181
Hiraide, M., see Mizuike, A. 305
Hughes, H. C., see Adeloju, S. B. 59

Izvekov, V. P., see Kopytin, A. V. 35

Johnson, D. C., see Pratt, K. W., Jr. 87

Kalvoda, R., see Langmaier, J. 19
Kamachi, S.
—, Wakabayashi, K., Yamaguchi, M. and Ohkura, Y.
Orange-I laurate, a new chromogenic substrate for the assay of lipase in blood 255
Kister, J., see Davin, E. 271
Koldashov, V. N., see Gribov, L. A. 159
Kopytin, A. V.
—, Gábor-Klatsmányi, P., Izvekov, V. P., Pungor, E. and Yagodin, G. A.
A trichloromercurate(II) ion-selective electrode based on the tetradecylphosphonium salt in polyvinyl chloride 35
Krug, F. J., see Hansen, E. H. 111
Kulys, J. J.
—, Laurinavičius, V.-S.A., Pesliakiene, M. V. and Gurevičiene, V. V.
The determination of glucose, hypoxanthine and uric acid with use of bienzyme amperometric electrodes 13

Langmaier, J.
—, Štulík, K. and Kalvoda, R.
Some potentiometric sensors with low output impedance 19
Laurinavičius, V.-S. A., see Kulys, J. J. 13
Lo, J. M.
— and Wai, C. M.
Determination of extraction constant for polonium diethyldithiocarbamate by substoichiometric extraction 327
Łodzińska, A.
— and El-Seify, F. A.
Bisoxalato and bismalonato complexes of chromium(III) as acid—base indicators 321
Lomdahl, G. S.
—, McPherson, R. and Sullivan, J. V.
The atomic emission spectrometric determination of nonconducting materials with a boosted-output glow-discharge source 171
Lucas, B. E., see Evans, W. H. 203

Malofeeva, G. I., see Zolotov, Yu. A. 135
Marcheva, E. V., see Zolotov, Yu. A. 135
McClintock, S. A.
— and Purdy, W. C.
Dual working-electrode electrochemical detector for liquid chromatography 127
McPherson, R., see Lomdahl, G. S. 171
Mille, G., see Davin, E. 271
Miskar'yants, V. G., see Zolotov, Yu. A. 135
Miyawaki, M., see Uesugi, K. 315
Mizuike, A.
—, Hiraide, M. and Mizuno, K.
Preconcentration of trace heavy metals in large aqueous samples of coprecipitation—flotation in a flow system 305
Mizuno, K., see Mizuike, A. 305
Murinov, Yu. I., see Zolotov, Yu. A. 135

Nagahiro, T., see Uesugi, K. 315
Nefedov, V. I., see Zolotov, Yu. A. 135
Nikitin, Yu. E., see Zolotov, Yu. A. 135

Ohkura, Y., see Kamachi, S. 255

Pesliakiene, M. V., see Kulys, J. J. 13
Petrukhin, O. M., see Zolotov, Yu. A. 135
Pletnjov, I. V., see Gribov, L. A. 159
Pratt, K. W., Jr.
— and Johnson, D. C.
The vibrating wire electrode as an amperometric detector for flow-injection systems 87
Pungor, E., see Kopytin, A. V. 35
Purdy, W. C., see McClintock, S. A. 127

Rechnitz, G. A., see Di Paolantonio, C. L. 1
Růžička, J., see Hansen, E. H. 111

Salinas, F., see Grases, F. 245
Shabushnig, J. G.
— and Hieftje, G. M.
Microdrop sample application in electrothermal atomization for atomic absorption spectrometry 181
Shestakov, V. A., see Zolotov, Yu. A. 135
Shiryaeva, O. A., see Zolotov, Yu. A. 135
Štulík, K., see Langmaier, J. 19
Sullivan, J. V., see Lomdahl, G. S. 171

Takayanagi, K.
— and Wong, G. T. F.
Fluorimetric determination of selenium(IV) and total selenium in natural waters 263
Tominaga, M.
— and Umezaki, Y.
Evaluation of interference supressors in electrothermal atomic absorption spectrometry 285

Uesugi, K.
—, Nagahiro, T. and Miyawaki, M.
A highly sensitive spectrophotometric determination of uranium with chromal blue G in the presence of cetyltrimethylammonium chloride 315
Umezaki, Y., see Tominaga, M. 285

Wai, C. M., see Lo, J. M. 327
Wakabayashi, K., see Kamachi, S. 255
Wang, J.
— and Freiha, B. A.
Differential pulse voltammetry with medium-exchange for analytes strongly adsorbed on electrode surfaces 79
Wilson, S. A.
— and Gent, C. A.
Determination of chloride in geological samples by ion chromatography 299
Wong, G. T. F., see Takayanagi, K. 263

Yagodin, G. A., see Kopytin, A. V. 35
Yamaguchi, M., see Kamachi, S. 255
Yao, T.
A chemically-modified enzyme membrane electrode as an amperometric glucose sensor 27

Zagatto, E. A. G., see Hansen, E. H. 111
Zolotov, Yu. A.
—, Petrukhin, O. M., Malofeeva, G. I., Marcheva, E. V., Shiryaeva, O. A., Shestakov, V. A., Miskar'yants, V. G., Nefedov, V. I., Murinov, Yu. I. and Nikitin, Yu. E.
Determination of platinum metals by x-ray fluorescence, atomic emission and atomic absorption spectrometry after preconcentration with a polymeric thioether 135

ACA announcements

ANNOUNCEMENTS OF MEETINGS

EUROANALYSIS V, CRACOW, POLAND

The 5th European Conference on Analytical Chemistry will be held in Cracow, Poland, on Aug. 26–Sept. 1, 1984. On behalf of the Working Party on Analytical Chemistry of the Federation of European Chemical Societies, this conference will be organised by the Polish Chemical Society and the Committee for Analytical Chemistry of the Polish Academy of Sciences. The conference will aim, like earlier conferences, at the broadest possible coverage of analytical chemistry. The programme is being planned to appeal both to practising analytical chemists in industrial and control laboratories and to those teaching and doing research on analytical chemistry at universities and research institutes. Topics will encompass all classical and instrumental analytical techniques of determination and separation. Special sessions will be devoted to Computer-Based Analytical Chemistry (COBAC III) and to Speciation in Trace and Environmental Analysis. The official language of the conference will be English.

Further details may be obtained from Professor Zygmunt Kowalski, Secretary-General, Euroanalysis V, Academy of Mining and Metallurgy, Mickiewicza 30, 30-059 Kraków, Poland.

ISEC '83 – INTERNATIONAL SOLVENT EXTRACTION CONFERENCE, DENVER, COLORADO, U.S.A., AUGUST 26–SEPTEMBER 2, 1983

International Solvent Extraction Conferences (under the aegis of the International Committee for Solvent Extraction Chemistry and Technology) are now being held on three-year cycles. ISEC '77 in Toronto, Canada, and ISEC '80 in Liege, Belgium, each attracted some 500 delegates and 150 papers. The conferences offer a broad technical program covering all phases of solvent extraction and related technologies and feature plentiful social activities. The initial announcement of ISEC '83, sponsored by the American Institute of Chemical Engineers with the American Chemical Society (Industrial Chemistry Division) and The Metallurgical Society of the American Institute of Mining, Metallurgical and Petroleum Engineers as co-sponsors, generated great interest and additional details regarding ISEC '83 are now available. The AIChE Summer National Meeting will be held in Denver, CO, U.S.A., on Aug. 28–Sept. 1, 1983. Its technical sessions will be open to all ISEC delegates at no additional cost.

Further information may be obtained from: Dean C. Judson King, College of Chemistry, University of California, 420 Latimer Hall, Berkeley, CA 94720, U.S.A.

1st INTERNATIONAL SYMPOSIUM ON KINETICS IN ANALYTICAL CHEMISTRY, CORDOBA, SPAIN, SEPTEMBER 27–30, 1983

The symposium will reflect the rapid development and increasing importance of kinetic methods of analysis during recent years. The scientific programme will include catalytic methods (including enzyme-catalyzed applications), differential reaction rate methods, and any aspect of a kinetic nature with an impact on analytical methodology. The symposium will consist of five plenary lectures, contributed papers, and posters. The language of the symposium will be English (with instantaneous translation to Spanish). The social programme will include visits to places of historic interest.

Further information may be obtained from: Professor D. Perez-Bendito, Departamento de Quimica Analitica, Facultad de Ciencias, Universidad de Córdoba, Córdoba, Spain.

5th INTERNATIONAL BIOANALYTICAL FORUM

The 5th International Bioanalytical Forum will be held at the University of Surrey in Guildford (near London), Great Britain, on Sept. 6–9, 1983. The range of topics will include use of stable isotopes, anti-cancer (e.g., Pt-complex) and other drugs, forensic analytes (especially tissue-bound), ligand approaches, and chromatographic advances (e.g., high-performance liquid chromatography with electrochemical detection). Part-attendance is allowed.

Further information may be obtained from: Dr. E. Reid, Guildford Academic Associates, 72 The Chase, Guildford, Surrey GU2 5UL, Great Britain. Tel.: 0483-65324.

2nd INTERNATIONAL SYMPOSIUM ON CAPILLARY CHROMATOGRAPHY

The 2nd International Symposium on Capillary Chromatography will be held on Oct. 10–12, 1983, at the Westchester Marriott Hotel in Tarrytown, NY, U.S.A. The symposium will consist of invited and submitted papers on all aspects of capillary chromatography, given by leading authorities from throughout the world. Informal discussions will permit the free exchange of ideas on various current questions related to these techniques and their applications. There will also be an exhibition of chromatography instrumentation.

Further information may be obtained from: Dr. A. Zlatkis, Chemistry Department, University of Houston, Houston, TX 77004, U.S.A.

WORKSHOP ON HANDLING OF ENVIRONMENTAL AND BIOLOGICAL SAMPLES IN CHROMATOGRAPHY

This workshop will be held at the Lausanne Congress Centre in Lausanne, Switzerland, on Nov. 24–25, 1983, and is organized by the International Association of Environmental Analytical Chemistry and is sponsored by national organizations. The workshop is intended to bring together specialists in this field who can give a good account of the state-of-the-art in their particular specialty and to present first-hand experience in sample handling. Strong industrial participation and ample discussion time are planned. Poster contributions to the workshop can be submitted until October 15, 1983.

A short course on "sample handling in liquid chromatography" will be offered prior to the workshop on Nov. 22–23, 1983, in the same location.

For further information contact: Prof. R.W. Frei, The Free University of Amsterdam, Department of Analytical Chemistry, De Boelelaan 1083, 1081 HV Amsterdam, The Netherlands.

CALENDAR OF FORTHCOMING MEETINGS

April 26–28, 1983 Riva del Garda, Italy	**5th International Symposium on Capillary Chromatography** Contact: Dr. P. Sandra, Laboratory of Organic Chemistry, University of Ghent, Krijgslaan 281 (S4), B-9000 Ghent, Belgium
May 2–6, 1983 Baden-Baden, G.F.R.	**VIIth International Symposium on Column Liquid Chromatography** Contact: Gesellschaft Deutscher Chemiker, Abteilung Fachgruppen, Postfach 90 04 40, Varrentrappstrasse 40–42, D-6000 Frankfurt (Main) 90, G.F.R.
May 15–17, 1983 Indianapolis, IN, U.S.A.	**1983 Symposium on LCEC and Voltammetry** Contact: LCEC Symposium, P.O. Box 2206, West Lafayette, IN 47096, U.S.A.
June 1–3, 1983 Budapest, Hungary	**The Budapest Chromatography Conference** Contact: Dr. Tibor Devenyi, Institute of Enzymology, Hungarian Academy of Sciences, Budapest, Hungary, or Dr. Haleem J. Issaq, NCI-Frederick Cancer Research Facility, P.O. Box B, Frederick, MD 21701, U.S.A.

June 5–10, 1983 Cologne, G.F.R.	**29th Congress of the International Union of Pure and Applied Chemistry (IUPAC)** Contact: General Secretariat of the 29th IUPAC Congress, Dr. W. Fritsche, c/o Gesellschaft Deutscher Chemiker, Postfach 90 04 40, D-6000 Frankfurt (Main) 90, G.F.R. (Further details published in Vol. 142.)
June 7–10, 1983 Brussels, Belgium	**1st International Symposium on Drug Analysis** Contact: Ms. C. Van Kerchove, Secretary, Société Belge des Sciences Pharmaceutiques/Belgisch Genootschap voor Pharmaceutische Wetenschappen, rue Archimedesstraat 11, B-1040 Brussels, Belgium. Tel.: (02) 733 98 20, ext. 33.
June 13–17, 1983 Annapolis, MD, U.S.A.	**5th International Symposium on Affinity Chromatography and Biological Recognition** Contact: Fifth International Symposium Secretariat, 9650 Rockville Pike, Bethesda, MD 20814, U.S.A.
June 20–23, 1983 Montreux, Switzerland	**International Symposium on Chromatography and Mass Spectrometry in Nutrition Science and Food Safety** Contact: Secretariat, International Symposium on Chromatography and Mass Spectrometry in Nutrition Science and Food Safety, c/o Italian Group for Mass Spectrometry in Biochemistry and Medicine, Via Eritrea 62, 20157 Milan, Italy. Tel: (02) 35 54 546; Telex: 331268 Negri I.
June 26–July 1, 1983 Amsterdam, The Netherlands	**23rd Colloquium Spectroscopium Internationale** Contact: Conference Secretariat 23 CSI, c/o Organisatie Bureau Amsterdam BV, Europaplein, 1078 GZ Amsterdam, The Netherlands. Tel.: (020) 44 08 07. Telex: 13499 raico nl. (Further details published in Vol. 138.)
June 27–July 1, 1983 Gatlinburg, TN, U.S.A.	**3rd Symposium on Separation Science and Technology for Energy Applications** Contact: A.P. Malinauskas, Oak Ridge National Laboratory, P.O. Box X, Oak Ridge, TN 37830, U.S.A. (Further details published in Vol. 142.)
July 17–23, 1983 Edinburgh, Scotland, Great Britain	**SAC '83, 6th International Conference and Exhibition on Analytical Chemistry** Contact: Miss P.E. Hutchison, The Royal Society of Chemistry, Analytical Division, Burlington House, London W1V 0BN, Great Britain. Tel.: 01-734-9971. (Further details published in Vol. 132.)
Aug. 1–5, 1983 New Hampton, NH, U.S.A.	**Gordon Research Conference on Statistics in Chemistry and Chemical Engineering** Contact: Dr. A.M. Cruickshank, Director, Gordon Research Conferences, Pastore Chemical Laboratory, University of Rhode Island, Kingston, RI 02881, U.S.A. Tel.: (401) 783-4011.
Aug. 26–Sept. 2, 1983 Denver, CO, U.S.A.	**ISEC '83 – International Solvent Extraction Conference** Contact: Dean C. Judson King, College of Chemistry, University of California, 420 Latimer Hall, Berkeley, CA 94720, U.S.A.
Aug. 28–Sept. 2, 1983 Amsterdam, The Netherlands	**9th International Symposium on Microchemical Techniques** Contact: Symposium Secretariat, c/o Municipal Congress Bureau, Oudezijds Achterburgwal 199, 1012 DK Amsterdam, The Netherlands. Tel: (020) 552 3459. (Further details published in Vol. 135, No. 2.)
Aug. 29–Sept. 2, 1983 Bratislava, Czechoslovakia	**4th Danube Symposium on Chromatography and 7th International Symposium "Advances and Application of Chromatography in Industry"** Contact: Professor J. Garaj, Department of Analytical Chemistry, Faculty of Chemical Technology, Jánska 1, 81237 Bratislava, Czechoslovakia.

Sept. 5–9, 1983 Bucharest, Romania	**MACRO '83: 29th IUPAC International Symposium on Macromolecules** Contact: IUPAC MACRO'83, Calea Plevnei 139, R-77131 Bucharest, Romania.
Sept. 6–9, 1983 Guildford, Great Britain	**5th International Bioanalytical Forum** Contact: Dr. E. Reid, Guildford Academic Associates, 72 The Chase, Guildford, Surrey GU2 5UL, Great Britain. Tel.: 0483-65324.
Sept. 11–14, 1983 Linz, Austria	**2nd International Conference on Carbonaceous Particles in the Atmosphere** Contact: Doz. Dr. H. Puxbaum, Institute for Analytical Chemistry, Technical University of Vienna, Getreidemarkt 9, A-1060 Wien, Austria. (Further details published in Vol. 142.)
Sept. 12–15, 1983 London, Great Britain	**3rd BOC Priestley Conference – Oxygen and the Conversion of Future Feedstocks** Contact: Dr. John F. Gibson, The Royal Society of Chemistry, Burlington House, London W1V 0BN, Great Britain.
Sept. 19–22, 1983 Fukuoka, Japan	**International Meeting on Chemical Sensors** Contact: Professor Noboru Yamazoe, Secretary, International Meeting on Chemical Sensors, Department of Materials Science and Technology, Graduate School of Engineering Sciences, Kyushu University, Kasuga, Kasuga-shi, Fukuoka 816, Japan.
Sept. 21–29, 1983 Amsterdam, The Netherlands	**het instrument** Contact: het instrument, Birkstraat 108, Postbus 152, 3760 AD Soest, The Netherlands. Tel. (02155) 18204.
Sept. 27–30, 1983 Córdoba, Spain	**1st International Symposium on Kinetics in Analytical Chemistry** Contact: Professor D. Perez-Bendito, Departamento de Quimica Analitica, Facultad de Ciencias, Universidad de Córdoba, Córdoba, Spain.
Sept. 29–30, 1983 Schliersee, G.F.R.	**Symposium "Chiralität und Aktivität"** Contact: Gesellschaft Deutscher Chemiker, Geschäftsstelle, Postfach 90 04 40, D-6000 Frankfurt am Main 90, G.F.R. Tel.: 0611/7917-366.
Oct. 3–6, 1983 Amsterdam, The Netherlands	**20th Anniversary – International Symposium on Advances in Chromatography** Contact: Professor A. Zlatkis, Department of Chemistry, University of Houston, Houston, TX 77004, U.S.A. (Further details published in Vol. 146.)
Oct. 10–12, 1983 Tarrytown, NY, U.S.A.	**Capillary Chromatography – 2nd International Symposium** Contact: Professor A. Zlatkis, Department of Chemistry, University of Houston, Houston, TX 77004, U.S.A.
Oct. 12–14, 1983 London, Great Britain	**Analyticon 83** Contact: Mr. G.C. Young, SIMA, Leicester House, 8 Leicester Street, London WC2H 7BN, Great Britain.
Oct. 17–21, 1983 Neubrandenburg, G.D.R.	**Analytiktreffen 1983: Fortschritte in der Gas- und Flüssigkeits-Chromatographie** Contact: Dr. sc. W. Engewald, Karl-Marx-Universität Leipzig, Sektion Chemie, Leibigstrasse 18, DDR-7010 Leipzig, G.D.R.
Nov. 10–16, 1983 Düsseldorf, G.F.R.	**9th International Congress and Exhibition for Instrumentation and Automation (INTERKAMA 83)** Contact: INTERKAMA 83, Düsseldorfer Messegesellschaft mbH, NOWEA, Postfach 32 02 03, D-4000 Düsseldorf 30, G.F.R.

Nov. 14–16, 1983 Monte Carlo, Monaco	**3rd International Symposium on HPLC of Proteins, Peptides and Polynucleotides** Contact: Shirley E. Schlessinger, 400 East Randolph, Chicago, IL 60601, U.S.A. Tel.: (312) 527-2011.
Nov. 16–18, 1983 New York, NY, U.S.A.	**22nd Eastern Analytical Symposium** Contact: Norman Gardner, 73 Ethel Street, Metuchen, NJ 08840, U.S.A. Tel.: (201) 548-7377.
Nov. 24–25, 1983 Lausanne, Switzerland	**Workshop on Handling of Environmental and Biological Samples in Chromatography** Contact: Prof. R.W. Frei, The Free University of Amsterdam, Department of Analytical Chemistry, De Boelelaan 1083, 1081 HV Amsterdam, The Netherlands.
Dec. 7–10, 1983 Singapore, Singapore	**Chem Asia '83 Conference** Contact: Singapore Exhibition Services, Ltd., 601 Cathay Building, Singapore 0922, Singapore.
Jan. 2–6, 1984 San Diego, CA, U.S.A.	**1984 Winter Conference on Plasma Spectroscopy** Contact: Dr. Ramon M. Barnes, Conference Chairman, Department of Chemistry, GRC Towers, University of Massachusetts, Amherst, MA 01003-0035, U.S.A. Tel.: (413) 545-2294.
April 16–19, 1984 New York, NY, U.S.A.	**20th International Symposium on Chromatography** Contact: Professor A. Zlatkis, Chemistry Department, University of Houston, Houston, TX 77004, U.S.A.
May 9–11, 1984 Dourdan, France	**4th Weurman Flavour Research Symposium** Contact: J. Adda, Laboratoire de Recherches sur les Arômes, 17 rue Sully, 21034 Dijon Cedex, France.
May 20–26, 1984 New York, NY, U.S.A.	**8th International Symposium on Column Liquid Chromatography** Contact: Professor Cs. Horváth, Mason Laboratory, Yale University, P.O. Box 2159, Yale Station, New Haven, CT 06520, U.S.A. (Further details published in Vol. 146.)
Aug. 26–31, 1984 Philadelphia, PA, U.S.A.	**188th National Meeting of the American Chemical Society** Contact: A.T. Winstead, American Chemical Society, 1155 16th Street, NW, Washington, DC 20036, U.S.A.
Aug. 26–Sept. 1, 1984 Cracow, Poland	**EUROANALYSIS V – 5th European Conference on Analytical Chemistry** Contact: Professor Zygmunt Kowalski, Secretary-General, Euroanalysis V, Academy of Mining and Metallurgy, Mickiewicza 30, 30-059 Kraków, Poland.
Sept. 2–5, 1984 Hradec Králové, Czechoslovakia	**4th International Symposium on Isotachophoresis – ITP 84** Contact: ITP 84, Dr. Z. Prusik, C.Sc., Institute of Organic Chemistry and Biochemistry, Czechoslovak Academy of Sciences, Flemingovo nám. 2, CS-166 10 Praha 6, Czechoslovakia. (Further details published in Vol. 146.)
Sept. 23–28, 1984 Philadelphia, PA, U.S.A.	**11th Annual Meeting of the Federation of Analytical Chemistry and Spectroscopy Societies** Contact: R.F. Hirsch, Division of Analytical Chemistry, American Chemical Society, 304 Beach Wood, Orange, NJ 07050, U.S.A.
Oct. 1–5, 1984 Nürnberg, G.F.R.	**15th International Symposium on Chromatography** Contact: Gesellschaft Deutscher Chemiker, Abteilung Fachgruppen, Postfach 90 04 40, Varrentrappstrasse 40–42, D-6000 Frankfurt (Main) 90, G.F.R.

Nov. 22–24, 1984
Barcelona, Spain

14th Annual Symposium on Analytical Chemistry of Pollutants
Contact: 3rd International Congress on Analytical Techniques in Environmental Chemistry/EXPOQUIMIA, Av. Reina Ma. Christina, Palacio No. 1, Barcelona 4, Spain. Tel.: 223.31.01; telex: 50458 FOIMB-E.

Nov. 22–24, 1984
Barcelona, Spain

3rd International Congress on Analytical Techniques in Environmental Chemistry
Contact: 3rd International Congress on Analytical Techniques in Environmental Chemistry/EXPOQUIMIA, Av. Reina Ma. Christina, Palacio No. 1, Barcelona 4, Spain. Tel.: 223.31.01; telex: 50458 FOIMB-E.

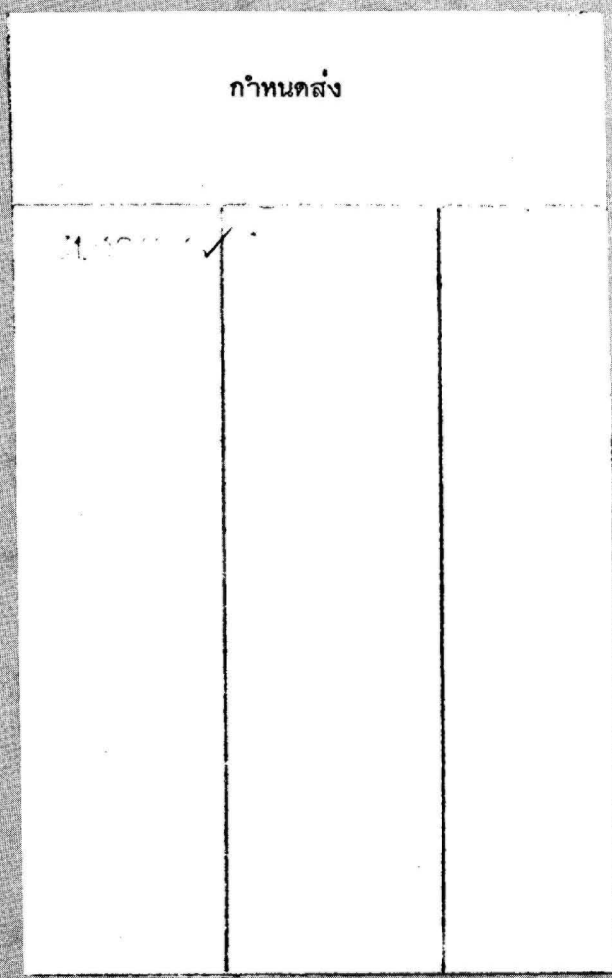

Continued from outside back cover)

Microdrop sample application in electrothermal atomization for atomic absorption spectrometry
J. G. Shabushnig and G. M. Hieftje (Bloomington, IN, U.S.A.) 181
Determination of trace metals in siliceous standard reference materials by electrothermal atomic absorption spectrometry after lithium tetraborate fusion
M. Bettinelli (Piacenza, Italy) 193
Evaluation of a method for determination of indium and thallium in foodstuffs
W. H. Evans, P. J. Brooke and B. E. Lucas (London, Gt. Britain) 203
Electrochemical separation and isotopic determination of thallium at the nanogram level by surface ionisation mass spectrometry
J. W. Arden (Oxford, Gt. Britain) 211
Determination of gold in natural waters by neutron activation–γ-spectrometry after preconcentration on activated charcoal
T. W. Hamilton, J. Ellis (Wollongong, N.S.W., Australia) and T. M. Florence (Lucas Heights, N.S.W., Australia) 225
Weighting scheme for regression analysis using pH data from acid–base titrations
A. Avdeef (Syracuse, NY, U.S.A.) 237
Some pyrazolines and isoxazolines as fluorimetric reagents. Kinetic–fluorimetric determination of vanadium
F. Grases, C. Genestar (Palma de Mallorca, Spain) and F. Salinas (Badajoz, Spain) 245
Orange-I laurate, a new chromogenic substrate for the assay of lipase in blood
S. Kamachi, K. Wakabayashi (Tokyo, Japan), M. Yamaguchi and Y. Ohkura (Fukuoka, Japan) . . . 225
Fluorimetric determination of selenium(IV) and total selenium in natural waters
K. Takayanagi and G. T. F. Wong (Norfolk, VA, U.S.A.) 263

Short Communications

Analyse quantitative de la transformation spiropyranne–mérocyanine par spectroscopie infrarouge de réflexion
E. Davin, M. Guiliano, H. Reymond, G. Mille et J. Kister (Marseille, France) 271
The S_2 calibration curve obtained by using molecular emission cavity analysis
A. C. Calokerinos and T. P. Hadjiioannou (Athens, Greece) 277
Evaluation of interference suppressors in electrothermal atomic absorption spectrometry
M. Tominaga and Y. Umezaki (Ibaraki, Japan) 285
The recovery of silver after lead collection and perchloric acid parting
A. Diamantatos (Germiston, South Africa) 293
Determination of chloride in geological samples by ion chromatography
S. A. Wilson and C. A. Gent (Denver, CO, U.S.A.) 299
Preconcentration of trace heavy metals in large aqueous samples by coprecipitation–flotation in a flow system
A. Mizuike, M. Hiraide and K. Mizuno (Nagoya, Japan) 305
Determination of total fluorine in blood by an open ashing technique
J. Alary, P. Bourbon and C. Balsa (Vigoulet Auzil, France) 311
A highly sensitive spectrophotometric determination of uranium with chromal blue G in the presence of cetyltrimethylammonium chloride
K. Uesugi, T. Nagahiro (Himeji, Japan) and M. Miyawaki (Kobe, Japan) 315
Oxoxalato and bismalonato complexes of chromium(III) as acid–base indicators
A. Łodzińska and F. A. El-Seify (Toruń, Poland) 321
Determination of extraction constant for polonium diethyldithiocarbamate by substoichiometric extraction
J. M. Lo and C. M. Wai (Moscow, ID, U.S.A.) 327

Author Index 331

CONTENTS

(Abstracted, Indexed in: Anal. Abstr.; Biol. Abstr.; Chem. Abstr.; Curr. Contents Phys. Chem. Earth Sci.; Life Sci.; Index Med.; Mass Spectrom. Bull.; Sci Citation Index; Excerpta Med.)

Stabilized bacteria-based potentiometric electrode for pyruvate
C. L. Di Paolantonio and G. A. Rechnitz (Newark, DE, U.S.A.) 1
The determination of glucose, hypoxanthine and uric acid with use of bi-enzyme amperometric electrodes
J. J. Kulys, V.-S. A. Laurinavičius, M. V. Pesliakiene and V. V. Gurevičiene (Vilnius, U.S.S.R.) 13
Some potentiometric sensors with low output impedance
J. Langmaier, K. Štulík and R. Kalvoda (Prague, Czechoslovakia) 19
A chemically-modified enzyme membrane electrode as an amperometric glucose sensor
T. Yao (Osaka, Japan) 27
A trichloromercurate(II) ion-selective electrode based on the tetradecylphosphonium salt in polyvinyl chloride
A. V. Kopytin, P. Gábor-Klatsmányi, V. P. Izvekov, E. Pungor (Budapest, Hungary) and G. A. Yagodin (Moscow, U.S.S.R.). 35
Direct potentiometry and potentiometric titration of mercury(II) with solid-state ion selective electrodes
G. A. East and I. A. Da Silva (Brasília, Brasil) 41
Determination of traces of metals by anodic stripping voltammetry at a rotating glassy carbon ring-disc electrode. Part 3. Evaluation of linear anodic stripping voltammetry with ring collection for the determination of cadmium, lead and copper in pure water and high-purity sodium chloride, and of cadmium, lead, copper, antimony and bismuth in sea water
C. Brihaye, G. Gillain and G. Duyckaerts (Liège, Belgium) 51
Determination of selenium, copper, lead and cadmium in biological materials by differential pulse stripping voltammetry
S. B. Adeloju, A. M. Bond (Waurn Ponds, Victoria, Australia) and H. C. Hughes (South Bentley, W.A., Australia). 59
Studies on the anodic stripping voltammetry of lead in polluted estuarine waters
S. A. Acebal and A. de Luca Rebello (Rio de Janeiro, Brasil) 71
Differential pulse voltammetry with medium-exchange for analytes strongly adsorbed on electrode surfaces
J. Wang and B. A. Freiha (Las Cruces, NM, U.S.A.). 79
The vibrating wire electrode as an amperometric detector for flow-injection systems
K. W. Pratt, Jr. and D. C. Johnson (Ames, IA, U.S.A.) 87
Amperometric determination of metal ions in a flow-injection system with a copper-amalgam electrode
P. W. Alexander and U. Akapongkul (Kensington, N.S.W., Australia). 103
Selectivity in flow injection analysis
E. H. Hansen, J. Růžička (Lyngby, Denmark), F. J. Krug and E. A. G. Zagatto (Piracicaba, Brasil) 111
Dual working-electrode electrochemical detector for liquid chromatography
S. A. McClintock and W. C. Purdy (Montreal, Quebec, Canada) 127
Determination of platinum metals by x-ray fluorescence, atomic emission and atomic absorption spectrometry after preconcentration with a polymeric thioether
Yu. A. Zolotov, O. M. Petrukhin, G. I. Malofeeva, E. V. Marcheva, O. A. Shiryaeva, V. A. Shestakov, V. G. Miskar'yants, V. I. Nefedov (Moscow, U.S.S.R.), Yu. I. Murinov and Yu. E. Nikitin (Ufa, U.S.S.R.) 135
A dialogue computer program system for structure recognition of complex molecules by spectroscopic methods
L. A. Gribov, M. E. Elyashberg, V. N. Koldashov and I. V. Pletnjov (Moscow, U.S.S.R.) 159
The atomic emission spectrometric determination of non-conducting materials with a boosted-output glow-discharge source
G. S. Lomdahl, R. McPherson and J. V. Sullivan (Clayton, Victoria, Australia) 171

(Continued on inside back cover)